INTEGRATIVE APPROACH TO PARKINSON'S DISEASE

EDITED BY: Hi-Joon Park, Xiaomin Wang and Seung-Nam Kim
PUBLISHED IN: Frontiers in Aging Neuroscience and Frontiers in Neuroscience

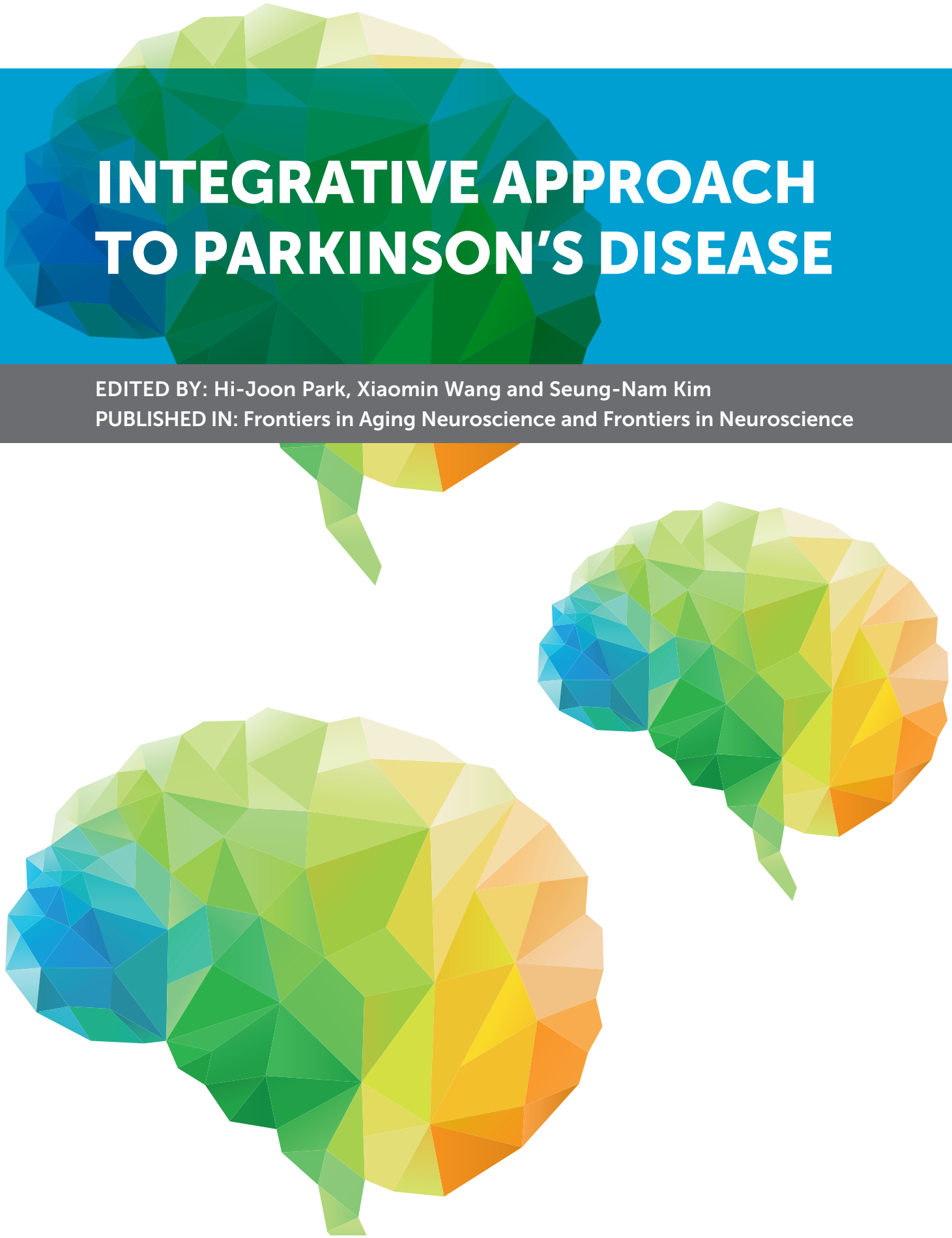

frontiers Research Topics

frontiers

ISSN 1664-8714
ISBN 978-2-88963-409-5
DOI 10.3389/978-2-88963-409-5

About Frontiers

Frontiers is more than just an open-access publisher of scholarly articles: it is a pioneering approach to the world of academia, radically improving the way scholarly research is managed. The grand vision of Frontiers is a world where all people have an equal opportunity to seek, share and generate knowledge. Frontiers provides immediate and permanent online open access to all its publications, but this alone is not enough to realize our grand goals.

Frontiers Journal Series

The Frontiers Journal Series is a multi-tier and interdisciplinary set of open-access, online journals, promising a paradigm shift from the current review, selection and dissemination processes in academic publishing. All Frontiers journals are driven by researchers for researchers; therefore, they constitute a service to the scholarly community. At the same time, the Frontiers Journal Series operates on a revolutionary invention, the tiered publishing system, initially addressing specific communities of scholars, and gradually climbing up to broader public understanding, thus serving the interests of the lay society, too.

Dedication to Quality

Each Frontiers article is a landmark of the highest quality, thanks to genuinely collaborative interactions between authors and review editors, who include some of the world's best academicians. Research must be certified by peers before entering a stream of knowledge that may eventually reach the public - and shape society; therefore, Frontiers only applies the most rigorous and unbiased reviews.
Frontiers revolutionizes research publishing by freely delivering the most outstanding research, evaluated with no bias from both the academic and social point of view. By applying the most advanced information technologies, Frontiers is catapulting scholarly publishing into a new generation.

What are Frontiers Research Topics?

Frontiers Research Topics are very popular trademarks of the Frontiers Journals Series: they are collections of at least ten articles, all centered on a particular subject. With their unique mix of varied contributions from Original Research to Review Articles, Frontiers Research Topics unify the most influential researchers, the latest key findings and historical advances in a hot research area! Find out more on how to host your own Frontiers Research Topic or contribute to one as an author by contacting the Frontiers Editorial Office: researchtopics@frontiersin.org

INTEGRATIVE APPROACH TO PARKINSON'S DISEASE

Topic Editors:
Hi-Joon Park, Kyung Hee University, South Korea
Xiaomin Wang, Beijing Institute for Brain Disorders, Capital Medical University, China
Seung-Nam Kim, Dongguk University,South Korea

Citation: Park, H.-J., Wang, X., Kim, S.-N., eds. (2020). Integrative approach to Parkinson's disease. Lausanne: Frontiers Media SA. doi: 10.3389/978-2-88963-409-5

Table of Contents

frontiers in Aging Neuroscience

EDITORIAL
published: 05 December 2019
doi: 10.3389/fnagi.2019.00339

Editorial: Integrative Approach to Parkinson's Disease

Seung-Nam Kim[1]*, *Xiaomin Wang*[2] and *Hi-Joon Park*[3]

[1] College of Korean Medicine, Dongguk University, Goyang, South Korea, [2] Beijing Institute for Brain Disorders, Capital Medical University, Beijing, China, [3] College of Korean Medicine, Kyung Hee University, Seoul, South Korea

Keywords: Parkinson's disease, complementary and alternative medicine, experimental model, clinical research, molecular mechanism

Editorial on the Research Topic

Integrative Approach to Parkinson's Disease

Parkinson's disease (PD) is a progressive neurodegenerative disease characterized by motor symptoms such as gait dysfunction, rigidity, involuntary tremor, and progressive postural instability (Demaagd and Philip, 2015). PD was first reported by Dr. James Parkinson in 1817 and knowledge of the disease is continuously increasing. Emerging evidence indicates that PD is currently the second most common neurological disorder, with a prevalence of ∼1% among individuals aged 60–70 years, increasing to ∼3% among those aged 80 years and older (Tanner and Goldman, 1996; Nussbaum and Ellis, 2003). Due to the increase in aging of the population, both the prevalence and incidence of PD are expected to rise by at least 30% by 2030, which will impose greater burden on society and the worldwide economy (Chen et al., 2001). Not only the pathology of PD is characterized by depletion of dopaminergic neurons in the substantia nigra pars compacta, but also involves other regions, related neural networks (Thomas and Beal, 2007). Treatment predominantly aims for symptom relief via drugs that increase dopamine levels in the striatum. Motor dysfunction is not the only symptom of PD, and drugs are used to relieve other symptoms such as mood disturbances and pain (Demaagd and Philip, 2015). Moreover, antioxidants, scavenging free radicals, apoptosis, and inflammation are also being studied to develop drugs that can prevent the death of dopaminergic neurons. However, novel therapies to reduce the rate of neurodegeneration, or to replenish lost neurons, are mainly in the laboratory research stage; there have been few early stage clinical trials.

Complementary and alternative medicine (CAM) encompasses diverse medical and health care systems, practices, and products that are not presently classified as conventional medicine. Complementary medicine refers to treatments used in conjunction with conventional medicine, while alternative medicine refers to treatments used instead of standard medical care. Integrative medicine is a combinatorial approach to medical care that integrates conventional medicine with CAM practices for which safety and efficacy have been demonstrated. CAM includes many techniques, such as acupuncture, herbal therapies, massage, and moxibustion. CAM has been used to relieve various ailments, including neurological diseases. Recently, the use of CAM has been increasing worldwide, as has the number of PD patients who favor integrative approaches. Reportedly, ∼40% of PD patients use CAM, including herbs, acupuncture, and qigong exercises (Ghaffari and Kluger, 2014). Nonetheless, scientific evidence supporting the efficacy of CAM remains insufficient. Therefore, in this review, recent research showing how CAM is useful for treating PD patients is discussed.

This editorial includes two review articles and four original *in vivo*/*in vitro* studies on herbal therapies for PD. Ding et al. analyzed the natural molecules present in Chinese herbs. In their study, positive effects on PD of the natural antioxidant molecules present in Chinese herbs were

OPEN ACCESS

Edited by:
P. Hemachandra Reddy, Texas Tech University Health Sciences Center, United States

Reviewed by:
Xudong Huang, Massachusetts General Hospital, Harvard Medical School, United States

***Correspondence:**
Seung-Nam Kim
snkim@dongguk.edu

Received: *30 September 2019*
Accepted: *22 November 2019*
Published: *05 December 2019*

Citation:
Kim S-N, Wang X and Park H-J (2019) Editorial: Integrative Approach to Parkinson's Disease. Front. Aging Neurosci. 11:339. doi: 10.3389/fnagi.2019.00339

suggested to be due to modulatory effects on mitochondrial function, intracellular antioxidant activity, dopamine metabolism, and iron levels. In another study, the phytochemical and pharmacological actions of *Radix Glycyrrhizae* in health and disease states were reviewed (Ramalingam et al.). The authors isolated the main components from *Radix Glycyrrhizae* and reported in detail on its pharmacological activities against neurodegenerative diseases, including PD. Kim et al. performed an *in vitro* study and observed that the mitochondrial dysfunction induced by MPP was rescued by *Sophora flevescens*. Korean red ginseng has also been studied and showed neurogenic effects in the subventricular zone of the brain in a mouse model of PD (Ryu et al.). Adult neurogenesis is important in the context of PD, and their study is informative for clinicians by showing the possible utility of red ginseng in the treatment of PD patients. Elsewhere, two herbal formulas were studied in terms of their potential beneficial effects on PD. Ahn et al. reported that Gami-Chunggan formula prevented motor dysfunction in animal models of PD *via* the induction of DJ-1 and BDNF expression. In an MPTP/p-induced and overexpressed A53T α-synuclein mouse model of PD, Gami-Chunggan formula conferred protection against neurotoxicity. In another study, performed by Huh et al., Ukgansan was shown to have synergistic effects with a conventional drug, aiding in the repair of dopamine neurons damaged by L-dopa.

Acupuncture was reported to have neuroprotective effects in rodent models of PD (Park et al., 2017). However, no review of the neuroprotective effects of acupuncture had been reported until Ko et al. performed a systematic review of animal studies on PD, published up to 2018, to determine the protective effects of acupuncture on PD. Although their review had some limitations, the authors concluded that both manual acupuncture and electroacupuncture showed statistical improvement in tyrosine hydroxylase-positive dopaminergic neurons, including MPTP, 6-OHDA, and in a genetic mutant. Zhao et al. reported that electroacupuncture ameliorated MPTP-induced motor dysfunction and rescued dopamine neuron depletion *via* activation of the TrkB pathway. In recent studies, the potential effects of bee venom for the treatment of PD were demonstrated (Cho et al., 2018). Baek et al. assessed the neuroprotective effects of bee venom according to the route of administration, while Kim et al. demonstrated dose-dependent beneficial effects of standardized bee venom phospholipase A2 in an animal model of PD. These studies both indicate that bee venom acupuncture has beneficial effects in PD patients.

This editorial also includes two articles pertaining to the clinical application of CAM. Woo and Hyun analyzed the effectiveness of integrative therapy for management of PD cases in the Republic of Korea. Although their study had some limitations, the authors concluded that integrative therapy is a better treatment for PD patients compared to conventional monotherapy. In another study, Cho et al. developed CAM practice guidelines for idiopathic PD patients. The guidelines were developed by experienced practitioners drawn from numerous centers, using an evidence-based approach based on registered clinical trials. The authors noted that even though they had several limitations, these initial CAM guidelines for PD patients would facilitate the use of integrative approaches. Potential biomarkers for PD diagnosis are also detailed in this editorial. Decreased serum amyloid alpha levels were found in the peripheral tissues of PD patients (Kurvits et al.). Elsewhere, the reliability of DJ-1 promoter polymorphisms as PD biomarkers was extensively studied (He et al.), while peripheral blood levels of Nurr1 and cytokines were also suggested as putative PD biomarkers (Li et al.). Due to the development of blood diagnostic tests, data can be generated to accelerate the development of integrative approaches to PD.

This review provided strong evidence for the efficacy of integrative approaches to the clinical treatment of PD patients. However, several issues remain to be evaluated. For example, an individualized approach, characterized by personalized diagnosis and treatment, is an important advantage of integrative medicine over conventional medicine. Differences in diagnoses based on symptoms, even among cases all diagnosed with PD, should be further investigated in the context of integrative medicine. Also, the relationship between integrative diagnosis and genetic information needs to be further explored. Additional studies are necessary to gain more insight into these topics. Nevertheless, integrative medicine is a promising approach that could yield clinically effective treatments for PD.

AUTHOR CONTRIBUTIONS

S-NK, XW, and H-JP wrote the manuscript.

FUNDING

This work was supported by National Research Foundation of Korea funded by the Korea government (MSIT) (NRF-2017R1C1B5018061, NRF-2015M3A9E3052338, and 2017R1A2B4009963) and from the Korea Institute of Oriental Medicine (grant K18182).

REFERENCES

Chen, R. C., Chang, S. F., Su, C. L., Chen, T. H., Yen, M. F., Wu, H. M., et al. (2001). Prevalence, incidence, and mortality of PD: a door-to-door survey in Ilan county, Taiwan. *Neurology* 57, 1679–1686. doi: 10.1212/wnl.57.9.1679

Cho, S. Y., Lee, Y. E., Doo, K. H., Lee, J. H., Jung, W. S., Moon, S. K., et al. (2018). Efficacy of combined treatment with acupuncture and bee venom acupuncture as an adjunctive treatment for Parkinson's disease. *J. Altern. Complement. Med.* 24, 25–32. doi: 10.1089/acm.2016.0250

Demaagd, G., and Philip, A. (2015). Parkinson's disease and its management: Part 1: disease entity, risk factors, pathophysiology, clinical presentation, and diagnosis. *P T* 40, 504–532.

Ghaffari, B. D., and Kluger, B. (2014). Mechanisms for alternative treatments in Parkinson's disease: acupuncture, tai chi, and other treatments. *Curr. Neurol. Neurosci. Rep.* 14:451. doi: 10.1007/s11910-014-0451-y

Nussbaum, R. L., and Ellis, C. E. (2003). Alzheimer's disease and Parkinson's disease. *N. Engl. J. Med.* 348, 1356–1364. doi: 10.1056/NEJM2003ra020003

Park, J. Y., Kim, S. N., Yoo, J., Jang, J., Lee, A., Oh, J. Y., et al. (2017). Novel neuroprotective effects of melanin-concentrating hormone in Parkinson's disease. *Mol. Neurobiol.* 54, 7706–7721. doi: 10.1007/s12035-016-0258-8

Tanner, C. M., and Goldman, S. M. (1996). Epidemiology of Parkinson's disease. *Neurol. Clin.* 14, 317–335.

Thomas, B., and Beal, M. F. (2007). Parkinson's disease. *Hum. Mol. Genet.* 16 Spec No. 2, R183–194. doi: 10.1093/hmg/ddm159

Conflict of Interest: The authors declare that the research was conducted in the absence of any commercial or financial relationships that could be construed as a potential conflict of interest.

frontiers in Aging Neuroscience

ORIGINAL RESEARCH
published: 24 April 2018
doi: 10.3389/fnagi.2018.00119

Sophora flavescens Aiton Decreases MPP^+-Induced Mitochondrial Dysfunction in SH-SY5Y Cells

*Hee-Young Kim[1], Hyongjun Jeon[2], Hyungwoo Kim[3], Sungtae Koo[1,2] and Seungtae Kim[1,2]**

[1]Korean Medicine Research Center for Healthy Aging, Pusan National University, Yangsan, South Korea, [2]Department of Korean Medical Science, School of Korean Medicine, Pusan National University, Yangsan, South Korea, [3]Division of Pharmacology, School of Korean Medicine, Pusan National University, Yangsan, South Korea

Sophora flavescens Aiton (SF) has been used to treat various diseases including fever and inflammation in China, South Korea and Japan. Several recent reports have shown that SF has anti-inflammatory and anti-apoptotic effects, indicating that it is a promising candidate for treatment of Parkinson's disease (PD). We evaluated the protective effect of SF against neurotoxin 1-methyl-4-phenylpyridinium ion (MPP^+)-induced mitochondrial dysfunction in SH-SY5Y human neuroblastoma cells, an *in vitro* PD model. SH-SY5Y cells were incubated with SF for 24 h, after which they were treated with MPP^+. MPP^+-induced cytotoxicity and apoptosis were confirmed by 3-(4,5-dimethyl-thiazol-2-yl)-2,5-diphenyl tetrazolium bromide assay and terminal deoxynucleotidyl transferase-mediated biotinylated UTP nick end labeling assay. MitoSOX red mitochondrial superoxide indicator, tetramethylrhodamine methyl ester perchlorate and Parkin, PTEN-induced putative kinase 1 (PINK1), and DJ-1 immunofluorescent staining were conducted to confirm the mitochondrial function. In addition, western blot was performed to evaluate apoptosis factors (Bcl-2, Bax, caspase-3 and cytochrome c) and mitochondrial function-related factors (Parkin, PINK1 and DJ-1). SF suppressed MPP^+-induced cytotoxicity, apoptosis and collapse of mitochondrial membrane potential by inhibiting the increase of reactive oxidative species (ROS) and DNA fragmentation, and controlling Bcl-2, Bax, caspase-3 and cytochrome *c* expression. Moreover, it attenuated Parkin, PINK1 and DJ-1 expression from MPP^+-induced decrease. SF effectively suppressed MPP^+-induced cytotoxicity, apoptosis and mitochondrial dysfunction by regulating generation of ROS, disruption of mitochondrial membrane potential, mitochondria-dependent apoptosis and loss or mutation of mitochondria-related PD markers including Parkin, PINK1 and DJ-1.

Keywords: Parkinson's disease, *Sophora flavescens* Aiton, SH-SY5Y, MPP^+, mitochondrial dysfunction

OPEN ACCESS

Edited by:
Seung-Nam Kim,
Dongguk University Seoul,
South Korea

Reviewed by:
Julnar A. R. Usta,
American University of Beirut,
Lebanon
Magdalena Alicja Maj,
Baylor College of Medicine,
United States
Suowen Xu,
University of Rochester,
United States

***Correspondence:**
Seungtae Kim
kimst@pusan.ac.kr

Received: *08 January 2018*
Accepted: *06 April 2018*
Published: *24 April 2018*

Citation:
Kim H-Y, Jeon H, Kim H, Koo S and Kim S (2018) Sophora flavescens Aiton Decreases MPP^+-Induced Mitochondrial Dysfunction in SH-SY5Y Cells. Front. Aging Neurosci. 10:119. doi: 10.3389/fnagi.2018.00119

INTRODUCTION

Parkinson's disease (PD) is an incurable neurodegenerative disorder characterized by bradykinesia, muscle rigidity, tremor and postural instability (Olanow and Tatton, 1999). These features of PD are associated with the appearance of Lewy bodies in the neuronal cytoplasm and progressive degeneration and death of dopaminergic neurons (DA) in the substantia nigra pars compacta (Moore et al., 2005). Although the exact etiology of PD has yet

to be elucidated, many recent studies have reported that oxidative stress and mitochondrial dysfunction are involved in progression of PD (Requejo-Aguilar and Bolaños, 2016). A neurotoxin, 1-methyl-4-phenyl-1,2,3,6-tetrahydropyridine (MPTP), is widely used for PD research because it selectively destroys DA in animals (Fernández-Moriano et al., 2015). MPTP is metabolized into 1-methyl-4-phenylpyridinium ion (MPP^+) by monoamine oxidase B in the brain, and MPP^+ disturbs mitochondrial respiration by inhibiting mitochondrial complex I. This process leads to abnormal mitochondrial metabolism and generation of reactive oxygen species (ROS) like pathogenesis of PD (Cleeter et al., 1992). In addition, increased cellular ROS production has been implicated in neurodegenerative diseases such as PD and Alzheimer's disease (Fernández-Moriano et al., 2015). According to several recent studies, MPP^+ causes opening of mitochondrial permeability transition pores, mitochondrial membrane potential disruption, impairment of ATP production and ROS generation, which induces apoptosis of DA (Lee et al., 2011; Requejo-Aguilar and Bolaños, 2016). Several PD-related substances, such as α-Synuclein, Parkin, PTEN-induced putative kinase 1 (PINK1), DJ-1 and Leucine-rich repeat kinase 2 (LRRK2), are involved in mitochondrial function in DA; therefore, loss or mutation of these substances causes cell death (Um et al., 2009; Fernández-Moriano et al., 2015; Requejo-Aguilar and Bolaños, 2016).

Currently, prospective drugs for PD do not exist. Several effective drugs, such as levodopa, can enhance clinical symptoms, but these drugs not only suppress progression of PD, but also induce side effects (Hu et al., 2011). Therefore, alternative medicine, curative foods, and phytochemicals are considered to have the potential for prevention or treatment of PD. Recently, beneficial effects of herbal medicines (Chen et al., 2007; Kim et al., 2009), ginseng (Kim et al., 2016), astaxanthin (Lee et al., 2011), and lycopene (Yi et al., 2013) in PD-like experimental models have been demonstrated.

Sophora flavescens Aiton (SF), a kind of deciduous shrub, is widespread in East Asia (He et al., 2015). Diverse flavonoids, alkaloids, and terpenoids have been found in SF, with flavonoids (e.g., kushenol, kurarinone and sophoflavescenol) and alkaloids (e.g., matrine and oxymatrine) comprising the major active components of SF (He et al., 2015). SF has been used for treatment of fever, pain, inflammation, ulcer, numbness and several skin diseases as traditional medicine in China, South Korea and Japan (Kim et al., 2012; He et al., 2015). Moreover, SF or its compounds have been shown to have anti-oxidative (Piao et al., 2006), anti-cancer (Sun et al., 2007; Liu et al., 2010), anti-arthritic (Jin et al., 2010), anti-ulcerative (Yamahara et al., 1990) and anti-dermatitis (Kim et al., 2012) effects, and recent studies have shown that it has neuroprotective effects. Extract of SF suppressed sodium nitroprusside-induced apoptosis in SH-SY5Y cells, while focal cerebral ischemia induced neuronal death in rats (Park et al., 2009) and enhanced axonal growth in mice (Tanabe et al., 2015), and oxymatrine extracted from SF prevented neuronal cell death in rat brains subjected to cerebral ischemia-reperfusion damage (Li et al., 2011). However, it is still not known if SF can also protect DA. Therefore, in the present study, we examined the protective effects of SF against MPP^+-induced cytotoxicity and mitochondrial dysfunction in human neuroblastoma SH-SY5Y cells.

MATERIALS AND METHODS

Preparation of SF Extract

SF was purchased from Kwangmyungdang Medical Herbs (Ulsan, South Korea). For extraction, 50 mg SF was immersed in absolute methanol (1000 mL) and sonicated for 30 min, extracted for 24 h, filtered through filter paper, and dried in a vacuum evaporator (Eyela, Japan). Finally, the extract was lyophilized by freeze-drying (Labconco, Kansas City, MO, USA). The yield value of powdered SF was 12.9%. The methanol extract of SF has been deposited at the Division of Pharmacology, School of Korean Medicine, Pusan National University (Voucher No. MH2010-004). The dark green colored SF extract was used to dissolve in phosphate-buffered saline (PBS) in all of experiments.

Cell Culture

SH-SY5Y cells, a human neuroblastoma cell line (KCLB, Korean cell line bank, Seoul, South Korea), were cultured in Dulbecco's Modified Eagle's Medium (Welgene, Daegu, South Korea) supplemented with 10% (v/v) heat-inactivated fetal bovine serum (Welgene) and 100 units/mL penicillin/streptomycin (Welgene). Cells were maintained at 37°C in a humidified 95% air and 5% CO_2 atmosphere.

Cell Viability Assay

Cell viability was determined by 3-(4,5-dimethyl-thiazol-2-yl)-2,5-diphenyl tetrazolium bromide (MTT; Duchefa Biochemie, Haarlem, Netherlands) assay. Cells were pre-incubated in 96-well plates at a confluence of 1×10^5 cells/mL, then treated with SF for 24 h, after which they were treated with MPP^+ for 24 h. Then, they were grown in 0.5 mg/mL MTT for 4 h. After medium was aspirated, 100 μL of dimethyl sulfoxide was added to dissolve the purple formazan crystals. Following incubation for 30 min, plates were read at 540 nm.

TUNEL Assay

Terminal deoxynucleotidyl transferase-mediated biotinylated UTP nick end labeling (TUNEL) assay was performed using a fluorometric TUNEL assay kit (Promega, Madison, WI, USA). Cells were grown in 8-well chamber slides (SPL Life Sciences, Pocheon, Korea) to a confluence of 3×10^4 cells/mL. Next, cells were incubated with or without SF for 24 h, then incubated with or without MPP^+ for 24 h. The, medium was then aspirated and fixed with 4% (v/v) paraformaldehyde for 30 min at 4°C, after which cells were stained by TUNEL and DAPI according to the manufacturer's protocols. Finally, fluorescence was detected by LSM 700 confocal laser scanning microscope (Zeiss, Oberkochen, Germany).

Western Blot

Cells were cultured in 6-well plates to a confluence of 1×10^5 cells/mL. Next, the cells were incubated with or without SF for 24 h, re-incubated with or without MPP^+ for 24 h, then

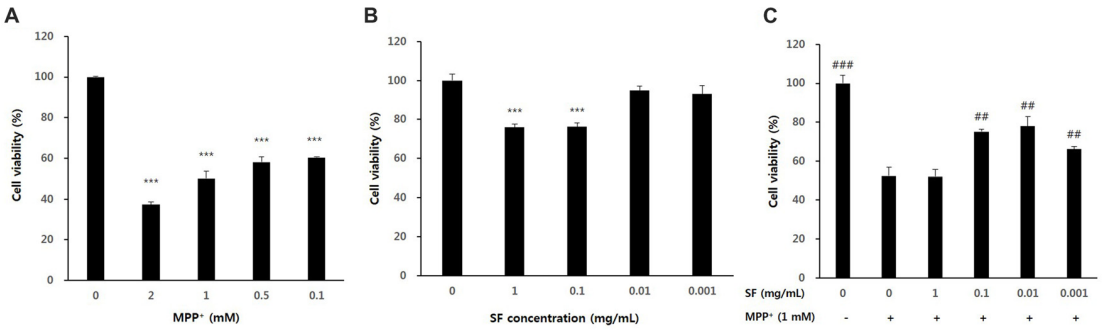

FIGURE 1 | Cell viability after 1-methyl-4-phenylpyridinium ion (MPP^+) or *Sophora flavescens* Aiton (SF) treatment of SH-SY5Y cells. Dose-dependent effects were observed in SH-SY5Y cells treated with MPP^+ **(A)**, SF **(B)**, or both SH-SY5Y and MPP^+ **(C)**. Values are the means ± SD ($n = 6$). In **(A,B)**, $^{***}p < 0.001$, compared with control (untreated group). In **(C)**, $^{\#\#}p < 0.01$ and $^{\#\#\#}p < 0.001$, compared with the group treated by MPP^+ alone.

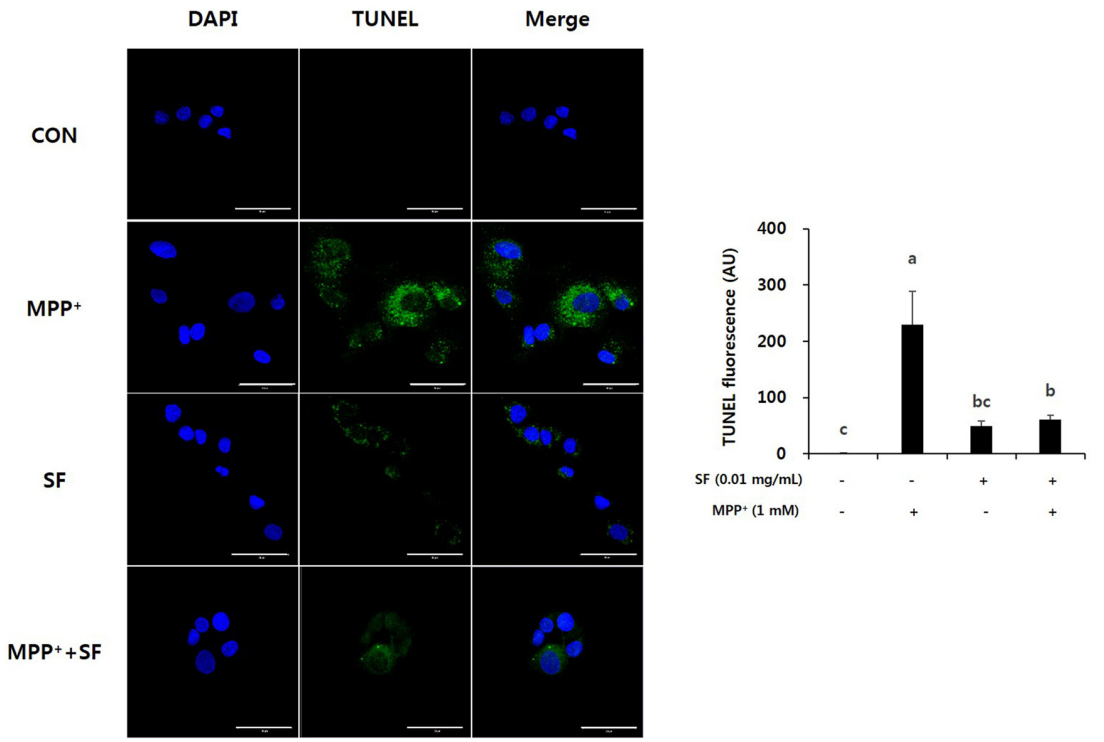

FIGURE 2 | SF attenuated MPP^+-induced apoptosis in SH-SY5Y cells. Cells were treated with 0.01 mg/mL SF for 24 h, then exposed to 1 mM MPP^+ for 24 h and stained with DAPI and TUNEL. TUNEL staining showed that MPP^+ increased apoptotic DNA fragmentation, but SF suppressed it. Scale bar = 50 μm. Values are the means ± SD (three slides per group). $^{a–c}$Means with different letters are significantly different ($p < 0.05$) by Duncan's multiple-range test.

detached with ice cold RIPA buffer (Armnesco, Solon, OH, USA) and centrifuged at 13,000 rpm for 15 min at 4°C. The protein concentration was subsequently determined using a BioRad protein assay kit (Hercules, CA, USA). Protein samples (20 μg) were then separated by sodium dodecyl sulfate–polyacrylamide gel electrophoresis and electrotransferred onto a 0.45 μm nitrocellulose blotting membrane (GE Healthcare UK Ltd, Little Chalfont, UK). The blots were incubated with anti-Bcl-2 (diluted 1:200), anti-Bax (1:1000), anti-cytochrome c (1:200), anti-cleaved caspase-3 (1:1000), anti-Parkin (1:1000), anti-PINK1 (1:200), anti-DJ-1 (1:1000) or anti-β-actin (1:200) primary antibodies while immersed in 5% skim milk or 5% Bovine serum albumin overnight at 4°C, after which they were incubated with secondary antibodies for 1 h at room temperature. The membranes were then washed several times with PBS containing 0.05% (v/v) Tween 20, after which they were visualized with ECL reagent (Thermo Fisher Scientific Inc., Rochford, IL, USA). All primary antibodies were purchased from Santa Cruz Biotechnology (Santa Cruz, CA, USA) except anti-cleaved caspase-3 and anti-DJ-1 (Cell Signaling Technology, Inc., Beverly, MA, USA).

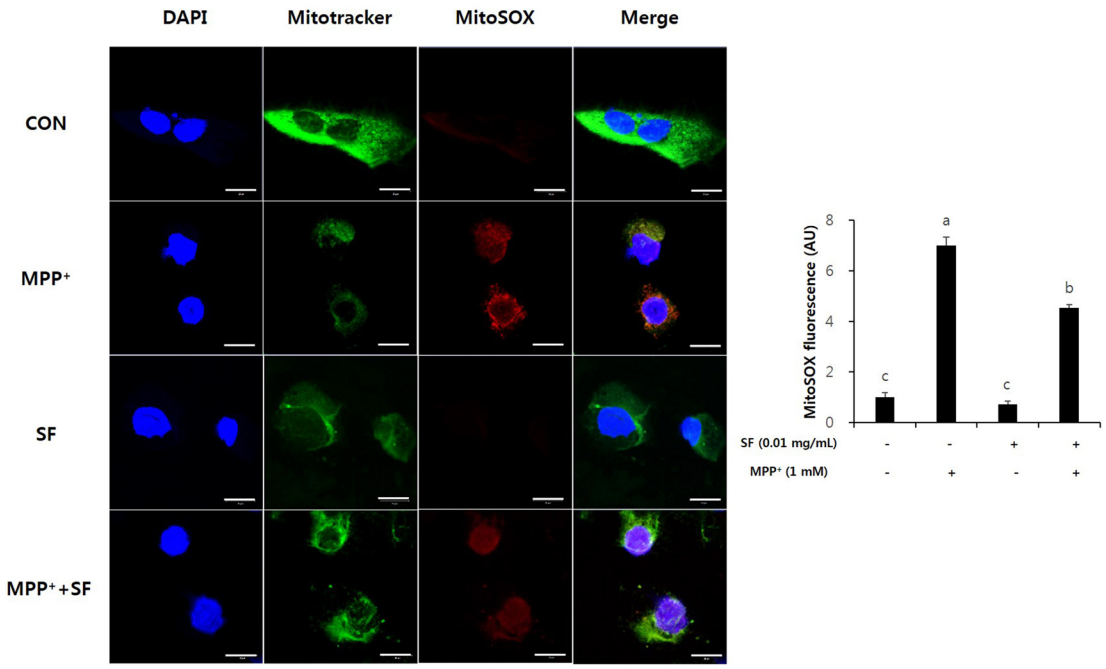

FIGURE 3 | SF attenuated MPP^+-mediated reactive oxidative species (ROS) generation in SH-SY5Y cells. Cells were exposed to 1 mM MPP^+ for 24 h in the absence or presence of 0.01 mg/mL SF for 24 h, then stained with DAPI, MitoSOX and Mitotracker. MPP^+ increased mitochondria-derived ROS generation, which was suppressed by SF. Scale bar = 50 μm. Values are the means ± SD (three slides per group). $^{a-c}$Means with different letters are significantly different ($p < 0.05$) by Duncan's multiple-range test.

Measurement of Mitochondrial Membrane Potential and Mitochondrial Reactive Oxygen Species

Cells were cultured in eight well-chamber slides with or without SF for 24 h, then re-incubated with or without MPP^+ for 24 h, after which 250 nM tetramethylrhodamine methyl ester perchlorate (TMRM; Invitrogen, Carlsbad, CA, USA) or 5 μM MitoSOX red mitochondrial superoxide indicator (MitoSOX; Invitrogen) was treated and the samples were incubated for 30 min or 10 min, respectively at 37°C. Cells were washed three times with PBS, after which they were counterstained with mitotracker green (Invitrogen, Carlsbad, CA, USA). Following counterstaining, the cells were fixed with 4% (v/v) paraformaldehyde (25 min, 4°C), and mounted with Vectashield mounting medium with DAPI (Vector, Burlingame, CA, USA). Finally, images of the slides were captured using a LSM 700 confocal laser scanning microscope (Zeiss).

Immunofluorescent Staining

Cells cultured in eight well-chamber slides were fixed with 4% (v/v) paraformaldehyde in PBS for 20 min, then permeabilized with 0.1% (v/v) Triton X-100 in PBS for 15 min at room temperature. Next, the cells blocked with 10% normal goat serum (NGS) in PBS for 1 h at room temperature. The cells were subsequently incubated with primary antibodies (anti-Parkin, anti-PINK1 and anti-DJ-1) dissolved in 10% NGS at 4°C, overnight, after which they were incubated with fluorophore-conjugated secondary antibodies anti-rabbit Alexa-488 IgG or anti-mouse Alexa-594 IgG (Molecular Probes, Eugene, OR, USA) for 1 h at room temperature in the dark. The cells were rinsed with 1% NGS and mounted with Vectashield mounting medium with DAPI (Vector), after which images of the cells were captured using a LSM 700 confocal laser scanning microscope (Zeiss). The numbers of Parkin, PINK1, or DJ-1-positive cells were counted on each capture. All cell counts were confirmed three times.

Statistical Analysis

All data are drawn from triplicate experiments, and presented as the means ± SD. Differences between the mean values were assessed by independent *t*-test in MTT assay, and one-way analysis of variance (ANOVA) with Duncan's multiple-range tests in other experiments. All statistical analyses were performed using IBM SPSS Statistics Ver. 22 (IBM Co., Armonk, NY, USA). Differences with a $p < 0.05$, was considered statistically significant.

RESULTS

SF Protects SH-SY5Y Cells Against MPP^+-Induced Cytotoxicity and Apoptosis

SH-SY5Y cells were treated with various concentrations of SF and MPP^+ to confirm their cytotoxicity. When the cells were

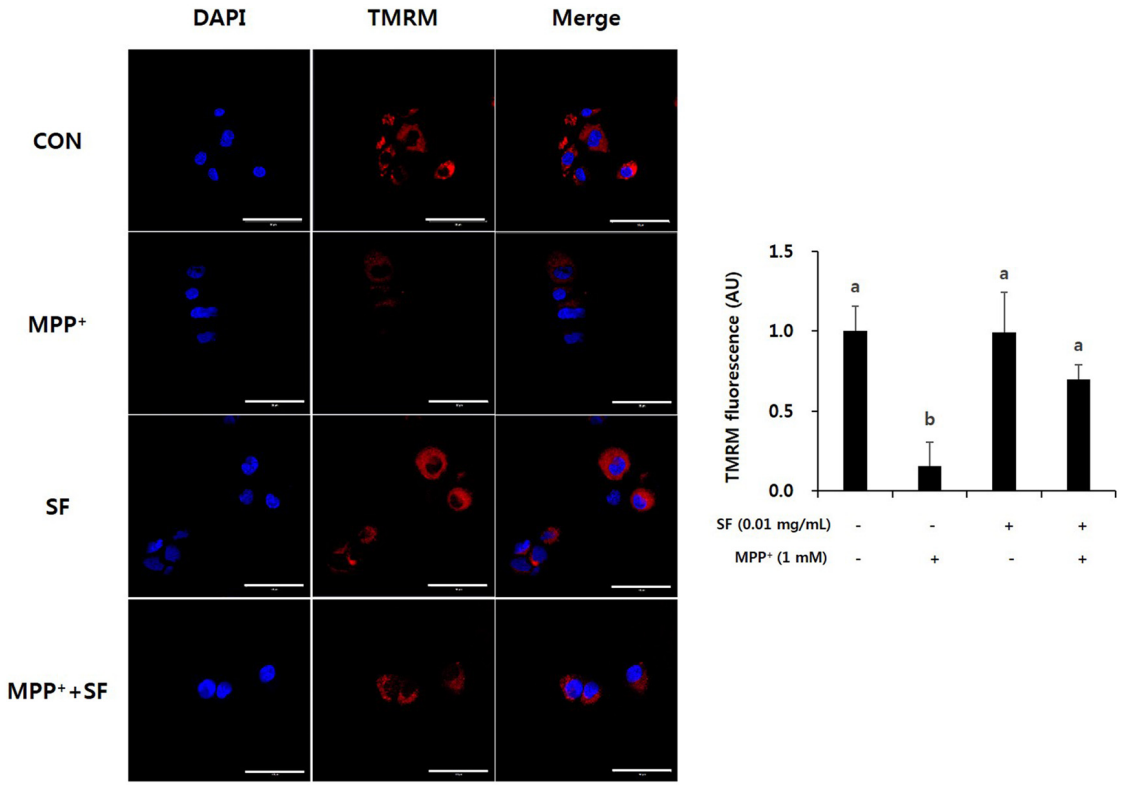

FIGURE 4 | SF attenuated MPP^+-mediated collapse of mitochondrial membrane permeability in SH-SY5Y cells. Cells were exposed to 1 mM MPP^+ for 24 h in the absence or presence of 0.01 mg/mL SF for 24 h, stained with tetramethylrhodamine methyl ester perchlorate (TMRM), then visualized by fluorescence microscopy and the intensity of fluorescence was calculated. MPP^+ collapsed mitochondrial membrane permeability, which was prevented by SF. Scale bar = 50 μm. Values are the means ± SD (three slides per group). [a,b]Means with different letters are significantly different ($p < 0.05$) by Duncan's multiple-range test.

exposed to MPP^+ for 24 h, cell viability was significantly decreased in a dose-dependent manner. When compared with the control cells, cells exposed to 1 mM MPP^+ for 24 h showed 50.1 ± 3.4% of the cell viability. The dose of 1 mM MPP^+ was also used in previous studies (Lee et al., 2011; Janhom and Dharmasaroja, 2015); therefore, a dose of 1 mM MPP^+ was used for further experiments (**Figure 1A**). SH-SY5Y cells treated with 0.001, 0.01, 0.1 or 1 mg/mL of SF showed 93.0 ± 4.5, 94.8 ± 2.3%, 76.3 ± 2.0, and 76.0 ± 1.6% cell viability relative to the control, respectively (**Figure 1B**). Pretreatment of SH-SY5Y cells with SF at 0.001, 0.01, or 0.1 mg/mL for 24 h followed by 1 mM MPP^+ for 24 h significantly attenuated MPP^+-evoked toxicity ($p < 0.01$), with 0.01 mg/mL SF pretreatment resulting in the highest cell viability (77.9 ± 5.0%; **Figure 1C**). Therefore, a dose of 0.01 mg/mL SF was used further experiments.

To confirm the protective effects of SF on MPP^+-induced apoptosis, a TUNEL assay was performed on SH-SY5Y cells. As shown in **Figure 2**, cells incubated with MPP^+ alone showed the highest level of TUNEL positive fluorescence. However, cells treated with SF (presence or absence of MPP^+) showed significantly lower apoptotic fluorescence than those treated with MPP^+ alone. These results indicate that SF reduced MPP^+-induced apoptotic DNA fragmentation in SH-SY5Y cells.

SF Suppresses MPP^+-Mediated Intracellular ROS Generation and Disruption of Mitochondrial Membrane Potential

MitoSOX selectively targets the mitochondria and exhibits red fluorescence in the mitochondria of live cells after oxidation by superoxide. MPP^+-treated SY-SH5Y cells showed significant increases of MitoSOX red fluorescence emission, indicating an increase of superoxide in mitochondria. However, the SF and MPP^+-treated cells showed lower red fluorescence emission than cells treated with only MPP^+. In addition, the intensity of the red signal in SF-only treated cells was similar to that in control cells. These results suggest that SF diminished MPP^+-induced ROS generation in mitochondria (**Figure 3**).

The cell-permeant dye TMRM is accumulated in active mitochondria with intact membrane potentials; thus, bright red fluorescence exists in the healthy mitochondria of live cells. Induction of MPP^+ causes abnormal mitochondrial membrane potential, so cells treated with MPP^+ alone showed lower levels of TMRM positive signal than control cells. However, the SF and MPP^+-treated cells showed significantly stronger signals than cells treated only with MPP^+ (**Figure 4**). These findings indicate that SF attenuated MPP^+-induced mitochondrial membrane

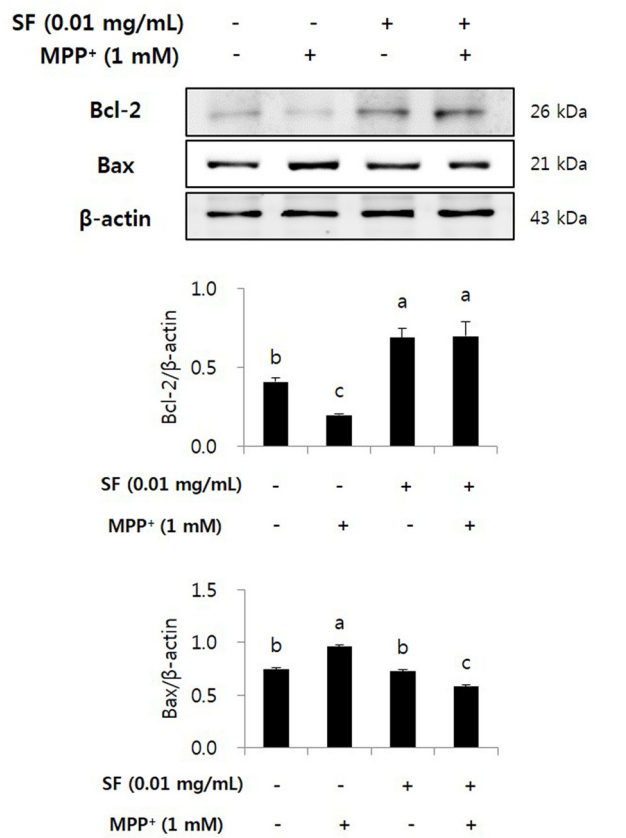

FIGURE 5 | SF regulated MPP^+-induced changes in Bcl-2 and Bax expression in SH-SY5Y cells. Cells were exposed to 1 mM MPP^+ for 24 h in the absence or presence of 0.01 mg/mL SF for 24 h, then harvested and subjected to Western blotting using the antibodies against Bcl-2 and Bax. SF alleviated MPP^+-induced down-regulation of Bcl-2 and up-regulation of Bax. Values are the means ± SD (n = 3). $^{a–c}$Means with different letters are significantly different ($p < 0.05$) by Duncan's multiple-range test.

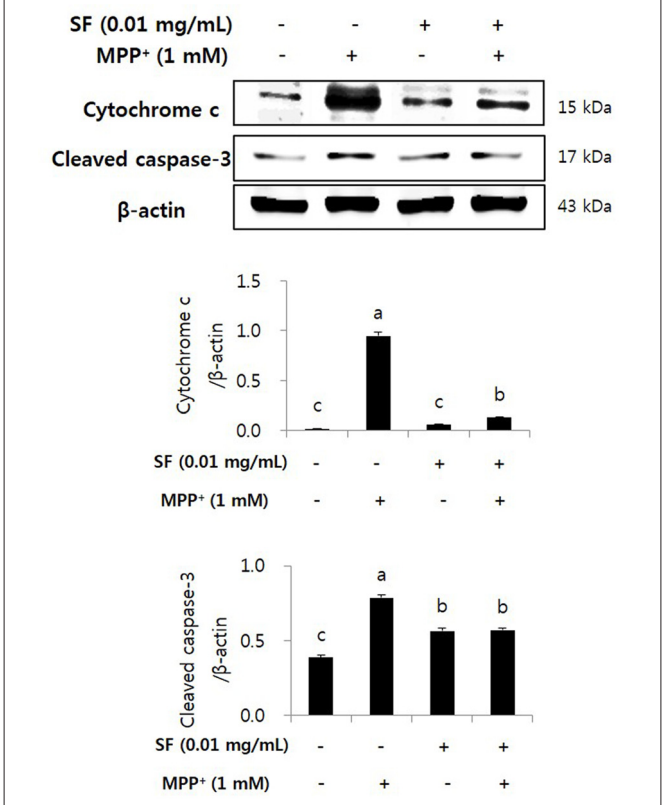

FIGURE 6 | SF inhibited MPP^+-induced release of cytochrome c and activation of caspase-3 in SH-SY5Y cells. Cells were exposed to 1 mM MPP^+ for 24 h in the absence or presence of 0.01 mg/mL SF for 24 h. Cells were harvested and subjected to Western blotting using antibodies against cytochrome c and cleaved caspase-3. SF suppressed MPP^+-induced release of cytochrome c and activation of caspase-3. Values are the means ± SD (n = 3). $^{a–c}$Means with different letters are significantly different ($p < 0.05$) by Duncan's multiple-range test.

depolarization. The signal in cells treated with SF alone did not differ significantly from the control cells.

SF Regulates Protein Expression of Bcl-2 and Bax

The expression of anti- and pro-apoptotic proteins Bcl-2 and Bax on SF and/or MPP^+ treated SH-SY5Y cells was confirmed by western blotting. The expression of anti-apoptotic Bcl-2 decreased significantly in response to MPP^+ treatment; however, SF pretreatment prevented the decrease significantly. Moreover, MPP^+ led to up-regulation of Bax expression, which was significantly suppressed by SF pretreatment (**Figure 5**).

SF Inhibits MPP^+-Mediated Activation of Cytochrome c and Caspase-3

Cytochrome c release and caspase cascades play major roles in apoptosis. Cytochrome c released from mitochondria stimulates caspase-9 and caspase-3, which causes apoptosis of cells (Fernández-Moriano et al., 2015). MPP^+-treated cells showed significantly higher level of cytochrome c than the other groups, however, the cells treated with MPP^+ and SF showed significantly lower level than the MPP^+ alone. MPP^+ increased cleaved caspase-3 expression; however, SF significantly attenuated it ($p < 0.05$) and the level was similar to that of the SF alone (**Figure 6**).

SF Suppresses MPP^+-Mediated Reduction of Parkin, PINK1 and DJ-1

Parkin, PINK1 and DJ-1 are involved in mitochondrial function and play important roles in the pathophysiology of PD. Immunofluorescent staining revealed that the levels of Parkin and PINK1 in SF-treated cells with no MPP^+ were higher than those in control cells. Moreover, MPP^+ treatment reduced the levels of Parkin and PINK1 compared with no MPP^+ treatment, but SF pretreatment attenuated the MPP^+-induced reduction significantly (**Figure 7**). The level of DJ-1 was also decreased in MPP^+-treated cells compared control cells; however, SF prevented the decrease (**Figure 8**).

We confirmed the levels of Parkin, PINK1, and DJ-1 by Western blotting. MPP^+ treatment reduced the levels of Parkin, PINK1, and DJ-1 in SH-SY5Y cells; however, SF pretreatment

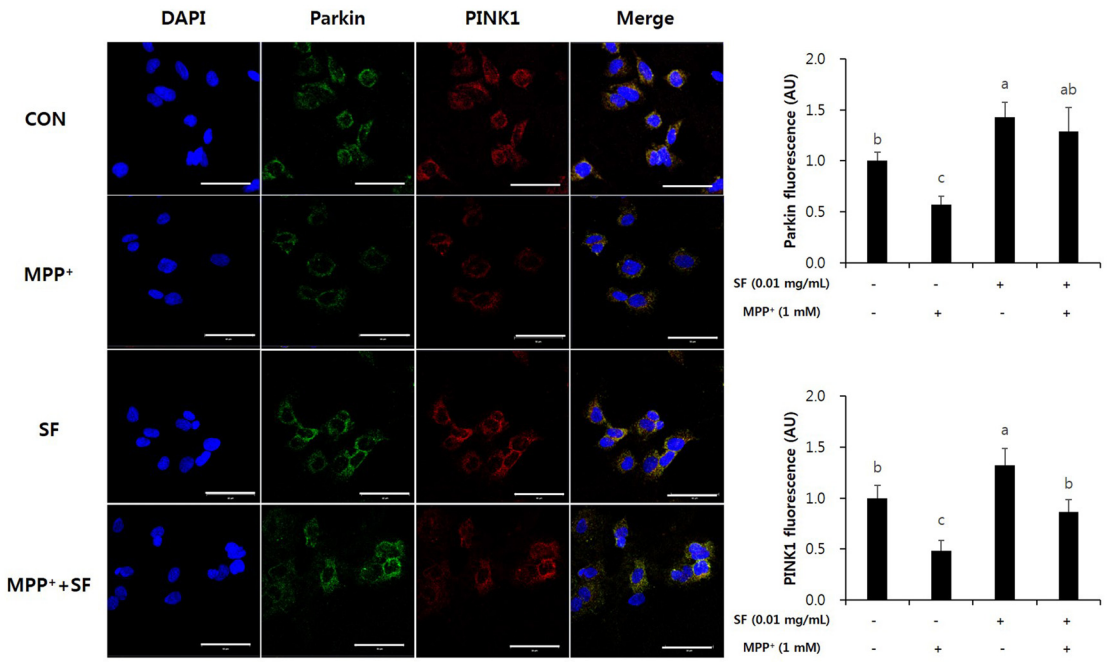

FIGURE 7 | SF suppressed MPP^+-mediated loss of Parkin and PTEN-induced putative kinase 1 (PINK1) in SH-SY5Y cells. Cells were exposed to 1 mM MPP^+ for 24 h in the absence or presence of 0.01 mg/mL SF for 24 h, after which they were subjected to immunofluorescent staining using antibodies against Parkin and PINK1. MPP^+ suppressed Parkin and PINK1 expression, while SF enhanced them. Scale bar = 50 μm. Values are the means ± SD (three slides per group). $^{a-c}$Means with different letters are significantly different ($p < 0.05$) by Duncan's multiple-range test.

significantly attenuated these decreases. Both the SF-treated and the SF and MPP^+-treated cells showed comparable protein expression of Parkin and DJ-1 compared to the control cells and higher expression of PINK1 compared to the control and the MPP^+-only treated cells (**Figure 9**).

DISCUSSION

In the present study, we demonstrated neuroprotective effect of SF in an *in vitro* PD model using neurotoxin MPP^+ and SH-SY5Y human neuroblastoma cells. The SH-SY5Y human neuroblastoma cell line is widely used for PD research because the cells have many characteristics of human DA (Sheehan et al., 1997). MPP^+, a metabolite of MPTP, has been used for PD research because it induces PD-like symptoms and degeneration of DA *in vitro* and *in vivo* (Langston et al., 1984). MPP^+-induced cell death is related to several factors such as oxidative stress (Jung et al., 2007), opening of mitochondrial permeability transition pores, and disruption of the mitochondrial membrane potential make sound it better in English.(Seaton et al., 1997). These abnormal mitochondrial conditions can cause production of ROS, impairment of energy production and cell death (Saporito et al., 2000; Alcaraz-Zubeldia et al., 2001).

We confirmed the protective effects of SF against MPP^+-induced neurotoxicity and apoptosis in SH-SY5Y cells by MTT and TUNEL assay. MPP^+ is known as a ROS generative neurotoxin (Johannessen et al., 1986). ROS generated by MPP^+ are involved in DNA and mitochondrial damage, as well as apoptotic cell death (Cassarino et al., 1999). In this study, MPP^+ induced cell death as previously reported. In addition, we found that SF pretreatment significantly attenuated DNA fragmentation and apoptosis (**Figures 1**, **2**), suggesting that SF can prevent MPP^+-induced apoptosis in SH-SY5Y cells. And partially SF treated cells showed a little unhealthy during the TUNEL assay (**Figure 2**). SF contains alkaloids including matrine and oxymatrine, the two alkaloids has been demonstrated to possess strong anti-tumor activities (Liu et al., 2014). SH-SY5Y is a human derived cell line and a kind of neuroblastoma, therefore the unhealthy cells treated with SF might be due to the anti-tumor activity of matrine and oxymatrine. However the influence of them was limited because 0.01 mg/mL SF showed 94.8% of cell viability and it is not significantly different level comparing to control cells (**Figure 1B**).

Oxidative stress is a major factor inducing apoptosis in cells (Zhang et al., 2000) and associated with neuronal damage and behavioral impairment in PD (Venkatesh Gobi et al., 2018). Mitochondria are vulnerable to oxidative stress; thus, excessive production of ROS leads to abnormal mitochondrial morphology, opening of the mitochondrial transition pore, and collapse of mitochondrial membrane potential (Cassarino et al., 1999; Büeler, 2009; Yao and Wood, 2009). These changes in mitochondrial membrane cause critical event in the process leading to apoptosis (Dispersyn et al., 1999). The oxidative stress-mediated apoptosis is

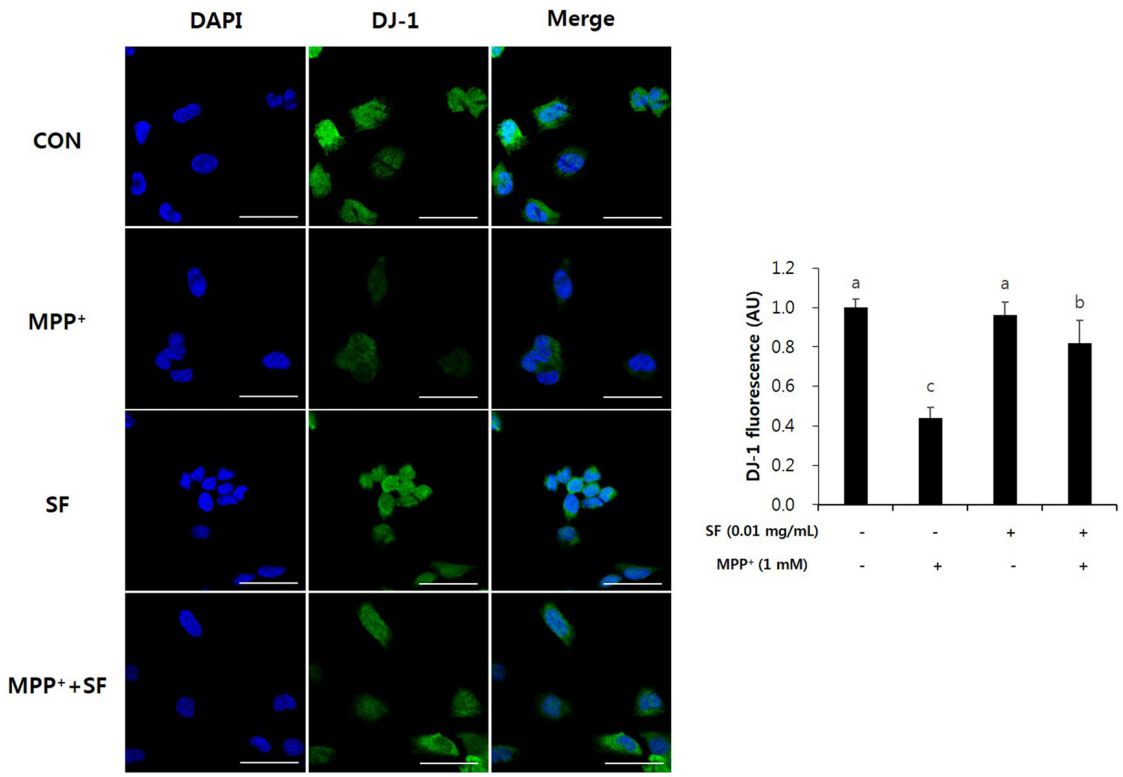

FIGURE 8 | SF attenuated MPP^+-mediated loss of DJ-1 in SH-SY5Y cells. Cells were exposed to 1 mM MPP^+ for 24 h in the absence or presence of 0.01 mg/mL SF for 24 h, then subjected to immunofluorescent staining using antibody against DJ-1. SF enhanced the MPP^+-induced decrease of DJ-1. Scale bar = 50 μm. Values are the means ± SD (three slides per group). $^{a–c}$Means with different letters are significantly different ($p < 0.05$) by Duncan's multiple-range test.

related to the activation of Bcl-2 family proteins, release of cytochrome c, and activation of caspase cascades (O'Malley et al., 2003; Ahn et al., 2009). Bcl-2 and Bax are members of the Bcl-2 family that serve as important apoptosis-related factors. Anti-apoptotic Bcl-2 and pro-apoptotic Bax regulate the membrane permeability of mitochondria as well as discharge of cytochrome c from mitochondria to cytosol (Crompton, 2000), especially Bcl-2 stabilizes inner mitochondrial transmembrane (Dispersyn et al., 1999) and prevents the release of cytochrome c (Yang et al., 1997). Caspase-3 is an important factor in downstream mitochondrial dysfunction related cell apoptosis (Strasser et al., 2000) that is activated by several apoptotic pathways, including the cytochrome c-dependent pathway. In the present study, MPP^+ treatment accumulated ROS in the mitochondria of SH-SY5Y cells, but SF pretreatment significantly prevented this ($p < 0.05$; **Figure 3**). Moreover, SF up-regulated Bcl-2 and down-regulated Bax in cells (**Figure 5**) and SF inhibited MPP^+-induced activation of cytochrome c and caspase-3 (**Figure 6**), which suggests that SF effectively suppressed mitochondria-dependent apoptosis in MPP^+-treated SH-SY5Y cells. In addition, mitochondrial membrane potential levels in the SF-treated cells were similar to those in control cells, regardless of MPP^+ treatment (**Figure 4**), indicating that SF effectively suppressed ROS generation and disruption of mitochondrial membrane potential.

Several genetic problems are involved in PD, especially mutations of Parkin, PINK1, and DJ-1, which are related to autosomal-recessive PD (Kitada et al., 1998; Bonifati et al., 2003; Valente et al., 2004). These genes play roles in neuronal cell apoptosis and mitochondrial functions such as ROS production, changes in mitochondrial morphology, mitochondrial respiration, and mitochondrial transportation (Requejo-Aguilar and Bolaños, 2016). In addition, Parkin, PINK1, and DJ-1 are involved in up-regulation of ATP production, mitochondrial membrane potential and mitophagy, as well as down-regulation of the mitochondrial permeability transition pore (Requejo-Aguilar and Bolaños, 2016). Parkin prevents DA death by suppression of α-synuclein aggregation (Bian et al., 2012). When mitochondrial membrane potential collapses, PINK1 recruits Parkin, and Parkin-mediated mitophagy is triggered to maintain a normal condition of mitochondria (Geisler et al., 2010). Ca^{2+} transfer is important process for mitochondrial respiration in neuronal cells, and Parkin, PINK1 and DJ-1 are involved in Ca^{2+} homeostasis by controlling connection of the endoplasmic reticulum-mitochondria and efflux of Ca^{2+} in the mitochondria (Calì et al., 2013a,b). Loss of DJ-1 causes mitochondrial fragmentation and increases sensibility against toxins including MPTP and paraquat; however, high levels of DJ-1 expression

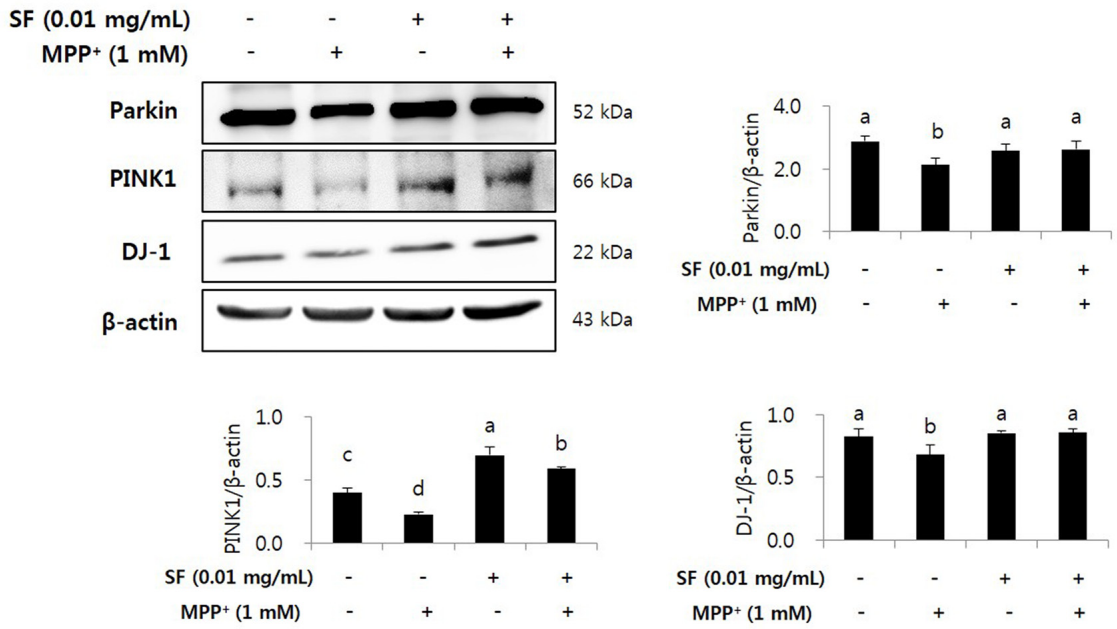

FIGURE 9 | SF inhibited loss of Parkinson's disease (PD) related markers Parkin, PINK1 and DJ-1 in MPP^+-induced SH-SY5Y cells. Cells were exposed to 1 mM MPP^+ for 24 h in the absence or presence of 0.01 mg/mL SF for 24 h, then harvested and subjected to Western blotting using antibodies against Parkin, PINK1 and DJ-1 with whole cell lysate. MPP^+ suppressed Parkin, PINK1 and DJ-1 expression, while SF enhanced them. Values are the means ± SD ($n = 3$). $^{a–d}$Means with different letters are significantly different ($p < 0.05$) by Duncan's multiple-range test.

protect the cells from the toxins (Kim et al., 2005; Yang et al., 2007; Requejo-Aguilar and Bolaños, 2016). In the present study, MPP^+ treatment significantly reduced the levels of Parkin, PINK1, and DJ-1 expression; however, SF attenuated these reductions. Moreover, SF treatment with no MPP^+ increased the levels of Parkin and PINK1 significantly (**Figures 7–9**). These results suggest that SF not only protects cells against MPP^+ toxicity, but also recovers Parkin, PINK1 and DJ-1 expression from MPP^+-induced downregulation.

Regulation of intracellular ROS and normalization of mitochondrial function can control neurodegenerative events, especially apoptosis, in PD. In the present study, SF significantly suppressed MPP^+-induced ROS generation, collapse of mitochondrial membrane potential, mitochondria-dependent apoptosis and mitochondria-related factors in SH-SY5Y cells, indicating that the protective effects of SF are due to alleviation of MPP^+-induced mitochondrial dysfunctions. However, it should be noted that there were several limitations that should be addressed in future studies. First, the active compound in SF was not investigated in this study. Second, SH-SY5Y is neuroblastoma cell line, so additional *ex vivo* or *in vivo* study is necessary to confirm that SF actually alleviates PD symptoms and that the protective mechanism works in normal neurons.

CONCLUSION

The results of the present study showed that SF has neuroprotective effects against MPP^+-induced cell death in SH-SY5Y cells. Specifically, SF suppressed MPP^+-mediated ROS generation and collapse of mitochondrial membrane potential. Moreover, SF controlled apoptosis-related protein expression of Bcl-2 and Bax, caspase-3, release of cytochrome c and PD-related factors including Parkin, PINK1 and DJ-1 in SH-SY5Y cells. These results suggest that SF has the potential for use in neuroprotective therapeutics of PD.

AUTHOR CONTRIBUTIONS

H-YK performed MTT assay, the acquisition of Western blotting and immunofluorescent data, conducted statistical analysis and drafted the manuscript. HJ assisted with acquisition of immunofluorescent data and manuscript preparation. HK and SKoo assisted with protocol development and experimental setup. SKim conceived and designed the study, coordinated the acquisition of all study data, performed analysis and interpretation of results and drafted the manuscript. All co-authors were involved in critical revision of initial drafts.

FUNDING

This research was supported by the Basic Science Research Program through the National Research Foundation of Korea (NRF) funded by the Ministry of Education (NRF-2016R1D1A3B03930920) and Ministry of Science ICT and Future Planning (MSIP; NRF-2014R1A5A2009936).

REFERENCES

Ahn, K. H., Kim, Y. S., Kim, S. Y., Huh, Y., Park, C., and Jeong, J. W. (2009). Okadaic acid protects human neuroblastoma SH-SY5Y cells from 1-methyl-4-phenylpyridinium ion-induced apoptosis. *Neurosci. Lett.* 449, 93–97. doi: 10.1016/j.neulet.2008.10.103

Alcaraz-Zubeldia, M., Rojas, P., Boll, C., and Rios, C. (2001). Neuroprotective effect of acute and chronic administration of copper (II) sulfate against MPP^+ neurotoxicity in mice. *Neurochem. Res.* 26, 59–64. doi: 10.1023/A:1007680616056

Bian, M., Liu, J., Hong, X., Yu, M., Huang, Y., Sheng, Z., et al. (2012). Overexpression of parkin ameliorates dopaminergic neurodegeneration induced by 1- methyl-4-phenyl-1,2,3,6-tetrahydropyridine in mice. *PLoS One* 7:e39953. doi: 10.1371/journal.pone.0039953

Bonifati, V., Rizzu, P., van Baren, M. J., Schaap, O., Breedveld, G. J., Krieger, E., et al. (2003). Mutations in the DJ-1 gene associated with autosomal recessive early-onset parkinsonism. *Science* 299, 256–259. doi: 10.1126/science.1077209

Büeler, H. (2009). Impaired mitochondrial dynamics and function in the pathogenesis of Parkinson's disease. *Exp. Neurol.* 218, 235–246. doi: 10.1016/j.expneurol.2009.03.006

Calì, T., Ottolini, D., and Brini, M. (2013a). Calcium and endoplasmic reticulum-mitochondria tethering in neurodegeneration. *DNA Cell Biol.* 32, 140–146. doi: 10.1089/dna.2013.2011

Calì, T., Ottolini, D., Negro, A., and Brini, M. (2013b). Enhanced parkin levels favor ER-mitochondria crosstalk and guarantee Ca^{2+} transfer to sustain cell bioenergetics. *Biochim. Biophys. Acta* 1832, 495–508. doi: 10.1016/j.bbadis.2013.01.004

Cassarino, D. S., Parks, J. K., Parker, W. D. Jr., and Bennett, J. P. Jr. (1999). The parkinsonian neurotoxin MPP^+ opens the mitochondrial permeability transition pore and releases cytochrome c in isolated mitochondria via an oxidative mechanism. *Biochim. Biophys. Acta* 1453, 49–62. doi: 10.1016/s0925-4439(98)00083-0

Chen, L. W., Wang, Y. Q., Wei, L. C., Shi, M., and Chan, Y. S. (2007). Chinese herbs and herbal extracts for neuroprotection of dopaminergic neurons and potential therapeutic treatment of Parkinson's disease. *CNS Neurol. Disord. Drug Targets* 6, 273–281. doi: 10.2174/187152707781387288

Cleeter, M. W., Cooper, J. M., and Schapira, A. H. (1992). Irreversible inhibition of mitochondrial complex I by 1-methyl-4-phenylpyridinium: evidence for free radical involvement. *J. Neurochem.* 58, 786–789. doi: 10.1111/j.1471-4159.1992.tb09789.x

Crompton, M. (2000). Bax, Bid and the permeabilization of the mitochondrial outer membrane in apoptosis. *Curr. Opin. Cell Biol.* 12, 414–419. doi: 10.1016/s0955-0674(00)00110-1

Dispersyn, G., Nuydens, R., Connors, R., Borgers, M., and Geerts, H. (1999). Bcl-2 protects against FCCP-induced apoptosis and mitochondrial membrane potential depolarization in PC12 cells. *Biochim. Biophys. Acta* 1428, 357–371. doi: 10.1016/s0304-4165(99)00073-2

Fernández-Moriano, C., González-Burgos, E., and Gómez-Serranillos, M. P. (2015). Mitochondria-targeted protective compounds in Parkinson's and Alzheimer's diseases. *Oxid. Med. Cell. Longev.* 2015:408927. doi: 10.1155/2015/408927

Geisler, S., Holmström, K. M., Treis, A., Skujat, D., Weber, S. S., Fiesel, F. C., et al. (2010). The PINK1/Parkin-mediated mitophagy is compromised by PD-associated mutations. *Autophagy* 6, 871–878. doi: 10.4161/auto.6.7.13286

He, X., Fang, J., Huang, L., Wang, J., and Huang, X. (2015). *Sophora flavescens* Ait.: traditional usage, phytochemistry and pharmacology of an important traditional Chinese medicine. *J. Ethnopharmacol.* 172, 10–29. doi: 10.1016/j.jep.2015.06.010

Hu, S., Han, R., Mak, S., and Han, Y. (2011). Protection against 1-methyl-4-phenylpyridinium ion (MPP^+)-induced apoptosis by water extract of ginseng (Panax ginseng C.A. Meyer) in SH-SY5Y cells. *J. Ethnopharmacol.* 135, 34–42. doi: 10.1016/j.jep.2011.02.017

Janhom, P., and Dharmasaroja, P. (2015). Neuroprotective effects of alpha-mangostin on MPP^+-induced apoptotic cell death in neuroblastoma SH-SY5Y cells. *J. Toxicol.* 2015:919058. doi: 10.1155/2015/919058

Jin, J. H., Kim, J. S., Kang, S. S., Son, K. H., Chang, H. W., and Kim, H. P. (2010). Anti-inflammatory and anti-arthritic activity of total flavonoids of the roots of *Sophora flavescens*. *J. Ethnopharmacol.* 127, 589–595. doi: 10.1016/j.jep.2009.12.020

Johannessen, J. N., Adams, J. D., Schuller, H. M., Bacon, J. P., and Markey, S. P. (1986). 1-methyl-4-phenylpyridine (MPP^+) induces oxidative stress in the rodent. *Life Sci.* 38, 743–749. doi: 10.1016/0024-3205(86)90589-8

Jung, T. W., Lee, J. Y., Shim, W. S., Kang, E. S., Kim, S. K., Ahn, C. W., et al. (2007). Rosiglitazone protects human neuroblastoma SH-SY5Y cells against MPP^+ induced cytotoxicity via inhibition of mitochondrial dysfunction and ROS production. *J. Neurol. Sci.* 253, 53–60. doi: 10.1016/j.jns.2006.11.020

Kim, D., Jeon, H., Ryu, S., Koo, S., Ha, K. T., and Kim, S. (2016). Proteomic analysis of the effect of korean red ginseng in the striatum of a Parkinson's disease mouse model. *PLoS One* 11:e0164906. doi: 10.1371/journal.pone.0164906

Kim, I. S., Koppula, S., Park, P. J., Kim, E. H., Kim, C. G., Choi, W. S., et al. (2009). Chrysanthemum morifolium Ramat (CM) extract protects human neuroblastoma SH-SY5Y cells against MPP^+-induced cytotoxicity. *J. Ethnopharmacol.* 126, 447–454. doi: 10.1016/j.jep.2009.09.017

Kim, H., Lee, M. R., Lee, G. S., An, W. G., and Cho, S. I. (2012). Effect of *Sophora flavescens* Aiton extract on degranulation of mast cells and contact dermatitis induced by dinitrofluorobenzene in mice. *J. Ethnopharmacol.* 142, 253–258. doi: 10.1016/j.jep.2012.04.053

Kim, R. H., Smith, P. D., Aleyasin, H., Hayley, S., Mount, M. P., Pownall, S., et al. (2005). Hypersensitivity of DJ-1-deficient mice to 1-methyl-4-phenyl-1,2,3,6-tetrahydropyrindine (MPTP) and oxidative stress. *Proc. Natl. Acad. Sci. U S A* 102, 5215–5220. doi: 10.1073/pnas.0501282102

Kitada, T., Asakawa, S., Hattori, N., Matsumine, H., Yamamura, Y., Minoshima, S., et al. (1998). Mutations in the parkin gene cause autosomal recessive juvenile parkinsonism. *Nature* 392, 605–608. doi: 10.1038/33416

Langston, J. W., Irwin, I., Langston, E. B., and Forno, L. S. (1984). 1-Methyl-4-phenylpyridinium ion (MPP^+): identification of a metabolite of MPTP, a toxin selective to the substantia nigra. *Neurosci. Lett.* 48, 87–92. doi: 10.1016/0304-3940(84)90293-3

Lee, D. H., Kim, C. S., and Lee, Y. J. (2011). Astaxanthin protects against MPTP/MPP^+-induced mitochondrial dysfunction and ROS production *in vivo* and *in vitro*. *Food Chem. Toxicol.* 49, 271–280. doi: 10.1016/j.fct.2010.10.029

Li, M., Zhang, X., Cui, L., Yang, R., Wang, L., Liu, L., et al. (2011). The neuroprotection of oxymatrine in cerebral ischemia/reperfusion is related to nuclear factor erythroid 2-related factor 2 (nrf2)-mediated antioxidant response: role of nrf2 and hemeoxygenase-1 expression. *Biol. Pharm. Bull.* 34, 595–601. doi: 10.1248/bpb.34.595

Liu, T., Song, Y., Chen, H., Pan, S., and Sun, X. (2010). Matrine inhibits proliferation and induces apoptosis of pancreatic cancer cells *in vitro* and *in vivo*. *Biol. Pharm. Bull.* 33, 1740–1745. doi: 10.1248/bpb.33.1740

Liu, Y., Xu, Y., Ji, W., Li, X., Sun, B., Gao, Q., et al. (2014). Anti-tumor activities of matrine and oxymatrine: literature review. *Tumour Biol.* 35, 5111–5119. doi: 10.1007/s13277-014-1680-z

Moore, D. J., West, A. B., Dawson, V. L., and Dawson, T. M. (2005). Molecular pathophysiology of Parkinson's disease. *Annu. Rev. Neurosci.* 28, 57–87. doi: 10.1146/annurev.neuro.28.061604.135718

Olanow, C. W., and Tatton, W. G. (1999). Etiology and pathogenesis of Parkinson's disease. *Annu. Rev. Neurosci.* 22, 123–144. doi: 10.1146/annurev.neuro.22.1.123

O'Malley, K. L., Liu, J., Lotharius, J., and Holtz, W. (2003). Targeted expression of BCL-2 attenuates MPP^+ but not 6-OHDA induced cell death in dopaminergic neurons. *Neurobiol. Dis.* 14, 43–51. doi: 10.1016/s0969-9961(03)00013-5

Park, S. J., Nam, K. W., Lee, H. J., Cho, E. Y., Koo, U., and Mar, W. (2009). Neuroprotective effects of an alkaloid-free ethyl acetate extract from the root of *Sophora flavescens* Ait. Against focal cerebral ischemia in rats. *Phytomedicine* 16, 1042–1051. doi: 10.1016/j.phymed.2009.03.017

Piao, X. L., Piao, X. S., Kim, S. W., Park, J. H., Kim, H. Y., and Cai, S. Q. (2006). Identification and characterization of antioxidants from *Sophora flavescens*. *Biol. Pharm. Bull.* 29, 1911–1915. doi: 10.1248/bpb.29.1911

Requejo-Aguilar, R., and Bolaños, J. P. (2016). Mitochondrial control of cell bioenergetics in Parkinson's disease. *Free Radic. Biol. Med.* 100, 123–137. doi: 10.1016/j.freeradbiomed.2016.04.012

Saporito, M. S., Thomas, B. A., and Scott, R. W. (2000). MPTP activates c-Jun NH_2-terminal kinase (JNK) and its upstream regulatory kinase MKK4 in nigrostriatal neurons *in vivo*. *J. Neurochem.* 75, 1200–1208. doi: 10.1046/j.1471-4159.2000.0751200.x

Seaton, T. A., Cooper, J. M., and Schapira, A. H. (1997). Free radical scavengers protect dopaminergic cell lines from apoptosis induced by complex I inhibitors. *Brain Res.* 777, 110–118.

Sheehan, J. P., Palmer, P. E., Helm, G. A., and Tuttle, J. B. (1997). MPP^+ induced apoptotic cell death in SH-SY5Y neuroblastoma cells: an electron microscope study. *J. Neurosci. Res.* 48, 226–237. doi: 10.1002/(sici)1097-4547(19970501)48:3<226::aid-jnr5>3.0.co;2-h

Strasser, A., O'Connor, L., and Dixit, V. M. (2000). Apoptosis signaling. *Annu. Rev. Biochem.* 69, 217–245. doi: 10.1146/annurev.biochem.69.1.217

Sun, M., Han, J., Duan, J., Cui, Y., Wang, T., Zhang, W., et al. (2007). Novel antitumor activities of Kushen flavonoids *in vitro* and *in vivo*. *Phytother. Res.* 21, 269–277. doi: 10.1002/ptr.2066

Tanabe, N., Kuboyama, T., Kazuma, K., Konno, K., and Tohda, C. (2015). The extract of roots of *Sophora flavescens* enhances the recovery of motor function by axonal growth in mice with a spinal cord injury. *Front. Pharmacol.* 6:326. doi: 10.3389/fphar.2015.00326

Um, J. W., Stichel-Gunkel, C., Lübbert, H., Lee, G., and Chung, K. C. (2009). Molecular interaction between parkin and PINK1 in mammalian neuronal cells. *Mol. Cell. Neurosci.* 40, 421–432. doi: 10.1016/j.mcn.2008.12.010

Valente, E. M., Abou-Sleiman, P. M., Caputo, V., Muqit, M. M., Harvey, K., Gispert, S., et al. (2004). Hereditary early-onset Parkinson's disease caused by mutations in PINK1. *Science* 304, 1158–1160. doi: 10.1126/science.1096284

Venkatesh Gobi, V., Rajasankar, S., Ramkumar, M., Dhanalakshmi, C., Manivasagam, T., Justin Thenmozhi, A., et al. (2018). Agaricus blazei extract attenuates rotenone-induced apoptosis through its mitochondrial protective and antioxidant properties in SH-SY5Y neuroblastoma cells. *Nutr. Neurosci.* 21, 97–107. doi: 10.1080/1028415X.2016.1222332

Yamahara, J., Mochizuki, M., Fujimura, H., Takaishi, Y., Yoshida, M., Tomimatsu, T., et al. (1990). Antiulcer action of *Sophora flavescens* root and an active constituent. I. *J. Ethnopharmacol.* 29, 173–177. doi: 10.1016/0378-8741(90)90053-v

Yang, W., Chen, L., Ding, Y., Zhuang, X., and Kang, U. J. (2007). Paraquat induces dopaminergic dysfunction and proteasome impairment in DJ-1-deficient mice. *Hum. Mol. Genet.* 16, 2900–2910. doi: 10.1093/hmg/ddm249

Yang, J., Liu, X., Bhalla, K., Kim, C. N., Ibrado, A. M., Cai, J., et al. (1997). Prevention of apoptosis by Bcl-2: release of cytochrome c from mitochondria blocked. *Science* 275, 1129–1132. doi: 10.1126/science.275.5303.1129

Yao, Z., and Wood, N. W. (2009). Cell death pathways in Parkinson's disease: role of mitochondria. *Antioxid. Redox Signal.* 11, 2135–2149. doi: 10.1089/ARS.2009.2624

Yi, F., He, X., and Wang, D. (2013). Lycopene protects against MPP^+-induced cytotoxicity by maintaining mitochondrial function in SH-SY5Y cells. *Neurochem. Res.* 38, 1747–1757. doi: 10.1007/s11064-013-1079-z

Zhang, Y., Dawson, V. L., and Dawson, T. M. (2000). Oxidative stress and genetics in the pathogenesis of Parkinson's disease. *Neurobiol. Dis.* 7, 240–250. doi: 10.1006/nbdi.2000.0319

Conflict of Interest Statement: The authors declare that the research was conducted in the absence of any commercial or financial relationships that could be construed as a potential conflict of interest.

frontiers in Aging Neuroscience

ORIGINAL RESEARCH
published: 11 June 2018
doi: 10.3389/fnagi.2018.00179

Comparison of Administration Routes on the Protective Effects of Bee Venom Phospholipase A2 in a Mouse Model of Parkinson's Disease

*Hyunjung Baek, Hyun Il Jang, Hat Nim Jeon and Hyunsu Bae**

Department of Physiology, College of Korean Medicine, Kyung Hee University, Seoul, South Korea

Parkinson's disease (PD) is the second most common neurodegenerative disorder worldwide. Progressive loss of dopaminergic neurons in the substantia nigra (SN) and their synaptic terminal connections in the striatum are main characterizations of PD. Although many efforts have been made to develop therapeutics, no treatment has been proven effective. We previously demonstrated that bvPLA2 can protect dopaminergic neurons by modulating neuroinflammatory responses in an MPTP (1-methyl-4-phenyl-1,2,3,6-tetrahydropyridine)-induced mouse model of PD. The cellular basis for the neuroprotective response of bvPLA2 was the induction of $CD4^+CD25^+$ regulatory T cells (Tregs), a population known to suppress immune activation and maintain homeostasis and tolerance to self-antigen. The aim of the present study was to investigate the effects of different routes of bvPLA2 administration in a PD mouse model. Neurobehavioral assessment revealed progressive deterioration in locomotor functions of the MPTP group compared with the control group. However, such functions were improved following subcutaneous (s.c.) bvPLA2 administration. The results showed that the s.c. route of bvPLA2 administration contributed to the induction of Treg cells and the reduction of Th1 and Th17 populations, demonstrating that the neuroprotective effects were associated with reduced tyrosine hydroxylase (TH)-positive dopaminergic neurons and microglia. These results suggested that the s.c. bvPLA2 injection could be beneficial for treating aspects of PD.

Keywords: Parkinson's disease, bee venom phospholipase A2 (bvPLA2), route of administration, tyrosine hydroxylase, regulatory T cells (Tregs)

OPEN ACCESS

Edited by:
Seung-Nam Kim,
Dongguk University Seoul,
South Korea

Reviewed by:
Dora Reglodi,
University of Pécs, Hungary
Petr A. Slominsky,
Institute of Molecular Genetics,
Czechia

****Correspondence:***
Hyunsu Bae
hbae@khu.ac.kr

Received: *14 February 2018*
Accepted: *24 May 2018*
Published: *11 June 2018*

Citation:
Baek H, Jang HI, Jeon HN and Bae H (2018) Comparison of Administration Routes on the Protective Effects of Bee Venom Phospholipase A2 in a Mouse Model of Parkinson's Disease. Front. Aging Neurosci. 10:179. doi: 10.3389/fnagi.2018.00179

INTRODUCTION

Parkinson's disease (PD) is a common degenerative disease of the central nervous system that affects motor functions, such as muscular rigidity, onset of tremor, slowness of voluntary movements and difficulty maintaining balance. PD is caused by the progressive loss of dopaminergic neurons in the substantia nigra (SN). Current symptomatic therapy for PD can provide a benefit to slow disease progression and may cause motor complications, such as motor fluctuation and dyskinesia. Therefore, therapeutic strategies to delay the onset or slow progression of PD are needed. Functional links between adaptive immunity and neurodegenerative disorders have been well studied for PD, Alzheimer's disease (AD) and multiple sclerosis (Bar-Or et al., 2003; Casal et al., 2003; Baba et al., 2005). A specific population of T cells currently recognized as $CD4^+CD25^+Foxp3^+$ regulatory T cells (Tregs) suppress immune activation and maintain immune homeostasis and tolerance.

Tregs mediate neuroprotection through the modulation of inflammatory responses, suppression of microglial activation, and promotion of neuronal survival in animal models of PD (Reynolds et al., 2007, 2010). Therefore, the development of fast and effective methods of generating Tregs is likely to play a key role in the development of therapies for PD patients.

Bee venom (BV) extracted from honeybees is commonly used in Korean medicine. Previous studies have reported that BV therapy has anti-nociceptive and anti-inflammatory effects on pain, arthritis, cancer and skin disease (Kwon et al., 2001, 2002). Recent studies suggest that BV treatment possesses beneficial effects on the loss of dopaminergic neurons in PD and motor neurons in amyotrophic lateral sclerosis (ALS; Yang et al., 2010; Kim et al., 2011). BV therapy can be used in a cream, liniment, ointment, via injection, acupuncture or even direct administration of live bee stings. The most commonly used method is BV acupuncture, which involves a subcutaneous injection of diluted BV into acupoints. BV acupuncture has long been employed for numerous disorders including arthritis, pain syndrome, and multiple sclerosis (Shinto et al., 2004; Kim et al., 2005; Lee et al., 2005). Recently, several randomized controlled trials (RCTs) patients with idiopathic PD evaluated the safety and efficacy of BV therapy, including BV acupuncture and subcutaneous injection (Cho et al., 2012; Doo et al., 2015; Hartmann et al., 2016). Considering the findings reported on BV therapy for PD, the different efficacy reported to date may be due to the therapeutic protocol used, the severity of PD, in addition to potential time and dose-dependent properties. Interestingly, another recently published study compared the effects of BV treatment using different administration routes for the symptomatic hSOD1^{G93A} transgenic model of ALS (Cai et al., 2015). Taken together, these findings are requested further well designed RCTs for the therapeutic potential of BV treatment, including the most effective doses and mode of administration, and comparison its effects in different stages of PD patients.

BV contains several bioactive compounds, including melittin, phospholipase A2 (PLA2), apamin and peptides (Lariviere and Melzack, 1996). Studies have shown that bvPLA2 possesses protective effects by inducing Treg populations in neurodegenerative diseases, such as AD and PD murine models (Chung et al., 2015; Ye et al., 2016). Chung et al. (2015) reported the neuroprotective effects of bvPLA2 in controlling the generation of Tregs in MPTP-induced mouse model of PD. These authors demonstrated that bvPLA2 could promote the survival of dopaminergic neurons by suppressing microglial activation and reducing the infiltration of CD4$^+$ T cells in a PD mouse model. However, it is unclear which route of bvPLA2 administration would be more relevant for the treatment of PD. Therefore, the purpose of the present study was to investigate which route of bvPLA2 administration would be more effective for protecting dopaminergic neurons in MPTP-induced PD models. Intraperitoneal (i.p.), subcutaneous (s.c.), intramuscular (i.m.) and intravenous (i.v.) injection routes were examined. The findings highlight the optimum route of bvPLA2 administration to exert its neuroprotective effects on MPTP-induced PD in a mouse model by controlling the generation of Treg populations.

MATERIALS AND METHODS

Animals

All experiments were performed in accordance with the approved animal protocols and guidelines established by Kyung Hee University. Seven to eight-week-old male C57BL/6J mice (19–23 g) were purchased from The Jackson Laboratory (Bar Harbor, ME, USA). The mice were maintained on a 12 h light/dark cycle and temperature-controlled conditions (21 ± 2°C), with food and water *ad libitum*.

Animal Experiments

For MPTP intoxication, the mice received four i.p. injections of MPTP-HCl (20 mg/kg free base in saline; Sigma-Aldrich, St. Louis, MO, USA) at 2-h intervals as previously described (Chung et al., 2011). Twelve hours after the last MPTP injection, the mortality rate of mice was 30.4%. Then, live mice were divided into five groups and received i.p., s.c., i.m., or i.v. injections of bvPLA2 (0.5 mg/kg) for 6 days. Some mice were injected with vehicle alone as controls.

Measurement of Motor Activity by Pole Test

Twenty-four hours after the last bvPLA2 injection, a pole test was performed to determine forelimb and hindlimb motor coordination and balance. Briefly, the mice were place on the top of a gauze-banded wooden pole (50 cm in length and 0.8 cm in diameter) facing upwards. The animals were allowed to climb down to the base of the pole. The time to turn completely downward (T-turn) and the total time taken for the mouse to reach the floor (locomotion activity time [T-LA]) were recorded, with a cut-off limit of 30 s. Each mouse was examined in five trials, and the average of the best three measurements was calculated. Trials with the mouse jumping or sliding down the pole were excluded.

Flow Cytometric Analysis of Th1, Th2, Th17 and Treg Populations

Flow cytometric analysis of T-helper cell subsets was performed by using fluorescein isothiocyanate (FITC)-conjugated anti-mouse CD4 (clone GK1.5; eBioscience, San Diego, CA, USA), phycoerythrin (PE)-conjugated anti-mouse CD25 (clone PC61.5; eBioscience), Alexa Fluor 647 anti-mouse/rat Foxp3 (clone MF23; BD Biosciences), PE-conjugated anti-mouse IFN-γ (clone SMG1.2; eBioscience) PE-conjugated anti-mouse IL-4 (clone 11B11; eBioscience), and PerCP-Cyanine5.5-conjugated anti-mouse/rat IL-17A (clone eBio17B7; eBioscience) antibodies. For Treg staining, single-cell splenocytes at a concentration of 2×10^6 cells/ml were collected, washed twice with phosphate-buffered saline (PBS), and stained with FITC-conjugated anti-CD4 and PE-labeled anti-CD25 antibodies in staining buffer for 30 min on ice in the dark. The cells were subsequently washed twice with PBS and fixed in fixation/permeabilization

buffer (eBioscience) for 1 h at 4°C in the dark. Subsequently, the cells were washed twice with PBS and stained with Alexa Fluor 647 anti-Foxp3 antibody overnight at 4°C in the dark. After washing, the cells were fixed in 1% paraformaldehyde and stored at 4°C in the dark for subsequent detection. For intracellular cytokine staining, single-cell splenocytes at a concentration of 2×10^6 cells/ml were stimulated with 50 ng/ml of phorbol myristate acetate (PMA; Sigma-Aldrich) and 1000 ng/ml of ionomycin (Sigma-Aldrich) for 1 h, and then incubated with GolgiStop (BD Biosciences) for 4 h. The cells were collected, washed twice with PBS, and stained with FITC-labeled anti-CD4 antibody for 30 min on ice in the dark. After washing with PBS, the cells were fixed in IC fixation buffer (BD Biosciences) for 30 min at room temperature in the dark. The cells were then stained with PE-conjugated anti-IFN-γ, PE-conjugated anti-IL-4 and PerCP-Cyanine5.5-conjugated anti-IL-17A antibodies overnight at 4°C (Lee et al., 2016). After washing with PBS, the cells were fixed in 1% paraformaldehyde and stored at 4°C in the dark for subsequent detection. After the samples were analyzed with a FACSCalibur flow cytometer (BD Biosciences), the data were generated in graphical and tabular formats by using FLOWJO software (Tree star, Ashland, OR, USA).

Tissue Processing and Immunohistochemistry

The mice were anesthetized with isoflurane (Forane solution; ChoongWae Pharma, Seoul, South Korea) and transcardially perfused with PBS followed by perfusion with a fixative solution containing 4% paraformaldehyde dissolved in 0.1 M phosphate buffer. The brain was dissected, postfixed in 4% paraformaldehyde at 4°C overnight, transferred to 30% sucrose solution, and subsequently frozen. The tissues were embedded in OCT compound and serially cut on a cryostat into 30-μm thick coronal sections by using a sliding microtome. All sections were collected in six separate series and processed for immunohistochemical staining. Primary antibody was directed against tyrosine hydroxylase (TH; 1:2000, Pel-Freez Clinical System, Brown Deer, WI, USA) and Iba-1 (1:2000), Wako Pure Chemic Industries, Osaka, Japan). After washing with PBS, the sections were incubated with the appropriate biotinylated secondary antibody and processed with an avidin-biotin complex kit (Vectastain ABC kit; Vector Laboratories, Burlingame, CA, USA). The reaction product was visualized with 0.05% diaminobenzidine-HCL (DAB) and 0.003% hydrogen peroxide in 0.1 M phosphate buffer. The labeled tissue sections were subsequently mounted and analyzed under a bright field microscope (Nikon, Tokyo, Japan).

Stereological Cell Counts

Unbiased stereological estimation of the total number of TH-positive dopaminergic neurons in the SN was performed by using an optical fractionator method on an Olympus CAST (computer-assisted stereological toolbox) system version 2.1.4. (Olympus, Ballerup, Denmark) as previously described (Chung et al., 2011). Sections used for counting covered the entire SN from the rostral tip of the pars compacta to the caudal end of the pars reticulate (anteroposterior, from −2.06 mm to −4.16 mm from bregma). Actual counting was performed by using a 100× oil objective. The total number of cells was estimated according to the optical fractionator equation. More than 300 points were analyzed for all sections of each specimen.

Statistical Analysis

All data were analyzed using GraphPad Prism 5.01 (GraphPad Software Inc., San Diego, CA, USA). The data are presented as the means ± standard error of the mean (SEM) where indicated. Statistical significance of each variable was evaluated by one-way analysis of variance (ANOVA), followed by Newman-Keuls multiple comparison test for multiple comparison or by two-tailed Student's *t*-test for single comparisons. All experiments were performed in a blind manner and repeated independently under identical conditions. Statistical significance was set at $P < 0.05$.

RESULTS

Effects of Different Routes of bvPLA2 Administration on Motor Function in MPTP-Induced Neurotoxicity

To evaluate the effects of different routes of bvPLA2 administration on MPTP-induced neurotoxicity, mice were administered MPTP and received a single daily injection via i.p., s.c., i.m. and i.v. of bvPLA2 or saline for 6 days commencing 12 h after the last MPTP injection. Various behavioral tests have been routinely used to qualify PD mouse models, including locomotor activity, rotarod test, forepaw stride length, and the pole test (Taylor et al., 2010). In the present study, the neuroprotective effect of bvPLA2 against PD-related motor deficits was evaluated by the pole test in an MPTP-induced mouse model. MPTP treatment significantly extended the time of T-turn and T-LA compared to those in the control group (**Figure 1**). T-turn and T-LA were significantly shortened in the SC group compared to those in the MPTP group. IP and IV administration of bvPLA2 showed moderate recovery of motor coordination and balance. However, there were no significant differences in the time of T-turn and T-LA between the MPTP and IM groups.

Effects of Different Routes of bvPLA2 Treatment on Treg Populations in MPTP-Injected Mice

In a previous report, the proportion of Treg cells was decreased in PD patients compared to that in the control group (Chen et al., 2015). Furthermore, the impaired ability of Tregs from PD patients to suppress effector T cell functions was observed. The effects of different injection routes of bvPLA2 on the proportions of Tregs were assessed by flow cytometric analysis. No significant difference in the $CD4^+CD25^+Foxp3^+$ Treg populations was detected between the control and MPTP groups. However, a more than 30% increase in the number of Treg cells was detected in the SC group compared to that in the control group (**Figure 2**). The other routes of bvPLA2 injection did not induce

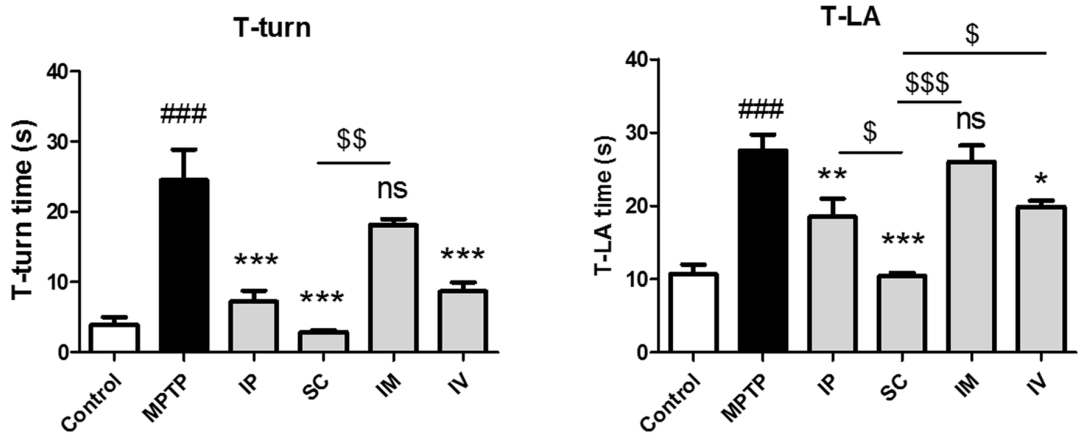

FIGURE 1 | Effects of the administration routes of Bee Venom Phospholipase A2 (bvPLA2) on T-turn and T-total time values in (1-methyl-4-phenyl-1,2,3,6-tetrahydropyridine; MPTP)-injected mice. The pole test was performed at 24 h after the last bvPLA2 injection. Behavioral function was improved when bvPLA2 was subcutaneously administered. Error bars represent the means ± standard error of the mean (SEM). The significance was determined by Student's *t*-test. $^{###}P < 0.001$ vs. the respective phosphate-buffered saline (PBS) control. $^{*}P < 0.05$, $^{**}P < 0.01$, $^{***}P < 0.001$, significantly different from the substantia nigra (SN) of MPTP-injected mice. $^{\$}P < 0.05$, $^{\$\$}P < 0.01$, $^{\$\$\$}P < 0.001$ vs. the SC group. IP, intraperitoneal injection; SC, subcutaneous injection; IM, intramuscular injection; IV, intravenous injection.

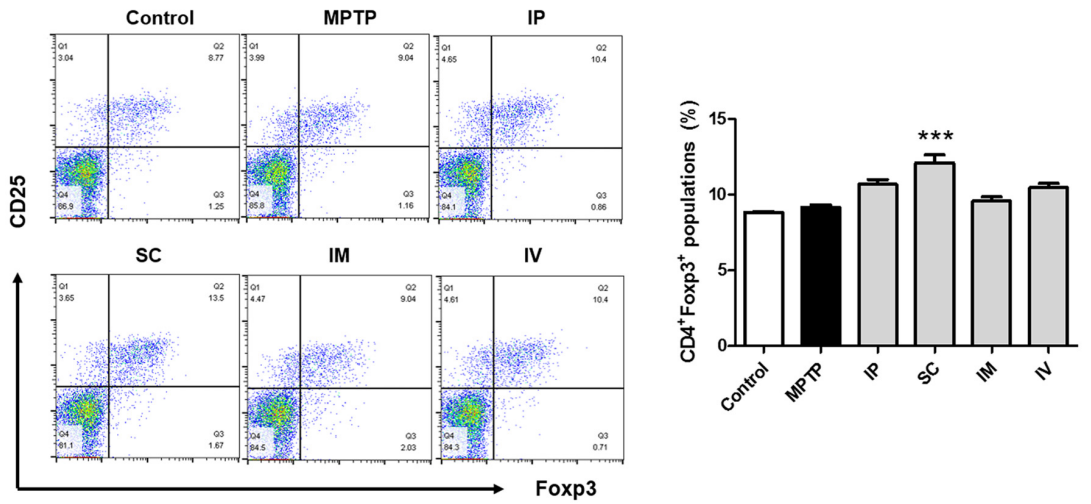

FIGURE 2 | Differentiation of Treg cells induced by bvPLA2 depending on routes of administration for MPTP-injected mice. Treg differentiation in splenocytes was assessed by flow cytometry for cells expressing CD4, CD25 and Foxp3. The bar graph depicts the statistics of Tregs in splenocytes. The number of Treg cells was increased when bvPLA2 was subcutaneously administered. Error bars represent the means ± SEM. The significance was determined by Student's *t*-test. $^{***}P < 0.001$, significantly different from MPTP-injected mice. IP, intraperitoneal injection; SC, subcutaneous injection; IM, intramuscular injection; IV, intravenous injection.

any significant difference in the number of Tregs within this population.

Effects of Different Routes of bvPLA2 Treatment on Th1/2/17 Populations in MPTP-Induced PD Mice

The effects of different routes of bVPLA2 administration on T-helper cell phenotypes were subsequently determined. Changes in IFN-γ, IL-4 and IL-17A expression suggest an alternative status of Th1, Th2 and Th17 cells. The prevalence of these cells was then further determined by flow cytometric analysis. As shown in **Figure 3A**, the Th1 population was increased and the Th1/Th2 balance was shifted toward Th1 in the MPTP group, indicating an enhanced Th1-type response. The present study also found that Th17 cells were increased in the MPTP group. Compared to the MPTP group, flow cytometric analysis indicated that polarized Th1 and Th17 cells showed the decreased IFN-γ and IL-17A expression in the IP and SC

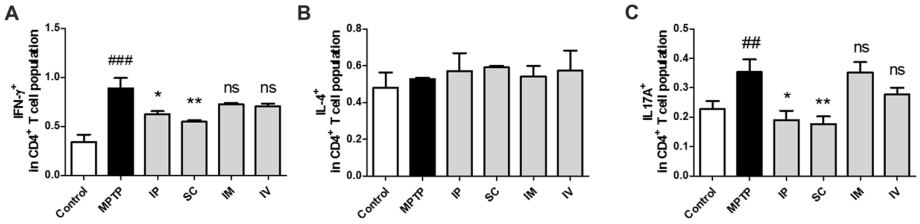

FIGURE 3 | Differentiation of Th1/2/17 cells induced by bvPLA2 depending on the routes of administration to MPTP-injected mice. Th1/2/17 differentiation in splenocytes was assessed by flow cytometry for **(A)** Th1 ($CD4^+IFN\text{-}\gamma^+$), **(B)** Th2 ($CD4^+IL\text{-}4^+$) and **(C)** Th17 ($CD4^+IL\text{-}17A^+$) populations. The bar graph depicts the statistics of Th1 cells in splenocytes. The error bars represent the means ± SEM. The significance was determined by Student's *t*-test. $^{\#\#}P < 0.01$ and $^{\#\#\#}P < 0.001$ vs. the respective PBS control. $^{*}P < 0.05$ and $^{**}P < 0.01$, significantly different from MPTP-injected mice. IP, intraperitoneal injection; SC, subcutaneous injection; IM, intramuscular injection; IV, intravenous injection.

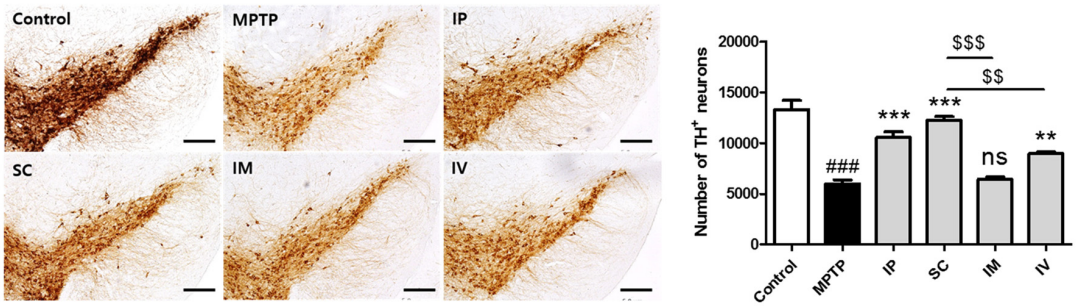

FIGURE 4 | Immunohistochemical staining for tyrosine hydroxylase (TH) in striatum tissue samples from bvPLA2-administered groups by different routes. Brain tissues were stained with TH for the analysis of damage on dopaminergic neurons. The number of TH-positive neurons in the SN was quantified by using a semi-quantitative scale. All randomly selected histological images were scored. These data are representatives of three separate experiments. Data are shown as the means ± SEM. $^{\#\#\#}P < 0.001$ vs. the CON group, $^{**}P < 0.01$ and $^{***}P < 0.001$ vs. the MPTP group, and $^{\$\$}P < 0.01$ and $^{\$\$\$}P < 0.001$ vs. the SC group. Scale bars: 5.0 μm. IP, intraperitoneal injection; SC, subcutaneous injection; IM, intramuscular injection; IV, intravenous injection.

group (**Figure 3C**). No significant differences were detected for Th2 polarization between all groups (**Figure 3B**).

Effects of Routes of bvPLA2 Administration on Dopaminergic Neurons in the SN Against MPTP Neurotoxicity

To assess the protective effect of each administration route of bvPLA2 on dopaminergic neurons, TH-positive neurons were counted (**Figure 4**). Treatment with MPTP reduced the number of TH-positive neurons more than two-fold compared to that in the control group. However, analysis of surviving dopaminergic neurons in TH-immunostained striatum after MPTP and bvPLA2 treatments revealed that i.p., s.c., and i.v. injections of bvPLA2 increased the number of surviving TH-positive neurons within the SN, whereas i.m. injection of bvPLA2 remarkably diminished dopaminergic neurons within the striatum (**Figure 4**).

Effects of Routes of bvPLA2 Injection on Microglial Activation From MPTP-Derived Neurotoxicity

Microglia are the resident immunocompetent and phagocytic cells in the brain that play a neuroprotective function. Microglia are rapidly activated in response to neuronal damage and produce various potentially neurotoxic compounds under neuropathological conditions. Therefore, we analyzed the level of Iba-1 as the specific marker of microglia in the model group. **Figure 5** shows that i.p., s.c., and i.v. injections of bvPLA2 dramatically reduced the number of Iba-1^+ microglia in the brains of MPTP-induced PD mice compared to those of the MPTP group. In contrast, compared with s.c. injection, i.m. injection increased Iba-1 expression.

DISCUSSION

In the present study, the best route of bvPLA2 administration to prevent the temporal progression of PD pathology was investigated. The results of a previous study revealed that the i.p. injection of bvPLA2 protected dopaminergic neurons by modulating neuroinflammatory responses in an MPTP-induced PD mouse model (Chung et al., 2015). In the present study to identify the optimum route of bvPLA2 administration to ameliorate the pathophysiology of PD, as shown in the previous article, the i.p. injection of bvPLA2 showed the neuroprotective effects. However, the s.c. injection of bvPLA2 showed the best neuroprotective effects, including enhanced motor functions, decreased Th1 and Th17 polarization, increased TH-positive

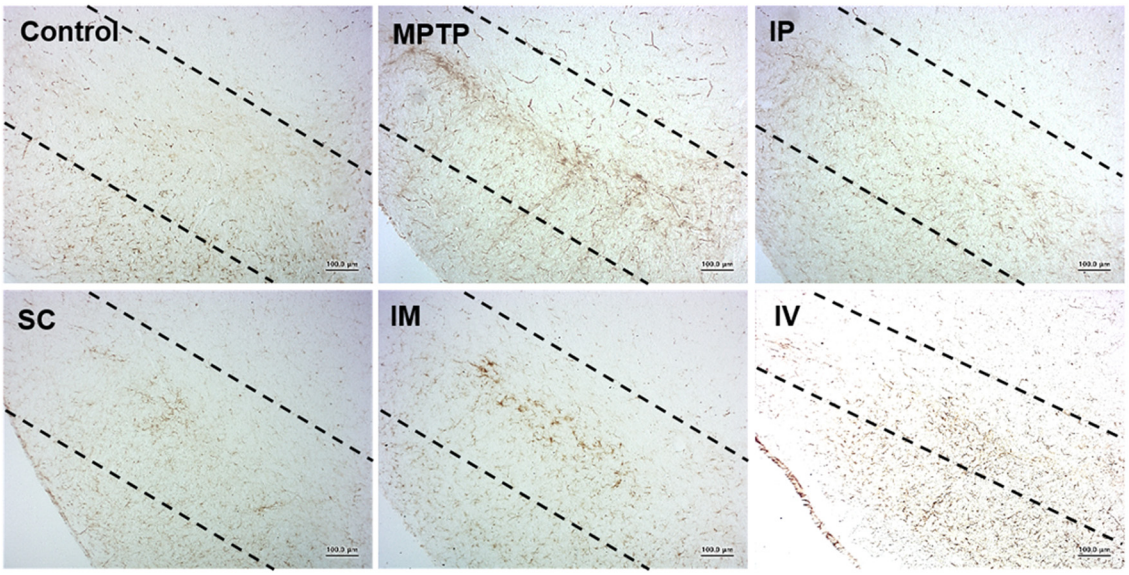

FIGURE 5 | Effects of different routes of bvPLA2 administration on microglial activation in an MPTP-induced neurotoxicity model. The activation of microglia was detected by Iba-1 immunostaining. Data show that s.c. injection of bvPLA2 could inhibit the elevated levels of Iba-1. Images were obtained from the SN. Scale bars: 200 μm. IP, intraperitoneal injection; SC, subcutaneous injection; IM, intramuscular injection; IV, intravenous injection.

dopaminergic neurons and reduced number of Iba-1-positive microglia in the SN of an MPTP toxicity model.

Different routes of administration were selected to achieve either the systemic or local delivery of medications in an active form. The route of administration in pharmacology and toxicology is determined by the physical characteristics of the drug, the speed at which the drug is absorbed, and the need to bypass hepatic metabolism and achieve high concentration at particular sites (Bruno et al., 2013). For therapeutic drugs, there are various routes for drug administration, including parenteral, oral, nasal, ocular, transmucosal and transdermal injections. From a clinical point of view, it is important to consider the route of drug administration that shows the most therapeutic effects. We compared the four clinically applicable routes of injection. The results of the present study suggested that the s.c. injection of bvPLA2 was the most effective for the attenuation of MPTP-induced neurotoxicity. Subcutaneous injection is administered below the epidermis and dermis layers into the subcutaneous tissue and is easily performed with a lower risk of damage to blood vessels and other structures. Insulin and hormones are commonly administered by s.c. injections. The s.c. route is generally preferred over the i.v. route because it offers more convenience to patients, improves quality of life and reduces health care costs. These findings have significant implications toward the development of a clinical protocol for PD.

Over the past few decades, many efforts have been made to identify new drug targets focusing on CNS disease, including AD, PD and Huntington disease (Trojanowski and Hampel, 2011; Harikrishna Reddy et al., 2014; Lim et al., 2017). Despite the progress in neuroscience, numerous candidate drugs for neurodegenerative diseases have shown encouraging results *in vitro* and *in vivo*, but failed to lead to clinical trials. The glial cell line-derived neurotrophic factor (GDNF) is an effective and potent neuroprotective agent for PD. However, GDNF drug development has failed, because the neurotrophic factor does not cross the blood-brain barrier (BBB; Bartus and Johnson, 2017a,b). The small lipid-soluble drug as an index of BBB transport is only valid when the molecular weight (MW) is less than or approximately equal to 400–600 Da. The majority of the therapeutic agents are larger than the size limit and thus cannot be transported across the BBB. Because bvPLA2 is a small, 15 kDa enzyme which belongs to group III secreted PLA2, bvPLA2 cannot directly reach the brain across the BBB. The presence of activated central memory T lymphocytes has been reported at blood-cerebrospinal fluid barrier (CSF) of the choroid plexus, which act as a site of immune surveillance process that allows immune cell entry to the brain in response to acute injury of inflammation (Baruch et al., 2013). In the previous and present study, we showed the bvPLA2-mediated induction of the $CD4^+CD25^+Foxp3^+$ Treg populations. We suggested that the neuroprotective effects of bvPLA2 treatment in MPTP-induced PD model resulted from the increased infiltration of memory T lymphocytes through choroid plexus instead of direct across the BBB.

A growing body of evidence suggests that cellular and humoral immune responses are changed in the peripheral immune system of PD patients (Dauer and Przedborski, 2003). In a previous report, the adoptive transfer of splenocytes from mice immunized with Copolymer-1 (Cop-1) suppressed microglial responses, leading to the protection of dopaminergic neurons in MPTP-intoxicated mice (Benner et al., 2004). $CD4^+$ T cells isolated from Cop-1 immunized mice evoked a robust neuroprotective response (Laurie et al., 2007).

In contrast, the depletion of these cells abrogated this protection. These reports represent the primary role of $CD4^+$ T cells in protective responses in PD. Furthermore, Reynold et al. have reported that the adoptive transfer of $CD4^+CD25^+$ Tregs can modulate immune responses in the brain, resulting in significant neuroprotection in a PD mouse model (Reynolds et al., 2007). These authors suggested that the use of immunomodulatory strategies by inducing Treg responses attenuates neuroinflammation and inhibits dopaminergic neurodegeneration to treat PD patients.

In PD, autoreactive Th1 or Th17 cells are important for the promotion of neurodegeneration. A shift in the Th1/Th2 balance toward Th1 is closely associated with motor function. Th17 cells play critical roles in the protection against mucosal inflammation. Recent studies on the neurotoxic properties of Th17 populations have reported that the infiltration of Th17 cells into the SN can exacerbate dopaminergic neuronal loss in MPTP intoxication models (Liu et al., 2017). Consistent with this finding, increased Th1 and Th17 populations in the MPTP group indicated enhanced PD-associated inflammation. Furthermore, the decreased Th17 population in s.c. injection of bvPLA2 indicated weakened PD-associated inflammation, whereas increased Tregs in the SC group suggested the enhanced suppression of inflammation.

The present study reported an optimized route of bvPLA2 administration to prevent neuronal damage in an MPTP-induced PD mouse model. The s.c. injection of bvPLA2 represented the best route of administration among i.p., s.c., i.m., and i.v. injections. The results from the present study suggest that the s.c. route of bvPLA2 administration might have potential application for the treatment of PD patients.

AUTHOR CONTRIBUTIONS

HNJ and HIJ performed the experiments and conducted the statistical analysis. HBaek drafted the first version of the manuscript. HNJ and HBaek drafted sections of the manuscript. HBae supervised the project and edited the manuscript. All authors contributed to the manuscript revision and have read and approved the submitted version.

FUNDING

This work was supported by the Basic Science Research Program through the National Research Foundation (NRF) of South Korea funded by the Ministry of Science, ICT and Future Planning (NRF-2017R1A2B3009574), the Korea Health Technology R&D Project through the Korea Health Industry Development Institute (KHIDI), funded by the Ministry of Health & Welfare, Republic of Korea (HI17C0978).

REFERENCES

Baba, Y., Kuroiwa, A., Uitti, R. J., Wszolek, Z. K., and Yamada, T. (2005). Alterations of T-lymphocyte populations in Parkinson disease. *Parkinsonism Relat. Disord.* 11, 493–498. doi: 10.1016/j.parkreldis.2005.07.005

Bar-Or, A., Nuttall, R. K., Duddy, M., Alter, A., Kim, H. J., Ifergan, I., et al. (2003). Analyses of all matrix metalloproteinase members in leukocytes emphasize monocytes as major inflammatory mediators in multiple sclerosis. *Brain* 126, 2738–2749. doi: 10.1093/brain/awg285

Bartus, R. T., and Johnson, E. M. Jr. (2017a). Clinical tests of neurotrophic factors for human neurodegenerative diseases, part 1: where have we been and what have we learned? *Neurobiol. Dis.* 97, 156–168. doi: 10.1016/j.nbd.2016.03.027

Bartus, R. T., and Johnson, E. M. Jr. (2017b). Clinical tests of neurotrophic factors for human neurodegenerative diseases, part 2: where do we stand where must we go next? *Neurobiol. Dis.* 97, 169–178. doi: 10.1016/j.nbd.2016.03.026

Baruch, K., Ron-Harel, N., Gal, H., Deczkowska, A., Shifrut, E., Ndifon, W., et al. (2013). CNS-specific immunity at the choroid plexus shifts toward destructive Th2 inflammation in brain aging. *Proc. Natl. Acad. Sci. U S A* 110, 2264–2269. doi: 10.1073/pnas.1211270110

Benner, E. J., Mosley, R. L., Destache, C. J., Lewis, T. B., Jackson-Lewis, V., Gorantla, S., et al. (2004). Therapeutic immunization protects dopaminergic neurons in a mouse model of Parkinson's disease. *Proc. Natl. Acad. Sci. U S A* 101, 9435–9440. doi: 10.1073/pnas.0400569101

Bruno, B. J., Miller, G. D., and Lim, C. S. (2013). Basics and recent advances in peptide and protein drug delivery. *Ther. Deliv.* 4, 1443–1467. doi: 10.4155/tde.13.104

Cai, M., Choi, S. M., and Yang, E. J. (2015). The effects of bee venom acupuncture on the central nervous system and muscle in an animal hSOD1G93A mutant. *Toxins* 7, 846–858. doi: 10.3390/toxins7030846

Casal, J. A., Robles, A., and Tutor, J. C. (2003). Serum markers of monocyte/macrophage activation in patients with Alzheimer's disease and other types of dementia. *Clin. Biochem.* 36, 553–556. doi: 10.1016/s0009-9120(03)00093-6

Chen, Y., Qi, B., Xu, W., Ma, B., Li, L., Chen, Q., et al. (2015). Clinical correlation of peripheral CD4+cell subsets, their imbalance and Parkinson's disease. *Mol. Med. Rep.* 12, 6105–6111. doi: 10.3892/mmr.2015.4136

Cho, S. Y., Shim, S. R., Rhee, H. Y., Park, H. J., Jung, W. S., Moon, S. K., et al. (2012). Effectiveness of acupuncture and bee venom acupuncture in idiopathic Parkinson's disease. *Parkinsonism Relat. Disord.* 18, 948–952. doi: 10.1016/j.parkreldis.2012.04.030

Chung, Y. C., Kim, S. R., Park, J. Y., Chung, E. S., Park, K. W., Won, S. Y., et al. (2011). Fluoxetine prevents MPTP-induced loss of dopaminergic neurons by inhibiting microglial activation. *Neuropharmacology* 60, 963–974. doi: 10.1016/j.neuropharm.2011.01.043

Chung, E. S., Lee, G., Lee, C., Ye, M., Chung, H. S., Kim, H., et al. (2015). Bee venom phospholipase A_2, a novel $Foxp3^+$ regulatory T cell inducer, protects dopaminergic neurons by modulating neuroinflammatory responses in a mouse model of Parkinson's disease. *J. Immunol.* 195, 4853–4860. doi: 10.4049/jimmunol.1500386

Dauer, W., and Przedborski, S. (2003). Parkinson's disease: mechanisms and models. *Neuron* 39, 889–909. doi: 10.1016/S0896-6273(03)00568-3

Doo, K. H., Lee, J. H., Cho, S. Y., Jung, W. S., Moon, S. K., Park, J. M., et al. (2015). A prospective open-label study of combined treatment for idiopathic Parkinson's disease using acupuncture and bee venom acupuncture as an adjunctive treatment. *J. Altern. Complement. Med.* 21, 598–603. doi: 10.1089/acm.2015.0078

Harikrishna Reddy, D., Misra, S., and Medhi, B. (2014). Advances in drug development for Parkinson's disease: present status. *Pharmacology* 93, 260–271. doi: 10.1159/000362419

Hartmann, A., Müllner, J., Meier, N., Hesekamp, H., van Meerbeeck, P., Habert, M. O., et al. (2016). Bee venom for the treatment of parkinson disease—a randomized controlled clinical trial. *PLoS One* 11:e0158235. doi: 10.1371/journal.pone.0158235

Kim, Y. S., Jun, H., Chae, Y., Park, H. J., Kim, B. H., Chang, I. M., et al. (2005). The practice of Korean medicine: an overview of clinical trials in acupuncture. *Evid. Based Complement. Alternat. Med.* 2, 325–352. doi: 10.1093/ecam/neh102

Kim, J. I., Yang, E. J., Lee, M. S., Kim, Y. S., Huh, Y., Cho, I. H., et al. (2011). Bee venom reduces neuroinflammation in the MPTP-induced model of Parkinson's disease. *Int. J. Neurosci.* 121, 209–217. doi: 10.3109/00207454.2010.548613

Kwon, Y. B., Lee, H. J., Han, H. J., Mar, W. C., Kang, S. K., Yoon, O. B., et al. (2002). The water-soluble fraction of bee venom produces antinociceptive and

anti-inflammatory effects on rheumatoid arthritis in rats. *Life Sci.* 71, 191–204. doi: 10.1016/s0024-3205(02)01617-x

Kwon, Y. B., Lee, J. D., Lee, H. J., Han, H. J., Mar, W. C., Kang, S. K., et al. (2001). Bee venom injection into an acupuncture point reduces arthritis associated edema and nociceptive responses. *Pain* 90, 271–280. doi: 10.1016/s0304-3959(00)00412-7

Lariviere, W. R., and Melzack, R. (1996). The bee venom test: a new tonic-pain test. *Pain* 66, 271–277. doi: 10.1016/0304-3959(96)03075-8

Laurie, C., Reynolds, A., Coskun, O., Bowman, E., Gendelman, H. E., and Mosley, R. L. (2007). CD4+ T cells from Copolymer-1 immunized mice protect dopaminergic neurons in the 1-methyl-4-phenyl-1,2,3,6-tetrahydropyridine model of Parkinson's disease. *J. Neuroimmunol.* 183, 60–68. doi: 10.1016/j.jneuroim.2006.11.009

Lee, E. J., Lee, G., Sohn, S. H., and Bae, H. (2016). Extract of *Rhus verniciflua* Stokes enhances Th1 response and NK cell activity. *Mol. Cell. Toxicol.* 12, 399–407. doi: 10.1007/s13273-016-0044-8

Lee, J. D., Park, H. J., Chae, Y., and Lim, S. (2005). An overview of bee venom acupuncture in the treatment of arthritis. *Evid. Based Complement. Alternat. Med.* 2, 79–84. doi: 10.1093/ecam/neh070

Lim, R. G., Salazar, L. L., Wilton, D. K., King, A. R., Stocksdale, J. T., Sharifabad, D., et al. (2017). Developmental alterations in Huntington's disease neural cells and pharmacological rescue in cells and mice. *Nat. Neurosci.* 20, 648–660. doi: 10.1038/nn.4532

Liu, Z., Huang, Y., Cao, B. B., Qiu, Y. H., and Peng, Y. P. (2017). Th17 cells induce dopaminergic neuronal death via LFA-1/ICAM-1 interaction in a mouse model of Parkinson's disease. *Mol. Neurobiol.* 54, 7762–7776. doi: 10.1007/s12035-016-0249-9

Reynolds, A. D., Banerjee, R., Liu, J., Gendelman, H. E., and Mosley, R. L. (2007). Neuroprotective activities of $CD4^{+}CD25^{+}$ regulatory T cells in an animal model of Parkinson's disease. *J. Leukoc. Biol.* 82, 1083–1094. doi: 10.1189/jlb.0507296

Reynolds, A. D., Stone, D. K., Hutter, J. A., Benner, E. J., Mosley, R. L., and Gendelman, H. E. (2010). Regulatory T cells attenuate Th17 cell-mediated nigrostriatal dopaminergic neurodegeneration in a model of Parkinson's disease. *J. Immunol.* 184, 2261–2271. doi: 10.4049/jimmunol.0901852

Shinto, L., Calabrese, C., Morris, C., Sinsheimer, S., and Bourdette, D. (2004). Complementary and alternative medicine in multiple sclerosis: survey of licensed naturopaths. *J. Altern. Complement. Med.* 10, 891–897. doi: 10.1089/acm.2004.10.891

Taylor, T. N., Greene, J. G., and Miller, G. W. (2010). Behavioral phenotyping of mouse models of Parkinson's disease. *Behav. Brain Res.* 211, 1–10. doi: 10.1016/j.bbr.2010.03.004

Trojanowski, J. Q., and Hampel, H. (2011). Neurodegenerative disease biomarkers: guideposts for disease prevention through early diagnosis and intervention. *Prog. Neurobiol.* 95, 491–495. doi: 10.1016/j.pneurobio.2011.07.004

Yang, E. J., Jiang, J. H., Lee, S. M., Yang, S. C., Hwang, H. S., Lee, M. S., et al. (2010). Bee venom attenuates neuroinflammatory events and extends survival in amyotrophic lateral sclerosis models. *J. Neuroinflammation* 7:69. doi: 10.1186/1742-2094-7-69

Ye, M., Chung, H. S., Lee, C., Yoon, M. S., Yu, A. R., Kim, J. S., et al. (2016). Neuroprotective effects of bee venom phospholipase A2 in the 3xTg AD mouse model of Alzheimer's disease. *J. Neuroinflammation* 13:10. doi: 10.1186/s12974-016-0476-z

Conflict of Interest Statement: The authors declare that the research was conducted in the absence of any commercial or financial relationships that could be construed as a potential conflict of interest.

frontiers in Aging Neuroscience

MINI REVIEW
published: 28 August 2018
doi: 10.3389/fnagi.2018.00246

Natural Molecules From Chinese Herbs Protecting Against Parkinson's Disease via Anti-oxidative Stress

Yaqi Ding[1], Chenqi Xin[1], Cheng-Wu Zhang[1], Kah-Leong Lim[2,3], Hang Zhang[1], ZhenQian Fu[1], Lin Li[1]* and Wei Huang[1]*

[1] *Key Laboratory of Flexible Electronics – Institute of Advanced Materials, Jiangsu National Synergistic Innovation Center for Advanced Materials, Nanjing Tech University, Nanjing, China,* [2] *Neurodegeneration Research Laboratory, National Neuroscience Institute, Singapore, Singapore,* [3] *Department of Physiology, Yong Loo Lin School of Medicine, National University of Singapore, Singapore, Singapore*

Parkinson's disease (PD) is the second most common neurodegenerative disease after Alzheimer's disease, affecting about 7–10 million patients worldwide. The major pathological features of PD include loss of dopaminergic (DA) neurons in the substantia nigra pars compacta (SNpc) of the midbrain and the presence of α-synuclein-enriched Lewy bodies. Although the mechanism underlying PD pathogenesis remains to be elucidated, oxidative stress induced by the overproduction of reactive oxygen species (ROS) is widely accepted to be a key pathogenic factors. ROS cause oxidative damage to proteins, lipids, and DNA, which subsequently lead to neurodegeneration. Great efforts have been made to slow or stop the progress of PD. Unfortunately there is no effective cure for PD till now. Compounds with good antioxidant activity represent the promising candidates for therapeutics of PD. Some natural molecules from Chinese herbs are found to have good antioxidant activity. Both *in vitro* and *in vivo* studies demonstrate that these natural molecules could mitigate the oxidative stress and rescue the neuronal cell death in PD models. In present review, we summarized the reported natural molecules that displayed protective effects in PD. We also addressed the possible signal pathway through which natural molecules achieved their antioxidative effects and mitigate PD phenotypes. Hopefully it will pave the way to better recognize and utilize Chinese herbs for the treatment of PD.

Keywords: Parkinson's disease, dopaminergic neurons, oxidative stress, natural molecules, Chinese herb

OPEN ACCESS

Edited by:
Hi-Joon Park,
Kyung Hee University, South Korea

Reviewed by:
Yu Tang,
Central South University, China
Maria Shadrina,
Institute of Molecular Genetics (RAS), Russia

****Correspondence:***
Cheng-Wu Zhang
iamcwzhang@njtech.edu.cn
Lin Li
iamlli@njtech.edu.cn

Received: *25 December 2017*
Accepted: *26 July 2018*
Published: *28 August 2018*

Citation:
Ding Y, Xin C, Zhang C-W, Lim K-L, Zhang H, Fu Z, Li L and Huang W (2018) Natural Molecules From Chinese Herbs Protecting Against Parkinson's Disease via Anti-oxidative Stress. Front. Aging Neurosci. 10:246. doi: 10.3389/fnagi.2018.00246

INTRODUCTION

Parkinson's disease (PD) is a devastating neurodegenerative disorder characterized by progressive loss of DA neurons in the SNpc of the midbrain, affecting 1–3% of the elderly population over 60 years (De Lau and Breteler, 2006). Currently, PD remains incurable and exerts heavy socio-economic burden to the society (Whetten-Goldstein et al., 1997; Lindgren et al., 2005; Winter et al., 2010). Although the precise molecular events underlying the pathogenesis of PD remain to be elucidated, the etiology of PD is found to involve environmental factors as well as genetic predisposition (Thomas and Beal, 2007). Regardless of exogenous or endogenous factors, oxidative stress is thought to play a pivotal role in the pathogenesis of PD (Jenner, 2003; Przedborski, 2017).

Oxidative stress is caused by imbalance of pro-oxidants and anti-oxidants in the cells (Barnham et al., 2004). Major reactive oxygen species (ROS) are produced in the process of adenosine triphosphate (ATP) synthesis which occurs in the mitochondria (Shadel and Horvath, 2015). DA neurons need relatively high amount of ATP to synthesize and release dopamine (Mamelak, 2018).

Hence, more ROS are produced in DA neurons compared to other types of neurons. Additionally, mitochondria are believed to contribute to the generation of ROS as a result of the accumulation of mitochondrial DNA (mtDNA) mutations during the aging process (Gredilla et al., 2012). The accumulation of mtDNA mutations could decrease the capability of the electron transport chain (ETC), triggering decreased ATP production and increased ROS production (Cha et al., 2015). Rotenone, a selective inhibitor of complex I of mitochondrial respiratory chain, was been proved to cause mitochondrial dysfunction as well as ROS accumulation. Moreover, reduced level or activity of antioxidants such as superoxide dismutase (SOD), catalase (CAT), glutathione (GSH), and glutathione peroxidase (Gpx) is another contributor to the build-up of oxidative stress (Koppula et al., 2012). Mutation of mitochondria homeostasis-related genes, including parkin, DJ-1, PTEN-induced putative kinase 1 (PINK1), peroxisome proliferator-activated receptor gamma coactivator-1α (PGC-1α), and leucine-rich repeat kinase 2 (LRRK2) has also been reported to lead to familial PD (Finck and Kelly, 2006; Handschin and Spiegelman, 2006; Aquilano et al., 2008; Schapira, 2008). Taken together, compelling evidence implicates the involvement of ROS-related stress in the pathogenesis of PD.

Currently there is no effective treatment for PD. Although L-DOPA, as the substitute of dopamine, has been widely used in clinic, the poisonous and side effect over time limits its application. Chinese herbs, which have been used for thousands of years to treat various diseases in China, represent an alternative strategy given their higher efficacy and relatively modest side effects. In PD treatment, the reported effects of Chinese herbs including antioxidant, anti-inflammatory, free radicals-scavenging, anti-apoptosis, and chelating harmful metals (Fu et al., 2015). In this review, we will discuss the role of oxidative stress in PD pathogenesis, summarize the anti-ROS effects of natural molecules from Chinese herbs and its possible mechanisms, with the view to position Chinese herbs as an alternative or complementary approach in treating PD patients.

OXIDATIVE STRESS AND PD

Oxygen is the prerequisite for nearly all forms of living organisms, but it is the source of oxidative stress also (Uttara et al., 2009). Oxidative stress results from excessive ROS, which is the consequence of imbalance between pro-oxidant and anti-oxidant homeostasis. ROS mainly comprise hydrogen peroxide (H_2O_2), superoxide anions (O_2^-) and the highly reactive hydroxyl radicals ($OH^\bullet$). Normally, the generation and elimination of ROS is well coordinated to maintain the redox status. Once the balance broken, oxidative stress will be induced, and subsequently diseases such as PD might occur. The concept of ROS involving the PD pathogenesis has been supported by multiple evidences (**Figure 1**).

Aging, iron accumulations, mitochondrial dysfunction, dopamine metabolism, which are all the established PD causative factors, meanwhile render oxidative stress. For example, incidence of PD is increased with aging, especially in elders. This is in accordance with that aged neuronal cells show hypersensitive toward oxidative stress (Floyd and Carney, 1992). The surveillance of antioxidants was also found compromised with aging (Lepoivre et al., 1994; Schulz et al., 2000). Active iron metals involved in generation of ROS through Fenton reaction and iron accumulation was attributed to PD pathogenesis (Takahashi et al., 2001; Maynard et al., 2002). Metabolism of dopamine produced many reactive molecules hence DA neurons were particularly susceptible to oxidative stress (Segura-Aguilar et al., 2014). Dopamine was synthesized in the cytoplasm and immediately sequestered into monoaminergic vesicles (Herrera et al., 2017). If not secreted, dopamine could be auto-oxidized or deaminated by monoamine oxidase (MAO), during which several cytotoxic molecules, including dopamine–quinone species ($SQ^\bullet$), $OH^\bullet$, and H_2O_2 are generated (Graham, 1978; Maker et al., 1981). Notably, 1-methyl-4-phenyl-1,2,3,6-tetrahydropyridine (MPTP) is commonly used to induce oxidative stress-related Parkinsonism in animal models. The active metabolite of MPTP, MPP^+, was selectively taken up into dopaminergic terminals by the plasma-membrane dopamine transporter (DAT) (Choi et al., 2015). MPP^+ would block complex I activity of the mitochondrial respiratory chain and result in the oxidative stress (Del Zompo et al., 1992; Peter et al., 1994; Lotharius and O'Malley, 2000).

Mitochondrial dysfunction, resulting from various malgenic factors, has been implicated in ROS generation and oxidative stress in PD. mtDNA mutations contributed to mitochondrial dysfunction due to impaired capability of the ETC, triggering ROS production (Gredilla et al., 2012; Yan et al., 2013; Cha et al., 2015). ROS in turn resulted in the collapse of the mitochondrial membrane potential (MMP) and disruption of the mitochondrial respiratory chain complex I, which ultimately leaded to increased cytosolic concentrations of Ca^{2+} and mitochondrial cytochrome c that initiated apoptosis signaling pathways (Du et al., 2010). Mutation of genes involved in mitochondrial homeostasis was known to induce familial PD (Schapira, 2007). Parkin, an E3 ubiquitin ligase, was mitochondria key regulator of mitophagy (Narendra et al., 2008). Not surprisingly, Drosophila deficient in parkin, exhibited mitochondrial dysfunction and higher vulnerability to oxidative stress (Whitworth et al., 2005; Ng et al., 2012). Parkin knockout mice showed decreased amounts of several proteins involved in mitochondrial function and enhanced oxidative stress (Palacino et al., 2004). PINK1, together with Parkin, were tightly coordinated to the controlling of mitochondrial dynamics (Scarffe et al., 2014). PINK1 accumulates on the outer membrane of damaged mitochondria and recruits Parkin to the dysfunctional mitochondrion (Pickrell and Youle, 2015). It was showed that the lack of PINK1 resulted in the mitochondrial defects and loss of SNpc DA neurons, and these phenomena could be ameliorated by the enhanced expression of Parkin (Yang et al., 2006; Gautier et al., 2008). Many lines of evidence suggested that DJ-1, another gene reported to cause a familial early onset PD, functions as an antioxidant protein. DJ-1 bonded to subunits of mitochondrial complex I and regulates its activity (Hayashi et al., 2009). DJ-1 mutation promoted its accumulation in mitochondria and was implicated as a cellular monitor of oxidative stress

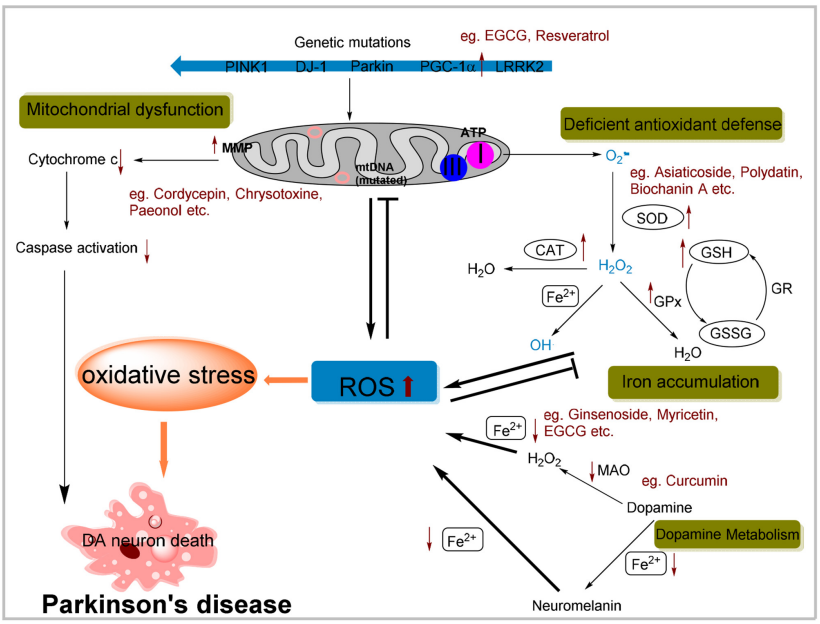

FIGURE 1 | Possible cellular mechanisms attributed to oxidative stress in Parkinson's disease (PD) and possible effects of natural antioxidants on specific pathway. Mitochondrial dysfunction by complex I inhibition and mtDNA mutation resulting in the ROS overproduction or mutation of genes involved in mitochondrial homeostasis can lead to an increased oxidative stress. ROS in turn results in the collapse of MMP and then initiates apoptosis signaling pathways contributing to DA neurons death. Also, the deficiency of antioxidant defense system may contribute to increased level of ROS. Additionally, dopamine metabolism can generate some active molecules contributing to ROS generation. Iron aggregation also enhances oxidative stress through the Fenton and Haber-Weiss reactions. In summary, all these cellular mechanisms due to the oxidative stress are implicated in the selective degeneration of dopaminergic neurons. Moreover, anti-oxidative effects of a portion of natural compounds mentioned above have been listed within specific pathway.

(Mitsumoto and Nakagawa, 2001; Bonifati et al., 2002). DJ-1 knockout mice displayed compromised mitochondrial function and then nigrostriatal DA neuron loss (Goldberg et al., 2005; Giaime et al., 2012). Furthermore, dysfunction of PGC-1α, the key transcriptional modulator of mitochondrial biogenesis and oxidative metabolism, was also implicated in PD (Arany et al., 2005; Lin et al., 2005). PGC-1α regulated the mitochondrial function and provides homeostatic control of cellular ATP (Rohas et al., 2007). It was revealed that inhibited expression of PGC-1α resulting from methylation of its gene contributed to the mitochondrial defects in substantia nigra of PD patients (Su et al., 2015). Dominant mutations in LRRK2 are currently recognized to be the most prevalent cause of late-onset familial PD (Kumari and Tan, 2009). Actually LRRK2 patient-derived cells exhibited altered mitochondrial dynamics that was accompanied by reduction in MMP and intracellular ATP levels (Mortiboys et al., 2010). Moreover, Drosophila with LRRK2 G2019S mutant induced marked mitochondrial pathological alternation both in flight muscles and DA neurons (Ng et al., 2012).

NATURAL ANTI-OXIDANT MOLECULES AND THEIR APPLICATIONS IN PD MODELS

Vast territory of China has brought about abundant natural resources. One precious natural resource is Chinese herb, which has been used throughout history to improve quality of human life. In recent years, traditional Chinese herbs attract more interests due to its impressive curative effect for a variety of diseases, coupled with lower toxicity and side effects (Fu et al., 2015). As mentioned above, oxidative stress damage is one of the most important characteristics of PD. Natural antioxidants, which are enriched in Chinese herbs, provide neuroprotective effects in PD through a variety of biological pathways (Obrenovich et al., 2010; Soobrattee et al., 2010). In this review, polyphenols, flavone (baicalein), flavonols (quercetin, kaempferol, morin, and myricetin), dihydroflavones (hesperetin and naringenin), isoflavone (biochanin A), and flavane (epigallocatechin gallate), and other non-flavonoids phenolic compounds (resveratrol, curcumin, and paeonol) from Chinese herbs against PD will be discussed. Moreover, the well-known glycoside derivatives [mangiferin, salidroside, asiaticoside, polydatin, gypenoside (GP), and ginsenoside], and other compounds (nerolidol, chrysotoxine, DL-3-n-butylphthalide, cordycepin, and ursolic acid) from natural resources with good antioxidant properties will also be addressed to discuss their possible mechanisms of against PD (**Table 1**).

Natural Molecules Modulating Mitochondrial Function

Mitochondrial dysfunction-induced oxidative stress is widely accepted to be the key driver of PD. Epigallocatechin gallate

TABLE 1 | Natural anti-oxidant molecules from Chinese herbs against PD.

Substances	Studied models *in vivo* or *in vitro*	Possible mechanisms	Reference
1. Modulate mitochondrial function			
Epigallocatechin gallate (EGCG)	MPP^+-treated PC12 cells	Up-regulates PGC-1α and improves mitochondrial function.	Ye et al., 2012
	Drosophila with mutant LRRK2 and null parkin	Attenuates mitochondrial-associated pathway in LRRK2 and parkin-related pathogenesis.	Ng et al., 2012
Resveratrol	Primary fibroblast from PD patients with PARK2 mutation	Raises the expression of PGC-1α's target genes (TFAM, cytochrome c and COX I).	Ferretta et al., 2014
Cordycepin	6-OHDA-induced PC12 cells	Maintains mitochondrial membrane potential (MMP) and reduce activation of caspase-3.	Olatunji et al., 2016
Baicalein	6-OHDA-induced SH-SY5Y cells	Attenuates mitochondrial dysfunction, oxidative injury, JNK and caspase activation.	Lee et al., 2005
Curcumin	MPP^+-induced PC12 cells	Mediates the toxicity of PC12 through Bcl-2-mitochondria-ROS-iNOS pathway.	Chen et al., 2006
Chrysotoxine	6-OHDA-induced SH-SY5Y cells	Attenuates the decrease of MMP, release of cytochrome c, imbalance of Bax/Bcl-2 ratio and activation of caspase-3.	Song et al., 2010
DL-3-n-butylphthalide (NBP)	MPP^+-induced PC12 cells	Retains mitochondrial function and suppresses ROS generation.	Huang et al., 2010
Mangiferin	Rotenone-induced SK-N-SH cells	Rectifies oxidative imbalance and protects mitochondrial function.	Kavitha et al., 2014
Morin	Excitotoxic neuron with NMDA receptor over-activation	Reduces ROS by restoring the MMP.	Campos-Esparza et al., 2009
Paeonol	MPP^+-induced mice	Restores MMP and reduces cytochrome c release and caspase-3 activity.	Lu et al., 2015
Ursolic acid	Parkin-mutant fibroblasts	Rescues mitochondrial function by the activation of the glucocorticoid receptor with increased phosphorylation of Akt.	Mortiboys et al., 2013
Salidroside	MPP^+-induced PC12 cells	Regulates the ratio of Bcl-2/Bax, decrease cytochrome c and Smac release, and inhibit caspase activation.	Wang S. et al., 2015
2. Activate intracellular antioxidants			
Asiaticoside	MPTP-induced rats	Attenuates the reduction of GSH level in the substantia nigra.	Xu et al., 2012
Polydatin	Rotenone-induced rats	Increases the level of GSH and manganese superoxide dismutases (MnSOD) in the striatum.	Chen Y. et al., 2015
Biochanin A	Lipopolysaccharide (LPS)-induced rat	Increases SOD and Gpx activities in the midbrain tissue.	Wang J. et al., 2015
	L-glutamate-treated PC12 cells	Increases total GSH activities.	Tan et al., 2012
Gypenosides (GP)	MPTP-induced mice	Attenuates the decrease of GSH content and SOD activities in the substantia nigra.	Wang et al., 2010
Mangiferin	MPP^+-induced N2A cells	Restores the GSH content and down-regulates both SOD1 and CAT mRNA expression.	Amazzal et al., 2007
Nerolidol	Rotenone-induced rats	Increases the level of SOD, CAT, and GSH in midbrain cells.	Javed et al., 2016
Quercetin	6-OHDA-induced rats	Restores the level of GSH in the striatum.	Haleagrahara et al., 2011
	H_2O_2-induced PC12 cells	Reduces CAT, SOD and Gpx level.	Chen L. et al., 2015
Kaempferol	MPTP-induced mice	Increases SOD and Gpx activities in the substantia nigra.	Żuk et al., 2011
Cordycepin	6-OHDA-induced PC12 cells	Increases SOD and Gpx activities.	Olatunji et al., 2016
Resveratrol	6-OHDA-induced rats	Up-regulates GPx, GR, CAT, and SOD activities.	Khan et al., 2010
Paeonol	MPTP-induced mice	Enhances the levels of SOD, CAT, and GSH.	Shi et al., 2016
Gastrodin	MPP^+-induced oxidative PD model	Increases antioxidant enzyme HO-1 expression.	Jiang et al., 2014
Hesperetin	6-OHDA-lesioned rats	Enhances striatal CAT and GSH content.	Kiasalari et al., 2016
3. Mediate metabolism of dopamine			
Curcumin	MPTP-induced rats	Inhibits MOA-B activity.	Rajeswari and Sabesan, 2008

(Continued)

TABLE 1 | Continued

Substances	Studied models *in vivo* or *in vitro*	Possible mechanisms	Reference
4. Decrease iron metal levels			
Curcumin	6-OHDA-induced rats	Chelates iron metals in the substantia nigra.	Du et al., 2012
Ginsenoside	6-OHDA-induced MES23.5 cells	Inhibits up-regulation of an iron importer protein DMT1 with iron IRE.	Xu et al., 2010
Myricetin	6-OHDA-induced rats	Prevents the increase of iron-staining cells in the substantia nigra.	Ma et al., 2007
EGCG	Iron-induced SH-SY5Y cells	Alleviates the iron accumulation through affecting IRE.	Reznichenko et al., 2006
Naringenin	Iron-induced rats	Chelates iron metals in the cerebral cortex.	Chtourou et al., 2014

(EGCG) is an important component of green tea and it has lots of biological effects, such as antioxidation, scavenging of free radicals and anti-apoptosis. In MPP^+-treated PC12 cells, EGCG caused up-regulation of PGC-1α, resulting in improved mitochondrial function and DA neuronal survival (Ye et al., 2012). In addition, EGCG was reported to act as a suppressor of mitochondrial dysfunction in both mutant LRRK2 and parkin-null flies through activation of the AMP-activated protein kinase (AMPK) signaling pathway (Ng et al., 2012). Resveratrol, a polyphenolic compound enriched in grapes, was shown to improve mitochondrial activity via affecting energy metabolic sensors through mediation of autophagy signals and activation of NAD-dependent deacetylase sirtuin-1 (SIRT1) and PGC-1α (Lagouge et al., 2006; Jeong et al., 2012). Resveratrol could also enhanced the mRNA level of a number of PGC-1α target genes such as mitochondrial transcription factor A (TFAM), cyclooxygenase-1 (COX I), resulting in mitochondrial biogenesis (Ferretta et al., 2014). Cordycepin, a nucleoside isolated from *Cordyceps* species displayed antioxidant property. Pretreatment of cordycepin helped to maintain MMP and reduced activation of caspase-3 in 6-OHDA induced PD model (Olatunji et al., 2016). The flavone baicalein, isolated from *Scutellaria baicalensis*, was reported to protect against 6-OHDA-induced neurotoxicity both *in vivo* and *in vitro* via confronting mitochondrial dysfunction, oxidative injury, JNK activation and caspase activation (Lee et al., 2005). Curcumin, the natural polyphenol compound derived from the curry spice turmeric, displayed neuroprotective effects on the MPTP induced PD cellular model through mediating Bcl-2-mitochondria-ROS-iNOS pathway (Chen et al., 2006). Chrysotoxine, a bioactive bibenzyl compounds isolated from medicinal *Dendrobium* species, was reported to be free radical scavengers (Zhang et al., 2007). Pretreatment with Chrysotoxine protected against 6-OHDA-induced intracellular generation of ROS and mitochondrial dysfunctions, including the decrease of MMP, increase of intracellular free Ca^{2+}, release of cytochrome c, and imbalance of Bax/Bcl-2 ratio (Song et al., 2010). DL-3-n-butylphthalide (NBP), derived from l-3-n-butylphthalidec extracted from the seeds of *Apium graveolens* Linn (Chinese celery), was found to be a natural free radical scavenger (Li et al., 2009). In a cellular PD model, pretreatment with NBP mitigated the toxicity of MPP^+ by retaining the mitochondrial function, and suppressing ROS generation (Huang et al., 2010). Two polyphenols, mangiferin and morin, specifically enriched in fruit, vegetables, plant extracts, wine, and tea, were reported to reduce the formation of ROS by restoring the MMP in excitotoxic induced cell model (Campos-Esparza et al., 2009; Kavitha et al., 2014). Paeonol, a major phenolic compound of the Chinese herb, *Cortex Moutan*, is known for its antioxidant, anti-inflammatory and antitumor properties. Paeonol has been shown to attenuate the intracellular ROS accumulation and associated mitochondrial cell death pathway including MMP disruption, cytochrome c release and caspase-3 activation in MPP^+-induced cellular PD model (Lu et al., 2015). From high throughput screening, the natural compound ursolic acid, a pentacyclic triterpenoid, was found to rescue mitochondrial function in parkin-mutant fibroblasts via the activation of the glucocorticoid receptor that is associated with increased phosphorylation of Akt (Mortiboys et al., 2013). Salidroside (Sal), a phenylpropanoid glycoside isolated from *Rhodiola rosea L.*, had potent antioxidant properties. Sal pretreatment protected DA neurons against MPP^+-induced toxicity by reducing the production of ROS or NO, regulating the ratio of Bcl-2/Bax, decreasing cytochrome c and Smac release, and inhibiting caspase activation (Wang J. et al., 2015).

Natural Molecules Regulating Endogenous Antioxidants and Dopamine Metabolism

Cells have endogenous defense mechanisms against oxidative stress, including enzymatic and non-enzymatic systems (Gilgun-Sherki et al., 2001). The capacity of antioxidant defenses declined with aging and in pathological state (Sohal and Weindruch, 1996; Lotharius et al., 2002). It was reported that polyphenols could modulate the activity of enzymes involved in oxidative stress (Ebrahimi and Schluesener, 2012). Xu et al. (2012) showed that asiaticoside, a triterpenoid saponin isolated from *Centella asiatica* attenuated the MPTP-induced the reduction of GSH in a rat model of Parkinsonism. Polydatin, a glycosylated derivative of resveratrol, significantly prevented the rotenone-induced decreased levels of GSH and the manganese superoxide dismutases (MnSOD) in the striatum of rodent models of PD (Chen Y. et al., 2015). Biochanin A, an *O*-methylated isoflavone found in chickpea, increased SOD and Gpx activities in lipopolysaccharide (LPS) induced rat PD model (Wang J. et al., 2015). Another research group reported that pretreatment with biochanin A could lead to the increase in the total GSH level in the L-glutamate-treated PC12 cells (Tan et al., 2012). Treatment

with GPs, saponins extracted from *Gynostemma pentaphyllum*, attenuated MPTP-induced decrease of GSH and reduced SOD activity in the SNpc of the mice (Wang et al., 2010). Pretreatment with mangiferin protected N2A cells against MPP^+-induced cytotoxicity, restored the GSH, and down-regulated both SOD1 and CAT mRNA expression (Amazzal et al., 2007). Nerolidol, a sesquiterpene alcohol, significantly increased the level of SOD, CAT, and GSH in a rotenone-induced PD experimental model (Javed et al., 2016). Quercetin, enriched in abundance in fruits and vegetables, onions, red wine and olive oil, restored level of GSH in the striatum of rats induced by 6-OHDA (Miean and Mohamed, 2001; Haleagrahara et al., 2011). In H_2O_2-induced PC12 cells, pretreatment with quercetin markedly reduced the antioxidant enzyme SOD and Gpx level (Chen L. et al., 2015). Kaempferol, a prototype flavonol presented in tea, broccoli, grapefruit, brussel sprouts and apple, was reported to have strong antioxidant and anti-inflammatory properties, and enhanced SOD and Gpx activity in the mouse model of PD (Żuk et al., 2011; Li and Pu, 2011). Cordycepin, resveratrol, hesperetin rendered up-regulation of the level and activity of antioxidants such as, SOD, GPx, CAT, GSH in 6-OHDA induced PD models (Khan et al., 2010; Kiasalari et al., 2016; Olatunji et al., 2016). Treatment with paeonol improved the MPTP-induced the oxidative stress, as determined by enhancing the activity levels of SOD, CAT, and GSH in the mouse PD model (Shi et al., 2016). Gastrodin, the major active component in the *Gastrodia elata*, has been demonstrated to have many pharmacological effects, such as antioxidative and neuroprotective properties. In MPP^+-induced oxidative cellular PD model, pretreatment with gastrodin increased antioxidant enzyme heme oxygenase-1 (HO-1) expression (Jiang et al., 2014) and activation of HO-1 resulted in increased levels of antioxidant substrates such as biliverdin, bilirubin, and ferritin (Doré et al., 1999). Curcumin and its metabolite tetrahydrocurcumin (ThC) exerted neuroprotection against MPTP induced neurotoxicity via inhibiting MAO-B activity (Rajeswari and Sabesan, 2008).

Natural Molecules Chelating Metal Iron

Iron, which accumulated in the aging brain especially the SNpc, is thought to promote PD pathogenesis (Devos et al., 2014). Iron enhances ROS generation through the Fenton and Haber-Weiss reactions (Barnham et al., 2004). Curcumin pretreatment reversed iron-induced degeneration of nigral DA neurons by its iron chelating activity (Du et al., 2012). Ginsenoside, the active component isolated from ginseng, was reported to decrease the 6-OHDA-induced iron influx by inhibiting up-regulation of an iron importer protein divalent metal transporter 1 with iron responsive element (DMT1+IRE), which was rendered via its antioxidant effect (Xu et al., 2010). Myricetin, a natural flavonoid found in fruits, vegetables, and herbs (Kang et al., 2010), was reported to suppress iron induced toxicity in the 6-OHDA induced PD model (Ma et al., 2007). EGCG served as iron chelator inhibiting the formation of transition metal catalyzed free radicals and displaying its antioxidant and neuroprotective effects (Weinreb et al., 2009; Singh et al., 2016). EGCG could also alleviate the iron accumulation in PD through affecting the iron responsive element (Reznichenko et al., 2006). Administration of naringenin (NGEN), a natural flavonoid compound, attenuated oxidative damages in the cerebral cortex of iron treatment induced PD model, due to its iron chelating activity (Chtourou et al., 2014).

CONCLUSION AND PERSPECTIVES

In recent years, given the limitations of current PD treatment, more attention has been given to the potential therapeutic effects of Chinese herbs (Song et al., 2012). In this review, we summarized natural antioxidants from Chinese herbs that were reported to protect against toxins-induced PD in preclinical animal models. These natural antioxidants achieve their protective effects mainly through regulating cellular oxidative homeostasis either directly or indirectly. Of them, resveratrol and EGCG, showed prominent antioxidative effect in PD models and could be a promising candidate for treating PD. Notwithstanding that, there are several challenges to overcome before natural molecules from Chinese Herbs could serve as alternative medicine for PD. How to efficiently screen and select the candidates that can be used for treatment of PD from the massive number of Chinese herbs available? What are the intracellular targets of the natural molecules? How to help the molecules pass through the blood–brain barrier (BBB) in order to directly protect the DA neurons in the SNpc? Clearly, it is promising but a lot of work needs to be done to ultimately achieve the goals of making natural molecules to be accepted and applied in PD patient treatment.

AUTHOR CONTRIBUTIONS

YD prepared the manuscript. CX, HZ, ZF, and WH provided help in the manuscript preparation. CW-Z, LL, and K-LL did the revision.

FUNDING

This work was financially supported by the National Natural Science Foundation of China (81672508 and 61505076), Jiangsu Provincial Foundation for Distinguished Young Scholars (BK20170041), Key University Science Research Project of Jiangsu Province (Grant 16KJA180004), and China-Sweden Joint Mobility Project (51661145021).

REFERENCES

Amazzal, L., Lapôtre, A., Quignon, F., and Bagrel, D. (2007). Mangiferin protects against 1-methyl-4-phenylpyridinium toxicity mediated by oxidative stress in N2A cells. *Neurosci. Lett.* 418, 159–164. doi: 10.1016/j.neulet.2007.03.025

Aquilano, K., Baldelli, S., Rotilio, G., and Ciriolo, M. R. (2008). Role of nitric oxide synthases in Parkinson's disease: a review on the antioxidant and

anti-inflammatory activity of polyphenols. *Neurochem. Res.* 33, 2416–2426. doi: 10.1007/s11064-008-9697-6

Arany, Z., He, H., Lin, J., Hoyer, K., Handschin, C., Toka, O., et al. (2005). Transcriptional coactivator PGC-1 alpha controls the energy state and contractile function of cardiac muscle. *Cell Metab.* 1, 259–271. doi: 10.1016/j.cmet.2005.03.002

Barnham, K. J., Masters, C. L., and Bush, A. I. (2004). Neurodegenerative diseases and oxidative stress. *Nat. Rev. Drug Discov.* 3, 205–214. doi: 10.1038/nrd1330

Bonifati, V., Rizzu, P., van, Baren MJ, Schaap, O., Breedveld, G. J., Krieger, E., et al. (2002). Mutations in the DJ-1 gene associated with autosomal recessive early-onset parkinsonism. *Science* 299, 256–259. doi: 10.1126/science.1077209

Campos-Esparza, M. R., Sánchez-Gómez, M. V., and Matute, C. (2009). Molecular mechanisms of neuroprotection by two natural antioxidant polyphenols. *Cell Calcium* 45, 358–368. doi: 10.1016/j.ceca.2008.12.007

Cha, M. Y., Kim, D. K., and Mook-Jung, I. (2015). The role of mitochondrial DNA mutation on neurodegenerative diseases. *Exp. Mol. Med.* 47:e150. doi: 10.1038/emm.2014.122

Chen, J., Tang, X. Q., Zhi, J. L., Cui, Y., Yu, H. M., Tang, E. H., et al. (2006). Curcumin protects PC12 cells against 1-methyl-4-phenylpyridinium ion-induced apoptosis by bcl-2-mitochondria-ROS-iNOS pathway. *Apoptosis* 11, 943–953. doi: 10.1007/s10495-006-6715-5

Chen, L., Sun, L., Liu, Z., Wang, H., and Xu, C. (2015). Protection afforded by quercetin against H2O2-induced apoptosis on PC12 cells via activating PI3K/Akt signal pathway. *J. Recept. Signal Transduct. Res.* 36, 98–102. doi: 10.3109/10799893.2015.1049363

Chen, Y., Zhang, D. Q., Liao, Z., Wang, B., Gong, S., Wang, C., et al. (2015). Anti-oxidant polydatin (piceid) protects against substantia nigral motor degeneration in multiple rodent models of Parkinson's disease. *Mol. Neurodegener.* 10:4. doi: 10.1186/1750-1326-10-4

Choi, S. J., Panhelainen, A., Schmitz, Y., Larsen, K. E., Kanter, E., Wu, M., et al. (2015). Changes in neuronal dopamine homeostasis following 1-methyl-4-phenylpyridinium (MPP^+) exposure. *J. Biol. Chem.* 290, 6799–6809. doi: 10.1074/jbc.M114.631556

Chtourou, Y., Fetoui, H., and Gdoura, R. (2014). Protective effects of naringenin on iron-overload-induced cerebral cortex neurotoxicity correlated with oxidative Stress. *Biol. Trace Elem. Res.* 158, 376–383. doi: 10.1007/s12011-014-9948-0

De Lau, L. M., and Breteler, M. M. (2006). Epidemiology of Parkinson's disease. *Lancet Neurol.* 5, 525–535. doi: 10.1016/S1474-4422(06)70471-9

Del Zompo, M., Piccardi, M. P., Ruiu, S., Corsini, G. U., and Vaccari, A. (1992). Characterization of a putatively vesicular binding site for [3H]MPP^+ in mouse striatal membranes. *Brain Res.* 571, 354–357. doi: 10.1016/0006-8993(92)90677-2

Devos, D., Moreau, C., Devedjian, J. C., Kluza, J., Petrault, M., Laloux, C., et al. (2014). Targeting chelatable iron as a therapeutic modality in Parkinson's disease. *Antioxid. Redox Signal.* 2, 195–210. doi: 10.1089/ars.2013.5593

Doré, S., Takahashi, M., Ferris, C. D., Zakhary, R., Hester, L. D., Guastella, D., et al. (1999). Bilirubin, formed by activation of heme oxygenase-2, protects neurons against oxidative stress injury. *Proc. Natl. Acad. Sci. U.S.A.* 96, 2445–2450. doi: 10.1073/pnas.96.5.2445

Du, T., Li, L., Song, N., Xie, J., and Jiang, H. (2010). Rosmarinic acid antagonized 1-Methyl-4-phenylpyridinium(MPP^+)-induced neurotoxicity in MES23.5 dopaminergic cells. *Int. J. Toxicol.* 29, 625–633. doi: 10.1177/1091581810383705

Du, X. X., Xu, H. M., Jiang, H., Song, N., Wang, J., and Xie, J. X. (2012). Curcumin protects nigral dopaminergic neurons by iron-chelation in the 6-hydroxydopamine rat model of Parkinson's disease. *Neurosci. Bull.* 28, 253–258. doi: 10.1007/s12264-012-1238-2

Ebrahimi, A., and Schluesener, H. (2012). Natural polyphenols against neurodegenerative disorders: potentials and pitfalls. *Ageing Res. Rev.* 11, 329–345. doi: 10.1016/j.arr.2012.01.006

Ferretta, A., Gaballo, A., Tanzarella, P., Piccoli, C., Capitanio, N., Nico, B., et al. (2014). Effect of resveratrol on mitochondrial function: implications inparkin-associated familiar Parkinson's disease. *Biochim. Biophys. Acta* 1842, 902–915. doi: 10.1016/j.bbadis.2014.02.010

Finck, B. N., and Kelly, D. P. (2006). PGC-1 coactivators: inducible regulators of energy metabolism in health and disease. *J. Clin. Invest.* 116, 615–622. doi: 10.1172/JCI27794

Floyd, R. A., and Carney, J. M. (1992). Free radical damage to protein and DNA: mechanisms involved and relevant observations on brain undergoing oxidative stress. *Ann. Neurol.* 32, 22–27. doi: 10.1002/ana.410320706

Fu, W., Zhuang, W., Zhou, S., and Wang, X. (2015). Plant-derived neuroprotective agents in Parkinson's disease. *Am. J. Transl. Res.* 7, 1189–1202.

Gautier, C. A., Kitada, T., and Shen, J. (2008). Loss of PINK1 causes mitochondrial functional defects and increased sensitivity to oxidative stress. *Proc. Natl. Acad. Sci. U.S.A.* 105, 11364–11369. doi: 10.1073/pnas.0802076105

Giaime, E., Yamaguchi, H., Gautier, C. A., Kitada, T., and Shen, J. (2012). Loss of DJ-1 does not affect mitochondrial respiration but increases ROS production and mitochondrial permeability transition pore opening. *PLoS One* 7:e40501. doi: 10.1371/journal.pone.0040501

Gilgun-Sherki, Y., Melamed, E., and Offen, D. (2001). Oxidative stress induced-neurodegenerative diseases: the need for antioxidants that penetrate the blood brain barrier. *Neuropharmacology* 40, 959–975. doi: 10.1016/S0028-3908(01)00019-3

Goldberg, M. S., Pisani, A., Haburcak, M., Vortherms, T. A., Kitada, T., Costa, C., et al. (2005). Nigrostriatal dopaminergic deficits and hypokinesia caused by inactivation of the familial Parkinsonism-linked gene DJ-1. *Neuron* 45, 489–496. doi: 10.1016/j.neuron.2005.01.041

Graham, D. G. (1978). Oxidative pathways for catecholamines in the genesis of neuromelanin and cytotoxic quinones. *Mol. Pharmacol.* 14, 633–643.

Gredilla, R., Weissman, L., Yang, J. L., Bohr, V. A., and Stevnsner, T. (2012). Mitochondrial base excision repair in mouse synaptosomes during normal aging and in a model of Alzheimer's disease. *Neurobiol. Aging* 33, 694–707. doi: 10.1016/j.neurobiolaging.2010.06.019

Haleagrahara, N., Siew, C. J., Mitra, N. K., and Kumari, M. (2011). Neuroprotective effect of bioflavonoid quercetin in 6-hydroxydopamine-induced oxidative stress biomarkers in the rat striatum. *Neurosci. Lett.* 500, 139–143. doi: 10.1016/j.neulet.2011.06.021

Handschin, C., and Spiegelman, B. M. (2006). Peroxisome proliferator-activated receptor γ coactivator 1 coactivators, energy homeostasis, and metabolism. *Endocr. Rev.* 27, 728–735. doi: 10.1210/er.2006-0037

Hayashi, T., Ishimori, C., Takahashi-Niki, K., Taira, T., Kim, Y., Maita, H., et al. (2009). DJ-1 binds to mitochondrial complex I and maintains its activity. *Biochem. Biophys. Res. Commun.* 390, 667–672. doi: 10.1016/j.bbrc.2009.10.025

Herrera, A., Muñoz, P., Steinbusch, H. W. M., and Segura-Aguilar, J. (2017). Are dopamine oxidation metabolites involved in the loss of dopaminergic neurons in the nigrostriatal system in Parkinson's disease? *ACS Chem. Neurosci.* 8, 702–711. doi: 10.1021/acschemneuro.7b00034

Huang, J. Z., Chen, Y. Z., Su, M., Zheng, H. F., Yang, Y. P., Chen, J., et al. (2010). DL-3-n-butylphthalide prevents oxidative damage and reduces mitochondrial dysfunction in an MPP^+-induced cellular model of Parkinson's disease. *Neurosci. Lett.* 475, 89–94. doi: 10.1016/j.neulet.2010.03.053

Javed, H., Azimullah, S., AbulKhair, S. B., Ojha, S., and Haque, M. E. (2016). Neuroprotective effect of nerolidol against neuroinflammation and oxidative stress induced by rotenone. *BMC Neurosci.* 17:58. doi: 10.1186/s12868-016-0293-4

Jenner, P. (2003). Oxidative stress in Parkinson's disease. *Ann. Neurol.* 53, 26–38. doi: 10.1002/ana.10483

Jeong, J. K., Moon, M. H., Bae, B. C., Lee, Y. J., Seol, J. W., Kang, H. S., et al. (2012). Autophagy induced by resveratrol prevents human prion protein-mediated neurotoxicity. *Neurosci. Res.* 73, 99–105. doi: 10.1016/j.neures.2012.03.005

Jiang, G., Hu, Y., Liu, L., Cai, J., Peng, C., and Li, Q. (2014). Gastrodin protects against MPP^+ -induced oxidative stress by up regulates heme oxygenase-1 expression through p38 MAPK/Nrf2 pathway in human dopaminergic cells. *Neurochem. Int.* 75, 79–88. doi: 10.1016/j.neuint.2014.06.003

Kang, K. A., Wang, Z. H., Zhang, R., Piao, M. J., Kim, K. C., Kang, S., et al. (2010). Myricetin protects cells against oxidative stress-induced apoptosis via regulation of PI3K/Akt and MAPK signaling pathways. *Int. J. Mol. Sci.* 11, 4348–4360. doi: 10.3390/ijms11114348

Kavitha, M., Manivasagam, T., Essa, M. M., Tamilselvam, K., Selvakumar, G. P., Karthikeyan, S., et al. (2014). Mangiferin antagonizes rotenone: induced apoptosis through attenuating mitochondrial dysfunction and oxidative stress in SK-N-SH neuroblastoma cells. *Neurochem. Res.* 39, 668–676. doi: 10.1007/s11064-014-1249-7

Khan, M. M., Ahmad, A., Ishrat, T., Khan, M. B., Hoda, M. N., Khuwaja, G., et al. (2010). Resveratrol attenuates 6-hydroxydopamine-induced oxidative damage

and dopamine depletion in rat model of Parkinson's disease. *Brain Res.* 1328, 139–151. doi: 10.1016/j.brainres.2010.02.031

Kiasalari, Z., Khalili, M., Baluchnejadmojarad, T., and Roghani, M. (2016). Protective effect of oral hesperetin against unilateral striatal 6-hydroxydopamine damage in the rat. *Neurochem. Res.* 41, 1065–1072. doi: 10.1007/s11064-015-1796-6

Koppula, S., Kumar, H., More, S. V., Lim, H. W., Hong, S. M., and Choi, D. K. (2012). Recent updates in redox regulation and free radical scavenging effects by herbal products in experimental models of Parkinson's disease. *Molecules* 17, 11391–11420. doi: 10.3390/molecules171011391

Kumari, U., and Tan, E. K. (2009). LRRK2 in Parkinson's disease: genetic and clinical studies from patients. *FEBS J.* 276, 6455–6463. doi: 10.1111/j.1742-4658.2009.07344.x

Lagouge, M., Argmann, C., Gerhart-Hines, Z., Meziane, H., Lerin, C., Daussin, F., et al. (2006). Resveratrol improves mitochondrial function and protects against metabolic disease by activating SIRT1 and PGC-1α. *Cell* 127, 1109–1122. doi: 10.1016/j.cell.2006.11.013

Lee, H. J., Noh, Y. H., Lee, D. Y., Kim, Y. S., Kim, K. Y., Chung, Y., et al. (2005). Baicalein attenuates 6-hydroxydopamine-induced neurotoxicity in SH-SY5Y cells. *Eur. J. Cell. Biol.* 84, 897–905. doi: 10.1016/j.ejcb.2005.07.003

Lepoivre, M., Flaman, J. M., Bobé, P., Lemaire, G., and Henry, Y. (1994). Quenching of the tyrosyl free radical of ribonucleotide reductase by nitric oxide. Relationship to cytostasis induced in tumor cells by cytotoxic macrophages. *J. Biol. Chem.* 269, 21891–21897.

Li, L., Zhang, B., Tao, Y., Wang, Y., Wei, H., Zhao, J., et al. (2009). DL-3-n-butylphthalide protects endothelial cells against oxidative/nitrosative stress, mitochondrial damage and subsequent cell death after oxygen glucose deprivation in vitro. *Brain Res.* 1290, 91–101. doi: 10.1016/j.brainres.2009.07.020

Li, S., and Pu, X. P. (2011). Neuroprotective effect of kaempferol against a 1-methyl-4-phenyl-1,2,3,6- tetrahydropyridine-induced mouse model of Parkinson's disease. *Biol. Pharm. Bull.* 34, 1291–1296. doi: 10.1248/bpb.34.1291

Lin, J., Handschin, C., and Spiegelman, B. M. (2005). Metabolic control through the PGC-1 family of transcription coactivators. *Cell Metab.* 1, 361–370. doi: 10.1016/j.cmet.2005.05.004

Lindgren, P., Von Campenhausen, S., Spottke, E., Siebert, U., and Dodel, R. (2005). Cost of Parkinson's disease in Europe. *Eur. J. Neurol.* 12, 68–73. doi: 10.1111/j.1468-1331.2005.01197.x

Lotharius, J., Barg, S., Wiekop, P., Lundberg, C., Raymon, H. K., and Brundin, P. (2002). Effect of mutant α-synuclein on dopamine homeostasis in a new human mesencephalic cell line. *J. Biol. Chem.* 277, 38884–38894. doi: 10.1074/jbc.M205518200

Lotharius, J., and O'Malley, K. L. (2000). The Parkinsonism-inducing drug 1-Methyl-4-phenylpyridinium triggers intracellular dopamine oxidation. *J. Biol. Chem.* 275, 38581–38588. doi: 10.1074/jbc.M005385200

Lu, X. L., Lin, Y. H., Wu, Q., Su, F. J., Ye, C. H., Shi, L., et al. (2015). Paeonolum protects against MPP^+-induced neurotoxicity in zebrafish and PC12 cells. *BMC Complement. Altern. Med.* 15:137. doi: 10.1186/s12906-015-0661-0

Ma, Z. G., Wang, J., Jiang, H., Liu, T. W., and Xie, J. X. (2007). Myricetin reduces 6-hydroxydopamine-induced dopamine neuron degeneration in rats. *Neuroreport* 18, 1181–1185. doi: 10.1097/WNR.0b013e32821c51fe

Maker, H. S., Weiss, C., Silides, D. J., and Cohen, G. (1981). Coupling of dopamine oxidation (monoamine oxidase activity) to glutathione oxidation via the generation of hydrogen peroxide in rat brain homogenates. *J. Neurochem.* 36, 589–593. doi: 10.1111/j.1471-4159.1981.tb01631.x

Mamelak, M. (2018). Parkinson's disease, the dopaminergic neuron and gammahydroxybutyrate. *Neurol. Ther.* 7, 5–11. doi: 10.1007/s40120-018-0091-2

Maynard, C. J., Cappai, R., Volitakis, I., Cherny, R. A., White, A. R., Beyreuther, K., et al. (2002). Overexpression of Alzheimer's disease amyloid- β opposes the age-dependent elevations of brain copper and iron. *J. Biol. Chem.* 277, 44670–44676. doi: 10.1074/jbc.M204379200

Miean, K. H., and Mohamed, S. (2001). Flavonoid (myricetin, quercetin, kaempferol, luteolin, and apigenin) content of edible tropical plants. *J. Agric. Food Chem.* 49, 3106–3112. doi: 10.1021/jf000892m

Mitsumoto, A., and Nakagawa, Y. (2001). DJ-1 is an indicator for endogenous reactive oxygen species elicited by endotoxin. *Free Radic. Res.* 35, 885–893. doi: 10.1080/10715760100301381

Mortiboys, H., Aasly, J., and Bandmann, O. (2013). Ursocholanic acid rescues mitochondrial function in common forms of familial Parkinson's disease. *Brain* 136, 3038–3050. doi: 10.1093/brain/awt224

Mortiboys, H., Johansen, K. K., Aasly, J. O., and Bandmann, O. (2010). Mitochondrial impairment inpatients with Parkinson disease with the G2019S mutation in LRRK2. *Neurology* 75, 2017–2020. doi: 10.1212/WNL.0b013e3181ff9685

Narendra, D., Tanaka, A., Suen, D. F., and Youle, R. J. (2008). Parkin is recruited selectively to impaired mitochondria and promotes their autophagy. *J. Cell. Biol.* 183, 795–803. doi: 10.1083/jcb.200809125

Ng, C. H., Guan, M. S., Koh, C., Ouyang, X., Yu, F., Tan, E. K., et al. (2012). AMP kinase activation mitigates dopaminergic dysfunction and mitochondrial abnormalities in drosophila models of Parkinson's disease. *J. Neurosci.* 32, 14311–14317. doi: 10.1523/Jneurosci.0499-12.2012

Obrenovich, M. E., Nair, N. G., Beyaz, A., Aliev, G., and Reddy, V. P. (2010). The role of polyphenolic antioxidants in health, disease, and aging. *Rejuvenation Res.* 13, 631–643. doi: 10.1089/rej.2010.1043

Olatunji, O. J., Feng, Y., Olatunji, O. O., Tang, J., Ouyang, Z., and Su, Z. (2016). Cordycepin protects PC12 cells against 6-hydroxydopamine induced neurotoxicity via its antioxidant properties. *Biomed. Pharmacother.* 81, 7–14. doi: 10.1016/j.biopha.2016.03.009

Palacino, J. J., Sagi, D., Goldberg, M. S., Krauss, S., Motz, C., Wacker, M., et al. (2004). Mitochondrial dysfunction and oxidative damage in parkin-deficient mice. *J. Biol. Chem.* 279, 18614–18622. doi: 10.1074/jbc.M401135200

Peter, D., Jimenez, J., Liu, Y., Kim, J., and Edwards, R. H. (1994). The chromaffin granule and synaptic vesicle amine transporters differ in substrate recognition and sensitivity to inhibitors. *J. Biol. Chem.* 269, 7231–7237.

Pickrell, A. M., and Youle, R. J. (2015). The roles of PINK1, parkin, and mitochondrial fidelity in Parkinson's disease. *Neuron* 85, 257–273. doi: 10.1016/j.neuron.2014.12.007

Przedborski, S. (2017). The two-centry journey of Parkinson disease research. *Nat. Rev. Neurosci.* 18, 251–259. doi: 10.1038/nrn.2017.25

Rajeswari, A., and Sabesan, M. (2008). Inhibition of monoamine oxidase-B by the polyphenolic compound, curcumin and its metabolite tetrahydrocurcumin in a model of Parkinson's disease induced by MPTP neurodegeneration in mice. *Inflammopharmacology* 16, 96–99. doi: 10.1007/s10787-007-1614-0

Reznichenko, L., Amit, T., Zheng, H., Avramovich-Tirosh, Y., Youdim, M. B., Weinreb, O., et al. (2006). Reduction of iron-regulated amyloid precursor protein and β-amyloid peptide by (-)-epigallocatechin-3-gallate in cell cultures: implications for iron chelation in Alzheimer's disease. *J. Neurochem.* 97, 527–536. doi: 10.1111/j.1471-4159.2006.03770.x

Rohas, L. M., St-Pierre, J., Uldry, M., Jäger, S., Handschin, C., and Spiegelman, B. M. (2007). A fundamental system of cellular energy homeostasis regulated by PGC-1alpha. *Proc. Natl. Acad. Sci. U.S.A.* 104, 7933–7938. doi: 10.1073/pnas.0702683104

Scarffe, L. A., Stevens, D. A., Dawson, V. L., and Dawson, T. M. (2014). Parkin and PINK1: much more than mitophagy. *Trends Neurosci.* 37, 315–324. doi: 10.1016/j.tins.2014.03.004

Schapira, A. H. (2007). Mitochondrial dysfunction in Parkinson's disease. *Cell Death Differ.* 14, 1261–1266. doi: 10.1038/sj.cdd.4402160

Schapira, A. H. (2008). Mitochondria in the aetiology and pathogenesis of Parkinson's disease. *Lancet Neurol.* 7, 97–109. doi: 10.1016/S1474-4422(07)70327-7

Schulz, J. B., Lindenau, J., Seyfried, J., and Dichgans, J. (2000). Glutathione, oxidative stress and neurodegeneration. *Eur. J. Biochem.* 267, 4904–4911. doi: 10.1046/j.1432-1327.2000.01595.x

Segura-Aguilar, J., Paris, I., Muñoz, P., Ferrari, E., Zecca, L., and Zucca, F. A. (2014). Protective and toxic roles of dopamine in Parkinson's disease. *J. Neurochem.* 129, 898–915. doi: 10.1111/jnc.12686

Shadel, G. S., and Horvath, T. L. (2015). Mitochondrial ROS signaling in organismal homeostasis. *Cell* 163, 560–569. doi: 10.1016/j.cell.2015.10.001

Shi, X., Chen, Y. H., Liu, H., and Qu, H. D. (2016). Therapeutic effects of paeonol on methyl-4-phenyl-1,2,3,6-tetrahydropyridine/probenecid-induced Parkinson's disease in mice. *Mol. Med. Rep.* 14, 2397–2404. doi: 10.3892/mmr.2016.5573

Singh, N. A., Mandal, A. K., and Khan, Z. A. (2016). Potential neuroprotective properties of epigallocatechin-3-gallate (EGCG). *Nutr. J.* 15:60. doi: 10.1186/s12937-016-0179-4

Sohal, R. S., and Weindruch, R. (1996). Oxidative stress, caloric restriction, and aging. *Science* 273, 59–63. doi: 10.1126/science.273.5271.59

Song, J. X., Shaw, P. C., Sze, C. W., Tong, Y., Yao, X. S., Ng, T. B., et al. (2010). Chrysotoxine, a novel bibenzyl compound, inhibits 6-hydroxydopamine induced apoptosis in SH-SY5Y cells via mitochondria protection and NF-kB modulation. *Neurochem. Int.* 57, 676–689. doi: 10.1016/j.neuint.2010.08.007

Song, J. X., Sze, S. C., Ng, T. B., Lee, C. K., Leung, G. P., Shaw, P. C., et al. (2012). Anti-Parkinsonian drug discovery from herbal medicines: what have we got from neurotoxic models. *J. Ethnopharmacol.* 139, 698–711. doi: 10.1016/j.jep.2011.12.030

Soobrattee, M. A., Bahorun, T., and Aruoma, O. I. (2010). Chemopreventive actions of polyphenolic compounds in cancer. *Biofactors* 27, 19–35. doi: 10.1002/biof.5520270103

Su, X., Chu, Y., Kordower, J. H., Li, B., Cao, H., Huang, L., et al. (2015). PGC-1α promoter methylation in Parkinson's disease. *PLoS One* 8:e0134087. doi: 10.1371/journal.pone.0134087

Takahashi, S., Takahashi, I., Sato, H., Kubota, Y., Yoshida, S., and Muramatsu, Y. (2001). Age-related changes in the concentrations of major and trace elements in the brain of rats and mice. *Biol. Trace Elem. Res.* 80, 145–158. doi: 10.1385/BTER:80:2:145

Tan, J. W., Tham, C. L., Israf, D. A., Lee, S. H., and Kim, M. K. (2012). Neuroprotective effects of biochanin A against glutamate-induced cytotoxicity in PC12 cells via apoptosis inhibition. *Neurochem. Res.* 38, 512–518. doi: 10.1007/s11064-012-0943-6

Thomas, B., and Beal, M. F. (2007). Parkinson's disease. *Hum. Mol. Genet.* 16, 183–194. doi: 10.1093/hmg/ddm159

Uttara, B., Singh, A. V., Zamboni, P., and Mahajan, R. T. (2009). Oxidative stress and neurodegenerative diseases: A review of upstream and downstream antioxidant therapeutic options. *Curr. Neuropharmacol.* 7, 65–74. doi: 10.2174/157015909787602823

Wang, J., He, C., Wu, W. Y., Chen, F., Wu, Y. Y., Li, W. Z., et al. (2015). Biochanin A protects dopaminergic neurons against lipopolysaccharide-induced damage and oxidative stress in a rat model of Parkinson's disease. *Pharmacol. Biochem. Behav.* 138, 96–103. doi: 10.1016/j.pbb.2015.09.013

Wang, P., Niu, L., Gao, L., Li, W. X., Jia, D., Wang, X. L., et al. (2010). Neuroprotective effect of gypenosides against oxidative injury in the substantia nigra of a mouse model of Parkinson's disease. *J. Int. Med. Res.* 38, 1084–1092. doi: 10.1177/147323001003800336

Wang, S., He, H., Chen, L., Zhang, W., Zhang, X., and Chen, J. (2015). Protective effects of salidroside in the MPTP/MPP$^+$-induced model of Parkinson's disease through ROS–NO-Related mitochondrion pathway. *Mol. Neurobiol.* 51, 718–728. doi: 10.1007/s12035-014-8755-0

Weinreb, O., Amit, T., Mandel, S., and Youdim, M. B. (2009). Neuroprotective molecular mechanisms of (2)-epigallocatechin- 3-gallate: a reflective outcome of its antioxidant, iron chelating and neuritogenic properties. *Genes Nutr.* 4, 283–296. doi: 10.1007/s12263-009-0143-4

Whetten-Goldstein, K., Sloan, F., Kulas, E., Cutson, T., and Schenkman, M. (1997). The burden of Parkinson's disease on society, family, and the individual. *J. Am Geriatr. Soc.* 45, 844–849. doi: 10.1111/j.1532-5415.1997.tb01512.x

Whitworth, A. J., Theodore, D. A., Greene, J. C., Benes, H., Wes, P. D., and Pallanck, L. J. (2005). Increased glutathione S-transferase activity rescues dopaminergic neuron loss in a Drosophila model of Parkinson's disease. *Proc. Natl. Acad. Sci. U.S.A.* 102, 8024–8029. doi: 10.1073/pnas.0501078102

Winter, Y., von Campenhausen, S., Brozova, H., Skoupa, J., Reese, J. P., Bötzel, K., et al. (2010). Costs of Parkinson's disease in Eastern Europe: a Czech cohort study. *Parkinsonism Relat. Disord.* 16, 51–56. doi: 10.1016/j.parkreldis.2009.07.005

Xu, C. L., Wang, Q. Z., Sun, L. M., Li, X. M., Deng, J. M., Li, L. F., et al. (2012). Asiaticoside: attenuation of neurotoxicity induced by MPTP in a rat model of Parkinsonism via maintaining redox balance and up-regulating the ratio of Bcl-2/Bax. *Pharmacol. Biochem. Behav.* 100, 413–418. doi: 10.1016/j.pbb.2011.09.014

Xu, H., Jiang, H., Wang, J., and Xie, J. (2010). Rg1 protects iron-induced neurotoxicity through antioxidant and iron regulatory proteins in 6-OHDA-treated MES23.5 cells. *J. Cell. Biochem.* 111, 1537–1545. doi: 10.1002/jcb.22885

Yan, M. H., Wang, X., and Zhu, X. (2013). Mitochondrial defects and oxidative stress in Alzheimer disease and Parkinson disease. *Free Radic. Biol. Med.* 62, 90–101. doi: 10.1016/j.freeradbiomed.2012.11.014

Yang, Y., Gehrke, S., Imai, Y., Huang, Z., Ouyang, Y., Wang, J.-W., et al. (2006). Mitochondrial pathology and muscle and dopaminergic neuron degeneration caused by inactivation of Drosophila Pink1 is rescued by Parkin. *Proc. Natl. Acad. Sci. U.S.A.* 103, 10793–10798. doi: 10.1073/pnas.0602493103

Ye, Q., Ye, L., Xu, X., Huang, B., Zhang, X., Zhu, Y., et al. (2012). Epigallocatechin-3-gallate suppresses 1-methyl-4-phenyl-pyridine-induced oxidative stress in PC12 cells via the SIRT1/PGC-1alpha signaling pathway. *BMC Complement. Altern. Med.* 12:82. doi: 10.1186/1472-6882-12-82

Zhang, X., Xu, J. K., Wang, J., Wang, N. L., Kurihara, H., Kitanaka, S., et al. (2007). Bioactive bibenzyl derivatives and fluorenones from dendrobium nobile. *J. Nat. Prod.* 70, 24–28. doi: 10.1021/np060449r

Żuk, M., Kulma, A., Dymińska, L., Szołtysek, K., Prescha, A., Hanuza, J., et al. (2011). Flavonoid engineering of flax potentiate its biotechnological application. *BMC Biotechnol.* 12:47. doi: 10.1186/1472-6750-12-47

Conflict of Interest Statement: The authors declare that the research was conducted in the absence of any commercial or financial relationships that could be construed as a potential conflict of interest.

frontiers in Aging Neuroscience

ORIGINAL RESEARCH
published: 15 October 2018
doi: 10.3389/fnagi.2018.00323

Complementary and Alternative Medicine for Idiopathic Parkinson's Disease: An Evidence-Based Clinical Practice Guideline

Ki-Ho Cho[1], Tae-Hun Kim[2], Seungwon Kwon[1], Woo-Sang Jung[1], Sang-Kwan Moon[1], Chang-Nam Ko[1,3], Seung-Yeon Cho[1,3], Chan-Yong Jeon[4], Sang-Ho Lee[5], Tae Young Choi[6], Ji Hee Jun[6], Jiae Choi[7], Myeong Soo Lee[6] and Eun Kyoung Chung[8]*

[1] Department of Cardiology and Neurology, College of Korean Medicine, Kyung Hee University, Seoul, South Korea, [2] Korean Medicine Clinical Trial Center, Korean Medicine Hospital, Kyung Hee University, Seoul, South Korea, [3] Stroke and Neurological Disorders Center, Kyung Hee University Hospital at Gangdong, Seoul, South Korea, [4] Department of Korean Internal Medicine, College of Korean Medicine, Gachon University, Seongnam, South Korea, [5] Gangdong Mokhuri Oriental Medical Hospital, Seoul, South Korea, [6] Clinical Medicine Division, Korea Institute of Oriental Medicine, Daejeon, South Korea, [7] Integrative Health Promotion Team, Korea Health Promotion Institute, Seoul, South Korea, [8] Division of Clinical Pharmacy, Department of Pharmacy, College of Pharmacy, Kyung Hee University, Seoul, South Korea

OPEN ACCESS

Edited by:
Seung-Nam Kim,
Dongguk University, South Korea

Reviewed by:
Nevena Divac,
University of Belgrade, Serbia
Julien Rossignol,
Central Michigan University, United States
Vinita Agarwal,
Salisbury University, United States

***Correspondence:**
Tae-Hun Kim
taehunkim@khu.ac.kr;
rockandmineral@gmail.com

Received: 07 June 2018
Accepted: 24 September 2018
Published: 15 October 2018

Citation:
Cho K-H, Kim T-H, Kwon S, Jung W-S, Moon S-K, Ko C-N, Cho S-Y, Jeon C-Y, Lee S-H, Choi TY, Jun JH, Choi J, Lee MS and Chung EK (2018) Complementary and Alternative Medicine for Idiopathic Parkinson's Disease: An Evidence-Based Clinical Practice Guideline. Front. Aging Neurosci. 10:323. doi: 10.3389/fnagi.2018.00323

Patients with idiopathic Parkinson's disease (IPD) require long-term care and are reported to use complementary and alternative medicine (CAM) interventions frequently. This CAM-specific clinical practice guideline (CPG) makes recommendations for the use of CAM, including herbal medicines, acupuncture, moxibustion, pharmaco-acupuncture, and qigong (with Tai chi) in patients with IPD. This guideline was developed using an evidence-based approach with randomized controlled trials currently available. Even though this CPG had some limitations, mainly originating from the bias inherent in the research on which it is based, it would be helpful when assessing the value of the CAM interventions frequently used in patients with IPD.

Keywords: idiopathic Parkinson's disease, complementary and alternative medicine, evidence-based medicine, clinical practice guideline, recommendations

INTRODUCTION

Idiopathic Parkinson's disease is a chronic neurodegenerative disease which presents progressive loss of dopaminergic neurons in substantia nigra. Generally, long-term medical care is often required after first diagnosis of IPD. The prevalence of IPD rises with age but there could be geographic difference in the prevalence among 70–79-year-old population between Asian countries and North America–Europe countries (Pringsheim et al., 2014). Because disease modifying therapy for IPD is absent and patients with IPD have unmet needs which are introduced from undesirable symptoms related to the conventional levodopa therapy and various non-motor symptoms (Bastide et al., 2015), many IPD patients use various complementary and alternative therapies currently.

Abbreviations: CAM, complementary and alternative medicine; CI, confidence interval; CPG, clinical practice guideline; GPP, good practice point; GRADE, Grading of Recommendation Assessment, Development, and Evaluation; IPD, idiopathic Parkinson's disease; KM, Korean medicine; MD, mean difference; OR: odds ratio; RCT, randomized controlled trials; RR, relative risk; SMD, standardized mean difference; UPDRS, Unified Parkinson's Disease Rating Scale.

It has been reported that 25.6–76% of patients with IPD have experience of CAM treatment (Wang et al., 2013). Although types of interventions that are frequently used were reported to be a little bit different between in Asia (acupuncture and herbal medication are most frequently used two interventions) and in United States (dietary supplements and massage are most frequently used two interventions) (Wang et al., 2013), many CAM interventions have been shown to be effective in motor function and balancing of IPD patients in clinical studies (Lee et al., 2008; Kim et al., 2012; Yang et al., 2014). However, there is no specific CPG currently available for CAM interventions in patients with the disease. Several interventions, including acupuncture, biofeedback, and manual therapy, were mentioned in part of a CPG endorsed by the Canadian Neurological Sciences Federation and Parkinson Society Canada in 2011, but with the caveat that the evidence for their use was insufficient and in need of update (Grimes et al., 2012). Another CPG for integrative interventions published in 2015 included a comprehensive CAM intervention-specific CPG for IPD but was a consensus-based guideline that was not developed on the basis of the current best clinical evidence (Pan et al., 2015). An up-to-date, evidence-based, specific CPG on CAM interventions for IPD is needed to provide clinical evidence that can assist both health care professionals and patients when making a decision whether to include CAM interventions in their long-term strategy for management of the disease.

This CAM-specific CPG for IPD was developed to provide reliable recommendations for health care professionals and patients based on current best clinical evidence on the benefits and harms of CAM interventions.

The scope covered in this guideline contained any modalities which are originated from outside of conventional biomedicine and can be used together with main-stream medical practice (Clarke et al., 2015). In the course of developing this guideline, we aimed to suggest recommendations the interventions that are commonly used in Korea in the highest priority, considering the reality of Korea. We plan to expand the scope of complementary medicine in future revisions to cover various interventions not covered in this guideline.

MATERIALS AND METHODS

This CAM-specific CPG for IPD was developed by the Society of Stroke on KM (**Figure 1**). In September 2016, the society organized a steering committee to oversee the development of the guideline, a development committee to synthesize the evidence and draft the CPG, and an advisory committee to review the proposed CPG. The steering committee included six society members, the development committee was multidisciplinary and consisted of four disease specialists, five methodology experts, one statistician, and one economic analysis specialist. The advisory committee included seven KM physicians working in primary and secondary care and recommended by the Society of Stroke on KM and two KM physicians recommended by the panel of physicians at the Guideline center for KM.

The development committee identified the primary clinical questions involving herbal medicines, acupuncture, moxibustion, qigong, and Tai chi which were reported to be most common and clinically important CAM interventions for IPD patients (Kim et al., 2009; Wang et al., 2013) and developed a search strategy and inclusion/exclusion criteria for application to the relevant literature. The PubMed, Cochrane CENTRAL, EMBASE, CNKI, Oriental Medicine Advanced Searching Integrated System, and National Digital Science Library databases were searched up to February 2017 to identify eligible RCTs. The details of the search strategy used for each intervention is shown in **Supplement 1**.

Multiple members of the development committee selected the literature, extracted the relevant data, and performed the risk of bias assessment and meta-analysis. Any disagreement was resolved by group discussion. The evidence for each clinical question was qualitatively and quantitively synthesized. In case of multiple clinical trials using the same specific intervention such as specific type of herbal medications or acupuncture, clinical questions for specific interventions were generated through panel discussion and synthesized too. Levels of evidence and the strength of the recommendations were then evaluated using the GRADE approach (Guyatt et al., 2008). Validated, Parkinson's disease-specific outcomes including the UPDRS, levodopa dose, 39-Item Parkinson's disease questionnaire (PDQ-39), Total effectiveness rate, Webster scale score, Berg balance scale, Parkinson Disease Sleep Scale, and adverse events were assessed for GRADE. The level of evidence for each outcome was classified as high, moderate, low, or insufficient based on the overall risk of bias, inconsistency, indirectness, imprecision, and other considerations in the included studies as suggested by the GRADE working group (**Table 1**). The strength of the recommendations was graded according to the level of evidence and its clinical importance, such as the risk and benefit of the intervention and its value to the patient, as A, B, C, D, or GPP (**Table 2**). Based on the level of evidence and strength of the recommendations, a draft recommendation for each clinical question was prepared by the development committee.

The Delphi method was used to achieve formal consensus between experts and clinicians and required all contributors to complete an on-line web survey[1]. A questionnaire concerning the initial draft of the recommendations was prepared, and a panel of nine multidisciplinary experts was established on the recommendation of the advisory committee. The experts on the panel were asked to grade their degree of agreement with each recommendation on a nine-point Likert scale (1, totally disagree; 9, fully agree). A median value of ≥ 7 indicated that agreement was reached and a median value <7 implied disagreement that required a further round of the Delphi process. The expert panel answered two rounds of questionnaires, after which the final recommendation for the CPG was drafted (**Supplementary Table 1**). The Guideline center for KM then approved the final draft of the CPG to be implemented by the end of 2018.

[1]https://ko.surveymonkey.com

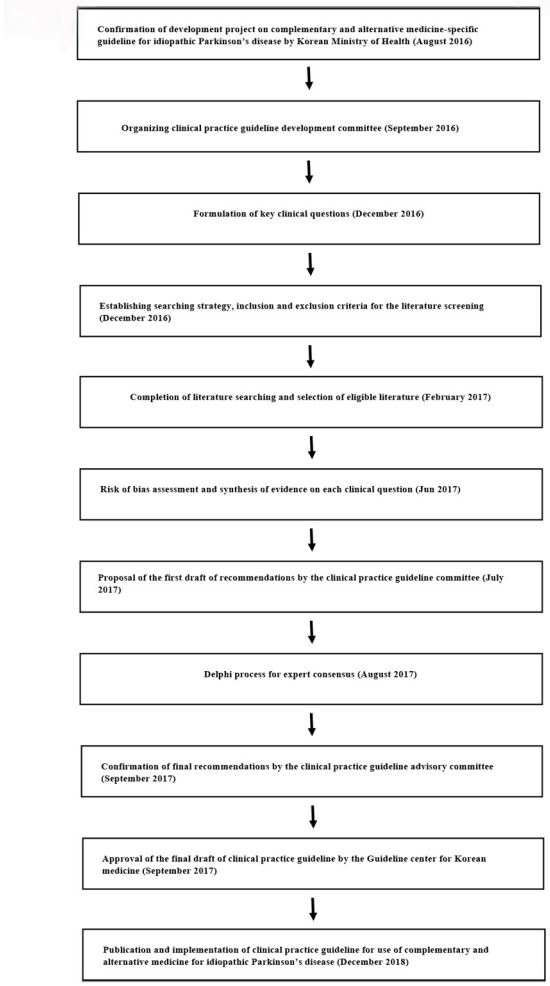

FIGURE 1 | The clinical practice guideline development process.

TABLE 1 | Levels of evidence.

Level	Description
High	We are very confident that the true effects lie close to that of the estimate of effect.
Moderate	We are moderately confident in the effect estimate: the true effect is likely to be close to the estimate of effect, but there is a possibility that it is substantially different.
Low	Our confidence in the effect estimate is limited: The true effect may be substantially different from the estimate of the effect.
Insufficient	We have very little confidence in the effect estimate: The true effect is likely to be substantially different from the estimate of effect.

TABLE 2 | Grade of recommendation.

Grade	Definition	Notation
A	Recommended when the level of evidence is "high," there is a clear benefit and the level of use in clinical settings is high.	Is recommended
B	Assigned when the level of evidence is "moderate," the benefits are reliable, and the level of use in clinical settings is high or moderate. Although relevant studies providing evidence supporting the recommendation may be lacking, the clinical benefit is clear.	Should be considered
C	Assigned when the level of evidence is "low," the benefits are not reliable, but the recommendation's level of use in clinical settings is high or moderate.	May be considered
D	Assigned when the level of evidence is "low" or "insufficient," the benefits are unreliable, harmful results may arise, and the recommendation's level of use in clinical settings is low.	Is not recommended
GPP	Due to the lack of evidence-based medical information, the level of evidence is "low" or "insufficient" and the benefits cannot be evaluated. This rating is assigned based on the clinical experience of the group that developed the CPG and a high level of use in clinical settings.	Is recommended based on the clinical experience of the group that developed the CPG

CPG, clinical practice guideline; GPP, good practice point.

RESULTS

Herbal Medicine

Clinical Question 1

Is concomitant administration of herbal medicines and anti-parkinsonian drug therapy a more effective symptomatic treatment for IPD than monotherapy with anti-parkinsonian agents?

This clinical question was intended to assess the overall clinical evidence for combination therapy using herbal medicines of any type and anti-parkinsonian agents. Although inclusion of multiple prescriptions when assessing the clinical evidence for herbal medicine is controversial, it is considered necessary at the present stage. In addition, the benefits and risks of treatment are similar between the herbal medicines available, and there was a consensus among the group of experts that the values and preferences for these medicines are similar. After assessing the overall evidence for herbal medicine regardless of the type of prescription, we evaluated the clinical evidence for several herbal prescriptions that have been evaluated in previous clinical trials using the following clinical questions in below sections.

Seventy-five studies (including 5430 patients with IPD) that evaluated the UPDRS total score were included. The score was significantly lower in the combination therapy group than in the anti-parkinsonian monotherapy group (MD −6.06, 95% CI [−6.82, −5.3]). The results of 44 RCTs (including 3100 patients with IPD) that evaluated the UPDRS part I score for mentation, behavior, and mood favored combination

therapy (MD −1.6, 95% CI [−1.94, −1.26]). Fifty-nine RCTs (including 4311 patients with IPD) that evaluated the UPDRS part II score for activities of daily living found a significant difference between the combination therapy group and the anti-parkinsonian drug monotherapy group (MD −2.2, 95% CI [−2.67, −1.76]). Seventy RCTs (including 4909 patients with IPD) that evaluated the UPDRS part III score for motor examination were included, and combination treatment achieved better results (MD −3.41, 95% CI [−4.23, −2.59]). When the UPDRS part IV score for motor complications was assessed, the results of 40 studies (including 3078 patients with IPD) indicated a significant difference in favor of combination treatment (MD −1.41, 95% CI [−1.72, −1.10]). The PDQ-39 summary index was assessed in 20 studies (including 1490 patients with IPD). The MD in the summary effect estimate for the PDQ-39 summary score was 9.29 (95% CI [−10.83, −7.75]) in favor of combination therapy. Twenty-seven RCTs (including 2043 patients with IPD) included information on the concomitant dose of levodopa. The SMD in levodopa consumption was −0.77 (95% CI [−0.99, −0.56]) when the group that received combination therapy was compared with the group that received anti-parkinsonian drug therapy alone, suggesting that lowering the dose of levodopa in the combination group was more effective. Forty-nine RCTs (including 3463 patients with IPD) included an assessment of adverse events; the RR for total incidence was estimated to be 0.44 (95% CI [0.3, 0.52]) in the group that received combination therapy when compared with the group that received anti-parkinsonian drug therapy alone. However, the overall level of evidence for these analyses was assessed as low, and the results of future studies will have a significant impact on the degree of confidence in the summary effect estimates. A combination of herbal medicine and anti-parkinsonian drug therapy should be considered in patients with IPD; however, the strength of this recommendation may change according to the outcomes of future research (strength of recommendation, B). The evidence in this section suggests a comprehensive recommendation for combination therapy using various herbal medicines and anti-parkinsonian drugs (**Supplementary Table 2.1**).

Recommendation

Concomitant treatment with herbal medicines and anti-parkinsonian drugs should be considered in patients with IPD (strength of recommendation: B/level of evidence: low).

Clinical Question 1-1

Does administration of Bosin-yanggan-sigpung-bang herbal medicine with anti-parkinsonian drug therapy improve symptoms more than anti-parkinsonian drugs alone in patients diagnosed with IPD?

Bosin-yanggan-sigpung-bang has been one of the most frequently evaluated herbal medicines in clinical trials and consists mainly of *Rehmannia glutinosa*, *Paeonia lactiflora*, and *Polygonum multiflorum*. Four RCTs (including 289 patients with IPD) that compared Bosin-yanggan-sigpung-bang and levodopa combination therapy and levodopa monotherapy were included. The MD in the summary effect estimate for the UPDRS total score was −11.39 (95% CI [−16.2, −6.57]) and the SMD for consumption of levodopa was −1.04 (95% CI [−1.49, −0.58]), which suggests a statistically significant difference in favor of combination treatment. There was no significant difference in the incidence of adverse events between the two groups. The levels of evidence for the UPDRS total score and the dose of levodopa were inadequate (**Supplementary Table 2.2**).

Recommendation

Concomitant administration of Bosin-yanggan-sigpung-bang herbal medicine and anti-parkinsonian drug therapy may be considered in patients with IPD (strength of recommendation: C/level of evidence: insufficient).

Clinical Question 1-2

Does administration of Bosin-hwalhyeol-cheobang herbal medicine with anti-parkinsonian drug therapy improve symptoms more than anti-parkinsonian drug therapy alone in patients diagnosed with IPD?

Bosin-hwalhyeol-cheobang contains mainly *Cornus officinalis*, *P. multiflorum*, and *Salvia miltiorrhiza*. Ten studies that were included in the analysis were used to answer this clinical question. The summary effect estimates for the UPDRS total score (MD −6.32, 95% CI [−8.6, −4.05]) and PDQ-39 (MD −9.01, 95% CI [−2.52, 0.25]) were in favor of combination therapy. The RR for the overall incidence of adverse events was 0.46 (95% CI [0.21, 1.03]; **Supplementary Table 2.3**).

Recommendation

Concomitant use of Bosin-hwalhyeol-cheobang herbal medicine and anti-parkinsonian drug therapy may be considered in patients with IPD (strength of recommendation: C/level of evidence: moderate).

Clinical Question 1-3

Does administration of Bosin-hwalhyeol-tonglag-cheobang herbal medicine with anti-parkinsonian drug therapy improve symptoms more than anti-parkinsonian drug therapy alone in patients diagnosed with IPD?

Bosin-hwalhyeol-tonglag-cheobang is mainly composed of *Lycium chinense*, *C. officinalis*, *P. multiflorum*, *S. miltiorrhiza*, and *Buthus martensi*. Three studies could be included in the analysis. When comparing combination therapy and levodopa monotherapy, the MD for the UPDRS total score was −15.40 (95% CI [−19.80, −11.00]) and the MD for the PDQ-39 was −7.05 (95% CI [−11.80, −2.30]) in favor of combination therapy. The overall level of evidence was moderate. None of the studies included information on adverse events (**Supplementary Table 2.4**).

Recommendation

Concomitant administration of Bosin-hwalhyeol-tonglag-cheobang herbal medicine and anti-parkinsonian drug therapy may be considered in patients with IPD (strength of recommendation: C/level of evidence: moderate).

Clinical Question 1-4

Does administration of Sugji-pyeongjeon-tang herbal medicine with anti-parkinsonian drugs improve symptoms more than anti-parkinsonian drug therapy alone in patients diagnosed with IPD?

Sugji-pyeongjeon-tang is a herbal prescription that consists mainly of *R. glutinosa*, *L. chinense*, *Loranthus parasiticus*, and *Gastrodia elata*. Three studies could be included in the analysis. The summary effect estimates for the UPDRS part II score for activities of daily living (MD −1.59, 95% CI [−2.51, −0.67]) and those for the UPDRS part III score for motor examination (MD −2.51, 95% CI [−3.89, −1.13]) favored combination therapy. The MD in the summary effect estimates for the amount of levodopa used was 0.05 (95% CI [−0.26, 0.36]). The estimated incidence of total adverse events favored combination treatment (RR 0.80, 95% CI [0.25, 2.52]). The level of evidence was low (**Supplementary Table 2.5**).

Recommendation

Concomitant use of Sugji-pyeongjeon-tang herbal medicine and anti-parkinsonian drug therapy should be considered in patients with IPD (strength of recommendation: B/level of evidence: low).

Acupuncture

Clinical Question 2

Does a combination of anti-parkinsonian drug therapy and acupuncture improve symptoms more than anti-parkinsonian drug therapy alone in patients diagnosed with IPD?

This clinical question was intended to assess the overall clinical evidence for combination therapy with acupuncture and anti-parkinsonian medications regardless of type of acupuncture intervention. After addressing this clinical question, we assessed the clinical evidence for the frequently used acupuncture interventions in the following clinical questions. Twenty-one RCTs were included. A meta-analysis of clinical trials comparing combination treatment with acupuncture and anti-parkinsonian drug therapy with anti-parkinsonian drug therapy alone suggested that combination therapy had better overall clinical effectiveness than anti-parkinsonian drug therapy alone (RR 1.2, 95% CI [1.08, 1.33]). In addition, there was a statistically significant difference in the Webster scale score (MD −3.09, 95% CI [−4.8, −1.38]) in favor of combination treatment. The UPDRS total score suggested that combination therapy with acupuncture and anti-parkinsonian drug administration was more effective in improving symptoms than anti-parkinsonian drug therapy alone (MD −6.72, 95% CI [−10.24, −3.2]). Only two studies reported adverse events, with no serious adverse events occurring in either study. The overall level of evidence is low, and future studies will have a significant impact on the degree of confidence in the summary effect estimates. This section suggests a comprehensive recommendation for various acupuncture interventions, and recommendations for individual type of acupuncture are suggested below (**Supplementary Table 3.1**).

Recommendations

Concomitant use of acupuncture and anti-parkinsonian drug therapy should be considered in patients with IPD (strength of recommendation: B/level of evidence: low).

Acupuncture points such as GB20, LR3, GB34, LI4, GV20, KI39, LI11, GV16, BL10, BL40, GB6, GV1, and PC6 can be considered for use in acupuncture.

Clinical Question 2-1

Does combination treatment with anti-parkinsonian drug therapy and manual acupuncture improve symptoms more than anti-parkinsonian drug therapy alone in patients diagnosed with IPD?

Seven RCTs were available to address this clinical question. The anti-parkinsonian therapy used in the control groups was a fixed combination of levodopa and benserazide in all cases. Significant improvement in the Webster scale score (MD −3.75, 95% CI [−5.27, −2.23]) was observed in favor of combination therapy when compared with the fixed combination as monotherapy. Adverse events were only reported in two of the seven studies. There were no serious adverse events in either of these studies. The level of evidence from the literature is low and the results of future studies are likely to have a significant impact on the degree of confidence in the summary effect estimates (**Supplementary Table 3.2**).

Recommendation

Concomitant use of manual acupuncture and anti-parkinsonian drug therapy should be considered in patients with IPD (strength of recommendation: B/level of evidence: low).

Clinical Question 2-2

Does combination treatment with anti-parkinsonian drug therapy and electroacupuncture improve symptoms more than anti-parkinsonian drug therapy alone in patients diagnosed with IPD?

In three RCTs, electroacupuncture and anti-parkinsonian drugs were compared with anti-parkinsonian drug therapy alone and there was no significant difference in overall clinical effectiveness (RR 1.22, 95% CI [0.91, 1.63]), Webster scale score (MD −2.98, 95% CI [−6.11, 0.15]), or UPDRS total score (MD −3.8, 95% CI [−7.74, 0.15]) between the two groups. However, the level of evidence was low and the results of future studies are likely to have a significant impact on the degree of confidence in the summary effect estimates (**Supplementary Table 3.3**).

Recommendation

Concomitant use of electroacupuncture and anti-parkinsonian drug therapy may be considered in patients with IPD (strength of recommendation: C/level of evidence: low).

If the patient's chief complaints are tremor and rigidity, electroacupuncture should be applied carefully so as not to trigger overstimulation.

Clinical Question 2-3

Does a combination of anti-parkinsonian drug therapy and scalp acupuncture improve symptoms more that anti-parkinsonian drug therapy alone in patients with IPD?

Three RCTs were available to answer this clinical question. The fixed combination of levodopa and benserazide was used as the anti-parkinsonian drug therapy in all the control groups. There was significant improvement in the Webster scale score (MD −1.97, 95% CI [−3.73, −0.21) in favor of combination therapy. There was no description of the adverse events that occurred in any of the studies. The level of evidence in the literature is insufficient but combination treatment is recommended based on the clinical experience of the development committee (**Supplementary Table 3.4**).

Recommendation

Concomitant use of scale acupuncture and anti-parkinsonian drugs may be considered in patients with IPD (strength of recommendation: GPP/level of evidence: insufficient).

Moxibustion

Clinical Question 3

Does moxibustion improve symptoms in patients with IPD?

Five studies (including 293 patients with IPD) were included in the comparison of the effectiveness of moxibustion with that of other interventions in terms of the UPDRS total score. The UPDRS total score was lower in the moxibustion group than in the control group (MD −8.75, 95% CI [−12.54, −4.95]). Three RCTs (including 174 patients with IPD) were included in the assessment of the UPDRS part III score for motor examination, and a significant difference was observed in favor of moxibustion (MD −1.92, 95% CI [−3.00, −0.84]). Only one study reported adverse events and none of the studies reported side effects. The overall level of evidence was low. Although moxibustion could potentially be a treatment for patients with IPD, there is a lack of concrete evidence for its efficacy and safety (**Supplementary Table 4.1**).

Recommendation

Moxibustion may be considered in patients with IPD (strength of recommendation: C/level of evidence: low).

Care should be taken not to cause adverse events by excessive stimulation if the main symptoms are tremor and rigidity.

Clinical Question 3-1

Does combination treatment with direct moxibustion, acupuncture, and anti-parkinsonian drug therapy improve symptoms in patients diagnosed with IPD?

Only one RCT could be included in the analysis to answer this clinical question. Sixty patients with IPD were included in this study and the UPDRS total score was assessed by comparing the combination of direct moxibustion, acupuncture, and anti-parkinsonian drug therapy with anti-parkinsonian drug monotherapy alone. The UPDRS total score was significantly improved in the combination group in comparison with the anti-parkinsonian drug monotherapy group (MD −7.07, 95% CI [−11.30, −2.84]). There was no description of adverse events in this study. The level of evidence is low; however, summary effect estimates may change according to the findings of future research. Care should be taken to avoid adverse events by excessive stimulation if the patient's main symptoms are tremor and rigidity (**Supplementary Table 4.2**).

Recommendation

A combination of direct moxibustion, acupuncture, and anti-parkinsonian drug therapy may be considered in patients with IPD (strength of recommendation: C/level of evidence: low). Care should be taken not to cause adverse events by excessive stimulation if the patient's main symptoms are tremor and rigidity.

Clinical Question 3-2

Does a combination of Moxa-stick moxibustion and anti-parkinsonian drug therapy improve symptom in patients diagnosed with IPD?

One RCT would be included in the analysis to answer this clinical question. There was no significant difference in the UPDRS total score between combination therapy and a fixed combination of levodopa and benserazide (MD −5.48, 95% CI [−11.64, 0.68]). No information on adverse events was available. The overall level of evidence is low. Care should be taken not to cause adverse events by excessive stimulation if the patient's main symptoms are tremor and rigidity (**Supplementary Table 4.3**).

Recommendation

Concomitant treatment with Moxa-stick moxibustion and anti-parkinsonian drug therapy may be considered in patients with IPD (strength of recommendation: C/level of evidence: low).

Care should be taken not to cause adverse events by excessive stimulation if the patient's main symptoms are tremor and rigidity.

Clinical Question 3-3

Does combination treatment with warm-needling acupuncture and swallowing exercises improve dysphagia symptoms in patients diagnosed with IPD?

One RCT comparing a combination of warm-needling acupuncture and swallowing exercises with swallowing exercises alone was included in the analysis to address this clinical question. The total effectiveness rate was significantly higher in the combination treatment group (RR 1.67, 95% CI [1.11, 2.50]) but there was no report on adverse events. The overall level of evidence was low (**Supplementary Table 4.4**).

Recommendation

Combination treatment with warm-needling acupuncture and swallowing exercises may be considered for the treatment of dysphagia in patients with IPD (strength of recommendation: C/level of evidence: low).

Pharmaco-acupuncture

Clinical Question 4-1

Does a combination of bee venom acupuncture and anti-parkinsonian drug therapy improve symptoms in patients diagnosed with IPD?

One RCT was available to address this clinical question. When comparing a combination of bee venom acupuncture and anti-parkinsonian drug therapy with anti-parkinsonian drug therapy alone, there was a significant difference in UPDRS total score in favor of combination therapy. One participant reported an itching event after bee venom acupuncture. The overall level of evidence was insufficient, but the development committee decided to make a GPP recommendation based on the prevalent use of this treatment modality in current clinical practice and the opinion of the expert committee.

Recommendation

Concomitant treatment with bee venom acupuncture and anti-parkinsonian drug therapy is recommended in patients with IPD (strength of recommendation: GPP/level of evidence: insufficient).

Clinical Question 4-2

Does a combination of pharmaco-acupuncture and anti-parkinsonian drug therapy improve symptoms in patients diagnosed with IPD?

One RCT could be included in the analysis to answer this clinical question. There was no significant difference in the total effectiveness rate between a combination comprising Puerarin pharmaco-acupuncture and anti-parkinsonian therapy and single anti-parkinsonian drug therapy alone (RR 1.06, 95% CI [0.90, 1.26]). No adverse events were reported. The overall level of evidence was insufficient, but the development committee decided to make a GPP recommendation based on the prevalent use in current clinical practice and the opinion of the expert committee (**Supplementary Table 5**).

Recommendation

Concomitant treatment with pharmaco-acupuncture and anti-parkinsonian drug therapy is recommended in patients with IPD (strength of evidence: GPP/level of evidence: insufficient).

Qigong and Tai Chi

Clinical Question 5-1

Does a combination of Qigong, walking exercise, and anti-parkinsonian drug therapy improve motor function and sleep quality in patients diagnosed with IPD?

Two RCTs (including 141 patients with IPD) were included to answer this clinical question. The group of patients that received combination therapy (qigong, walking exercise, anti-parkinsonian drugs) had a better UPDRS part III score for motor examination (MD −4.17, 95% CI [−5.43, −2.92]) and a better Berg balance scale score (MD 3.30, 95% CI [2.62, 3.98]). In addition, the combination therapy group showed better results in several domains on the Parkinson Disease Sleep Scale-2, including sleep quality (MD −11.47, 95% CI [−15.77, −7.17]), motor symptoms at night (MD −4.63, 95% CI [−6.02, −3.24]), symptoms of Parkinson's disease at night (MD −3.1, 95% CI [−4.37, −1.83]), and disturbed sleep (MD −3.44, 95% CI [−5.09, −1.79]) compared with the groups without qigong. However, the overall level of evidence was low (**Supplementary Table 6.1**).

Recommendation

Concomitant treatment with qigong, walking exercise, and anti-parkinsonian drug therapy should be considered in patients with IPD (strength of recommendation: B/level of evidence: low).

Clinical Question 5-2

Does Tai chi improve motor function in patients diagnosed with IPD?

Three RCTs (including 216 patients with IPD) were included for evaluation of this clinical question. When compared with exercise or stretching movement, Tai chi had a better effect on the UPDRS part III score for motor examination (MD −3.1, 95% CI [−3.86, −2.34]) and Berg balance scale score (MD 3.52, 95% CI [1.92, 5.12]). In addition, there was a significant decrease in the number of falls recorded in the Tai chi training group (OR 0.38, 95% CI [0.19, 5.12]). However, the overall level of evidence was low (**Supplementary Table 6.2**).

Recommendations

Tai chi can be considered in patients with IPD (strength of recommendation: B/level of evidence: low).

DISCUSSION

This evidence-based CPG on CAM interventions for IPD outlines the currently available evidence and makes recommendations for the commonly used CAM interventions, i.e., herbal medicines, acupuncture, moxibustion, pharmaco-acupuncture, and qigong (with Tai chi). This CPG mainly addresses combination treatment using individual CAM interventions and anti-parkinsonian drug therapy because of the current lack of clinical evidence for use of CAM interventions alone. In this sense, CAM interventions need to be considered for concomitant use only until new and conclusive evidence of their efficacy as monotherapy emerges. In addition to this, about CAM interventions usage, communication between physician and patients is very important to prevent potential adverse events, which should be reminded when CAM interventions get started (Wang et al., 2013).

Limitations

The development committee acknowledges that this CPG has several limitations, the most important one being that the overall level of evidence for each intervention as assessed by GRADE approach is low or insufficient because of the high risk of bias introduced by methodologic problems and inaccuracies arising from the small numbers of participants in the included studies. Indeed, there could be considerable

publication bias because most of the relevant studies were performed in Asian countries. Additionally, we did not intend to limit target population of this CPG but most clinical studies included only Asian population who showed different characteristics in ages, sex, and region across the studies. Second, most of the recommendations focus on the overall benefit and harm of combination treatment with CAM interventions and antiparkinsonian drugs. CPGs that focus on specific symptoms or long-term complications related to IPD need to be developed in the future. In addition, this CPG dose not include detailed information on the methods for usage of individual CAM interventions, which would be updated in the future CPG. Third, this CPG is based on evidence for combination treatment with CAM interventions and anti-parkinsonian drug therapy. As already mentioned, there is no clear evidence regarding whether individual CAM interventions are effective and safe enough to be recommended in this CPG. Therefore, in principle, we recommend that most CAM interventions be used in combination with conventional anti-parkinsonian drug therapy at this stage. Third, there was no participation of consumer groups in the Delphi process, which means that no patient perspectives or preferences were taken into account in the development of this CPG. Fourth, no cost or economic analysis was performed. Finally, only limited interventions were assessed in this review. As we described in the "Materials and Methods" section, interventions which were frequently used in Asian countries were included for this CPG. Actually, frequently used CAM modalities are reported to be different between countries (Wang et al., 2013) so other interventions such as natural products, mind–body interventions, or Ayurveda should be assessed. In the future updated CPG, we will include these frequently used interventions which was not discussed in the CPG.

Implications for Clinical Studies and Updates to the CPG

Rigorous RCTs for individual CAM interventions with adequate statistical power should be conducted, especially in the United States and Europe. The safety and effectiveness of CAM as monotherapy and when used as part of combination therapy should be evaluated in the IPD population. Comparative ranking between included CAM modalities would be helpful which can be suggested through indirect comparison using network meta-analysis method. A consumer group should be included in the Delphi process when updating this CPG in the future. Inclusion of a cost-effectiveness analysis should also be considered when updating this CPG. Finally, when clinically implementing recommendations of the interventions included in this CPG outside Korea, physicians and patients need to consider accessibility and feasibility of the interventions in their medical environment and context.

Development of this guideline was funded by the Ministry of Health & Welfare through the Korea Health Industry Development Institute. None of the members of the Society of Stroke on Korean Medicine or members of each committee and expert panel that participated in the Delphi process has any conflicts of interests in this research.

This guideline will be updated in 2020. In the future update, various CAM interventions not covered in this guideline will be included.

AUTHOR CONTRIBUTIONS

K-HC, T-HK, SK, W-SJ, S-KM, C-NK, S-YC, C-YJ, S-HL, TC, JJ, JC, ML, and EC participated in the CPG development committee and devised the CPG development project. K-HC, T-HK, SK, W-SJ, S-KM, C-NK, S-YC, C-YJ, and S-HL involved in the clinical question development. TC, JJ, JC, and ML conducted systematic literature searching and conducted electronic Delphi surveys. T-HK, TC, JJ, and JC conducted evidence synthesis and made draft of the recommendations. T-HK drafted this manuscript.

FUNDING

This research was supported by the Traditional KM R&D program funded by the Ministry of Health and Welfare through the Korea Health Industry Development Institute (KHIDI, HB16C0051).

ACKNOWLEDGMENTS

We express our sincere gratitude to the Society of Stroke on KM, the panel of physicians, and the Guideline center for KM that have actively supported this CPG development.

SUPPLEMENTARY MATERIAL

The Supplementary Material for this article can be found online at: https://www.frontiersin.org/articles/10.3389/fnagi.2018.00323/full#supplementary-material

REFERENCES

Bastide, M. F., Meissner, W. G., Picconi, B., Fasano, S., Fernagut, P.-O., Feyder, M., et al. (2015). Pathophysiology of L-dopa-induced motor and non-motor complications in Parkinson's disease. *Prog. Neurobiol.* 132, 96–168. doi: 10.1016/j.pneurobio.2015.07.002

Clarke, T. C., Black, L. I., Stussman, B. J., Barnes, P. M., and Nahin, R. L. (2015). Trends in the use of complementary health approaches among adults: United States, 2002–2012. *Natl. Health Stat. Rep.* 10, 1–16.

Grimes, D., Gordon, J., Snelgrove, B., Lim-Carter, I., Fon, E., Martin, W., et al. (2012). Canadian guidelines on Parkinson's Disease. *Can. J. Neurol. Sci.* 39:S1. doi: 10.1017/S031716710001516X

Guyatt, G. H., Oxman, A. D., Vist, G. E., Kunz, R., Falck-Ytter, Y., Alonso-Coello, P., et al. (2008). GRADE: an emerging consensus on rating quality of evidence and strength of recommendations. *BMJ* 336, 924–926. doi: 10.1136/bmj.39489.470347.AD

Kim, S. R., Lee, T. Y., Kim, M. S., Lee, M. C., and Chung, S. J. (2009). Use of complementary and alternative medicine by Korean patients with Parkinson's

disease. *Clin. Neurol. Neurosurg.* 111, 156–160. doi: 10.1016/j.clineuro.2008.09.011

Kim, T.-H., Cho, K.-H., Jung, W.-S., and Lee, M. S. (2012). Herbal medicines for Parkinson's disease: a systematic review of randomized controlled trials. *PLoS One* 7:e35695. doi: 10.1371/journal.pone.0035695

Lee, M. S., Shin, B. C., Kong, J. C., and Ernst, E. (2008). Effectiveness of acupuncture for Parkinson's disease: a systematic review. *Mov. Disord.* 23, 1505–1515. doi: 10.1002/mds.21993

Pan, W., Liu, J., Chen, X., Wang, Q., Wu, Y., Bai, Y., et al. (2015). A practical consensus guideline for the integrative treatment of Parkinson's disease in Shanghai, China. *Integr. Med. Int.* 2, 56–62. doi: 10.1159/000435813

Pringsheim, T., Jette, N., Frolkis, A., and Steeves, T. D. (2014). The prevalence of Parkinson's disease: a systematic review and meta-analysis. *Mov. Disord.* 29, 1583–1590. doi: 10.1002/mds.25945

Wang, Y., Xie, C.-L., Wang, W.-W., Lu, L., Fu, D.-L., Wang, X.-T., et al. (2013). Epidemiology of complementary and alternative medicine use in patients with Parkinson's disease. *J. Clin. Neurosci.* 20, 1062–1067. doi: 10.1016/j.jocn.2012.10.022

Yang, Y., Li, X.-Y., Gong, L., Zhu, Y.-L., and Hao, Y.-L. (2014). Tai Chi for improvement of motor function, balance and gait in Parkinson's disease: a systematic review and meta-analysis. *PLoS One* 9:e102942. doi: 10.1371/journal.pone.0102942

Conflict of Interest Statement: The authors declare that the research was conducted in the absence of any commercial or financial relationships that could be construed as a potential conflict of interest.

frontiers in Aging Neuroscience

REVIEW
published: 01 November 2018
doi: 10.3389/fnagi.2018.00348

Phytochemical and Pharmacological Role of Liquiritigenin and Isoliquiritigenin From Radix Glycyrrhizae in Human Health and Disease Models

Mahesh Ramalingam[1], Hyojung Kim[2], Yunjong Lee[2] and Yun-Il Lee[1,3]**

[1] Well Aging Research Center, Daegu Gyeongbuk Institute of Science and Technology, Daegu, South Korea, [2] Division of Pharmacology, Department of Molecular Cell Biology, Samsung Biomedical Research Institute, Sungkyunkwan University School of Medicine, Suwon, South Korea, [3] Companion Diagnostics and Medical Technology Research Group, Daegu Gyeongbuk Institute of Science and Technology, Daegu, South Korea

The increasing lifespan in developed countries results in age-associated chronic diseases. Biological aging is a complex process associated with accumulated cellular damage by environmental or genetic factors with increasing age. Aging results in marked changes in brain structure and function. Age-related neurodegenerative diseases and disorders (NDDs) represent an ever-growing socioeconomic challenge and lead to an overall reduction in quality of life around the world. Alzheimer's disease (AD) and Parkinson's disease (PD) are most common degenerative neurological disorders of the central nervous system (CNS) in aging process. The low levels of acetylcholine and dopamine are major neuropathological feature of NDDs in addition to oxidative stress, intracellular calcium ion imbalance, mitochondrial dysfunction, ubiquitin-proteasome system impairment and endoplasmic reticulum stress. Current treatments minimally influence these diseases and are ineffective in curing the multifunctional pathological mechanisms. Synthetic neuroprotective agents sometimes have negative reactions as an adverse effect in humans. Recently, numerous ethnobotanical studies have reported that herbal medicines for the treatment or prevention of NDDs are significantly better than synthetic drug treatment. Medicinal herbs have traditionally been used around the world for centuries. Radix Glycyrrhizae (RG) is the dried roots and rhizomes of *Glycyrrhiza uralensis* or *G. glabra* or *G. inflata* from the Leguminosae/Fabaceae family. It has been used for centuries in traditional medicine as a life enhancer, for the treatment of coughs and influenza, and for detoxification. Diverse chemical constituents from RG have reported including flavanones, chalcones, triterpenoid saponins, coumarines, and other glycosides. Among them, flavanone liquiritigenin (LG) and its precursor and isomer chalcone isoliquiritigenin (ILG) are the main bioactive constituents of RG. In the present review, we summarize evidence in the literature on the structure and phytochemical properties and pharmacological applications of LG and ILG in age-related diseases to establish new therapeutics to improve human health and lifespan.

Keywords: isoliquiritigenin, liquiritigenin, memory, Parkinson's disease, Radix Glycyrrhizae

OPEN ACCESS

Edited by:
Seung-Nam Kim,
Dongguk University Seoul,
South Korea

Reviewed by:
Youngmin Bu,
Kyuung Hee University, South Korea
Seung-Mann Paek,
Gyeongsang National University,
South Korea

****Correspondence:***
Yunjong Lee
ylee69@skku.edu
Yun-Il Lee
ylee56@dgist.ac.kr

Received: *26 June 2018*
Accepted: *15 October 2018*
Published: *01 November 2018*

Citation:
Ramalingam M, Kim H, Lee Y and Lee Y-I (2018) Phytochemical and Pharmacological Role of Liquiritigenin and Isoliquiritigenin From Radix Glycyrrhizae in Human Health and Disease Models. Front. Aging Neurosci. 10:348. doi: 10.3389/fnagi.2018.00348

INTRODUCTION

The average life expectancy at birth in developed countries was about 47 years at the beginning of the 20th century and increased to 77.8 years in the beginning of the 21st century (Oeppen and Vaupel, 2002). Senescence or biological aging is neither irreversible nor inevitable fate of all organisms and significantly delayed (da Costa et al., 2016). The rate of dying prematurely has decreased, whereas the rate of death from aging-associated chronic diseases such as diabetes mellitus, cancer, and heart, kidney, and neurological diseases has increased (Fontana, 2009). The aging process in biological systems is complex (Gottfries, 1990) and is proving to be a major risk factor for all of the common chronic and lethal conditions. Aging results in marked changes in brain structure and function (Cole and Franke, 2017). Age-related neurodegenerative disorders (NDDs) represent an ever-growing socioeconomic challenge and lead to an overall reduction in quality of life around the world (Tarailo-Graovac et al., 2016).

Alzheimer's disease (AD) and Parkinson's disease (PD) are most common age-related neurological disorders of the central nervous system (CNS). AD is characterized by insoluble extracellular β-amyloid peptide (Aβ) forming senile plaques deposition, intraneuronal tau accumulation and hyperphosphorylated microtubule-associated fibrillary tangles. It may contribute to progressive neuronal degeneration with memory loss and cognitive impairment in brain during normal aging (Dickson et al., 1988). PD is characterized by loss of dopamine(DA)-rgic neurons and the presence of intracytoplasmic aggregated α-synuclein Lewy bodies in the substantia nigra pars compacta of the brain eventually leads to bradykinesia, rigidity, slowing of movement and postural instability (Gibb and Lees, 1988). In addition, low levels of brain neurotransmitter acetylcholine (ACh) (Houghton and Howes, 2005), oxidative stress, intracellular calcium ion imbalance, mitochondrial dysfunction, ubiquitin-proteasome system impairment and endoplasmic reticulum stress are involved in the pathogenesis of NDDs (Ramalingam and Kim, 2016b). Aging enables the development of chronic diseases, and anti-aging mechanisms not only increase lifespan but also preserve function resembling a more youthful state (Fontana, 2009). Therefore, there is a focus on developing novel multi-disease preventative and therapeutic approaches (Kennedy et al., 2014). At present, there are no cures for NDDs. The existing therapies are focused on increasing the amount of ACh and DA by inhibiting acetylcholinesterase and monoamine oxidase (MAO) inhibition, respectively or elevating the concentration of the precursor levodopa (L-DOPA) (Houghton and Howes, 2005).

The brain is the body's most complex organ and not all drugs are sanctioned for the treatment of age-related NDDs. The currently available treatments have proven ineffective in curing the multi-functional pathological conditions of NDDs (Vijayakumar et al., 2016). Synthetically manufactured drugs have certain side effects, such as dry mouth, tiredness, sleepiness, sluggishness, drowsiness, anxiety, tension, nervousness, and trouble with balance in humans (Phani Kumar et al., 2015). Recently, increasing scientific researches on medicinal plants have widespread interest and their active ingredients may help to identify new multi-functional therapeutic agents. Numerous plant-based natural and their manufactured synthetic neuroprotective drugs have been permitted by the U.S. Food and Drug Administration (FDA) over the past 30 years (Kumar et al., 2012; Cragg and Newman, 2013). Plants have been used for many centuries in traditional medicines to treat NDDs (Abushouk et al., 2017). Dietary compounds present in daily foods such as fruits, seeds, vegetables, and beverages have been reported for neuroprotective by various signaling pathways against NDDs (Asthana et al., 2016). Although there are many medicinal plants documented in pharmacopeias, only a few have been extensively studied to understanding their potential effectiveness in the treatment of NDDs (Vijayakumar et al., 2016).

Glycyrrhiza uralensis Fisch.

Glycyrrhiza uralensis, commonly known as licorice (or liquorice), is one of the most popular herbal medicines, used as antitussive, expectorant, and antipyretic in traditional prescriptions, foods, beverages, brewing, tobacco, and cosmetics for its effects of relieving cough, pharyngitis, bronchitis, and bronchial asthma (Cao et al., 2004; Kao et al., 2014). It is a perennial glandular herb, 30–100 cm high, with an erect stem with short whitish hairs and echinate glandular hairs; the lower part of the stem is woody. Leaves are alternate and imparipinnate, with 7–17 leaflets. Leaves are ovate-elliptical in shape and 2–5.5 cm long by 1–3 cm wide (WHO, 1999). The apex is obtuse-rounded and the base is rounded and both surfaces are covered with glandular hairs and short hairs. Stipules are lanceolate and inflorescence is an axillary cluster. Flowers are purplish and papilionaceous with villous calyx. The fruit is a flat oblong pod, 6–9 mm wide, that is sometimes falcate and is densely covered with brownish echinate glandular hairs. Each pod contains 2–8 seeds. The root is cylindrical, fibrous, flexible, 20–22 cm long and 15 mm in diameter, with or without cork, which is reddish, furrowed, and light yellow inside (WHO, 1999).

Classification

Kingdom: Plantae (Plants)
Subkingdom: Tracheobionta (Vascular Plants)
Superdivision: Spermatophyta (Seed Plants)
Division: Magnoliophyta (Flowering Plants)
Class: Magnoliopsida (Dicotyledons)
Subclass: Rosidae
Order: Fabales
Family: Leguminosae/Fabaceae
Genus: *Glycyrrhiza*
Species: *G. uralensis* Fisch.
Binomial: *Glycyrrhiza uralensis* Fisch. Ex DC. (Theplantlist, 2013; Wikipedia, 2018)

Synonyms

Glycyrrhiza asperrima var. *desertorum* Regel
Glycyrrhiza asperrima var. *uralensis* Regel
Glycyrrhiza glandulifera Ledeb. (Theplantlist, 2013)

Vernacular Names

Chinese : Gan Cao (甘草)
Korean : Gam Cho (감초)
Japanese : Uraru-kanzou (ウラルカンゾウ)

RADIX GLYCYRRHIZAE

Radix Glycyrrhizae (RG) is the dried roots and rhizomes of three Glycyrrhiza species—*G. uralensis* Fisch. ex DC., *G. glabra* L, and *G. inflata* Batalin—that is prescribed as licorice in Pharmacopeias (Liu et al., 2013; Wang et al., 2015). Among these species, *G. uralensis* is the most frequently used species for RG in Korea, China and Japan that constitutes 90% of total licorice production around the world (Zhang and Ye, 2009). Moreover, *G. uralensis* known as Far East Asian licorice and *G. glabra* as Western licorice (Davis and Morris, 1991), this review is limited to *G. uralensis*. The roots and rhizomes are cylindrical, fibrous, flexible, 20–100 cm long and 0.6–3.5 cm in diameter, with or without cork. Roots are externally reddish brown or grayish brown, longitudinally wrinkled, furrowed, and lenticellate, with sparse rootlet scars (WHO, 1999). The texture is compact and slightly fibrous, and the interior is yellowish white and starchy. The cambium ring is distinct and the rays radiate, some with clefts. Rhizomes are cylindrical with external bud scars, and pith is present in the center of the fracture (WHO, 1999).

RG is one of the most commonly used and oldest herbal medicines documented in the pharmacopeias (Liu et al., 2013). The earliest Chinese written literature *Shennong's Classic of Materia Medica* describing the use of licorice dates from 2100 BC for its life-enhancing properties (Wang et al., 2015). Its clinical practice against cough, influenza, liver damage and for detoxification values has received considerable attention throughout the world (Ji et al., 2016). Recent researches revealed its antioxidant, anti-inflammatory, anti-viral, anti-diabetic, cytotoxic, skin-whitening and cholinergic activities (Mae et al., 2003; Isbrucker and Burdock, 2006; Nassiri and Hossein, 2008; Ahn et al., 2010). It is used as a natural sweetener and food additive in snacks, candies, cookies, seasoning sauce, soy sauce, and drinks (Kitagawa, 2002).

QUALITY AND SAFETY

Use of herbal medicines is an important tradition in rural communities for health and disease prevention (Fennell et al., 2004). However, there is always a risk of ineffectiveness, side effects, or misadministration of toxic plants. Identification, collection, processing, storage and contaminants in the natural plant products have also contributed to the deleterious effect in human body (Street et al., 2008). Quality, safety, and efficacy are the main concerns that must be evaluated in crude or fractionated extracts and their individual compounds and documented before they are prescribed for use as herbal medicines and botanical dietary supplements.

Licorice species have a unique profile of secondary metabolites and distinct biological activities (Li et al., 2016). Glycyrrhizin, present in all three species, is a sweet-tasting saponin that can cause hypertension, sodium salt and water retention, and reduced potassium ion levels (WHO, 1999; Farag et al., 2012), but the aqueous extract has less negative effects compared to glycyrrhizin pure compound (Bernardi et al., 1994; Cantelli-Forti et al., 1994). High doses of glycyrrhizic acid (400 mg/day) have risk of side effects, such as cardiac dysfunction, edema, and hypertension (Størmer et al., 1993).

The chemical ingredients may change during the extraction process of the herbs due to the solvents interaction or heating process is considered for their altered pharmacological effects (Wang et al., 2013). RG combined with Sargassum, Herba Cirsii Japonici, Euphorbia Kansui, and Flos Genkwa might cause cardiac toxicity (Huang et al., 2001). In contrast, RG reduces the toxicity of hydroxysafflor yellow A from Flos Carthami, strychnine and brucine from Semen Strychni, and aconite from Radix Aconiti Lateralis Praeparata (Wang et al., 2013). Therefore, systematic safety evaluation of prolonged use or overdose of compounds and potential drug–drug interactions is needed before the use of herbal medicine as a nutritional supplement and/or therapeutic drugs.

ISOLIQUIRITIGENIN AND LIQUIRITIGENIN

The medicinal plants lies in their chemical constituents to produce physiological actions to have various health benefits in the human body (Sharma et al., 2018). As a result of genetic, ecological, and environmental differences, herbal medicines generally vary in their quality and chemical constituents (Bopana and Saxena, 2007). RG contains at least 400 different chemical constituents including triterpenoid saponins, flavanones, chalcones, coumarines, and their glycosides (Fujii et al., 2014; Kao et al., 2014). As there are many phytochemicals present in each plant, it is necessary to identify a single phytochemical that might be useful in the treatment of human health and diseases (Ramalingam and Kim, 2016a). However, little is known about the effective chemical constituents responsible for biological activities isolated from RG (Ji et al., 2016). More than 25% of the components in RG have been identified as active constituents through oral bioavailability, virtual screening and drug-likeness (Liu et al., 2013).

The chalcone isoliquiritigenin (ILG; 2′,4,4′-trihydroxychalcone) is biosynthetically and structurally interrelated to the flavanone liquiritigenin (LG; 4′,7-dihydroxyflavanone) (Simmler et al., 2013). These two polyphenols are the main bioactive constituents of RG (**Table 1**). ILG is the isomeric precursor of LG (Jayaprakasam et al., 2009). In flavonoid biosynthesis, chalcone isomerase (CHI) promotes enzymatic isomerization through which the ionized 2′-hydroxychalcones (e.g., ILG) is stereochemically converted to 2-S flavanone (e.g., LG). During this process, the ionized chalcone interacts with amino acid side chains in the CHI active site to produce flavanone by high enantioselectivity (Jez et al., 2000; Jez and Noel, 2002). Moreover, studies have reported that ILG and LG are interchangeable by pH and temperature. Chalcones

TABLE 1 | Chemical and interchangeable properties of ILG and LG.

Particulars	ILG	LG
Chemical properties		
Structure	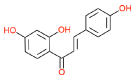	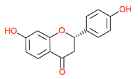
IUPAC name	(E)-1-(2,4-dihydroxyphenyl)-3-(4-hydroxyphenyl)prop-2-en-1-one	(2S)-7-hydroxy-2-(4-hydroxyphenyl)-2,3-dihydrochromen-4-one
MeSH entry term	2′,4′,4-trihydroxychalcone	7,4′-dihydroxyflavanone
CAS number	961-29-5	578-86-9
Molecular formula	$C_{15}H_{12}O_4$	$C_{15}H_{12}O_4$
Molecular weight	256.257 g/mol	256.257 g/mol
Hydrogen bond donor count	3	2
Hydrogen bond acceptor count	4	4
Classification	Flavonoids → chalcones	Flavonoids → flavanones
Interchangeable properties		
Neutral pH[1,2]	ILG ⟶ LG	
Acidic pH[1,2]	ILG ⟶ LG	
Basic pH[3,4]	ILG ⟵ LG	
DMEM or RPMI1640[5] (37°C, 5% CO_2, pH 7.4)	ILG ⟵ (9.6%) / ⟶ (90.4%) LG	
PBS(0–4°C, pH 7.4)[5]	ILG ⟵✕⟶ LG	

ILG, isoliquiritigenin; LG, liquiritigenin; DMEM, Dulbecco's modified Eagle's medium; RPMI 1640, Roswell Park Memorial Institute 1640 medium. [1](Cisak and Mielczarek, 1992); [2](Furlong and Nudelman, 1988); [3](Nudelman and Furlong, 1991); [4](Andújar et al., 2003); [5](Simmler et al., 2013).

undergo rapid cyclization into flavanones at neutral and lower acidic pH whereas flavones isomers undergo a reversible reaction to their chalcones at basic pH. This interconversion between chalcone and flavanone represents temperature dependent isomerization and racemization of these active compounds (Furlong and Nudelman, 1988; Miles and Main, 1989; Nudelman and Furlong, 1991; Cisak and Mielczarek, 1992; Yamín et al., 1997; Andújar et al., 2003). Interestingly, these chemical conditions match the cell culture-based assays also. LG and ILG were incubated in cell culture mediums such as RPMI 1640 or DMEM/F12 supplemented with 5 or 10% heat-inactivated fetal bovine serum maintained at pH around 7.4 in 5% CO_2 at 37°C (with or without MCF-7 cells). ILG began isomerization and reached interconversion ratio of 10.4% ILG and 89.6% LG after 96 h. It suggests that LG and ILG have interconnected biological activities and the biological activity of ILG can be linked to its flavanone LG (Simmler et al., 2013).

PHARMACOLOGICAL ACTIVITIES AGAINST NDDs

Studies on bioactivities revealed that LG and ILG have some valuable pharmacological activities against NDDs.

Antidepressant and Antianxiety Activities

Major depression is a severe life-threatening disorder caused by a complex pathophysiological process related to a person's knowledge (Su et al., 2016; Tao et al., 2016). Lipopolysaccharide (LPS) has been used to cause acute depressive behavior as well as inflammation. Unpredictable chronic mild stress (UCMS) has been used as a model for chronic anxiety/depressive-like behavior. Male ICR mice were pretreated with LG at 7.5 and 15 mg/kg intragastrically for 7 days followed by subcutaneous injection of 0.5 mg/kg LPS. LG pretreatment significantly reduced the LPS-induced significant increase in immobility duration in forced swimming and tail suspension tests. Moreover, levels of the pro-inflammatory cytokines interleukin (IL)-6 (IL-6) and tumor necrosis factor-α (TNF-α) in serum and hippocampus were decreased in the LG group compared with the control LPS group. LG also decreased the expression of p-p65NF-κB, p-IκBα, brain-derived neurotrophic factor (BDNF), and p-TrkB (tropomyosin receptor kinase B). These results indicated that the antidepressant and antianxiety activities of LG might be associated with anti-inflammatory and BDNF/TrkB pathways (Su et al., 2016).

For the chronic type of anxiety, mice were exposed to UCMS for 6 weeks and intragastrically treated with LG (7.5 and 15 mg/kg) from the third week. LG-treated mice showed a reduced immobility time in forced swimming test (FST) and tail suspension test (TST) and a reduction in sucrose preference test (SPT). There were no significant changes in spontaneous locomotor activities. Levels of pro-inflammatory cytokines IL-6, IL-1β, and TNF-α in serum and hippocampus were downregulated by LG treatment. The elevated concentrations of glucocorticoids (GC) in plasma and serum malondialdehyde (MDA) were decreased, together with improved superoxide dismutase (SOD) and catalase (CAT) activity and glutathione (GSH) content. LG also upregulated the concentrations of 5-hydroxytryptamine (serotonin; 5-HT) and

norepinephrine (NE) in hippocampus of mice. Different degrees of attenuation in BDNF and phosphorylated phosphoinositide 3-kinase (PI3K), protein kinase B (Akt), mammalian target of rapamycin (mTOR), and TrkB were observed. Collectively, these data showed that LG could alleviate depressive-like symptoms, possibly through regulation of the PI3K/Akt/mTOR–mediated BDNF/TrkB pathway in the hippocampus (Tao et al., 2016).

Anti-psychostimulant Activities

Dopamine (DA) is a neurotransmitter in the CNS activated by drugs of abuse and psychostimulants such as cocaine (Jang et al., 2008; Jeon et al., 2008). It increases extracellular DA levels from dopaminergic neurons, resulting in spontaneous hyperlocomotion and other neurobehavioral changes. ILG inhibited cocaine-induced DA release in the nucleus accumbens of rat brain (Jeon et al., 2008). In addition, ILG caused alterations of a protooncogene protein c-Fos expression in cocaine-treated rat brain (White and Gall, 1987; Jang et al., 2008). Moreover, ILG treatment was associated with differences in gene expression patterns for 56 proteins including gamma enolase, glial fibrillary acidic protein (GFAP), and ubiquitin carboxyl-terminal hydrolase isozyme L1. These data suggest that ILG might be a potential agent against cocaine-induced neuronal cell injury and death (Jeon et al., 2008).

Activation of dopamine neurons by continued cocaine drug abuse that originate in the ventral tegmental area cause D1 and D2 DA receptor signaling dysfunction then leads to upregulation of c-Fos in the nucleus accumbens and prefrontal cortex (Bardo, 1998; Anderson and Pierce, 2005). Oral administration of ILG for 1 h prior to an injection of cocaine (20 mg/kg, i.p.) in male Sprague-Dawley rats suppressed the extracellular DA level in the nucleus accumbens in a dose-dependent manner and attenuated the expression of c-Fos. Gamma-aminobutyric acid (GABA)-β receptors attenuate the reinforcing effect of drugs. These effects of ILG were entirely stopped by a GABAβ receptor antagonist SCH 80911. These results suggest that ILG might be effective by modulating the GABAβ receptor to block the cocaine effects, and may be used in pharmacotherapy for drug addiction (Jang et al., 2008).

Inhibitory Activities Against Monoamine Oxidases

The monoamine oxidases (MAOA and MAOB) catalyze the oxidative deamination of monoamines in the CNS and peripheral nervous system (PNS). MAO inhibitors are used in therapy for disorders of the CNS (Kanazawa, 1994). Licorice extracts (30 μg/ml) from different specimens were showed inhibitory effects on MAO without characterization of their active constituents (Hatano et al., 1991). LG (IC_{50}: 32 μM) and ILG (IC_{50}: 13.9 μM) inhibited the activity of MAOA in a dose-dependent manner, but non-competitively with the positive control clorgyline (IC_{50}: 0.198 μM). The IC_{50} values for MAOB inhibition for LG, ILG, and positive control deprenyl were 104.6, 47.2, and 0.251 μM, respectively (Pan et al., 2000). These reports indicate that LG and ILG might be major MAO inhibitors in RG and useful for the treatment of anxiety and depression and the treatment and prevention of PD.

Activities Against Parkinson's Disease

PD is a progressive NDD described by the selective loss of dopaminergic (DArgic) neurons and formation of intracellular Lewy bodies such as α-synuclein (α-syn) within the substantia nigra. The α-syn monomers misfold into toxic oligomers of α-syn aggregates that subsequently increase the reactive oxygen species (ROS) level and induce apoptosis, resulting in dopaminergic neuronal injury in PD. *G. uralensis* is one of the main herbs in approximately 40% of traditional medical prescriptions described in pharmacopeias for the treatment of PD. ILG showed inhibitory effects against membrane toxicity in *in vitro* aggregated α-syn and disaggregated preformed mature fibrils in a transgenic *Caenorhabditis elegans* PD model (Liao et al., 2016).

Treatment of dopaminergic neuronal SN4741 cells with ILG at 0.1, 0.5, and 1 μM did not affect cell viability. Pretreatment with ILG (1 μM) attenuated 6-hydroxydopamine (6-OHDA)–induced cell death. ILG pretreatment significantly inhibited 6-OHDA–induced nuclear condensation, fragmentation and apoptosis, in accordance with inhibition of caspase-3 activation. ILG pretreatment completely attenuated generation of ROS and reactive nitrogen species (RNS), in addition to suppressing mitochondrial membrane potential (MMP) dissipation and cytochrome c in the cytosol. The protective effects of ILG appear to be mediated through attenuation of c-Jun N-terminal kinase (JNK), p38, and Akt by modulating the Bcl-2/Bax ratio, whereas the extracellular signal-regulated kinase 1/2 (ERK1/2) signaling pathway is not affected. ILG significantly enhanced production of BDNF, a neurotrophic factor, and reduced the downregulation of BDNF release that increases the survival and the morphological differentiation of dopaminergic neurons (Hwang and Chun, 2012). ILG (1 μM) pretreatment for 20 h followed for 24-h treatment with rotenone (3 μM) or sodium nitroprusside (SNP; 0.4 mM) in PC12 cells significantly improved MMP, adenosine triphosphate (ATP) level, and cell viability as well as cell proliferation (Denzer et al., 2016).

An E3 ubiquitin ligase, RNF146 recognizes its substrates through poly(ADP-ribosyl)ation (PARsylation) of proteins mediated by poly(ADP-ribose) polymerases (PARPs) (Kang et al., 2011; Zhou et al., 2011; Fatokun et al., 2014; DaRosa et al., 2015). RNF146 can disturb PARP1-regulated cellular processes and has neuroprotective activity against *N*-methyl-D-aspartate (NMDA)–induced excitotoxicity, DNA damage, and stroke. LG treatment at 10 μM increased 3-fold of RNF146 mRNA and protein expressions in SH-SY5Y cells and caused a nuclear translocation of endogenous estrogen receptor β (ERβ). Tamoxifen, an ER antagonist, blocked the LG-induced increase in RNF146 expression, indicating that ER activation was responsible for RNF146 induction. In addition, LG failed to induce RNF146 expression in an ERβ deletion model (Kim et al., 2017).

LG up to a concentration of 100 μM did not affect the viability of SH-SY5Y cells. In addition, LG completely eliminated the hydrogen peroxide (H_2O_2)–induced oxidative injury in SH-SY5Y cells. LG treatment (10 μM, 48 h) showed substantial protective effects on cell viability against PD-associated toxins 6-OHDA

(70 μM, 24 h) and rotenone (20 μM, 24 h). In a model of H_2O_2 toxicity, primary mouse cortical neurons exposed to LG showed a 4-fold increase in RNF146 expression and reversed cellular ATP content and mitochondrial membrane potential. H_2O_2 induces robust PARP1 activation, which was largely abolished by LG treatment (Kim et al., 2017). AIMP2, a parkin substrate, enhances cell toxicity, and the levels of PAR-conjugated proteins were significantly reduced by LG-induced RNF146 expression. These effects collectively indicate that LG has various cytoprotective abilities against multiple PARP1-activating stimuli. shRNA-mediated silencing of RNF146 expression annihilated the LG-mediated cytoprotection against H_2O_2 injury in SH-SY5Y cells. Moreover, the shRNA-RNF146 expression knocked down the endogenous RNF146 expression by more than 80% and resulted in a sustained increase in PAR activity and depletion of ATP following H_2O_2 toxicity. Similarly, CRISPR-Cas9–mediated ERβ ablation eliminated the LG-induced neuroprotection against H_2O_2 toxicity. Taken together, these data indicate that LG-induced activations of ERβ and RNF146 inhibit PARP1 and confer neuroprotection (Kim et al., 2017).

As previously reported, LG can penetrate into the brain and exert neuroprotective activity (Yang E.J. et al., 2013). Intraperitoneal administration of LG to mice for 3 consecutive days resulted an increased levels of RNF146 mRNA and protein expressions in ventral midbrain, striatum, and cerebellum. In a 6-OHDA–induced PD-like model, LG pretreatment markedly enhanced tyrosine hydroxylase (TH)-positive DArgic neurons and almost completely inhibited PARP1 activity. Moreover, LG was shown to selectively activate ERβ, but not ERα, thus avoiding aberrant tumor growth *in vivo* (Mersereau et al., 2008) and improving the safety profile of long-term LG treatment for NDDs (Kim et al., 2017). Therefore, ILG and LG are potential candidates against PD in *in vitro* and *in vivo* models and their working mechanisms are diagrammatically represented in **Figure 1**.

Memory Enhancing Activities

N-methyl-D-aspartic acid receptors (NMDARs) in the CNS have been allied to learning and memory (Nakazawa et al., 2004). Administration of LG at 20 mg/kg to ICR mice resulted in an increased level of spontaneous alternation behavior without an alternation in the number of arm entries. LG also significantly improved longer step-through latency time in a passive avoidance test. Regarding cognitive enhancement, LG influenced on hippocampal NMDAR subunits 1, 2A, and 2B expressions in ICR mice. For NMDAR downstream targets, LG significantly increased PSD-95 expression and phosphorylation of Ca^{2+}/calmodulin-dependent protein kinase II (CaMKII), ERK, and cAMP response element binding protein (CREB) in the hippocampus (Ko et al., 2018). LG promotes neurogenesis within the CNS via Notch-2 signaling pathway inhibition by ERβ dependent learning and memory. LG inhibits expression of Notch-2 mRNA and protein in progenitor cells, which may explain the high number of neurons with overexpression of ERβ (Liu et al., 2010b).

Treatment of ICR mice fed a high-fat diet (HFD) with ILG at 30 and 60 mg/kg/day increased the time spent in the target quadrant where the platform was located in a Morris water maze task. ILG also ameliorated the HFD-induced peripheral insulin resistance, which may results to neuronal damage and cognitive deficits, as measured by decreased plasma insulin and glucose levels. ILG treatment decreased the expression of TNF-α, p-JNK, IL-1β, p-IRSSer307 to reverse inflammation and insulin resistance (Ma et al., 2015). This suggests that ILG has protective activity against the HFD caused learning and memory deficits through inhibition of the TNF-α/JNK/IRS pathway. Based on these findings, LG might be used to enhance cognitive performance in neurological disorders such as AD.

Anti-Alzheimer's Activities

Alzheimer's disease is a chronic NDD and most common cause of dementia characterized by the increasing age-related impairment of learning and memory (Weon et al., 2016). The pathological hallmarks of AD are amyloid beta (Aβ) accumulation, senile plaques, neurofibrillary tangles, dystrophic neurites, and neuronal loss (Lin et al., 2012; Ko et al., 2017). LG in the dose range of 0.2–2 μM to rat hippocampal neurons prevented $A\beta_{25-35}$-induced cell death as shown by 3-(4,5-dimethylthiazol-2-yl)-2,5-diphenyltetrazolium bromide (MTT) and lactate dehydrogenase (LDH) detection assays. LG blocked the significant increase in $[Ca^{2+}]_i$ and ROS accumulation induced by $A\beta_{25-35}$. LG also exerted an anti-apoptotic role against $A\beta_{25-35}$ toxicity by increasing the Bcl-2 expression LG probably has some neurotropic actions, including increasing the expression of nuclear respiratory factor 3 (Ntf-3) at both the gene and protein levels. LG downregulated Aβ A4 precursor protein-binding family B member 1 (Apbb-1), a peptide that forms the extracellular amyloid fibrils, explaining the mechanism of inhibited Aβ accumulation in rat primary hippocampal neurons (Liu et al., 2009).

Multiple factors can be attributed to the learning and memory deficiency in AD. LG (2.3, 7, and 21 mg/kg/day) effectively attenuated Aβ-induced learning and memory impairment in Wistar rats determined by Morris water maze and shuttle box test. Treatment with LG had no effect on Aβ expression caused by injection of $A\beta_{25-35}$. LG treatment markedly attenuated the CA1 hippocampal neuronal loss in AD model rats as indicated by microtubule-associated protein 2 (MAP2) immunostaining and Nissl's staining. Moreover, Notch signaling affects CNS, inhibits neuronal differentiation and triggers downstream reactions. The expression of Notch-2 mRNA and protein levels in the AD model rat brains were inhibited by LG treatment (Liu et al., 2010a). Study suggest that LG may serve as a NeuroSERM, an molecule that acts on estrogen mechanisms in the brain while avoiding peripheral estrogen receptors (Liu et al., 2009).

Treatment of Tg2576 mice with LG at 30 mg/kg showed a greater improvement in learning and memory than doses of 3 and 10 mg/kg in Morris water maze and shuttle box test. LG did not alter the levels of amyloid precursor protein (APP); however, levels of an oligomeric form of Aβ protein in Tg2576 mice were significantly reduced in a dose-dependent manner. GFAP levels by immunostaining and immunoblotting were decreased significantly by treatment with 10 and 30 mg/kg LG compared with vehicle treatment in Tg2576 mice. Levels of the active

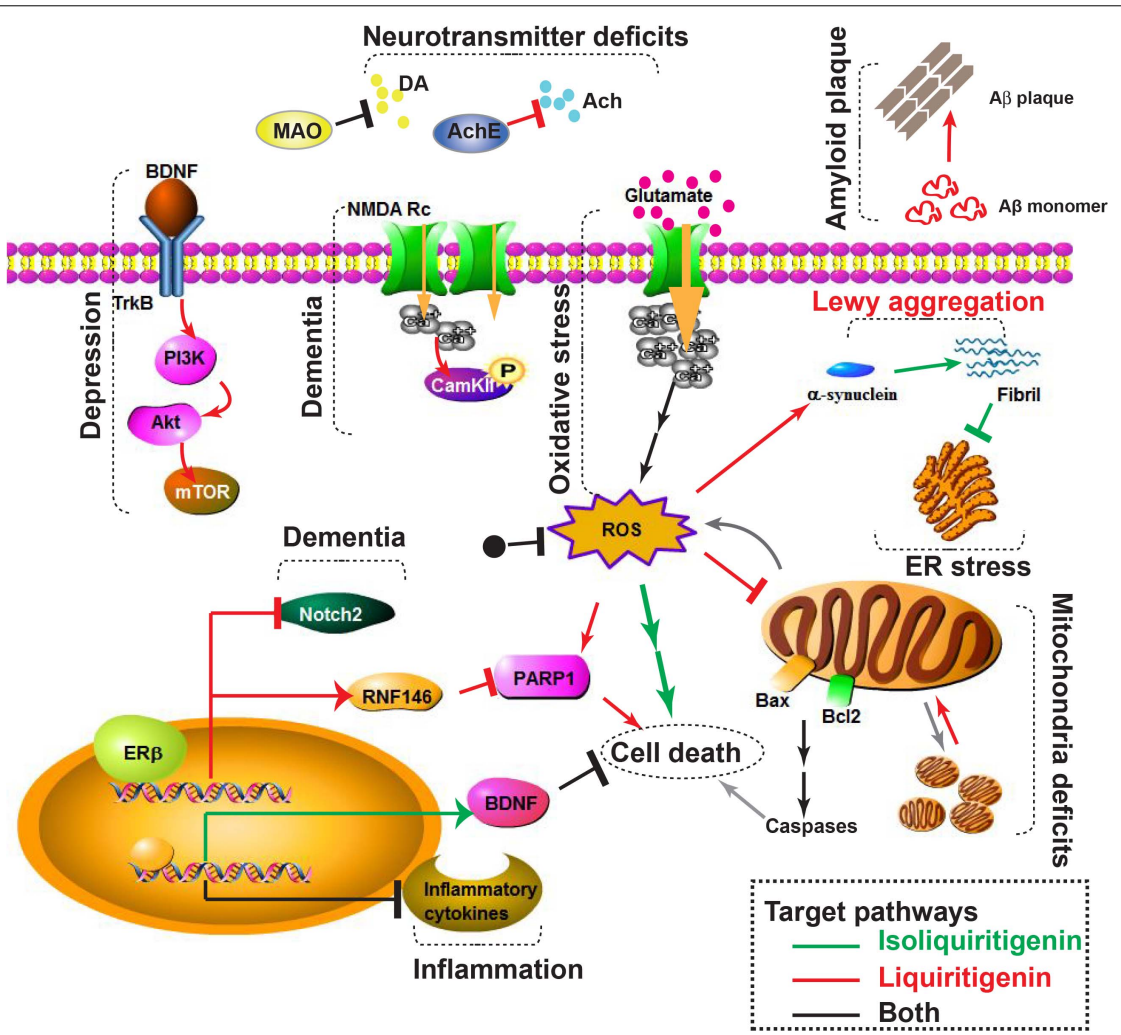

FIGURE 1 | Diagrammatic representation of pathological phenotypes (depression, dementia, inflammation, oxidative stress, amyloid plaque, neurotransmitter deficits, Lewy aggregation, ER stress, mitochondrial deficits, and cell death) and underlying molecular pathways that could be involved in Alzheimer's and Parkinson's disease. Pathways regulated by isoliquiritigenin (ILG) and liquiritigenin (LG) were labeled as green and red lines, respectively. Pathways targeted by both ILG and LG were colored as black line. Arrows (↓) denote stimulation and bars (⊥) denote inhibition by ILG (green), LG (red), and both (black). PD related pathways include MAO (monoamine oxidase), and Lewy aggregation. AD related pathways include amyloid plaque formation and AChE (acetylcholine esterase). Other pathological processes are related to both AD and PD, thus could be therapeutic targets by ILG or LG. The scheme was generated by using Pathway Builder Tool.

fragment of Notch-2^{IC} were significantly decreased in LQ-treated Tg2576 mice (Liu et al., 2011).

Mitochondria are powerhouses that continuously undergo fusion, fission, transport, and degradation for regulation of their functions. Mitochondrial fission is controlled by dynamin-related protein-1 (DRP-1) while fusion is regulated by mitofuscin 1 and 2 (Mfn1/2) and optic atrophy protein 1 (Opa1). LG treatment of SK-N-MC cells stably expressing YFP resulted in highly elongated and aggregated mitochondria, suggesting that LG induces mitochondrial fusion in a dose- and time-dependent manner (Jo et al., 2016). Pretreatment with LG effectively restored mitochondrial fragmentation in Mfn1 and Mfn2 knockout MEF cells, but had no effect on Opa1 knockout cells. Treatment of SK-N-MC/mito-YFP with LG inhibited Aβ-induced mitochondrial fragmentation. These data suggest that LG treatment might be a best therapeutic strategy against mitochondrial dysfunction (Jo et al., 2016).

Sopolamine is a muscarinic cholinergic receptor antagonist that causes disturbances in the cholinergic system in association with cognitive decline (Haider et al., 2016) by formation of ROS and free radicals (El-Sherbiny et al., 2003). The scopolamine-induced spontaneous alternation behavior, cognitive deficit, and discrimination index of recognition memory were significantly reversed by LG at 20 mg/kg in 4-week-old male CD-1 mice. Scopoamine significantly increased the level of acetylcholinesterase (AChE) and MDA whereas treatment with LG inhibited these increases, suggesting that LG improves cognitive dysfunction. Moreover, LG treatment ameliorated the scopolamine-induced hippocampal expression of BDNF, ERK, and CREB related to cognitive function. Therefore, LG may have

potential learning and memory enhancement effects in mice (Ko et al., 2017). The above reports show that the ERβ agonist LG has a promising future as a principal active constituent for the treatment of AD.

Neuroprotection Against Glutamate-Induced Toxicity

High concentrations of neurotransmitter glutamate can persuade neuronal cell death by receptor-induced cytotoxicity or ROS-mediated oxidative stress, leading to the learning and memory deficits in NDDs (Yang E.J. et al., 2013). Oxidative stress can be induced by 5 mM glutamate in the mouse hippocampal neuronal cell line, HT22, which lacks ionotropic glutamate receptors. Glutamate concentrations greater than millimolar levels can cause oxidative stress through inhibition of cysteine uptake, leading to glutathione reduction in the cells (Murphy et al., 1989).

Pretreatment with LG (10 and 50 μM) and ILG (5 and 10 μM) for 12 h showed protective efficacy against cell cytotoxicity and ROS production induced by 12-h treatment with glutamate. LG effectively recovered the glutamate and calcium chloride ($CaCl_2$) toxicity in a concentration-dependent manner (Yang E.J. et al., 2013). The Bid level was increased and phosphorylation of mitogen-activated protein kinases (MAPKs) upon glutamate induction was decreased by 50 μM LG or 5 μM ILG (Yang E.J. et al., 2013; Yang et al., 2016). These results showed that LG and ILG effectively prevented glutamate-induced toxicity by attenuation of mitochondrial dysfunction, and may help to prevent NDDs.

Neuroprotection Against Stroke

Stroke, with predominant clinical manifestations of ischemia of the brain and hemorrhagic injury, is a major cause of mortality worldwide (Li et al., 2015). The blood-brain barrier (BBB) is a diffusion barrier that selectively blocks influx and efflux of most compounds between blood and brain (Ballabh et al., 2004). However, following a stroke the BBB is disrupted and LG and ILG were detected in plasma and brain tissue with the onset of reperfusion in male Sprague-Dawley rats, suggesting that LG and ILG are able to penetrate the BBB and become distributed in the brain tissue, where they exhibit a protective effect (Li et al., 2015). Zhan and Yang demonstrated that ILG exerted protective effects against rat model of transient middle cerebral artery occlusion (MCAO)-induced focal cerebral ischemia (Zhan and Yang, 2006).

Neuroprotection Against Brain Glioma

Gliomas are the most common and extremely serious type of primary intracranial neoplasm results in higher mortality and morbidity (Lacroix et al., 2001). The loss of ERβ expression in high-grade glioma tumors suggests the potential tumor suppressor role of ERβ. Treatment of temozolomide (TMZ)-resistant U138 glioma cells with LG significantly increased ERβ expression and synergistically inhibited the U138 glioma cells to TMZ-induced proliferation. In addition, ERβ knockdown or activation of the PI3K/Akt/mTOR pathway by IGF-1 eradicated the function of LG (Liu et al., 2015). These results suggest that the ERβ agonist LG significantly inhibits the PI3K/Akt/mTOR pathways representing a possible therapy for TMZ susceptibility in gliomas.

Activity Against HIV-1-Associated Neurocognitive Disorders

HIV-1 in CNS results in an array of deficits known as HIV-1-associated neurocognitive disorders (HAND) allied with dendritic simplification and synaptic loss (Antinori et al., 2007). Treatment with HIV-1 transactivating protein (Tat) at 50 nM for 24 h resulted in a significant reduction of F-actin-labeled dendritic puncta and loss of dendrites in brain primary neuronal cultures. LG treatment against Tat 1-86B toxicity protects cell viability, prevents cumulative injury to the dendritic network, and aids recovery from HAND (Bertrand et al., 2014). Results suggest that LG acts via an ERβ-dependent mechanism to avert synaptodendritic damage induced by HIV-1 Tat 1-86B (Bertrand et al., 2014).

Anti-nociception Activities

Transient receptor potential melastatin 3 (TRPM3) is a calcium-permeable nonselective cation channel member of the large superfamily of TRP ion channels (Straub et al., 2013) expressed in sensory neurons of trigeminal and dorsal root ganglia (DRG). Activation of TRPM3 by the neurosteroid pregnenolone sulfate (PregS) and heat is linked to neuronal myelination (Hoffmann et al., 2010). Incubation of human embryonic kidney 293 (HEK293) cells stably expressing TRPM3 (HEK_{mTRPM3}) with LG at 25 μM abrogated PregS (35 μM)-induced $[Ca^{2+}]_i$ entry. LG elicited a half-maximal block with an IC_{50} of 500 nM. Moreover, LG had no impact on capsaicin (2 μM)-induced transient receptor potential vanilloid-related (TRPV)1 activation, but concentration dependently inhibited allyl isothiocyanate (AITC)-induced TRPA1 activation. In addition, TRPM7-dependent inward or outward currents were affected by LG (20 μM) treatment in HEK293 cells without impairing cell proliferation and viability. Moreover, activation of TRPM3 in DRG neurons is linked to thermosensation. LG at 10 μM strongly counteracted the PregS-induced calcium entry in rat DRG neurons, suggesting that its TRP channel-inhibiting properties and/or TRPM3 inhibition may be useful in the development of novel and tolerable analgesic therapies (Straub et al., 2013).

Neurogenesis Activities

Recent studies focused on the identification of compounds such as phytoestrogens that are neuro-selective estrogen receptor agonists (NeuroSERMs) (Zhao et al., 2005) and mimic the actions of estrogen in the brain but have insignificant effects on non-neuronal estrogen-responsive tissues (Zhao et al., 2002). ERβ is also reported for learning and memory functions (Liu et al., 2008; Walf et al., 2008). Liu et al. (2010a) reported the effects of LG on newborn Sparague-Dawley rat brain-derived progenitor cells. Study reported that stem and progenitor cells were differentiated into mature neurons by inhibition of Notch proteins (Woo et al., 2009). Decreased Notch-2 mRNA and

protein expression in progenitor cells after LG treatment explains the increased neurogenesis and higher number of neurons. In addition, LG promotes neurogenesis by ERβ dependent Notch-2 protein inhibition in SH-SY5Y cells. ERβ gene silencing using RNAi indicated the relationships between Notch receptors, ERs, and neurogenesis (Liu et al., 2010b).

OTHER PHARMACOLOGICAL ACTIVITIES

In addition to the neuropharmacological activities of ILG and LG mentioned above, numerous studies have revealed additional potential therapeutic effects such as radical scavenging, antimicrobial, anti-inflammatory, and antitumor activities.

Radical Scavenging Activities

Reactive oxygen species induced by oxidative stress result in damage to cellular proteins, lipids, and nucleic acids. RG extract G9315 containing six flavonoids showed good radical scavenging activity against superoxide ($O_2^{\cdot -}$), hydroxyl ($^{\cdot}OH$), H_2O_2, and singlet oxygen ($^1O_2$) species (Fu and Liu, 1995). In structure-activity relationship studies ILG showed higher activity than LG (Zhang et al., 2012). The $^{\cdot}OH$ and $^{\cdot}OOH$ radical scavenging activity of ILG was by radical adduct formation and that of LG was through hydrogen atom transfer methods. ILG showed more efficient radical scavenging activity than LG because of its nearly planar conjugated conformation (Wang et al., 2017). LG at 100 μM showed the potential to scavenge 2,2-diphenyl-1-picrylhydrazyl (DPPH) free radicals (Yu et al., 2015).

Antibacterial Activities

The antibacterial activity of ILG and LG have similar minimal inhibitory concentration (MIC) at 25 μg/ml against *Mycobacterium tuberculosis* (Chokchaisiri et al., 2009). ILG inhibited growth of *Mycobacterium bovis* at 50 μg/ml (Brown et al., 2007), whereas 250 μg/ml was needed for growth inhibition of *Staphylococcus aureus*, *Staphylococcus epidermidis*, and *Staphylococcus hemolyticus* (de Barros Machado et al., 2005).

Estrogen Receptor Signaling Activities

The ERα and ERβ are nuclear transcription factors that regulate the transcription of target genes (Paterni et al., 2015). LG in RG shows 20-fold greater affinity for ERβ than ERα determined by competitive binding assays. Although LG binds ERα, it induced minimal transcriptional activation of receptor genes at higher concentration of 2.5 μM. From above results, steroid receptor coactivator-2 (SRC-2) engaged to ER target genes proposing that transcriptional potency and ligand binding are not interrelated after LG treatment (Mersereau et al., 2008). In another study, LG treatment to luciferase reporter plasmid transfected MCF-7 and T47D cells induced a higher differentiation at 5×10^{-7} M (Lecomte et al., 2017).

Anti-inflammatory Activities

Inflammation is an immune system response against harmful stimuli and is characterized by redness, swelling, heat, and pain and macrophages play a vital role in the inflammatory response (Iontcheva et al., 2004). ILG and LG significantly inhibited nitric oxide (NO) production in RAW 264.7 macrophages. LG (30 μM) and ILG (1.6 μM) almost completely suppressed the LPS (1 μg/ml)-induced inducible nitric oxide synthase (iNOS) expression by inhibiting NF-κB/IκBa activation in RAW264.7 macrophages in a dose-dependent manner (Kim J.Y. et al., 2008; Kim Y.W. et al., 2008). In addition, ILG suppressed the LPS-induced phosphorylation of ERK and P38 MAPK, but not JNK1/2 (Kim J.Y. et al., 2008). Treatment of rats with LG (50 mg/kg/day for 3 days p.o. or 15 mg/kg/day for 2 days i.v.) significantly reduced paw swelling induced by carrageenan (Kim Y.W. et al., 2008). These results suggest that LG and ILG have been considered as possible anti-inflammatory agents.

The anti-inflammatory properties of LG were studied in a LPS-stimulated BV-2 microglial cell model and *tert*-butyl hydrogen peroxide (*t*-BHP)-treated ICR male mice model. LG (25, 50, and 100 μM) inhibited LPS-stimulated NO levels in a dose-dependent manner. LG inhibited expressions of iNOS, Cox-2, and pro-inflammatory genes IL-1β and IL-6, but had no effect on TNF-α expression. t-BHP toxicity induced a significant increase in alanine aminotransferase (ALT) and aspartate aminotransferase (AST) levels in serum and TNF-α, IL-1β, IL-6 mRNA expression in the liver of mice, whereas these levels were diminished by LG treatment (Yu et al., 2015). These results suggest that LG inhibits various inflammatory mediators and suppresses inflammation in the liver.

Anti-periodontitis Activities

Periodontal diseases (gum disease) and dental caries (tooth decay) are the most common human oral infections. *Mutans streptococci* such as *Streptococcus mutans* and *Streptococcus sobrinus* are associated with dental caries through their aciduric, acidogenic, and adhesion properties (Liljemark and Bloomquist, 1996). Different concentrations of ILG and LG were used to determine the MICs for *P. gingivalis*, *F. nucleatum*, *P. intermedia*, *S. mutans*, and *S. sobrinus*. ILG and LG displayed significant growth inhibition in gram-negative periodontal bacteria, but had no effect on gram-positive streptococci. ILG was found to be a effective inhibitor of *P. gingivalis* collagenase and MMP-9 compared with LG. ILG also suppressed dimerization of the inflammatory mediator toll-like receptor 4 (TLR4), which correlated with NF-κB p65 inhibition, activator protein-1 (AP-1) activation and subsequently reduced expression of cytokines in LPS-induced inflammation (Feldman et al., 2011).

Anti-asthmatic Effects

Asthma is a common long-term inflammatory airway disease characterized by the polarized Th2 cell secretion of Th2 cytokines (Yang E.J. et al., 2013). *G. uralensis* was reported for its protective responsiveness in asthma patients (Wang et al., 1998). An anti-asthma formula, ASHMI^{TM}, containing *G. uralensis*, has been reported for improvement in lung function and reduced airway hyperresponsiveness in allergic asthma (Wen et al., 2005). In addition, LG and ILG had high ability in eotaxin secretion suppression compared to glycyrrhizin (Jayaprakasam et al., 2009). Yang N. et al. (2013) reported that the ASHMI

formula contains LG, ILG, and 7,4′-DHF. These flavonoids suppress CA-stimulated synthesis of Th2 cytokine and levels of IL-4 and IL-5 in D10 cell culture media supernatants in a concentration-dependent manner without affecting cell viabilities (Yang N. et al., 2013).

Anti-diabetic Activities

Diabetes is a major metabolic disease with a rapidly increasing prevalence worldwide. In type 2 diabetes, a chronic increase in lipotoxicity and insulin deficiency contributes to increased beta-cell dysfunction and death (Oh, 2015). LG treatment (5 μM) to rat INS-1 insulinoma cells showed increased cell viability and insulin secretion. LG also increased cell viability and decreased apoptosis associated with palmitate (PA)-induced lipotoxicity. In addition, LG suppressed PA-induced endoplasmic reticulum stress markers such as C/EBP homologous protein (CHOP), eukaryotic initiation factor 2α (eIF-2α) and protein kinase RNA-like endoplasmic reticulum kinase (PERK), but had no effect on X-box binding protein (XBP), JNK and activating transcription factor 6 (ATF-6). In addition, LG activated phosphorylation of Akt by ER and subsequently inactivated the PERK pathway, highlighting its therapeutic value in the prevention of diabetes progression (Bae et al., 2018).

Diabetes is characterized by abnormally high blood glucose levels. Oral administration of ILG (10 and 20 mg/kg) to streptozotocin (STZ)-induced diabetic rats for 2 weeks or 2.5 and 5 μM to glucose (30 mM)-insulted N2a cells significantly caused an activation of sirutin (SIRT1, a metabolic sensor of the cellular NAD^+/NADH ratio) in a dose-dependent manner. In addition, ILG mimics the effects of PGC-1α-mediated mitochondrial biogenesis, calorie restriction, 5′ AMP-activated protein kinase (AMPK)–mediated autophagy and Forkhead box O3a (FOXO3a) mediated stress resistance to counteract experimental diabetic neuropathy (Yerra et al., 2017).

ILG was found to be effective at 100 mg/kg b.w. after 120 min in an oral glucose tolerance test (OGTT), but LG was inefficient in lowering blood glucose levels in the STZ-induced diabetic mice model. In the glucose tolerance test, improvement was observed for ILG at 200 mg/kg b.w. post-administered after 15, 30, 60, 90, and 120 min. Hyperglycemic albino mice treated with 200 mg/kg b.w. of ILG for 14 days showed significant (53%) recovery of random blood glucose level and significant modification of liver glycogen content to 49.92% (Gaur et al., 2014).

Anti-osteoporosis Activities

Osteoporosis is a disease results from altered bone mass have impact on life expectancy and the quality of life (Lane and Kelman, 2003). Osteoblasts can markedly enhance bone formation (Choi, 2012). LG stimulated cell growth of MC3T3-E1 cells in addition to increasing calcium ion deposition, ALP activity and collagen content, suggesting that LG may induce early and later phases of osteogenic differentiation. The increased osteoblast function was also associated with LG-induced GSH content. In osteoblastic MC3T3-E1 cells, antimycin A (70 μM)–induced production of ROS, cytokines TNF-α and IL-6 and receptor activator of nuclear factor kappa-B ligand (RANKL) was significantly inhibited by treatment with LG (0.04, 0.4, and 4 μM) (Choi, 2012). These data suggest that LG may act as a potential therapeutic candidate against oxidative stress-induced dysfunction in osteoblasts.

Hepatoprotective Activities

Cadmium (Cd), an environmental heavy metal, largely accumulates in the liver and kidney and induces pulmonary, hepatic, and renal tubular diseases. LG (10–100 μM) treatment to Cd (10 μM) or Cd (1 μM) + buthionine sulfoximine (BSO; 50 μM) exposed H4IIE rat-derived hepatocyte cells showed more active in protecting cells than ILG (0.1–10 μM) treatment. LG also prevented the GSH content reduction induced by BSO, suggesting that LG, but not ILG, have cytoprotection in Cd-induced cellular damages (Kim et al., 2004).

Nitric oxide, an inflammatory mediator, plays a pathophysiological role in various diseases (Colasanti and Suzuki, 2000). Treatment of primary hepatocytes isolated from the liver of male Wistar rats with RG extract and its constituents ILG and LG significantly blocked NO levels in the presence of IL-1β without cytotoxicity. ILG showed an IC_{50} of 11.9 μM. Furthermore, ILG and LG reduced the levels of both iNOS mRNA and protein in primary rat hepatocytes. Moreover, TNF-α and IL-6 mRNA levels were downregulated by ILG and LG, supporting anti-inflammatory effects in hepatocytes (Tanemoto et al., 2015).

The toxicity of acetaminophen, mostly used as analgesic and antipyretic agent, results in massive hepatic necrosis and causes major morbidity and mortality (Zakin and Boyer, 1990). Sprague-Dawley rats were orally administered LG dissolved in 40% PEG administered and then given a single oral dose of acetaminophen in 40% PEG (1.2 g/kg b.w.). LG treatment at 50 mg/kg/day p.o. for 4 days or 15 mg/kg i.v. for 2 days significantly reduced the plasma ALT, improved plasma LDH, and ameliorated liver necrosis induced by acetaminophen. LQ administered i.v. had greater protective effects than p.o. against acetaminophen toxicity (Kim et al., 2006). In addition, LG showed a choleretic effect by increased hepatic bile flow, phase II enzymes and hepatic transporters against in a GalN/LPS-induced rat hepatitis model (Kim et al., 2009).

Phase II drug metabolism enzymes, nuclear receptors and other transcription factors in liver stimulates the toxic substances detoxification and excretion processes. Nuclear factor erythroid 2–related factor 2 (Nrf2) plays major role in drug disposition and phase II drug metabolism enzymes (Zollner et al., 2010). Nrf2 dissociates from Keap1 and translocates into the nucleus leading to expression of target genes under stress conditions. ILG significantly induces Nrf2, UGT1A1, BSEB, MRP2 and GCLS in HepG2 cells. In addition, ILG induces UGT1A1, GCLC, and MRP2 in Nrf2 WT mice but not in Nrf2 KO mice, concluding that ILG has Nrf2-dependent protective activities (Gong et al., 2015).

Hepatocellular carcinoma (HCC) is one of the most common malignant tumors with low recovery rates, and currently available conventional and modified therapies are rarely effective (Kern et al., 2002). Treatment of the human hepatocarcinoma cell line SMMC-7721 with LG resulted in a concentration-dependent decrease in cell viability and apoptosis. The free radical scavenger, *N*-acetyl-cysteine (NAC),

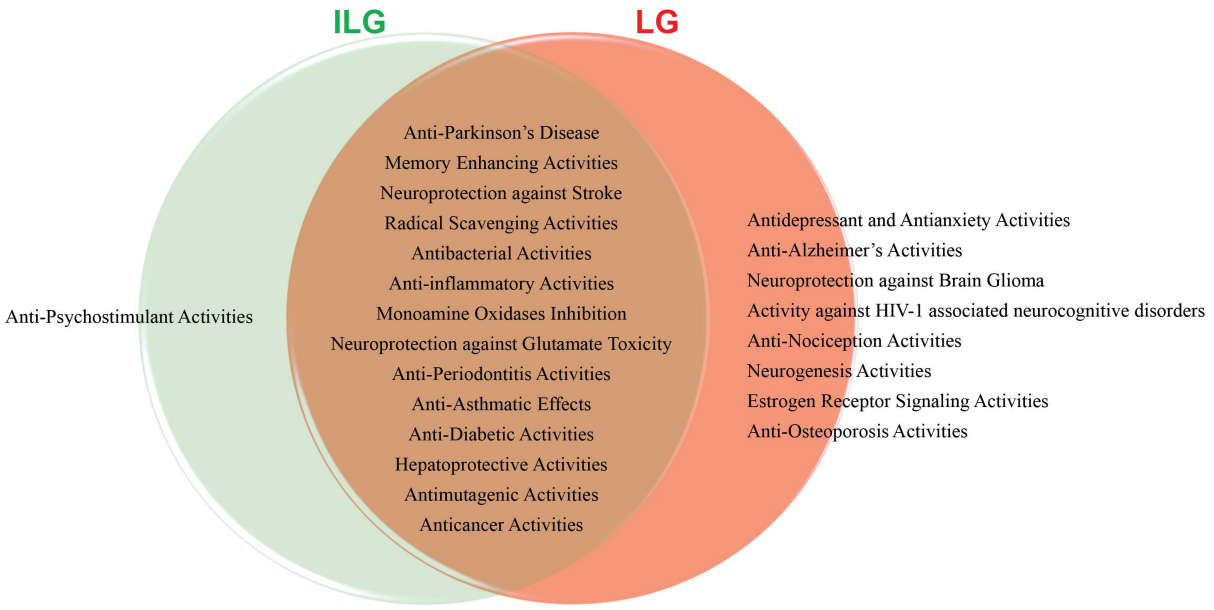

FIGURE 2 | Diagrammatic representation of various pharmacological activities of isoliquiritigenin (ILG) and liquiritigenin (LG).

suppressed both LG-induced apoptosis and ROS production. Expression of caspase-3, the principal caspase associated with apoptotic nuclear changes, significantly increased in a time-dependent manner, with a 7-fold induction at 72 h after LG (0.4 mM) treatment. Furthermore, LG treatment increased tumor suppressor p53 protein and decreased anti-apoptotic Bcl-2 protein through ROS production and mitochondrial membrane potential loss, in agreement with decreased activities of antioxidant enzymes SOD, GSH, and glutathione peroxidase (GPx) in SMMC-7721 cells. These effects have been proven to be cell-specific as LG at 0.4 mM did not cause significant cell death in human hepatic L-02 cells (Zhang et al., 2009).

Anti-mutagenic and Anti-cancer Activities

The human osteosarcoma U2OS cell line (which does not express endogenous ERs), human breast MCF-7 cancer cell line (which express ERα), and human cervical HeLa cancer cell line were treated with different doses of LG (0.5, 1, 2, and 2.5 μM). LG treatment at 2 μM stimulated the ERE-tk-luciferase, and ER regulatory elements CECR6, NKG2E, and NKD in ERβ transfected cells due to its greater selectivity, but not with ERα transfected cells. LG (2 mg; 2.5 μl/h) infused for 30 days to nude mice did not involve in uterine enlargement or MCF-7 breast cancer cells induced xenograft (Mersereau et al., 2008). RG extract G9315 containing ILG and LG significantly inhibited the Cytoxan induced mouse bone-marrow micronuclei formation suggesting an antimutagenic activity (Fu and Liu, 1995).

LG was shown to inhibit breast (MDA-MB-231, MCF7, SKBR3) and colon (LoVo, HCT) cancer cells proliferation (Paterni et al., 2015). LG also showed an IC_{50} of 88.3 μM *in vitro* in glioma U87 cells and in an *in vivo* study of U87 glioma cells induced nude mice xenografts (Paterni et al., 2015). ILG treatment blocked the cell growth and induced apoptosis on mouse RCN-9 and human COLO-320DM colon cancer cells (Takahashi et al., 2004). Furthermore, ILG treated at 15 ppm *at libitum* to azoxymethane (AOM; 10 mg/kg b.w. s.c.)-induced colon carcinogenesis in ddY mice inhibited the preneoplastic aberrant crypt foci (ACF) induction (Baba et al., 2002). ILG mixed at 100 ppm in diet fed against AOM (15 mg/kg b.w., 3 times/weekly) induced for 3 weeks effectively reduced the ACF in the colon of male F344 rats (Takahashi et al., 2004).

CONCLUSION AND FUTURE PROSPECTS

Aging process is considered major risk factor for age-related diseases such as AD and PD become main concerns in the challenge to improve health. Aging effects cause a cascade of stressors that weaken energy metabolism, mitochondrial functions, and gene expression. The current synthetic drugs treatments to multi-functional age-related NDDs have proven ineffective in curing and have certain side effects. On the other hand, botanical drugs are multicomponent complex systems that might interact with multiple signaling pathways and targets in the human body. This new era on botanical research has provide many opportunities to develop new therapies for patients with age-related diseases. RG have been used widely in traditional medicines throughout the world because of its rich components such as triterpenoids, flavanones, chalcones, coumarines and their glycosides. These active components suggest that RG may be an effective herb for the treatment of different

kinds of disease. The main bioactive constituents ILG and LG showed prominent effects in AD, PD and other NDDs models by numerous *in vitro* and *in vivo* experimental studies. The various pharmacological abilities of ILG and LG clearly establish a protective role in human health and disease model(s) (**Figure 2**). The chemically interconnected structures of ILG and LG attributed for their linked bioactivities offers the greatest potential as therapeutic compounds for age-related degenerative diseases. From this viewpoint, authenticating the traditional herbal remedies will provide clues in the search of new active single specific or combined compounds in the future and scientific evaluation in clinical development use will support their use in health care systems. Therefore, medicinal plants and their active constituents are an excellent source of information in the discovery of new therapeutics to improve human health and lifespan.

AUTHOR CONTRIBUTIONS

MR, YL and Y-IL searched the related literature, conceptualized, designed and wrote the manuscript. HK conceptualized, designed the figures in the manuscript. All authors edited and revised the manuscript.

FUNDING

This research was supported by grants from DGIST (2018010112, 18-LC-01 and 18-BT-01) and the NRF (NRF-2017M3C7A1043848), which is funded by the Korea Ministry of Science, ICT, and Future Planning (MSIP). This work was also supported by Samsung Research Funding & Incubation Center for Future Technology (SRFC-IT1701-10).

REFERENCES

Abushouk, A. I., Negida, A., Ahmed, H., and Abdel-Daim, M. M. (2017). Neuroprotective mechanisms of plant extracts against MPTP induced neurotoxicity: future applications in Parkinson's disease. *Biomed. Pharmacother.* 85, 635–645. doi: 10.1016/j.biopha.2016.11.074

Ahn, J. Y., Kim, S., Jung, S. E., and Ha, T. Y. (2010). Effect of licorice (*Glycyrrhiza uralensis* fisch) on amyloid-β-induced neurotoxicity in PC12 cells. *Food Sci. Biotechnol.* 19, 1391–1395. doi: 10.1007/s10068-010-0198-4

Anderson, S. M., and Pierce, R. C. (2005). Cocaine-induced alterations in dopamine receptor signaling: implications for reinforcement and reinstatement. *Pharmacol. Ther.* 106, 389–403. doi: 10.1016/j.pharmthera.2004.12.004

Andújar, S. A., Filippa, M. A., Ferretti, F. H., and Blanco, S. E. (2003). Isomerization of 4′-methoxy-flavanone in alkaline medium. Determination of the enolate formation constant. *J. Mol. Struct.* 636, 157–166. doi: 10.1016/S0166-1280(03)00474-3

Antinori, A., Arendt, G., Becker, J. T., Brew, B. J., Byrd, D. A., Cherner, M., et al. (2007). Updated research nosology for HIV-associated neurocognitive disorders. *Neurology* 69, 1789–1799. doi: 10.1212/01.WNL.0000287431.88658.8b

Asthana, J., Mishra, B. N., and Pandey, R. (2016). Acacetin promotes healthy aging by altering stress response in *Caenorhabditis elegans*. *Free Radic. Res.* 50, 861–874. doi: 10.1080/10715762.2016.1187268

Baba, M., Asano, R., Takigami, I., Takahashi, T., Ohmura, M., Okada, Y., et al. (2002). Studies on cancer chemoprevention by traditional folk medicines XXV. Inhibitory effect of isoliquiritigenin on azoxymethane-induced murine colon aberrant crypt focus formation and carcinogenesis. *Biol. Pharm. Bull.* 25, 247–250. doi: 10.1248/bpb.25.247

Bae, G. D., Park, E. Y., Baek, D. J., Jun, H. S., and Oh, Y. S. (2018). Liquiritigenin prevents palmitate-induced beta-cell apoptosis via estrogen receptor-mediated AKT activation. *Biomed. Pharmacother.* 101, 348–354. doi: 10.1016/j.biopha.2018.02.097

Ballabh, P., Braun, A., and Nedergaard, M. (2004). The blood-brain barrier: an overview: structure, regulation, and clinical implications. *Neurobiol. Dis.* 16, 1–13. doi: 10.1016/j.nbd.2003.12.016

Bardo, M. T. (1998). Neuropharmacological mechanisms of drug reward: beyond dopamine in the nucleus accumbens. *Crit. Rev. Neurobiol.* 12, 37–67. doi: 10.1615/CritRevNeurobiol.v12.i1-2.30

Bernardi, M., D'intino, P. E., Trevisani, F., Cantelli-Forti, G., Raggi, M. A., Turchetto, E., et al. (1994). Effects of prolonged ingestion of graded doses of licorice by healthy volunteers. *Life Sci.* 55, 863–872. doi: 10.1016/0024-3205(94)90042-6

Bertrand, S. J., Mactutus, C. F., Aksenova, M. V., Espensen-Sturges, T. D., and Booze, R. M. (2014). Synaptodendritic recovery following HIV Tat exposure: neurorestoration by phytoestrogens. *J. Neurochem.* 128, 140–151. doi: 10.1111/jnc.12375

Bopana, N., and Saxena, S. (2007). *Asparagus racemosus*–ethnopharmacological evaluation and conservation needs. *J. Ethnopharmacol.* 110, 1–15. doi: 10.1016/j.jep.2007.01.001

Brown, A. K., Papaemmanouil, A., Bhowruth, V., Bhatt, A., Dover, L. G., and Besra, G. S. (2007). Flavonoid inhibitors as novel antimycobacterial agents targeting Rv0636, a putative dehydratase enzyme involved in *Mycobacterium tuberculosis* fatty acid synthase II. *Microbiology* 153, 3314–3322. doi: 10.1099/mic.0.2007/009936-0

Cantelli-Forti, G., Maffei, F., Hrelia, P., Bugamelli, F., Bernardi, M., D'intino, P., et al. (1994). Interaction of licorice on glycyrrhizin pharmacokinetics. *Environ. Health Perspect.* 102, 65–68. doi: 10.1289/ehp.94102s965

Cao, Y., Wang, Y., Ji, C., and Ye, J. (2004). Determination of liquiritigenin and isoliquiritigenin in *Glycyrrhiza uralensis* and its medicinal preparations by capillary electrophoresis with electrochemical detection. *J. Chromatogr. A* 1042, 203–209. doi: 10.1016/j.chroma.2004.05.049

Choi, E. M. (2012). Liquiritigenin isolated from *Glycyrrhiza uralensis* stimulates osteoblast function in osteoblastic MC3T3-E1 cells. *Int. Immunopharmacol.* 12, 139–143. doi: 10.1016/j.intimp.2011.11.003

Chokchaisiri, R., Suaisom, C., Sriphota, S., Chindaduang, A., Chuprajob, T., and Suksamrarn, A. (2009). Bioactive flavonoids of the flowers of *Butea monosperma*. *Chem. Pharm. Bull.* 57, 428–432. doi: 10.1248/cpb.57.428

Cisak, A., and Mielczarek, C. (1992). Practical and theoretical aspects of flavanone-chalcone isomerisations. *J. Chem. Soc. Perkin. Trans.* 2, 1603–1607. doi: 10.1039/P29920001603

Colasanti, M., and Suzuki, H. (2000). The dual personality of NO. *Trends Pharmacol. Sci.* 21, 249–252. doi: 10.1016/S0165-6147(00)01499-1

Cole, J. H., and Franke, K. (2017). Predicting age using neuroimaging: innovative brain ageing biomarkers. *Trends Neurosci.* 40, 681–690. doi: 10.1016/j.tins.2017.10.001

Cragg, G. M., and Newman, D. J. (2013). Natural products: a continuing source of novel drug leads. *Biochim. Biophys. Acta* 1830, 3670–3695. doi: 10.1016/j.bbagen.2013.02.008

da Costa, J. P., Vitorino, R., Silva, G. M., Vogel, C., Duarte, A. C., and Rocha-Santos, T. (2016). A synopsis on aging-Theories, mechanisms and future prospects. *Ageing Res. Rev.* 29, 90–112. doi: 10.1016/j.arr.2016.06.005

DaRosa, P. A., Wang, Z., Jiang, X., Pruneda, J. N., Cong, F., Klevit, R. E., et al. (2015). Allosteric activation of the RNF146 ubiquitin ligase by a poly(ADP-ribosyl)ation signal. *Nature* 517, 223–226. doi: 10.1038/nature13826

Davis, E. A., and Morris, D. J. (1991). Medicinal uses of licorice through the millennia: the good and plenty of it. *Mol. Cell. Endocrinol.* 78, 1–6. doi: 10.1016/0303-7207(91)90179-V

de Barros Machado, T., Leal, I. C., Kuster, R. M., Amaral, A. C., Kokis, V., De Silva, M. G., et al. (2005). Brazilian phytopharmaceuticals–evaluation against hospital bacteria. *Phytother. Res.* 19, 519–525. doi: 10.1002/ptr.1696

Denzer, I., Münch, G., Pischetsrieder, M., and Friedland, K. (2016). S-allyl-l-cysteine and isoliquiritigenin improve mitochondrial function in cellular

models of oxidative and nitrosative stress. *Food Chem.* 194, 843–848. doi: 10.1016/j.foodchem.2015.08.052

Dickson, D. W., Farlo, J., Davies, P., Crystal, H., Fuld, P., and Yen, S. H. (1988). Alzheimer's disease. A double-labeling immunohistochemical study of senile plaques. *Am. J. Pathol.* 132, 86–101.

El-Sherbiny, D. A., Khalifa, A. E., Attia, A. S., and Eldenshary Eel, D. (2003). *Hypericum perforatum* extract demonstrates antioxidant properties against elevated rat brain oxidative status induced by amnestic dose of scopolamine. *Pharmacol. Biochem. Behav.* 76, 525–533. doi: 10.1016/j.pbb.2003.09.014

Farag, M. A., Porzel, A., and Wessjohann, L. A. (2012). Comparative metabolite profiling and fingerprinting of medicinal licorice roots using a multiplex approach of GC-MS, LC-MS and 1D NMR techniques. *Phytochemistry* 76, 60–72. doi: 10.1016/j.phytochem.2011.12.010

Fatokun, A. A., Dawson, V. L., and Dawson, T. M. (2014). Parthanatos: mitochondrial-linked mechanisms and therapeutic opportunities. *Br. J. Pharmacol.* 171, 2000–2016. doi: 10.1111/bph.12416

Feldman, M., Santos, J., and Grenier, D. (2011). Comparative evaluation of two structurally related flavonoids, isoliquiritigenin and liquiritigenin, for their oral infection therapeutic potential. *J. Nat. Prod.* 74, 1862–1867. doi: 10.1021/np200174h

Fennell, C. W., Lindsey, K. L., Mcgaw, L. J., Sparg, S. G., Stafford, G. I., Elgorashi, E. E., et al. (2004). Assessing African medicinal plants for efficacy and safety: pharmacological screening and toxicology. *J. Ethnopharmacol.* 94, 205–217. doi: 10.1016/j.jep.2004.05.012

Fontana, L. (2009). Modulating human aging and age-associated diseases. *Biochim. Biophys. Acta* 1790, 1133–1138. doi: 10.1016/j.bbagen.2009.02.002

Fu, N., and Liu, Z. (1995). Antipromoting, antimutagenic and antioxidant action of glycyrrhizae flavonoids. *Chin. J. Cancer Res.* 7, 163–167. doi: 10.1007/BF03023467

Fujii, S., Morinaga, O., Uto, T., Nomura, S., and Shoyama, Y. (2014). Development of a monoclonal antibody-based immunochemical assay for liquiritin and its application to the quality control of licorice products. *J. Agric. Food Chem.* 62, 3377–3383. doi: 10.1021/jf404731z

Furlong, J. J. P., and Nudelman, N. S. (1988). Cyclization of substituted 2'-hydroxychalcones to flavanones. Solvent and isotope effects. *J. Chem. Soc. Perkin. Trans.* 2, 1213–1217. doi: 10.1039/P29880001213

Gaur, R., Yadav, K. S., Verma, R. K., Yadav, N. P., and Bhakuni, R. S. (2014). *In vivo* anti-diabetic activity of derivatives of isoliquiritigenin and liquiritigenin. *Phytomedicine* 21, 415–422. doi: 10.1016/j.phymed.2013.10.015

Gibb, W. R., and Lees, A. J. (1988). The relevance of the Lewy body to the pathogenesis of idiopathic Parkinson's disease. *J. Neurol. Neurosurg. Psychiatry* 51, 745–752. doi: 10.1136/jnnp.51.6.745

Gong, H., Zhang, B. K., Yan, M., Fang, P. F., Li, H. D., Hu, C. P., et al. (2015). A protective mechanism of licorice (*Glycyrrhiza uralensis*): isoliquiritigenin stimulates detoxification system via Nrf2 activation. *J. Ethnopharmacol.* 162, 134–139. doi: 10.1016/j.jep.2014.12.043

Gottfries, C. G. (1990). Neurochemical aspects on aging and diseases with cognitive impairment. *J. Neurosci. Res.* 27, 541–547. doi: 10.1002/jnr.490270415

Haider, S., Tabassum, S., and Perveen, T. (2016). Scopolamine-induced greater alterations in neurochemical profile and increased oxidative stress demonstrated a better model of dementia: a comparative study. *Brain Res. Bull.* 127, 234–247. doi: 10.1016/j.brainresbull.2016.10.002

Hatano, T., Fukuda, T., Liu, Y. Z., Noro, T., and Okuda, T. (1991). Phenolic constituents of licorice. IV. Correlation of phenolic constituents and licorice specimens from various sources, and inhibitory effects of licorice extracts on xanthine oxidase and monoamine oxidase. *Yakugaku Zasshi* 111, 311–331. doi: 10.1248/yakushi1947.111.6_311

Hoffmann, A., Grimm, C., Kraft, R., Goldbaum, O., Wrede, A., Nolte, C., et al. (2010). TRPM3 is expressed in sphingosine-responsive myelinating oligodendrocytes. *J. Neurochem.* 114, 654–665. doi: 10.1111/j.1471-4159.2010.06644.x

Houghton, P. J., and Howes, M. J. (2005). Natural products and derivatives affecting neurotransmission relevant to Alzheimer's and Parkinson's disease. *Neurosignals* 14, 6–22. doi: 10.1159/000085382

Huang, W., Cheng, X., Xiao, H., Shao, H., and Xu, Z. (2001). Experimental toxicology study on part of forbidden medicine of Eighteen Antagonisms of TCM. *Chengdu Univ. Tradit. Chin. Med.* 24, 45–47.

Hwang, C. K., and Chun, H. S. (2012). Isoliquiritigenin isolated from licorice *Glycyrrhiza uralensis* prevents 6-hydroxydopamine-induced apoptosis in dopaminergic neurons. *Biosci. Biotechnol. Biochem.* 76, 536–543. doi: 10.1271/bbb.110842

Iontcheva, I., Amar, S., Zawawi, K. H., Kantarci, A., and Van Dyke, T. E. (2004). Role for moesin in lipopolysaccharide-stimulated signal transduction. *Infect. Immun.* 72, 2312–2320. doi: 10.1128/IAI.72.4.2312-2320.2004

Isbrucker, R. A., and Burdock, G. A. (2006). Risk and safety assessment on the consumption of licorice root (*Glycyrrhiza* sp.), its extract and powder as a food ingredient, with emphasis on the pharmacology and toxicology of glycyrrhizin. *Regul. Toxicol. Pharmacol.* 46, 167–192. doi: 10.1016/j.yrtph.2006.06.002

Jang, E. Y., Choe, E. S., Hwang, M., Kim, S. C., Lee, J. R., Kim, S. G., et al. (2008). Isoliquiritigenin suppresses cocaine-induced extracellular dopamine release in rat brain through GABA(B) receptor. *Eur. J. Pharmacol.* 587, 124–128. doi: 10.1016/j.ejphar.2008.03.054

Jayaprakasam, B., Doddaga, S., Wang, R., Holmes, D., Goldfarb, J., and Li, X.-M. (2009). Licorice flavonoids inhibit Eotaxin-1 secretion by human fetal lung fibroblasts in vitro. *J. Agric. Food Chem.* 57, 820–825. doi: 10.1021/jf802601j

Jeon, J. P., Buono, R. J., Han, B. G., Jang, E. Y., Kim, S. C., Yang, C. H., et al. (2008). Proteomic and behavioral analysis of response to isoliquiritigenin in brains of acute cocaine treated rats. *J. Proteome Res.* 7, 5094–5102. doi: 10.1021/pr800237s

Jez, J. M., Bowman, M. E., Dixon, R. A., and Noel, J. P. (2000). Structure and mechanism of the evolutionarily unique plant enzyme chalcone isomerase. *Nat. Struct. Biol.* 7, 786–791. doi: 10.1038/79025

Jez, J. M., and Noel, J. P. (2002). Reaction mechanism of chalcone isomerase. pH dependence, diffusion control, and product binding differences. *J. Biol. Chem.* 277, 1361–1369. doi: 10.1074/jbc.M109224200

Ji, S., Li, Z., Song, W., Wang, Y., Liang, W., Li, K., et al. (2016). Bioactive constituents of *Glycyrrhiza uralensis* (Licorice): discovery of the effective components of a traditional herbal medicine. *J. Nat. Prod.* 79, 281–292. doi: 10.1021/acs.jnatprod.5b00877

Jo, D. S., Shin, D. W., Park, S. J., Bae, J. E., Kim, J. B., Park, N. Y., et al. (2016). Attenuation of Abeta toxicity by promotion of mitochondrial fusion in neuroblastoma cells by liquiritigenin. *Arch. Pharm. Res.* 39, 1137–1143. doi: 10.1007/s12272-016-0780-2

Kanazawa, I. (1994). Short review on monoamine oxidase and its inhibitors. *Eur. Neurol.* 34(Suppl 3), 36–39. doi: 10.1159/000119540

Kang, H. C., Lee, Y. I., Shin, J. H., Andrabi, S. A., Chi, Z., Gagne, J. P., et al. (2011). Iduna is a poly(ADP-ribose) (PAR)-dependent E3 ubiquitin ligase that regulates DNA damage. *Proc. Natl. Acad. Sci. U.S.A.* 108, 14103–14108. doi: 10.1073/pnas.1108799108

Kao, T. C., Wu, C. H., and Yen, G. C. (2014). Bioactivity and potential health benefits of licorice. *J. Agric. Food Chem.* 62, 542–553. doi: 10.1021/jf404939f

Kennedy, B. K., Berger, S. L., Brunet, A., Campisi, J., Cuervo, A. M., Epel, E. S., et al. (2014). Geroscience: linking aging to chronic disease. *Cell* 159, 709–713. doi: 10.1016/j.cell.2014.10.039

Kern, M. A., Breuhahn, K., and Schirmacher, P. (2002). Molecular pathogenesis of human hepatocellular carcinoma. *Adv. Cancer Res.* 86, 67–112. doi: 10.1016/S0065-230X(02)86003-1

Kim, H., Ham, S., Lee, J. Y., Jo, A., Lee, G. H., Lee, Y. S., et al. (2017). Estrogen receptor activation contributes to RNF146 expression and neuroprotection in Parkinson's disease models. *Oncotarget* 8, 106721–106739. doi: 10.18632/oncotarget.21828

Kim, J. Y., Park, S. J., Yun, K. J., Cho, Y. W., Park, H. J., and Lee, K. T. (2008). Isoliquiritigenin isolated from the roots of *Glycyrrhiza uralensis* inhibits LPS-induced iNOS and COX-2 expression via the attenuation of NF-kappaB in RAW 264.7 macrophages. *Eur. J. Pharmacol.* 584, 175–184. doi: 10.1016/j.ejphar.2008.01.032

Kim, Y. W., Zhao, R. J., Park, S. J., Lee, J. R., Cho, I. J., Yang, C. H., et al. (2008). Anti-inflammatory effects of liquiritigenin as a consequence of the inhibition of NF-kappaB-dependent iNOS and proinflammatory cytokines production. *Br. J. Pharmacol.* 154, 165–173. doi: 10.1038/bjp.2008.79

Kim, S. C., Byun, S. H., Yang, C. H., Kim, C. Y., Kim, J. W., and Kim, S. G. (2004). Cytoprotective effects of *Glycyrrhizae radix* extract and its active component liquiritigenin against cadmium-induced toxicity (effects on bad translocation and cytochrome c-mediated PARP cleavage). *Toxicology* 197, 239–251. doi: 10.1016/j.tox.2004.01.010

Kim, Y. W., Kang, H. E., Lee, M. G., Hwang, S. J., Kim, S. C., Lee, C. H., et al. (2009). Liquiritigenin, a flavonoid aglycone from licorice, has a choleretic effect and the ability to induce hepatic transporters and phase-II enzymes. *Am. J. Physiol. Gastrointest. Liver Physiol.* 296, G372–G381. doi: 10.1152/ajpgi.90524.2008

Kim, Y. W., Ki, S. H., Lee, J. R., Lee, S. J., Kim, C. W., Kim, S. C., et al. (2006). Liquiritigenin, an aglycone of liquiritin in *Glycyrrhizae radix*, prevents acute liver injuries in rats induced by acetaminophen with or without buthionine sulfoximine. *Chem. Biol. Interact.* 161, 125–138. doi: 10.1016/j.cbi.2006.03.008

Kitagawa, I. (2002). Licorice root. A natural sweetener and an important ingredient in Chinese medicine. *Pure Appl. Chem.* 74, 1189–1198. doi: 10.1351/pac200274071189

Ko, Y. H., Kwon, S. H., Hwang, J. Y., Kim, K. I., Seo, J. Y., Nguyen, T. L., et al. (2018). The memory-enhancing effects of liquiritigenin by activation of NMDA receptors and the CREB signaling pathway in mice. *Biomol. Ther.* 26, 109–114. doi: 10.4062/biomolther.2016.284

Ko, Y. H., Kwon, S. H., Lee, S. Y., and Jang, C. G. (2017). Liquiritigenin ameliorates memory and cognitive impairment through cholinergic and BDNF pathways in the mouse hippocampus. *Arch. Pharm. Res.* 40, 1209–1217. doi: 10.1007/s12272-017-0954-6

Kumar, S., Madaan, R., Bansal, G., Jamwal, A., and Sharma, A. (2012). Plants and plant products with potential anticonvulsant activity - a review. *Pharmacogn. Commn.* 2, 3–99. doi: 10.5530/pc.2012.suppl1.2

Lacroix, M., Abi-Said, D., Fourney, D. R., Gokaslan, Z. L., Shi, W., Demonte, F., et al. (2001). A multivariate analysis of 416 patients with glioblastoma multiforme: prognosis, extent of resection, and survival. *J. Neurosurg.* 95, 190–198. doi: 10.3171/jns.2001.95.2.0190

Lane, N. E., and Kelman, A. (2003). A review of anabolic therapies for osteoporosis. *Arthritis Res. Ther.* 5, 214–222. doi: 10.1186/ar797

Lecomte, S., Lelong, M., Bourgine, G., Efstathiou, T., Saligaut, C., and Pakdel, F. (2017). Assessment of the potential activity of major dietary compounds as selective estrogen receptor modulators in two distinct cell models for proliferation and differentiation. *Toxicol. Appl. Pharmacol.* 325, 61–70. doi: 10.1016/j.taap.2017.04.005

Li, G., Nikolic, D., and Van Breemen, R. B. (2016). Identification and chemical standardization of licorice raw materials and dietary supplements using UHPLC-MS/MS. *J. Agric. Food Chem.* 64, 8062–8070. doi: 10.1021/acs.jafc.6b02954

Li, H., Ye, M., Zhang, Y., Huang, M., Xu, W., Chu, K., et al. (2015). Blood-brain barrier permeability of Gualou Guizhi granules and neuroprotective effects in ischemia/reperfusion injury. *Mol. Med. Rep.* 12, 1272–1278. doi: 10.3892/mmr.2015.3520

Liao, M., Zhao, Y., Huang, L., Cheng, B., and Huang, K. (2016). Isoliquiritigenin and liquiritin from *Glycyrrhiza uralensis* inhibit α-synuclein amyloid formation. *RSC Adv.* 6, 86640–86649. doi: 10.1039/C6RA17770K

Liljemark, W. F., and Bloomquist, C. (1996). Human oral microbial ecology and dental caries and periodontal diseases. *Crit. Rev. Oral Biol. Med.* 7, 180–198. doi: 10.1177/10454411960070020601

Lin, Z., Gu, J., Xiu, J., Mi, T., Dong, J., and Tiwari, J. K. (2012). Traditional Chinese medicine for senile dementia. *Evid. Based Complement. Alternat. Med.* 2012:692621. doi: 10.1155/2012/692621

Liu, F., Day, M., Muniz, L. C., Bitran, D., Arias, R., Revilla-Sanchez, R., et al. (2008). Activation of estrogen receptor-beta regulates hippocampal synaptic plasticity and improves memory. *Nat. Neurosci.* 11, 334–343. doi: 10.1038/nn2057

Liu, H., Wang, J., Zhou, W., Wang, Y., and Yang, L. (2013). Systems approaches and polypharmacology for drug discovery from herbal medicines: an example using licorice. *J. Ethnopharmacol.* 146, 773–793. doi: 10.1016/j.jep.2013.02.004

Liu, R. T., Tang, J. T., Zou, L. B., Fu, J. Y., and Lu, Q. J. (2011). Liquiritigenin attenuates the learning and memory deficits in an amyloid protein precursor transgenic mouse model and the underlying mechanisms. *Eur. J. Pharmacol.* 669, 76–83. doi: 10.1016/j.ejphar.2011.07.051

Liu, R. T., Zou, L. B., Fu, J. Y., and Lu, Q. J. (2010a). Effects of liquiritigenin treatment on the learning and memory deficits induced by amyloid beta-peptide (25-35) in rats. *Behav. Brain Res.* 210, 24–31. doi: 10.1016/j.bbr.2010.01.041

Liu, R. T., Zou, L. B., Fu, J. Y., and Lu, Q. J. (2010b). Promotion of rat brain-derived progenitor cell neurogenesis by liquiritigenin treatment: underlying mechanisms. *Neurosci. Lett.* 481, 139–143. doi: 10.1016/j.neulet.2010.06.065

Liu, R.-T., Zou, L.-B., and Lü, Q.-J. (2009). Liquiritigenin inhibits Aβ25–35-induced neurotoxicity and secretion of Aβ1–40 in rat hippocampal neurons. *Acta Pharmacol. Sin.* 30, 899–906. doi: 10.1038/aps.2009.74

Liu, X., Wang, L., Chen, J., Ling, Q., Wang, H., Li, S., et al. (2015). Estrogen receptor beta agonist enhances temozolomide sensitivity of glioma cells by inhibiting PI3K/AKT/mTOR pathway. *Mol. Med. Rep.* 11, 1516–1522. doi: 10.3892/mmr.2014.2811

Ma, X., Fang, F., Song, M., and Ma, S. (2015). The effect of isoliquiritigenin on learning and memory impairments induced by high-fat diet via inhibiting TNF-alpha/JNK/IRS signaling. *Biochem. Biophys. Res. Commun.* 464, 1090–1095. doi: 10.1016/j.bbrc.2015.07.081

Mae, T., Kishida, H., Nishiyama, T., Tsukagawa, M., Konishi, E., Kuroda, M., et al. (2003). A licorice ethanolic extract with peroxisome proliferator-activated receptor-γ ligand-binding activity affects diabetes in KK-Ay mice, abdominal obesity in diet-induced obese C57BL mice and hypertension in spontaneously hypertensive rats. *J. Nutr.* 133, 3369–3377. doi: 10.1093/jn/133.11.3369

Mersereau, J. E., Levy, N., Staub, R. E., Baggett, S., Zogovic, T., Chow, S., et al. (2008). Liquiritigenin is a plant-derived highly selective estrogen receptor beta agonist. *Mol. Cell. Endocrinol.* 283, 49–57. doi: 10.1016/j.mce.2007.11.020

Miles, C. O., and Main, L. (1989). Kinetics and mechanism of the cyclisation of 2',6'-dihydroxychalcone and derivatives. *J. Chem. Soc. Perkin. Trans.* 2, 1623–1632. doi: 10.1039/P29890001623

Murphy, T. H., Miyamoto, M., Sastre, A., Schnaar, R. L., and Coyle, J. T. (1989). Glutamate toxicity in a neuronal cell line involves inhibition of cystine transport leading to oxidative stress. *Neuron* 2, 1547–1558. doi: 10.1016/0896-6273(89)90043-3

Nakazawa, K., Mchugh, T. J., Wilson, M. A., and Tonegawa, S. (2004). NMDA receptors, place cells and hippocampal spatial memory. *Nat. Rev. Neurosci.* 5, 361–372. doi: 10.1038/nrn1385

Nassiri, A. M., and Hossein, H. (2008). Review of pharmacological effects of *Glycyrrhiza* sp. and its bioactive compounds. *Phytother Res* 22, 709–724. doi: 10.1002/ptr.2362

Nudelman, N. S., and Furlong, J. J. P. (1991). Conversion of flavanones into chalcones in alkaline medium. Kinetic and spectroscopic studies. *J. Phys. Org. Chem.* 4, 263–270. doi: 10.1002/poc.610040502

Oeppen, J., and Vaupel, J. W. (2002). Demography. Broken limits to life expectancy. *Science* 296, 1029–1031. doi: 10.1126/science.1069675

Oh, Y. S. (2015). Mechanistic insights into pancreatic beta-cell mass regulation by glucose and free fatty acids. *Anat. Cell Biol.* 48, 16–24. doi: 10.5115/acb.2015.48.1.16

Pan, X., Kong, L. D., Zhang, Y., Cheng, C. H., and Tan, R. X. (2000). *In vitro* inhibition of rat monoamine oxidase by liquiritigenin and isoliquiritigenin isolated from *Sinofranchetia chinensis*. *Acta Pharmacol. Sin.* 21, 949–953.

Paterni, I., Bertini, S., Granchi, C., Tuccinardi, T., Macchia, M., Martinelli, A., et al. (2015). Highly selective salicylketoxime-based estrogen receptor beta agonists display antiproliferative activities in a glioma model. *J. Med. Chem.* 58, 1184–1194. doi: 10.1021/jm501829f

Phani Kumar, G., Anila Kumar, K. R., and Naveen, S. (2015). Phytochemicals having neuroprotective properties from dietary sources and medicinal herbs. *Pharmacogn. J.* 7, 1–17. doi: 10.5530/pj.2015.7.1

Ramalingam, M., and Kim, S. J. (2016a). Pharmacological activities and applications of Spicatoside A. *Biomol. Ther.* 24, 469–474. doi: 10.4062/biomolther.2015.214

Ramalingam, M., and Kim, S. J. (2016b). The neuroprotective role of insulin against MPP^+-induced Parkinson's disease in differentiated SH-SY5Y cells. *J. Cell. Biochem.* 117, 917–926. doi: 10.1002/jcb.25376

Sharma, V., Katiyar, A., and Agrawal, R. C. (2018). "*Glycyrrhiza glabra*: chemistry and pharmacological activity," in *Sweeteners: Pharmacology, Biotechnology, and Applications*, eds J.-M. Mérillon and K. G. Ramawat (Cham: Springer International Publishing), 87–100. doi: 10.1007/978-3-319-27027-2_21

Simmler, C., Hajirahimkhan, A., Lankin, D. C., Bolton, J. L., Jones, T., Soejarto, D. D., et al. (2013). Dynamic residual complexity of the isoliquiritigenin-liquiritigenin interconversion during bioassay. *J. Agric. Food Chem.* 61, 2146–2157. doi: 10.1021/jf304445p

Størmer, F. C., Reistad, R., and Alexander, J. (1993). Glycyrrhizic acid in liquorice—Evaluation of health hazard. *Food Chem. Toxicol.* 31, 303–312. doi: 10.1016/0278-6915(93)90080-I

Straub, I., Krugel, U., Mohr, F., Teichert, J., Rizun, O., Konrad, M., et al. (2013). Flavanones that selectively inhibit TRPM3 attenuate thermal nociception in vivo. *Mol. Pharmacol.* 84, 736–750. doi: 10.1124/mol.113.086843

Street, R. A., Stirk, W. A., and Van Staden, J. (2008). South African traditional medicinal plant trade-Challenges in regulating quality, safety and efficacy. *J. Ethnopharmacol.* 119, 705–710. doi: 10.1016/j.jep.2008.06.019

Su, Q., Tao, W., Huang, H., Du, Y., Chu, X., and Chen, G. (2016). Protective effect of liquiritigenin on depressive-like behavior in mice after lipopolysaccharide administration. *Psychiatry Res.* 240, 131–136. doi: 10.1016/j.psychres.2016.04.002

Takahashi, T., Takasuka, N., Iigo, M., Baba, M., Nishino, H., Tsuda, H., et al. (2004). Isoliquiritigenin, a flavonoid from licorice, reduces prostaglandin E2 and nitric oxide, causes apoptosis, and suppresses aberrant crypt foci development. *Cancer Sci.* 95, 448–453. doi: 10.1111/j.1349-7006.2004.tb03230.x

Tanemoto, R., Okuyama, T., Matsuo, H., Okumura, T., Ikeya, Y., and Nishizawa, M. (2015). The constituents of licorice (*Glycyrrhiza uralensis*) differentially suppress nitric oxide production in interleukin-1beta-treated hepatocytes. *Biochem. Biophys. Rep.* 2, 153–159. doi: 10.1016/j.bbrep.2015.06.004

Tao, W., Dong, Y., Su, Q., Wang, H., Chen, Y., Xue, W., et al. (2016). Liquiritigenin reverses depression-like behavior in unpredictable chronic mild stress-induced mice by regulating PI3K/Akt/mTOR mediated BDNF/TrkB pathway. *Behav. Brain Res.* 308, 177–186. doi: 10.1016/j.bbr.2016.04.039

Tarailo-Graovac, M., Shyr, C., Ross, C. J., Horvath, G. A., Salvarinova, R., Ye, X. C., et al. (2016). Exome sequencing and the management of neurometabolic disorders. *N. Engl. J. Med.* 374, 2246–2255. doi: 10.1056/NEJMoa1515792

Theplantlist (2013). *Glycyrrhiza uralensis Fisch*. Available: http://www.theplantlist.org/tpl1.1/record/ild-32406 [accessed March 14, 2018].

Vijayakumar, S., Prabhu, S., Rajalakhsmi, S., and Manogar, P. (2016). Review on potential phytocompounds in drug development for Parkinson disease: a pharmacoinformatic approach. *Inform. Med. Unlocked* 5, 15–25. doi: 10.1016/j.imu.2016.09.002

Walf, A. A., Koonce, C. J., and Frye, C. A. (2008). Estradiol or diarylpropionitrile administration to wild type, but not estrogen receptor beta knockout, mice enhances performance in the object recognition and object placement tasks. *Neurobiol. Learn. Mem.* 89, 513–521. doi: 10.1016/j.nlm.2008.01.008

Wang, A., Lu, Y., Shi, P., and Zhang, H. (2017). Hydroxyl and hydroperoxyl radicals scavenging by isoliquiritigenin and liquiritigenin: a quantum chemical study. *Struct. Chem.* 28, 1181–1186. doi: 10.1007/s11224-017-0924-0

Wang, H., Chang, B., and Wang, B. (1998). [The effect of herbal medicine including *Astragalus membranaceus* (fisch) bge, *Codonpsis pilosula* and *Glycyrrhiza uralensis* fisch on airway responsiveness]. *Zhonghua Jie He He Hu Xi Za Zhi* 21, 287–288.

Wang, L., Yang, R., Yuan, B., Liu, Y., and Liu, C. (2015). The antiviral and antimicrobial activities of licorice, a widely-used Chinese herb. *Acta Pharm. Sin. B* 5, 310–315. doi: 10.1016/j.apsb.2015.05.005

Wang, X., Zhang, H., Chen, L., Shan, L., Fan, G., and Gao, X. (2013). Liquorice, a unique "guide drug" of traditional Chinese medicine: a review of its role in drug interactions. *J. Ethnopharmacol.* 150, 781–790. doi: 10.1016/j.jep.2013.09.055

Wen, M. C., Wei, C. H., Hu, Z. Q., Srivastava, K., Ko, J., Xi, S. T., et al. (2005). Efficacy and tolerability of anti-asthma herbal medicine intervention in adult patients with moderate-severe allergic asthma. *J. Allergy Clin. Immunol.* 116, 517–524. doi: 10.1016/j.jaci.2005.05.029

Weon, J. B., Jung, Y. S., and Ma, C. J. (2016). Cognitive-enhancing effect of *Dianthus superbus* var. *longicalycinus* on scopolamine-induced memory impairment in mice. *Biomol. Ther.* 24, 298–304. doi: 10.4062/biomolther.2015.083

White, J. D., and Gall, C. M. (1987). Differential regulation of neuropeptide and proto-oncogene mRNA content in the hippocampus following recurrent seizures. *Brain Res.* 427, 21–29. doi: 10.1016/0169-328X(87)90040-4

WHO (ed.). (1999). "Radix glycyrrhizae," in *WHO Monographs on Selected Medicinal Plants*. (Geneva: World Health Organization), 183–194.

Wikipedia (2018). *Glycyrrhiza uralensis. [Online]. Wikipedia, The Free Encyclopedia*. Available at: https://en.wikipedia.org/w/index.php?title=Glycyrrhiza_uralensis&oldid=831892972 [accessed July 03, 2018].

Woo, S. M., Kim, J., Han, H. W., Chae, J. I., Son, M. Y., Cho, S., et al. (2009). Notch signaling is required for maintaining stem-cell features of neuroprogenitor cells derived from human embryonic stem cells. *BMC Neurosci.* 10:97. doi: 10.1186/1471-2202-10-97

Yamín, L. J., Blanco, S. E., Luco, J. M., and Ferretti, F. H. (1997). Theoretical study of cyclization of 2′-hydroxychalcone. *J. Mol. Struct. THEOCHEM* 390, 209–215. doi: 10.1016/S0166-1280(96)04776-8

Yang, E. J., Kim, M., Woo, J. E., Lee, T., Jung, J. W., and Song, K. S. (2016). The comparison of neuroprotective effects of isoliquiritigenin and its Phase I metabolites against glutamate-induced HT22 cell death. *Bioorg. Med. Chem. Lett.* 26, 5639–5643. doi: 10.1016/j.bmcl.2016.10.072

Yang, E. J., Park, G. H., and Song, K. S. (2013). Neuroprotective effects of liquiritigenin isolated from licorice roots on glutamate-induced apoptosis in hippocampal neuronal cells. *Neurotoxicology* 39, 114–123. doi: 10.1016/j.neuro.2013.08.012

Yang, N., Patil, S., Zhuge, J., Wen, M. C., Bolleddula, J., Doddaga, S., et al. (2013). *Glycyrrhiza uralensis* flavonoids present in anti-asthma formula, ASHMI, inhibit memory Th2 responses *in vitro* and *in vivo*. *Phytother. Res.* 27, 1381–1391. doi: 10.1002/ptr.4862

Yerra, V. G., Kalvala, A. K., and Kumar, A. (2017). Isoliquiritigenin reduces oxidative damage and alleviates mitochondrial impairment by SIRT1 activation in experimental diabetic neuropathy. *J. Nutr. Biochem.* 47, 41–52. doi: 10.1016/j.jnutbio.2017.05.001

Yu, J. Y., Ha, J. Y., Kim, K. M., Jung, Y. S., Jung, J. C., and Oh, S. (2015). Anti-Inflammatory activities of licorice extract and its active compounds, glycyrrhizic acid, liquiritin and liquiritigenin, in BV2 cells and mice liver. *Molecules* 20, 13041–13054. doi: 10.3390/molecules200713041

Zakin, D., and Boyer, T. D. (1990). "Drug-induced liver disease," in *Hepatology*, ed. W. Lamsback (Philadelphia, PA: W.B. Saunders Company), 759–762.

Zhan, C., and Yang, J. (2006). Protective effects of isoliquiritigenin in transient middle cerebral artery occlusion-induced focal cerebral ischemia in rats. *Pharmacol. Res.* 53, 303–309. doi: 10.1016/j.phrs.2005.12.008

Zhang, Q., and Ye, M. (2009). Chemical analysis of the Chinese herbal medicine Gan-Cao (licorice). *J. Chromatogr. A* 1216, 1954–1969. doi: 10.1016/j.chroma.2008.07.072

Zhang, S. P., Zhou, Y. J., Liu, Y., and Cai, Y. Q. (2009). Effect of liquiritigenin, a flavanone existed from Radix glycyrrhizae on pro-apoptotic in SMMC-7721 cells. *Food Chem. Toxicol.* 47, 693–701. doi: 10.1016/j.fct.2008.12.015

Zhang, X., Yang, Y. J., and Ly, Q. Z. (2012). Density functional theory calculations on antioxidation activity of four flavones from radix glycyrrhizae. *Comput. Appl. Chem.* 29, 656–660.

Zhao, L., Chen, Q., and Diaz Brinton, R. (2002). Neuroprotective and neurotrophic efficacy of phytoestrogens in cultured hippocampal neurons. *Exp. Biol. Med.* 227, 509–519. doi: 10.1177/153537020222700716

Zhao, L., O'neill, K., and Diaz Brinton, R. (2005). Selective estrogen receptor modulators (SERMs) for the brain: current status and remaining challenges for developing NeuroSERMs. *Brain Res. Brain Res. Rev.* 49, 472–493. doi: 10.1016/j.brainresrev.2005.01.009

Zhou, Z. D., Chan, C. H., Xiao, Z. C., and Tan, E. K. (2011). Ring finger protein 146/Iduna is a poly(ADP-ribose) polymer binding and PARsylation dependent E3 ubiquitin ligase. *Cell Adh. Migr.* 5, 463–471. doi: 10.4161/cam.5.6.18356

Zollner, G., Wagner, M., and Trauner, M. (2010). Nuclear receptors as drug targets in cholestasis and drug-induced hepatotoxicity. *Pharmacol. Ther.* 126, 228–243. doi: 10.1016/j.pharmthera.2010.03.005

Conflict of Interest Statement: The authors declare that the research was conducted in the absence of any commercial or financial relationships that could be construed as a potential conflict of interest.

frontiers in Aging Neuroscience

ORIGINAL RESEARCH
published: 06 November 2018
doi: 10.3389/fnagi.2018.00355

Korean Red Ginseng Enhances Neurogenesis in the Subventricular Zone of 1-Methyl-4-Phenyl-1,2,3,6-Tetrahydropyridine-Treated Mice

Sun Ryu[1], *Hyongjun Jeon*[2], *Sungtae Koo*[1,2] *and Seungtae Kim*[1,2]*

[1]Korean Medicine Research Center for Healthy Aging, Pusan National University, Yangsan, South Korea, [2]Department of Korean Medical Science, School of Korean Medicine, Pusan National University, Yangsan, South Korea

Regulation of adult neurogenesis plays an important role in therapeutic strategies for various neurodegenerative diseases. Recent studies have suggested that the enhancement of adult neurogenesis can be helpful in the treatment of Parkinson's disease (PD). In this study, we investigated whether Korean red ginseng (KRG) can enhance neurogenesis in the subventricular zone (SVZ) of a PD mouse model. To accomplish this, male 8-week-old C57BL/6 mice were injected with vehicle or 20 mg/kg of 1-methyl-4-phenyl-1,2,3,6-tetrahydropyridine (MPTP) four times at 2 h intervals. After the final injection, they were administered water or 100 mg/kg of KRG extract and injected intraperitoneally with 50 mg/kg of 5'-bromo-2'-deoxyuridine-monophosphate (BrdU) once a day for 14 consecutive days. After the last pole test, dopaminergic neuronal survival in the striatum and the substantia nigra (SN), cell proliferation in the SVZ and mRNA expression of neurotrophic factors and dopamine receptors in the striatum were evaluated. KRG administration suppressed dopaminergic neuronal death induced by MPTP in the striatum as well as the SN, augmented the number of BrdU- and BrdU/doublecortin (Dcx)-positive cells in the SVZ and enhanced the expression of proliferation cell nuclear antigen, brain derived neurotrophic factor (BDNF), glial cell derived neurotrophic factor (GDNF), cerebral dopamine neurotrophic factor (CDNF), ciliary neurotrophic factor (CNTF), dopamine receptor D3 (DRD3) and D5 mRNAs. These results suggest that KRG administration augments neurogenesis in the SVZ of the PD mouse model.

Keywords: Parkinson's disease, Korean red ginseng, neurogenesis, 1-methyl-4-phenyl-1,2,3,6-tetrahydropyridine, subventricular zone, ginseng

OPEN ACCESS

Edited by:
Seung-Nam Kim,
Dongguk University Seoul,
South Korea

Reviewed by:
Ji-Yeun Park,
Daejeon University, South Korea
Songhee Jeon,
Chonnam National University Medical School, South Korea

***Correspondence:**
Seungtae Kim
kimst@pusan.ac.kr

Received: *29 June 2018*
Accepted: *18 October 2018*
Published: *06 November 2018*

Citation:
Ryu S, Jeon H, Koo S and Kim S (2018) Korean Red Ginseng Enhances Neurogenesis in the Subventricular Zone of 1-Methyl-4-Phenyl-1,2,3,6-Tetrahydropyridine-Treated Mice. Front. Aging Neurosci. 10:355. doi: 10.3389/fnagi.2018.00355

INTRODUCTION

Adult neurogenesis is the process through which functional, mature neurons are formed from adult neural precursors in specific brain regions, the subventricular zone (SVZ) and the subgranular zone (SGZ) in mammals (Ming and Song, 2011). The regulation of adult endogenous neurogenesis plays an important role in therapeutic strategies for various neurodegenerative conditions such as Parkinson's disease (PD), Alzheimer's disease and stroke (Geraerts et al., 2007; Ryu et al., 2016b) because adult neurogenesis may act as an endogenous repair mechanism in the adult brain (Ming and Song, 2011).

It has been suggested that neurotransmitters and neurotrophic factors play an important role in the regulation of endogenous neurogenesis (Abdipranoto et al., 2008). Recent reports have demonstrated that alteration of neurotransmitter levels in PD patients affects adult neurogenesis in the SGZ as well as SVZ and that increases in adult neurogenesis can repair the dopaminergic system in the nigrostriatal pathway (Borta and Höglinger, 2007). Neurochemical deficit of dopamine suppresses neurogenic activity (Borta and Höglinger, 2007), whereas dopamine-enhancing drugs increase neurogenic activity in the SVZ (Hoglinger et al., 2004; Chiu et al., 2015). Increases in brain derived neurotrophic factor (BDNF) have been found to enhance endogenous neurogenesis in the SVZ and the SGZ (Zhao et al., 2008), while the release of neurotrophic factors such as glial cell-derived neurotrophic factor (GDNF) has been shown to promote neurogenesis and synaptic connectivity (Borta and Höglinger, 2007). In addition to neurotrophic factors, dopamine receptor D3 (DRD3) and dopamine receptor D5 (DRD5) are known to be involved in adult neurogenesis as well as the pathophysiology of PD (Borta and Höglinger, 2007; Chen et al., 2013; Chetrit et al., 2013; Lao et al., 2013; Elgueta et al., 2017).

Korean red ginseng (KRG), which is the steamed root of *Panax ginseng* Meyer, is a valuable herb in Asian countries. Recent studies have shown that KRG exerts positive effects in the brain. Specifically, KRG alleviates the decline of learning and memory in aged mice (Lee and Oh, 2015), suppresses inflammatory cytokines in the brain of a stroke rat model (Lee et al., 2011), increases cognitive function in Alzheimer's disease patients (Heo et al., 2016) and enhances neuronal survival and development in the nigrostriatal pathway of a PD mouse model (Jun et al., 2015; Kim et al., 2016, 2018). Moreover, it has been reported that ginsenosides, which are components of KRG, enhance cell proliferation. Specifically, ginsenoside Rd was found to promote neural stem cell (NSC) proliferation in the brain of an ischemia animal model (Lin et al., 2012) and to alleviate lead-impaired neurogenesis in the brains of aging rats (Wang et al., 2013). Additionally, ginsenoside Rg1 influenced modulation of the proliferation of progenitor cells in the hippocampus (Shen and Zhang, 2004). However, it is still not clear if KRG administration can enhance neurogenesis in the brain of a PD animal model.

We previously demonstrated that KRG exerts neuroprotective properties and improves motor function in PD models through various mechanisms (Jun et al., 2015; Kim et al., 2016, 2018; Ryu et al., 2016a). In the present study, we investigated whether KRG can modulate neurogenesis in the SVZ and the expression of neurotrophic factors in the striatum using a mouse model of PD induced by 1-methyl-4-phenyl-1,2,3,6-tetrahydropyridine (MPTP).

MATERIALS AND METHODS

Animals and Groups

This study was approved by the Pusan National University Institutional Animal Care and Use Committee and animals were handled in accordance with the current guidelines established by the Pusan National University Institutional Animal Care and Use Committee. Male 8-week-old C57BL/6 mice weighing 20–22 g were purchased from Orientbio Inc. (Seongnam, Korea) and housed at a standard temperature (22 ± 2°C) in a light-controlled environment (lights on from 8:00 AM to 8:00 PM) with free access to food and water.

After a 7-day adjustment period, mice were randomly assigned to four groups (n = 11 in each group): a vehicle-injected and water-treated control group (Veh), a vehicle-injected and 100 mg/kg KRG-treated group (KRG), a MPTP-injected and water-treated group (MPTP) and a MPTP-injected and KRG-treated group (MPTP+KRG).

MPTP and Bromodeoxyuridine Injection and KRG Administration

Mice in the MPTP and the MPTP+KRG groups were injected with MPTP-HCl (20 mg/kg; Sigma, St. Louis, MO, USA) intraperitoneally four times at 2 h intervals (total, 80 mg/kg). Mice in the Veh and KRG groups were injected with vehicle (normal saline) on the same schedule. The KRG extract used in this study was acquired from the Korea Ginseng Corporation (Daejeon, Korea). The KRG extract was diluted with sterilized mineral water. One hour after the first MPTP injection, mice in the KRG and the MPTP+KRG group received oral administration of the KRG extract (100 mg/kg) once a day for 14 consecutive days because this dose was found to have the best neuroprotective effect against MPTP toxicity in our previous study (Jun et al., 2015). Mice in the Veh and the MPTP group were administered the same amount of vehicle (sterilized water) on the same schedule. Immediately after the oral administration, all mice were intraperitoneally injected with 50 mg/kg of 5'-bromo-2'-deoxyuridine-monophosphate (BrdU; Sigma, St. Louis, MO, USA) once a day for 14 consecutive days to detect cell mitosis.

Pole Test

The pole test was performed by modifying the method established by Abe et al. (2001). Briefly, mice (n = 6 in each group) were positioned head downwards near the top of a rough-surfaced wood pole (10 mm in diameter; 55 cm in height) and the time taken to arrive at the floor was recorded. The test was repeated three times at 30 s time intervals and behavioral changes were evaluated according to the average of the three descending times. The tests were conducted 1 day before the first KRG administration (day 0), and 2 h after KRG administration on days 7 and 14.

Immunohistochemistry

After the last behavioral test, mice (n = 6 at each group) were deeply anesthetized by isoflurane (JW Pharmaceutical, Seoul, Korea) and then perfused transcardially with 4% paraformaldehyde (PFA) dissolved in 0.1 M phosphate buffer (PFA). Next, brains were quickly harvested, postfixed in 4% PFA for 24 h, and immersed in 30% sucrose in 0.1 M sodium phosphate buffer (pH 7.4) at 4°C for 3 days. Frozen sections were cut to a thickness of 25 μm using a cryostat (Leica Microsystems, Wetzlar, Germany).

To evaluate dopaminergic neuronal death in the nigrostriatal pathway, sections were placed in normal serum for 2 h at room temperature for blocking. Sections were then incubated with mouse anti-tyrosine hydroxylase (TH, 1:200; Santa Cruz Biotechnology, Santa Cruz, CA, USA) primary antibody overnight at 4°C. After washing, the sections were incubated with Alexa 568-conjugated goat anti-mouse IgG (1:200; Molecular Probes, Eugene, OR, USA) secondary antibody for 2 h at room temperature.

To identify cell proliferation, sections were placed into 2 N HCl at 37°C for 10 min and then 0.1 M boric acid at room temperature for 3 min. After blocking in normal serum for 2 h at room temperature, the sections were incubated with mouse anti-BrdU (1:200; Abcam, Cambridge, UK) and rabbit anti-doublecortin (Dcx; 1:100; Abcam) primary antibodies overnight at 4°C. After washing, the sections were incubated with Alexa 488-conjugated goat anti-rabbit IgG (1:200; Molecular Probes) and Alexa 568-conjugated donkey anti-mouse IgG (1:200; Molecular Probes) secondary antibodies for 2 h at room temperature.

The stained sections were captured with a LSM700 confocal microscope (Carl ZEISS, Oberkochen, Germany). To evaluate the changes in dopaminergic neuronal fibers in the striatum, the mean values of optical density (OD) of the TH in the striatum were determined using Image-Pro Plus 6.0 (Media Cybernetics, Silver Spring, MD, USA). The number of TH-positive neuronal cells in the substantia nigra (SN) was manually counted to evaluate the survival of dopaminergic neurons. Additionally, the numbers of BrdU-positive cells and BrdU/Dcx double-labeled cells in the SVZ were counted manually on each capture. To minimize the possibility of observer bias, an independent observer that did not know the expected results manually counted the cells bilaterally in three continuous striatal sections, and the cell counts were confirmed three times.

Quantitative Real Time PCR

After the last behavioral test, mice (n = 5 at each group) were sacrificed and the bilateral striata were quickly removed, frozen in liquid nitrogen and then homogenized using a Polytron homogenizer. Real time PCR analysis was subsequently conducted to examine the proliferating cell nuclear antigen (PCNA), BDNF, GDNF, cerebral dopamine neurotrophic factor (CDNF), ciliary neurotrophic factor (CNTF), DRD3 and DRD5. Total RNA was isolated using a RNeasy Lipid Tissue Kit (Qiagen, Valencia, CA, USA) and treated with DNase. Reverse transcription was performed using a High-Capacity cDNA Reverse Transcription Kit (Applied Biosystems, Foster City, CA, USA) based on the manufacturer's protocols. Primer sequences were designed using a software program (Applied Biosystems) and synthesized commercially (Bioneer, Korea). The PCR primers used in this study were as follows: PCNA (forward, 5′-TTTGAGGCACGCCTGATCC-3′; reverse, 5′-GG AGACGTGAGACGAGTCCAT-3′), BDNF (forward, 5′-GG ATGAGGACCAGAAGGTTGC-3′; reverse, 5′-TTGTCTAT GCCCCTGCAGCCT-3′), GDNF (forward, 5′-ATGGGATG TCGTGGCTGTCTG-3′; reverse, 5′-TCTCTGGAGCCAGG GTCAGAT-3′), CDNF (forward, 5′-GGTCGCTAAAATTG CAGAGC-3′; reverse, 5′-AAGGTAGCCCAGCCCACTAT-3′), CNTF (forward, 5′-GGGACCTCTGTAGCCGCTCTATCTG-3′; reverse, 5′-GTTCCAGAAGCGCCATTAACTCCTC-3′), DRD3 (forward, 5′-TTTGGCAACGGTCTGGTATGT-3′; reverse, 5′-CCAGGCTCACCACTAGGTAG-3′), DRD5 (forward, 5′-TC TGGCCGTCTCAGACCTC-3′; reverse, 5′-GGGTCATCTTGC GCTCGTA-3′) and glyceraldehyde-3-phosphatedehydrogenase (GAPDH; forward, 5′-GGCATTGCTCTCAATGGACAA-3′; reverse, 5′-CCGAGGTTGGGATAGGGCC-3′). GAPDH was used as the reference standard to normalize the expression levels of the target genes. cDNA amplification was performed using the Maxima SYBR Green qPCR Master Mix (Applied Biosystems) and the following conditions: 20 s denaturation at 94°C followed by 40 cycles of 1 min annealing and extension at 60°C in an ABI 7700 sequence detector system (Applied Biosystems).

Statistical Analysis

The behavioral data of the pole test were expressed as the means ± the standard error of the mean and analyzed by two-way ANOVA (group × time) with Bonferroni's multiple comparison test. The cell counts, optical densities and mRNA expressions among the four groups were expressed as the means ± the standard deviation and analyzed by one-way ANOVA with Tukey's multiple comparison tests. Prism five for Windows (GraphPad Software Inc., La Jolla, CA, USA) was used for all statistical analyses and a $p < 0.05$ was considered statistically significant.

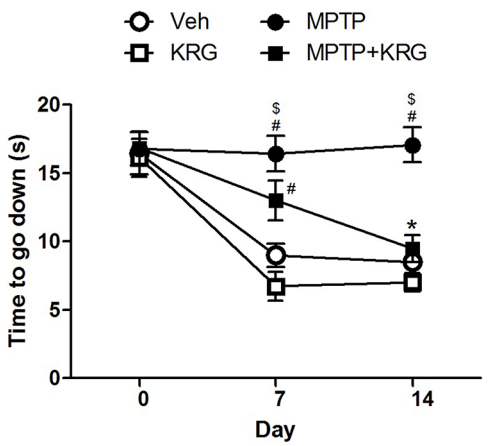

FIGURE 1 | Result of the pole test. On day 7, the descending time in the methyl-4-phenyl-1,2,3,6-tetrahydropyridine (MPTP) group was significantly higher than that in the Veh and the KRG groups and that in the MPTP+KRG group was also significantly higher than that in the KRG group. On day 14, the descending time in the MPTP group was still higher than those of the other groups, but that in the MPTP+KRG group was significantly lower than that in the MPTP group. Data are presented as the means ± the standard error of the mean (n = 6 in each group). All results were determined by two-way ANOVA (group × time) with Bonferroni's multiple comparison test. $^{\#}p < 0.05$ compared with the Veh group. $^{\$}p < 0.05$ compared with the KRG group. $^{*}p < 0.05$ compared with the MPTP group. Veh, a vehicle-treated control group; KRG, Korean red ginseng treated group; MPTP, MPTP-injected and vehicle-treated group; MPTP+KRG, MPTP-injected and KRG-treated group.

RESULTS

KRG Administration Alleviates MPTP-Induced Behavioral Dysfunction

A pole test was performed to evaluate the influence of KRG administration on motor function. There were no significant differences in the descending times among groups before KRG administration (day 0). On day 7, the descending time in the MPTP group was significantly longer than those in the Veh and the MPTP groups ($p < 0.05$ in each group). Additionally, the descending time in the MPTP+KRG group was lower than that in the MPTP group and higher than those in the Veh and the MPTP groups, but was only significantly different from that in the KRG group ($p < 0.05$). On day 14, the descending time in the MPTP group was significantly higher than those in the other three groups ($p < 0.05$ in each group), but the times were not significantly different among the Veh, MPTP and MPTP+KRG groups (**Figure 1**). These results indicate that MPTP injection induces motor dysfunction, but KRG administration can alleviate it.

KRG Administration Suppresses MPTP-induced Dopaminergic Neuronal Loss

The OD of TH-positive neurons in the striatum of the MPTP group was significantly decreased relative to that of the Veh and the KRG groups ($p < 0.01$ in each group). However, the density in the striatum of the MPTP+KRG group was significantly increased when compared to that in the MPTP group ($p < 0.05$). The number of TH-positive neurons in the SN of the MPTP group was significantly decreased relative to those in the Veh and KRG groups ($p < 0.001$ in each group). However, the number in the SN of the MPTP+KRG group was significantly increased when compared to that in the MPTP group ($p < 0.05$, **Figure 2**). These findings suggest that KRG administration protects dopaminergic neurons in the nigrostriatal pathway from MPTP toxicity.

MPTP Promotes Neurogenesis in the SVZ

To detect MPTP-induced cell proliferation in the SVZ, the number of BrdU-positive cells was measured 14 days after MPTP injection (day 14). The number was significantly increased in the MPTP group compared to the Veh group ($p < 0.05$, **Figures 3A,B**) and the level of PCNA mRNA in the MPTP group was significantly higher than that in the Veh group ($p < 0.05$, **Figure 4A**).

To analyze the differentiation potential of endogenous NSCs in the SVZ, we performed double labeling with the antibodies against BrdU and against Dcx, a marker for migrating neuronal cells. The number of BrdU/Dcx-positive cells in the MPTP group was significantly higher than that in the Veh group ($p < 0.05$,

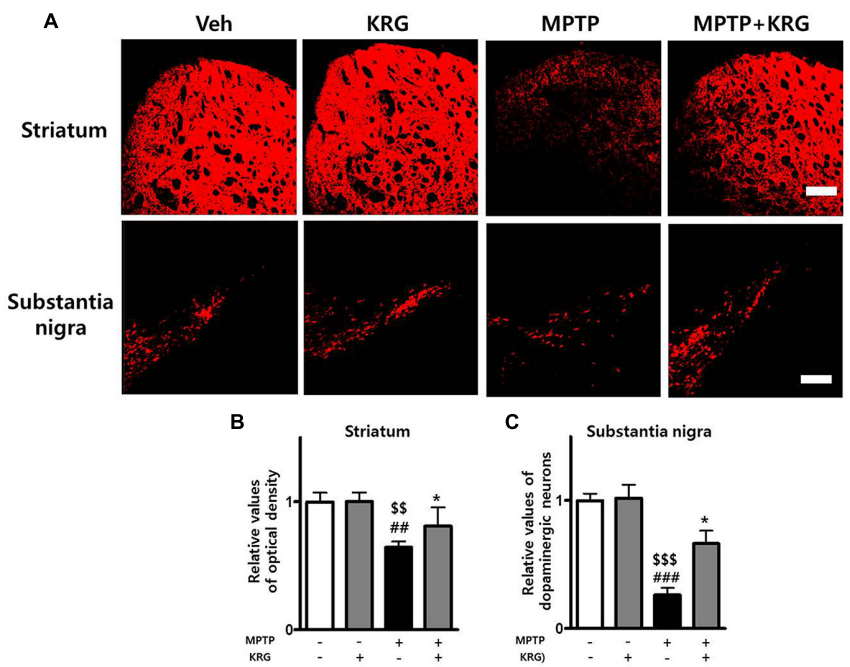

FIGURE 2 | Effects of KRG on MPTP-induced dopaminergic neuronal death in the nigrostriatal pathway. MPTP treatment significantly decreased dopaminergic neurons in the striatum and the substantia nigra (SN), whereas KRG administration significantly suppressed the MPTP-induced dopaminergic neuronal death. **(A)** Tyrosine hydroxylase (TH)-specific immunohistochemical staining in the striatum and the SN. **(B)** Relative value of the optical density (OD) in the striatum. **(C)** Relative value of the number of dopaminergic neurons in the SN. Scale bar: 200 μm. Data are presented as the means ± standard deviation ($n = 6$ in each group). All results were determined by one-way analysis of variance with Bonferroni's multiple comparison test. $^{\#\#}p < 0.01$ and $^{\#\#\#}p < 0.001$ compared with the Veh group. $^{\$\$}p < 0.01$ and $^{\$\$\$}p < 0.001$ compared with the KRG group. $^{*}p < 0.05$ compared with the MPTP group.

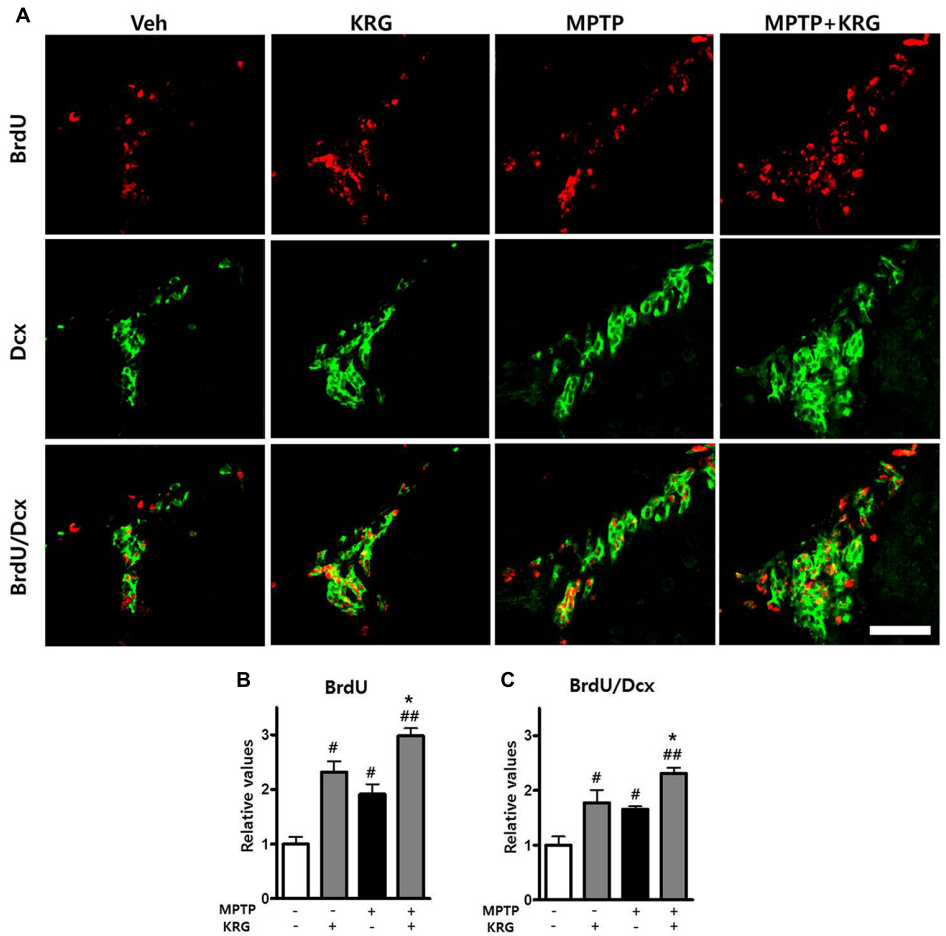

FIGURE 3 | Effects of KRG on cell proliferation in the subventricular zone (SVZ) of the vehicle-or MPTP-treated mice. MPTP promoted proliferation and differentiation of endogenous neural stem cells (NSCs) in the SVZ and KRG administration further enhanced proliferation and differentiation of endogenous NSCs in the SVZ. **(A)** BrdU (red) and Dcx (green)-specific immunohistochemical staining in the SVZ. **(B)** Number of BrdU-positive cells in the SVZ. **(C)** Number of BrdU/Dcx-positive cells in the SVZ. Data are expressed as the mean ± SD ($n = 6$) and were analyzed using one-way analysis of variance with Bonferroni's multiple comparison test. $^{\#}p < 0.05$ and $^{\#\#}p < 0.01$ compared with the Veh group. $^{*}p < 0.05$ compared with the MPTP group. Scale bars: 50 μm. BrdU, 5-bromo-2′-deoxyuridine; Dcx, doublecortin.

Figures 3A,C), suggesting that MPTP induces the expansion and differentiation of endogenous NSCs in the SVZ.

KRG Enhances Neurogenesis in the SVZ

To determine if KRG can enhance cell proliferation in the SVZ, the number of BrdU-positive cells was measured 14 days after MPTP injection. In the KRG group, the number of cells was significantly increased compared to the Veh group ($p < 0.05$), while the number in the MPTP+KRG group was significantly increased compared to the Veh and the MPTP groups ($p < 0.01$ and $p < 0.05$, respectively, **Figures 3A,B**). To explore the influence of KRG administration on cell proliferation in detail, the level of PCNA mRNA in the SVZ was measured. At 14 days after the KRG treatments, the level of PCNA mRNA in the KRG group was significantly higher than that in the Veh group ($p < 0.05$), while the level in the MPTP+KRG group was significantly higher than those in the Veh and MPTP groups ($p < 0.01$ and $p < 0.05$, respectively, **Figure 4A**).

To determine if the cells differentiated in response to KRG administration were immature neuronal cells, the number of BrdU/DCX-positive cells was measured in the SVZ. The number of BrdU/DCX-positive cells in the KRG group was significantly greater than that in the Veh group ($p < 0.05$), while the number in the MPTP+KRG group was significantly greater than those in the Veh and the MPTP groups ($p < 0.01$ and $p < 0.05$, respectively, **Figure 3C**). These findings suggest that KRG administration enhances the expansion and differentiation of NSCs in the SVZ.

MPTP Increases Neurotropic Factors in the Striatum and KRG Multiples

Growth factors and neurotrophic factors are potent regulators of endogenous adult neurogenesis. Real time qPCR analysis was

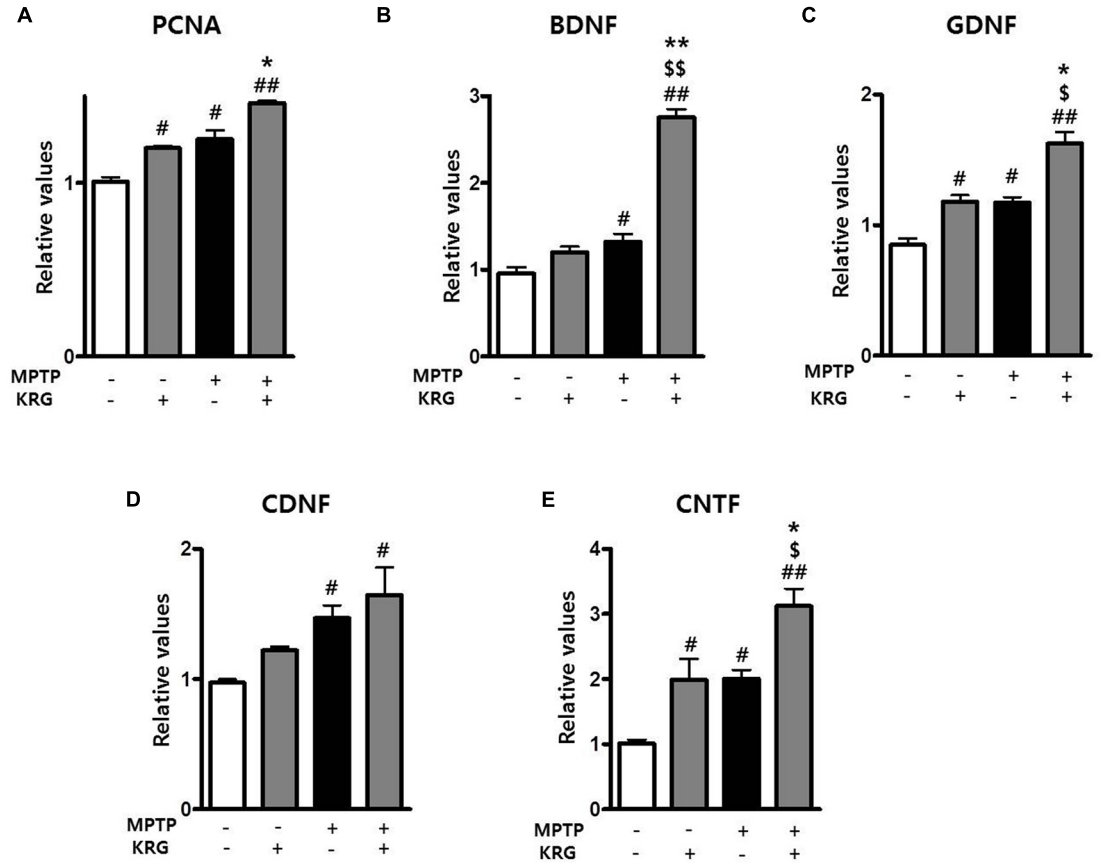

FIGURE 4 | Effects of KRG on neurotropic factors in the striatum of the vehicle-or MPTP-treated mice. Expression of PCNA **(A)**, BDNF **(B)**, GDNF **(C)**, CDNF **(D)** and CNTF **(E)** mRNAs in the SVZ was quantified using real time qPCR. GAPDH was used as an internal control. The data are presented as the mean ± SD of five independent experiments ($n = 5$ in each group). Data were analyzed using one-way analysis of variance with Bonferroni's multiple comparison test. $^{\#}p < 0.05$ and $^{\#\#}p < 0.01$ compared with the Veh group. $^{\$}p < 0.05$ and $^{\$\$}p < 0.01$ compared with the KRG group. $^{*}p < 0.05$ and $^{**}p < 0.01$ compared with the MPTP group. PCNA, proliferation cell nuclear antigen; BDNF, brain derived neurotrophic factor; GDNF, glial cell derived neurotrophic factor; CDNF, cerebral dopamine neurotrophic factor; CNTF, ciliary neurotrophic factor.

utilized to investigate changes in neurotrophic factors induced by MPTP and/or KRG in the striatum. Fourteen days after MPTP injection, the mRNA levels of BDNF, GDNF, CDNF and CNTF in the MPTP group were significantly higher than those in the Veh group ($p < 0.05$ for each neurotrophic factor, **Figures 4B–E**). Additionally, the mRNA levels of GDNF and CNTF in the KRG group were significantly higher than those in the Veh group ($p < 0.05$ in each neurotrophic factor), while the mRNA levels of BDNF, GDNF and CNTF in the MPTP+KRG group were significantly higher than those in the Veh ($p < 0.01$ in each neurotrophic factor), KRG ($p < 0.01$ in BDNF and $p < 0.05$ in GDNF and CNTF) and MPTP ($p < 0.01$ in BDNF and $p < 0.05$ in GDNF and CNTF) groups (**Figure 4**), suggesting that the KRG would affect the increase of neurogenesis in the SVZ through increases in the neurotrophic factors in the striatum.

MPTP Increases Dopamine Receptor 3 and 5 in the Striatum and KRG Multiples

DRD3 and DRD5 are involved in adult neurogenesis and the pathophysiology of PD. To investigate the changes of DRD3 and DRD5 induced by MPTP and KRG, the mRNA expressions of DRD3 and DRD5 in the striatum were evaluated using real-time qPCR. Fourteen days after MPTP injection, the mRNA levels of DRD3 and DRD5 in the MPTP group were significantly higher than in the Veh group ($p < 0.01$ in each dopamine receptor, **Figure 4**). Additionally, the mRNA levels of DRD3 and DRD5 in the KRG group were significantly higher than those in the Veh group ($p < 0.01$ in each dopamine receptor), while the mRNA levels in the MPTP+KRG group were significantly higher than those in the Veh ($p < 0.01$ in each dopamine receptor) and the MPTP ($p < 0.05$ in each dopamine receptor) groups (**Figure 5**), suggesting that the KRG would affect the increase of neurogenesis by enhancing DRD3 and DRD5 in the striatum.

DISCUSSION

This study demonstrated that KRG administration alleviated MPTP-induced behavioral dysfunction and increased cell differentiation and proliferation of NSCs in the SVZ of

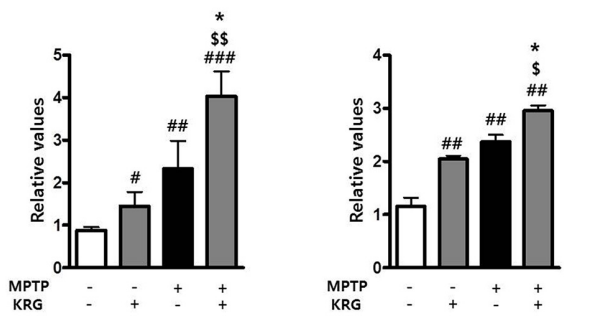

FIGURE 5 | Effects of KRG on dopamine receptors in the striatum of the vehicle-or MPTP-treated mice. Expressions of dopamine receptor D3 (DRD3) **(A)** and D5 **(B)** mRNAs in the striatum were quantified using real time qPCR. GAPDH was used as an internal control. The data are presented as the mean ± SD of five independent experiments ($n = 5$ in each group). Data were analyzed using one-way analysis of variance with Bonferroni's multiple comparison test. $^{\#}p < 0.05$, $^{\#\#}p < 0.01$ and $^{\#\#\#}p < 0.001$ compared with the Veh group. $^{\$}p < 0.05$ and $^{\$\$}p < 0.01$ compared with the KRG group. $^{*}p < 0.05$ compared with the MPTP group.

MPTP-treated mice. Moreover, KRG administration increased the mRNA expressions of the neurotropic factors and the dopamine receptors in the striatum of both vehicle- and MPTP-injected mice.

MPTP-injected mice are a widely used animal model for PD studies. In this study, behavioral functions of mice gradually depreciated and dopaminergic neuronal cell death progressed after MPTP administration. However, KRG administration significantly alleviated MPTP-induced behavioral dysfunction and reduced MPTP-induced dopaminergic neuronal death in the striatum and the SN, indicating that the alleviation of the behavioral impairment with the KRG treatment was due to protection of dopaminergic neurons in the nigrostriatal pathway.

It is not clear whether MPTP enhances or suppress cell proliferation in the SVZ and DG. Hoglinger et al. (2004) reported that MPTP injection resulted in a decrease of PCNA-positive cells among DG and BrdU-positive cells in the SVZ. In contrast, Park and Enikolopov (2010) reported that PCNA-positive cells and BrdU-positive cells increased transiently 14 days after MPTP injection, while Peng et al. (2008) showed that MPTP injection induced dopaminergic neuronal death, but increased striatal neurogenesis. Conversely, chronic MPTP injections (25 mg/kg, bi-weekly for 5 weeks) did not alter cell proliferation in the SVZ (van den Berge et al., 2011). But studies conducted to investigate whether MPTP enhances cell proliferation concluded that the enhancement is a self-repairing process (He and Nakayama, 2009; Park and Enikolopov, 2010). In this study, MPTP injection increased BrdU-positive cells as well as BrdU/Dcx positive cells in the SVZ, as well as PCNA mRNA expression in the striatum; therefore, it is believed that the enhanced neurogenesis in the SVZ in response to MPTP injections may be a compensative mechanism of MPTP-induced cell death.

In the present study, KRG significantly enhanced neurogenesis in the SVZ of vehicle- as well as MPTP-injected mice and significantly increased the levels of BDNF, GDNF, CDNF and CNTF mRNAs in the striatum. The neurotrophic factors are important regulators of adult neurogenesis (Lichtenwalner and Parent, 2006; Zhao et al., 2008); therefore, they can promote neurogenesis and synaptic connectivity (Borta and Höglinger, 2007). Increased BDNF enhanced endogenous neurogenesis in the SVZ and SGZ of the adult brain (Zhao et al., 2008), while GDNF promoted survival of grafted midbrain-derived NSCs in a PD rat model (Lei et al., 2011) and CDNF and CNTF enhanced memory function, neurogenesis and synaptic plasticity in the SGZ (Chohan et al., 2011). These results suggest that KRG would enhance neurogenic activity via modulation of the expression of endogenous neurotrophic factors.

KRG administration increased mRNA expression of DRD3 and DRD5 in the striatum of MPTP-treated mice in this study. Activation of DRD3 reduced the MPTP-induced behavioral impairment and neuronal death (Chen et al., 2013; Elgueta et al., 2017) and enhanced proliferation of neural progenitor cells in the SVZ (Lao et al., 2013). Activation of DRD5 also protected dopaminergic neurons in a PD rat model (Chetrit et al., 2013), promoted neurogenesis in an Alzheimer's disease mouse model (Shen et al., 2016) and regulated BDNF expression in the rodent brain (Perreault et al., 2013). These results indicate that the KRG-induced increase of DRD3 and DRD5 mRNAs may influence dopaminergic neuronal survival in the nigrostriatal pathway and the increase of neurogenesis in the SVZ.

In conclusion, the present study showed that KRG administration significantly protected against dopaminergic neuronal death in the nigrostriatal pathway and enhanced endogenous adult neurogenesis in the SVZ of MPTP-treated mice by increasing the mRNA expression of BDNF, GDNF, CDNF, CNTF, DRD3 and DRD5. These results suggest KRG would be useful in future strategies for PD treatment via modulation of endogenous adult neurogenesis.

AUTHOR CONTRIBUTIONS

SR conducted the immunohistochemistry, quantitative real time PCR and statistical analyses and drafted the manuscript. HJ performed the pole test and assisted with acquisition of immunofluorescent and real time PCR data. SuK assisted with design of the study, coordinated the acquisition of all study data and performed the analysis. SeK designed the experimental setup, interpreted the results, drafted the manuscript and supervised the study. All co-authors were involved in critical revision of the initial drafts.

FUNDING

This research was supported by the Basic Science Research Program through the National Research Foundation of Korea (NRF) funded by the Ministry of Education (No. NRF-2016R1D1A3B03930920) and MSIP (No. NRF-2014R1A5A2009936).

REFERENCES

Abdipranoto, A., Wu, S., Stayte, S., and Vissel, B. (2008). The role of neurogenesis in neurodegenerative diseases and its implications for therapeutic development. *CNS Neurol. Disord. Drug Targets* 7, 187–210. doi: 10.2174/187152708784083858

Abe, K., Taguchi, K., Wasai, T., Ren, J., Utsunomiya, I., Shinohara, T., et al. (2001). Biochemical and pathological study of endogenous 1-benzyl-1,2,3,4-tetrahydroisoquinoline-induced parkinsonism in the mouse. *Brain Res.* 907, 134–138. doi: 10.1016/s0006-8993(01)02573-2

Borta, A., and Höglinger, G. U. (2007). Dopamine and adult neurogenesis. *J. Neurochem.* 100, 587–595. doi: 10.1111/j.1471-4159.2006.04241.x

Chen, Y., Ni, Y.-Y., Liu, J., Lu, J.-W., Wang, F., Wu, X.-L., et al. (2013). Dopamine receptor 3 might be an essential molecule in 1-methyl-4-phenyl-1,2,3,6-tetrahydropyridine-induced neurotoxicity. *BMC Neurosci.* 14:76. doi: 10.1186/1471-2202-14-76

Chetrit, J., Taupignon, A., Froux, L., Morin, S., Bouali-Benazzouz, R., Naudet, F., et al. (2013). Inhibiting subthalamic D5 receptor constitutive activity alleviates abnormal electrical activity and reverses motor impairment in a rat model of Parkinson's disease. *J. Neurosci.* 33, 14840–14849. doi: 10.1523/JNEUROSCI.0453-13.2013

Chiu, W.-H., Depboylu, C., Hermanns, G., Maurer, L., Windolph, A., Oertel, W. H., et al. (2015). Long-term treatment with L-DOPA or pramipexole affects adult neurogenesis and corresponding non-motor behavior in a mouse model of Parkinson's disease. *Neuropharmacology* 95, 367–376. doi: 10.1016/j.neuropharm.2015.03.020

Chohan, M. O., Li, B., Blanchard, J., Tung, Y.-C., Heaney, A. T., Rabe, A., et al. (2011). Enhancement of dentate gyrus neurogenesis, dendritic and synaptic plasticity and memory by a neurotrophic peptide. *Neurobiol. Aging* 32, 1420–1434. doi: 10.1016/j.neurobiolaging.2009.08.008

Elgueta, D., Aymerich, M. S., Contreras, F., Montoya, A., Celorrio, M., Rojo-Bustamante, E., et al. (2017). Pharmacologic antagonism of dopamine receptor D3 attenuates neurodegeneration and motor impairment in a mouse model of Parkinson's disease. *Neuropharmacology* 113, 110–123. doi: 10.1016/j.neuropharm.2016.09.028

Geraerts, M., Krylyshkina, O., Debyser, Z., and Baekelandt, V. (2007). Concise review: therapeutic strategies for Parkinson disease based on the modulation of adult neurogenesis. *Stem Cells* 25, 263–270. doi: 10.1634/stemcells.2006-0364

He, X. J., and Nakayama, H. (2009). Neurogenesis in neurotoxin-induced animal models for Parkinson's disease-a review of the current status. *J. Toxicol. Pathol.* 22, 101–108. doi: 10.1293/tox.22.101

Heo, J.-H., Park, M.-H., and Lee, J.-H. (2016). Effect of korean red ginseng on cognitive function and quantitative EEG in patients with Alzheimer's disease: a preliminary study. *J. Altern. Complement. Med.* 22, 280–285. doi: 10.1089/acm.2015.0265

Hoglinger, G. U., Rizk, P., Muriel, M. P., Duyckaerts, C., Oertel, W. H., Caille, I., et al. (2004). Dopamine depletion impairs precursor cell proliferation in Parkinson disease. *Nat. Neurosci.* 7, 726–735. doi: 10.1038/nn1265

Jun, Y. L., Bae, C.-H., Kim, D., Koo, S., and Kim, S. (2015). Korean Red Ginseng protects dopaminergic neurons by suppressing the cleavage of p35 to p25 in a Parkinson's disease mouse model. *J. Ginseng Res.* 39, 148–154. doi: 10.1016/j.jgr.2014.10.003

Kim, D., Jeon, H., Ryu, S., Koo, S., Ha, K. T., and Kim, S. (2016). Proteomic analysis of the effect of Korean red ginseng in the striatum of a Parkinson's disease mouse model. *PLoS One* 11:e0164906. doi: 10.1371/journal.pone.0164906

Kim, D., Kwon, S., Jeon, H., Ryu, S., Ha, K. T., and Kim, S. (2018). Proteomic change by Korean red ginseng in the substantia nigra of a Parkinson's disease mouse model. *J. Ginseng Res.* 42, 429–435. doi: 10.1016/j.jgr.2017.04.008

Lao, C. L., Lu, C. S., and Chen, J. C. (2013). Dopamine D3 receptor activation promotes neural stem/progenitor cell proliferation through AKT and ERK1/2 pathways and expands type-B and -C cells in adult subventricular zone. *Glia* 61, 475–489. doi: 10.1002/glia.22449

Lee, J. S., Choi, H. S., Kang, S. W., Chung, J. H., Park, H. K., Ban, J. Y., et al. (2011). Therapeutic effect of Korean red ginseng on inflammatory cytokines in rats with focal cerebral ischemia/reperfusion injury. *Am. J. Chin. Med.* 39, 83–94. doi: 10.1142/s0192415x1100866x

Lee, Y., and Oh, S. (2015). Administration of red ginseng ameliorates memory decline in aged mice. *J. Ginseng Res.* 39, 250–256. doi: 10.1016/j.jgr.2015.01.003

Lei, Z., Jiang, Y., Li, T., Zhu, J., and Zeng, S. (2011). Signaling of glial cell line-derived neurotrophic factor and its receptor GFRα1 induce Nurr1 and Pitx3 to promote survival of grafted midbrain-derived neural stem cells in a rat model of Parkinson disease. *J. Neuropathol. Exp. Neurol.* 70, 736–747. doi: 10.1097/nen.0b013e31822830e5

Lichtenwalner, R. J., and Parent, J. M. (2006). Adult neurogenesis and the ischemic forebrain. *J. Cereb. Blood Flow Metab.* 26, 1–20. doi: 10.1038/sj.jcbfm.9600170

Lin, T., Liu, Y., Shi, M., Liu, X., Li, L., Liu, Y., et al. (2012). Promotive effect of ginsenoside Rd on proliferation of neural stem cells *in vivo* and *in vitro*. *J. Ethnopharmacol.* 142, 754–761. doi: 10.1016/j.jep.2012.05.057

Ming, G. L., and Song, H. (2011). Adult neurogenesis in the mammalian brain: significant answers and significant questions. *Neuron* 70, 687–702. doi: 10.1016/j.neuron.2011.05.001

Park, J. H., and Enikolopov, G. (2010). Transient elevation of adult hippocampal neurogenesis after dopamine depletion. *Exp. Neurol.* 222, 267–276. doi: 10.1016/j.expneurol.2010.01.004

Peng, J., Xie, L., Jin, K., Greenberg, D. A., and Andersen, J. K. (2008). Fibroblast growth factor 2 enhances striatal and nigral neurogenesis in the acute 1-methyl-4-phenyl-1,2,3,6-tetrahydropyridine model of Parkinson's disease. *Neuroscience* 153, 664–670. doi: 10.1016/j.neuroscience.2008.02.063

Perreault, M. L., Jones-Tabah, J., O'Dowd, B. F., and George, S. R. (2013). A physiological role for the dopamine D5 receptor as a regulator of BDNF and Akt signalling in rodent prefrontal cortex. *Int. J. Neuropsychopharmacol.* 16, 477–483. doi: 10.1017/s1461145712000685

Ryu, S., Koo, S., Ha, K.-T., and Kim, S. (2016a). Neuroprotective effect of Korea Red Ginseng extract on 1-methyl-4-phenylpyridinium-induced apoptosis in PC12 cells. *Anim. Cells Syst.* 20, 363–368. doi: 10.1080/19768354.2016.1257510

Ryu, S., Lee, S.-H., Kim, S., and Yoon, B.-W. (2016b). Human neural stem cells promote proliferation of endogenous neural stem cells and enhance angiogenesis in ischemic rat brain. *Neural Regen. Res.* 11, 298–304. doi: 10.4103/1673-5374.177739

Shen, L., Yan, M., and He, L. (2016). D5 receptor agonist 027075 promotes cognitive function recovery and neurogenesis in a Aβ1–42-induced mouse model. *Neuropharmacology* 105, 72–83. doi: 10.1016/j.neuropharm.2016.01.008

Shen, L. H., and Zhang, J. T. (2004). Ginsenoside Rg1 promotes proliferation of hippocampal progenitor cells. *Neurol. Res.* 26, 422–428. doi: 10.1179/016164104225016047

van den Berge, S. A., van Strien, M. E., Korecka, J. A., Dijkstra, A. A., Sluijs, J. A., Kooijman, L., et al. (2011). The proliferative capacity of the subventricular zone is maintained in the parkinsonian brain. *Brain* 134, 3249–3263. doi: 10.1093/brain/awr256

Wang, B., Feng, G., Tang, C., Wang, L., Cheng, H., Zhang, Y., et al. (2013). Ginsenoside Rd maintains adult neural stem cell proliferation during lead-impaired neurogenesis. *Neurol. Sci.* 34, 1181–1188. doi: 10.1007/s10072-012-1215-6

Zhao, C., Deng, W., and Gage, F. H. (2008). Mechanisms and functional implications of adult neurogenesis. *Cell* 132, 645–660. doi: 10.1016/j.cell.2008.01.033

Conflict of Interest Statement: The authors declare that the research was conducted in the absence of any commercial or financial relationships that could be construed as a potential conflict of interest.

frontiers in Aging Neuroscience

SYSTEMATIC REVIEW
published: 08 November 2018
doi: 10.3389/fnagi.2018.00349

Herbal Medicine Formulas for Parkinson's Disease: A Systematic Review and Meta-Analysis of Randomized Double-Blind Placebo-Controlled Clinical Trials

Chun-Shuo Shan†, Hong-Feng Zhang†, Qing-Qing Xu, Yi-Hua Shi, Yong Wang, Yan Li, Yan Lin and Guo-Qing Zheng**

Department of Neurology, The Second Affiliated Hospital and Yuying Children's Hospital of Wenzhou Medical University, Wenzhou, China

Background: Parkinson's disease (PD) is a debitlitating, chronic, progressive neurodegenerative disorder without modifying therapy. Here, we aimed to evaluate the available evidence of herbal medicine (HM) formulas for patients with PD according to randomized double-blind placebo-controlled clinical trials.

Methods: HM formulas for PD were searched in eight main databases from their inception to February 2018. The methodological quality was assessed using Cochrane Collaboration risk of bias tool. Meta-analysis was performed using RevMan 5.3 software.

Results: Fourteen trials with Seventeen comparisons comprising 1,311 patients were identified. Compared with placebo groups, HM paratherapy (n = 16 comparisons) showed significant better effects in the assessments of total Unified Parkinson's Disease Rating Scale (UPDRS) (WMD: −5.43, 95% CI:−8.01 to −2.86; $P < 0.0001$), UPDRS I (WMD: −0.30, 95% CI: −0.54 to −0.06; $P = 0.02$), UPDRS II (WMD: −2.21, 95% CI: −3.19 to −1.22; $P < 0.0001$), UPDRS III (WMD: −3.26, 95% CI:−4.36 to −2.16; $P < 0.00001$), Parkinson's Disease Quality of Life Questionnaire ($p < 0.01$) and Parkinson's Disease Questionnaire-39 (WMD: −7.65, 95% CI: −11.46 to −3.83; $p < 0.0001$), Non-motor Symptoms Questionnaire ($p < 0.01$) and Non-Motor Symptoms Scale (WMD: −9.19, 95% CI: −13.11 to −5.28; $P < 0.00001$), Parkinson's Disease Sleep Scale (WMD: 10.69, 95% CI: 8.86 to 12.53; $P < 0.00001$), and Hamilton depression rating scale (WMD: −5.87, 95% CI: −7.06 to −4.68; $P < 0.00001$). The efficiency of HM monotherapy ($n = 1$ comparison) was not superior to the placebo according to UPDRS II, UPDRS III and total UPDRS score in PD patients who never received levodopa treatment, all $P > 0.05$. HM formulas paratherapy were generally safe and well tolerated for PD patients (RR: 0.41, 95% CI: 0.21 to 0.80; $P = 0.009$).

Conclusion: The findings of present study supported the complementary use of HM paratherapy for PD patients, whereas the question on the efficacy of HM monotherapy in alleviating PD symptoms is still open.

Keywords: Parkinson's disease, randomized double-blind placebo-controlled clinical trial, traditional Chinese medicine, meta-analysis, systematic review

OPEN ACCESS

Edited by:
Seung-Nam Kim,
Dongguk University Seoul,
South Korea

Reviewed by:
Hyangsook Lee,
Kyung Hee University, South Korea
Seung-Yeon Cho,
Kyung Hee University, South Korea
Song-Yi Kim,
Gachon University, South Korea

****Correspondence:***
Yan Lin
linyanm@vip.sina.com
Guo-Qing Zheng
gq_zheng@sohu.com

†These authors have contributed equally to this work

Received: *07 June 2018*
Accepted: *15 October 2018*
Published: *08 November 2018*

Citation:
Shan C-S, Zhang H-F, Xu Q-Q, Shi Y-H, Wang Y, Li Y, Lin Y and Zheng G-Q (2018) Herbal Medicine Formulas for Parkinson's Disease: A Systematic Review and Meta-Analysis of Randomized Double-Blind Placebo-Controlled Clinical Trials. Front. Aging Neurosci. 10:349. doi: 10.3389/fnagi.2018.00349

INTRODUCTION

Parkinson's disease (PD) is a common chronic neurodegenerative disease characterized by the degeneration of dopaminergic neurons in the substantia nigra (SN) (Kalia and Lang, 2015), and presents with non-motor or/and motor syndrome (Rogers et al., 2017). In the Global Burden of Diseases, Injuries, and Risk Factors Study (GBD) 2016, PD was the second leading cause in neurological disorders of years lived with disability (YLDs), contributing to 6.1 million of patients (GBD, 2016 Disease and Injury Incidence and Prevalence Collaborators, 2017). From 2005 to 2015, global deaths due to PD increased by 42.4%, to 117.4 thousands deaths (GBD, 2015 Mortality and Causes of Death Collaborators, 2016), as a result of population aging. With the growing incidence, PD seriously hurt the physical and mental health of the elderly, also produced a heavy economic burden on both families and society. The average annual cost per PD patient was $22,800 in the United States (Kowal et al., 2013) and $36,085 in the UK (Findley et al., 2011). Current conventional treatment for PD is based on the dopamine (DA) replacement therapies and reduction of DA degradation, including levodopa, DA receptor agonists, monoamine oxidase-B inhibitors, catechol-O-methyltransferase inhibitors and other types of drugs (Rogers et al., 2017). However, all the current therapeutic approaches remain palliative and can't inhibit or reverse the progression of PD (Athauda and Foltynie, 2015). Furthermore, frequently with these treatments can lead to obvious adverse events and efficacies diminished, as well as induce therapy-related motor complications such as dyskinesia, choreoathetosis, and fluctuations in motor function (Jenner, 2015). A safer and more effective alternative treatment of PD is increasingly demanded.

The therapy of herbal medicine (HM) for PD is particularly common. In China, HM could be traced in the Huangdi Neijing (Inner Canon of Yellow Emperor) (Zheng, 2009), the earliest existing classics in Chinese herbal medicine (CHM). Up to now, HM is still very popular in the treatment of PD especially in Asian countries (Wang et al., 2011, 2013). Previous reviews (Wang et al., 2012; Zhang et al., 2015) found lack of evidence of supporting the use of HM for PD patients because of the generally low-quality studies included. Here, we performed a systematic review and meta-analysis of randomized double-blind placebo-controlled clinical trials of HM formulas for PD patients and further explored the mechanisms of high-frequently used herbs against PD.

METHODS

This systematic review and meta-analysis is conducted according to the Preferred Reporting Items for Systematic Reviews and Meta-Analyses: The PRISMA Statement (Moher et al., 2010b) and our previous study (Yang et al., 2017).

Search Strategy

Randomized double-blind placebo-controlled clinical trials of HM formulas for PD were searched in eight databases from their inception to February 2018. They are PubMed, EMBASE, Cochrane Central Register of Controlled Trials (CENTRAL), Web of science, Chinese National Knowledge Infrastructure (CNKI), Chinese VIP Information, Wanfang database and Chinese Biological Medical Literature Database (CBM). Moreover, we hand searched additional relevant studies using the reference list of previous reviews. The search strategy of PubMed was as follows, and was modified to suit other English or Chinese databases.

PubMed search strategy:

#1. Parkinson disease [mh]
#2. Parkinson*[tiab]
#3. #1OR #2
#4. Medicine, Chinese Traditional [mh]
#5. Herbal Medicine [mh]
#6. Integrative Medicine [mh]
#7. traditional Chinese medicine [tiab]
#8. herb* [tiab]
#9. #4 OR #5 OR #6 OR #7 OR #8
#10. #3 And #9

Study Selection

Two authors (CS-S and H-FZ) independently engaged in the selection of studies by reading study titles, abstracts and full texts. The disagreement was resolved by the corresponding author (GZ) or repeated discussion.

Inclusion Criteria

Type of study: the articles were randomized double-blind placebo-controlled clinical trials.

Type of participants: participants were of any age or sex with a confirmed diagnosis of PD according to the UK Brain Bank criteria (Hughes et al., 1992), Chinese National Diagnosis Standard (CNDS) for PD in 1984 (Wang, 1985), CNDS updated version in 2006 for PD (Zhang, 2006) or other formal comparable criteria.

Type of intervention: Analyzed interventions were HM formulas or HM formulas plus western conventional medicine (WCM) according to PD treatment guidelines, [2] regardless of the form of the drug, dosage, frequency or duration of the treatment. Comparator interventions were placebo or placebo plus WCM.

Type of outcome measures: the primary outcomes were total Unified Parkinson's Disease Rating Scale (UPDRS) score, UPDRS I (Mental Score), UPDRS II (Activities of Daily Life), UPDRS III (Motor Score), and UPDRS IV (Complications of treatment). The secondary outcomes were: (1) Parkinson's Disease Quality of Life Questionnaire (PDQL) and Parkinson's Disease Questionnaire-39 (PDQ-39); (2) Non-motor Symptoms Questionnaire (NMSQuest) and Non-Motor Symptoms Scale (NMSS); (3) Parkinson's Disease Sleep Scale (PDSS); (4) Hamilton depression rating scale (HAMD); (5) Adverse events.

Exclusion Criteria

Studies were excluded if they were any one of the followings: (1) clinical trials evaluating the other alternative and complementary medicines mixed in the experimental group or control group

in the treatment of PD; (2) single herb, herbal extracts and herbal components; (3) case series, reviews, comments and protocols; (4) animal studies and *in vitro* studies; (5) duplicated publications.

Quality Assessment

The methodological quality was evaluated by using the Cochrane Collaboration's risk of bias tool (Higgins et al., 2011). The quality of each study was assessed by following seven biases: adequate sequence generation, allocation concealment, blinding of participants and personnel, blinding of outcome assessors, incomplete outcome data addressed (ITT analysis), free of selective reporting and other bias. Each domain can be rated as "+" (low risk of bias), "-" (high risk of bias), or "?" (unclear risk of bias), which were the three categories for the degree of each potential bias.

Data Extraction

Two authors (CS-S and HF-Z) independently extracted the data according to predefined extraction form as follows: (1) General information: the first author's name, publication year, and publication language; (2) Participants: diagnostic criteria, study design, total number and number in comparison groups, gender and mean age; (3) Intervention: herbal preparations, dose, frequency, course of treatment, follow-up; (4) Outcome measures. If the study had multiple comparison groups, we chosen the most relevant groups for analysis. The original authors were contacted if further information was needed. Disagreements were resolved through discussing with corresponding author (GZ).

The constituent of HM formulas for PD in each included study was recorded. The herbs with cumulative frequencies over 50% are documented and ranked.

Data Synthesis and Statistical Analysis

We synthesized all data and performed meta-analyses on RevMan 5.3 software. Continuous outcomes were using weighted mean differences (WMD) or standardized mean differences (SMD) with 95% confidence intervals (CIs), while dichotomous outcomes were summarized using risk ratio (RR) with 95% confidence intervals (CIs). Heterogeneity among studies was detected by I^2 and Chi^2 tests. If substantial statistical heterogeneity existed ($I^2 \geq 50\%$, $P < 0.10$), a random-effects model was used. If there was no observed heterogeneity ($I^2 < 50\%$, $P > 0.10$), a fixed-effect model was applied. Possible sources of heterogeneity were explored by subsequent sensitivity analyses. If more than ten trials were identified in each outcome, publication bias was detected by funnel plot analyses and Egger's test.

RESULTS

Description of the Screening Process

The detailed screening process was summarized in the PRISMA flow diagram (**Figure 1**). A total of 7,521 potentially relevant hits were initially yielded from the eight databases and other sources, in which 6,570 records were remained after removal of duplicates. Through screening titles and abstracts, we excluded 5,824 papers because they were studies with no relevance to PD ($n = 3292$), nonclinical trials ($n = 1007$), case reports, reviews, comments OR protocols ($n = 1525$). After full-text evaluation, 732 papers were excluded, including 234 that were not CHM studies, 142 that contained mixed interventions, 38 that aimed at single herb, herbal extracts or components, 305 that were not randomized double-blind placebo-controlled trials, and 13 that observed no outcome of interest. Ultimately, 14 eligible studies (Pan et al., 2009, 2011, 2013; Zhao et al., 2009, 2013; Guo, 2010; Kum et al., 2011; Chen M. Y. et al., 2014; Guo et al., 2014; Wen et al., 2015; Li et al., 2016; Yu, 2016; Cai et al., 2017; Yang, 2017) were selected in our study.

STUDY CHARACTERISTICS

The general characteristics of the included studies are summarized in **Table 1**. Fourteen included studies (Pan et al., 2009, 2011, 2013; Zhao et al., 2009, 2013; Guo, 2010; Kum et al., 2011; Chen M. Y. et al., 2014; Guo et al., 2014; Wen et al., 2015; Li et al., 2016; Yu, 2016; Cai et al., 2017; Yang, 2017) were published between 2009 and 2017. Among them, 4 studies (Kum et al., 2011; Pan et al., 2011, 2013; Li et al., 2016) were published in English and 10 studies (Pan et al., 2009; Zhao et al., 2009, 2013; Guo, 2010; Chen M. Y. et al., 2014; Guo et al., 2014; Wen et al., 2015; Yu, 2016; Cai et al., 2017; Yang, 2017) in Chinese. The most used diagnostic criterion of PD was UK Brain Bank criteria, which was referred in 11 studies (Guo, 2010; Kum et al., 2011; Pan et al., 2011, 2013; Zhao et al., 2013; Chen M. Y. et al., 2014; Guo et al., 2014; Wen et al., 2015; Li et al., 2016; Cai et al., 2017; Yang, 2017). Comparison of HM monotherapy vs. placebo was performed in one trial (Zhao et al., 2009). Comparisons of CHM plus WCM versus placebo plus WCM were conducted in 14 trials (Pan et al., 2009, 2011, 2013; Zhao et al., 2009, 2013; Guo, 2010; Kum et al., 2011; Chen M. Y. et al., 2014; Guo et al., 2014; Wen et al., 2015; Li et al., 2016; Yu, 2016; Cai et al., 2017; Yang, 2017), of whom 7 trials used Madopar (Zhao et al., 2009; Guo, 2010; Guo et al., 2014; Li et al., 2016; Yu, 2016; Cai et al., 2017; Yang, 2017). All studies involved a total of 1,311 patients with 675 in the treatment group vs. 636 in the placebo group, ranging in age from 51 to 79 years old. The sample size of the included studies ranged from 47 to 242. The male-to-female ratio was between 1.0 and 2.1. Duration of disease ranged from 2.2 months to 11.3 years. The total intervention period varied from 8 weeks to 6 months. The most common duration was 12 weeks. Two studies (Pan et al., 2013; Li et al., 2016) mentioned the follow-up times were 4 weeks and 6 months, respectively.

Description of the HM Formulas

Fourteen studies reported a wide range of TCM formulas, including Bushen Huoxue granule ($n = 2$), Zengxiao Anshen Zhichan 2 capsule ($n = 1$), Zengxiao Anshen Zhichan 2 granule ($n = 1$), Zhichan decoction ($n = 1$), Zhichan granule ($n = 1$), Guilu Dihuang capsule ($n = 1$), Jiawei Liujunzi Tang granule ($n = 1$), Yangxue Qingnao granule ($n = 1$), Congwu Qufeng granule ($n = 1$), Yishen Chuchan decoction ($n = 1$), Naokang granule ($n = 1$), Guiling Pa'an capsule ($n = 1$), and Guiling

TABLE 1 | Characteristics of the included studies.

Included studies	Publication language	Diagnostic criteria	Study designs	No. of participants (male/female); mean age (years)		Course of disease		Interventions		Course of treatment	Follow up	Outcome index	Intergroup differences
				Trial	Control	Trial	Control	Trial	Control				
Cai et al., 2017	Chinese	UK brain bank standard	Randomized double-blind and placebo-controlled parallel study	43 (25/18) 57.24 ± 3.36	43 (23/20) 58.14 ± 4.12	4.45 ± 1.36 years	4.75 ± 1.68 years	1. Zhichan decoction (1 package, bid) 2. Madopar and Sinemet (NR)	1.Placebo (1 package, bid) 2. Madopar and Sinemet (NR)	12 weeks	NR	1. UPDRS I 2. UPDRS II 3. UPDRS III 4. UPDRS IV 5. Total UPDRS Score 6. PDQL 7. NMSQuest 8. PDSS 9. HAMD 10. Adverse events	1. $P < 0.05$ 2. $P < 0.05$ 3. $P < 0.05$ 4.$P > 0.05$ 5. $P < 0.05$ 6. $P < 0.01$ 7. $P < 0.01$ 8. $P < 0.01$ 9. $P < 0.01$ 10. $P < 0.05$
Chen M. Y. et al., 2014	Chinese	UK brain bank standard	Randomized, double-blind and placebo-controlled parallel study	57 (38/19) 66.44 ± 7.64	51 (35/16) 65.63 ± 7.37	4.41 ± 2.45 years	4.39 ± 3.07 years	1.Zhichan granule (1 package, bid) 2.WCM (NR)	1.Placebo (1 package, bid) 2. WCM (NR)	12 weeks	NR	1. UPDRS I 2. UPDRS II 3. UPDRS III 4. UPDRS IV 5. Total UPDRS Score 6. Adverse events	1.$P > 0.05$ 2.$P > 0.05$ 3.$P < 0.05$ 4.$P > 0.05$ 5. $P < 0.05$ 6.$P > 0.05$
Guo, 2010	Chinese	UK brain bank standard	Randomized, double-blind and placebo-controlled parallel study	30 (20/10) 68.23 ± 7.22	30 (16/14) 67.47 ± 8.12	47.4 ± 33.98 months	39.67 ± 24.33 months	1.Guilu Dihuang capsule (1.5 g, tid) 2. Madopar (125 mg, tid)	1.Placebo (1.5 g, tid) 2. Madopar (125 mg, tid)	8 weeks	NR	1. Adverse events	1. $P > 0.05$
Guo et al., 2014	Chinese	UK brain bank standard	Randomized, double-blind and placebo-controlled parallel study	35 (NR) NR	30 (NR) NR	NR	NR	1. Bushen Huoxue granules (1 package, bid) 2. Madopar (NR)	1. Placebo (1 package, bid) 2. Madopar (NR)	6 months	NR	1. HAMD 2. Adverse Events	1. $P > 0.01$ 2. $P > 0.05$
Kum et al., 2011	English	UK brain bank standard	Randomized, double-blind and placebo-controlled parallel study	22 (14/8) 64.82 ± 8.88	25 (17/8) 60.88 ± 9.41	5.44 ± 5.26 years	6.37 ± 4.93 years	1.Jiawei Liujunzi Tang granule (1 package, qd) 2.Levodopa (NR)	1.Placebo (1 package, qd) 2.Levodopa (NR)	24 weeks	NR	1. UPDRS IV 2. PDQ-39 3. Adverse Events	1. $P < 0.05$ 2. $P < 0.05$ 3. $P > 0.05$
Li et al., 2016	English	UK brain bank Standard	Multi-center randomized, double-blind and placebo-controlled parallel study	60 (31/27) 66.6 ± 1.2	60 (42/20) 67.3 ± 1.2	5.2 ± 0.4 years	5.1 ± 0.5 years	1.Bushen Huoxue granule (1 package, bid) 2. Madopar (NR)	1.Placebo (1 package, bid) 2. Madopar (NR)	3 months	6 months	1. UPDRS II 2. UPDRS III 3. PDQ-39 4. PDSS 5. Adverse Events	1. $P > 0.05$ 2. $P > 0.05$ 3. $P > 0.05$ 4. $P > 0.05$ 5. $P > 0.05$
Pan et al., 2009	Chinese	JDS for PD in 1997	Randomized, double-blind and placebo-controlled parallel study	32 (18/14) 64.9 ± 10.2	18 (10/8) 65.3 ± 10.2	4.9 ± 4 years	5.1 ± 2.5 years	1.Zengxiao Anshen Zhichan 2 granule (5 g, bid) 2. WCM (NR)	1.Placebo (5 g, bid) 2. WCM (NR)	3 months	NR	1. UPDRS I 2. UPDRS II 3. UPDRS III 4. UPDRS IV 5. Total UPDRS Score	1. $P > 0.05$ 2. $P > 0.05$ 3. $P > 0.05$ 4. $P > 0.05$ 5. $P > 0.05$
				30 (16/14) 65.1 ± 9.4	16 (8/8) 63.7 ± 11.1	6.1 ± 3.8 years	6.3 ± 2.9 years	1.Zengxiao Anshen Zhichan 2 granule (5 g, bid) 2. WCM (NR)	1.Placebo (5 g, bid) 2. WCM (NR)	3 months	NR	1. UPDRS I 2. UPDRS II 3. UPDRS III 4. UPDRS IV 5. Total UPDRS Score	1. $P > 0.05$ 2. $P > 0.05$ 3. $P > 0.05$ 4. $P > 0.05$ 5. $P > 0.05$

(Continued)

TABLE 1 | Continued

Included studies	Publication language	Diagnostic criteria	Study designs	No. of participants (male/female); mean age (years)		Course of disease		Interventions		Course of treatment	Follow up	Outcome index	Intergroup differences
				Trial	Control	Trial	Control	Trial	Control				
Pan et al., 2011	English	UK brain bank standard	Randomized, double-blind and placebo-controlled parallel study	56 (34/22) 62.82 ± 10.31	54 (32/22) 63.1 ± 10.2	5.73 ± 4.81 years	5.81 ± 3.24 years	1.Zengxiao Anshen Zhichan 2 granule (1 package, tid) 2. WCM (NR)	1. Placebo (1 package, tid) 2. WCM (NR)	3 months	NR	1. UPDRS I 2. UPDRS II 3. UPDRS III 4. UPDRS IV 5. Total UPDRS Score 6. Adverse Events	1. $P > 0.05$ 2. $P < 0.05$ 3. $P > 0.05$ 4. $P < 0.05$ 5. $P < 0.05$ 6. $P > 0.05$
Pan et al., 2013	English	UK brain bank standard	Randomized, double-blind and placebo-controlled parallel study	31 (18/13) 68.6 ± 9.2	30 (19/11) 67.1 ± 10.2	5.9 ± 4.7 years	6.1 ± 4.9 years	1.Yangxue Qingnao granule (1 package, tid) 2. WCM (NR)	1.Placebo (1 package, tid) 2. WCM (NR)	12 weeks	4 weeks	1. PDSS 2. Adverse events	1. $P < 0.05$ 2. $P > 0.05$
Wen et al., 2015	Chinese	UK brain bank standard	Randomized, double-blind and placebo-controlled parallel study	29 (15/14) 70.79 ± 7.5	28 (16/12) 71.21 ± 5.96	34.48 ± 12.70 m	34.78 ± 11.63 m	1.Congwu Qufeng granule (1 package, tid) 2. WCM (NR)	1.Placebo (1 package, tid) 2. WCM (NR)	3 months	NR	1. PDQ-39	1. $P < 0.05$
Yang, 2017	Chinese	UK brain bank standard	Randomized, double-blind and placebo-controlled parallel study	40 (19/21) 65.24 ± 12.53	39 (21/18) 63.28 ± 11.26	7.02 ± 3.63 years	6.24 ± 2.16 years	1.Yishen Chuchan decoction (0.5 dose, bid) 2. Madopar (NR)	1.Placebo (0.5 dose, bid) 2. Madopar (NR)	2 months	NR	1. UPDRS III 2. PDQ-39 3. NMSS 4. Adverse Events	1.$P < 0.05$ 2. $P < 0.01$ 3. $P < 0.01$ 4. $P > 0.05$
Yu, 2016	Chinese	CNDS for PD in 2006	Randomized, double-blind and placebo-controlled parallel study	34 (19/15) 70.765 ± 7.836	34 (17/17) 69.706 ± 9.137	24.176 ± 10.715 months	26.029 ± 11.371 months	1.Naokang granule (1 package, tid) 2. Madopar (125 mg, tid)	1.Placebo (1 package, bid) 2. Madopar (125 mg, tid)	2 months	NR	1. UPDRS II 2. UPDRS III 3. NMSS 4. Adverse Events	1. $P < 0.05$ 2. $P < 0.05$ 3. $P < 0.05$ 4. $P > 0.05$
Zhao et al., 2009	Chinese	CNDS for PD in 1984	Multi-center randomized, double-blind and placebo-controlled parallel study	28 (15/13) 65.40 ± 8.16	25 (15/10) 63.14 ± 11.58	3.69 ± 1.82 years	4.19 ± 3.39 years	Guiling Pa'an capsule (1.5 g, tid)	Placebo (1.5 g, tid)	12 weeks	NR	1. UPDRS II 2. UPDRS III 3. Total UPDRS Score	1. $P > 0.05$ 2. $P > 0.05$ 3. $P > 0.05$
				75 (46/29) 64.86 ± 9.85	79 (47/32) 65.63 ± 8.51	4.7 ± 3.44 years	4.59 ± 3.82 years	1.Guiling Pa'an capsule (3 g, tid) 2. Madopar and Sinemet (NR)	1.Placebo (3 g, tid) 2. Madopar and Sinemet (NR)	12 weeks	NR	1. UPDRS II 2. UPDRS III 3. Total UPDRS Score	1. $P > 0.05$ 2. $P > 0.05$ 3. $P > 0.05$
				19 (8/11) 67.24 ± 9.54	16 (12/4) 66.l 0 ± 7.61	6.24 ± 4.31 years	6.26 ± 2.53 years	1.Guiling Pa'an capsule (3 g, tid) 2. Madopar and Sinemet (NR)	1,Placebo (3 g, tid) 2. Madopar and Sinemet (NR)	12 weeks	NR	1. UPDRS II 2. UPDRS III 3. Total UPDRS Score	1. $P > 0.05$ 2. $P > 0.05$ 3. $P > 0.05$
Zhao et al., 2013	Chinese	UK brain bank standard	Multicenter randomized, double-blind and placebo-controlled parallel study	54 (42/16) 68.64 ± 8.00	58 (27/27) 68.46 ± 8.80	2–18 years	2–21 years	1.Guiling Pa'an granule (6 g, tid) 2. WCM (NR)	1.Placebo (6 g,tid) 2. WCM (NR)	6 months	NR	1. Adverse Events	1. $P > 0.05$

bid, bis in die; CNDS, Chinese National Diagnosis Standard; HAMD, Hamilton depression rating scale; JDS, Japnese Diagnosis Standard; m, month; NMSQuest, Non-motor Symptoms Questionnaire; NMSS, Non-Motor Symptoms Scale; NR, not reported; PDQ-39, Parkinson's Disease Questionnaire-39; PDQL, Parkinson's Disease Quality of Life Questionnaire; PDSS, Parkinson's Disease Sleep Scale; qd, quaque die; tid, ter in die; UPDRS, Unified Parkinson's Disease Rating Scale; w, week; WCM, western conventional medication; y, year.

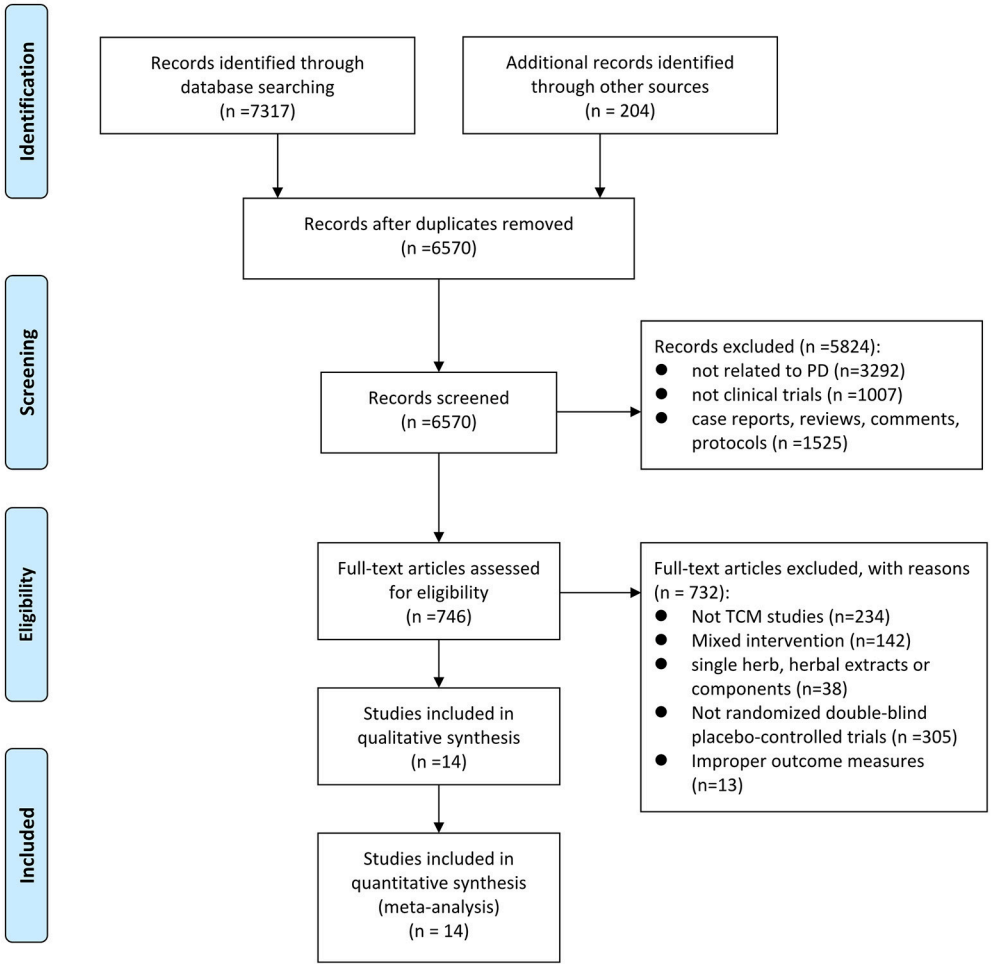

FIGURE 1 | Flow diagram of the search process.

Pa'an granule ($n = 1$). The ingredients of TCM formulas in each included studies were presented in **Table 2**. A total of 52 herbs were used in these TCM formulas. High-frequency herbs in HM formulas were ranked in **Table 3**. The top 11 most frequently used herbs were Radix Salviae Miltiorrhizae (Dan Shen), Radix Paeoniae Alba (Bai Shao), Ramulus Uncariae Cum Uncis (Gou Teng), Radix Rehmanniae (Di Huang), Herba Cistanches (Rou Cong Rong), Radix Polygoni Multiflori (He Shou Wu), Rhizoma Ligustici Chuanxiong (Chuan Xiong), Fructus Corni (Shan Zhu Yu), Radix Angelicae Sinensis (Dang Gui), Rhizoma Acori Tatarinowii (Shi Chang Pu), and Radix Astragali seu Hedysari (Huang Qi).

Assessing the Quality of Studies

The methodological quality of all included studies was detailed in the **Figure 2**. All included studies were randomized studies with explicit description. Specifically, seven studies (Pan et al., 2009, 2011; Guo et al., 2014; Wen et al., 2015; Yu, 2016; Cai et al., 2017; Yang, 2017) used random number tables. Four studies (Zhao et al., 2009; Kum et al., 2011; Pan et al., 2013; Chen M. Y. et al., 2014) used computer-generated lists of random numbers. Two studies (Zhao et al., 2013; Li et al., 2016) employed online center distribution, while only one study (Guo, 2010) stated the method for sequence generation by simple randomization. Eleven studies (Zhao et al., 2009, 2013; Kum et al., 2011; Pan et al., 2011, 2013; Chen M. Y. et al., 2014; Wen et al., 2015; Li et al., 2016; Yu, 2016; Cai et al., 2017; Yang, 2017) reported adequate allocation concealment. Four (Kum et al., 2011; Chen M. Y. et al., 2014; Yu, 2016; Cai et al., 2017) adopted opaque and sealed envelopes. The remaining studies (Zhao et al., 2009, 2013; Pan et al., 2011, 2013; Wen et al., 2015; Li et al., 2016; Yang, 2017) adopted center distribution. Of 14 included studies, 8 studies (Pan et al., 2009; Zhao et al., 2009, 2013; Guo, 2010; Guo et al., 2014; Wen et al., 2015; Yu, 2016; Yang, 2017) applied double blinding and 6 studies (Kum et al., 2011; Pan et al., 2011, 2013; Chen M. Y. et al., 2014; Li et al., 2016; Cai et al., 2017) had triple blinding. All studies had low risk of bias in the incomplete out-come data. Four studies (Guo, 2010; Guo et al., 2014; Yu, 2016; Yang, 2017) had unclear risk of bias in selective reporting because of no available protocols. Other

TABLE 2 | Ingredients of TCM formula.

Included studies	Prescription	Ingredients		
		Latin name	**English name**	**Chinese name**
Cai et al., 2017	Zhichan decoction	Radix Astragali seu Hedysari, Radix Paeoniae Alba, Radix Salviae Miltiorrhizae, Rhizoma Anemarrhenae, Ramulus Uncariae Cum Uncis, Rhizoma Cimicifugae, Rhizoma Polygoni Cuspidati.	Milkvetch root, debark peony root, danshen root, common anemarrhena rhizome, gambir plant nod, largetrifoliolious bugbane rhizome, giant knotweed rhizome.	Huang Qi, Bai Shao, Dan Shen, Zhi Mu, Gou Teng, Sheng Ma, Hu Zhang.
Chen M. Y. et al., 2014	Zhichan granule	Radix Astragali seu Hedysari, Ramulus Uncariae Cum Uncis, Radix Polygoni Multiflori Preparata, Radix Paeoniae Alba, Rhizoma Anemarrhenae, et al.	Milkvetch root, gambir plant nod, prepared fleeceflower root, debark peony root, common anemarrhena rhizome, et al.	Huang Qi, Gou Teng, Zhi He Shou Wu, Bai Shao, Zhi Mu, et al.
Guo, 2010	Guilu Dihuang capsule	Radix Rehmanniae Preparata, Chinemys reevesii, Colla Corni Cervi, et al.	Prepared rehmannia root, tortoise plastron glue, deerhorn glue, et al.	Shu Di Huang, Gui Ban Jiao, Lu Jiao Jiao, et al.
Guo et al., 2014	Bushen Huoxue granule	Fructus Corni, Herba Cistanches, Radix Polygoni Multiflori, Rhizoma Ligustici Chuanxiong, Radix Angelicae Sinensis, Radix Salviae Miltiorrhizae, Scolopendra, et al.	Asiatic cornelian cherry fruit, desertliving cistanche, fleeceflower root, sichuan lovage rhizome, Chinese angelica, danshen root, centipede, et al.	Shan Zhu Yu; Rou Cong Rong; He Shou Wu; Chuan Xiong; Dang Gui; Dan Shen; Wu Gong , et al.
Kum et al., 2011	Jiawei Liujun Zi Tang granule	Radix Codonopsis, Radix Rehmanniae Recens, Poria, Ramulus Uncariae Cum Uncis, Rhizoma Atractylodis Macrocephalae, Radix Angelicae Sinensis, Rhizoma Pinelliae Preparatum, Rhizoma Ligustici Chuanxiong, Radix Achyranthis Bidentatae, Pericarpium Citri Reticulatae, Radix Glycyrrhizae.	Tangshen, unprocessed rehmannia root, Indian bread, gambir plant nod, largehead atractylodes rhizome, Chinese angelica, processed pinellia tuber, sichuan lovage rhizome, twotoothed achyranthes root, dried tangerine peel, liquorice root.	Dang shen; Sheng di huang; Fu ling; Gou Teng; Bai Zhu; Dang Gui; Fa ban xia; Chuan Xiong; niu xi; Chen pi; Gan cao.
Li et al., 2016	Bushen Huoxue granule	Fructus Corni, Rhizoma Acor tatarinowii, Radix Polygoni multiflori, Herba Cistanches, Raix Angelicae sinensis, Radix Salviae miltiorrhizae, Scolopendra.	Asiatic cornelian cherry fruit, grassleaf sweetflag rhizome, fleeceflower root, desertliving cistanche, Chinese angelica, danshen root, centipede.	Shan Zhu Yu, Shi Chang Pu, He Shou Wu; Rou Cong Rong, Dang Gui; Dan Shen; Wu Gong.
Pan et al., 2009	Zeng-xiao An-shen Zhi-chan 2 capsule	Radix Rehmanniae Preparata, Fructus Corni, Os Draconis, Radix Asparagi, Radix Paeoniae Alba, Carapax et Plastrum Testudinis, Herba Cistanches, Radix Puerariae, Rhizoma Arisaematis Cum Bile, Scorpio, Radix Salviae Miltiorrhizae, Lumbricus, Rhizoma Acori Tatarinowii, Rhizoma Curcumae Longae.	Prepared rehmannia root, asiatic cornelian cherry fruit, bone fossil of big mammals, cochinchinese asparagus root, debark peony root, tortoise carapace and plastron, desertliving cistanche, kudzuvine root, bile arisaema, scorpion, Danshen root, earthworm, grassleaf sweetflag rhizome, turmeric.	Shu Di Huang; Shan Zhu Yu; Long Gu; Tian Dong; Shao Yao; Gui Jia; Rou Cong Rong; Ge Gen; Dan Nan Xing; Quan Xie; Dan Shen; Di Long; Shi Chang Pu; Jiang Huang.
Pan et al., 2011	Zengxiao Anshen Zhichan 2 granule	Ramulus Uncariae Cum Uncis, Radix Rehmanniae Recens, Fructus Corni, Radix Asparagi, Radix Paeoniae Alba, Herba Cistanches, Radix Puerariae, Rhizoma Arisaematis, Radix Salviae Miltiorrhizae, Rhizoma Acori Tatarinowii, Rhizoma Curcumae Longae, Radix Morindae Officinalis, Rhizoma Gastrodiae, Rhizoma Ligustici Chuanxiong,	Gambir plant nod, unprocessed rehmannia root, asiatic cornelian cherry fruit, cochinchinese asparagus root, debark peony root, desertliving cistanche, kudzuvine root, jackinthepulpit tuber, danshen root, grassleaf sweetflag rhizome, turmeric, morinda root, tall gastrodia tuber, sichuan lovage rhizome.	Gou Teng; Sheng Di Huang; Shan Zhu Yu; Tian Dong; Bai Shao; Rou Cong Rong; Ge Gen; Tian Nan Xing; Dan Shen; Shi Chang Pu; Jiang Huang; Ba Ji Tian; Tian Ma; Chuan Xiong.
Pan et al., 2013	Yangxue Qingnao granule	Radix Angelicae Sinensis, Rhizoma Ligustici Chuanxiong, Radix Paeoniae Alba, Ramulus Uncariae Cum Uncis, Caulis Spatholobi, Spica Prunellae, Concha Margaritifera, Radix Rehmanniae Recens, Semen Cassiae, Rhizoma Corydalis, Herba Asari.	Chinese angelica, sichuan lovage Rhizome, debark peony root, gambir plant nod, suberect spatholobus stem, common selfheal fruit-spike, nacre, unprocessed rehmannia root, cassia seed, yanhusuo, manchurian wildginger.	Dang Gui; Chuan Xiong; Bai shao; Gou Teng; Ji Xue Teng; Xia Ku Cao; Zhen Zhu Mu; Di Huang; Jue Ming Zi; Yan Hu Suo; Xi Xin

(Continued)

TABLE 2 | Continued

Included studies	Prescription	Ingredients		
		Latin name	English name	Chinese name
Wen et al., 2015	Congwu Xifeng granule	Radix Polygoni Multiflori Preparata, Herba Cistanches, Cortex Eucommiae, Rhizoma Gastrodiae Ramulus Uncariae Cum Uncis, Rhizoma Atractylodis Macrocephalae, Radix Paeoniae Alba, Rhizoma Polygoni Cuspidati, Radix et Rhizoma Rhei,	Prepared fleeceflower root, desertliving cistanche, eucommia bark, tall gastrodia tuber, gambir plant nod, largehead atractylodes rhizome, debark peony root, giant knotweed rhizome, rhubarb root and rhizome.	Zhi He Shou Wu; Rou Cong Rong; Du Zhong; Tian Ma , Gou Teng; Bai Zhu; Bai Shao; Hu Zhang; Jiu Da Huang.
Yang et al., 2017	Yishen Chuchan decoction	Radix Polygoni Multiflori Preparata,Radix Rehmanniae Recens, Rhizoma Gastrodiae, Radix Paeoniae Alba, Concha Ostreae, Bombyx Batryticatus, Radix et Rhizoma Rhei, Radix Linderae, Rhizoma Dioscoreae, Fructus Alpiniae oxyphyllae.	PREPARED fleeceflower root, unprocessed rehmannia root, tall gastrodia tuber, debark peony root, oyster shell, stiff silkworm, rhubarb root and rhizome, combined spicebush root, common yam rhizome, sharp-leaf glangal fruit.	Zhi He Shou Wu, Sheng Di Huang, Tian Ma, Bai Shao, Mu Li, Jiang Can, Da Huang, wu Yao, Shan yao, Yi Zhi.
Yu, 2016	Naokang granule	Herba Cistanches, Radix Notoginseng, Rhizoma Ligustici Chuanxiong, Radix Salviae Miltiorrhizae, Rhizoma Acori Tatarinowii, Radix Polygalae, Scolopendra, Lumbricus, Bombyx Batryticatus, Scorpio, Radix Astragali seu Hedysari, Radix Codonopsis, Herba Epimedii.	Desertliving cistanche, sanqi, sichuan lovage rhizome, danshen root, grassleaf sweetflag rhizome, milkwort root, centipede, earthworm, stiff silkworm, scorpion, milkvetch root, tangshen, epimedium herb.	Rou Cong Rong, San Qi, Chuan Xiong, Dan Shen, Shi Chang Pu, Yuan Zhi, Wu Gong, Di Long, Jiang Can, Quan Xie, Huang qi, Dang Shen, Yin Yang Huo.
Zhao et al., 2009, 2013	Guiling Pa'an capsule Guiling Pa'an granule	Carapax et Plastrum Testudinis, Cornu Saigae Tataricae, et al.	Tortoise carapace and plastron, antelope horn, et al.	Gui Jia; Ling Yang Jiao, et al.

TABLE 3 | The 11 high-frequency used herbs for PD in the 14 trials included.

Herb name			Frequency	The total frequency %	Cumulative percentiles %
Latin name	English name	Chinese name			
Radix Salviae Miltiorrhizae	Danshen root	Dan Shen	7	6.1	6.1
Radix Paeoniae Alba	Debark peony root	Bai Shao	7	6.1	12.2
Ramulus Uncariae Cum Uncis	Gambir plant nod	Gou Teng	6	5.2	17.4
Radix Rehmanniae	Rehmannia root	Di Huang	6	5.2	22.6
Herba Cistanches	Desertliving cistanche	Rou Cong Rong	6	5.2	27.8
Radix Polygoni Multiflori	Fleeceflower root	He Shou Wu	5	4.3	32.2
Rhizoma Ligustici Chuanxiong	Sichuan lovage rhizome	Chuan Xiong	5	4.3	36.5
Fructus Corni	Asiatic cornelian cherry fruit	Shan Zhu Yu	4	3.5	40.0
Radix Angelicae Sinensis	Chinese angelica	Dang Gui	4	3.5	43.5
Rhizoma Acori Tatarinowii	Grassleaf sweetflag rhizome	Shi Chang Pu	4	3.5	47.0
Radix Astragali seu Hedysari	Milkvetch root	Huang Qi	3	2.6	49.6

risks of bias were described in one study (Li et al., 2016), which reported significant differences in baseline values of some outcome variables.

Effect Estimation

HM Monotherapy vs. Placebo

One study (Zhao et al., 2009) showed that the efficacy of HM monotherapy was similar to placebo according to UPDRS II ($P > 0.05$), UPDRS III ($P > 0.05$) and total UPDRS score ($P > 0.05$) in PD patients who never received levodopa treatment.

HM Plus WCM vs. Placebo Plus WCM

UPDRS I: Four studies (Pan et al., 2009, 2011; Chen M. Y. et al., 2014; Cai et al., 2017) with 5 comparisons showed that the HM paratherapy significantly improved UPDRS I compared with control groups (WMD: −0.30, 95% CI: −0.54 to −0.06, $P = 0.02$; heterogeneity: $Chi^2 = 3.21$, $P = 0.52$, $I^2 = 0\%$; **Figure 3A**).

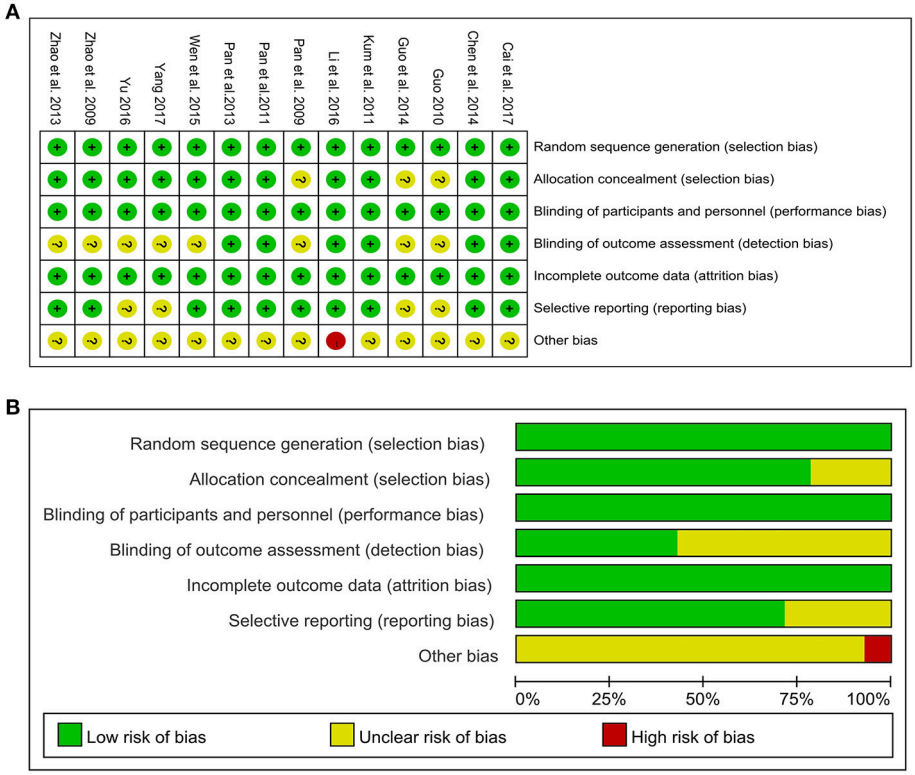

FIGURE 2 | Risk of bias of the included studies. **(A)** Risk of bias summary: judgements about each risk of bias item for each included study. **(B)** Risk of bias graph: judgements about each risk of bias item presented as percentages across all included studies. +, low risk of bias; -, high risk of bias; ?, unclear risk of bias.

UPDRS II: Seven studies (Pan et al., 2009, 2011; Zhao et al., 2009; Chen M. Y. et al., 2014; Li et al., 2016; Yu, 2016; Cai et al., 2017) with 9 comparisons assessed UPDRS II. Compared with the placebo, meta-analysis of 9 comparisons showed that HM paratherapy significantly improved UPDRS II (WMD: −1.53, 95% CI −2.76 to −0.30, $P = 0.01$; heterogeneity: $Chi^2 = 19.42$, $P = 0.01$, $I^2 = 59\%$). Sensitivity analyses conducted to explore potential sources of heterogeneity. A trial (Li et al., 2016) had imbalanced baseline comparing HM with placebo. After removing the trial, meta-analysis of 8 comparisons (Pan et al., 2009, 2011; Zhao et al., 2009; Chen M. Y. et al., 2014; Yu, 2016; Cai et al., 2017) showed that HM paratherapy was still superior to the placebo (WMD: −2.21, 95% CI: −3.19 to −1.22, $P < 0.0001$; heterogeneity: $Chi^2 = 3.46$, $P = 0.84$, $I^2 = 0\%$; **Figure 3B**).

UPDRS III: Eight studies (Pan et al., 2009, 2011; Zhao et al., 2009; Chen M. Y. et al., 2014; Li et al., 2016; Yu, 2016; Cai et al., 2017; Yang, 2017) with 10 comparisons used UPDRS III as outcome measure. Compared with the placebo, meta-analysis of 10 comparisons showed that HM paratherapy had no significance for improving UPDRS III (WMD = −2.13, 95% CI:−4.92 to 0.66, $P = 0.19$; heterogeneity: $Chi^2 = 87.10$, $P < 0.00001$, $I^2 = 90\%$). A trial (Li et al., 2016) had imbalanced baseline comparing HM with placebo. After removing the trial, meta-analysis of 9 comparisons (Pan et al., 2009, 2011; Zhao et al., 2009; Chen M. Y. et al., 2014; Yu, 2016; Cai et al., 2017; Yang, 2017) showed that HM paratherapy was superior to the placebo (WMD: −3.26, 95% CI:−4.36 to −2.16, $P < 0.00001$; heterogeneity: $Chi^2 = 1.88$, $P = 0.98$, $I^2 = 0\%$; **Figure 3C**).

UPDRS IV: Meta-analysis of 5 studies (Pan et al., 2009, 2011; Kum et al., 2011; Chen M. Y. et al., 2014; Cai et al., 2017) with 6 comparisons revealed that HM paratherapy did not significantly improve UPDRS IV relative to placebo (WMD: −0.18, 95% CI: −0.37 to −0.01, $P = 0.06$; heterogeneity: $Chi^2 = 5.76$, $P = 0.33$, $I^2 = 13\%$; **Figure 3D**).

Total UPDRS Score: Meta-analysis of 4 studies (Pan et al., 2009, 2011; Zhao et al., 2009; Chen M. Y. et al., 2014) with 6 comparisons revealed that HM paratherapy significantly improved the total UPDRS scores relative to placebo (WMD: −5.43, 95% CI:−8.01 to −2.86, $P < 0.0001$; heterogeneity: $Chi^2 = 2.59$, $P = 0.76$, $I^2 = 0\%$; **Figure 3E**).

Quality of Life: Compared with the placebo, meta-analysis of 4 studies (Kum et al., 2011; Wen et al., 2015; Li et al., 2016; Yang, 2017) showed that HM paratherapy had no significance for improving PDQ-39 (WMD: −4.65, 95% CI: −10.97 to 1.68, $P = 0.15$; heterogeneity: $Chi^2 = 19.19$, $P = 0.0002$, $I^2 = 84\%$). A trial (Li et al., 2016) had imbalanced baseline comparing HM with placebo. After removing the trial, meta-analysis of 3 studies (Kum et al., 2011; Wen et al., 2015; Yang, 2017) showed that HM paratherapy was superior to the placebo (WMD: −7.65, 95% CI: −11.46 to −3.83, $p < 0.0001$; heterogeneity: $Chi^2 = 0.12$, $P = 0.94$, $I^2 = 0\%$; **Figure 4A**). One randomized

controlled trial (RCT) (Cai et al., 2017) showed HM paratherapy was a significant superiority to placebo according to PDQL (P <0.01).

NMSQuest and NMSS: One trial (Cai et al., 2017) showed that HM paratherapy produced greater reduction in NMSQuest score than that of placebo ($P < 0.01$). Meta-analysis of 2 studies (Yu, 2016; Yang, 2017) showed that HM paratherapy was favor of NMSS compared with placebo (WMD: −9.19, 95% CI: −13.11 to −5.28, $P < 0.00001$; heterogeneity: $Chi^2 = 0.56$, $P = 0.45$, $I^2 = 0\%$; **Figure 4B**).

PDSS: Compared with the placebo, meta-analysis of 3 studies (Pan et al., 2013; Li et al., 2016; Cai et al., 2017) showed that HM paratherapy had no significance for improving PDSS (WMD: 7.10, 95% CI: −2.26 to 16.45, $P = 0.14$; heterogeneity: $Chi^2 = 101.02$, $P = 0.14$, $I^2 = 98\%$). A trial (Li et al., 2016) had imbalanced baseline comparing HM with placebo. After removing the trial, meta-analysis of 2 studies (Pan et al., 2013; Cai et al., 2017) showed that HM paratherapy was superior to the placebo (WMD: 10.69, 95% CI: 8.86 to 12.53, $P < 0.00001$; heterogeneity: $Chi^2 = 0.48$, $P = 0.49$, $I^2 = 0\%$; **Figure 4C**).

HAMD: Meta-analysis of 2 studies (Guo et al., 2014; Cai et al., 2017) showed that HM paratherapy was superior to the placebo according to HAMD (WMD: −5.87, 95% CI: −7.06 to −4.68, $p < 0.00001$) with mild heterogeneity ($Chi^2 = 1.51$, $P = 0.22$, $I^2 = 34\%$; **Figure 4D**).

Adverse Events

HM Monotherapy vs. Placebo

In the only one study (Zhao et al., 2009), neither the experimental group nor the control group provide any information about adverse events.

HM Plus WCM vs. Placebo Plus WCM

Eleven RCTs (Guo, 2010; Kum et al., 2011; Pan et al., 2011, 2013; Zhao et al., 2013; Chen M. Y. et al., 2014; Guo et al., 2014; Li et al., 2016; Yu, 2016; Cai et al., 2017; Yang, 2017) reported adverse events, among them 3 studies (Pan et al., 2011, 2013; Guo et al., 2014) reported no adverse events. However, the other 3 studies did not provide any information on adverse event (Pan et al., 2009; Zhao et al., 2009; Wen et al., 2015). Meta-analysis of 8 studies (Guo, 2010; Kum et al., 2011; Zhao et al., 2013; Chen M. Y. et al., 2014; Li et al., 2016; Yu, 2016; Cai et al., 2017; Yang, 2017) showed that HM paratherapy was significant benefit in reducing adverse events compared with control group (RR: 0.41, 95% CI: 0.21 to 0.80, $P = 0.009$; heterogeneity: $Chi^2 = 6.36$, $P = 0.38$, $I^2 = 6\%$; **Figure 5**). The most reported adverse events were gastrointestinal symptoms, such as nausea, vomiting, diarrhea, and abdominal distention in both the HM groups and placebo groups. No life-threatening adverse event was noted in all studies.

Publication Bias

We did not performed the Funnel plot and Egger's test because the number of studies in each meta-analysis was less than ten.

DISCUSSION

Summary of Evidence

This is first systematic review of randomized double-blind placebo-controlled clinical trials to assess the efficacy and safety of HM formulas for PD. Fourteen high-quality randomized controlled trials (Pan et al., 2009, 2011, 2013; Zhao et al., 2009, 2013; Guo, 2010; Kum et al., 2011; Chen M. Y. et al., 2014; Guo et al., 2014; Wen et al., 2015; Li et al., 2016; Yu, 2016; Cai et al., 2017; Yang, 2017) involving 1,316 patients suffering from PD were identified. HM paratherapy was significant for improving motor symptoms and non-motor functions, whereas there was a negative result of complications of treatment. One trail (Zhao et al., 2009) indicated that HM monotherapy was not superior to the placebo. Eleven out of fourteen studies (Guo, 2010; Kum et al., 2011; Pan et al., 2011, 2013; Zhao et al., 2013; Chen M. Y. et al., 2014; Guo et al., 2014; Li et al., 2016; Yu, 2016; Cai et al., 2017; Yang, 2017) reported no serious adverse events relevant with HM formulas, indicating that HM formulas were generally safe and well tolerated for PD patients. Thus, the findings of present study supported the complementary use of HM paratherapy for PD patients, whereas HM monotherapy for PD is still lack of evidence.

LIMITATIONS

First, the members of the International Committee of Medical Journal Editors published a statement requiring that all clinical trials must be registered in order to be considered for publication (DeAngelis et al., 2004). However, most of included studies didn't formally register. Protocols were not available to confirm free of selective reporting. Thus, further clinical trials must register prospectively in international clinical trials registry platform. Second, although we included randomized double-blind placebo-controlled trials, some inherent and methodological weaknesses still existed in the primary studies: (1) An adequate sample size is crucial to the design of RCTs (Lewis, 1999), but only 4 trials (Kum et al., 2011; Zhao et al., 2013; Li et al., 2016; Yu, 2016) applied pre-trial sample size estimation; (2) PD is a chronic degenerative disease. Long-term efficacy and safety are important assessments to decide the clinical usefulness of an agent in treatment, but only one trial (Li et al., 2016) had the long-term duration of follow-up at 6 month; (3) Intention-to-treat (ITT) analysis could avoid bias and false-positive results, which is the recommended standard approach to analyse data from RCTs (Abraha et al., 2017). However, only two studies (Kum et al., 2011; Li et al., 2016) adopted ITT analysis. (4) In the present study, only 6 trials conducted assessor blinding. Considering the characteristics of outcome measurement of PD patients (e.g., UPDRS), assessor blinding successfully eliminates assessment bias and increases the accuracy and objectivity of outcomes results. Triple blindness is needed in further PD trials. Thus, CONSORT 2010 statement (Moher et al., 2010a) and CONSORT Extension for Chinese Herbal Medicine Formulas 2017 (Cheng et al., 2017) should be applied in trial reporting and publication. Third, the herbal composition, drug formulation

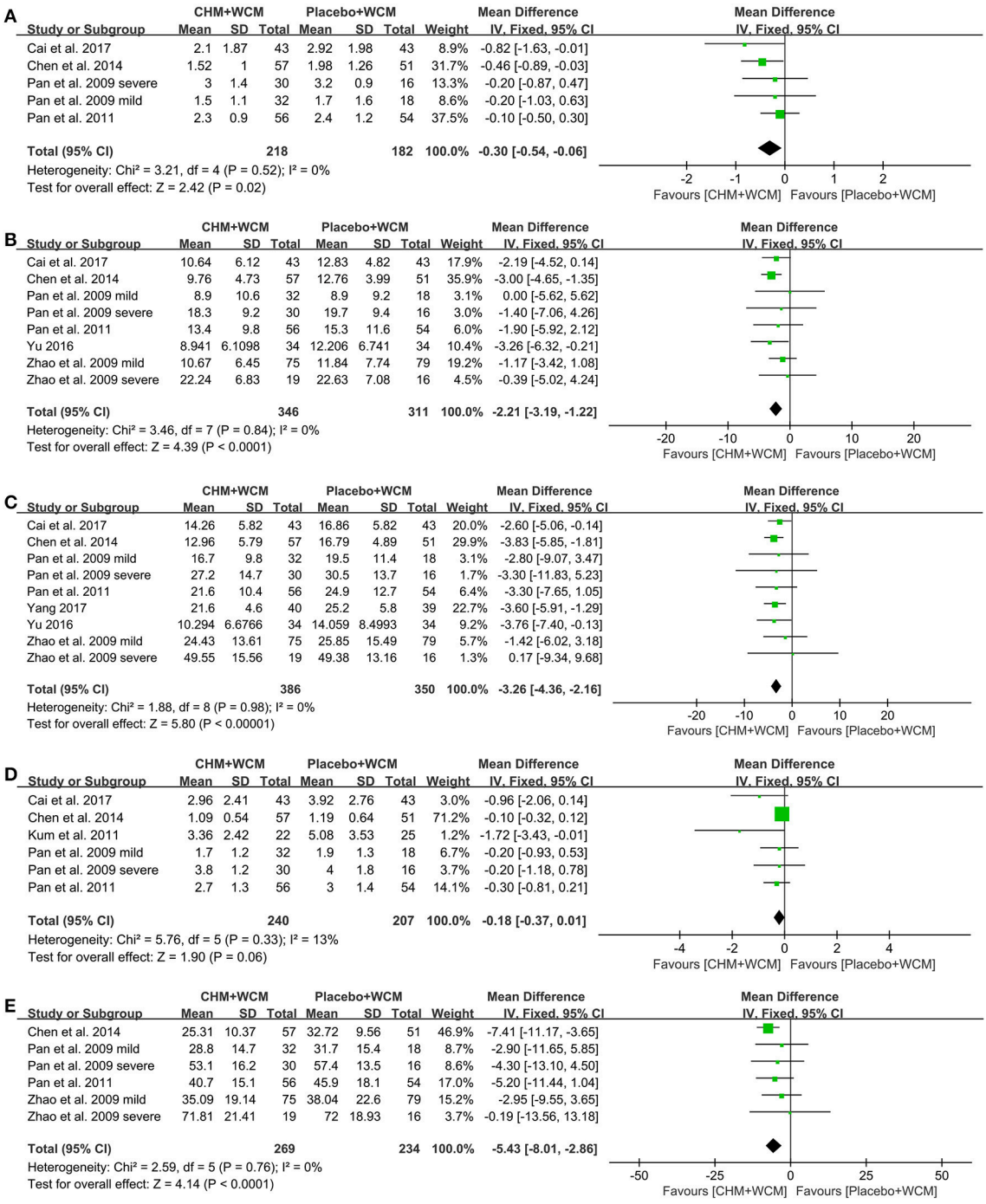

FIGURE 3 | Forest plot of HM plus WCM vs. placebo plus WCM in terms of **(A)** UPDRS I, **(B)** UPDRS II, **(C)** UPDRS III, **(D)** UPDRS IV, and **(E)** Total UPDRS Score. (HM, herbal medicine; WCM, western conventional medicine; UPDRS, Unified Parkinson's Disease Rating Scale).

and dose of the intervention were not exact same, which would lead to clinical heterogeneity. To assess the efficacy and safety of HMs in a clinical trial, all subjects should be given exactly the same intervention in terms of product identity, purity, dosage, and formulation. Fourth, our study only included trials published in the English and Chinese languages and all the included studies were conducted in China, which may affect the generalizability of present findings. In the further studies, the international coliaboration is needed in order to get more qualified stuidies. Finally, different types and stages of PD can influence disease progression and response to treatment (Reinoso et al., 2015). It is difficult to differentiate the effectiveness of

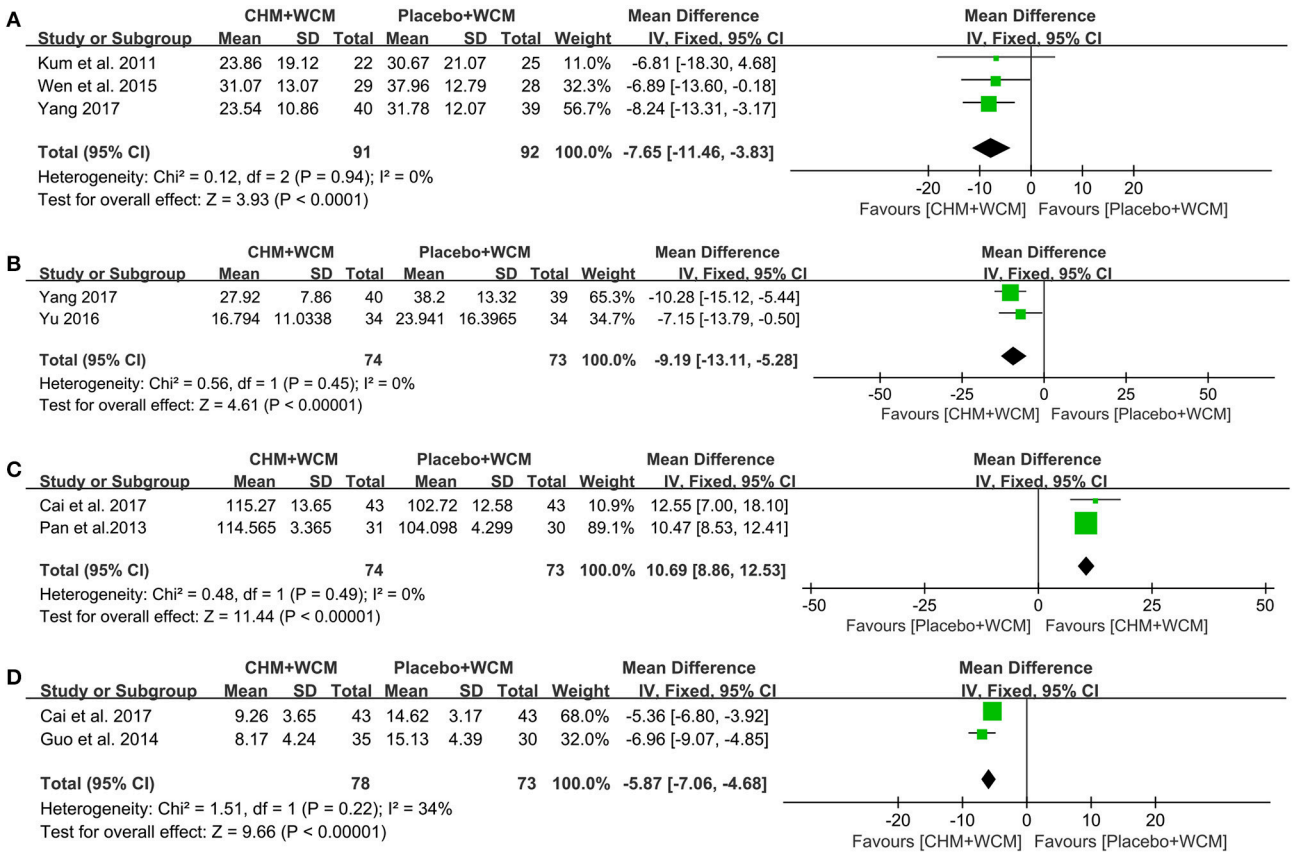

FIGURE 4 | Forest plot of HM plus WCM vs. placebo plus WCM in terms of **(A)** PDQ-39, **(B)** NMSS, **(C)** PDSS, and **(D)** HAMD. (HM, herbal medicine; WCM, western conventional medicine; PDQ-39, Parkinson's Disease Questionnaire-39; NMSS, Non-Motor Symptoms Scale; PDSS, Parkinson's Disease Sleep Scale; HAMD, Hamilton depression rating scale).

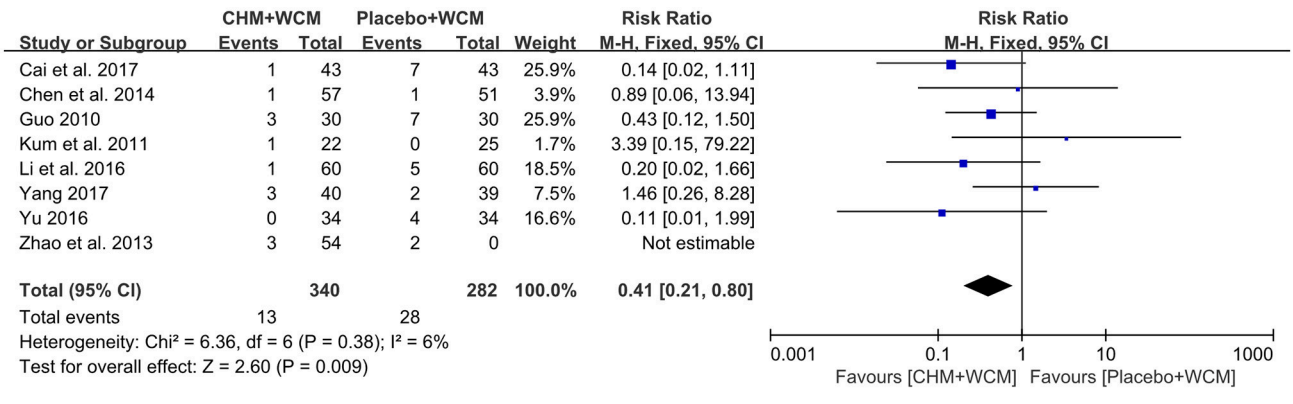

FIGURE 5 | Forest plot of HM plus WCM vs. placebo plus WCM in terms of adverse events.

HM formulas targeting these subgroups due to insufficient data of primary studies. The pertinent research should be conducted in future clinical trials, which would contribute significantly to explore the responsiveness of specific PD subgroup to interventions.

Implications

Up to now, several systematic reviews of traditional medicine for PD (Kim et al., 2012; Wang et al., 2012; Zhang et al., 2014, 2015) have been performed. However, low-quality of included primary studies hindered our conclusions. For example, the

two articles written by Kim et al. (2012) and Zhang et al. (2015) belong to high-quality systematic reviews; however, the inherent limitations existed in the included low-quality primary studies. The present study only included randomized double-blind placebo-controlled trials, which remains the gold standard of trial design (Athauda and Foltynie, 2016). These trials reported the detailed randomized methods; placebo-controlled group accounts for the placebo effects that don't depend on the treatment itself (Chen et al., 2017), and thus increasing the reliability of experiment results. The present study provided the evidence to support HM paratherapy for PD, whereas there is still lack of available evidence for HM monotherapy for PD. However, it should be remembered that a lack of scientific evidence does not necessarily mean that the treatment is ineffective (Kotsirilos, 2005). To explore the efficacy of HM monotherapy for PD is needed in the future.

Currently, most available PD therapies are mainly aimed at motor symptoms (Fox et al., 2018). Non-motor symptoms (NMS) are common in PD patients across all disease stages and are a key determinant of QOL (Martinez-Martin et al., 2012). However, NMS have received limited attention and targeted treatments remain a challenge (Kulisevsky et al., 2018). The present systematic review provided the sportive evidence for the effectiveness and safety of HM paratherapy for NMS of PD patients. Thus, it is worthy of further studies.

Although the exact pathogenic mechanisms underlying selective dopaminergic neurons loss in PD remain unknown, it is believed that oxidative stress and mitochondrial dysfunction, protein misfolding and aggregation, inflammation, and apoptotic cell death play central roles in PD pathogenesis (Sarkar et al., 2016). Obviously, PD is not a result of dysfunction of one specific pathway but rather a combination of interconnected events (Lim and Zhang, 2013). The urgent need in PD is the development of neuroprotective therapy targeting more potential signal pathways (Kalia et al., 2015). However, clinical neuroprotective effects of current agents in PD remain unproven (Löhle and Reichmann, 2010). The most frequently used herbs of HM formulas were selected in the present study, including Radix Salviae Miltiorrhizae, Radix Paeoniae Alba, Ramulus Uncariae Cum Uncis, Radix Rehmanniae, Herba Cistanches, Radix Polygoni Multiflori, Rhizoma Ligustici Chuanxiong, Fructus Corni, Radix Angelicae Sinensis, Rhizoma Acori Tatarinowii, and Radix Astragali seu Hedysari. Based on the high-frequency used herbs, the anti-PD mechanisms of the main active ingredients of herbs *in vivo or in vitro* trails are as follows: (1) Antioxidant: Danshensu (from *Radix Salviae Miltiorrhizae*), catalpol (from *Radix Rehmanniae*), 2,3,5,4′-Tetrahydroxystilbene-2-O-β-D-Glucoside (TSG) (from *Radix Polygoni Multiflori*), morroniside (from Fructus Corni) and astragaloside IV (AS-IV) (from *Radix Astragali seu Hedysari)* were shown to alleviate oxidative stress through reducing reactive oxygen species (ROS) level (Bi et al., 2008a; Sun et al., 2011; Chong et al., 2013; Liu et al., 2017; Zhang et al., 2017). Catalpol, and tetramethylpyrazine (TMP) (from Rhizoma Ligustici Chuanxiong) prevented the decrease in the activities of superoxide dismutase, catalase and glutathione peroxidase, and inhibited malondialdehyde overproduction (Bi et al., 2008a; Lu et al., 2014; Li et al., 2016). The Regulation of I3K/Akt/Nrf2 signaling pathway by Danshensu (Chong et al., 2013) and the inhibition of Nrf2/HO-1 pathway by TMP (Michel et al., 2017) contributed to their antioxidant role; (2) Anti-inflammatory: Echinacoside (ECH) (from *Herba Cistanches*) and catalpol showed a stronger inhibition on the productions and/or expressions of several pro-inflammatory cytokine, including nitric oxide (Tian et al., 2006), tumor necrosis factor-α (Tian et al., 2006), interleukin (IL)-1α (Tian et al., 2006), IL-1β and IL-6 (Wang et al., 2015). TMP (Michel et al., 2017) may inhibit the expression of neuroinflammation markers: nuclear factor κB (NF-κB), inducible nitric oxide synthase, cyclooxygenase-2, and glial fibrillary acidic protein; (3) Anti-apoptotic: ECH, TSG, morroniside, paeoniflorin (PF) (from *Radix Paeoniae Alba*), TMP, n-Butylidenephthalide (BP) (from *Radix Angelicae Sinensis*), or AS-IV exerted anti-apoptotic capacity in different aspects, including suppressing the upregulation of the ratio of Bax/Bcl-2 (Sun et al., 2012; Lu et al., 2014; Liu et al., 2017; Michel et al., 2017), the activation of caspase-3 and caspase-8 (Geng et al., 2007; Sun et al., 2011; Lu et al., 2014; Michel et al., 2017) and the expression of Proapoptotic Gene egl-1 (Fu et al., 2014). TSG (Qin et al., 2011) reduced MPP+-induced apoptotic that mediated via PI3K/Akt signaling pathway; (4) The Regulation of mitochondrial dysfunction: ECH, TSG, PF or catalpol attenuated mitochondrial dysfunction not only by suppressing the decrease of cellular ATP levels (Wang et al., 2015), mitochondrial membrane potential (Bi et al., 2008b; Sun et al., 2011, 2012; Wang et al., 2015), the activity of mitochondrial complex I (Bi et al., 2008b), but also decreasing mitochondrial permeability transition pore opening (Bi et al., 2008b); (5) DA and dopaminergic neuron protection: Danshensu, ECH, BP, TMP, AS- IV or β-asarone (from *Rhizoma Acori Tatarinowii*) could enhance the content of DA as well as its metabolites and reduce dopaminergic neuron degeneration (Geng et al., 2007; Chong et al., 2013; Fu et al., 2014; Lu et al., 2014), and led to a marked increase in Tyrosine hydroxylase expression (Geng et al., 2007; Lu et al., 2014; Zhang et al., 2016; Liu et al., 2017). Furthermore, catalpol (Bi et al., 2008b) was found to be a strong inhibitor of MAO-B,which may weaken the biotransformation of 1-methyl-4-phenyl-1,2,3,6-tetrahydropyridine to 1-methyl-4-phenylpyridinium and the metabolism of DA; (6) Reduce α-synuclein accumulation: α-synuclein (α-syn) is a major component of lewy bodies that plays an important role in the pathogenesis of PD (Rocha et al., 2018). Corynoxine (Chen L. L. et al., 2014) (from *Ramulus Uncariae Cum Uncis*) down regulated α-syn in PC12 cells by inducing autophagy. AS-IV (Liu et al., 2017) inhibited the expression of the α-syn via the p38 MAPK signaling pathway. Furthermore, β-asarone (Zhang et al., 2016) promoted the clearance of α-syn via regulating long non-coding RNA Metastasis associated lung adenocarcinoma transcript 1. Because of their advantage of multi-component, multi-target and multi-pathway, HM formulas have great potential application value in neuroprotection. Furthermore, based on the high-frequency used herbs, we can explore the best formula combination, which also ignite the HM treatment method for PD patients.

CONCLUSION

The findings of present study showed that HM paratherapy can effectively improve the motor symptoms and non motor symptoms of PD and is well tolerated for PD patients. Thus, the available evidence supported the complementary use of HM paratherapy for PD patients; however, the question on the efficacy of HM monotherapy in alleviating PD symptoms is still open.

AUTHOR CONTRIBUTIONS

G-QZ and C-SS: study conception and design; C-SS, H-FZ, Q-QX, Y-HS, YW, YLi, YLin, and G-QZ: acquisition, analysis and/or interpretation of data; G-QZ: final approval and overall responsibility for this published work.

FUNDING

This work was financially supported by the grant of National Natural Science Foundation of China (81573750/81473491/81173395/H2902); the Young and Middle-Aged University Discipline Leaders of Zhejiang Province, China (2013277); Zhejiang Provincial Program for the Cultivation of High-level Health talents (2015).

REFERENCES

Abraha, I., Cozzolino, F., Orso, M., Marchesi, M., Germani, A., Lombardo, G., et al. (2017). A systematic review found that deviations from intention-to-treat are common in randomized trials and systematic reviews. *J. Clin. Epidemiol.* 84, 37–46. doi: 10.1016/j.jclinepi.2016.11.012

Athauda, D., and Foltynie, T. (2015). The ongoing pursuit of neuroprotective therapies in Parkinson disease. *Nat. Rev. Neurol.* 11, 25–40. doi: 10.1038/nrneurol.2014.226

Athauda, D., and Foltynie, T. (2016). Challenges in detecting disease modification in Parkinson's disease clinical trials. *Parkinson. Relat. Disord.* 32, 1–11. doi: 10.1016/j.parkreldis.2016.07.019

Bi, J., Jiang, B., Liu, J. H., Lei, C., Zhang, X. L., and An, L. J. (2008a). Protective effects of catalpol against H2O2-induced oxidative stress in astrocytes primary cultures. *Neurosci Lett.* 442, 224–227. doi: 10.1016/j.neulet.2008.07.029

Bi, J., Wang, X.B., Chen, L., Hao, S., An, L.J., Jiang, B., et al. (2008b). Catalpol protects mesencephalic neurons against MPTP induced neurotoxicity via attenuation of mitochondrial dysfunction and MAO-B activity. *Toxicol in vitro* 22, 1883–1889. doi: 10.1016/j.tiv.2008.09.007

Cai, L., Liu, Y., and Li, W.T. (2017). Combination of Zhichan decoction and western medicine for the treatment of 43 cases of Parkinson's disease: a randomized double-blind controlled trial. *Jiangsu J. Tradit. Chin. Med.* 49, 33–35. doi: 10.3969/j.issn.1672-397X.2017.11.013

Chen, L. L., Song, J. X., Lu, J. H., Yuan, Z. W., Liu, L. F., Durairajan, S. S., et al. (2014). Corynoxine, a natural autophagy enhancer, promotes the clearance of alpha-synuclein via Akt/mTOR pathway. *J. Neuroimmune Pharmacol.* 9, 380–387. doi: 10.1007/s11481-014-9528-2

Chen, M. Y., Liu, Y., Ruan, K. F., Zhang, J. Q., Hong, Y. L., Zhu, J. Y., et al. (2014). Combination of Zhichan granules and western medicine for the treatment of Parkinson's disease of liver kidney deficiency pattern and qi blood deficiency pattern: a randomized double-blind placebo-controlled clinical trial. *Shanghai J. Tradit. Chin. Med.* 28, 27–30. doi: 10.16305/j.1007-1334.2014.10.034

Chen, Z. X., Li, Y., Zhang, X. G., Chen, S., Yang, W. T., Zheng, X. W., et al. (2017). Sham electroacupuncture methods in randomized controlled trials. *Sci. Rep.* 7:40837. doi: 10.1038/srep40837

Cheng, C.W., Wu, T.X., Shang, H.C., Li, Y.P., Altman, D.G., Moher, D., et al. (2017). CONSORT extension for Chinese herbal medicine formulas 2017: recommendations, explanation, and elaboration (simplified Chinese version). *Ann. Intern. Med.* 167, W21–W34. doi: 10.7326/M16-2977

Chong, C. M., Zhou, Z. Y., Razmovski-Naumovski, V., Cui, G. Z., Zhang, L. Q., Sa, F., et al. (2013). Danshensu protects against 6-hydroxydopamine-induced damage of PC12 cells *in vitro* and dopaminergic neurons in zebrafish. *Neurosci. Lett.* 543, 121–125. doi: 10.1016/j.neulet.2013.02.069

DeAngelis, C., Drazen, J. M., Frizelle, F. A., Haug, C., Hoey, J., Horton, R., et al. (2004). Clinical trial registration: a statementfrom the International committee of medical journal editors. *Med. J. Aust.* 181, 293–294. doi: 10.1001/jama.292.11.1363

Findley, L.J., Wood, E., Lowin, J., Roeder, C., Bergman, A., and Schifflers, M. (2011). The economic burden of advanced Parkinson's disease: an analysis of a UK patient dataset. *J. Med. Econ.* 14, 130–139. doi: 10.3111/13696998.2010.551164

Fox, S. H., Katzenschlager, R., Lim, S. Y., Barton, B., de Bie, R. M. A., Seppi, K., et al. (2018). International Parkinson and movement disorder society evidence-based medicine review: update on treatments for the motor symptoms of Parkinson's disease. *Mov. Disord.* 33, 1248–1266. doi: 10.1002/mds.27372

Fu, R. H., Harn, H. J., Liu, S. P., Chen, C. S., Chang, W. L., Chen, Y. M., et al. (2014). n-butylidenephthalide protects against dopaminergic neuron degeneration and α-synuclein accumulation in *Caenorhabditis elegans* models of Parkinson's disease. *PLoS ONE* 9:e85305. doi: 10.1371/journal.pone.0085305

GBD, 2015 Mortality and Causes of Death Collaborators (2016). Global, regional, and national life expectancy, all-cause mortality, and cause-specific mortality for 249 causes of death, 1980-2015: a systematic analysis for the Global Burden of Disease Study 2015. *Lancet* 388, 1459–1544. doi: 10.1016/S0140-6736(16)31012-1

GBD, 2016 Disease and Injury Incidence and Prevalence Collaborators (2017). Global, regional, and national incidence, prevalence, and years lived with disability for 328 diseases and injuries for 195 countries, 1990-2016: a systematic analysis for the Global Burden of Disease Study 2016. *Lancet* 390, 1211–1259. doi: 10.1016/S0140-6736(17)32154-2

Geng, X., Tian, X., Tu, P., and Pu, X. (2007). Neuroprotective effects of echinacoside in the mouse MPTP model of Parkinson's disease. *Eur. J. Pharmacol.* 564, 66–74. doi: 10.1016/j.ejphar.2007.01.084

Guo, C.H. (2010). *Observation of Clinical Curation Effect on Gui Lu Di Huang Capsule for the Treatment of Parkinson's Disease Which is Liver-Kidney yin Deficiency Type*. Dissertation, Guangzhou: Guangzhou University of Chinese Medicine (in Chinese).

Guo, Y. X., Li, S. D., and Yang, M. H. (2014). Bushen Huoxue Granule (BSHXG) for clinical studies of Parkinson's disease with depression. *Glob. Traditional Chinese Med.* 7, 275–278. doi: 10.3969/j.issn.1674-1749.2014.04.009

Higgins, J. P., Altman, D. G., Gøtzsche, P. C., Jüni, P., Moher, D., Oxman, A. D., et al. (2011). The Cochrane collaboration's tool for assessing risk of bias in randomised trials. *BMJ* 343:d5928. doi: 10.1136/bmj.d5928

Hughes, A. J., Daniel, S. E., Kilford, L., and Lees, A. J. (1992). Accuracy of clinical diagnosis of idiopathic Parkinson's disease: a clinico-pathological study of 100 cases. *J. Neurol. Neurosurg. Psychiatry* 55, 181–184. doi: 10.1136/jnnp.55.3.181

Jenner, P. (2015). Treatment of the later stages of Parkinson's disease - pharmacological approaches now and in the future. *Transl. Neurodegener.* 4:3. doi: 10.1186/2047-9158-4-3

Kalia, L. V., Kalia, S. K., and Lang, A. E. (2015). Disease-modifying strategies for Parkinson's disease. *Mov. Disord.* 30, 1442–1450. doi: 10.1002/mds.26354

Kalia, L. V., and Lang, A. E. (2015). Parkinson's disease. *Lancet* 386, 896–912. doi: 10.1016/S0140-6736(14)61393-3

Kim, T. H., Cho, K. H., Jung, W. S., and Lee, M. S. (2012). Herbal medicines for Parkinson's disease: a systematic review of randomized controlled trials. *PLoS ONE* 7:e35695. doi: 10.1371/journal.pone.0035695

Kotsirilos, V. (2005). Complementary and alternative medicine. Part 2–evidence and implications for GPs. *Aust. Fam. Physician* 34, 689–691.

Kowal, S. L., Dall, T. M., Chakrabarti, R., Storm, M. V., and Jain, A. (2013). The current and projected economic burden of Parkinson's disease in the United States. *Mov. Disord.* 28, 311–318. doi: 10.1002/mds.25292

Kulisevsky, J., Oliveira, L., and Fox, S. H. (2018). Update in therapeutic strategies for Parkinson's disease. *Curr. Opin. Neurol.* 31, 439–47. doi: 10.1097/WCO.0000000000000579

Kum, W. F., Durairajan, S. S., Bian, Z. X., Man, S. C., Lam, Y. C., Xie, L. X., et al. (2011). Treatment of idiopathic Parkinson's disease with traditional chinese herbal medicine: a randomized placebo-controlled pilot clinical study. *Evid. Based Complement. Alternat. Med.* 2011:724353. doi: 10.1093/ecam/nep116

Lewis, J. A. (1999). Statistical principles for clinical trials (ICH E9): an introductory note on an international guideline. *Stat Med.* 18, 1903–1942. doi: 10.1002/(SICI)1097-0258(19990815)18:15<1903::AID-SIM188>3.0.CO;2-F

Li, M., Yang, H. M., Luo, D. X., Chen, J. Z., and Shi, H. J. (2016). Multi-dimensional analysis on Parkinson's disease questionnaire-39 in Parkinson's patients treated with Bushen Huoxue Granule: a multicenter, randomized, double-blinded and placebo controlled trial. *Complement Ther. Med.* 29, 116–120. doi: 10.1016/j.ctim.2016.09.008

Lim, K. L., and Zhang, C. W. (2013). Molecular events underlying Parkinson's disease-an interwoven tapestry. *Front. Neurol.* 4:33. doi: 10.3389/fneur.2013.00033

Liu, X., Zhang, J., Wang, S., Qiu, J., and Yu, C. (2017). Astragaloside IV attenuates the H2O2-induced apoptosis of neuronal cells by inhibiting α-synuclein expression via the p38 MAPK pathway. *Int. J. Mol. Med.* 40, 1772–1780. doi: 10.3892/ijmm.2017.3157

Löhle, M., and Reichmann, H. (2010). Clinical neuroprotection in Parkinson's disease-still waiting for the breakthrough. *J. Neurol. Sci.* 289, 104–114. doi: 10.1016/j.jns.2009.08.025

Lu, C., Zhang, J., Shi, X., Miao, S., Bi, L., Zhang, S., et al. (2014). Neuroprotective effects of tetramethylpyrazine against dopaminergic neuron injury in a rat model of Parkinson's disease induced by MPTP. *Int. J. Biol. Sci.* 10, 350–357. doi: 10.7150/ijbs.8366

Martinez-Martin, P., Falup Pecurariu, C., Odin, P., van Hilten, J. J., Antonini, A.,Rojo-Abuin, J. M., et al. (2012). Gender-related differences in the burden of non-motor symptoms in Parkinson's disease. *J. Neurol.* 259, 1639–1647. doi: 10.1007/s00415-011-6392-3

Michel, H. E., Tadros, M. G., Esmat, A., Khalifa, A. E., and Abdel-Tawab, A. M. (2017). Tetramethylpyrazine ameliorates rotenone-induced parkinson's disease in rats: involvement of its anti-inflammatory and anti-apoptotic actions. *Mol. Neurobiol.* 54, 4866–4878. doi: 10.1007/s12035-016-0028-7

Moher, D., Hopewell, S., Schulz, K. F., Montori, V., Gøtzsche, P. C., Devereaux, P. J., et al. (2010a). CONSORT 2010 explanation and elaboration: updated guidelines for reporting parallel group randomised trials. *J. Clin. Epidemiol.* 63, e1–e37. doi: 10.1136/bmj.c869

Moher, D., Liberati, A., Tetzlaff, J., Altman, D. G., and PRISMA Group (2010b). Preferred reporting items for systematic reviews and meta-analyses: the PRISMA statement. *Int. J. Surg.* 8, 336–341. doi: 10.1016/j.ijsu.2010.02.007

Pan, W., Kwak, S., Li, G., Chen, Y., and Cai, D. (2013). Therapeutic effect of Yang-Xue-Qing-Nao granules on sleep dysfunction in Parkinson's disease. *Chin Med.* 8:14. doi: 10.1186/1749-8546-8-14

Pan, W., Kwak, S., Liu, Y., Sun, Y., Fang, Z., Qin, B., et al. (2011). Traditional chinese medicine improves activities of daily living in Parkinson's disease. *Parkinsons Dis.* 2011:789506. doi: 10.4061/2011/789506

Pan, W. D., Yuan, W. A., Fang, Z. L., Liu, Y., and Guo, S. (2009). Effects of Zengxiao Anshen Zhichan 2 Decoction on motor and non-motor symptoms in Parkinson's disease. *Acta Univ. Tradit. Med. Sin. Pharmacol.* 23, 29–34. doi: 10.16306/j.1008-861x.2009.04.024

Qin, R., Li, X., Li, G., Tao, L., Li, Y., Sun, J., et al. (2011). Protection by tetrahydroxystilbene glucoside against neurotoxicity induced by MPP+: the involvement of PI3K/Akt pathway activation. *Toxicol. Lett.* 202, 1–7. doi: 10.1016/j.toxlet.2011.01.001

Reinoso, G., Allen, J. C. Jr., Au, W. L., Seah, S. H., Tay, K. Y., and Tan, L. C. (2015). Clinical evolution of Parkinson's disease and prognostic factors affecting motor progression: 9-year follow-up study. *Eur. J. Neurol.* 22, 457–463. doi: 10.1111/ene.12476

Rocha, E. M., de Miranda, B., and Sanders, L. H. (2018). Alpha-synuclein: pathology, mitochondrial dysfunction and neuroinflammation in Parkinson's disease. *Neurobiol. Dis.* 109, 249–257. doi: 10.1016/j.nbd.2017.04.004

Rogers, G., Davies, D., Pink, J., and Cooper, P. (2017). Parkinson's disease: summary of updated NICE guidance. *BMJ* 358:j1951. doi: 10.1136/bmj.j1951

Sarkar, S., Raymick, J., and Imam, S. (2016). Neuroprotective and therapeutic strategies against Parkinson's disease: recent perspectives. *Int. J. Mol. Sci.* 17:E904. doi: 10.3390/ijms17060904

Sun, F. L., Zhang, L., Zhang, R. Y., and Li, L. (2011). Tetrahydroxystilbene glucoside protects human neuroblastoma SH-SY5Y cells against MPP+-induced cytotoxicity. *Eur. J. Pharmacol.* 660, 283–290. doi: 10.1016/j.ejphar.2011.03.046

Sun, R., Wang, K., Wu, D., Li, X., and Ou, Y. (2012). Protective effect of paeoniflorin against glutamate-induced neurotoxicity in PC12 cells via Bcl-2/Bax signal pathway. *Folia Neuropathol.* 50, 270–276. doi: 10.5114/fn.2012.30527

Tian, Y.Y., An, L.J., Jiang, L., Duan, Y.L., Chen, J., and Jiang, B. (2006). Catalpol protects dopaminergic neurons from LPS-induced neurotoxicity in mesencephalic neuron-glia cultures. *Life Sci.* 80, 193–199. doi: 10.1016/j.lfs.2006.09.010

Wang, X.D. (1985). Standard for diagnosing and distinguishing Parkinson's disease and Parkinsonian syndromes. *Chin. J. Neurol.* 18:256. (in Chinese)

Wang, Y., Lin, X.M., and Zheng, G.Q. (2011). Traditional Chinese medicine for Parkinson's disease in China and beyond. *J. Altern. Complement Med.* 17, 385–388. doi: 10.1089/acm.2011.0025

Wang, Y., Xie, C. L., Lu, L., Fu, D. L., and Zheng, G. Q. (2012). Chinese herbal medicine paratherapy for Parkinson's disease: a meta-analysis of 19 randomized controlled trials. *Evid. Based Complement. Alternat. Med.* 2012:534861. doi: 10.1155/2012/534861

Wang, Y., Xie, C. L., Wang, W. W., Lu, L., Fu, D. L., Wang, X. T., et al. (2013). Epidemiology of complementary and alternative medicine use in patients with Parkinson's disease. *J. Clin. Neurosci.* 20, 1062–1067. doi: 10.1016/j.jocn.2012.10.022

Wang, Y. H., Xuan, Z. H., Tian, S., and Du, G. H. (2015). Echinacoside protects against 6-hydroxydopamine-induced mitochondrial dysfunction and inflammatory responses in PC12 cells via reducing ROS production. *Evid. Based Complement Alternat. Med.* 2015:189239. doi: 10.1155/2015/189239

Wen, L. L., He, Y., and Ji, L. (2015). Congwu Extinguish Wind Granule on movement of syndromes symptoms of Parkinson's disease and auality of life of intervention study. *J. Liaoning Univ. Tradit. Chin. Med.* 17, 130–132. doi: 10.13194/j.issn.1673-842x.2015.04.045

Yang, N. (2017). *The Research on the Distribution of "Elements of Syndrome and Pathogenesis" of Parkinson's Disease and the Clinical Observation of Yishen Chuchan Decoction on Treating 40 cases.* Dissertation, Nanjing: Nanjing University of Chinese Medicine (in Chinese).

Yang, W. T., Zheng, X. W., Chen, S., Shan, C. S., Xu, Q. Q., Zhu, J. Z., et al. (2017). Chinese herbal medicine for Alzheimer's disease: clinical evidence and possible mechanism of neurogenesis. *Biochem. Pharmacol.* 141, 143–155. doi: 10.1016/j.bcp.2017.07.002

Yu, T. (2016). *Clinical Study on the Treatment of Parkinson's Disease With Syndrome of Wind Stirring due to Blood Stasis by Naokang Granules.* Dissertation, Guangzhou: Guangzhou University of Chinese Medicine (in Chinese).

Zhang, G., Xiong, N., Zhang, Z., Liu, L., Huang, J., Yang, J., et al. (2015). Effectiveness of traditional Chinese medicine as an adjunct therapy for Parkinson's disease: a systematic review and meta-analysis. *PLoS ONE* 10: e0118498. doi: 10.1371/journal.pone.0118498

Zhang, J. X., Wang, R., Xi, J., Shen, L., Zhu, A.Y., Qi, Q., et al. (2017). Morroniside protects SK-N-SH human neuroblastoma cells against H2O2-induced damage. *Int. J. Mol. Med.* 39, 603–612. doi: 10.3892/ijmm.2017.2882

Zhang, Q. S., Wang, Z. H., Zhang, J. L., Duan, Y. L., Li, G. F., and Zheng, D. L. (2016). Beta-asarone protects against MPTP-induced Parkinson's disease via regulating long non-coding RNA MALAT1 and inhibiting α-synuclein protein expression. *Biomed. Pharmacother.* 83, 153–159. doi: 10.1016/j.biopha.2016.06.017

Zhang, Y., Wang, Z. Z., Sun, H. M., Li, P., Li, Y. F., and Chen, N. H. (2014). Systematic review of traditional chinese medicine for depression in Parkinson's disease. *Am. J. Chin. Med.* 42, 1035–1051. doi: 10.1142/S0192415X14500657

Zhang, Z.X. (2006). The diagnosis of Parkinson's disease. *Chin. J. Neurol.* 39, 408–409. doi: 10.3760/j.issn:1006-7876.2006.06.024

Zhao, G. H., Meng, Q. G., Yu, X. D., Bai, J. Y., Luo, X. D., Yuan, C. X., et al. (2009). A multicentered randomized double-blinded controlled linical study on efficacy of Guiling Pa'an capsule in treating Parkinson's disease. *Chin. J. Integer. Tradit. West Med.* 29, 590–594. doi: 10.3321/j.issn:1003-5370.2009.07.006

Zhao, G. H., Sun, F., Feng, X. G., and Gao, M. (2013). Treatment of non-motor symptoms of Parkinson's disease patients of Gan-Shen deficiency syndrome by Guling Pa'an Granule:a multi-center double-blinded randomized controlled trial. *Chin. J. Integer. Tradit. West Med.* 33, 476–479 (in Chinese).

Zheng, G. Q. (2009). Therapeutic history of Parkinson's disease in Chinese medical treatises. *J. Altern. Complement. Med.* 15, 1223–1230. doi: 10.1089/acm.2009.0101

Conflict of Interest Statement: The authors declare that the research was conducted in the absence of any commercial or financial relationships that could be construed as a potential conflict of interest.

frontiers in Aging Neuroscience

ORIGINAL RESEARCH
published: 29 November 2018
doi: 10.3389/fnagi.2018.00392

Alterations of *NURR1* and Cytokines in the Peripheral Blood Mononuclear Cells: Combined Biomarkers for Parkinson's Disease

*Tianbai Li[1,2], Zhaofei Yang[1,2], Song Li[1,2], Cheng Cheng[1,2], Bairong Shen[3] and Weidong Le[1,2]**

[1] Center for Clinical Research on Neurological Diseases, The First Affiliated Hospital, Dalian Medical University, Dalian, China, [2] Liaoning Provincial Key Laboratory for Research on the Pathogenic Mechanisms of Neurological Diseases, The First Affiliated Hospital, Dalian Medical University, Dalian, China, [3] Institute for Systems Genetics, West China Hospital, Sichuan University, Chengdu, China

Nuclear receptor related 1 protein (*NURR1*), a transcription factor as key player for maintaining dopamine neuron functions and regulating neuroinflammation in the central nerves system, is a potential susceptibility gene for Parkinson's disease (PD). To ascertain whether the expression levels of *NURR1* gene and inflammatory cytokines are altered in patients with PD, we measured their mRNA levels in the peripheral blood mononuclear cells (PBMCs) in 312 PD patients, 318 healthy controls (HC), and 332 non-PD neurological disease controls (NDCs) by quantitative real-time PCR. Our data showed that *NURR1* gene expression was significantly decreased in the PBMCs of PD as compared with that of HC and NDC ($p < 0.01$). Since *NURR1* was reported to have regulating effects on neuroinflammation, we assessed the expression levels of cytokines (*TNF-α*, *IL-1β*, *IL-4*, *IL-6,* and *IL-10*) in the PBMCs of PD and controls (HC and NDC). Our results showed that the expression levels of those cytokines were significantly higher than those of controls. Statistical analysis revealed that *NURR1* expression presented a negative correlation with the expression of *TNF-α*, *IL-1β*, *IL-6,* and *IL-10*, and collectively the measurements of *NURR1* plus those cytokines significantly improve the diagnostic accuracy. All these findings suggested that *NURR1* is likely to be involved in the process of PD by mediating the neuroinflammation, and the combination of *NURR1* and cytokines assessment in the PBMCs can be potential biomarkers for PD diagnosis.

Keywords: *NURR1*, Parkinson's disease, biomarkers, cytokines, neuroinflammation

OPEN ACCESS

Edited by:
Hi-Joon Park,
Kyung Hee University, South Korea

Reviewed by:
Franc Llorens,
Centro de Investigación Biomédica en Red sobre Enfermedades Neurodegenerativas (CIBERNED), Spain
Liu Jun,
Shanghai Jiao Tong University, China

***Correspondence:**
Weidong Le
wdle@sibs.ac.cn

Received: *27 June 2018*
Accepted: *12 November 2018*
Published: *29 November 2018*

Citation:
Li T, Yang Z, Li S, Cheng C, Shen B and Le W (2018) Alterations of NURR1 and Cytokines in the Peripheral Blood Mononuclear Cells: Combined Biomarkers for Parkinson's Disease. Front. Aging Neurosci. 10:392. doi: 10.3389/fnagi.2018.00392

INTRODUCTION

Parkinson's disease (PD) is a chronic and progressive neurodegenerative disorder occurring as a result of the loss of dopamine (DA) neurons within the substantia nigra (SN) (Dickson, 2012). As the second most common neurodegenerative disorder, PD affects 1% of people older than age 60, and 3% at the age 80 years or older (Erkkinen et al., 2018). Although many important discoveries have been made during the 200 years of PD research history (Li and Le, 2017), PD diagnosis is still mainly based on the identification of motor symptoms whereas pathological

changes and non-motor manifestations emerge years prior to motor symptoms, indicating that earlier diagnosis and treatments are necessary (Van Laar and Jain, 2004). Currently, an increasing number of studies focus on the peripheral biomarkers utilizing biofluids, which may reflect the disease related molecular changes in the brain. Commonly peripheral blood mononuclear cells (PBMCs) have been used to measure specific alteration in DA components, enzyme activities, DA receptors, and transporters in PD (Caronti et al., 2001; Pellicano et al., 2007; Buttarelli et al., 2011), gene expression profile in PBMCs was widely investigated to identify potential biomarkers of PD.

Causal genes for Mendelian-inherited PD have been reported, including *SNCA, PRKN, UCH-L1, PINK1, DJ-1, LRRK2, GBA,* and *VPS35* (Mizuta et al., 2006; Martin et al., 2011; Williams-Gray and Worth, 2016). Among the potential susceptibility genes which may act as molecular biomarkers of PD, we were particular interested in *NURR1*, a transcription factor belonging to the nuclear receptor 4 family (Wang et al., 2003; Huang et al., 2004). *NURR1* is not only highly expressed in midbrain DA neurons (Castillo et al., 1998; Sakurada et al., 1999), but also in other tissues, such as PBMCs (Mages et al., 1994; Jankovic et al., 2005). *NURR1* is known to play a crucial role in the development and differentiation of midbrain DA neurons (Jankovic et al., 2005; Decressac et al., 2013; Dong et al., 2016). Our previously study has shown that *Nurr1*-null mice have selective agenesis of DA neurons in the SN and ventral tegmental area (Le et al., 1999). Several studies also suggested that dysfunction in *NURR1* gene may play a role in PD (Le et al., 2003; Chu et al., 2006). Our earlier study has documented that *NURR1* gene expression is significantly decreased in the PBMCs of PD as compared with healthy control (HC) and neurological disease control (NDC) (Le et al., 2008; Liu et al., 2012). Based on those reports, it is believed that alteration in *NURR1* could be a potential molecular biomarker of PD.

NURR1 has also been considered to be a part of anti-inflammatory pathway in microglia, which protects DA neurons against inflammation-induced death (Saijo et al., 2009; Decressac et al., 2013). Mounting evidence supports the role of inflammation as a measurable driving force of PD pathology (Deleidi and Gasser, 2013). Neuroinflammation is associated with activated microglia and altered levels of inflammatory mediators in the brain of PD (Heneka et al., 2014). Many researches have revealed that significantly higher levels of inflammatory cytokines, such as tumor necrosis factor (TNF)-α, interleukin (IL)-1β, IL-4, IL-6 are found in the brain and cerebrospinal fluid (CSF) of PD (Mogi et al., 1996; Nagatsu and Sawada, 2005; Sawada et al., 2006). The pathological effects in the brain may have an implication in the peripheral blood, therefore, detecting the levels of inflammatory cytokines in the peripheral blood may be able to evaluate the inflammatory status of PD (Chen et al., 2008; Reale et al., 2009).

In the present study, we recruited 312 patients with diagnosed PD, 318 HC and 332 non-PD NDC, and measured the levels of *NURR1* and inflammatory cytokines (*TNF-α*, *IL-1β*, *IL-4*, *IL-6,* and *IL-10*) mRNA in their PBMCs. The purpose of this study was to determine whether the expression levels of *NURR1* gene and inflammatory cytokines in their PBMCs were specifically altered in PD as compared with HC and NDC in a relatively larger number of Chinese population, and to evaluate the relationship between *NURR1* and cytokines expression levels in the PBMCs, which may provide further evidence that *NURR1* is involved in the process of PD by mediating the neuroinflammation pathway.

MATERIALS AND METHODS

Participants and Blood Sampling

In this study, we collected a total of 962 PBMCs samples: 312 from patients with sporadic PD, 318 from HC, and 332 from patients with various NDC (**Table 1**). Among 312 PD patients, 82 were of recent-onset without any anti-PD treatment, the other 230 patients were treated with anti-PD medications. NDC consisted of 48 cerebrovascular diseases, 42 Alzheimer disease (AD), 40 epilepsy, 36 peripheral neuropathy, 31 migraine, 24 myasthenia gravis, 22 essential tremor, 21 parkinsonism (including 11 vascular parkinsonism and 10 multiple system atrophy), 21 anxiety/sleep disorders, 17 restless legs syndrome, 12 motor neuron disease, 11 multiple sclerosis, 4 myelopathy, and 3 chorea minor. PD patients were examined and diagnosed by at least two experienced neurologists from the First Affiliated Hospital of Dalian Medical University according to the Movement Disorder Society Clinical Diagnostic Criteria for Parkinson's disease (Postuma et al., 2015). PD disease severity was assessed by Modified Hoehn – Yahr (H-Y) staging (Goetz et al., 2004). PD patients were excluded if they had any other major neurological, ongoing infectious/autoimmune, or serious metabolic disorders. HC subjects were recruited from the Health Examination Center of the First Affiliated Hospital of Dalian Medical University, showing they did not have any obvious neurological disorders or non-neurological disorders. All subjects (or their caregivers) recruited to our studies provided a written informed consent agreeing to participate the project. This study has been granted ethical approval by the Ethics Committee of the First Affiliated Hospital of Dalian Medical University (approval number: LCKY2014-29).

Peripheral blood samples were collected by direct venipuncture at the First Affiliated Hospital of Dalian Medical University. Peripheral blood (2 ml) was drawn from cubital vein into ethylene diamine tetra-acetic acid (EDTA) containing blood collection tubes. PBMCs were separated from Human Peripheral Lymphocyte Separation Medium (Haoyang, Tianjin, China) by centrifugation at 450*g* for 20 min at room temperature (20 ± 2°C) no later than 4 h and were stored at −80°C immediately until RNA preparation.

PBMCs mRNA Extraction and Quantification

Total RNAs from PBMCs were extracted using the mirVana miRNA Isolation Kit (Ambion, Carlsbad, CA, United States). The mRNA levels of *NURR1*, *TNF-α*, *IL-1β*, *IL-4*, *IL-6,* and *IL-10* in PBMCs were also measured by quantitative real-time PCR.

TABLE 1 | Demographic characteristics of subjects enrolled in the present study.

Groups	Number (%)	Gender Male:Female	*P*-value	*P*-value	Age (years) (mean ± SD)	*P*-value	*P*-value
HC	318(33.1)	178:140	Ref		67.61 ± 8.93	Ref	
PD	312(32.4)	176:136	NS	Ref	67.47 ± 9.56	NS	Ref
NDC	332(34.5)	188:144	NS	NS	67.6 ± 10.2	NS	NS

Chi-square test and Student's t-test. SD, standard deviation; Ref, reference; NS, not significant; HC, healthy controls; PD, Parkinson's disease; NDC, neurological disease control.

TABLE 2 | List of primers used for quantitative real-time PCR assays.

mRNA	Primer sequence
NURR1	Forward: 5′-TCCAACGAGGGGCTGTGCG-3′
	Reverse: 5′-CACTGTGCGCTTAAAGAAGC-3′
TNF-α	Forward: 5′-GAGCTGAGAGATAACCAGCTGGTG-3′
	Reverse: 5′-CAGATAGATGGGCTCATACCAGGG-3′
IL-1β	Forward: 5′-CTCGCCAGTGAAATGATGGCT-3′
	Reverse: 5′-GTCGGAGATTCGTAGCTGGAT-3′
IL-4	Forward: 5′-ACAAAGCCCAGAGAGAACACA-3′
	Reverse: 5′-TCCAACGTACTCTGGTTGGC-3′
IL-6	Forward: 5′-AGGACTGGAGATGTCTGAGGCTC-3′
	Reverse: 5′-GCGCTTGTGCAGAAGGAGTTC-3′
IL-10	Forward: 5′-CGAGATGCCTTCAGCAGAGT-3′
	Reverse: 5′-GGCAACCCAGGTAACCCTTA-3′
GAPDH	Forward: 5′-GAA GGT GAA GGT CGG AGT C-3′
	Reverse: 5′-GAA GAT GGT GAT GGG ATT TC-3′

PCR was carried out using ABI 7500 fast real-time PCR system (Applied Biosystems, Foster City, CA, United States) in a total volume of 20 μl for each reaction. *GAPDH* gene was used as an internal control. The specific primers targeting PBMCs *NURR1*, *TNF-α*, *IL-1β*, *IL-4*, *IL-6,* and *IL-10* were presented in **Table 2**. After 94°C for 30 s, the experimental reaction consisted of 40 cycles of 94°C for 5 s and 60°C for 34 s, the target genes as well as *GAPDH* gene was detected by the fluorescent dye SYBR Green I (TransGen, Beijing, China). The value of threshold cycle (Ct) was generated at every cycle during a run. Fluorescent reading from real-time PCR reaction was quantitatively analyzed by determining the difference of Ct (delta Ct) between Ct of the target genes and *GAPDH*, and the target genes expression were determined using the 2^{-dCt} method.

Statistical Analysis

Quantitative data were expressed as mean ± standard error of mean (SEM). The dichotomous variables were compared by using chi-square test and continuous variables were compared with independent *t*-test. A one-way ANOVA followed by a Tukey-Kramer test as a *post hoc* analysis was performed using the GraphPad Prism software version 7 (GraphPad Inc., San Diego, CA, United States) to evaluate the differences in the mean value of the relative *NURR1* and cytokines expression. Correlations were evaluated using Spearman's correlation coefficient (R). The correlations were reported at an α level of 0.05. Receiver operating characteristic (ROC) curves and areas under the curves (AUC) were used to evaluate the prediction performance of the potential biomarkers. The other statistical analysis in this research was performed with the SPSS software version 13.0 (SPSS Inc., Chicago, IL, United States). All statistical checks were carried out two-sided and a p-value <0.05 was considered as statistical significance.

RESULTS

Characteristics of Study Population

All subjects we collected were ethnic Chinese. The demographic characteristics of PD patients and control subjects were summarized in **Table 1**. No significant difference in both gender and age was found among patients with PD, HC, and NDC.

NURR1 Gene Expression in PBMCs of All Three Groups

We determined the *NURR1* mRNA level in the PBMCs of all three groups by quantitative real-time PCR technique. We found that the *NURR1* mRNA level in the PBMCs of patients with PD was significantly lower than that of HC (decreased by 61%, $p < 0.01$), and NDC (decreased by 54%, $p < 0.01$). There was no difference of *NURR1* expression between HC and NDC groups (**Figure 1**). In the individual groups of NDC, some changes were found in the expression levels of NURR1 as compared with PD, but no statistical differences were reached (**Supplementary Table S1**).

The Impacts of Disease Duration, Severity, and Medications on *NURR1* Expression in PD

We analyzed disease duration (years after onset of disease symptoms) and severity (H-Y scores) in 312 patients with PD. We divided disease duration into four stages: 1–2 years ($n = 82$), 3–5 years ($n = 83$), 6–10 years ($n = 105$), and 10–20 years ($n = 42$) and demonstrated that the level of *NURR1* expression was slightly down-regulated during the disease progression, but no significant statistical difference (**Figure 2A**). The disease severity of PD was divided into five stages: H-Y 1–1.5 ($n = 59$), H-Y 2 ($n = 89$), H-Y 2.5 ($n = 93$), H-Y 3 ($n = 55$) and H-Y 4–5 ($n = 16$). Again, a slightly down-regulation of *NURR1* expression with higher H-Y scores was found, there was no significant statistical difference (**Figure 2B**).

We also divided the PD patients into four groups according to the use of medications. Among the 312 PD patients, 82 were untreated with any anti-PD medications, the remaining patients

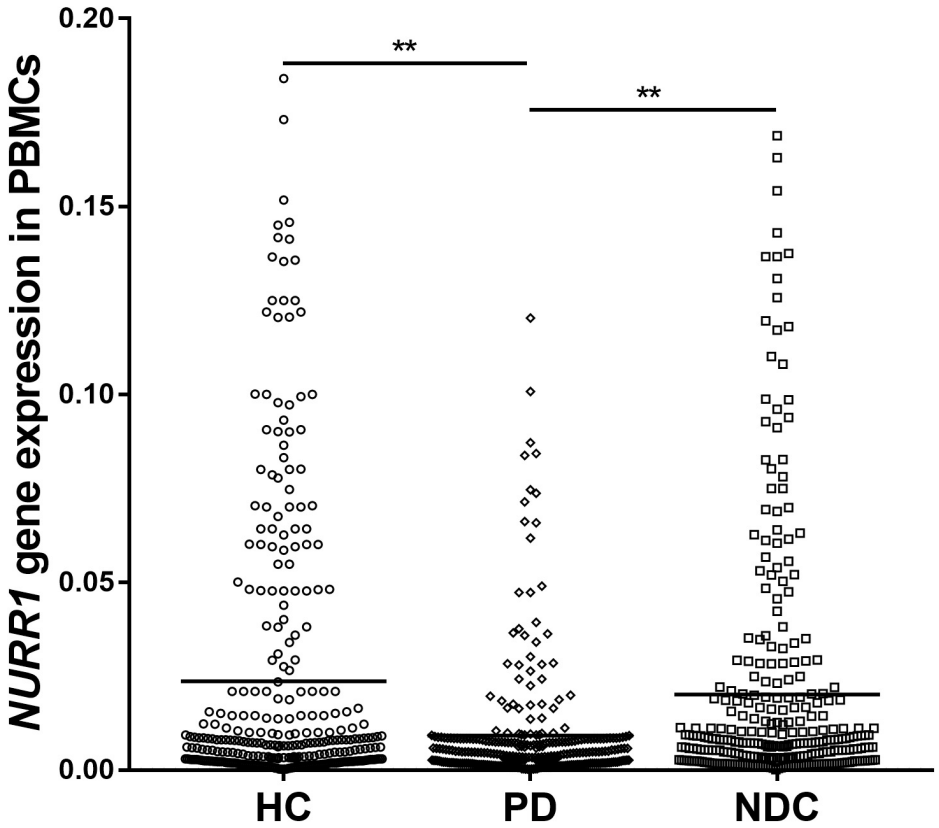

FIGURE 1 | Scatter plots of *NURR1* gene relative mRNA expression level in the PBMCs of HC (n = 318), PD (n = 312), and NDC (n = 332), which was determined using real-time PCR assays. Horizontal bars represent mean value. The *NURR1* gene mRNA level in the PBMCs was markedly low in patients with PD (mean ± SEM, 0.009 ± 0.0009) as compared with HC (mean ± SEM, 0.023 ± 0.0021) and various NDC (mean ± SEM, 0.019 ± 0.002). $^{**}p < 0.01$.

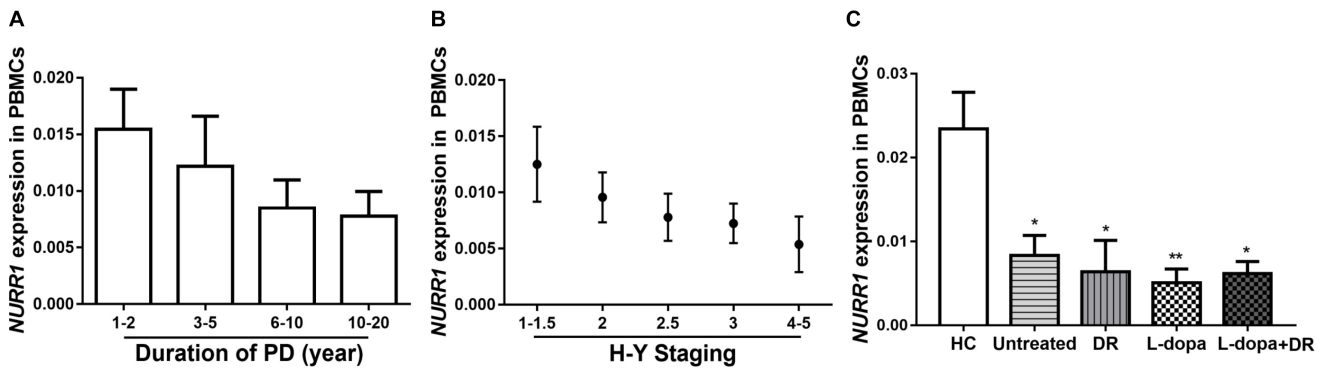

FIGURE 2 | The expression level of *NURR1* in PD and HC. The effects of **(A)** disease course, **(B)** disease severity, and **(C)** medication on the expression level of *NURR1* in PBMCs. The results are the mean ± SEM values. $^{*}p < 0.05$ and $^{**}p < 0.01$ relative to HC.

were treated with anti-PD medications, including 89 were treated with l-dopa monotherapy, 28 treated with DA receptor agonists (DR) monotherapy, and other 113 patients were treated with the combination of DA agonists and l-dopa. All these four groups were significantly lower expression level of NURR1 than HC, but there was no significant difference among the four groups (**Figure 2C**).

TNF-α, *IL-1β*, *IL-4*, *IL-6*, and *IL-10* Expressions in the PBMCs of All Recruited Subjects

Since *NURR1* plays important role in regulating neuroinflammation, we then measured mRNA levels of several cytokines in their PBMCs. Our data showed significantly higher levels of *TNF-α* ($p < 0.001$), *IL-1β* ($p < 0.001$), *IL-4* ($p < 0.01$),

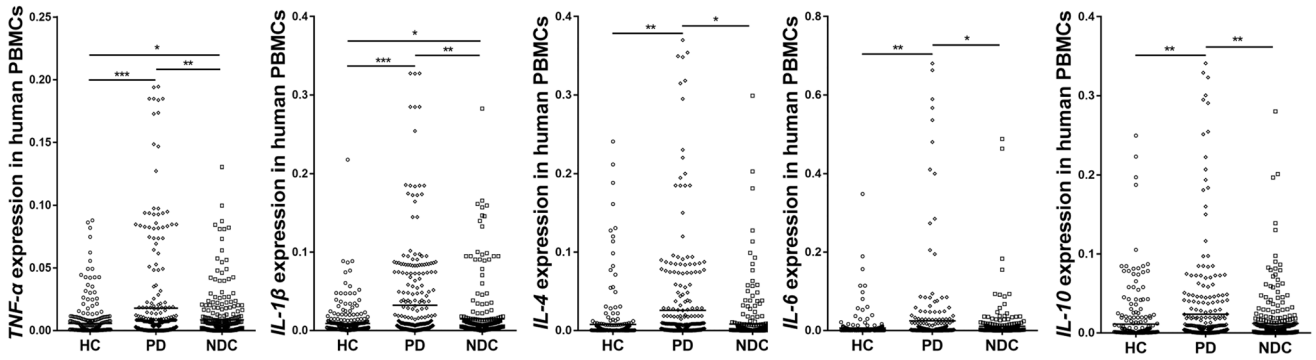

FIGURE 3 | Scatter plots of *TNF*-α, *IL-1*β, *IL-4*, *IL-6*, and *IL-10* relative mRNA expression levels in the PBMCs of HC (n = 318), PD (n = 312), and NDC (n = 332). Significantly higher levels of *TNF*-α ($p < 0.001$), *IL-1*β ($p < 0.001$), *IL-4* ($p < 0.01$), *IL-6* ($p < 0.05$), and *IL-10* ($p < 0.01$) were seen in PD patients than those in HC. The levels of *TNF*-α ($p < 0.01$), *IL-1*β ($p < 0.01$), *IL-4* ($p < 0.05$), *IL-6* ($p < 0.05$), and *IL-10* ($p < 0.01$) expression were also markedly higher in PD than NDC. Horizontal bars represent mean value. *$p < 0.05$, **$p < 0.01$, and ***$p < 0.001$.

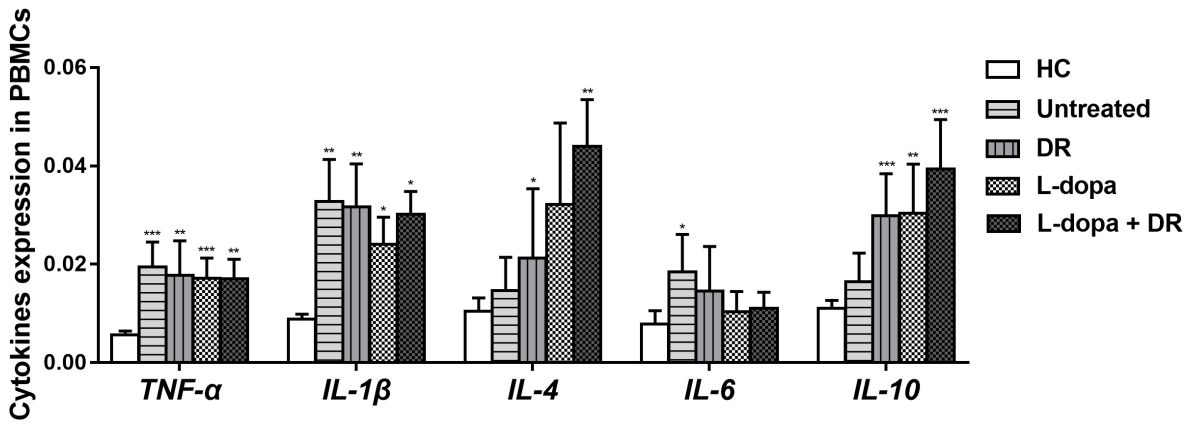

FIGURE 4 | The levels of *TNF*-α, *IL-1*β, *IL-4*, *IL-6,* and *IL-10* expression in PD patients with different anti-PD medications. The results are the mean ± SEM values. *$p < 0.05$, **$p < 0.01$, and ***$p < 0.001$ relative to HC. DR: DA receptor agonists monotherapy; L-dopa: l-dopa monotherapy; L-dopa+DR: combination of DA agonists and l-dopa.

IL-6 ($p < 0.05$) and *IL-10* ($p < 0.05$) in PD than those in HC. Moreover, the levels of *TNF*-α ($p < 0.05$), *IL-1*β ($p < 0.01$), *IL-4* ($p < 0.05$), *IL-6* ($p < 0.05$), and *IL-10* ($p < 0.05$) expression were also markedly higher in PD than NDC (**Figure 3**). In the NDC group, there were slight to moderate differences among different diseases regarding the five cytokines expression levels, but no statistical differences were reached (**Supplementary Table S2**).

We further analyzed the expression levels of cytokines in different disease duration and severity of PD, no significant differences were found among different groups (**Supplementary Figures S1, S2**).

The Influence of Medications on Cytokines Expression

Generally, the influence of anti-PD medications on PBMCs cytokines expression was minimal. Our results showed that the levels of *TNF*-α, *IL-1*β, and *IL-6* expression in PD patients with anti-PD medications were slightly lower than that of untreated patients, while the levels of *IL-4* and *IL-10* expression in PD with all types of anti-PD medications were slightly higher than that of untreated PD. However, there was no statistical difference between them (**Figure 4**).

Correlations Between the Expression Levels of *NURR1*, *TNF-*α, *IL-1*β, *IL-4*, *IL-6*, and *IL-10*

We performed a correlation analysis between expressions of *NURR1* and *TNF*-α, *IL-1*β, *IL-4*, *IL-6*, and *IL-10*. Our results showed that the level of *NURR1* presented a negative correlation with *TNF*-α ($r = -0.232$, $p < 0.01$), *IL-1*β ($r = -0.101$, $p < 0.05$), *IL-6* ($r = -0.123$, $p < 0.05$) and *IL-10* ($r = -0.129$, $p < 0.05$). Moreover, positive correlations were also found among the expression levels of *TNF*-α, *IL-1*β, *IL-4*, *IL-6,* and *IL-10* (**Table 3**).

TABLE 3 | Spearman correlation coefficient (R) between the expression levels of *NURR1*, *TNF-α*, *IL-1β*, *IL-4*, *IL-6,* and *IL-10* in the PBMCs of PD.

	TNF-α	***IL-1β***	***IL-4***	***IL-6***	***IL-10***
NURR1	−0.232**	−0.101*	−0.058	−0.123*	−0.129*
TNF-α		0.372**	0.528**	0.439**	0.337*
IL-1β			0.532**	0.489**	0.411**
IL-4				0.608**	0.462**
IL-6					0.649**

*$p < 0.05$; **$p < 0.01$.

Performance of Combined Expression Levels of *NURR1*, *TNF-α*, *IL-1β*, *IL-4*, *IL-6*, and *IL-10* for PD Diagnosis

We evaluated the performance of combined expression of PBMCs *NURR1*, *TNF-α*, *IL-1β*, *IL-4*, *IL-6*, and *IL-10* for the PD diagnosis by the AUC values based on the ROC curve analysis. The AUCs of *NURR1*, *TNF-α*, *IL-1β*, *IL-4*, *IL-6*, and *IL-10* were 0.64 (95% CI, 0.6–0.69), 0.62 (95% CI, 0.58–0.67), 0.65 (95% CI, 0.61–0.7), 0.65 (95% CI, 0.61–0.7), 0.6 (95% CI, 0.55–0.65), 0.64 (95% CI, 0.59–0.68), respectively. The combination of PBMCs *NURR1* with these cytokines significantly enhanced the discriminatory accuracy between PD and HC, with an increased AUC as 0.73 (95% CI, 0.69–0.77) ($p < 0.05$, **Figure 5**).

DISCUSSION

In this study, we measured the levels of *NURR1* and inflammatory cytokines (*TNF-α*, *IL-1β*, *IL-4*, *IL-6*, and *IL-10*) mRNA in the PBMCs of a relatively larger number of Chinese population. In order to determine the alterations of PBMCs *NURR1* and cytokines in PD are specific, we particularly recruited 332 various NDC and compared the expression levels of *NURR1* and inflammatory cytokines in PD with not only HC but also NDC. We carried out the assays of five key inflammatory cytokines simultaneously in the PBMCs to assess the complex inflammatory changes in PD. Although there were numerous reports of cytokine changes in PD, a comprehensive analysis of *NURR1* and cytokines expression changes has, to the best of our knowledge, not been performed. We demonstrated for the first

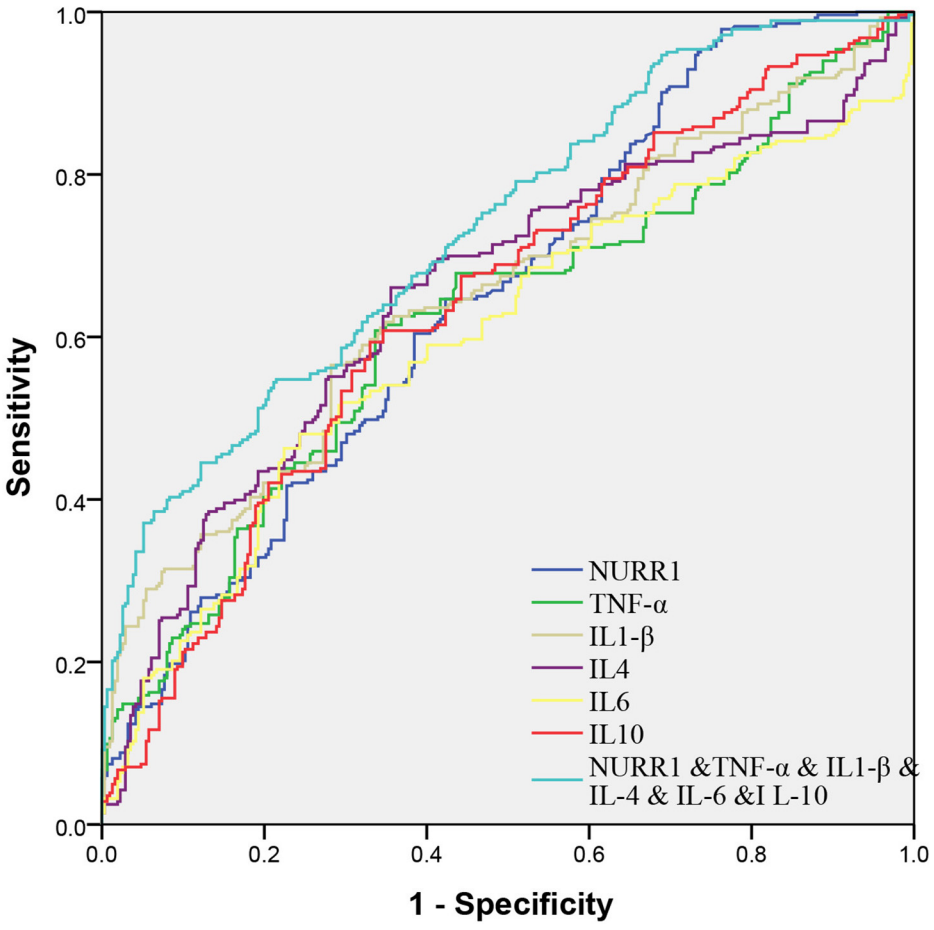

FIGURE 5 | Receiver operating characteristic curves for *NURR1*, *TNF-α*, *IL-1β*, *IL-4*, *IL-6,* and *IL-10* of PD versus HC. The AUCs value of the combination of *NURR1* with cytokines was 0.73 (95% CI, 0.69–0.77; $p < 0.05$), which was out performed those of *NURR1*, *TNF-α*, *IL-1β*, *IL-4*, *IL-6*, and *IL-10* alone.

time that the level of *NURR1* presented a negative correlation with cytokines in the PBMCs of PD, and the combination of PBMCs *NURR1* and cytokines assessment may improve the diagnostic performance of PD.

Our study confirmed that the expression level of *NURR1* in the PBMCs of PD was significantly lower than that of HC and NDC, which is consistent with our previous reports (Le et al., 2008; Liu et al., 2012). The genetic variant resulting in reduced expression of *NURR1* was reported to be associated with PD (Le et al., 2003; Hering et al., 2004; Jacobsen et al., 2008). *NURR1* has not only been found to be down-regulated in the brains of PD patients (Chu et al., 2006), but also in the peripheral blood of PD patients (Montarolo et al., 2016). These results indicating that *NURR1* dysfunction may contribute to the PD pathogenesis and the disease progression, acting in the brain and in peripheral inflammatory cells.

Based on the evidence that *NURR1* is able to prevent DA neurons from inflammation-induced death through the anti-inflammatory pathway (Bensinger and Tontonoz, 2009; Saijo et al., 2009), we suspected that the decreased level of *NURR1* gene in the pathogenesis of PD may give rise to the expression of inflammatory cytokines. Our study documented that the levels of all measured cytokines were significantly higher in the PBMCs of PD in comparison to the controls. Recently a numerous of studies have reported similar findings in protein levels from samples of serum or plasma (Chen et al., 2008; Hofmann et al., 2009; Reale et al., 2009; Koziorowski et al., 2012). Cytokines are considered key players in the neuroinflammatory cascades associated with the degenerative process in PD (Litteljohn and Hayley, 2012). However, the exact mechanisms by which cytokine levels are elevated in the peripheral blood of PD patients remain controversial. It is believed that neuroinflammation in the central nervous system of PD may induces a systemic inflammatory response to activate mononuclear cells in the peripheral blood to express and produces more cytokines during the disease development and progression of PD (Neumann and Wekerle, 1998; Reale et al., 2009). In the various diseases of NDC, some changes were found in the expression levels of cytokines as compared with PD, but no statistical differences were reached. This could be because of the small number of patients enrolled in the individual groups of NDC. As to the influence of medications on cytokines expression in PD, no statistical difference was found between the anti-PD medications groups and the untreated group, indicating that anti-PD medications may have a minimal effect on the immunological processes of PD.

In this study, we documented that *NURR1* presented a negative correlation with those of *TNF-α*, *IL-1β*, *IL-6,* and *IL-10* in the PBMCs of PD patients. Consistent with our findings, Saijo et al. (2009) showed that *NURR1* acted in microglia and astrocytes to suppress the production of inflammatory mediators and protect against DA neuron degeneration. Another study suggested that the levels of pro-inflammatory cytokines produced by primary microglia was significantly decreased in the presence of *NURR1* overexpression (Chen et al., 2018). These reports suggest that *NURR1* may play a significant role in regulating inflammation in PD. Although statistical analysis showed a negative correlation between *NURR1* and cytokines in our study, it is still unclear how *NURR1* mediates the neuroinflammation in peripheral circulation, and more experiments are needed in the future to clarify that. Furthermore, we also found that the combination of PBMCs *NURR1* and cytokines can enhance the discriminatory accuracy between PD and HC, indicating that combination of *NURR1* and cytokines expression in PBMCs could be utilized as collective biomarkers for PD diagnosis.

CONCLUSION

This study may draw the following conclusions: (1) *NURR1* gene expression is significantly decreased in the PBMCs PD patients as compared with HC and NDC. (2) The levels of inflammatory cytokines (*TNF-α*, *IL-1β*, *IL-4*, *IL-6,* and *IL-10*) were significantly higher in the PBMCs of PD patients in comparison to the controls (HC and NDC). (3) *NURR1* presented a negative correlation with *TNF-α*, *IL-1β*, *IL-6,* and *IL-10*. (4) The combination of PBMCs *NURR1* and cytokines assessment could be used as biomarkers and improve the performance of PD diagnosis.

AUTHOR CONTRIBUTIONS

TL, ZY, SL, CC, BS, and WL designed the project of this manuscript and revised the paper. TL and ZY carried out all the experiments. TL, ZY, CC, and BS contributed to statistical analyses and results interpretation. TL, ZY, SL, CC, and BS contributed to drafting of the manuscript. WL contributed to research concept and research administration. All authors edited and approved the final version of the manuscript.

FUNDING

This work was supported by the National Basic Research Program of China (81430021 and 81771521).

SUPPLEMENTARY MATERIAL

The Supplementary Material for this article can be found online at: https://www.frontiersin.org/articles/10.3389/fnagi.2018.00392/full#supplementary-material

REFERENCES

Bensinger, S., and Tontonoz, P. (2009). A Nurr1 pathway for neuroprotection. *Cell* 137, 26–28. doi: 10.1016/j.cell.2009.03.024

Buttarelli, F., Fanciulli, A., Pellicano, C., and Pontieri, F. (2011). The dopaminergic system in peripheral blood lymphocytes: from physiology to pharmacology and potential applications to neuropsychiatric disorders. *Curr. Neuropharmacol.* 9, 278–288. doi: 10.2174/157015911795596612

Caronti, B., Antonini, G., Calderaro, C., Ruggieri, S., Palladini, G., Pontieri, F., et al. (2001). Dopamine transporter immunoreactivity in peripheral blood lymphocytes in Parkinson's disease. *J. Neural. Transm.* 108, 803–807. doi: 10.1007/s007020170030

Castillo, S., Baffi, J., Palkovits, M., Goldstein, D., Kopin, I., Witta, J., et al. (1998). Dopamine biosynthesis is selectively abolished in substantia nigra/ventral tegmental area but not in hypothalamic neurons in mice with targeted disruption of the Nurr1 gene. *Mol. Cell. Neurosci.* 11, 36–46. doi: 10.1006/mcne.1998.0673

Chen, H., O'Reilly, E., Schwarzschild, M., and Ascherio, A. (2008). Peripheral inflammatory biomarkers and risk of Parkinson's disease. *Am. J. Epidemiol.* 167, 90–95. doi: 10.1093/aje/kwm260

Chen, X., Qian, Y., Wang, X., Tang, Z., Xu, J., Lin, H., et al. (2018). Nurr1 promotes neurogenesis of dopaminergic neuron and represses inflammatory factors in the transwell coculture system of neural stem cells and microglia. *CNS Neurosci. Ther.* (Suppl. 1), doi: 10.1111/cns.12825 [Epub ahead of print].

Chu, Y., Le, W., Kompoliti, K., Jankovic, J., Mufson, E., and Kordower, J. (2006). Nurr1 in Parkinson's disease and related disorders. *J. Comp. Neurol.* 494, 495–514. doi: 10.1002/cne.20828

Decressac, M., Volakakis, N., Bjorklund, A., and Perlmann, T. (2013). NURR1 in Parkinson disease–from pathogenesis to therapeutic potential. *Nat. Rev. Neurol.* 9, 629–636. doi: 10.1038/nrneurol.2013.209

Deleidi, M., and Gasser, T. (2013). The role of inflammation in sporadic and familial Parkinson's disease. *Cell. Mol. Life Sci.* 70, 4259–4273. doi: 10.1007/s00018-013-1352-y

Dickson, D. (2012). Parkinson's disease and parkinsonism: neuropathology. *Cold Spring Harb. Perspect. Med.* 2:a009258. doi: 10.1101/cshperspect.a009258

Dong, J., Li, S., Mo, J., Cai, H., and Le, W. (2016). Nurr1-based therapies for Parkinson's disease. *CNS Neurosci. Ther.* 22, 351–359. doi: 10.1111/cns.12536

Erkkinen, M., Kim, M., and Geschwind, M. (2018). Clinical neurology and epidemiology of the major neurodegenerative diseases. *Cold Spring Harb. Perspect. Biol.* 10:a033118. doi: 10.1101/cshperspect.a033118

Goetz, C., Poewe, W., Rascol, O., Sampaio, C., Stebbins, G., Counsell, C., et al. (2004). Movement disorder society task force report on the Hoehn and Yahr staging scale: status and recommendations. *Mov. Disord.* 19, 1020–1028. doi: 10.1002/mds.20213

Heneka, M., Kummer, M., and Latz, E. (2014). Innate immune activation in neurodegenerative disease. *Nat. Rev. Immunol.* 14, 463–477. doi: 10.1038/nri3705

Hering, R., Petrovic, S., Mietz, E., Holzmann, C., Berg, D., Bauer, P., et al. (2004). Extended mutation analysis and association studies of Nurr1 (NR4A2) in Parkinson disease. *Neurology* 62, 1231–1232. doi: 10.1212/01.wnl.0000118285.18383.90

Hofmann, K., Schuh, A., Saute, J., Townsend, R., Fricke, D., Leke, R., et al. (2009). Interleukin-6 serum levels in patients with Parkinson's disease. *Neurochem. Res.* 34, 1401–1404. doi: 10.1007/s11064-009-9921-z

Huang, Y., Cheung, L., Rowe, D., and Halliday, G. (2004). Genetic contributions to Parkinson's disease. *Brain Res. Rev.* 46, 44–70. doi: 10.1016/j.brainresrev.2004.04.007

Jacobsen, K., MacDonald, H., Lemonde, S., Daigle, M., Grimes, D., Bulman, D., et al. (2008). A Nurr1 point mutant, implicated in Parkinson's disease, uncouples ERK1/2-dependent regulation of tyrosine hydroxylase transcription. *Neurobiol. Dis.* 29, 117–122. doi: 10.1016/j.nbd.2007.08.003

Jankovic, J., Chen, S., and Le, W. (2005). The role of Nurr1 in the development of dopaminergic neurons and Parkinson's disease. *Prog. Neurobiol.* 77, 128–138. doi: 10.1016/j.pneurobio.2005.09.001

Koziorowski, D., Tomasiuk, R., Szlufik, S., and Friedman, A. (2012). Inflammatory cytokines and NT-proCNP in Parkinson's disease patients. *Cytokine* 60, 762–766. doi: 10.1016/j.cyto.2012.07.030

Le, W., Conneely, O., Zou, L., He, Y., Saucedo-Cardenas, O., Jankovic, J., et al. (1999). Selective agenesis of mesencephalic dopaminergic neurons in Nurr1-deficient mice. *Exp. Neurol.* 159, 451–458. doi: 10.1006/exnr.1999.7191

Le, W., Pan, T., Huang, M., Xu, P., Xie, W., Zhu, W., et al. (2008). Decreased NURR1 gene expression in patients with Parkinson's disease. *J. Neurol. Sci.* 273, 29–33. doi: 10.1016/j.jns.2008.06.007

Le, W., Xu, P., Jankovic, J., Jiang, H., Appel, S., Smith, R., et al. (2003). Mutations in NR4A2 associated with familial Parkinson disease. *Nat. Genet.* 33, 85–89. doi: 10.1038/ng1066

Li, S., and Le, W. (2017). Milestones of Parkinson's disease research: 200 years of history and beyond. *Neurosci. Bull.* 33, 598–602. doi: 10.1007/s12264-017-0178-2

Litteljohn, D., and Hayley, S. (2012). Cytokines as potential biomarkers for Parkinson's disease: a multiplex approach. *Methods Mol. Biol.* 934, 121–144. doi: 10.1007/978-1-62703-071-7_7

Liu, H., Wei, L., Tao, Q., Deng, H., Ming, M., Xu, P., et al. (2012). Decreased NURR1 and PITX3 gene expression in Chinese patients with Parkinson's disease. *Eur. J. Neurol.* 19, 870–875. doi: 10.1111/j.1468-1331.2011.03644.x

Mages, H., Rilke, O., Bravo, R., Senger, G., and Kroczek, R. (1994). NOT, a human immediate-early response gene closely related to the steroid/thyroid hormone receptor NAK1/TR3. *Mol. Endocrinol.* 8, 1583–1591. doi: 10.1210/mend.8.11.7877627

Martin, I., Dawson, V., and Dawson, T. (2011). Recent advances in the genetics of Parkinson's disease. *Annu. Rev. Genomics Hum. Genet.* 12, 301–325. doi: 10.1146/annurev-genom-082410-101440

Mizuta, I., Satake, W., Nakabayashi, Y., Ito, C., Suzuki, S., Momose, Y., et al. (2006). Multiple candidate gene analysis identifies α-synuclein as a susceptibility gene for sporadic Parkinson's disease. *Hum. Mol. Genet.* 15, 1151–1158. doi: 10.1093/hmg/ddl030

Mogi, M., Harada, M., Narabayashi, H., Inagaki, H., Minami, M., and Nagatsu, T. (1996). Interleukin (IL)-1β, IL-2, IL-4, IL-6 and transforming growth factor-α levels are elevated in ventricular cerebrospinal fluid in juvenile parkinsonism and Parkinson's disease. *Neurosci. Lett.* 211, 13–16. doi: 10.1016/0304-3940(96)12706-3

Montarolo, F., Perga, S., Martire, S., Navone, D., Marchet, A., Leotta, D., et al. (2016). Altered NR4A subfamily gene expression level in peripheral blood of Parkinson's and Alzheimer's disease patients. *Neurotox. Res.* 30, 338–344. doi: 10.1007/s12640-016-9626-4

Nagatsu, T., and Sawada, M. (2005). Inflammatory process in Parkinson's disease: role for cytokines. *Curr. Pharm. Des.* 11, 999–1016. doi: 10.2174/1381612053381620

Neumann, H., and Wekerle, H. (1998). Neuronal control of the immune response in the central nervous system: linking brain immunity to neurodegeneration. *J. Neuropathol. Exp. Neurol.* 57, 1–9. doi: 10.1097/00005072-199801000-00001

Pellicano, C., Buttarelli, F., Circella, A., Tiple, D., Giovannelli, M., Benincasa, D., et al. (2007). Dopamine transporter immunoreactivity in peripheral blood lymphocytes discriminates Parkinson's disease from essential tremor. *J. Neural Transm.* 114, 935–938. doi: 10.1007/s00702-006-0623-2

Postuma, R., Berg, D., Stern, M., Poewe, W., Olanow, C., Oertel, W., et al. (2015). MDS clinical diagnostic criteria for Parkinson's disease. *Mov. Disord.* 30, 1591–1601. doi: 10.1002/mds.26424

Reale, M., Iarlori, C., Thomas, A., Gambi, D., Perfetti, B., Nicola, M., et al. (2009). Peripheral cytokines profile in Parkinson's disease. *Brain Behav. Immun.* 23, 55–63. doi: 10.1016/j.bbi.2008.07.003

Saijo, K., Winner, B., Carson, C., Collier, J., Boyer, L., Rosenfeld, M., et al. (2009). A Nurr1/CoREST pathway in microglia and astrocytes protects dopaminergic neurons from inflammation-induced death. *Cell* 137, 47–59. doi: 10.1016/j.cell.2009.01.038

Sakurada, K., Ohshima-Sakurada, M., Palmer, T., and Gage, F. (1999). Nurr1, an orphan nuclear receptor, is a transcriptional activator of endogenous tyrosine hydroxylase in neural progenitor cells derived from the adult brain. *Development* 126, 4017–4026.

Sawada, M., Imamura, K., and Nagatsu, T. (2006). Role of cytokines in inflammatory process in Parkinson's disease. *J. Neural Transm. Suppl.* 70, 373–381. doi: 10.1007/978-3-211-45295-0

Van Laar, A., and Jain, S. (2004). Non-motor symptoms of Parkinson disease: update on the diagnosis and treatment. *Neurologist* 10, 185–194.

Wang, Z., Benoit, G., Liu, J., Prasad, S., Aarnisalo, P., Liu, X., et al. (2003). Structure and function of Nurr1 identifies a class of ligand-independent nuclear receptors. *Nature* 423, 555–560. doi: 10.1038/nature01645

Williams-Gray, C., and Worth, P. (2016). Parkinson's disease. *Medicine* 44, 542–546. doi: 10.1016/j.mpmed.2016.06.001

Conflict of Interest Statement: The authors declare that the research was conducted in the absence of any commercial or financial relationships that could be construed as a potential conflict of interest.

frontiers in Aging Neuroscience

ORIGINAL RESEARCH
published: 07 January 2019
doi: 10.3389/fnagi.2018.00431

An Integrative Approach to Treat Parkinson's Disease: Ukgansan Complements L-Dopa by Ameliorating Dopaminergic Neuronal Damage and L-Dopa-Induced Dyskinesia in Mice

Eugene Huh[1,2], *Jin Gyu Choi*[2,3], *Yeomoon Sim*[2] *and Myung Sook Oh*[2,4]*

[1] Department of Medical Science of Meridian, Graduate School, Kyung Hee University, Seoul, South Korea, [2] Department of Life and Nanopharmaceutical Sciences, Graduate School, Kyung Hee University, Seoul, South Korea, [3] BK21 PLUS Integrated Education and Research Center for Nature-inspired Drug Development Targeting Healthy Aging, Kyung Hee University, Seoul, South Korea, [4] Department of Oriental Pharmaceutical Science, College of Pharmacy, Kyung Hee East-West Pharmaceutical Research Institute, Kyung Hee University, Seoul, South Korea

OPEN ACCESS

Edited by:
Seung-Nam Kim,
Dongguk University Seoul,
South Korea

Reviewed by:
Chen Haibo,
Beijing Hospital, China
Mahsa H. Jahromy,
Azad University of Medical Sciences,
Iran

***Correspondence:**
Myung Sook Oh
msohok@khu.ac.kr

Received: 16 August 2018
Accepted: 14 December 2018
Published: 07 January 2019

Citation:
Huh E, Choi JG, Sim Y and Oh MS (2019) An Integrative Approach to Treat Parkinson's Disease: Ukgansan Complements L-Dopa by Ameliorating Dopaminergic Neuronal Damage and L-Dopa-Induced Dyskinesia in Mice. Front. Aging Neurosci. 10:431. doi: 10.3389/fnagi.2018.00431

Parkinson's disease (PD) is accompanied by motor impairments due to the loss of dopaminergic neurons in the nigrostriatal pathway. Levodopa (L-dopa) has been the gold standard therapy for PD since the 1960s; however, its neurotoxic features accelerate PD progression through auto-oxidation or the induction of dyskinetic movements. Ukgansan (UGS) is a well-known prescription for treating PD in traditional medicines of East Asia, and its anti-PD function has been experimentally evaluated. The present study investigated whether UGS attenuates (1) motor dysfunction and dopaminergic neuronal damage when co-treated with L-dopa and (2) L-dopa-induced dyskinesia (LID) in 6-hydroxydopamine (6-OHDA)-induced PD mice. Although L-dopa was found to reduce motor dysfunctions, it failed to decrease the dopaminergic neuronal damage and increased the expression of dopamine receptor 1 (D1R) and 2 (D2R) in the 6-OHDA-injected mouse striatum. Co-treatment with UGS resulted in normal striatal histology and ameliorated motor impairments. In addition, UGS suppressed the dyskinesia induced by chronic L-dopa treatment while restoring the dopaminergic neurons in the striatum. For the underlying mechanism, UGS reduced the overexpression of D1R-related signaling proteins, such as phosphorylated extracellular signal-regulated kinase, ΔFosB, and c-fos in the striatum. Overall, the results suggest that the effect of UGS could be complementary to L-dopa by ameliorating motor dysfunction, restoring the dopaminergic neurons, and suppressing the dyskinetic movements in PD.

Keywords: Parkinson's disease, levodopa, ukgansan, levodopa-induced dyskinesia, 6-hydroxydopamine

INTRODUCTION

Parkinson's disease (PD), one of the most typical neurodegenerative diseases, accounts for 1–2% of the population over 65 years of age, presenting motor dysfunctions such as bradykinesia, tremor, rigidity, and postural instability (Jankovic, 2008). These manifestations are caused by the lack of dopamine via loss of dopaminergic neurons in the substantia nigra pars compacta (SNpc) and the striatum (ST) (De Lau and Breteler, 2006). Most current treatments for PD mainly rely on dopaminergic substitution for the purpose of relieving symptoms (Schapira et al., 2014).

Levodopa (L-dopa), a precursor of dopamine, is the gold standard therapy for treating symptoms of PD via supplying exogenous dopamine, which reverses the distinctive behavioral indications of PD. However, there are some critical limitations of L-dopa since its effects are merely symptomatic and not as fundamental. One such limitation is that L-dopa may accelerate dopaminergic neuronal death during the progression of PD (Fahn et al., 2004). In addition, chronic treatment with L-dopa is accompanied by severe side effects that are induced by failure to control the concentration of exogenous dopamine. Up to90% of PD patients treated by L-dopa administration for 9–10 years have experienced L-dopa-induced dyskinesia (LID), which is the chief complaint (Connolly and Lang, 2014). LID involves abnormal involuntary movements (AIM) that represent a clinical therapeutic problem and worsen patients' quality of life. Though the mechanisms of LID have not been clearly revealed, it is closely related with the hyperactivation of the dopamine receptor 1 (D1R)-related signaling pathway in striatal projection neurons (Feyder et al., 2011; Fieblinger et al., 2014).

Herbal medicines have been widely utilized as traditional medicines since thousands of years. Their use is a promising approach to treating neurodegenerative diseases as they contain a variety of compounds that have a wider range of targets than conventional small-molecule drugs (Koehn and Carter, 2005; Choi et al., 2018). In a systematic approach, Kim et al. (2015) revealed that compounds derived from herbal medicines more closely resemble human metabolites than synthetic compounds. This suggests that herbal medicines may be more suitable for treating disease than conventional drugs and may offer an integrative approach required to treat multifactorial diseases such as PD.

Ukgansan (UGS) is composed of seven medicinal herbs and is the most used prescription for neurodegenerative diseases such as dementia and PD in traditional medicines of East Asia (Iwasaki et al., 2005). In PD patients, treatment with UGS for 4 weeks improved behavioral and psychological symptoms via regulating various neurotransmissions (Kawanabe et al., 2010). Similarly, 25 PD patients treated with UGS for 12 weeks showed significant reduction in neuropsychiatric symptoms (Hatano et al., 2014). UGS has been shown to reduce parkinsonism symptoms in drug-induced PD patients (Shim et al., 2015). Doo et al. (2010) revealed the neuroprotective effects of UGS against 1-methyl-4-phenyl-1,2,3,6-tetrahydropyridene (MPTP) neurotoxicity via upregulating PI3K/Akt pathway. In addition, it has been reported that UGS inhibits catechol-O-methyltransferase (COMT) to assist dopamine supplementation (Ishida et al., 2016). However, it is unclear whether UGS could support the effects of L-dopa on motor dysfunctions or suppress the hyperkinetic movements accompanied by chronic treatment with L-dopa in a PD mouse model.

This study aimed to investigate whether (1) UGS and L-dopa ameliorate motor dysfunction and dopaminergic neuronal damage induced by 6-hydroxydopamine (6-OHDA) when treated concurrently, and whether (2) UGS reduces LID and its related histological changes. To investigate the effects of UGS and L-dopa on 6-OHDA-induced motor impairments and dopaminergic neuronal loss, we performed the rotarod and apomorphine-induced rotation tests, and histological analysis of the ST and SNpc. To investigate the effect of UGS on dyskinetic movements in 6-OHDA-injected mice treated with L-dopa chronically, we measured the score of AIM scale (AIMs) and analyzed the concomitant histological changes in the ST.

MATERIALS AND METHODS

Animals

Animal maintenance and treatments were performed in accordance with the Animal Care and Use Guidelines of Kyung Hee University, Seoul, Korea (approved number; KHUASP(SE)-17-020). Male ICR mice (6 weeks old, 30–32 g) were purchased from the Daehan Biolink Co., Ltd. (Eumseong, Korea). The animals were housed 4 per cage (size 40 × 25 × 18 cm) with free access to water and food and were kept under constant temperature (23 ± 1°C) and humidity (60 ± 10%) and a 12-h light/dark cycle. Mice were adapted to their surroundings for 7 days and kept under the same conditions before the start of the study.

Surgery Procedure

Mice were anesthetized with tribromoethanol (312.5 mg/kg, i.p.) (Salazar et al., 2010) and placed on a stereotaxic apparatus (myNeuroLab, St. Louis, MO, USA). Each mouse received a unilateral injection of 2 μL vehicle (saline with 0.1% ascorbic acid, for sham-operated mice) or 6-OHDA (8 μg/μL) into the right ST (coordinates with respect to bregma in mm: AP 0.5, ML 2.0, DV−3.0), according to the stereotaxic atlas of mouse brain (Franklin and Paxinos, 2013). 6-OHDA solution was delivered by a microinjection pump at an injection rate of 0.5 μL/min, and the cannula was left in place for 4 min after the end of injection. After surgery, mice were allowed to recover from anesthesia in a temperature-controlled chamber and then placed in individual cages.

Preparation of UGS

UGS is composed of seven dried medicinal herbs: Atractylodes lancea rhizome (4.0 g, rhizome of *Atractylodes lancea* De Candolle), Poria sclerotium (4.0 g, sclerotium of *Poria cocos* Wolf), Cnidium rhizome (3.0 g, rhizome of *Cnidium officinale* Makino), Uncaria Hook (3.0 g, thorn of *Uncaria rhynchophylla* Miquel), Japanese Angelica Root (3.0 g, root of *Angelica acutiloba* Kitagawa), Bupleurum Root (2.0 g, root of *Bupleurum falcatum* Linne), and Glycyrrhiza (1.5 g, root and stolon of *Glycyrrhiza*

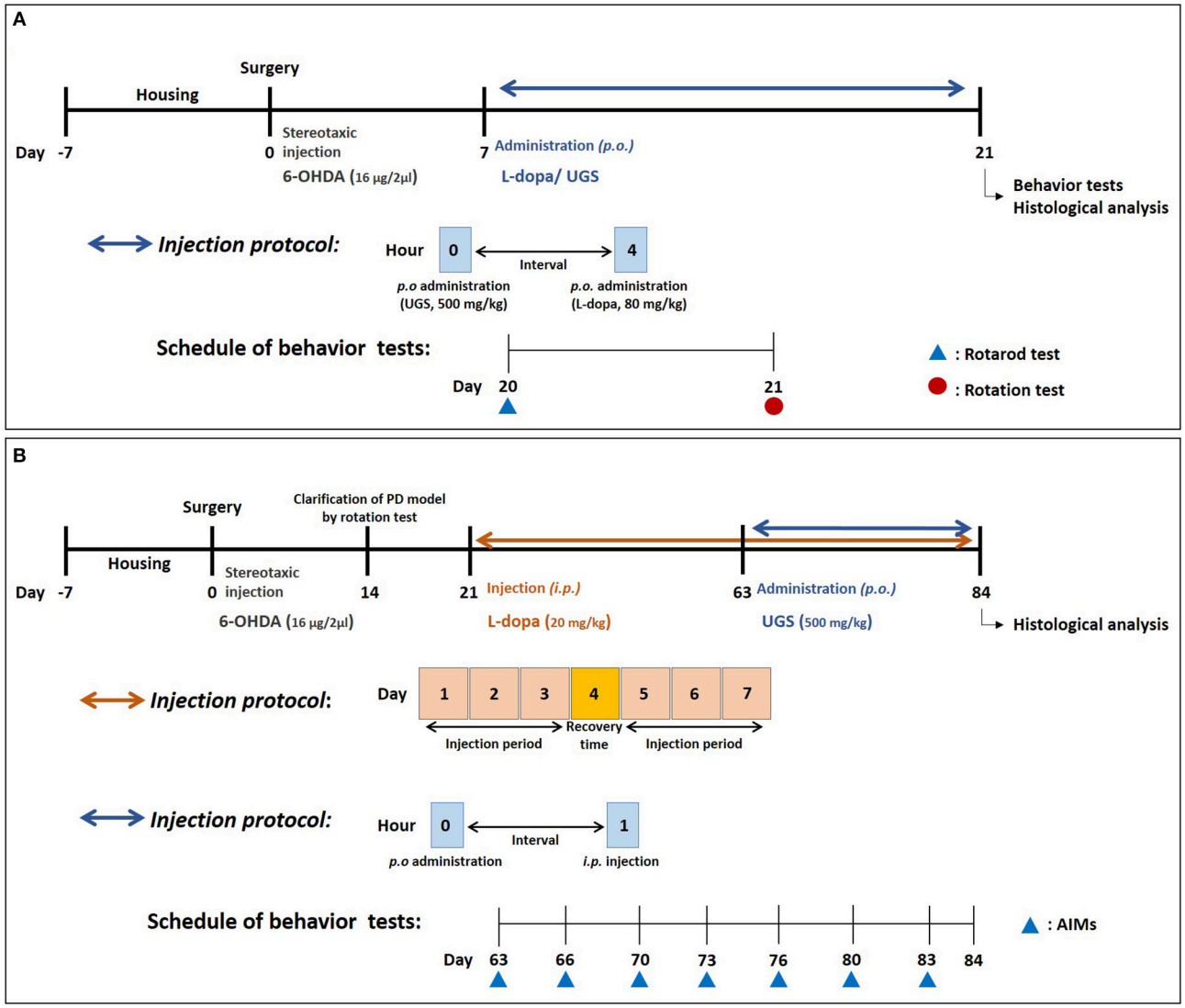

FIGURE 1 | Experimental schedule. The schedule for investigating the effects of UGS and L-dopa on motor dysfunctions **(A)** and for the effects of UGS on LID **(B)**.

uralensis Fisher). It was supplied by Tsumura & Co. (Tokyo, Japan) as a dry, powdered extract. Each plant used in the preparation of UGS was identified by its external morphology and authenticated against known specimens according to the methods of the Japanese Pharmacopoeia and the company's standards, previously reported (Mizukami et al., 2009).

Drug Administration

As shown in **Figure 1A**, drugs were administered once daily for 14 days starting from the 7th day after stereotaxic injection. The 56 animals used in the study were divided into 7 groups with 8 mice in each group: (1) Sham group (Sham-operated plus oral vehicle treatment), (2) L-dopa group (Sham-operated plus oral L-dopa treatment [80 mg/kg/day for 14 days]), (3) UGS group (Sham-operated plus oral UGS treatment [500 mg/kg/day for 14 days]), (4) 6-OHDA group (6-OHDA-lesioned plus oral vehicle treatment); (5) 6-OHDA + L-dopa group (6-OHDA-lesioned plus oral L-dopa treatment [80 mg/kg/day for 14 days]), (6) 6-OHDA + UGS group (6-OHDA-lesioned plus oral UGS treatment [500 mg/kg/day for 14 days]), and (7) 6-OHDA + L-dopa + UGS group (6-OHDA-lesioned plus oral L-dopa and UGS treatment [80 mg/kg/day and 500 mg/kg/day, respectively, for 14 days]). L-dopa (Sigma-Aldrich, MO, USA) and UGS were dissolved in normal saline. The administration of UGS was conducted at least 4 h after the administration of L-dopa. Equal volumes of the vehicle were administered to sham and 6-OHDA mice.

The scheme for investigating the effect of UGS on LID was as follows (**Figure 1B**): on the 14th day post-surgery, the rotation test was performed to assess coordination in the PD model. L-dopa (20 mg/kg with 10 mg/kg benserazide) was administered for 42 days starting on the 21st day after stereotaxic injection,

reflecting the clinical period of L-dopa administration. The administration schedule was as follows: 3 days for injection and 1 day for recovery. After the development of LID, 32 animals were divided into 4 groups with 8 mice in each group: (1) Sham group (Sham-operated plus intraperitoneal vehicle treatment), (2) PD group (6-OHDA-lesioned plus intraperitoneal vehicle treatment), (3) LID group (6-OHDA-lesioned plus intraperitoneal L-dopa treatment [20 mg/kg/day for 21 days]), and (4) LID + UGS (6-OHDA-lesioned plus intraperitoneal L-dopa treatment [20 mg/kg/day for 21 days] and oral UGS treatment [500 mg/kg/day for 21 days]) where L-dopa and UGS were dissolved in normal saline.

Behavioral Tests

Rotarod Test

To measure the bradykinesia and hypokinesia induced by 6-OHDA in mouse, we performed the rotarod test. The rotarod unit was made of a rotating spindle (7.3 cm diameter) and five individual compartments able to simultaneously test five mice. After two successive days of twice-daily training (4 rpm rotation speed on the first day and 12 rpm on the second day), the test rotation speed was increased to 14 rpm on the last day in a test session. The time each mouse remained on the rotating bar was recorded over three trials per mouse, at 5 min intervals and the maximum test time was limited up to 180 s. Data were shown as the mean time on the rotating bar over the three test trials.

Apomorphine-Induced Rotation Test

The mice were placed in hemispheric rotational bowl with a diameter of 40 cm. They were allowed to habituate to their environment for 5 min before the administration of apomorphine (4 mg/kg, *s.c.*). Full 360° turns in the direction opposite to the lesion (contralateral rotation) were counted and rotational behaviors were assessed for 25 min. Results were expressed as contralateral turns in 25 min.

AIMs Scoring Test

To evaluate the dyskinesia induced by L-dopa, AIMs scoring tests were performed and modified based on previous studies (Pavon et al., 2006; Dos-Santos-Pereira et al., 2016). A trained observer assessed each mouse for the presence of AIMs at 20-min intervals for 180 min after L-dopa administration. The assessment took place on days 0, 3, 7, 10, 13, 17, and 20 following the development of the LID model. Axial, limb, and orolingual AIMs subtypes were scored in 1-min periods. Each subtype was measured accordingly on a severity scale ranging from 0 to 4 (0 = absent, 1 = occasional, 2 = frequent, 3 = continuous but interrupted by sensory distraction, and 4 = continuous, severe, and insuppressible).

Western Blot Analysis

Brain tissues were lysed using a protein assay kit according to the manufacturer's instructions. Protein concentrations in each fraction were quantified by Bradford's assay by using kit according to the manufacture's instruction (Bio-rad, Hercules, CA, USA). Equal amount of protein in each sample was separated on 10 % sodium dodecyl sulfate–polyacrylamide gel electrophoresis, and then separated proteins were electrophoretically transferred to a membrane. The membranes were blocked with 5% skim milk in 25 mM tris-Cl, 150 mM NaCl, and 0.005% Tween-20 for 45 min. Thereafter, the membranes were incubated overnight with primary antibodies at 4°C. The primary antibodies were directed against D1R, dopamine receptor 2 (D2R) (Abcam, MA, USA), FosB, c-fos, extracellular signal-regulated kinase (ERK), phosphorylated ERK (p-ERK), and β-actin (Santa Cruz, CA, USA). The blots were washed three times for 10 min with tris-buffered saline with tween 20 (TBS-T). Then, the membranes were incubated with respective horseradish peroxidase-conjugated secondary antibodies for 1 h and washed with TBS-T again. Immunoreactive bands were developed using an enzyme-linked chemiluminescence detection kit and visualized using the ChemiDoc^{TM} XRS+ system (Bio-rad, CA, USA).

Immunohistochemistry and Quantification

Mice were anesthetized with tribromoethanol (312.5 mg/kg, *i.p.*), perfused transcardially with 0.05 M phosphate-buffered saline (PBS) and then fixed with cold 4% paraformaldehyde (PFA) in 0.1 M phosphate buffer (PB). Brains were removed and post-fixed in 0.1 M PB containing 4% PFA overnight at 4°C and then immersed in a solution containing 30% sucrose in 0.05 M PBS for cryoprotection. Serial 30 μm-thick coronal sections were cut on a freezing microtome (Leica Instruments GmbH, Nussloch, Germany) and stored in cryoprotectant (25% ethylene glycol, 25% glycerol, and 0.05 M PB) at −20°C until use for immunohistochemistry.

For each mouse, brain regions including ST (at Bregma 0.98 to 0.50 mm Li et al., 2000) and SN [at Bregma −2.92 to −3.52 mm (L'episcopo et al., 2013)] were used for the immunohistochemistry. Cell counting was conducted by an experimenter who did not know the treatment condition, and the result for each animal was the average of the number from its three sections.

Free floating brain sections were rinsed in PBS before immunostaining and then pretreated with 1% hydrogen peroxide for 15 min to remove endogenous peroxidase activity. Then, they were incubated overnight with a rabbit anti-tyrosine hydroxylase (TH) (1:1000 dilution) or anti-dopamine transporter (DAT) antibodies (1:500 dilution) (Abcam, MA, USA) in PBS containing 0.3% Triton X-100 and normal goat serum. They were then incubated with a biotinylated anti-rabbit IgG (1:200 dilution) for 1 h 20 min followed by incubation in avidin-biotin complex solution for 1 h at room temperature. The color of every section was developed with 3,3-diaminobenzidine for 30 sec to 1 min. Quantification of the brain tissue sections was performed by counting the number of TH-immunopositive neurons in the SNpc at × 200 magnification and measuring the optical density of TH-positive and DAT-positive fibers in the ST at × 40 magnification using Image J software (Bethesda, MD, USA). Data were presented as a percent of the contralateral side of each section values. The images were photographed using an optical light microscope (Olympus Microscope System BX51; Olympus, Tokyo, Japan).

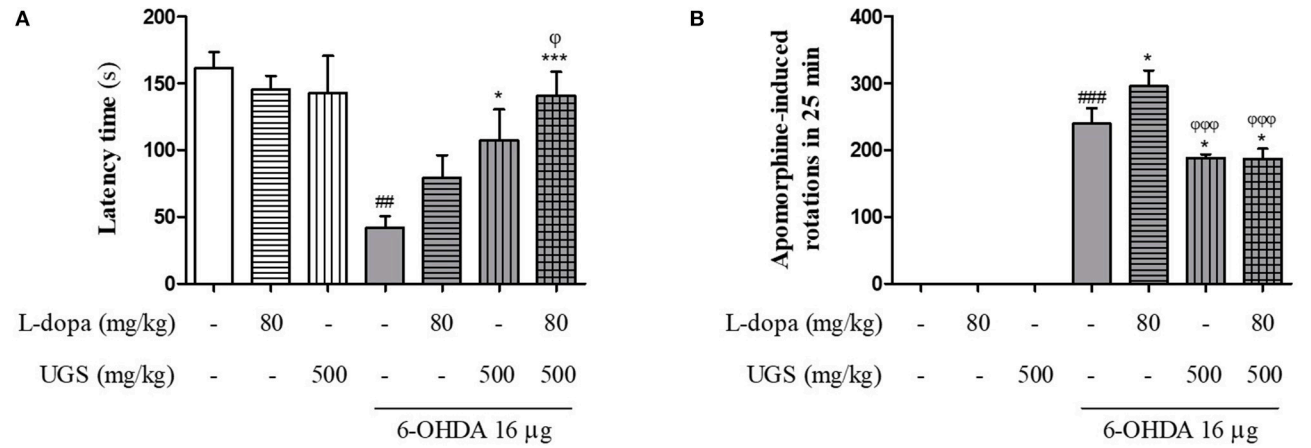

FIGURE 2 | UGS attenuated 6-OHDA-induced motor dysfunctions when co-treated with L-dopa. To evaluate the passive motor function, rotarod test was assessed **(A)**. For hemi-parkinsonian model, it can evaluate the effect of dopamine function via apomorphine-induced rotation tests **(B)**. Values are given as the mean ± S.E.M. ($N = 8$). The significance of differences was analyzed by one-way ANOVA followed by Bonferroni's Multiple Comparison Test: $^{\#\#}p < 0.01$ and $^{\#\#\#}p < 0.001$; mean values were significantly different from the sham group. $^{*}p < 0.05$ and $^{***}p < 0.001$; mean values were significantly different from the 6-OHDA group. $^{\phi}p < 0.05$ and $^{\phi\phi\phi}p < 0.001$; mean values were significantly different from the 6-OHDA + L-dopa group.

Statistical Analysis

All statistical parameters were calculated using GraphPad Prism 5.01 software (GraphPad Software Inc., San Diego, USA). Values were expressed as the mean ± standard error of the mean (S.E.M.). The results except AIMs scores were analyzed by one-way analysis of variance (ANOVA) followed by Bonferroni's multiple comparison test among all groups. AIMs scores were analyzed by repeated measures of ANOVA with Bonferroni's post hoc tests for pairwise multiple comparisons. Differences with a p value less than 0.05 were considered statistically significant.

RESULTS

UGS Attenuated 6-OHDA-Induced Motor Dysfunctions When Co-treated With L-Dopa

The rotarod test was performed to compare the effects of combined UGS and L-dopa treatment and L-dopa-only treatment. The latency time of the 6-OHDA group was significantly shortened compared with that of the sham group while those of the 6-OHDA + L-dopa, 6-OHDA + UGS, and 6-OHDA + L-dopa + UGS groups were longer than that of the 6-OHDA group. The latency time of the 6-OHDA + L-dopa + UGS group was significantly increased compared to that of the 6-OHDA + L-dopa group (**Figure 2A**). The apomorphine-induced rotation test was conducted to investigate the alterations in dopamine sensitivity when treated with L-dopa and UGS concurrently or separately. The number of rotations in the 6-OHDA + L-dopa group was higher than that in the 6-OHDA-lesioned group; however, the 6-OHDA + L-dopa + UGS group showed decreased number of rotations compared to the 6-OHDA group and the 6-OHDA + UGS group (**Figure 2B**).

UGS Reduced the Dopaminergic Neuronal Damage Induced by 6-OHDA in the Mouse ST and SNpc When Co-treated With L-Dopa, Reduction did not Occur in the L-Dopa Only Treatment

TH-immunohistochemistry was performed using the SNpc and ST of each mouse brain to test whether co-treatment of UGS with L-dopa reduces 6-OHDA-induced decrease in dopaminergic neuronal cells and fibers in SNpc and ST, respectively. The 6-OHDA group showed significantly decreased optical density of TH-positive fibers in the ST compared to the sham group. The 6-OHDA + UGS and 6-OHDA + L-dopa + UGS groups showed normal optical densities of TH-positive fibers in the ST when compared to the 6-OHDA group. Although the 6-OHDA + L-dopa group showed no improvement in the optical density of TH-positive fibers in the ST, the 6-OHDA + L-dopa + UGS group showed significantly increased TH-positive fibers when compared to the 6-OHDA + L-dopa group (**Figure 3A**). In the SNpc region, the number of TH-positive neuronal cells of the 6-OHDA group did not differ from that in the 6-OHDA + L-dopa group. However, the 6-OHDA + UGS and 6-OHDA + L-dopa + UGS groups showed significantly reduced dopaminergic neuronal damage. The 6-OHDA + L-dopa + UGS group also showed significantly increased number of TH-positive neuronal cells compared to the 6-OHDA + L-dopa group (**Figure 3C**).

DAT maintains the concentration of dopamine in the synaptic cleft via the uptake of dopamine into dopaminergic neurons, and its expression indirectly represents the abundance of dopaminergic neurons. To investigate the expression of DAT in the ST, DAT-immunohistochemistry was performed. The expression of DAT was significantly decreased in the 6-OHDA group. Moreover, there were no significant differences in DAT

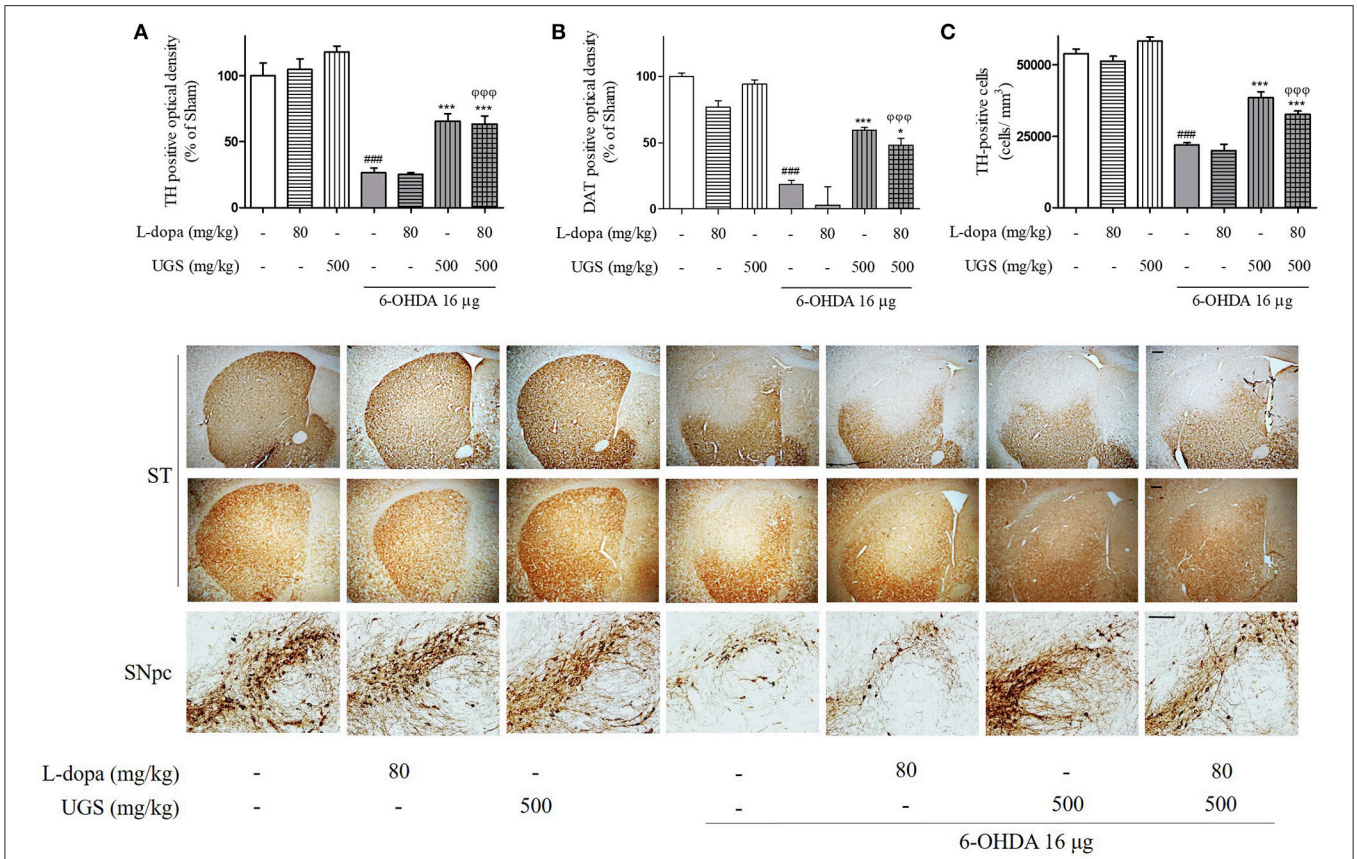

FIGURE 3 | UGS treated with L-dopa reduced the dopaminergic neuronal damage induced by 6-OHDA in the mouse ST and SNpc. To impede the progress of PD, drugs have to restore dopaminergic neurons against toxicity. To evaluate the restorative effect, dopaminergic neurons were visualized with TH and DAT-immunostaining in nigrostriatal pathway. The optical density of TH and DAT-positive fibers in the ST was measured **(A,B)**. The stereological TH-positive neurons in the SNpc were counted **(C)**. Scale bar = 100 μm. Values of quantification data are given as the mean ± S.E.M. ($N = 8$). The significance of differences was analyzed by one-way ANOVA followed by Bonferroni's Multiple Comparison Test: $^{###}p < 0.001$; mean values were significantly different from the sham group. $^{*}p < 0.05$ and $^{***}p < 0.001$; mean values were significantly different from the 6-OHDA group. $^{\phi\phi\phi}p < 0.001$; mean values were significantly different from the 6-OHDA + L-dopa group.

expression between the 6-OHDA + L-dopa group and the 6-OHDA group. However, the 6-OHDA + UGS and 6-OHDA + L-dopa + UGS groups showed significantly increased DAT. Moreover, the 6-OHDA + L-dopa + UGS group showed a higher optical density for DAT than the 6-OHDA + L-dopa group (**Figure 3B**).

UGS Reduced the Expression of D1R That Was Increased by L-Dopa in the ST of 6-OHDA Mice

L-dopa has been known to induce the upregulation of D1R. Upon chronic use, L-dopa causes an imbalance in dopamine regulatory systems. Therefore, it is important to modulate the activities of dopamine receptors to harmonize the dopaminergic transmission. To investigate the dopaminergic signaling modulation, the western blot was performed to detect whether the co-administration of L-dopa and UGS normalizes the expression of dopamine receptors in the ST. Results showed that the 6-OHDA group had decreased expression of D1R, but increased expression of D2R. Interestingly, the ratio of D1R/D2R was significantly increased in the 6-OHDA + L-dopa group, while the L-dopa group showed opposite results. The 6-OHDA + L-dopa + UGS group showed a normal ratio of D1R and D2R (**Figure 4**).

We confirmed that the co-administration of UGS with L-dopa significantly ameliorates motor dysfunction in 6-OHDA-injected mice, compared to L-dopa alone. Following this confirmation, we investigated whether UGS had an effect on dyskinesia induced by chronic treatment of L-dopa.

UGS Suppressed the Dyskinetic Movements in LID Mice

After 42 days of treatment with L-dopa, the PD mice exhibited apparent dyskinetic movements. The scores of axial, limb, and orolingual AIMs assessments had no significant differences between the LID and LID + UGS groups on the first day of assessment. During the 21-day administration period, both the total global and separated (axial, limb, and orolingual) AIMs

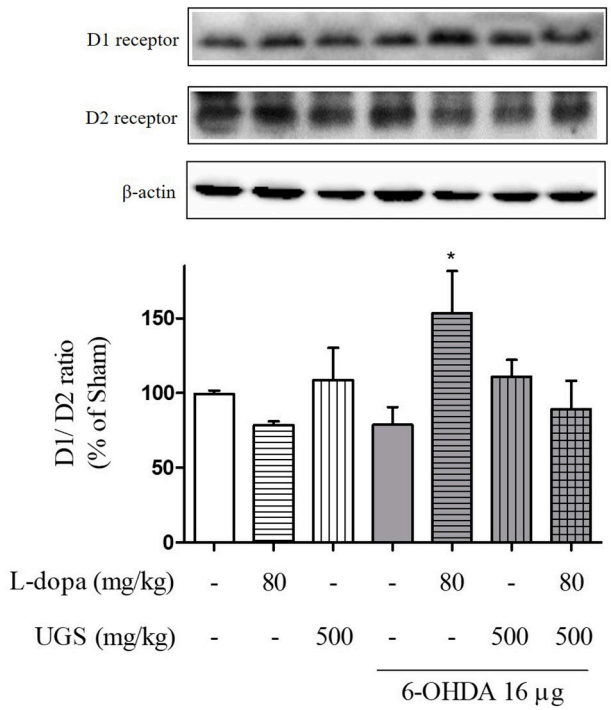

FIGURE 4 | UGS regulated the L-dopa-induced alterations in the expression of dopamine receptors in 6-OHDA-injected mouse ST**.** Representative band image of the expression of dopamine receptors from western blot analysis, quantification data of D1R and D2R. The D1R/D2R ratio was evaluated. Values of quantification data are given as the mean ± S.E.M. ($N = 6$). The significance of differences was analyzed by one-way ANOVA followed by Bonferroni's Multiple Comparison Test: *$p < 0.05$; mean values were significantly different from the 6-OHDA group.

scores were maintained in the LID group. In the UGS-treated group, all AIMs scores were significantly decreased from the 10th day of administration compared to those in the LID group. Repeated measures of ANOVA revealed a significant anti-dyskinetic effect of UGS [$F_{(3,168)}$ =12.728, $p < 0.001$] and a significant group*time interaction [$F_{(9,168)} = 6.301$, $p < 0.001$]. The dyskinetic behavior was not seen in the PD group (**Figure 5**).

To investigate the interaction between UGS and time after treatment with L-dopa, AIMs scores were measured on the 10th day of administration for 180 min after L-dopa injection. In the LID group, all AIMs scores peaked at 60 min after L-dopa injection. Mice treated with UGS showed significantly decreased dyskinetic movements at the peak time compared to LID-induced mice. Mice in both the LID and LID+UGS groups did not show dyskinetic movements 160 min after LID injection. Repeated measures of ANOVA was performed and revealed a significant main effect of UGS [$F_{(3,245)} = 25.693$, $p< 0.001$] and, a non-significant group*time interaction [$F_{(9,245)} = 0.735$, $p = 0.636$] (**Figure 6**).

UGS Attenuated the Dopaminergic Neuronal Loss in the ST of LID Mice

TH-immunohistochemistry in the ST of each mouse brain was performed to detect whether UGS reduced the dopaminergic neuronal damage in the ST of LID mice. The PD and LID groups showed significantly decreased optical density of TH-positive fibers in the ST compared to the sham group. The LID + UGS group showed normal optical densities of TH-positive fibers in the ST, which showed a tendency to be worse in the LID group (**Figure 7**).

UGS Normalized the Overexpression of D1R-Related Transmissions in the ST of LID Mice

Chronic administration of L-dopa leads to persistent and intermittent hyperactivation of the cAMP signaling cascade, which regulates several downstream effector targets such as ΔFosB and c-fos, responsible for the control of excitability of striatal neurons (Feyder et al., 2011). In the current study, western blot was performed to detect whether UGS normalized the L-dopa-induced overexpression of D1R and the phosphorylation of cAMP signaling-related protein, ERK, in the ST. The expression of D1R and p-ERK was significantly increased by L-dopa, while UGS reduced the overexpression in the lesioned section of the ST (**Figure 8**).

The proteins, ΔFosB and c-fos, are known as the downstream signaling proteins of ERK phosphorylation in the ST of the LID mouse model. The overexpression of ΔFosB and c-fos induced by D1R are implicated in various forms of synaptic plasticity, particularly in long-term potentiation (Chen et al., 2017). In the present study, the expression of transcriptional targets, such as ΔFosB and c-fos, was increased in the mouse ST of the LID group. UGS reduced the overexpression of ΔFosB and c-fos in the lesioned ST (**Figure 9**).

We confirmed that UGS inhibited dyskinetic movements induced by chronic administration of L-dopa in the 6-OHDA-injected PD mouse model. In addition, we found that UGS suppressed the D1R-ERK signaling pathway in the ST of the LID model.

DISCUSSION

In the current study, we investigated whether (1) the combined treatment of UGS with L-dopa attenuates motor functions in 6-OHDA-induced parkinsonian mice compared to L-dopa single treatment and whether (2) UGS ameliorates dyskinesia in response to chronic administration of L-dopa. This study clearly revealed that UGS increased the effects of L-dopa on motor dysfunction and inhibited L-dopa-induced dyskinetic movements. The effect of UGS on the survival of dopaminergic neurons in the SNpc and ST of 6-OHDA-induced parkinsonian mice and a reduction in D1R, p-ERK, ΔFosB, and c-fos levels in the ST of the LID mice were observed.

The unilaterally-lesioned 6-OHDA rodent model is the primary model used to reflect parkinsonian motor dysfunctions and LID; this surgical mouse model is referred to as "hemiparkinsonian syndrome." The model is associated with complete dopamine depletion and hypersensitivity of lesioned, striatal dopamine receptors with lateralized behavior disorders of the forelimb contralateral to the lesion (Amalric et al.,

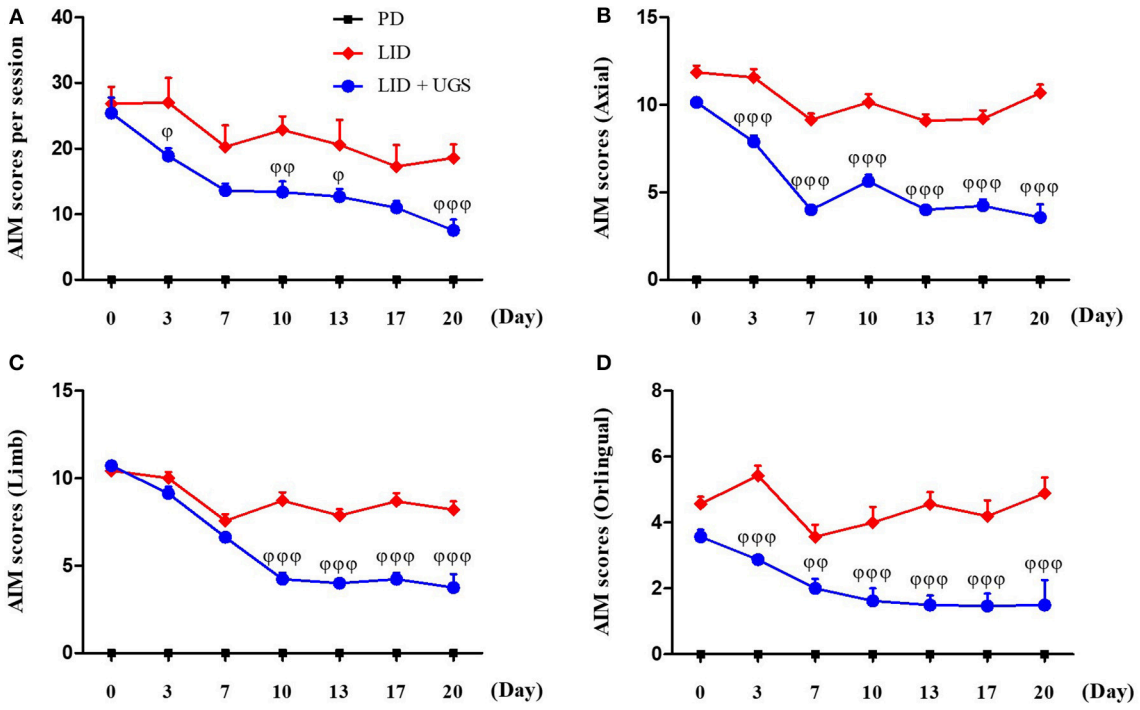

FIGURE 5 | UGS suppressed the dyskinetic movements in LID mice**.** 6-OHDA-lesioned mice treated with UGS ameliorates LID over the 21 days treatment period, which differed significantly from the LID groups in all testing sessions. The sum of axial, limb, and oroligual **(A)**, axial **(B)**, forelimb **(C)**, and oroligual **(D)** AIMs on each testing session were rated following the administration of UGS. Values are given as the mean ± S.E.M. ($N = 6$). The significance of differences was analyzed by repeated measures of ANOVA with Bonferroni's post hoc tests: $^{\Phi}p < 0.05$, $^{\Phi\Phi}p < 0.01$, and $^{\Phi\Phi\Phi}p < 0.001$; mean values were significantly different from the LID group.

1995). Upon chronic L-dopa treatment, 6-OHDA-lesioned mice showed AIM, and the biochemical mechanisms underlying the pathophysiology of LID are consistent with PD patients (Tronci and Francardo, 2017). Although the MPTP mouse model has been previously reported to replicate LID, it presents several drawbacks such as inconsistency in dyskinetic subtypes (hyperactive running and jumping) with clinical features of LID and variable degrees of behavioral and biochemical impairments (Nicholas, 2007). Therefore, the model used in this study is suitable for representing the clinical features of patients with PD and LID.

Since L-dopa is the precursor of dopamine, its effects merely supplement dopamine deficiency. In addition, the excessive supply of dopamine causes oxidative stress termed, auto-oxidation. Serra et al. (2000) found that the dopaminergic neuronal death by auto-oxidation of exogenous L-dopa occurs in both PC12 cells and the ST of rats. Administering L-dopa accelerates the progression of PD while temporarily mitigating symptoms of the disease. In the current study, UGS was selected for treatment along with L-dopa as it is one of the common drugs used to treat PD in East Asia and its mechanisms differ from those of L-dopa; the anti-parkinsonian effects of UGS are focused on neuroprotection and regulation of neurotransmissions (Doo et al., 2010; Kawanabe et al., 2010). This study revealed that combined treatment of UGS and L-dopa reduced the rigidity in 6-OHDA-lesioned mice compared to L-dopa alone and decreased dopaminergic neuronal damage in the nigrostriatal pathway as shown in **Figure 2**. Increased in the number of rotations upon combined treatment of UGS and L-dopa was also observed. Since dopamine depletion induces contralateral rotations in hemi-parkinsonian rodents, these results indicate that UGS influences the survival of dopaminergic neurons. Taken together, the behavioral manifestations after combined treatment seem to derived from the neuroprotective effects of UGS.

In the striatal projection neurons, the activation of D1R directly controls the excitatory signaling, whereas the activation of D2R indirectly regulates the excitatory signaling, which suppresses motor effects (Pavon et al., 2006). The expression of D1R is increased in response to the administration of L-dopa; therefore, its chronic use causes hypersensitivity or hyperactivation of D1R. In the current study, it was confirmed that the regulatory effects of UGS on D1R-related signaling are enhanced by L-dopa, which subsequently activates D2R in the ST.

Similarly, the overexpression of D1R in the dopamine-depleted ST of LID mice was observed. Pavon et al. (2006) and Fieblinger et al. (2014) have reported that overexpressing D1R results in an increase in related proteins while Feyder et al. (2016) reported that changes in mitogen-activated protein kinase signaling pathways are associated with increased D1R activation. Phosphorylation of ERK has also been shown to be involved in synaptic plasticity leading to long-term potentiation, which regulates the state of normal or abnormal form of

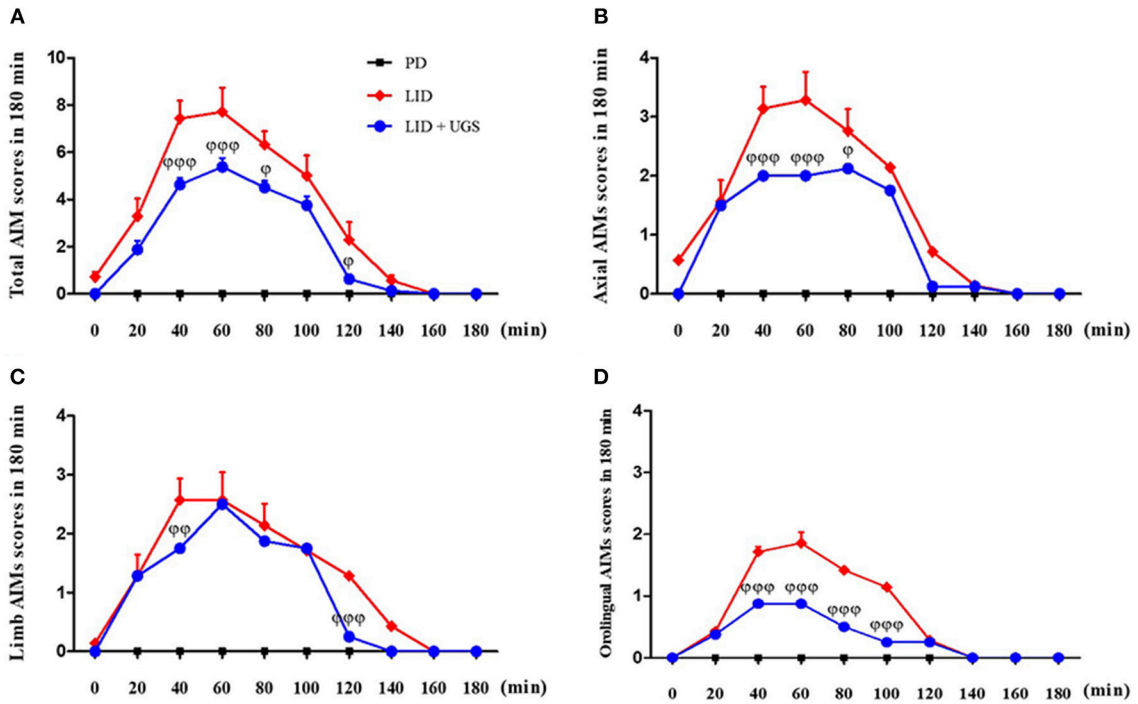

FIGURE 6 | UGS decreased the peak score of LID during 180 min after L-dopa injection. All testing sessions were performed at the 10th day of L-dopa treatment. The sum of axial, limb, and oroligual **(A)**, axial **(B)**, forelimb **(C)**, and oroligual **(D)** AIMs on each testing session were rated every 20 min. There is no significant difference of interaction time as treating UGS in LID mouse. Values are given as the mean ± S.E.M. ($N = 6$). The significance of differences was analyzed by repeated measures of ANOVA with Bonferroni's *post hoc* tests: $^{\phi}p < 0.05$, $^{\phi\phi}p < 0.01$, and $^{\phi\phi\phi}p < 0.001$; mean values were significantly different from the LID group.

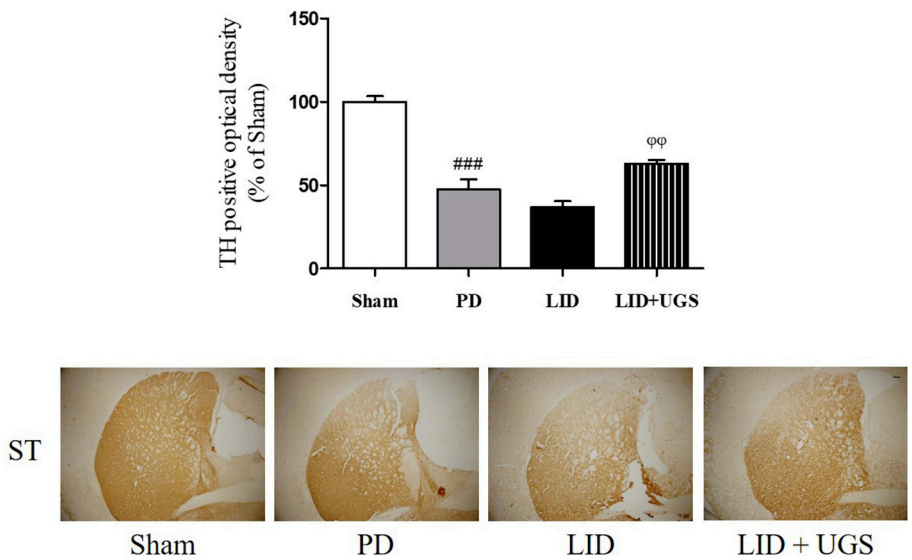

FIGURE 7 | UGS attenuated the dopaminergic neuronal loss in L-dopa chronically treated the mouse ST. The optical density of TH fibers in the ST was measured. Scale bar = 100 μm. Values of quantification data were given as the mean ± S.E.M. ($N = 6$). The significance of differences was analyzed by one-way ANOVA followed by Bonferroni's Multiple Comparison Test: $^{\#\#\#}p < 0.001$; mean values were significantly different from the sham group. $^{\phi\phi}p < 0.01$; mean values were significantly different from the LID group.

motor learning. The subsequent long-lasting overexpression of ΔFosB and c-fos induced by p-ERK may also mediate long-term potentiation in the dopamine-depleted ST (Pavon et al., 2006). It has been suggested that hyperactivation in the glutamatergic corticostriatal pathway is related to the development of dyskinesia. We confirmed increased ΔFosB and c-fos levels

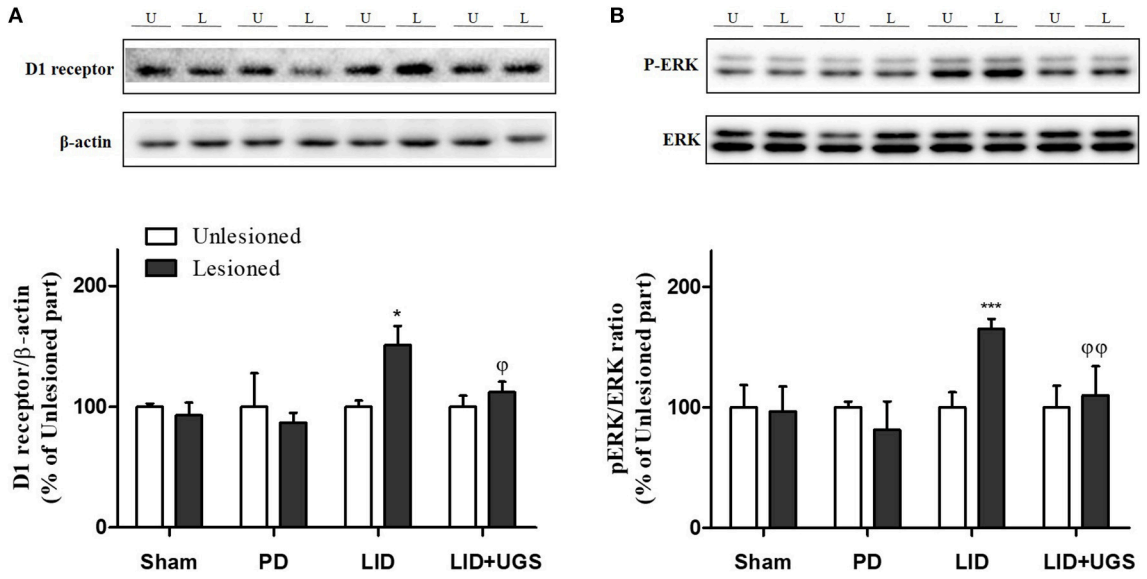

FIGURE 8 | UGS reduced the expression of D1R and the phosphorylation of ERK after development of LID. Representative band images and the quantification data of D1R **(A)** and p-ERK **(B)** for western blot analysis. Values of quantification data are given as the mean ± S.E.M. ($N = 6$). The significance of differences was analyzed by one-way ANOVA followed by Bonferroni's Multiple Comparison Test: $^{*}p < 0.05$ and $^{***}p < 0.001$; mean values were significantly different from the unlesioned part of each group. $^{\phi}p < 0.05$ and $^{\phi\phi}p < 0.01$; mean values were significantly different from the LID group.

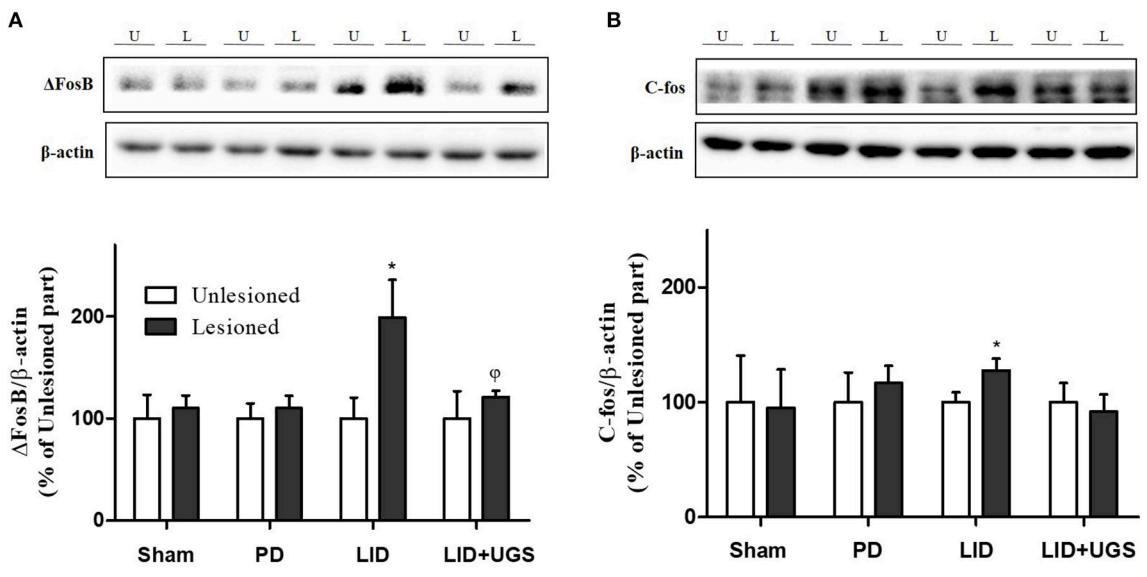

FIGURE 9 | UGS inhibited the expression of ΔFosB and c-fos after development of LID. Representative band images and the quantification data of expression of ΔFosB **(A)** and c-fos **(B)** for western blot analysis. Values of quantification data are given as the mean ± S.E.M. ($N = 6$). The significance of differences was analyzed by one-way ANOVA followed by Bonferroni's Multiple Comparison Test: $^{*}p < 0.05$; mean values were significantly different from the unlesioned part of each group. $^{\phi}p < 0.05$; mean values were significantly different from the LID group.

induced by p-ERK in the lesioned ST with chronic L-dopa treatment. In addition, UGS normalizing the increase may be related to the amelioration of D1R expression and dopamine depletion.

In the present study, we investigated the interaction between UGS and L-dopa over time using AIMs assessment. The results indicated that there was an interaction between UGS and L-dopa with signs of dyskinetic symptoms; however, there was no effect on the drug's prolonged duration. In previous study, Ishida et al. (2016) reported that UGS prolonged the effectiveness of L-dopa via inhibiting COMT. In addition, they evaluated the effectiveness of L-dopa with the AIMs test and showed the

prolonged duration of L-dopa when UGS was administered in rats. This is rather inconsistent with our results as duration was unaffected. In the previous study, the assessment was conducted on day 15 after L-dopa injection with a single injection of UGS; however, in this study, the interaction was estimated to take place on day 10 of UGS administration with chronic L-dopa. The differences between the two studies may be a result of the difference in the period of administration; however, further studies would be required to confirm.

D1R and D2R expression is also closely related to the activation of other receptors, such as metabotropic glutamate (mGlu) receptor or N-methyl-D-aspartate receptor in L-dopa-induced excitability. These receptors induce excessive Ca^{2+} influx and influence D1R activation while suppressing D2R activation (Morin et al., 2016). Among them, the mGlu5R and A2a-adrenoceptor interact with D2R, which regulates Akt/glycogen synthase kinase 3 beta and ERK signaling (Fieblinger et al., 2014; Zhang et al., 2016). It has been reported that UGS regulates adrenergic receptor activation. Nakagawa et al. (2012) suggested that the components in UGS inhibit morphine tolerance and physical dependence via suppressing A2a-adrenoceptor. It can be inferred that combining UGS with L-dopa normalizes both D1R and D2R via regulating the A2a-adrenoceptor; however, further studies on the mechanisms would be required to confirm.

In summary, UGS attenuated PD-like motor dysfunctions when treated with L-dopa via reduction of dopaminergic neuronal loss and normalization of D1R and D2R in 6-OHDA-injected mice. Moreover, UGS ameliorates dyskinetic movements induced by chronic administration of L-dopa via suppressing D1R-related signaling. These results suggest that UGS could be a promising agent for combination treatment with L-dopa for PD patients.

AUTHOR CONTRIBUTIONS

EH and MO designed and coordinated this study. EH, JC, and YS performed the experiments and analyzed the data. EH and MO wrote the manuscript. All the authors participated in discussion of the results and reviewed the final draft.

FUNDING

This study was supported by grants from Medical Research Center Program through the National Research Foundation of Korea funded by the Ministry of Science and ICT (NRF-2017R1A5A2014768).

REFERENCES

Amalric, M., Moukhles, H., Nieoullon, A., and Daszuta, A. (1995). Complex deficits on reaction time performance following bilateral intrastriatal 6-OHDA infusion in the rat. *Eur. J. Neurosci.* 7, 972–980. doi: 10.1111/j.1460-9568.1995.tb01085.x

Chen, G., Nie, S., Han, C., Ma, K., Xu, Y., Zhang, Z., et al. (2017). Antidyskinetic effects of MEK inhibitor are associated with multiple neurochemical alterations in the striatum of hemiparkinsonian rats. *Front. Neurosci.* 11:112. doi: 10.3389/fnins.2017.00112

Choi, J. G., Kim, S. Y., Jeong, M., and Oh, M. S. (2018). Pharmacotherapeutic potential of ginger and its compounds in age-related neurological disorders. *Pharmacol. Ther.* 182, 56–69. doi: 10.1016/j.pharmthera.2017.08.010

Connolly, B. S., and Lang, A. E. (2014). Pharmacological treatment of Parkinson disease: a review. *JAMA* 311, 1670–1683. doi: 10.1001/jama.2014.3654

De Lau, L. M., and Breteler, M. M. (2006). Epidemiology of Parkinson's disease. *Lancet Neurol.* 5, 525–535. doi: 10.1016/S1474-4422(06)70471-9

Doo, A. R., Kim, S. N., Park, J. Y., Cho, K. H., Hong, J., Eun-Kyung, K., et al. (2010). Neuroprotective effects of an herbal medicine, Yi-Gan San on MPP+/MPTP-induced cytotoxicity *in vitro* and *in vivo*. *J. Ethnopharmacol.* 131, 433–442. doi: 10.1016/j.jep.2010.07.008

Dos-Santos-Pereira, M., Da-Silva, C. A., Guimaraes, F. S., and Del-Bel, E. (2016). Co-administration of cannabidiol and capsazepine reduces L-DOPA-induced dyskinesia in mice: Possible mechanism of action. *Neurobiol. Dis.* 94, 179–195. doi: 10.1016/j.nbd.2016.06.013

Fahn, S., Oakes, D., Shoulson, I., Kieburtz, K., Rudolph, A., Lang, A., et al. (2004). Levodopa and the progression of Parkinson's disease. *N. Engl. J. Med.* 351, 2498–2508. doi: 10.1056/NEJMoa033447

Feyder, M., Bonito-Oliva, A., and Fisone, G. (2011). L-DOPA-induced dyskinesia and abnormal signaling in striatal medium spiny neurons: focus on dopamine D1 receptor-mediated transmission. *Front. Behav. Neurosci.* 5:71. doi: 10.3389/fnbeh.2011.00071

Feyder, M., Södersten, E., Santini, E., Vialou, V., Laplant, Q., Watts, E. L., et al. (2016). A role for mitogen- and stress-activated kinase 1 in L-DOPA-induced dyskinesia and FosB expression. *Biol. Psychiatry* 79, 362–371. doi: 10.1016/j.biopsych.2014.07.019

Fieblinger, T., Sebastianutto, I., Alcacer, C., Bimpisidis, Z., Maslava, N., Sandberg, S., et al. (2014). Mechanisms of dopamine D1 receptor-mediated ERK1/2 activation in the parkinsonian striatum and their modulation by metabotropic glutamate receptor type 5. *J. Neurosci.* 34, 4728–4740. doi: 10.1523/JNEUROSCI.2702-13.2014

Franklin, K. B. J., and Paxinos, G. (2013). *Paxinos and Franklin's The Mouse Brain in Stereotaxic Coordinates.* Amsterdam: Academic Press, an imprint of Elsevier.

Hatano, T., Hattori, N., Kawanabe, T., Terayama, Y., Suzuki, N., Iwasaki, Y., et al. (2014). An exploratory study of the efficacy and safety of yokukansan for neuropsychiatric symptoms in patients with Parkinson's disease. *J. Neural Transm.* 121, 275–281. doi: 10.1007/s00702-013-1105-y

Ishida, Y., Ebihara, K., Tabuchi, M., Imamura, S., Sekiguchi, K., Mizoguchi, K., et al. (2016). Yokukansan, a traditional Japanese medicine, enhances the L-DOPA-induced rotational response in 6-hydroxydopamine-Lesioned rats: possible inhibition of COMT. *Biol. Pharm. Bull.* 39, 104–113. doi: 10.1248/bpb.b15-00691

Iwasaki, K., Satoh-Nakagawa, T., Maruyama, M., Monma, Y., Nemoto, M., Tomita, N., et al. (2005). A randomized, observer-blind, controlled trial of the traditional Chinese medicine Yi-Gan San for improvement of behavioral and psychological symptoms and activities of daily living in dementia patients. *J. Clin. Psychiatry* 66, 248–252. doi: 10.4088/JCP.v66n0214

Jankovic, J. (2008). Parkinson's disease: clinical features and diagnosis. *J. Neurol. Neurosurg. Psychiatry* 79, 368–376. doi: 10.1136/jnnp.2007.131045

Kawanabe, T., Yoritaka, A., Shimura, H., Oizumi, H., Tanaka, S., and Hattori, N. (2010). Successful treatment with Yokukansan for behavioral and psychological symptoms of Parkinsonian dementia. *Prog. Neuropsychopharmacol. Biol. Psychiatry* 34, 284–287. doi: 10.1016/j.pnpbp.2009.11.019

Kim, H. U., Ryu, J. Y., Lee, J. O., and Lee, S. Y. (2015). A systems approach to traditional oriental medicine. *Nat. Biotechnol.* 33, 264–268. doi: 10.1038/nbt.3167

Koehn, F. E., and Carter, G. T. (2005). The evolving role of natural products in drug discovery. *Nat. Rev. Drug Discov.* 4, 206–220. doi: 10.1038/nrd1657

L'episcopo, F., Tirolo, C., Testa, N., Caniglia, S., Morale, M. C., Impagnatiello, F., et al. (2013). Aging-induced Nrf2-ARE pathway disruption in the subventricular zone drives neurogenic impairment in parkinsonian mice

via PI3K-Wnt/beta-catenin dysregulation. *J. Neurosci.* 33, 1462–1485. doi: 10.1523/JNEUROSCI.3206-12.2013

Li, Q., Wichems, C., Heils, A., Lesch, K. P., and Murphy, D. L. (2000). Reduction in the density and expression, but not G-protein coupling, of serotonin receptors (5-HT1A) in 5-HT transporter knock-out mice: gender and brain region differences. *J. Neurosci.* 20, 7888–7895. doi: 10.1523/JNEUROSCI.20-21-07888.2000

Mizukami, K., Asada, T., Kinoshita, T., Tanaka, K., Sonohara, K., Nakai, R., et al. (2009). A randomized cross-over study of a traditional Japanese medicine (kampo), yokukansan, in the treatment of the behavioural and psychological symptoms of dementia. *Int. J. Neuropsychopharmacol.* 12, 191–199. doi: 10.1017/S146114570800970X

Morin, N., Morissette, M., Grégoire, L., and Di Paolo, T. (2016). mGlu5, Dopamine D2 and Adenosine A2A Receptors in L-DOPA-induced dyskinesias. *Curr. Neuropharmacol.* 14, 481–493. doi: 10.2174/1570159X14666151201185652

Nakagawa, T., Nagayasu, K., Nishitani, N., Shirakawa, H., Sekiguchi, K., Ikarashi, Y., et al. (2012). Yokukansan inhibits morphine tolerance and physical dependence in mice: the role of alpha(2)A-adrenoceptor. *Neuroscience* 227, 336–349. doi: 10.1016/j.neuroscience.2012.09.079

Nicholas, A. P. (2007). Levodopa-induced hyperactivity in mice treated with 1-methyl-4-phenyl-1,2,3,6-tetrahydropyridine. *Mov. Disord.* 22, 99–104. doi: 10.1002/mds.21235

Pavon, N., Martin, A. B., Mendialdua, A., and Moratalla, R. (2006). ERK phosphorylation and FosB expression are associated with L-DOPA-induced dyskinesia in hemiparkinsonian mice. *Biol. Psychiatry* 59, 64–74. doi: 10.1016/j.biopsych.2005.05.044

Salazar, D. L., Uchida, N., Hamers, F. P., Cummings, B. J., and Anderson, A. J. (2010). Human neural stem cells differentiate and promote locomotor recovery in an early chronic spinal cord injury NOD-scid mouse model. *PLoS ONE* 5:e12272. doi: 10.1371/journal.pone.0012272

Schapira, A. H., Olanow, C. W., Greenamyre, J. T., and Bezard, E. (2014). Slowing of neurodegeneration in Parkinson's disease and Huntington's disease: future therapeutic perspectives. *Lancet* 384, 545–555. doi: 10.1016/S0140-6736(14)61010-2

Serra, P. A., Esposito, G., Enrico, P., Mura, M. A., Migheli, R., Delogu, M. R., et al. (2000). Manganese increases L-DOPA auto-oxidation in the striatum of the freely moving rat: potential implications to L-DOPA long-term therapy of Parkinson's disease. *Br. J. Pharmacol.* 130, 937–945. doi: 10.1038/sj.bjp.0703379

Shim, Y. H., Park, J. Y., Choi, W. W., Min, I. K., Park, S. U., Jung, W. S., et al. (2015). Herbal medicine treatment for drug-induced parkinsonism. *J. Altern. Complement Med.* 21, 273–280. doi: 10.1089/acm.2014.0124

Tronci, E., and Francardo, V. (2017). Animal models of L-DOPA-induced dyskinesia: the 6-OHDA-lesioned rat and mouse. *J. Neural Transm.* 125:1137–44. doi: 10.1007/s00702-017-1825-5

Zhang, X., Choi, B. G., and Kim, K. M. (2016). Roles of dopamine D(2) receptor subregions in interactions with beta-arrestin2. *Biomol. Ther.* 24, 517–522. doi: 10.4062/biomolther.2015.198

Conflict of Interest Statement: The authors declare that the research was conducted in the absence of any commercial or financial relationships that could be construed as a potential conflict of interest.

frontiers in Neuroscience

ORIGINAL RESEARCH
published: 29 January 2019
doi: 10.3389/fnins.2019.00013

Serum Amyloid Alpha Is Downregulated in Peripheral Tissues of Parkinson's Disease Patients

Lille Kurvits[1,2], Ene Reimann[3], Liis Kadastik-Eerme[1], Laura Truu[4], Külli Kingo[5,6], Triin Erm[7], Sulev Kõks[8,9], Pille Taba[1†] and Anu Planken[10†]*

[1] Department of Neurology and Neurosurgery, University of Tartu, Tartu, Estonia, [2] Department of Neurology, Charité – Universitätsmedizin Berlin, Berlin, Germany, [3] Institute of Pathophysiology, University of Tartu, Tartu, Estonia, [4] Laboratory of Bioenergetics, National Institute of Chemical Physics and Biophysics, Tallinn, Estonia, [5] Department of Dermatology, University of Tartu, Tartu, Estonia, [6] Dermatology Clinic, Tartu University Hospital, Tartu, Estonia, [7] Department of Pathology, Tartu University Hospital, Tartu, Estonia, [8] Centre for Comparative Genomics, Murdoch University, Perth, WA, Australia, [9] Perron Institute for Neurological and Translational Science, University of Western Australia, Perth, WA, Australia, [10] Oncology and Haematology Clinic, North-Estonian Medical Centre, Tallinn, Estonia

We report the changed levels of serum amyloid alpha, an immunologically active protein, in Parkinson's disease (PD) patients' peripheral tissues. We have previously shown that *Saa-1* and *-2* (serum amyloid alpha-1,-2, genes) were among the top downregulated genes in PD patients' skin, using whole-genome RNA sequencing. In the current study, we characterized the gene and protein expression profiles of skin and blood samples from patients with confirmed PD diagnosis and age/sex matched controls. qRT-PCR analysis of PD skin demonstrated downregulation of *Saa-1* and *-2* genes in PD patients. However, the lowered amount of protein could not be visualized using immunohistochemistry, due to low quantity of SAA (Serum Amyloid Alpha, protein) in skin. *Saa-1* and *-2* expression levels in whole blood were below detection threshold based on RNA sequencing, however significantly lowered protein levels of SAA1/2 in PD patients' serum were shown with ELISA, implying that SAA is secreted into the blood. These results show that SAA is differentially expressed in the peripheral tissues of PD patients.

Keywords: neurodegenarative disease, serum amyloid A (SAA), Parkinson's disease (PD), intrinsically disordered protein (IDP), skin biopsy

OPEN ACCESS

Edited by:
Hi-Joon Park,
Kyung Hee University, South Korea

Reviewed by:
Patrizia Longone,
Fondazione Santa Lucia (IRCCS), Italy
David Pozo,
Universidad de Sevilla, Spain

***Correspondence:**
Anu Planken
plankena@gmail.com

† These authors have contributed equally to this work

Specialty section:
This article was submitted to Neurodegeneration, a section of the journal Frontiers in Neuroscience

Received: *25 August 2018*
Accepted: *08 January 2019*
Published: *29 January 2019*

Citation:
Kurvits L, Reimann E, Kadastik-Eerme L, Truu L, Kingo K, Erm T, Kõks S, Taba P and Planken A (2019) Serum Amyloid Alpha Is Downregulated in Peripheral Tissues of Parkinson's Disease Patients. Front. Neurosci. 13:13. doi: 10.3389/fnins.2019.00013

INTRODUCTION

Parkinson's disease (PD) is a neurodegenerative disorder, characterized by motor symptoms, like resting tremor, hypo- and bradykinesia, rigidity and postural instability (Poewe et al., 2017). However, the clinical specter of affected functions is much wider due to the involvement of other central and peripheral organ systems. Pathologic neuronal lesions outside the central nervous system (CNS) have been demonstrated in PD patients (Gelpi et al., 2014), for example characteristic α-synuclein deposits have been found in dermal nerve fibers of PD patients skin (Wang et al., 2013). In addition, pathogenic biomolecular defects of PD occur in non-neuronal peripheral tissues (Braak et al., 2003; Auburger et al., 2012; Teves et al., 2018). PD patients have many dermatologic problems like seborrhoea, seborrheic dermatitis, hyperhidrosis and impaired wound healing (Gregory and Miller, 2015). As to date the affirmative diagnosis of PD can only be made based on the results of post-mortem autopsy, thus there is a great need for detailed understanding of disease biology, as

well as for studies investigating novel diagnostic and prognostic biomarkers. Peripheral blood has been widely used in the search for biomarkers in PD (Scherzer et al., 2007; Grünblatt et al., 2010; Borrageiro et al., 2017), however other peripheral tissues, such as skin, are promising models for investigating the pathogenic mechanisms of PD.

Serum amyloid alpha (SAA) is a protein that may be linked to PD due to its many functions in metabolic networks affected in PD. SAA plays a key role in the functioning of the immune system, being involved in inflammation, tumorigenesis, regulating skin homeostasis and accumulating as misfolded AA-amyloid protein (Artl et al., 2000; Urieli-Shoval et al., 2000). SAA1 and SAA2 expression is induced in the liver, which is the major site of synthesis. It is also produced extrahepatically, especially within dermal tissues by keratinocytes (Urieli-Shoval et al., 1998; Upragarin et al., 2005). Different types of cancers occur less frequently in PD patients, however the risk of melanoma is about 2-fold higher than for controls (Devine et al., 2011; Liu et al., 2011). Serum SAA has been shown to be elevated in melanoma patients through all stages of disease and is proposed to be a prognostic cancer biomarker (Findeisen et al., 2009).

The current study was undertaken based on observations from our previous transcriptomic analysis on PD patients' skin, which demonstrated serum amyloid alpha 1 and 2 genes (*Saa-1,-2)* to be one of the most significantly deregulated genes in PD skin (Planken et al., 2017). It was of interest, whether the changes in RNA levels are constant and transcribed into changed protein levels within different tissues.

MATERIALS AND METHODS

Study Subjects

We enrolled in total 86 PD patients who were diagnosed by neurology-board-certified movement disorders specialists and met the Queen Square Brain Bank diagnostic criteria (Gibb and Lees, 1988; Lees et al., 2009) from Tartu University Hospital. 72 healthy matched controls with no personal history of neurodegenerative diseases were also enrolled. Independent samples of PD patients with comparable age, gender, Movement Disorders Society's Unified Parkinson's Disease Rating Scale (MDS-UPDRS, Goetz et al., 2008) and the Hoehn and Yahr Scale (H&Y, Hoehn and Yahr, 1967) were randomly allocated for quantitative real time polymerase chain reaction (qRT-PCR), enzyme-linked immunosorbent assay (ELISA) and Immunohistochemistry. In total, the PD patients had an average age of 71.0 $\pm$ 7.8 years, MDS-UPDRS of 52.0 $\pm$ 14.0, H&Y of 2.7 $\pm$ 0.9 and 85.0% had no family history of PD. Clinical details of the participants are provided in **Table 1** (breakdown of clinical details of different groups in **Supplementary Table S1**). All PD patients received standard medications. As a limitation to our study, the inflammatory status of all subjects is not known, but those tested (4 PD patients) had serum CRP $<$ 1 mg/L and serum cholesterol $<$ 5.2 mmol/L. The study was approved by the local Ethics Committee and an informed consent was obtained from all patients and controls included in the study.

Tissue Sampling and RNA Extraction

Skin punch-biopsies of Ø 4 mm were taken from non-sun-exposed skin from the medial side of upper arm, instantly frozen in liquid nitrogen and stored at –80°C until RNA extraction. Biopsies were homogenized with Precellys24 homogenizer with the Cryolys system (Bertin Technologies). RNeasy Fibrous Tissue Mini Kit (Qiagen) was used for total RNA extraction, according to the manufacturer's protocol. During the purification on-column DNase I was applied (Qiagen). The RNA quality was assessed using Agilent 2100 Bioanalyzer, the RNA 6000 Nano kit (Agilent Technologies) and the Qubit fluorometer (Life Technologies). The lowest RIN of samples was 6.7.

Real-Time Quantitative PCR

Blood samples of 37 patients and 33 healthy controls were obtained. Total RNA from skin biopsies was converted to cDNA using random primers and High Capacity cDNA Reverse Transcription Kit with RNase Inhibitor (Applied Biosystems). For duplex qRT-PCR analysis TaqMan Gene Expression Assays were used: VIC (housekeeping gene ActinB) and FAM (gene of interest) probes and TaqMan Gene® Expression Master Mix (Applied Biosystems). The TaqMan® Gene Assay IDs were the following: Hs01060665_g1 (*ActinB*), Hs00761940_s1 (*Saa1*), Hs00754237_s1 (*Saa2*). qRT-PCR was performed using ABI PRISM 7900HT Fast Real-Time PCR System equipment (Applied Biosystems) and the ABI PRISM 7900 SDS 2.2.2 Software. Each reaction was performed in quadruplicate to minimize technical errors. Real-time PCR data for gene of interest was expressed as mean ΔCT value relative to housekeeping gene. ΔCT of controls was subtracted from ΔCT of PD to yield $\Delta\Delta$CT. Relative expression i.e. fold change was calculated using $2^{-\Delta CT}$-function. The data of studied genes following normal distribution were parametrically tested by unpaired *t*-test.

Enzyme-Linked Immunosorbent Assay of the Blood Samples

Blood samples of 36 patients and 27 healthy controls were obtained. Serum was extracted from blood samples and rapidly frozen to and stored at –80°C. Stored samples were defrosted and centrifuged at 1500 g at room temperature for 10 min. ELISA kit for human SAA1/2 (Invitrogen Corporation) was used. 200-fold diluted human serum SAA1/2 standard was calibrated to a highly purified *Escherichia coli*-expressed recombinant protein. The sample measurements were performed with Tecan GeniOS Pro luminometer in duplicate and repeated 3 times on separate plates. Optical density (450 nm) readings were used to quantitatively express serum SAA1/2 results. The Human SAA1/2 concentrations for samples and controls were plotted based on the standard curve. Values obtained for serum were multiplied by 200 to correct for the overall dilution. The data for mean concentration followed normal distribution, was plotted on a barplot and parametrically tested by unpaired *t*-test.

Skin Immunohistochemistry

Immunohistochemistry samples were obtained from 13 PD patients (6 male, 7 female, mean age of 72.0 $\pm$ 7.2 years) and 12

TABLE 1 | Demographic characteristics for total PD patients and controls.

Samples	PD qRT-PCR	PD ELISA	PD Immuno-histo	HC qRT-PCR	HC ELISA	HC immuno-histo	*P*
Age at enrolment (years, *SD*)	69.5 ± 7.3	72.1 ± 8.4	72.0 ± 7.2	72.1 ± 7.9	72.7 ± 9.6	71.8 ± 8.6	n.s.
Age of PD onset (years, *SD*)	61.4 ± 8.3	66.5 ± 10.8	65.6 ± 9.2	n/a	n/a	n/a	n.s.
Male gender (*n*, %)	18 (49)	12 (33)	6 (46)	12 (36)	10 (37)	3(25)	n.s.
1st degree relatives with PD (*n*, %)	3 (8.1)	4 (11.4)	0	n/a	n/a	n/a	n.s.
MDS-UPDRS (mean, *SD*)	62.7 ± 24.8	71.8 ± 30.7	65.8 ± 27.1	n/a	n/a	n/a	n.s.
H&Y (mean, *SD*)	2.5 ± 0.8	2.7 ± 1.0	3.1 ± 0.8	n/a	n/a	n/a	n.s.

There were no significant (n.s.; $p > 0.05$) differences between independent samples by analysis of variance with post hoc Tukey test.

controls (6 male, 6 female, mean age of 71.3 ± 7.1 years). The skin biopsies were deparaffinized with 2× 4 min. xylene, 4 min. isopropanol, 2× 4 min. 96% alcohol. Then they were blocked with 3% hydrogen peroxide for 7 min, and processed with proteinase K for 5 min. The slides were incubated with primary mouse monoclonal Serum Amyloid A antibody (Novus Biologicals) in 1:100 dilution for 30 min. and processed with detection antibodies (DAKO REAL EnVision+ Dual Link, Single Reagents, HRP Rabbit/Mouse) for 30 min. The sections were immersed in 3.3% diaminobenzidine (Dako Company) chromogen dye and hydrogen peroxide buffer solution for 4 min. This created a brownish staining in the location of detection antibody. The background was dyed with hematoxylin, dehydrated with 2x 96% alcohol and 2x xylene, covered with aqueous resin. The immunohistochemistry visual validation procedure was carried out by an independent pathologist. Within the publication data 1 PD patient (male, age 74) and 1 control (female, age 64) have been presented as representative images.

RESULTS

Our previous work with skin RNA-sequencing showed a significant downregulation of *Saa-1* and *-2* expression levels in PD patients (logFC -2,75 and -1,65, respectively, Planken et al., 2017). Further tests with 86 PD patients, who met the Queen Square Brain Bank diagnostic criteria (Gibb and Lees, 1988; Lees et al., 2009) and 72 healthy matched controls were performed. *Saa-1* and *-2* gene expression levels were measured using qRT-PCR from skin, followed by measurement of SAA1/2 protein levels from serum using ELISA and finally the SAA1/2 protein levels were assayed using immunohistochemistry from PD patients' skin.

Gene Expression Profiling of *Saa-1* and *-2* in Skin and Blood From PD Patients

The qRT-PCR analysis from 33 PD patients and 37 controls demonstrated a significant 1.68-fold downregulation of *Saa2* gene ($p = 0.0372$) and 1.34-fold downregulation of *Saa1* gene in PD patients skin, however the result was not statistically significant ($p = 0.2469$) (**Figure 1**).

SAA Protein Visualization in the Skin

The immunohistochemical analysis of 13 PD patients' and 12 controls' skins for expression of SAA 1/2 protein, demonstrated that no visually detectable protein or changes in protein levels can be observed in PD patients (**Figure 2**).

ELISA From Serum

ELISA analysis (from 36 PD patients and 27 controls) of serum for SAA 1/2 protein expression, demonstrated decreased protein concentration levels in the serum of PD patients by 50.9%

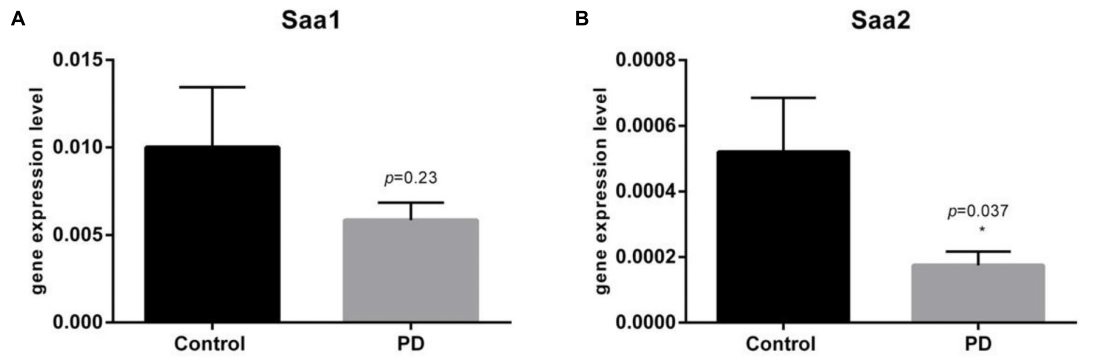

FIGURE 1 | qRT-PCR on relative gene expression levels of *Saa1* **(A)** and *Saa2* **(B)** genes in the skin of 33 PD patients and 37 controls. Barplots show mean fold changes with upper percentiles displayed in $2^{-\Delta CT}$ values. **(A)** Demonstrating not significantly ($p = 0.25$) lowered *Saa1* levels in PD patients by 1.34-fold. Mean relative gene expression for controls is 0.01001 (SEM = 0.003431) and for PD patients 0.005853 (SEM = 0.001007). **(B)** Demonstrating significantly ($p = 0.037$) lowered *Saa2* levels in PD patients by 1.68-fold. Mean relative gene expression for controls is 0.0005200 (SEM = 0.0001653) and for PD patients 0.0001749 (SEM = 4.242e-005).

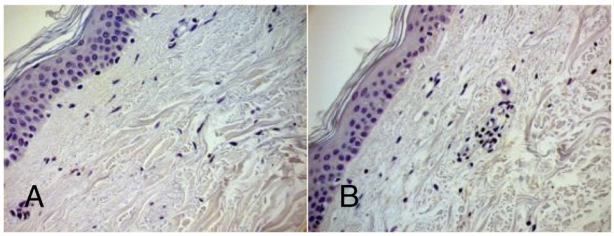

FIGURE 2 | Representative IHC for SAA 1/2. Control **(A)** and PD patient **(B)**. Magnification: 40×. Dye: Hematoxylin and immunohistochemical labeling for serum amyloid alpha. Both in control and PD patient no detectable visual staining can be demonstrated.

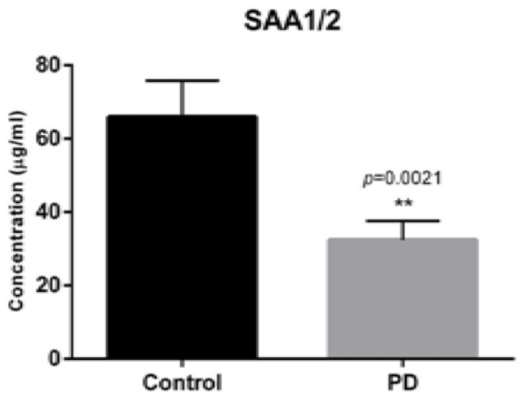

FIGURE 3 | Serum ELISA SAA1/2 concentration in 27 controls and 36 PD patients, respectively. Demonstrating decreased concentration of SAA1/2 by 50.9% (p = 0.0021). Bars show mean concentration with upper percentiles, 66.8 µg/ml for healthy controls and 32.8 µg/ml for PD patients (p = 0.0054).

compared to controls (**Figure 3**, p = 0.0021), with the mean protein concentrations being 32.8 and 66.8 µg/ml, respectively.

DISCUSSION

The qRT-PCR results of SAA downregulation in the skin mirrored the changes obtained in RNA-sequencing (Planken et al., 2017). *Saa-1* and *-2* RNA levels in whole-blood cells were below the detection levels using RNA-sequencing (unpublished data). In blood serum, SAA1/2 was downregulated, implying SAA1/2 is secreted into blood. In skin immunohistochemistry, SAA1/2 protein does not visualize, thus downregulation of the gene is not detectable using this method. As the quantity level for these proteins in the normal skin is physiologically low, this is to be expected. SAA is known as a marker for AA-amyloidosis and positive staining is seen only in patients suffering from chronic inflammation, certain cancers or genetic defects, in which case, the pathologic staining would be seen around basal membranes, blood vessel walls and collagenous connective tissue (James et al., 2011). In addition, Western blot analysis on the same subject samples were performed, however the levels of SAA in skin homogenates were also too low for detection (data not shown). Taken together, the findings show downregulated *Saa-1* and *-2* expression in skin and protein SAA1/2 levels in blood.

SAA as an Immunomodulator in the Skin

SAA in the skin tissue is an autocrine modulatory protein, induced by inflammatory signals like IL-11α, TNF-α, and IL-17A and stimulating the expressions of other cytokines, interleukins and metalloproteinases on the tissue level (Patel et al., 1998; Furlaneto and Campa, 2000; Vallon et al., 2001; de Seny et al., 2013). SAA upregulates its own expression, creating an autocrine self-maintaining regulation by positive feedback (Couderc et al., 2017). In our previous work with skin RNA-sequencing a large set of genes in PD skin were downregulated, which are involved in the process of epidermal cornification and desquamation (Planken et al., 2017). The downregulation of SAA, an important autocrine immunomodulator in PD skin, might contribute to the impaired epidermal renewal processes which are clinically associated with poor wound healing in PD patients. Moreover, serum SAA has been shown to be elevated in patients of all stages of melanoma (I to IV) and is proposed as a prognostic biomarker for the disease (Findeisen et al., 2009). Different types of cancers occur less frequently in PD patients, however the risk of melanoma is about 2-fold higher than in general population (Liu et al., 2011). These findings corroborate the role of SAA within the pathomechanistic link between melanoma and PD. It would be of interest to measure the levels of keratinocyte-derived SAA in patients diagnosed with both PD and melanoma to elaborate these findings.

SAA as an Intrinsically Disordered Protein

Intrinsically disordered proteins (IDPs) refer to proteins without fixed three-dimensional structures under physiological conditions, allowing the same polypeptide to undertake different interactions with different consequences (Zhang et al., 2013). This lack of proper fixed structure enables IDPs to interact with many ligands, but renders them vulnerable to environmental changes and causes them to misfold. IDPs are involved in neurodegenerative diseases (Uversky, 2009, 2015), which all exhibit characteristic accumulation of incorrectly folded proteins that hence form insoluble deposits (Takalo et al., 2013). SAA is an IDP (Ye et al., 2011; Colón et al., 2015) and therefore able to contribute to protein deposit formation in PD. Overexpression of IDPs, like a-synuclein, in the CNS is known to cause neurodegeneration in model organisms (Kirik and Björklund, 2003). It is suggestive that SAA acts similarly in the CNS of PD. In a mouse model of AD, systemic LPS was administered (Liu et al., 2016), which induced SAA expression that led to activation of brain microglia and to suppression of tau hyperphosphorylation, having a modifying effect on neurofibrillary tangle development. Acute SAA is shown to be elevated in human AD brains (Liang et al., 1997) and cerebrospinal fluid (Kindy et al., 1999). Neurodegenerative diseases, like AD and PD are associated with neuroinflammation, suggesting that also the levels of SAA, as one of acute phase reactants, are expected to be higher in the CNS. How SAA acts in the periphery in neurodegenerative diseases

is largely unknown. We now show that SAA is downregulated in the peripheral tissues like skin and blood, which could be a compensatory effect for excessive levels of aberrant SAA in the CNS.

Global Peripheral Downregulation of SAA Protein

Within this study we have also demonstrated significantly lowered protein levels of SAA in PD serum. This finding suggests that the downregulation of SAA proteins occurs in PD patients not only on the transcriptomic level in the skin, but more globally also in other tissues. Liver is the predominant synthesis place of SAA, from where SAA proteins are secreted into the circulation. The downregulated levels in serum indicate a reduced transcription of SAA in the liver tissue. In the skin, no SAA could be detected using immunohistochemistry and by Western blot method. This was expected, as the accumulation of misfolded SAA is known as AA-Amyloidosis and it seems to appear in the conditions of chronic inflammation with elevated serum levels of SAA. We showed, instead, downregulated levels of SAA in both skin and serum. In the normal brain tissue, SAA is not detectable, but it has been shown to be elevated in the CNS under induced inflammatory conditions and in case of Alzheimer's disease (Liang et al., 1997; Guo et al., 2002). How SAA acts in the CNS in case of PD and whether its expression in the periphery affects it, is largely unknown. We have now characterized the downregulation of SAA in PD skin and serum and demonstrated that no visible deposits of SAA protein in the skin of PD patients can be seen.

ETHICS STATEMENT

Research Ethics Committee of the University of Tartu 3-318 51003.

AUTHOR CONTRIBUTIONS

AP, LK, LT, TE, and ER carried out the laboratory work. LK-E performed patient selection and clinical analysis. KK contributed to study planning and reviewing the manuscript. SK and AP involved study planning, performed analysis of sequencing data, and wrote the manuscript. PT participated in writing and reviewing of the manuscript. All authors read and approved the final manuscript.

FUNDING

This study was supported by the Grant PUT1239 of the Estonian Research Council.

SUPPLEMENTARY MATERIAL

The Supplementary Material for this article can be found online at: https://www.frontiersin.org/articles/10.3389/fnins.2019.00013/full#supplementary-material

TABLE S1 | Breakdown of patient and control clinical characteristics.

REFERENCES

Artl, A., Marsche, G., Lestavel, S., Sattler, W., and Malle, E. (2000). Role of serum amyloid A during metabolism of acute-phase HDL by macrophages. *Arterioscler. Thromb. Vasc. Biol.* 20, 763–772. doi: 10.1161/01.ATV.20.3.763

Auburger, G., Klinkenberg, M., Drost, J., Marcus, K., Morales-Gordo, B., Kunz, W. S., et al. (2012). Primary skin fibroblasts as a model of parkinson's disease. *Mol. Neurobiol.* 46, 20–27. doi: 10.1101/gr.138032.112

Borrageiro, G., Haylett, W., Seedat, S., Kuivaniemi, H., and Bardien, S. (2017). A review of genome-wide transcriptomics studies in parkinson's disease. *Eur. J. Neurosci.* 7, 1–16. doi: 10.1111/ejn.13760

Braak, H., Tredici, K. D., Rüb, U., de Vos, R. A., Jansen Steur, E. N., and Braak, E. (2003). Staging of brain pathology related to sporadic parkinson?s disease. *Neurobiol. Aging* 24, 197–211. doi: 10.1016/S0197-4580(02)00065-9

Colón, W., Aguilera, J. J., and Srinivasan, S. (2015). "Intrinsic Stability, Oligomerization, and Amyloidogenicity of HDL-Free Serum Amyloid A," in *Lipids in Protein Misfolding*, ed. O. Gursky (New York, NY: Springer International Publishing).

Couderc, E., Morel, F., Levillain, P., Buffière-Morgado, A., Camus, M., Paquier, C., et al. (2017). Interleukin-17A-induced production of acute serum amyloid A by keratinocytes contributes to psoriasis pathogenesis. *PLoS One* 12:e0181486. doi: 10.1371/journal.pone.0181486

de Seny, D., Cobraiville, G., Charlier, E., Neuville, S., Esser, N., Malaise, D., et al. (2013). Acute-phase serum amyloid A in osteoarthritis: regulatory mechanism and proinflammatory properties. *PloS One* 8:e66769. doi: 10.1371/journal.pone.0066769

Devine, M. J., Plun-Favreau, H., and Wood, N. W. (2011). Parkinson's disease and cancer: two wars, one front. *Nat. Rev. Cancer* 24, 812–823. doi: 10.1038/nrc3150

Findeisen, P., Zapatka, M., Peccerella, T., Matzk, H., Neumaier, M., Schadendorf, D., et al. (2009). Serum amyloid A as a prognostic marker in melanoma identified by proteomic profiling. *J. Clin. Oncol.* 27, 2199–2208. doi: 10.1200/JCO.2008.18.0554

Furlaneto, C. J., and Campa, A. (2000). A novel function of serum amyloid A: a potent stimulus for the release of tumor necrosis factor-α, interleukin-1β, and interleukin-8 by human blood neutrophil. *Biochem. Biophys. Res. Commun.* 268, 405–408. doi: 10.1006/bbrc.2000.2143

Gelpi, E., Navarro-Otano, J., Tolosa, E., Gaig, C., Compta, Y., Rey, M. J., et al. (2014). Multiple organ involvement by alpha-synuclein pathology in lewy body disorders: peripheral alpha-synuclein in pd. *Mov. Disord.* 29, 1010–1018. doi: 10.1002/mds.25776

Gibb, W. R., and Lees, A. J. (1988). The relevance of the Lewy body to the pathogenesis of idiopathic parkinson's disease. *J. Neurol. Neurosurg. Psychiatry* 51, 745–752. doi: 10.1136/jnnp.51.6.745

Goetz, C. G., Tilley, B. C., Shaftman, S. R., Stebbins, G. T., Fahn, S., Martinez-Martin, P., et al. (2008). Movement disorder society-sponsored revision of the unified parkinson's disease rating scale (MDS-UPDRS): scale presentation and clinimetric testing results. *Mov. Disord.* 15, 2129–2170. doi: 10.1002/mds.22340

Gregory, R., and Miller, S. (2015). Parkinson's disease and the skin. *Pract. Neurol.* 15, 246–249. doi: 10.1136/practneurol-2015-001107

Grünblatt, E., Zehetmayer, S., Jacob, C. P., Müller, T., Jost, W. H., and Riederer, P. (2010). Pilot study: peripheral biomarkers for diagnosing sporadic Parkinson's disease. *J. Neural. Transm.* 117, 1387–1393. doi: 10.1007/s00702-010-0509-1

Guo, J.-T., Yu, J., Grass, D., de Beer, F. C., and Kindy, M. S. (2002). Inflammation-dependent cerebral deposition of serum amyloid A protein in a mouse model of amyloidosis. *J. Neurosci.* 15, 5900–5909. doi: 10.1523/JNEUROSCI.22-14-05900.2002

Hoehn, M. M., and Yahr, M. D. (1967). Parkinsonism: onset, progression and mortality. *Neurology* 17, 427–442. doi: 10.1212/WNL.17.5.427

James, W. D., Berger, T., and Elston, D. (2011). *Andrew's Diseases of the Skin: Clinical Dermatology*. London: Elsevier Health Sciences.

Kindy, M. S., Yu, J., Guo, J.-T., and Zhu, H. (1999). Apolipoprotein serum amyloid A in alzheimer's disease. *J. Alzheimers Dis. JAD* 1, 155–167. doi: 10.3233/JAD-1999-1303

Kirik, D., and Björklund, A. (2003). Modeling CNS neurodegeneration by overexpression of disease-causing proteins using viral vectors. *Trends Neurosci.* 26, 386–392. doi: 10.1016/S0166-2236(03)00164-4

Lees, A. J., Hardy, J., and Revesz, T. (2009). Parkinson's disease. *Lancet* 373, 2055–2066. doi: 10.1016/S0140-6736(09)60492-X

Liang, J. S., Sloane, J. A., Wells, J. M., Abraham, C. R., Fine, R. E., and Sipe, J. D. (1997). Evidence for local production of acute phase response apolipoprotein serum amyloid A in Alzheimer's disease brain. *Neurosci. Lett.* 4, 73–76. doi: 10.1016/S0304-3940(97)00196-1

Liu, J., Wang, D., Li, S.-Q., Yu, Y., and Ye, R. D. (2016). Suppression of LPS-induced tau hyperphosphorylation by serum amyloid A. *J. Neuroinflamm.* 13:28. doi: 10.1186/s12974-016-0493-y

Liu, R., Gao, X., Lu, Y., and Chen, H. (2011). Meta-analysis of the relationship between parkinson disease and melanoma. *Neurology* 7, 2002–2009. doi: 10.1212/WNL.0b013e31821e554e

Patel, H., Fellowes, R., Coade, S., and Woo, P. (1998). Human serum amyloid A has cytokine-like properties. *Scand. J. Immunol.* 48, 410–418. doi: 10.1046/j.1365-3083.1998.00394.x

Planken, A., Kurvits, L., Reimann, E., Kadastik-Eerme, L., Kingo, K., Kõks, S., et al. (2017). Looking beyond the brain to improve the pathogenic understanding of Parkinson's disease: implications of whole transcriptome profiling of patients' skin. *BMC Neurol.* 17:6. doi: 10.1186/s12883-016-0784-z

Poewe, W., Seppi, K., Tanner, C. M., Halliday, G. M., Brundin, P., Volkmann, J., et al. (2017). Parkinson disease. *Nat. Rev. Dis. Primer.* 23:17013. doi: 10.1038/nrdp.2017.13

Scherzer, C. R., Eklund, A. C., Morse, L. J., Liao, Z., Locascio, J. J., Fefer, D., et al. (2007). Molecular markers of early parkinson's disease based on gene expression in blood. *Proc. Natl. Acad. Sci.* 16, 955–960. doi: 10.1073/pnas.0610204104

Takalo, M., Salminen, A., Soininen, H., Hiltunen, M., and Haapasalo, A. (2013). Protein aggregation and degradation mechanisms in neurodegenerative diseases. *Am. J. Neurodegener. Dis.* 2, 1–14.

Teves, J. M. Y., Bhargava, V., Kirwan, K. R., Corenblum, M. J., Justiniano, R., Wondrak, G. T., et al. (2018). Parkinson's disease skin fibroblasts display signature alterations in growth, redox homeostasis, mitochondrial function, and autophagy. *Front. Neurosci.* 11:737. doi: 10.3389/fnins.2017.00737

Upragarin, N., Landman, W. J. M., Gaastra, W., and Gruys, E. (2005). Extrahepatic production of acute phase serum amyloid A. *Histol. Histopathol.* 20, 1295–1307. doi: 10.14670/HH-20.1295

Urieli-Shoval, S., Cohen, P., Eisenberg, S., and Matzner, Y. (1998). Widespread expression of serum amyloid A in histologically normal human tissues. predominant localization to the epithelium. *J. Histochem. Cytochem.* 46, 1377–1384. doi: 10.1177/002215549804601206

Urieli-Shoval, S., Linke, R. P., and Matzner, Y. (2000). Expression and function of serum amyloid A, a major acute-phase protein, in normal and disease states. *Curr. Opin. Hematol.* 7, 64–69. doi: 10.1097/00062752-200001000-00012

Uversky, V. N. (2009). Intrinsic disorder in proteins associated with neurodegenerative diseases. *Front. Biosci.* 14:5188-5238. doi: 10.1007/978-1-4020-9434-7-2

Uversky, V. N. (2015). Intrinsically disordered proteins and their (disordered) proteomes in neurodegenerative disorders. *Front. Aging Neurosci.* 7:18. doi: 10.3389/fnagi.2015.00018

Vallon, R., Freuler, F., Desta-Tsedu, N., Robeva, A., Dawson, J., Wenner, P., et al. (2001). Serum amyloid A (apoSAA) expression is up-regulated in rheumatoid arthritis and induces transcription of matrix metalloproteinases. *J. Immunol.* 166, 2801–2807. doi: 10.4049/jimmunol.166.4.2801

Wang, N., Gibbons, C. H., Lafo, J., and Freeman, R. (2013). α-Synuclein in cutaneous autonomic nerves. *Neurology* 29, 1604–1610. doi: 10.1212/WNL.0b013e3182a9f449

Ye, Z., Bayron Poueymiroy, D., Aguilera, J. J., Srinivasan, S., Wang, Y., Serpell, L. C., et al. (2011). Inflammation protein SAA2.2 spontaneously forms marginally stable amyloid fibrils at physiological temperature. *Biochemistry* 50, 9184–9191. doi: 10.1021/bi200856v

Zhang, T., Faraggi, E., Li, Z., and Zhou, Y. (2013). Intrinsically semi-disordered state and its role in induced folding and protein aggregation. *Cell Biochem. Biophys.* 67, 1193–1205. doi: 10.1007/s12013-013-9638-0

Conflict of Interest Statement: The authors declare that the research was conducted in the absence of any commercial or financial relationships that could be construed as a potential conflict of interest.

frontiers in Aging Neuroscience

ORIGINAL RESEARCH
published: 26 February 2019
doi: 10.3389/fnagi.2019.00040

Effectiveness of Integrative Therapy for Parkinson's Disease Management

Yeonju Woo[1] *and Min Kyung Hyun*[2]*

[1] Department of Preventive Medicine, College of Korean Medicine, Dongguk University Graduate School, Seoul, South Korea, [2] Department of Preventive Medicine, College of Korean Medicine, Dongguk University, Gyeongju, South Korea

Objectives: To investigate the effectiveness of integrative therapy on prevalence and length of hospitalization and management of major complications of Parkinson's disease (PD) in the South Korea.

Methods: This study was a retrospective cohort analysis conducted using the National Health Insurance Service-National Sample Cohort in the South Korea. Patients over 65 years old who were newly diagnosed with PD during 2007–2011 were identified. The integrative therapy group was defined as patients treated with both Korean medicine (KM) and biomedicine, and the monotherapy group consisted of patients treated with biomedicine alone. From PD diagnosis to 2013, the prevalence and annual length of hospitalization because of PD and major complications (dementia, depression and pneumonia/sepsis) were analyzed using logistic regression, ANOVA and *t*-tests after propensity score (PS) matching with a 1:1 ratio.

Results: After PS estimation and matching, the cohort used in the analysis included 228 subjects (114 integrative therapy group, 114 monotherapy group). Sex, age, index year, comorbidity, severity of disability, neurologic care, and anti-parkinsonism medication (levodopa, ropinirole, pramipexole, selegiline) were adjusted in both groups. The prevalence of hospitalization due to pneumonia/sepsis was 0.50 times (95% C.I.: 0.26–0.96) lower in the integrative therapy group than the monotherapy group, which was statistically significant (p = 0.038). The prevalence and annual length of total hospitalization and hospitalization because of PD, dementia, and depression in the integrative therapy group showed positive results compared to the monotherapy group, but these differences were not statistically significant.

Conclusion: It has not been clearly identified that integrative therapy with KM and biomedicine for PD management is better treatment for patients compared to biomedicine monotherapy; however, we found a clue of better result in integrated therapy. Therefore, further investigation by increasing the number of subjects is needed to confirm the findings presented herein.

Keywords: Parkinson's disease, integrative medicine, medicine, Korean traditional, complications, patient care

OPEN ACCESS

Edited by:
Hi-Joon Park,
Kyung Hee University, South Korea

Reviewed by:
Julien Rossignol,
Central Michigan University, United States
Joao Batista Teixeira da Rocha,
Universidade Federal de Santa Maria, Brazil

***Correspondence:**
Min Kyung Hyun
mk3three@dongguk.ac.kr;
mk3three@gmail.com

Received: *15 June 2018*
Accepted: *11 February 2019*
Published: *26 February 2019*

Citation:
Woo Y and Hyun MK (2019) Effectiveness of Integrative Therapy for Parkinson's Disease Management. Front. Aging Neurosci. 11:40. doi: 10.3389/fnagi.2019.00040

Abbreviations: CCI, Charlson Comorbidity Index; KM, Korean medicine; NHIS-NSC, National Health Insurance Service-National Sample Cohort; PD, Parkinson's disease; PDQ-39, Parkinson's Disease Questionnaire; SCOPA, Scales for Outcomes in Parkinson's Disease; UPDRS, Unified Parkinson's Disease Rating Scale.

INTRODUCTION

Parkinson's disease, which is the second most frequent neurodegenerative disease after Alzheimer's disease, is caused by an imbalance between the inhibitory action of dopamine and the excitatory action of acetylcholine because of decreases in dopamine (Rizek et al., 2016; Delamarre and Meissner, 2017). The incidence and prevalence of PD increases with age, especially after one reaches their 60s.

Parkinson's disease patients have motor symptoms including bradykinesia, rigidity, resting tremor, and postural instability; however, non-motor symptoms may also be prominent, including cognitive impairment, depression, and autonomic disturbances (Rogers et al., 2017). Generally, PD is caused by an interaction between genetic and environmental factors (Delamarre and Meissner, 2017). Pesticides, history of melanoma, and traumatic brain injury have also been reported as increased risk factors of PD, but the promotion of physical activity is known to prevent PD (Ascherio and Schwarzschild, 2016).

Levodopa is the gold-standard for treatment of motor symptoms of PD (Rizek et al., 2016). However, PD is progressive and worsens with time, and there is currently no cure; accordingly, it is necessary to treat and care for PD-related symptoms of patients (Elbaz et al., 2016). Therefore, about 40% of PD patients use alternative therapies including acupuncture, tai chi, and herbal medicine to complement their standard treatments (Ghaffari and Kluger, 2014). Indeed, previous studies have shown that herbal formulas, acupuncture and tai chi might be safe and beneficial to PD patients (Bega and Zadikoff, 2014; Cwiekala-Lewis et al., 2017; Lee and Lim, 2017; Noh et al., 2017; Shan et al., 2018). In addition, there have been studies to find out the benefit of using biomedicine and KM concurrently in PD patients (Leem, 2016; Yang et al., 2016; Jang et al., 2018; Lee et al., 2018).

In the present study, the effectiveness of integrative therapy consisting of both biomedicine and KM on the management of PD patients was investigated.

MATERIALS AND METHODS

Data Source

All citizens of the South Korea receive health insurance, and medical treatment and prescription data of all healthcare institutions and pharmacies has been loaded into a national database maintained and managed by the NHIS. The NHIS built the NHIS-NSC database, which consists of representative anonymized data extracted from national health insurance records pertaining to about 1,000,000 members of the total population in 2002 who were followed until 2013. The personal privacy of each participant was protected by de-identification of the data (Lee et al., 2017). The NHIS-NSC 2nd version (2002–2015) of the NHIS-NSC was generated in 2017, but the data masked 2,980 diagnoses, including those of cancer and infective diseases. Therefore, the 2nd version could not be used in this study.

Study Design

This was a retrospective cohort study. The eligibility period was set from January 2002 (the start date of the NHIS-NSC) to December 2006, while the cohort index was set from January 2007 to December 2011 and the follow-up period was set from January 2007 to December 2013 (the end of the NHIS-NSC data), or the expired date of the patients (**Figure 1**).

Subjects

From 2007 to 2011, a cohort of patients aged 65 years or older who were diagnosed with PD by the NHIS-NSC was established. The diagnosis was defined by the G20 code based on the Korean Standard Classification of Diseases (KCD), which is the same as the 10th revision of the International Classification of Diseases (ICD-10). Patients who were diagnosed with PD during the eligibility period were excluded; therefore, only those newly diagnosed with PD from 2007 to 2011 were included (**Figure 1**). Patients were divided into two groups by treatment type, an integrative therapy group that received both biomedicine and KM, and a monotherapy group that was only treated with biomedicine. When treatment history for PD was recorded at least twice in each form, the patient was considered to have received the treatment. However, patients who received the treatment only once were excluded (**Figure 2**).

Outcome Variables

Generally, the outcome of PD recovery or management is based on the UPDRS, SCOPA, or the PDQ-39 (Peto et al., 1995; Marinus et al., 2004; Goetz et al., 2008). However, the NHIS-NSC does not have survey or examination data such as health insurance claims data. Thus, this study used alternative outcomes to demonstrate that PD and its complications had been well-controlled through alternative outcomes. The outcome was defined as the prevalence of hospitalization and annual length of hospitalization after PD diagnosis. Hospitalization was classified as total hospitalization, hospitalization because of PD and hospitalization due to major complications of PD. In this study, dementia, depression, and pneumonia/sepsis were considered major complications. KCD F00–F09, G30–G32 for dementia, F30–F39 and U22 for depression, and A40–A41, J12–J18, J69 and J80–J84 for pneumonia/sepsis were applied.

Statistical Analysis

Confounders were controlled for comparison between the integrative therapy group and the monotherapy group. In this study, the CCI was calculated using the KCD code of the NHIS-NSC and had a possible score of 0 to 12 points. The CCI gives weight to several comorbidity factors that affect death, and has been mapped to ICD codes through clinical review (Quan et al., 2005). In addition, the severity of disability of the patients included in the NHIS-NSC was considered as a confounder. To adjust for biomedicine treatment in both treatment groups, the treatment period in neurology, hospitalization period in neurology and anti-parkinsonism medications (levodopa, ropinirole, pramipexole, selegiline) were also considered as confounders (Zhuo et al., 2017).

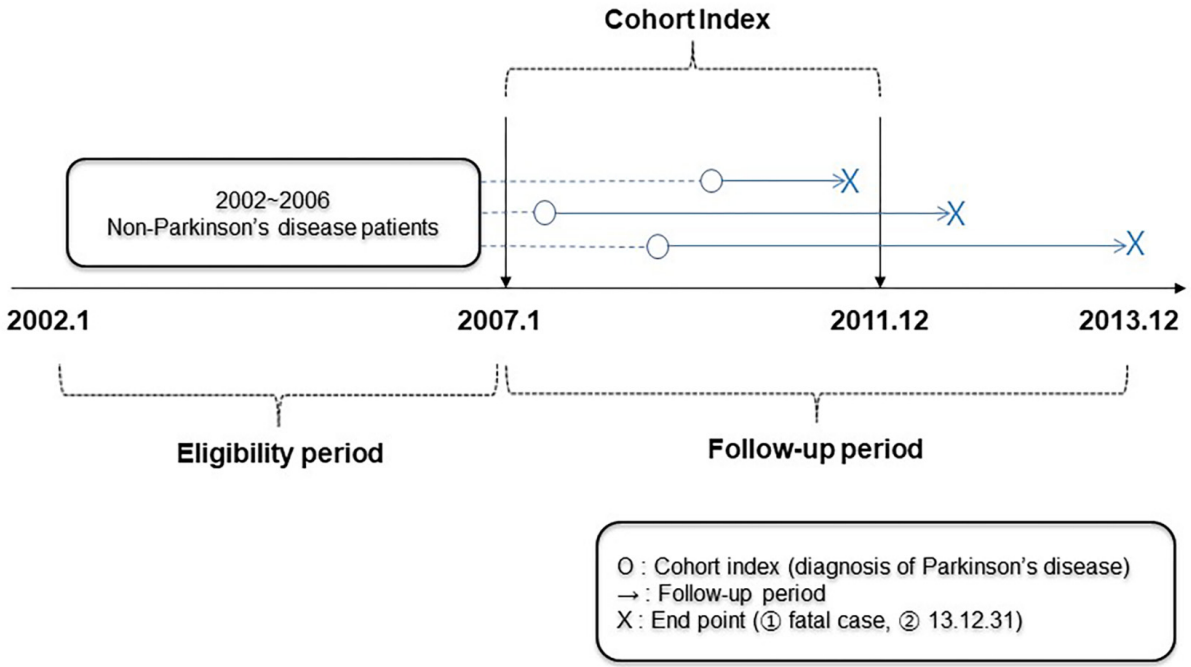

FIGURE 1 | Study design.

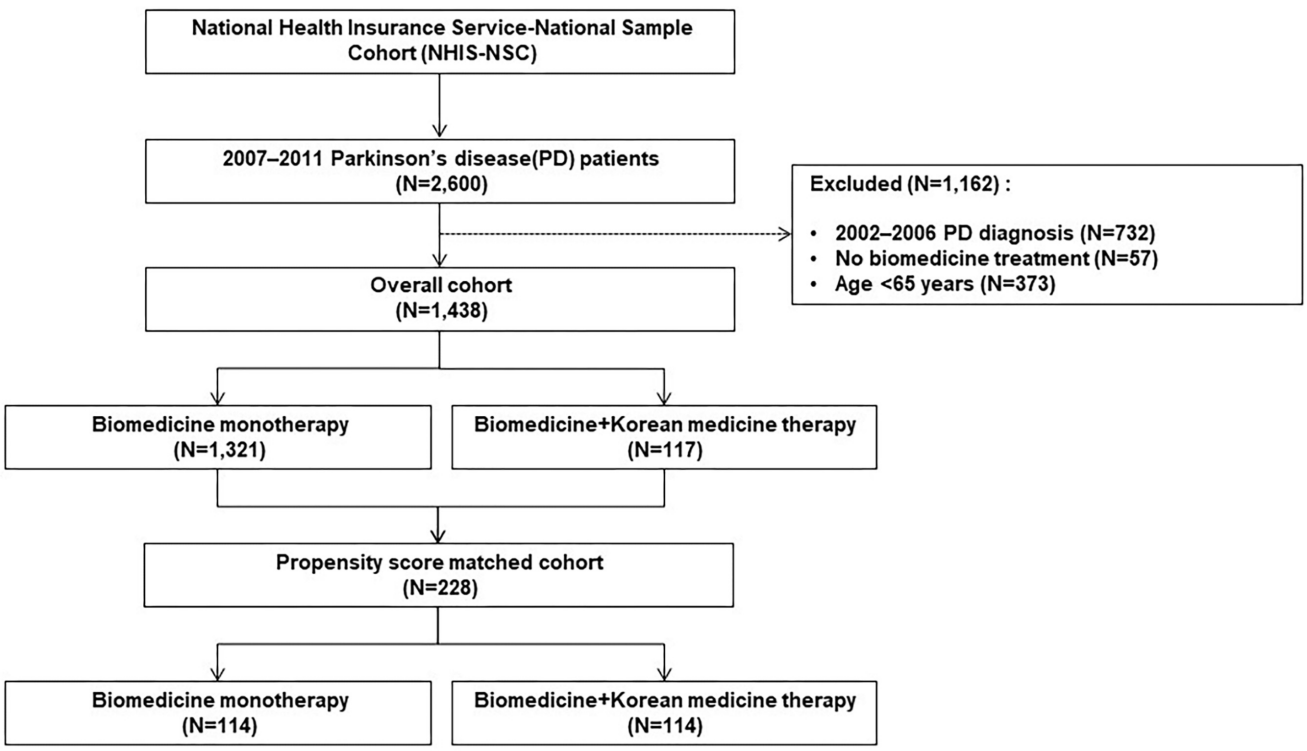

FIGURE 2 | Selection of subjects.

The propensity score (PS) was used to increase the level of causality revealed in the observational study (D'Agostino, 1998). Specifically, the PS was used to match the subjects with similar characteristics in the two groups. Several variables were used to create the PS index: age, sex, index year, CCI, treatment period in neurology, hospitalization period in neurology, severity of disability and anti-parkinsonism medication. Comparison of the PS between groups was repeated using the greedy algorithm and 1: 1 matching continued until there were no more matching pairs (Parsons, 2001). The PS fit was confirmed by c-statistics and the Hosmer and Lemeshow Goodness-of-Fit test. In the case of a c-statistic value over 0.5, the Hosmer

TABLE 1 | Comparison of characteristics between integrative therapy group and monotherapy group.

	Before PS matching			After PS matching		
	Integrative therapy group (*N* = 117)	**Monotherapy group (*N* = 1,321)**	***p*-Value**	**Integrative therapy group (*N* = 114)**	**Monotherapy Group (*N* = 114)**	***p*-Value**
Sex			0.512			0.487
Male	38 (32.5%)	469 (35.5%)		37 (32.5%)	42 (36.8%)	
Female	79 (67.5%)	852 (64.5%)		77 (67.5%)	72 (63.2%)	
Age			< 0.001*			0.686
65–69	37 (31.6%)	241 (18.2%)		34 (29.8%)	28 (24.6%)	
70–74	30 (25.6%)	374 (28.3%)		30 (26.3%)	27 (23.7%)	
75–79	35 (29.9%)	346 (26.2%)		35 (30.7%)	41 (36.0%)	
=80	15 (12.8%)	360 (27.3%)		15 (13.2%)	18 (15.8%)	
Index year			0.016*			0.491
2007	7 (6.0%)	225 (17.0%)		7 (6.1%)	5 (4.4%)	
2008	23 (19.7%)	279 (21.1%)		23 (20.2%)	23 (20.2%)	
2009	25 (21.4%)	278 (21.0%)		25 (21.9%)	16 (14.0%)	
2010	26 (22.2%)	236 (17.9%)		24 (21.1%)	26 (22.8%)	
2011	36 (30.8%)	393 (22.9%)		35 (30.7%)	44 (38.6%)	
Charlson Comorbidity Index			0.308			0.489
0	0 (0.0%)	5 (0.4%)		0 (0.0%)	0 (0.0%)	
1	17 (14.5%)	290 (22.0%)		17 (14.9%)	21 (18.4%)	
3	88 (75.2%)	900 (68.1%)		86 (75.4%)	87 (76.3%)	
4	2 (1.7%)	8 (0.6%)		1 (0.9%)	0 (0.0%)	
6	10 (8.6%)	117 (8.9%)		10 (8.8%)	6 (5.3%)	
9	0 (0.0%)	1 (0.1%)		0 (0.0%)	0 (0.0%)	
Treatment period in neurology (days)			< 0.001*			0.992
≤29	19 (16.2%)	664 (50.3%)		19 (16.7%)	18 (15.8%)	
30–179	29 (24.8%)	328 (24.8%)		29 (25.4%)	30 (26.3%)	
180–364	12 (10.3%)	82 (6.2%)		12 (10.5%)	11 (9.7%)	
≥365	57 (48.7%)	247 (18.7%)		54 (47.4%)	55 (48.3%)	
Hospitalization period in neurology (days)			< 0.001*			0.966
≤13	15 (12.8%)	616 (46.6%)		15 (13.2%)	15 (13.2%)	
14–29	26 (22.2%)	267 (20.2%)		25 (21.9%)	22 (19.3%)	
30–59	17 (14.5%)	208 (15.8%)		17 (14.9%)	17 (14.9%)	
>60	59 (50.4%)	230 (17.4%)		57 (50.0%)	60 (52.6%)	
Severity of disability			0.477			0.729
Normal	89 (76.1%)	1,005 (76.1%)		86 (75.4%)	91 (79.8%)	
Mild	22 (18.8%)	213 (16.1%)		22 (19.3%)	18 (15.8%)	
Severe	6 (5.1%)	103 (7.8%)		6 (5.3%)	5 (4.4%)	
Anti-parkinsonism medication						
Levodopa	68 (58.1%)	326 (24.7%)	< 0.001*	65 (57.0%)	58 (50.9%)	0.352
Ropinirole	34 (29.1%)	126 (9.5%)	< 0.001*	32 (28.1%)	27 (23.7%)	0.450
Pramipexole	18 (15.4%)	74 (5.6%)	< 0.001*	16 (14.0%)	15 (13.2%)	0.847
Selegiline	5 (4.3%)	26 (2.0%)	0.100	5 (4.4%)	3 (2.6%)	0.472

PS, propensity score; monotherapy group, treated by biomedicine only; integrative therapy group, treated by biomedicine and KM.
**Statistically significant ($p < 0.05$).*

and Lemeshow Goodness-of-Fit test was considered to be good when the *p*-value was 0.05 or higher (D'Agostino, 1998; Maldonado and Greenland, 2002).

The prevalence and annual length of hospitalization were analyzed using logistic regression analysis and *t*-tests. A *p*-value < 0.05 was considered significant. Additionally, the integrative therapy group was divided into two groups by treatment period, less than 30 days and over 30 days. The prevalence and annual length of hospitalization were analyzed using logistic regression analysis and ANOVA. After ANOVA, Duncan's *post hoc* test was applied. A *p*-value < 0.05 was considered significant. Finally, survival analysis of the integrative therapy group and monotherapy group was performed using the Cox proportional hazard analysis.

All statistical analyses were performed using SAS 9.4.

RESULTS

Characteristics of Patients

Except for patients diagnosed with PD prior to 2007, patients treated without biomedicine treatment and those younger than 65 years, a total of 1,438 patients were included in the cohort. Of these, 117 were treated using both biomedicine and Korean medicine, while 1,321 received biomedicine alone. After PS estimation and matching, the cohort used in the analysis included 228 subjects (114 in the integrative therapy group and 114 in the monotherapy group) (**Figure 2**). The PS matching was considered to be well-fitted based on a c-statistics value of 0.810 and a *p*-value of the Goodness-of-Fit Test of 0.141.

The patients' characteristics based on confounders in the two groups before and after PS matching were compared. After PS matching, the characteristics of both groups were statistically similar (**Table 1**).

Types of KM Used in the Integrative Group

Among 114 patients in the integrative group, 112 patients (98.2%) received acupuncture therapy at least two times, 49 (43.0%) received moxibustion therapy, 31 (27.2%) received cupping therapy, 15 (13.2%) received herbal medication, and 83 (72.8%) received other physical therapy or psychotherapy. The results of dividing the number of days on which KM was applied by 30 days are presented in **Figure 3**.

Comparison of Prevalence of Hospitalization

Comparison of the prevalence of hospitalization between the two groups was performed by logistic regression analysis, after which the odds ratio was calculated. The prevalence of hospitalization because of pneumonia/sepsis was 0.50 (95% C.I.: 0.26–0.96) times lower in the integrative therapy group than the monotherapy group ($p = 0.038$). The prevalence of total hospitalization, as well as hospitalization because of PD, dementia, and depression in the integrative therapy group was positive compared to the monotherapy group, but this difference was not significant.

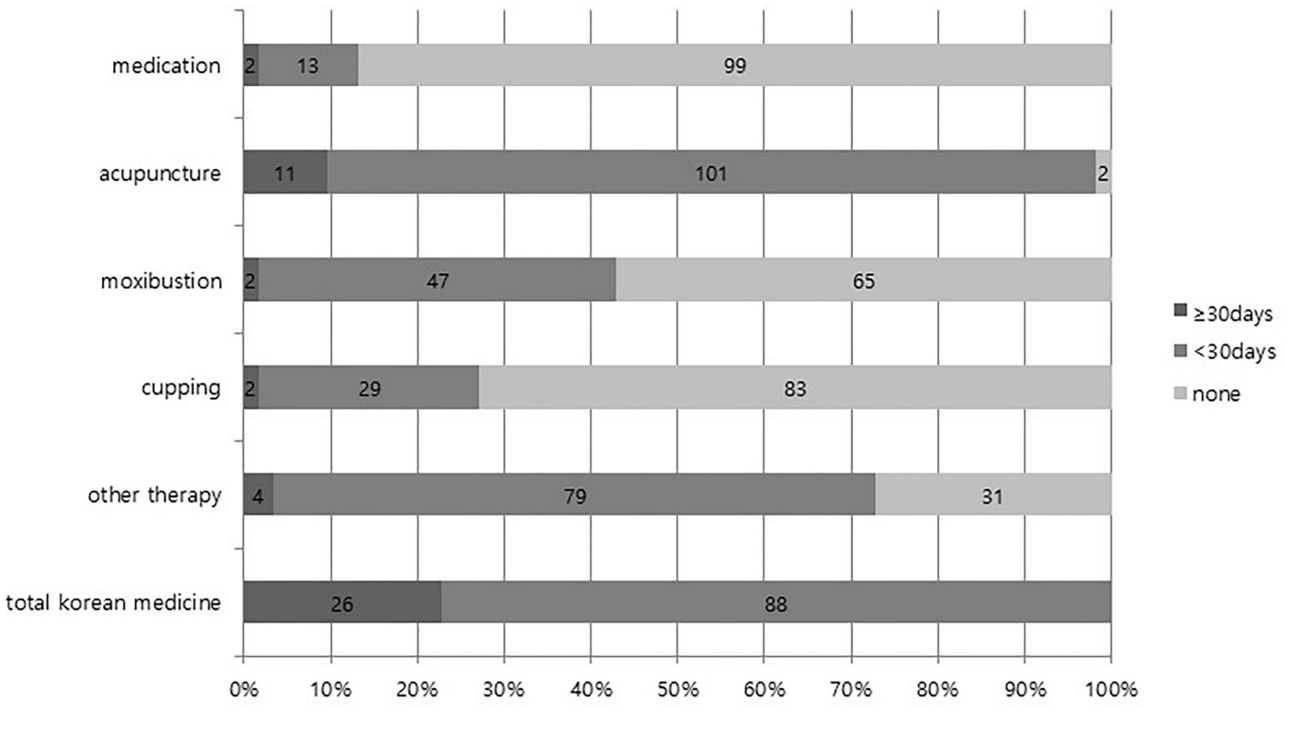

FIGURE 3 | Status of KM therapy in integrative therapy group.

Additionally, the prevalence of total hospitalization, hospitalization because of PD, dementia, depression, and pneumonia/sepsis showed positive results in the order of integrative group II (KM 30 days or more), integrative group I (KM less than 30 days), monotherapy group, but this difference was not significant (**Table 2**).

Comparison of Annual Length of Hospitalization

Comparison of the annual length of hospitalization between groups using a *t*-test revealed that total annual length of hospitalization, annual length of hospitalization due to PD, annual length of hospitalization due to dementia, annual length of hospitalization due to depression and annual length of hospitalization due to pneumonia/sepsis were shorter in the integrative therapy group than the monotherapy group; however, these differences were not statistically significant. The integrative therapy group was divided into two groups (over 30 days, less than 30 days) by treatment duration, and ANOVA was conducted to compare each of these with the monotherapy group. The prevalence of total hospitalization, as well as hospitalization because of PD, dementia, depression and pneumonia/sepsis showed positive results in the order of integrative group II (KM 30 days or more), integrative group I (KM less than 30 days), and monotherapy group, but these differences were not significant (**Figure 4**).

The cox proportional hazard model was used to compare the mortality between groups. The mortality of the integrative therapy group was found to be 4.51 patients per 1,000 person-years, while that of the monotherapy group was 9.21 patients per 1,000 person-years and the hazard ratio (HR) was 0.50. However, these differences were not significant.

DISCUSSION

The most typical medication for PD is levodopa; however, its long-term use results in decreased efficacy, motor fluctuation, and dyskinesia in about 75% of patients (Fahn et al., 2004).

TABLE 2 | Comparison of prevalence of hospitalization between integrative therapy group and monotherapy group (unit: no. of subjects).

	No. of subjects (%)	OR (95% C.I.)	*p*-Value
Total hospitalization			
Monotherapy group (*N* = 114)	103 (90.4%)	1	
Integrative therapy group (*N* = 114)	99 (86.8%)	0.71 (0.31–1.61)	0.406
Monotherapy group (*N* = 114)	103 (90.4%)	1	
Integrative therapy group I (*N* = 88)	77 (87.5%)	0.75 (0.31–1.81)	0.520
Integrative therapy group II (*N* = 26)	22 (84.6%)	0.59 (0.17–2.02)	0.398
Hospitalization d/t PD			
Monotherapy group (*N* = 114)	79 (69.3%)	1	
Integrative therapy group (*N* = 114)	74 (64.9%)	0.82 (0.47–1.43)	0.481
Monotherapy group (*N* = 114)	79 (69.3%)	1	
Integrative therapy group I (*N* = 88)	61 (69.3%)	1.00 (0.55–1.83)	0.998
Integrative therapy group II (*N* (=26)	13 (50.0%)	0.44 (0.19–1.05)	0.065
Hospitalization d/t dementia			
Monotherapy group (*N* = 114)	19 (16.7%)	1	
Integrative therapy group (*N* = 114)	10 (8.8%)	0.48 (0.21–1.09)	0.078
Monotherapy group (*N* = 114)	19 (16.7%)	1	
Integrative therapy group I (*N* = 88)	9 (10.2%)	0.57 (0.24–1.33)	0.193
Integrative therapy group II (*N* = 26)	1 (3.8%)	0.20 (0.03–1.57)	0.125
Hospitalization d/t depression			
Monotherapy group (*N* = 114)	5 (4.4%)	1	
Integrative therapy group (*N* = 114)	1 (0.9%)	0.19 (0.02–1.68)	0.136
Monotherapy group (*N* = 114)	5 (4.4%)	1	
Integrative therapy group I (*N* = 88)	1 (1.1%)	0.25 (0.03–2.19)	0.242
Integrative therapy group II (*N* = 26)	0 (0%)	-	–
Hospitalization d/t pneumonia/sepsis			
Monotherapy group (*N* = 114)	31 (27.2%)	1	
Integrative therapy group (*N* = 114)	18 (15.8%)	0.50 (0.26–0.96)	0.038*
Monotherapy group (*N* = 114)	31 (27.2%)	1	
Integrative therapy group I (*N* = 88)	15 (17.0%)	0.55 (0.28–1.10)	0.091
Integrative therapy group II (*N* = 26)	3 (11.5%)	0.35 (0.10–1.25)	0.105

OR, odds ratio; C.I., confidence interval; monotherapy group, treated by biomedicine only; integrative therapy group, treated by biomedicine and KM; integrative therapy group I, KM treatment less than 30 days; integrative therapy group II, KM treatment over than 30 days; d/t, due to; PD, Parkinson's disease.
**Statistically significant ($p < 0.05$).*

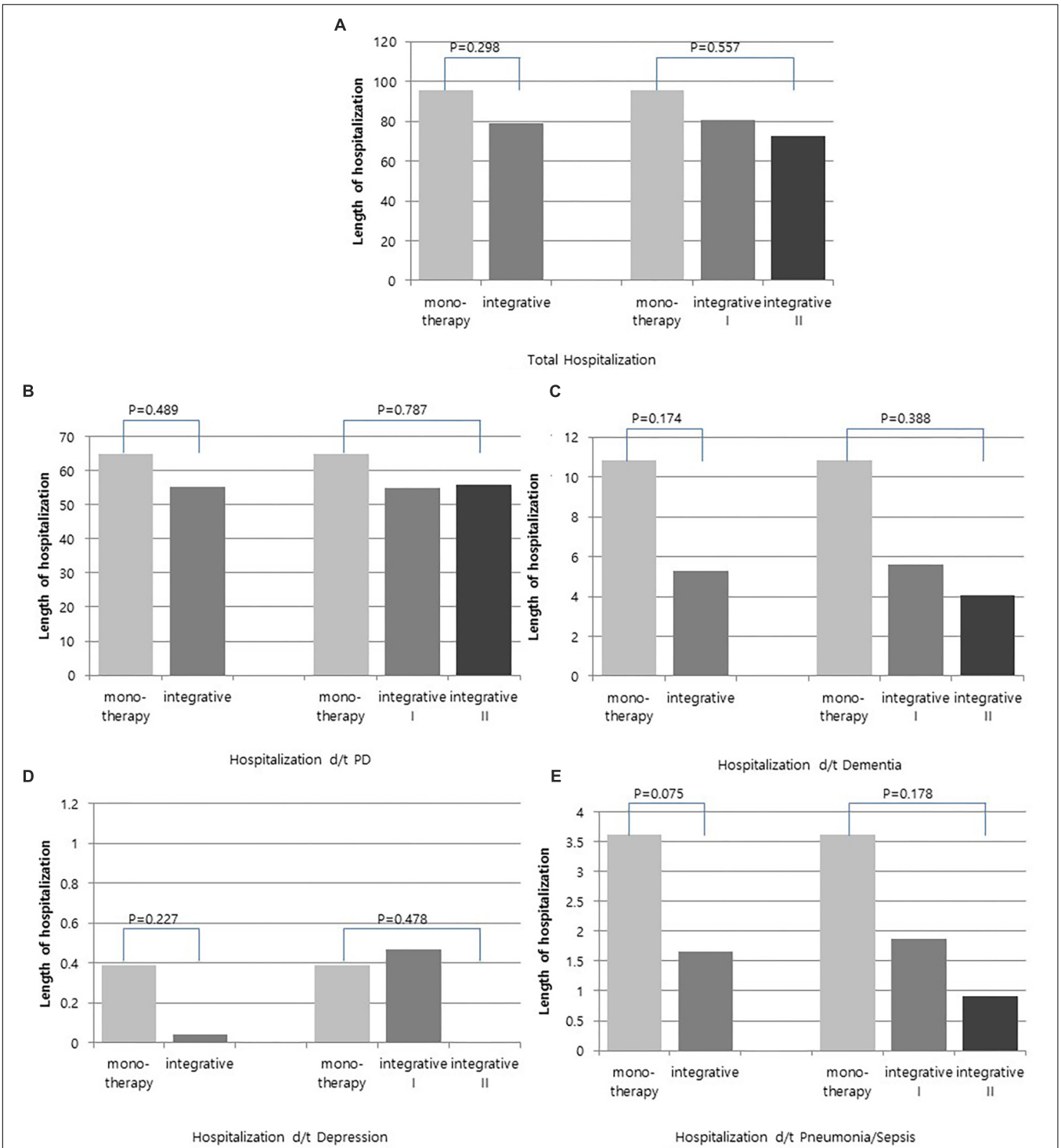

FIGURE 4 | Comparison of annual length of hospitalization between integrative therapy group and monotherapy group. **(A)** Total hospitalization, **(B)** Hospitalization d/t PD, **(C)** Hospitalization d/t dementia, **(D)** Hospitalization d/t depression, and **(E)** Hospitalization d/t pneumonia/sepsis.

The prevalence of melanoma in PD patients taking levodopa is significantly higher than that of the general population (Shalaby and Louis, 2016). Dementia in PD patients is a common complication of PD that makes treatment difficult and leads to disability. Depression is also a common complication of PD (Brown and Marsden, 1984; Cummings, 1992), and infectious diseases such as pneumonia are considered factors that increase mortality in PD patients (Pinter et al., 2015). Additionally,

patients with a longer duration of PD have more complications and lower quality of life (Ou et al., 2018). Subthalamic stimulation has been attempted to improve quality of life with positive results. However, surgery can be accompanied by unintended adverse events, even death (Dafsari et al., 2018). Therefore, the use of relatively safe treatment regimens such as CAM should be considered.

This study investigated whether KM could reduce hospitalization in the management of PD patients in the South Korea. Two groups of patients, an integrative therapy group using both biomedicine and KM and a monotherapy group using only biomedicine, were compared by PS estimation and matching based on confounders such as sex, age, comorbidity, and anti-parkinsonism medication. The prevalence of hospitalization because of pneumonia/sepsis was significantly lower (0.50 times) in the integrative therapy group than the monotherapy group. Traditional medicine may have beneficial immunomodulatory effects for preventing viral infections (Poon et al., 2006). For severe acute respiratory syndrome (SARS), advantages to treatment with integrative Chinese medicine and biomedicine were observed when compared with that of biomedicine alone, especially with respect to improvement of clinical symptoms, promotion of the recovery of immune function and reduction of treatment duration (Qiang et al., 2003). Hence, KM seems to have a positive effect on infectious diseases such as pneumonia and sepsis.

Other outcomes of the integrative therapy group also showed better results than the monotherapy group, but these differences were not significant. Although there were no significant differences in the outcomes observed in this study, the prevalence and duration of hospitalization tended to be lower in patients who received KM. Specifically, a KM treatment period of 30 days or more showed better results than that of less than 30 days.

Studies have shown that acupuncture is effective at the treatment of PD (Lee and Lim, 2017). For example, PD patients with acupuncture showed significant improvement in motor function compared to those without acupuncture. Moreover, brain imaging revealed that putamen and the primary motor cortex were activated in patients with acupuncture (Chae et al., 2009). Korean herbal formulas such as Chungsimyeolda-tang or Yeoldahanso-tang induce autophagy and prevent diseases associated with misfolded/aggregated proteins in various neurodegenerative disorders, including PD (Bae et al., 2011, 2015). In China, 48.6% of patients underwent CAM treatment and herbal medication, primarily rehabilitation exercise and acupuncture. These treatments were effective in half of the patients who received them, while they produced negative results in 11% of the patients (Pan et al., 2018). Additionally, the incidence and prevalence of PD in Asian countries, including South Korea, have been shown to be lower than in Europe and America (Pringsheim et al., 2014). This difference may result from genetic and ethnic differences, but the possibility of the effects of CAM, including KM, cannot be ruled out.

It should be noted that this paper had several limitations. First, the number of subjects was not sufficient because of data limitations; therefore, we cannot be sure of whether the non-significance of results is due to the absence of a relationship between the groups or to a lack of statistical power. Accordingly, comparative studies with increased duration and number of patients are required to clarify the effects KM on PD. Second, we assessed whether PD and its complications have been well-controlled by alternative outcomes-related measures such as the prevalence of hospitalization and annual length of hospitalization after PD diagnosis. Generally, the outcome of PD recovery or management is evaluated based on the UPDRS, SCOPA, or the PDQ-39. However, the NHIS-NSC does not contain this information because it consists of only health insurance claim data. Third, the number of KM monotherapy patients was very small. In the Korean health insurance system, PD is a serious rare disease that is registered and managed by the government. After PD patients are confirmed and registered 90% of the cost of treatment is supported by the government. In addition to receiving standard drug therapies such as levodopa, registered patients can also concurrently use KM such as herbal formulas and acupuncture if they desire. Therefore, further study is necessary to analyze the total national insurance dataset because the NHIS-NSC, which was used in our study, is equivalent to only 2.2% of the population of the South Korea.

CONCLUSION

It has not been clearly identified that integrative therapy with KM and biomedicine for PD management is better treatment for patients compared to biomedicine monotherapy; however, we found a clue of better result in integrated therapy. However, it should be noted that further investigation by increasing the number of subjects is needed.

ETHICS STATEMENT

This study was approved by the Institutional Review Board of Dongguk University, Gyeongju (DRG IRB 20170015). Patient consent was exempted because of the total anonymity of all research data used in this study.

AUTHOR CONTRIBUTIONS

YW and MH planned the study and wrote the manuscript.

FUNDING

This work was supported by the National Research Foundation of Korea (NRF) grant funded by the Korea government (Ministry of Science and ICT) (No. 2016R1C1B3006806).

ACKNOWLEDGMENTS

The authors alone are responsible for the content and writing of the article. This study used the NHIS-NSC (NHIS-2017-2-445) data provided by the NHIS.

REFERENCES

Ascherio, A., and Schwarzschild, M. A. (2016). The epidemiology of Parkinson's disease: risk factors and prevention. *Lancet Neurol.* 15, 1257–1272. doi: 10.1016/S1474-4422(16)30230-7

Bae, N., Ahn, T., Chung, S., Oh, M. S., Ko, H., Oh, H., et al. (2011). The neuroprotective effect of modified Yeoldahanso-tang via autophagy enhancement in models of Parkinson's disease. *J. Ethnopharmacol.* 134, 313–322. doi: 10.1016/j.jep.2010.12.016

Bae, N., Chung, S., Kim, H. J., Cha, J. W., Oh, H., Gu, M.-Y., et al. (2015). Neuroprotective effect of modified Chungsimyeolda-tang, a traditional Korean herbal formula, via autophagy induction in models of Parkinson×s disease. *J. Ethnopharmacol.* 159, 93–101. doi: 10.1016/j.jep.2014.11.007

Bega, D., and Zadikoff, C. (2014). Complementary & alternative management of Parkinson's disease: an evidence-based review of eastern influenced practices. *J. Mov. Disord.* 7, 57–66. doi: 10.14802/jmd.14009

Brown, R. G., and Marsden, C. D. (1984). How common is dementia in Parkinson's disease? *Lancet* 2, 1262–1265.

Chae, Y., Lee, H., Kim, H., Kim, C.-H., Chang, D.-I., Kim, K.-M., et al. (2009). Parsing brain activity associated with acupuncture treatment in parkinson's diseases. *Mov. Disord.* 24, 1794–1802. doi: 10.1002/mds.22673

Cummings, J. L. (1992). Depression and parkinson's disease: a review. *Am. J. Psychiatry* 149, 443–454. doi: 10.1176/ajp.149.4.443

Cwiekala-Lewis, K. J., Gallek, M., and Taylor-Piliae, R. E. (2017). The effects of Tai Chi on physical function and well-being among persons with parkinson's disease: a systematic review. *J. Bodyw. Mov. Ther.* 21, 414–421. doi: 10.1016/j.jbmt.2016.06.007

Dafsari, H. S., Reker, P., Stalinski, L., Silverdale, M., Rizos, A., Ashkan, K., et al. (2018). Quality of life outcome after subthalamic stimulation in parkinson's disease depends on age. *Mov. Disord.* 33, 99–107. doi: 10.1002/mds.27222

D'Agostino, R. B. Jr. (1998). Propensity score methods for bias reduction in the comparison of a treatment to a non-randomized control group. *Stat. Med.* 17, 2265–2281. doi: 10.1002/(SICI)1097-0258(19981015)17:19<2265::AID-SIM918>3.0.CO;2-B

Delamarre, A., and Meissner, W. G. (2017). Epidemiology, environmental risk factors and genetics of parkinson's disease. *Presse Med.* 46, 175–181. doi: 10.1016/j.lpm.2017.01.001

Elbaz, A., Carcaillon, L., Kab, S., and Moisan, F. (2016). Epidemiology of Parkinson's disease. *Rev. Neurol.* 172, 14–26. doi: 10.1016/j.neurol.2015.09.012

Fahn, S., Oakes, D., Shoulson, I., Kieburtz, K., Rudolph, A., Lang, A., et al. (2004). Levodopa and the progression of parkinson's disease. *N. Engl. J. Med.* 351, 2498–2508. doi: 10.1056/NEJMoa033447

Ghaffari, B. D., and Kluger, B. (2014). Mechanisms for alternative treatments in parkinson's disease: acupuncture, tai chi, and other treatments. *Curr. Neurol. Neurosci. Rep.* 14:451. doi: 10.1007/s11910-014-0451-y

Goetz, C. G., Tilley, B. C., Shaftman, S. R., Stebbins, G. T., Fahn, S., Martinez-Martin, P., et al. (2008). Movement Disorder Society-sponsored revision of the Unified Parkinson's Disease Rating Scale (MDS-UPDRS): scale presentation and clinimetric testing results. *Mov. Disord.* 23, 2129–2170. doi: 10.1002/mds.22340

Jang, J. H., Lee, J., Jung, I., and Yoo, H. (2018). Efficacy of Yokukansankachimpihange on sleep disturbance in Parkinson's disease: a study protocol of a randomized, double blind, placebo-controlled pilot trial. *Medicine* 97:e11298. doi: 10.1097/MD.0000000000011298

Lee, H. J., Kim, S. Y., Chae, Y., Kim, M. Y., Yin, C., Jung, W. S., et al. (2018). Turo (Qi Dance) program for parkinson's disease patients: randomized, assessor blind, waiting-list control, partial crossover study. *Explore* 14, 216–223. doi: 10.1016/j.explore.2017.11.002

Lee, J., Lee, J. S., Park, S. H., Shin, S. A., and Kim, K. (2017). Cohort profile: the National Health Insurance Service-National Sample Cohort (NHIS-NSC), South Korea. *Int. J. Epidemiol.* 46:e15.

Lee, S. H., and Lim, S. (2017). Clinical effectiveness of acupuncture on Parkinson disease: a PRISMA-compliant systematic review and meta-analysis. *Medicine* 96:e5836. doi: 10.1097/MD.0000000000005836

Leem, J. (2016). Acupuncture for motor symptom improvement in parkinson's disease and the potential identification of responders to acupuncture treatment. *Integr. Med. Res.* 5, 332–335. doi: 10.1016/j.imr.2016.06.006

Maldonado, G., and Greenland, S. (2002). Estimating causal effects. *Int. J. Epidemiol.* 31, 422–429. doi: 10.1093/intjepid/31.2.422

Marinus, J., Visser, M., Stiggelbout, A. M., Rabey, J. M., Martínez-Martín, P., Bonuccelli, U., et al. (2004). A short scale for the assessment of motor impairments and disabilities in parkinson's disease: the SPES/SCOPA. *J. Neurol. Neurosurg. Psychiatry* 75, 388–395. doi: 10.1136/jnnp.2003.017509

Noh, H., Kwon, S., Cho, S. Y., Jung, W. S., Moon, S. K., Park, J. M., et al. (2017). Effectiveness and safety of acupuncture in the treatment of parkinson's disease: a systematic review and meta-analysis of randomized controlled trials. *Complement. Ther. Med.* 34, 86–103. doi: 10.1016/j.ctim.2017.08.005

Ou, R., Hou, Y., Song, W., Wei, Q., Chen, Y., Cao, B., et al. (2018). Clinical characteristics and quality of life in Chinese patients with parkinson's disease beyond 20 years. *Neurol. Res.* 40, 312–317. doi: 10.1080/01616412.2018.1438227

Pan, X.-W., Zhang, X.-G., Chen, X.-C., Lu, Q., Hu, Y.-S., Han, L.-Y., et al. (2018). A survey of application of complementary and alternative medicine in chinese patients with parkinson's disease: a pilot study. *Chin. J. Integr. Med.* doi: 10.1007/s11655-018-2560-y [Epub ahead of print].

Parsons, L. (2001). "Reducing bias in a propensity score matched-pair sample using greedy matching techniques," in *Proceedings of the 26th Annual SAS Users Group International Conference*, (Long Beach, CA), 214–226.

Peto, V., Jenkinson, C., Fitzpatrick, R., and Greenhall, R. (1995). The development and validation of a short measure of functioning and well being for individuals with Parkinson's disease. *Qual. Life Res.* 4, 241–248. doi: 10.1007/BF02260863

Pinter, B., Diem-Zangerl, A., Wenning, G. K., Scherfler, C., Oberaigner, W., Seppi, K., et al. (2015). Mortality in parkinson's disease: a 38-year follow-up study. *Mov. Disord.* 30, 266–269. doi: 10.1002/mds.26060

Poon, P. M. K., Wong, C. K., Fung, K. P., Fong, C. Y. S., Wong, E. L. Y., Lau, J. T. F., et al. (2006). Immunomodulatory effects of a traditional chinese medicine with potential antiviral activity: a self-control study. *Am. J. Chin. Med.* 34, 13–21. doi: 10.1142/S0192415X0600359X

Pringsheim, T., Jette, N., Frolkis, A., and Steeves, T. D. (2014). The prevalence of parkinson's disease: a systematic review and meta-analysis. *Mov. Disord.* 29, 1583–1590. doi: 10.1002/mds.25945

Qiang, J., Biao, W., Rui-Lin, Z., Bao-Guo, W., Li-Min, F., Hai-Jian, W., et al. (2003). Clinical controlled study of integrative chinese and western medicine in treating 49 cases of SARS. *Chin. J. Integr. Med.* 9, 175–180. doi: 10.1007/BF02838027

Quan, H., Sundararajan, V., Halfon, P., Fong, A., Burnand, B., Luthi, J. C., et al. (2005). Coding algorithms for defining comorbidities in ICD-9-CM and ICD-10 administrative data. *Med. Care* 43, 1130–1139. doi: 10.1097/01.mlr.0000182534.19832.83

Rizek, P., Kumar, N., and Jog, M. S. (2016). An update on the diagnosis and treatment of parkinson disease. *CMAJ* 188, 1157–1165. doi: 10.1503/cmaj.151179

Rogers, G., Davies, D., Pink, J., and Cooper, P. (2017). Parkinson's disease: summary of updated NICE guidance. *BMJ* 358:j1951. doi: 10.1136/bmj.j1951

Shalaby, S. Y., and Louis, E. D. (2016). Increased odds of melanoma: parkinson's disease, essential tremor, dystonia versus controls. *Neuroepidemiology* 46, 128–136. doi: 10.1159/000443794

Shan, C. S., Zhang, H. F., Xu, Q. Q., Shi, Y. H., Wang, Y., Li, Y., et al. (2018). Herbal medicine formulas for parkinson's disease: a systematic review and meta-analysis of randomized double-blind placebo-controlled clinical trials. *Front. Aging Neurosci.* 10:349. doi: 10.3389/fnagi.2018.00349

Yang, S.-B., Kim, Y.-J., Lee, H.-M., Lee, H.-J., Cho, S.-Y., Park, J.-M., et al. (2016). Effects of korean medicine on patients with idiopathic parkinson's disease: a retrospective study. *J. Intern. Korean Med.* 37, 653–660. doi: 10.22246/jikm.2016.37.4.653

Zhuo, C., Zhu, X., Jiang, R., Ji, F., Su, Z., Xue, R., et al. (2017). Comparison for efficacy and tolerability among ten drugs for treatment of parkinson's disease: a network meta-analysis. *Sci. Rep.* 8:45865. doi: 10.1038/srep45865

Conflict of Interest Statement: The authors declare that the research was conducted in the absence of any commercial or financial relationships that could be construed as a potential conflict of interest.

frontiers in Aging Neuroscience

ORIGINAL RESEARCH
published: 26 February 2019
doi: 10.3389/fnagi.2019.00024

Lack of Association Between DJ-1 Gene Promoter Polymorphism and the Risk of Parkinson's Disease

Lu He[1†], Suzhen Lin[1†], Hong Pan[1,2], Ruinan Shen[1], Mengyan Wang[3], Zhihao Liu[3], Shiyao Sun[4], Yuyan Tan[1], Ying Wang[1], Shengdi Chen[1,2] and Jianqing Ding[1*]*

[1] Department of Neurology, Institute of Neurology, Ruijin Hospital, Shanghai Jiao Tong University School of Medicine, Shanghai, China, [2] Laboratory of Neurodegenerative Diseases, Institute of Health Science, Shanghai Institutes for Biological Sciences, Chinese Academy of Sciences, Shanghai Jiao Tong University School of Medicine, Shanghai, China, [3] Shanghai Jiao Tong University School of Medicine, Shanghai, China, [4] The University of Melbourne, Melbourne, VIC, Australia

OPEN ACCESS

Edited by:
Hi-Joon Park,
Kyung Hee University, South Korea

Reviewed by:
Pawan Gupta,
University of Illinois at Chicago, United States
Pau Pastor,
Mútua Terrassa University Hospital, Spain

***Correspondence:**
Jianqing Ding
jqding18@yahoo.com
Shengdi Chen
ruijincsd@126.com

[†] These authors have contributed equally to this work

Received: *10 August 2018*
Accepted: *28 January 2019*
Published: *26 February 2019*

Citation:
He L, Lin S, Pan H, Shen R, Wang M, Liu Z, Sun S, Tan Y, Wang Y, Chen S and Ding J (2019) Lack of Association Between DJ-1 Gene Promoter Polymorphism and the Risk of Parkinson's Disease. Front. Aging Neurosci. 11:24. doi: 10.3389/fnagi.2019.00024

Low DJ-1 protein level caused by DJ-1 gene mutation leads to autosomal recessive Parkinson's disease (PD) due to impaired antioxidative activity. In sporadic PD patients, although mutations were rarely found, lower DJ-1 protein level was also reported. Dysregulation of DJ-1 gene expression might contribute to low DJ-1 protein level. Since the promoter is the most important element to initiate gene expression, whether polymorphisms in the DJ-1 promoter result in the dysregulation of gene expression, thus leading to low protein level and causing PD, is worth exploring. The DJ-1 promoter region was sequenced in a Chinese cohort to evaluate possible links between DJ-1 promoter polymorphisms, PD risk and clinical phenotypes. Dual-luciferase reporter assay was conducted to evaluate the influence of promoter polymorphisms on DJ-1 transcriptional activity. Related information in an existing genome-wide association studies (GWAS) database were looked up, meta-analysis of the present study and other previous reports was conducted, and expression quantitative trait loci (eQTL) analysis was performed to further explore the association. Three single nucleotide polymorphisms (SNPs) (rs17523802, rs226249, and rs35675666) and one 18 bp deletion (rs200968609) were observed in our cohort. However, there was no significant association between the four detected genetic variations and the risk of PD either in allelic or genotype model, in single-point analysis or haplotype analysis. This was supported by the meta-analysis of this study and previous reports as well as that of GWAS database PDGene. Dual luciferase reporter assay suggested these promoter polymorphisms had no influence on DJ-1 transcriptive activity, which is consistent with the eQTL analysis results using the data from GTEx database. Thus, DJ-1 promoter polymorphisms may play little role in the dysregulation of DJ-1 expression and PD susceptibility in sporadic PD.

Keywords: PARK7/DJ-1, promoter, polymorphism, Parkinson's disease, eQTL

INTRODUCTION

Parkinson's disease (PD) is a common neurodegenerative disorder affecting approximately 1% of people over the age of 60 of the world and 1.7% of people over 65 in China (Zhang et al., 2005; de Lau and Breteler, 2006). Clinically, PD is manifested by classical motor symptoms, including tremor, rigidity, bradykinesia, and postural instability (Kalia and Lang, 2015). Increasing evidence has suggested that PD is probably caused by a combination of genetic and environmental risk factors (Kalia and Lang, 2015). During the past 20 years, more than 20 locis and 9 genes have been found associated with PD (Kalinderi et al., 2016). One such gene, PARK 7/DJ-1 aroused our interest since it played an important role in both familial and sporadic PD.

The human DJ-l gene is located on 1p36.23. DJ-1 protein acts as a molecular chaperone which plays a protective role in oxidative stress (Canet-Aviles et al., 2004). Loss of function mutations in the DJ-1 gene, including deletion of exon 1-5 (Bonifati et al., 2003), L166P (Bonifati et al., 2003), R98Q (Abou-Sleiman et al., 2003; Hague et al., 2003), M26I (Abou-Sleiman et al., 2003), E64D (Hering et al., 2004), and L172Q (Taipa et al., 2016), have been demonstrated to cause degeneration of dopamine neurons and autosomal recessive inherited PD. However, these causative mutations explained less than 10% of PD patients since about 90% of cases are sporadic without these mutations (Sutherland et al., 2009). Shen's group examined DJ-1 protein levels in SNc of 18 sporadic PD cases and found a lower level than that of normal control group (Nural et al., 2009). Similarly, lower DJ-1 protein level was also observed in cerebrospinal fluid (CSF) of sporadic PD patients compared with normal controls (Hong et al., 2010). These findings strongly indicated that a low level of DJ-1 might contribute to the pathogenesis of sporadic PD. The observation in our previous research that knockdown (KD) DJ-1 could increase MPP+ induced ROS production and cell death further supported the above hypothesis (Wang et al., 2011). However, the mechanism of low DJ-1 protein level in sporadic PD is still obscure.

Since DJ-1 gene mutations are rarely found in sporadic PD, we hypothesized that low DJ-1 protein levels in sporadic PD might be related to dysregulation of gene expression. The transcriptional initiation is the basic step of gene expression, and the promoter is the most fundamental element to initiate transcription. Polymorphic sites in the promoter may affect the binding and regulatory ability of transcription factors (TFs) to the promoter and influence transcriptional activity. Whether polymorphisms in the DJ-1 promoter affect the transcriptional activity and relate to the occurrence of PD is unknown. The promoter of DJ-1 is believed in a 2.1 kB area (−1015∼+1104) across the Transcription Start Site (TSS) (Taira et al., 2001). Taira et al. (2001) discovered a significant regulatory region in the promoter present at −109 to −101 from the TSS, and Duplan et al. (2013) showed a region located at −78 to −73 from the TSS (**Figure 1**), which could dramatically upregulate the expression of DJ-1. Considering that polymorphisms present at or near these regions might affect promoter activity and lead to low DJ-1 protein levels, we sequenced an area containing the above regions of DJ-1 promoter (NC_000001.11: 7961201-7962000) in 523 sporadic PD patients and 599 controls in Chinese Han population to screen the polymorphisms which may be associated with PD. To further analyze the genetic association, detected polymorphisms in the DJ-1 gene promoter region were looked up in existing public genome-wide association studies (GWAS) meta-analysis database PDGene. Meta-analysis of this study and previous reports was also conducted. Dual-luciferase assay was used to access the influences of detected polymorphisms on DJ-1 transcriptional activity. To further assess the association between detected polymorphisms and human brain DJ-1 expression level, expression quantitative trait loci (eQTL) analysis results were searched in GTEx Portal.

MATERIALS AND METHODS

Study Population

523 PD patients were recruited from movement disorders clinics in Ruijin Hospital, Shanghai, China. All patients were diagnosed with idiopathic PD by at least two movement disorders specialists according to the United Kingdom Parkinson's Disease Society (UKPDS) Brain Bank Clinical Diagnostic Criteria (Gibb and Lees, 1988). 599 unrelated controls were recruited from communities of Shanghai in epidemiologic investigation program. Each of the control had no evidence of neurodegenerative disease. All participants were Chinese Han residing in Shanghai. Any participants with a family history of PD were excluded. Demographic information [gender, age, age at onset, medication status, oral Levodopa Equivalent Dose (LED), disease duration, etc] and peripheral blood samples were collected from participants. The modified Hoehn and Yahr scale (H-Y) was rated in the OFF state of each patient. LED was computed according to the protocol provided by Tomlinson et al. (2010). Lifestyle factors including smoking and consumption of alcohol were also recorded. PD patients were divided into Tremor Dominant (TD), Akinetic/Rigid (AR) and Mixed (MX) subtypes by the criteria used in previous studies (Rajput et al., 2008). TD: rest tremor as sustained dominant symptom over bradykinesia and rigidity; Akinetic/Rigid dominant (AR): predominantly bradykinetic motor features with no or only mild rest tremor; Mixed motor feature group (MX): rest tremor, bradykinesia and rigidity present at the time of diagnosis or sustained comparable severity of tremor and bradykinetic motor features. Patients with age at onset <50 were classified as early-onset PD (EOPD), ≥ 50 years as late-onset PD (LOPD). The study was in accordance with the Helsinki Declaration of 1975. Written informed consents were obtained from all participants. Approval for the study was obtained from the Ethics Committee of Ruijin Hospital, Shanghai Jiao Tong University School of Medicine (2011-No. 13).

Blood Sample Collection and Genetic Analysis

Peripheral blood samples were collected in EDTA anticoagulant tubes and placed immediately on ice. After the lysis of erythrocytes, blood samples were centrifuged at 3000 rpm for 10 min to isolate leukocytes. DNA was extracted from leukocytes

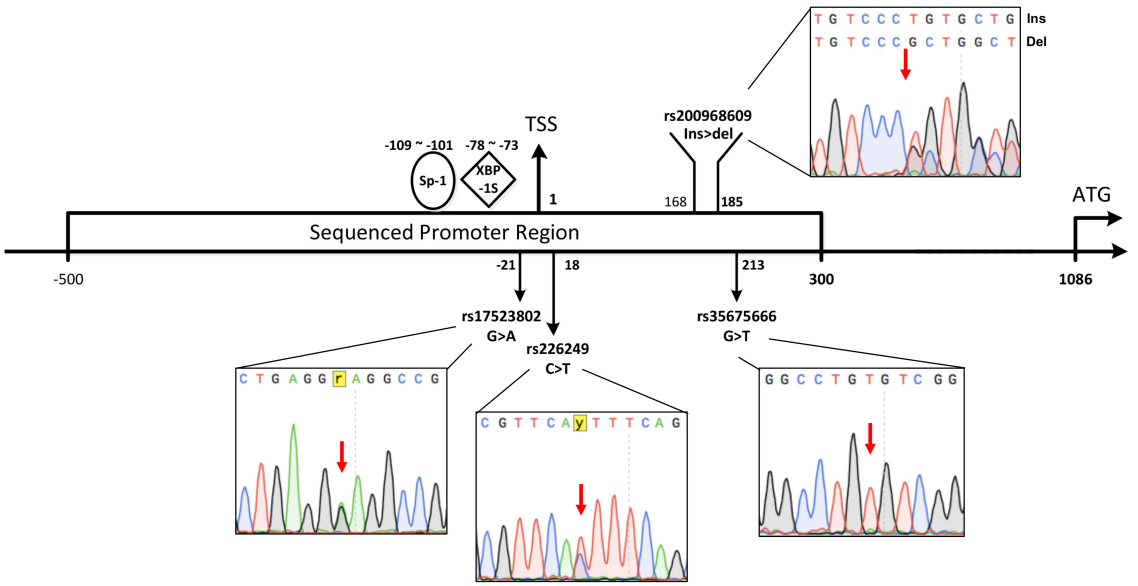

FIGURE 1 | Schematic view of relative positions of the polymorphisms investigated in the study. The first base of TSS was defined as 1, the first upstream base of TSS is −1, the relative positions of 4 polymorphisms observed in our cohort and previous reported functional sites (Sp-1 or XBP-1S binding site) were calculated based on TSS. The range of –500∼+300 across TSS (NC_000001.11: 7961201-7962000) containing the above functional areas of DJ-1 promoter was sequenced in the study. Representative sequence of rs17523802 G > A heterozygote, rs226249 heterozygote, rs200968609 heterozygote, and rs35675666 homozygote were shown.

through standardized phenol/chlorine extraction method. The range of −500∼+300 across TSS (NC_000001.11: 7961201–7962000) in DJ-1 promoter was amplified and sequenced (Schematic view of the area was shown in **Figure 1**). The primers used for polymerase chain reaction (PCR) amplification were as follows: forward 5′-ACTGCTCTAGTCCTGTGGGT-3′ and reverse 5′-CAGCTCGCCTCATGAC-ATCT-3′. With the PrimeSTAR DNA Polymerase (Takara, Dalian, China), following an initial denaturation at 94°C for 5 min, 30 PCR cycles were performed according to a 68–50°C touchdown PCR protocol (the first 12 cycles: 98°C for 15 s, 68–50°C for 15 s, 72°C for 1 min 50 s, the annealing temperature decreases by 1.5°C every cycle from 68 to 50°C; the next 18 cycles: 98°C for 15 s, 50°C for 15 s, 72°C for 1 min 50 s) with a final extension at 72°C for 5 min. After PCR amplification, the product was electrophoresed in 1.5% agarose gels containing ethidium bromide, purified and directly sequenced (Biosune, Shanghai, China). Sequences were aligned to the reference human genome sequence (NC_000001.11) using the SnapGene software (from GSL Biotech, available at[1]) and the Mutation Surveyor software (form SoftGenetics, available at[2]).

Meta-Analysis of the Association Between DJ-1 Promoter Polymorphisms and PD

The four variations were looked up in GWAS meta-analysis database PDGene[3]. Meta-analysis *p*-values and odds ratios (OR) of the four variations based on 13,708 PD cases and 95,282 controls from 13 independent GWAS datasets of European descent were obtained (Nalls et al., 2014). Due to privacy protection and data sharing restrictions, detailed genotype information of the four variations were not accessible. Thus, only Meta *p* values and Meta OR of the four variations in GWAS reports were listed in **Table 5**. Except for existing GWAS data, other related previous case-control studies were searched in PubMed, Embase and Web of Science, using the following terms "(polymorphism OR SNP) AND (DJ-1 OR PARK7) AND (PD OR Parkinson's disease)," "(rs17523802 OR rs226249 OR rs200968609 OR rs35675666) AND (PD OR Parkinson's disease)." Studies on irrelevant polymorphisms were eliminated, and finally, 6 independent case-control studies were selected. Genotype data were retrieved from the 6 studies and analyzed. Detailed information of the studies including race, minor allele frequencies (MAF) and sample counts were shown in **Table 6**. Meta-analysis was conducted with the Review Manager version 5.3.5 under the random effect model.

Construction of Luciferase Reporter Gene Vectors and Dual-Luciferase Reporter Assays

The DJ-1 promoter plasmid, containing the T or C allele at rs226249, or the A or G allele at rs17523802 (since rs17523802, rs200968609 and rs35675666 showed strong linkage pattern with $r^2 = 1$, three haplotypes were constructed: G-C-ins-G and G-T-ins-G to detect rs226249 function, G-C-ins-G and A-C-del-T to detect rs17523802, rs200968609 and rs35675666 function,

[1]snapgene.com

[2]softgenetics.com

[3]http://www.pdgene.org

alleles arrayed in order of rs17523802, rs226249, rs200968609 and rs35675666), were amplified from the genomic DNA of PD patients, using primers containing BglII in the forward primer and HindIII in the reverse primer for cloning (forward: 5′-GAAGATCTACTGCTCTAGTCCTGTGGGT-3′ and reverse: 5′-CCCAAGCTTCATTGCAACCCTGAGATACCCC-3′). PCR was performed: denatured at 94°C for 5 min, and amplified for 30 cycles at 98°C 15 s, 56°C 20 s, 72°C 1 min 45 s, with terminal extension at 72°C 5 min. After digested with Bgl II and HindIII (Takara, Dalian, China) and purified (Tiangen, Beijing, China), the fragments were cloned into the pGL3-basic luciferase plasmid (Promega, Beijing, China).

Human neuroblastoma cells (SH-SY5Y) were cultured in DMEM medium with 10% FBS (GIBCO/Invitrogen, Shanghai, China) and incubated at 37°C in a humidified environment with 5% CO2. SH-SY5Y cells were plated into 24-well culture plates 24 h prior to transfection, and cells were 80% confluent at transfection. 490 ng polymorphism plasmid or pGL3-basic empty plasmid (as a negative control) was transfected into SH-SY5Y cells using Lipofectamine 3000 (Invitrogen, Shanghai, China), with 10 ng Renilla pRL-TK plasmid (Promega, Beijing, China) cotransfected as a normalizing control. After 24 h, cells were rinsed with PBS and harvested with Passive Lysis buffer (Promega). Transcriptional activity was determined using the Dual-Luciferase Reporter Assay System (Promega, Beijing, China) on a Synergy^{TM} H4 Hybrid Microplate Reader (BioTek, Shanghai, China). For each plasmid construct, four independent transfection experiments were carried out and readings were taken in duplicate. The transcriptional activities were reported as relative luciferase activities, which was the ratio of firefly luciferase activities over renilla luciferase activities.

Analyzing the Effects of DJ-1 Promoter Polymorphisms on DJ-1 Gene Expression in Normal Human Brain

The potential impact of DJ-1 promoter SNPs on DJ-1 gene expression was evaluated by eQTL analysis. The data used for the analyses were obtained from the GTEx Portal[4] and dbGaP (accession number phs000424.vN.pN).

Statistical Analysis

All statistical analysis was performed using the SPSS software. For analyzing demographic statistics, a Mann–Whitney *U*-test was used for continuous variables and a Chi-squared test or Fisher's exact test was used for nominal data. The Chi-squared test or Fisher's exact test was used to assess the deviation of alleles in (HWE) and to evaluate the differences in genotype and allele distributions between groups. Measures of linkage disequilibrium (D' and r2) were computed from participants' genotypes with Haploview 4.1 (from Broad Institute, available at[5]). Each genotype was estimated by logistic regression analysis presuming additive mode of inheritance under correcting by confounders. A two-tailed $P < 0.05$ was considered statistically significant. For multiple statistical tests, the Bonferroni method was applied to correct the alpha level and *P* values accordingly.

[4]https://www.gtexportal.org

[5]broadinstitute.org

RESULTS

Demographic and Clinical Characteristics of Participants

Characteristics of 1122 participants were shown in **Table 1**. No significant statistical difference was observed for age and gender between PD and controls ($P > 0.05$). Compared to controls, PD patients were less likely to ever smoke cigarettes or drink alcohol ($P < 0.05$) (**Table 1**), which is consistent with several studies (Noyce et al., 2012; Zhang et al., 2014). Gender, disease duration, Hoehn and Yahr stage and oral LED/day showed different distribution among three PD motor subtypes: There were more male patients in the AR group; Tremor Dominant (TD) group consisted of more early stage PD patients compared to AR and MX group. Between EOPD and LOPD subgroups, the distribution of age and age at onset was as expected (**Table 1**).

Lack of Association Between DJ-1 Promoter Polymorphisms and PD in Single-Point Analysis

Three single nucleotide polymorphisms (SNPs) and one 18 bp deletion were observed in our cohort. Each of them already has a reference in the SNP database of NCBI (rs17523802, rs226249, rs200968609, and rs35675666). Schematic view of relative positions of these polymorphisms according to TSS was shown in **Figure 1**. All the four variations were in HWE among PD and controls ($P > 0.001$). There was no statistical difference in genotype or allele distribution of the four variations between the entire PD group and control (**Table 2**). When patients were stratified by life style factors (cigarette or alcohol intake), no significance of allele or genotype distribution was observed in all subgroups for the four variations (data not shown). Stratification analysis of age or gender also showed no statistical differences between PD and control among the four variations after Bonferroni adjustment (data not shown).

To investigate the association between polymorphisms and PD clinical phenotypes, genotype and allele distribution analysis between control and clinical subtypes of PD were further conducted. However, no significant difference was reached on either the genotype or allele distribution of the four variations among the entire control group and the motor subtypes of PD or among the EOPD (age of onset < 50), LOPD (age of onset ≥ 50) group and control group (**Table 3**).

Lack of Association Between DJ-1 Promoter Polymorphisms and PD in Haplotype Analysis

Since the four detected polymorphisms were located on the same chromosome, to explore whether they were in linkage disequilibrium (LD) linkage analysis was performed. Strong linkage patterns were observed among rs17523802, rs200968609, and rs35675666) ($r^2 = 1.0$, D' = 1.0, LOD = 206.52). The four

TABLE 1 | Demographic and clinical characteristics of controls and PD patients.

Characteristics[a]	Controls *N* = 599	Total PD *N* = 523	*p*	Subtypes of PD defined by motor symptoms				Subtypes of PD defined by onset age		
				TD *n* = 152	AR *n* = 225	MX *n* = 146	*p*	EOPD *n* = 99	LOPD *n* = 424	*p*
Gender										
Male	322 (53.8)	288 (55.1)	0.660	73 (48.0)	137 (60.9)	78 (53.4)	**0.043**	60 (60.6)	228 (53.8)	0.218
Female	277 (46.2)	235 (44.9)		79 (52.0)	88 (39.1)	68 (46.6)		39 (39.4)	196 (46.2)	
Age	63.94 ± 10.05	63.13 ± 9.51	0.388	63.48 ± 9.54	62.94 ± 9.70	63.07 ± 9.21	0.893	50.61 ± 8.24	66.06 ± 7.11	**<0.001**
Age at onset	NA	58.42 ± 9.76	NA	59.20 ± 9.77	58.45 ± 9.93	57.78 ± 9.48	0.670	44.06 ± 5.82	61.85 ± 7.05	**<0.001**
Disease duration (year)	NA	4.52 ± 4.29	NA	3.51 ± 3.87	4.66 ± 4.63	5.36 ± 3.96	**<0.001**	6.32 ± 6.20	4.10 ± 3.59	**0.003**
Hoehn and Yahr stage										
1–1.5	NA	233 (46.8)	NA	78 (52.0)	101 (48.6)	54 (38.6)	**0.025**	38 (40.8)	195 (48.1)	0.248
2–2.5	NA	193 (38.7)		60 (40.0)	75 (36.1)	58 (41.4)		37 (39.8)	156 (38.6)	
≥ 3	NA	72 (14.5)		12 (8.0)	32 (15.4)	28 (20.0)		18 (19.4)	54 (13.3)	
Oral LED/day (mg)	NA	366.64 ± 287.7	NA	263.61 ± 234.14	397.34 ± 299.85	423.87 ± 292.24	**<0.001**	424.46 ± 333.15	352.58 ± 274.23	0.104
Smokers (Yes/No)	163/436	74/449	**<0.001**	20/132	42/183	12/134	**0.017**	19/80	55/369	0.110
Alcohol drinkers (Yes/No)	102/497	62/461	**0.014**	14/138	35/190	13/133	0.075	12/87	50/374	0.927

TD, tremor dominant subtype of Parkinson's disease; AR, Akinetic/Rigid dominant subtype of Parkinson's disease; MX, mixed subtype of Parkinson's disease; EOPD, early onset Parkinson's disease; LOPD, late onset Parkinson's disease; SD, standard deviation; NA, not available. P-values that reach statistical significance were shown in bold. [a]Attributes data are presented as mean ± SD; variables data are presented as numbers (%).

TABLE 2 | Genotype and allele distribution between total PD patients and controls of polymorphisms in DJ-1 promoter region.

SNP ID[a]	Position[b]	Allele/Genotype	PD (*n* = 523)	Control (*n* = 599)	*p*[c]	OR (95% CI)[c]
Rs17523802	−21	G	982 (93.9)	1107 (92.4)	0.221	0.806 (0.570,1.139)
		A	64 (6.1)	91 (7.6)		
		GG	460 (87.9)	510 (85.2)	0.215	0.800 (0.562,1.139)
		GA	62 (11.9)	87 (14.5)		
		AA	1 (0.2)	2 (0.3)		
Rs226249	18	C	681 (65.1)	802 (66.9)	0.123	1.155 (0.962,1.386)
		T	365 (34.9)	396 (33.1)		
		CC	232 (44.4)	274 (45.7)	0.131	1.147 (0.96,1.369)
		CT	217 (41.5)	254 (42.4)		
		TT	74 (14.1)	71 (11.9)		
Rs200968609	168_185del	Ins	982 (93.9)	1107 (92.4)	0.221	0.806 (0.570,1.139)
		Del	64 (6.1)	91 (7.6)		
		Ins/ins	460 (87.9)	510 (85.2)	0.215	0.800 (0.562,1.139)
		Ins/del	62 (11.9)	87 (14.5)		
		Del/del	1 (0.2)	2 (0.3)		
Rs35675666	213	G	982 (93.9)	1107 (92.4)	0.221	0.806 (0.570,1.139)
		T	64 (6.1)	91 (7.6)		
		GG	460 (87.9)	510 (85.2)	0.215	0.800 (0.562,1.139)
		GT	62 (11.9)	87 (14.5)		
		TT	1 (0.2)	2 (0.3)		

OR, odds ratio; 95% CI, 95% confidence interval. [a]SNP ID represents the ID of each polymorphism recorded in the NCBI SNP database. [b]The first base of TSS was defined as 1, the first upstream base of TSS is −1, the relative position of each polymorphism was calculated based on TSS. [c]Adjusted for age, gender, cigarettes, and alcohol.

variations constitute one block of haplotype. Three Haplotypes with a frequency greater than 1% in all samples (G-T-ins-G, G-C-ins-G, and A-C-del-T, alleles arrayed in order of rs17523802, rs226249, rs200968609, and rs35675666) were selected to analyze. However, the frequency of the three Haplotypes showed no difference between PD and control (**Table 4**).

TABLE 3 | Allele distribution of DJ-1 promoter polymorphisms between controls and different PD subtypes classified by motor features or age at onset.

SNP ID	Allele/ genotype		Motor subtype of PD			AR vs. TD		Onset-age PD subtypes		EOPD vs. LOPD	
		Control *n* = 599	TD *n* = 152	AR *n* = 225	MX *n* = 146	*p*[a]	OR (95% CI)[a]	EOPD *n* = 99	LOPD *n* = 424	*p*[a]	OR (95% CI)[a]
rs17523802	G	1107 (92.4)	277 (91.1)	420 (93.3)	277 (94.9)	0.312	0.75 (0.44,1.3)	186 (93.9)	794 (93.9)	0.221	0.81 (0.57,1.14)
	A	91 (7.6)	27 (8.9)	30 (6.7)	15 (5.1)			12 (6.1)	52 (6.1)		
	GG	510 (85.2)	125 (82.2)	196 (87.1)	131 (89.7)	0.299	0.74 (0.42,1.3)	87 (87.9)	373 (88.0)	0.457	0.67 (0.24,1.92)
	GA	87 (14.5)	27 (17.8)	28 (12.4)	15 (10.3)			12 (12.1)	50 (11.8)		
	AA	2 (0.3)	0 (0)	1 (0.4)	0 (0)			0 (0)	1 (0.2)		
rs226249	C	802 (66.9)	200 (65.8)	285 (63.3)	196 (67.1)	0.525	1.11 (0.81,1.51)	136 (68.7)	544 (64.3)	0.12	1.16 (0.96,1.39)
	T	396 (33.1)	104 (34.2)	165 (36.7)	96 (32.9)			62 (31.3)	302 (35.7)		
	CC	274 (45.7)	64 (42.1)	99 (44)	69 (47.3)	0.540	1.10 (0.82,1.48)	50 (50.5)	182 (42.9)	0.88	1.04 (0.65,1.66)
	CT	254 (42.4)	72 (47.4)	87 (38.7)	58 (39.7)			36 (36.4)	181 (42.7)		
	TT	71 (11.9)	16 (10.5)	39 (17.3)	19 (13)			13 (13.1)	61 (14.4)		
rs200968609	Ins	1107 (92.4)	277 (91.1)	420 (93.3)	277 (94.9)	0.312	0.75 (0.44,1.3)	186 (93.9)	794 (93.9)	0.221	0.81 (0.57,1.14)
	Del	91 (7.6)	27 (8.9)	30 (6.7)	15 (5.1)			12 (6.1)	52 (6.1)		
	Ins/ins	510 (85.2)	125 (82.2)	196 (87.1)	131 (89.7)	0.299	0.74 (0.42,1.3)	87 (87.9)	373 (88.0)	0.45	0.67 (0.24,1.92)
	Ins/del	87 (14.5)	27 (17.8)	28 (12.4)	15 (10.3)			12 (12.1)	50 (11.8)		
	Del/del	2 (0.3)	0 (0)	1 (0.4)	0 (0)			0 (0)	1 (0.2)		
rs35675666	G	1107 (92.4)	277 (91.1)	420 (93.3)	277 (94.9)	0.312	0.75 (0.44,1.3)	186 (93.9)	794 (93.9)	0.22	0.81 (0.57,1.13)
	T	91 (7.6)	27 (8.9)	30 (6.7)	15 (5.1)			12 (6.1)	52 (6.1)		
	GG	510 (85.2)	125 (82.2)	196 (87.1)	131 (89.7)	0.299	0.74 (0.42,1.3)	87 (87.9)	373 (88.0)	0.46	0.67 (0.24,1.92)
	GT	87 (14.5)	27 (17.8)	28 (12.4)	15 (10.3)			12 (12.1)	50 (11.8)		
	TT	2 (0.3)	0 (0)	1 (0.4)	0 (0)			0 (0)	1 (0.2)		

TD, tremor dominant subtype of Parkinson's disease; AR, Akinetic/Rigid dominant subtype of Parkinson's disease; MX, mixed subtype of Parkinson's disease; EOPD, early onset Parkinson's disease; LOPD, late onset Parkinson's disease. [a]Adjusted for age, gender, cigarettes and alcohol.

Analyzing Effects of the Four Variations on PD With Public GWAS Database

To further evaluate the effect of these polymorphisms on PD, we looked up these polymorphisms in existing public genomic databases. As shown in **Table 5**, MAF of the four variations in our study were quite in accordance with the MAFs of East Asian population in 1000 Genome Project database, and lower than the MAFs of all population in either 1000 Genome Project database or TOPMED program database. We searched the meta-analysis results based on 13,708 PD cases and 95,282 controls from 13 independent GWAS datasets of European descent in PDGene database. Due to data sharing restrictions, detailed genotype information of the four variations were not accessible. Thus, only Meta *p* values and Meta OR of the four variations in GWAS reports were listed in **Table 5**. All the four variations showed Meta *P*-value > 0.05, which suggested, not only in Chinese as this study observed, the four variations may also not be associated with PD in European populations.

Meta-Analysis of DJ-1 Promoter Polymorphisms Based on This Study and Other Previous Reports

Except for meta-analysis on GWAS reports, a meta-analysis of the four variations with PD was performed based on this study and other related previous case-control studies (Eerola et al., 2003; Morris et al., 2003; De Marco et al., 2010; Sadhukhan et al., 2012; Sironi et al., 2013; Glanzmann et al., 2014). Detailed information of previous studies was shown in **Table 6**. Consistent with our results, no significant associations were observed between these polymorphisms and PD (rs17523902 $p = 0.777$, rs226249 $p = 0.816$, rs200968609 $p = 0.188$, and rs35675666 $p = 0.276$) at the allelic level under the random effect model (**Figure 2**), which indicated that DJ-1 promoter

TABLE 4 | Haplotype frequencies of the four variations in DJ-1 promoter region.

	Haplotype[a]	Total	PD	control	*p*	OR (95% CI)
		2N = 2244	2n = 1046	2n = 1198		
Block 1	1. G-C-ins-G	1320 (58.8)	609 (58.2)	711 (59.3)	0.588	0.96 (0.81, 1.13)
	2. G-T-ins-G	761 (33.9)	365 (34.9)	396 (33.1)	0.358	1.09 (0.91, 1.29)
	3. A-C-del-T	163 (7.3)	72 (6.9)	91 (7.6)	0.516	0.90 (0.65, 1.24)

OR, odds ratio; 95% CI, 95% confidence interval. [a]Alleles in haplotype are arrayed in order of rs17523802, rs226249, rs200968609, and rs35675666.

TABLE 5 | The frequencies of polymorphisms detected in present study and in public databases.

Polymorphisms	Minor allele frequency (%)							
	Present study		dbsnp147 database	1000 Genomes Project database		TOPMED program database	PDGene database	
	PD	Control		(All population)	(East Asian)		Meta *P*-value[a]	Meta OR[a]
−21 G > A	6.1	7.6	rs17523802	17.65	7	22.33	>0.05	>1
18 C > T	34.9	33.1	rs226249	36.26	33	29.18	>0.05[§]	>1[§]
168_185del	6.1	7.6	rs200968609	9.29	7	–	>0.05[§]	>1[§]
213 G > T	6.1	7.6	rs35675666	14.82	7	18.36	>0.05	>1

TOPMED, Trans-Omics for Precision Medicine Program. [a]The meta-analysis includes data up to 13,708 PD cases and 95,282 control from 15 independent GWAS datasets. The meta p-value ≥ 0.05 corresponds to p-values ≤ 1 and ≥0.05. [§] rs226249 and rs200968609 had no record in the database; Since rs226249 was in LD with rs2493215 (r^2 = 0.896 in 1000 Genome), we looked up rs2493215 to represent rs226249 in PDGene and found a Meta p-value > 0.05 with Meta OR > 1; considering rs200968609 was in LD with rs17523802 and rs35675666 (r^2 = 0.896 in 1000 Genome), the results of rs17523802 and rs35675666 could also represent that of rs200968609.

TABLE 6 | Detailed information of previous studies selected into meta-analysis.

Polymorphisms	Chr	Pos (hg38)	SNP ID	PD		Control		*P*-value	Ethnic background	Study
				MAF (%)	Cases	MAF (%)	Cases			
−21 G > A	1	7961680	rs17523802	2.5	163EOPD	6	100	0.039[a]	Italian	Sironi et al., 2013
				21.4	138PD	10.5	38	0.033[§]	Indian	Sadhukhan et al., 2012
				12.2	294PD	7.3	298	0.005	Italian	De Marco et al., 2010
18 C > T	1	7961718	rs226249	44.5	163EOPD	44	100	0.915[a]	Italian	Sironi et al., 2013
				56.2	138PD	67.1	38	0.086[§]	Indian	Sadhukhan et al., 2012
168_185del	1	7961913	rs200968609	8.9	163EOPD	10.5	100	0.543[a]	Italian	Sironi et al., 2013
				31	136sporadic PD	29	129	0.65	Finnish	Eerola et al., 2003
				11	308PD	8.7	248	0.19[§]	Indian	Sadhukhan et al., 2012
				23	46PD	18	96	0.362[§]	England	Morris et al., 2003
				13.8	294PD	6.9	298	<0.001	Italian	De Marco et al., 2010
				0.2	285PD	0	264	0.497	White	Glanzmann et al., 2014
				1	99PD	1.1	132	0.337	Mixed ancestry	Glanzmann et al., 2014
				5.6	18PD	1.1	132	0.111	Black African	Glanzmann et al., 2014
213 G > T	1	7961850	rs35675666	2.5	163EOPD	0.5	100	0.193[a]	Italian	Sironi et al., 2013
				22.1	86PD	5.1	39	<0.001[§]	Indian	Sadhukhan et al., 2012

Chr, chromosome; pos (hg38), SNP position on hg38 reference sequence; MAF, minor allele frequency. [a]Values were non-significant according to Bonferroni correction (p < 0.002). [§]P values calculated with provided data in the studies (which were not directly provided in the studies).

polymorphisms may play little role in PD susceptibility in different ethnic populations.

Effects of Promoter Polymorphisms on DJ-1 Promoter Transcriptional Activity

To test whether the four variations alter DJ-1 promoter transcriptional activity, dual-luciferase reporter gene assay was conducted. As shown in **Figure 3**, allele alteration of rs226249 or rs17523802/rs200968609/rs35675666 had no effect on DJ-1 promoter transcriptional activity.

EQTL (Expression Quantitative Trait Loci) Analysis of the Four Variations

To explore whether these DJ-1 promoter polymorphisms could impact human brain DJ-1 gene expression, eQTL analysis was conducted with data from dbGaP. As shown in **Figure 4**, rs17523802 (P = 0.62), rs226249 (P = 0.8), and rs35675666 (P = 0.75) showed no association with DJ-1 gene expression in human brain substantia nigra. In addition, other brain regions including amygdala, anterior cingulate cortex (BA24), Caudate (basal ganglia), Frontal Cortex (BA9), Hippocampus, Hypothalamus, nucleus accumbens (basal ganglia), putamen (basal ganglia), spinal cord (cervical c-1) were also analyzed and found negative results (**Table 7**).

DISCUSSION

The antioxidative effect of DJ-1 plays an important role in cell survival, deficiency or low level of DJ-1 protein makes neurons more susceptible to oxidative stress and result in the occurrence of PD. In familial PD, such deficiency is

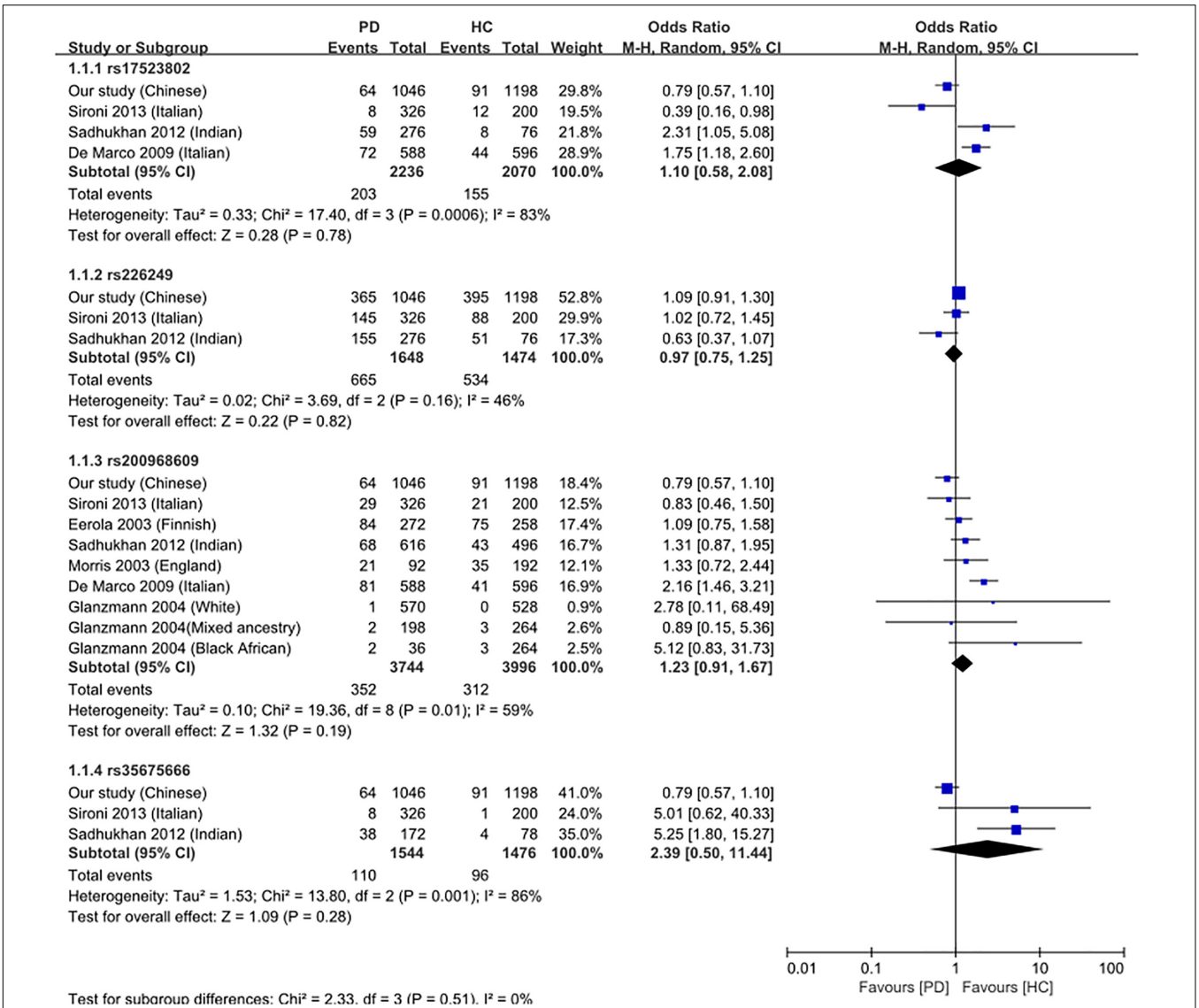

FIGURE 2 | Forest plots of the meta-analysis between DJ-1 promoter polymorphisms and PD under the allelic model. For meta-analysis, rs17523902 $p = 0.777$, rs226249 $p = 0.816$, rs200968609 $p = 0.188$, and rs35675666 $p = 0.276$. OR, odds ratio; CI, confidence interval; I-squared, heterogeneity.

caused by mutations in DJ-1 gene, whereas in sporadic PD, who lacks mutations in DJ-1, the reason of a low brain DJ-1 protein level remains obscure. This study attempted to reveal whether polymorphisms in DJ-1 promoter were associated with PD through affecting the regulation of DJ-1 expression. In the present study, we sequenced the core region of DJ-1 promoter in 523 sporadic PD patients and 599 controls in Chinese Han population of mainland, and finally found four variations (rs17523802, rs226249, rs200968609, and rs35675666). However, no significant association was found between all the four detected polymorphisms and the risk of PD either in the allelic model or genotype model, in single-point analysis or haplotype analysis. After stratification by age, gender, PD subtypes or habitude of cigarette or alcohol, we still failed to find any difference in the distribution of the four variations between PD and control or among subtypes. Searching results in PDGene GWAS database and meta-analysis of the present study and previous reports also showed no association between the four variations and PD. In addition, eQTL analysis demonstrated lack of association between the four DJ-1 promoter polymorphisms and normal human brain DJ-1 gene expression. All of these results suggested DJ-1 promoter polymorphisms may play little role in regulating brain DJ-1 gene expression level and PD susceptibility.

To our best knowledge, this is the first survey of the association between DJ-1 promoter polymorphisms and PD risk in a relatively large sample size of Chinese sporadic PD patients. Previous reports on DJ-1 promoter polymorphisms are very rare, and the results are not consistent. De Marco

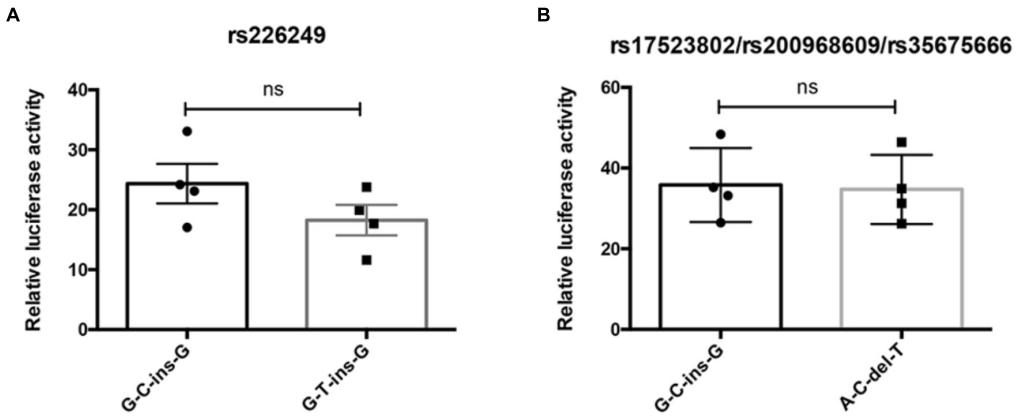

FIGURE 3 | The influence of promoter polymorphisms on DJ-1 promoter transcriptional activity. Dual-luciferase reporter assay was used to access whether rs226249 **(A)** or rs17523802/rs200968609/rs35675666 **(B)** affect DJ-1 promoter transcriptional activity. The haplotype alleles arrayed in order of rs17523802, rs226249, rs200968609, and rs35675666. The data were represented as mean ± SE from four independent transfection experiments, each in duplicate.

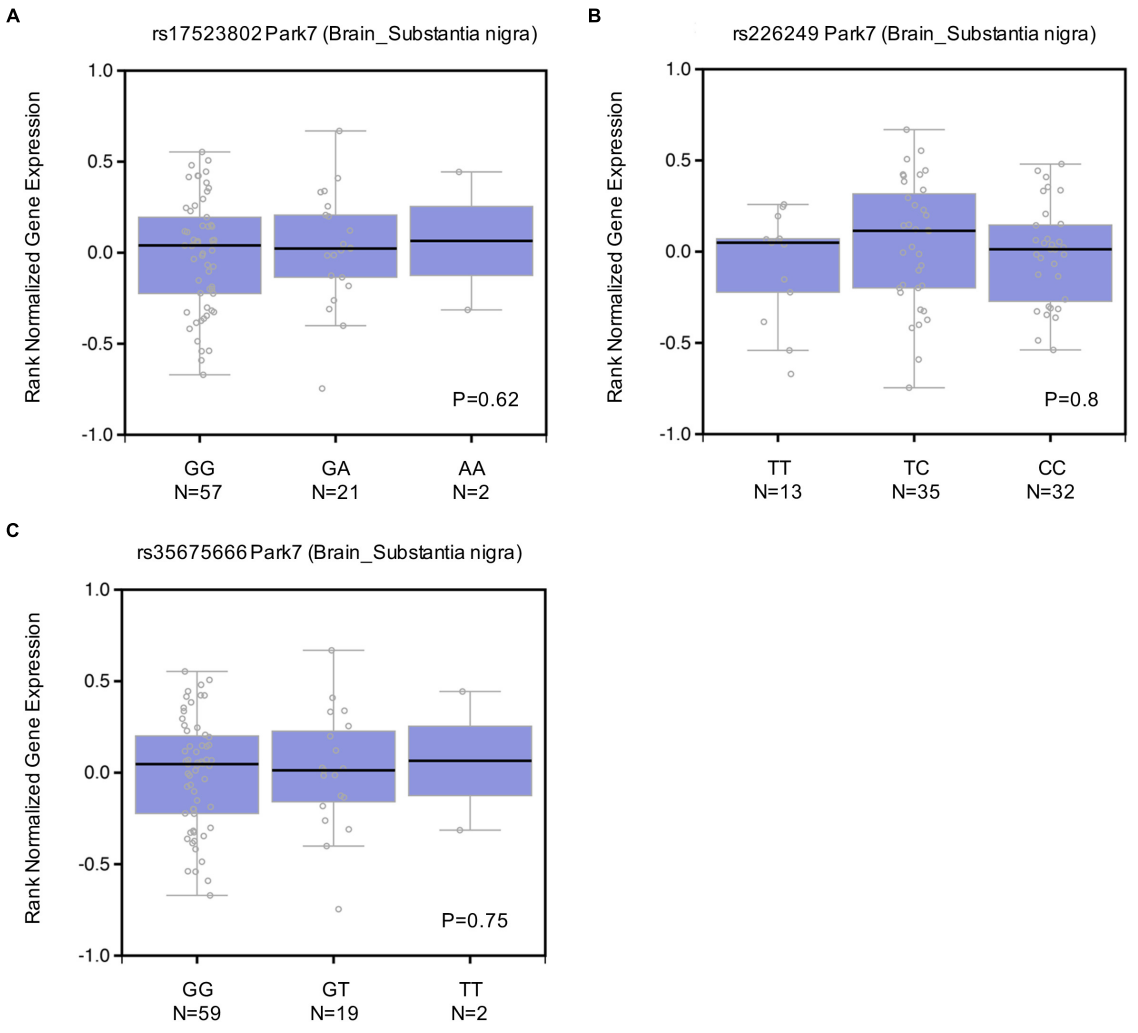

FIGURE 4 | Effect of rs17523802 **(A)**, rs226249 **(B)**, rs356756666 **(C)** genotype on DJ-1 mRNA expression in normal human brain substantia nigra. Data of rs200968609 were not found in dbGap.

TABLE 7 | Effect of rs17523802, rs226249, and rs356756666 on DJ-1 mRNA expression in different regions of normal human brain.

Polymorphisms	Gene	dbSNP number	Tissue	*P*-value	Effect size
−21 G > A	PARK7	rs17523802	Brain–Amygdala	0.19	−0.1
			Brain–Anterior cingulate cortex (BA24)	0.23	−0.089
			Brain–Caudate (basal ganglia)	0.81	−0.016
			Brain–Frontal Cortex (BA9)	0.18	−0.084
			Brain–Hippocampus	0.097	−0.092
			Brain–Hypothalamus	0.065	−0.11
			Brain–Nucleus accumbens (basal ganglia)	0.4	−0.052
			Brain–Putamen (basal ganglia)	0.55	0.047
			Brain–Spinal cord (cervical c-1)	0.38	0.066
			Brain–Substantia nigra	0.62	0.045
18 C > T	PARK7	rs226249	Brain–Amygdala	0.48	0.043
			Brain–Anterior cingulate cortex (BA24)	0.84	0.013
			Brain–Caudate (basal ganglia)	0.26	−0.06
			Brain–Frontal Cortex (BA9)	0.22	0.071
			Brain–Hippocampus	0.35	−0.044
			Brain–Hypothalamus	0.38	0.049
			Brain–Nucleus accumbens (basal ganglia)	0.51	0.032
			Brain–Putamen (basal ganglia)	0.33	−0.058
			Brain–Spinal cord (cervical c-1)	0.68	0.027
			Brain–Substantia nigra	0.8	−0.017
213 G > T	PARK7	rs35675666	Brain–Amygdala	0.27	−0.089
			Brain–Anterior cingulate cortex (BA24)	0.24	−0.087
			Brain–Caudate (basal ganglia)	0.64	−0.032
			Brain–Frontal Cortex (BA9)	0.11	−0.099
			Brain–Hippocampus	0.2	−0.072
			Brain–Hypothalamus	0.073	−0.11
			Brain–Nucleus accumbens (basal ganglia)	0.46	−0.046
			Brain–Putamen (basal ganglia)	0.61	0.041
			Brain–Spinal cord (cervical c-1)	0.4	0.064
			Brain–Substantia nigra	0.75	0.029

et al. (2010) found rs17523802 (P = 0.005) and rs200968609 (P < 0.001) were associated with PD risk in an Italian cohort (294PD and 298 control) (**Table 6**). Whereas, Sadhukhan et al. (2012) suggested rs35675666 (P < 0.001) was a risk factor of PD in an Indian population (86PD and 39 control), and rs17523802 and rs200968609 were not associated with PD (**Table 6**). Other studies (Eerola et al., 2003; Morris et al., 2003; Sironi et al., 2013; Glanzmann et al., 2014) failed to find association between these polymorphisms and PD (**Table 6**). Meta-analysis of previous reports and our present study suggested no association between the four variations and PD. The results of GWAS database and eQTL analysis further confirmed that polymorphisms in DJ-1 promoter region (rs17523802, rs226249, rs200968609, and rs35675666) were not associated with DJ-1 expression in human brain and the risk of PD.

Based on current findings, low DJ-1 protein level in sporadic PD patients is not a consequence of DJ-1 promoter polymorphisms. According to relevant researches, the low DJ-1 protein level in sporadic PD might be related to dysregulation of gene expression. On the transcriptional level, it might be caused by altered regulation of transcriptional factors or epigenetic regulation such as DNA methylation and histone modifications. Taira et al. (2001) and Duplan et al. (2013), respectively, found the transcription factor SP-1 (Taira et al., 2001) or XBP-1S (Duplan et al., 2013) could bind to the DJ-1 promoter region and increase its transcriptional activity, suggesting that expression or activity alterations of transcriptional factors might be associated with PD. Zhou et al. (2011) demonstrated that deacetylase inhibitors such as phenyl butyrate and sodium butyrate could increase DJ-1 mRNA and protein expression to protect cells against oxidative stress, which suggested alterations of acetylation of histone for DJ-1, might affect DJ-1 expression. However, in our previous study (Tan et al., 2016), we found that DNA methylation did not regulate DJ-1 expression. On the post-transcriptional level, microRNAs may have an effect on the expression of DJ-1 protein level. Our previous study (Chen et al., 2017) found that MircoRNA-4639 could downregulate DJ-1 expression and had the potential to be a biomarker for PD. Thus, low DJ-1 protein levels in sporadic PD might be a combination result of a variety of factors, future studies on detailed mechanisms would be needed.

In conclusion, our results implicated that DJ-1 promoter polymorphisms may not be associated with PD risk.

AUTHOR CONTRIBUTIONS

JD designed the project. SC, YW, and YT collected the samples. LH, SL, RS, HP, MW, ZL, and SS conducted genotyping and analyzed the data. JD, LH, and SC wrote the manuscript. All authors have approved the final version of the manuscript.

FUNDING

The project was supported by the National Natural Science Foundation of China #81630029, #81871005, the National Key R&D Program of China #2016YFC13060000, and the Science and Technology Commission of Shanghai Municipality #14XD1402700.

REFERENCES

Abou-Sleiman, P. M., Healy, D. G., Quinn, N., Lees, A. J., and Wood, N. W. (2003). The role of pathogenic DJ-1 mutations in Parkinson's disease. *Ann. Neurol.* 54, 283–286. doi: 10.1002/ana.10675

Bonifati, V., Rizzu, P., van Baren, M. J., Schaap, O., Breedveld, G. J., Krieger, E., et al. (2003). Mutations in the DJ-1 gene associated with autosomal recessive early-onset parkinsonism. *Science* 299, 256–259. doi: 10.1126/science.1077209

Canet-Aviles, R. M., Wilson, M. A., Miller, D. W., Ahmad, R., McLendon, C., Bandyopadhyay, S., et al. (2004). The Parkinson's disease protein DJ-1 is neuroprotective due to cysteine-sulfinic acid-driven mitochondrial localization. *Proc. Natl. Acad. Sci. U.S.A.* 101, 9103–9108. doi: 10.1073/pnas.0402959101

Chen, Y., Gao, C., Sun, Q., Pan, H., Huang, P., Ding, J., et al. (2017). MicroRNA-4639 Is a regulator of DJ-1 expression and a potential early diagnostic marker for Parkinson's disease. *Front. Aging Neurosci.* 9:232. doi: 10.3389/fnagi.2017.00232

de Lau, L. M. L., and Breteler, M. M. B. (2006). Epidemiology of Parkinson's disease. *Lancet Neurol.* 5, 525–535. doi: 10.1016/S1474-4422(06)70471-9

De Marco, E. V., Annesi, G., Tarantino, P., Nicoletti, G., Civitelli, D., Messina, D., et al. (2010). DJ-1 is a Parkinson's disease susceptibility gene in southern Italy. *Clin. Genet.* 77, 183–188. doi: 10.1111/j.1399-0004.2009.01310.x

Duplan, E., Giaime, E., Viotti, J., Sevalle, J., Corti, O., Brice, A., et al. (2013). ER-stress-associated functional link between Parkin and DJ-1 via a transcriptional cascade involving the tumor suppressor p53 and the spliced X-box binding protein XBP-1. *J. Cell Sci.* 126(Pt 9), 2124–2133. doi: 10.1242/jcs.127340

Eerola, J., Hernandez, D., Launes, J., Hellstrom, O., Hague, S., Gulick, C., et al. (2003). Assessment of a DJ-1 (PARK7) polymorphism in Finnish PD. *Neurology* 61, 1000–1002. doi: 10.1212/01.WNL.0000083992.28066.7E

Gibb, W. R., and Lees, A. J. (1988). The relevance of the Lewy body to the pathogenesis of idiopathic Parkinson's disease. *J. Neurol. Neurosurg. Psychiatry* 51, 745–752. doi: 10.1136/jnnp.51.6.745

Glanzmann, B., Lombard, D., Carr, J., and Bardien, S. (2014). Screening of two indel polymorphisms in the 5'UTR of the DJ-1 gene in South African Parkinson's disease patients. *J. Neural Transm.* 121, 135–138. doi: 10.1007/s00702-013-1094-x

Hague, S., Rogaeva, E., Hernandez, D., Gulick, C., Singleton, A., Hanson, M., et al. (2003). Early-onset Parkinson's disease caused by a compound heterozygous DJ-1 mutation. *Ann. Neurol.* 54, 271–274. doi: 10.1002/ana.10663

Hering, R., Strauss, K. M., Tao, X., Bauer, A., Woitalla, D., Mietz, E. M., et al. (2004). Novel homozygous p.E64D mutation in DJ1 in early onset Parkinson disease (PARK7). *Hum. Mutat.* 24, 321–329. doi: 10.1002/humu.20089

Hong, Z., Shi, M., Chung, K. A., Quinn, J. F., Peskind, E. R., Galasko, D., et al. (2010). DJ-1 and alpha-synuclein in human cerebrospinal fluid as biomarkers of Parkinson's disease. *Brain* 133(Pt 3), 713–726. doi: 10.1093/brain/awq008

Kalia, L. V., and Lang, A. E. (2015). Parkinson's disease. *Lancet* 386, 896–912. doi: 10.1016/S0140-6736(14)61393-3

Kalinderi, K., Bostantjopoulou, S., and Fidani, L. (2016). The genetic background of Parkinson's disease: current progress and future prospects. *Acta Neurol. Scand.* 134, 314–326. doi: 10.1111/ane.12563

Morris, C. M., O'Brien, K. K., Gibson, A. M., Hardy, J. A., and Singleton, A. B. (2003). Polymorphism in the human DJ-1 gene is not associated with sporadic dementia with Lewy bodies or Parkinson's disease. *Neurosci. Lett.* 352, 151–153. doi: 10.1016/j.neulet.2003.08.037

Nalls, M. A., Pankratz, N., Lill, C. M., Do, C. B., Hernandez, D. G., Saad, M., et al. (2014). Large-scale meta-analysis of genome-wide association data identifies six new risk loci for Parkinson's disease. *Nat. Genet.* 46, 989–993. doi: 10.1038/ng.3043

Noyce, A. J., Bestwick, J. P., Silveira-Moriyama, L., Hawkes, C. H., Giovannoni, G., Lees, A. J., et al. (2012). Meta-analysis of early nonmotor features and risk factors for Parkinson disease. *Ann. Neurol.* 72, 893–901. doi: 10.1002/ana.23687

Nural, H., He, P., Beach, T., Sue, L., Xia, W., and Shen, Y. (2009). Dissembled DJ-1 high molecular weight complex in cortex mitochondria from Parkinson's disease patients. *Mol. Neurodegener.* 4:23. doi: 10.1186/1750-1326-4-23

Rajput, A. H., Sitte, H. H., Rajput, A., Fenton, M. E., Pifl, C., and Hornykiewicz, O. (2008). Globus pallidus dopamine and Parkinson motor subtypes: clinical and brain biochemical correlation. *Neurology* 70(16 Pt 2), 1403–1410. doi: 10.1212/01.wnl.0000285082.18969.3a

Sadhukhan, T., Biswas, A., Das, S. K., Ray, K., and Ray, J. (2012). DJ-1 variants in Indian Parkinson's disease patients. *Dis. Markers* 33, 127–135. doi: 10.3233/dma-2012-0913

Sironi, F., Primignani, P., Ricca, S., Tunesi, S., Zini, M., Tesei, S., et al. (2013). DJ1 analysis in a large cohort of Italian early onset Parkinson disease patients. *Neurosci. Lett.* 557(Pt B), 165–170. doi: 10.1016/j.neulet.2013.10.048

Sutherland, G. T., Halliday, G. M., Silburn, P. A., Mastaglia, F. L., Rowe, D. B., Boyle, R. S., et al. (2009). Do polymorphisms in the familial Parkinsonism genes contribute to risk for sporadic Parkinson's disease? *Mov. Disord.* 24, 833–838. doi: 10.1002/mds.22214

Taipa, R., Pereira, C., Reis, I., Alonso, I., Bastos-Lima, A., Melo-Pires, M., et al. (2016). DJ-1 linked parkinsonism (PARK7) is associated with Lewy body pathology. *Brain* 139(Pt 6), 1680–1687. doi: 10.1093/brain/aww080

Taira, T., Takahashi, K., Kitagawa, R., Iguchi-Ariga, S. M., and Ariga, H. (2001). Molecular cloning of human and mouse DJ-1 genes and identification of Sp1-dependent activation of the human DJ-1 promoter. *Gene* 263, 285–292. doi: 10.1016/S0378-1119(00)00590-4

Tan, Y., Wu, L., Li, D., Liu, X., Ding, J., and Chen, S. (2016). Methylation status of DJ-1 in leukocyte DNA of Parkinson's disease patients. *Transl. Neurodegener.* 5:5. doi: 10.1186/s40035-016-0052-6

Tomlinson, C. L., Stowe, R., Patel, S., Rick, C., Gray, R., and Clarke, C. E. (2010). Systematic review of levodopa dose equivalency reporting in Parkinson's disease. *Mov. Disord.* 25, 2649–2653. doi: 10.1002/mds.23429

Wang, Z., Liu, J., Chen, S., Wang, Y., Cao, L., Zhang, Y., et al. (2011). DJ-1 modulates the expression of Cu/Zn-superoxide dismutase-1 through the Erk1/2-Elk1 pathway in neuroprotection. *Ann. Neurol.* 70, 591–599. doi: 10.1002/ana.22514

Zhang, D. F., Jiang, H., and Xie, J. X. (2014). Alcohol intake and risk of Parkinson's disease: a meta-analysis of observational studies. *Mov. Disord.* 29, 819–822. doi: 10.1002/mds.25863

Zhang, Z. X., Roman, G. C., Hong, Z., Wu, C. B., Qu, Q. M., Huang, J. B., et al. (2005). Parkinson's disease in China: prevalence in Beijing, Xian, and Shanghai. *Lancet* 365, 595–597. doi: 10.1016/s0140-6736(05)17909-4

Zhou, W., Bercury, K., Cummiskey, J., Luong, N., Lebin, J., and Freed, C. R. (2011). Phenylbutyrate up-regulates the DJ-1 protein and protects neurons in cell culture and in animal models of Parkinson disease. *J. Biol. Chem.* 286, 14941–14951. doi: 10.1074/jbc.M110.211029

Conflict of Interest Statement: The authors declare that the research was conducted in the absence of any commercial or financial relationships that could be construed as a potential conflict of interest.

frontiers in Aging Neuroscience

ORIGINAL RESEARCH
published: 05 April 2019
doi: 10.3389/fnagi.2019.00080

Dose-Dependent Neuroprotective Effect of Standardized Bee Venom Phospholipase A_2 Against MPTP-Induced Parkinson's Disease in Mice

*Kyung Hwa Kim[1], Seung Young Lee[1], Jaekwon Shin[1], Jae-Taeg Hwang[2], Hat Nim Jeon[1] and Hyunsu Bae[1]**

[1]Department of Physiology, College of Korean Medicine, Kyung Hee University, Seoul, South Korea, [2]Inist ST Co. Ltd., Seongnam-si, South Korea

Parkinson's disease (PD) is a chronic progressive neurodegenerative movement disorder characterized by the selective loss of dopaminergic neurons within the substantia nigra (SN). While the precise etiology of dopaminergic neuronal demise is elusive, multiple lines of evidence indicate that neuroinflammation is involved in the pathogenesis of PD. We have previously demonstrated that subcutaneous administration of bee venom (BV) phospholipase A_2 (bvPLA$_2$) suppresses dopaminergic neuronal cell death in a PD mouse model. In the present study, we established standardized methods for producing bvPLA$_2$ agent isolated from crude BV at good manufacturing practice (GMP) facility. The therapeutic efficacy of purified bvPLA2 agent was examined in MPTP-induced PD mice. Importantly, administration of purified bvPLA$_2$ in a dose-dependent manner reversed motor deficits in PD mice as well as inhibited loss of dopaminergic neurons within the SN of PD mice. The concentration-dependent action of standardized bvPLA$_2$ appeared to be related to the induction of $CD4^+CD25^+Foxp3^+$ regulatory T cells (Tregs), which, in part, inhibits T helper 1 (Th1) and Th17 polarization and suppresses microglial activation in PD mice. Taken together, these results suggest that standardized bvPLA$_2$ purified from BV shows a neuroprotective effect against PD and thus has a potential target for treatment of PD.

Keywords: Parkinson's disease, regulatory T cells, bee venom phospholipase A_2, neuroinflammation, dose-dependent response

OPEN ACCESS

Edited by:
Seung-Nam Kim, Dongguk University Seoul, South Korea

Reviewed by:
Craig Doupnik, USF Health, United States
Mohamed M. Abdel-Daim, Suez Canal University, Egypt
Roberta Marongiu, Cornell University, United States

****Correspondence:***
Hyunsu Bae
hbae@khu.ac.kr

Received: *31 October 2018*
Accepted: *19 March 2019*
Published: *05 April 2019*

Citation:
Kim KH, Lee SY, Shin J, Hwang J-T, Jeon HN and Bae H (2019) Dose-Dependent Neuroprotective Effect of Standardized Bee Venom Phospholipase A_2 Against MPTP-Induced Parkinson's Disease in Mice. Front. Aging Neurosci. 11:80. doi: 10.3389/fnagi.2019.00080

INTRODUCTION

Parkinson's disease (PD) is known as the second most common neurodegenerative disease to affect about 3% of the population over the age of 65 (Lang and Lozano, 1998; de Lau et al., 2004). It is generally characterized by the selective loss of dopaminergic neurons as significant neuropathological hallmarks (Bertram and Tanzi, 2005). Until recently, several animal models have been developed to discover PD pathogenesis as well as search for neuroprotective therapeutic targets (Wang et al., 2015). Among all of these models, MPTP model has been widely used to initiate PD in animal models by penetrating blood-brain barrier (BBB) and destroying dopaminergic neurons in the substantia nigra (SN; Sakaguchi et al., 2008).

While the etiology of PD is unclear, a considerable body of research suggests that inflammatory responses play an important role in the development and progression of PD (Tufekci et al., 2012). Emerging evidence indicates the enhanced inflammatory responses, infiltration of T cells into the brain and glial cell activation are prominent features of PD (Wang et al., 2015). Recently, significant efforts recently have been focused on developing novel anti-inflammatory agents for PD treatment (Samii et al., 2009).

Bee venom (BV) consists of a complex mixture of peptides, enzymes, lipids and bioactive amines. Accumulating evidence suggests a wide range of pharmaceutical properties of BV. Accordingly, BV therapy has been developed to treat various diseases, including inflammatory diseases (Lee et al., 2014) and neurodegenerative diseases (Hossen et al., 2017).

One of the major components of BV is phospholipase A_2 (PLA_2), comprising approximately 10%–12% of the dry weight of the venom in the European honeybee, *Apis mellifera* (Habermann, 1972). The PLA2 derived from BV ($bvPLA_2$) belongs to group III secretory PLA_2 ($sPLA_2$) that has been implicated in diverse cellular responses, such as signal transduction, host defense, blood coagulation, and pain relief (Hossen et al., 2016). Interestingly, several lines of evidence have indicated the therapeutic effect of $bvPLA_2$ in neurodegenerative diseases, including prion disease (Jeong et al., 2011). Consistent with this finding, we previously reported the neuroprotective effect of $bvPLA_2$ against neurodegenerative diseases including Alzheimer's disease (Ye et al., 2016) and PD (Chung et al., 2015). The cellular action of $bvPLA_2$ appeared to mainly suppress immune responses *via* stimulation of dendritic cells, ultimately enhancing the function of regulatory T cells which play an essential role in maintaining immune tolerance (Sakaguchi et al., 2008).

It appears that generating clinical-grade and sterile pharmaceutical products from BV is challenging, mostly related to identification, isolation, and purification of bioactive components from BV (Ameratunga et al., 1995; Lee et al., 2014). In the present study, we developed an effective strategy for therapeutic components based on $bvPLA_2$ which were isolated and purified from BV at good manufacturing practice (GMP) facility. To evaluate the translational relevance, we tested the neuroprotective effects of the standardized $bvPLA_2$ in MPTP-induced mouse model of PD. Additionally, dose-dependent effect of $bvPLA_2$ isolated from BV on MPTP-induced PD mice was investigated to determine an optimal dose. Thus, the present study may shed new light on developing new therapeutic targets for PD to provide a basis for standardization and GMP of $bvPLA_2$ drug.

MATERIALS AND METHODS

Animals

All experiments were performed in accordance with the approved animal protocols and guidelines established by Kyung Hee University. Briefly, 7- to 8-week-old male C57BL/6J mice were purchased from The Jackson Laboratory (Bar Harbor, ME, USA). All mice were maintained under pathogen-free conditions on a 12-h light/dark cycle and temperature-controlled conditions, with food and water *ad libitum*.

$BvPLA_2$ Isolation, Preparation, Manufacturing, and Quality Management

A standardized BV PLA2 was prepared by Inist St Co. Limited (Eumseong-gun, South Korea). For isolation and purification, raw BV was purchased from Bee Venom Lab LLC (Tbilisi, GA, USA) and dissolved in high performance liquid chromatography (HPLC) grade water at a concentration of 1 mg/ml. Then the diluted samples were applied to PTFE membrane filter (pore size 0.45 μm; Sigma-Aldrich, St Louis, MO, USA). To reduce the volume for the subsequent steps, the filtered mixtures were further concentrated by a tangential flow filtration (TFF) system, fitted with Pellicon 3 devices with Ultracel-10kDa membrane (Merck Millipore, Billerica, MA, USA). For manufacturing, the purified $bvPLA_2$ was dried with freeze-drying and was collected as a white powder. The $bvPLA_2$ content was determined using HPLC system and then diluted to a concentration of 0.1 mg/ml. Undesired substances including allergen were removed by membrane filters (pore size 0.22 μm PVDF sterile membrane filter; Jet Bio-Filtration Co., Ltd, Guangzhou, China). The separation and detection were carried out on reversed-phase (RP)-HPLC system on a C18 column (pore size: 180 Å; Sigma-Aldrich, St Louis, MO, USA) using a Waters 2695 liquid chromatograph and a Waters 2489 UV-visible detector (Waters Corporation, Milford, MA, USA). The sample was chromatographed at 25°C at a flow rate of 2 ml/min. The elution was performed with a linear gradient of 0%–80% acetonitrile in 0.1% trifluoroacetic acid (TFA; Sigma-Aldrich, St Louis, MO, USA) and the elution profile was monitored at 220 nm. The area of the peak detected was used to measure the recovery of $bvPLA_2$ and the separation profiles of purified $bvPLA_2$ were compared with those of commercial standard $bvPLA_2$ (Sigma-Aldrich, St Louis, MO, USA). The bioactivity of purified $bvPLA_2$ was compared with inactive mutated recombinant $bvPLA_2$-H34A (Lee et al., Manuscript submitted for publication). In order to measure bioactivity of purified $bvPLA_2$, PLA_2 activity was measured with EnzCheck PLA2 Assay Kit (Invitrogen, Carlsbad, CA, USA) according to the supplier's instructions. All these procedures were carried out at an aseptic GMP facility. For quality management, the purity test was performed to ensure that there was no detectable heavy metals, insoluble particulate matter, endotoxins, or microbes. A quality control using endotoxin assays was performed by Charles River Laboratories Korea (Incheon, South Korea). Certificate of Analysis, which specifies the pyrogenicity of the endotoxin assessed by kinetic turbidimetric assay, was supplied. The commercial standard endotoxin was dissolved and diluted with Limulus amebocyte lysate (LAL) reagent water (LRW) and tris aminomethane buffer in order to determine the endotoxin level of purified standard $bvPLA_2$. Changes in the $bvPLA_2$ content were examined for 3 months in stability test. Hence, based on these observations, the purified $bvPLA_2$ appeared to be appropriate as standardized $bvPLA_2$.

MPTP-Induced PD Mouse Model

1-Methyl-4-phenyl-1,2,3,6-tetrahydropyridine (MPTP; 20 mg/kg; Sigma-Aldrich, St Louis, MO, USA) was intraperitoneally (i.p.) administered to mice four times a day at 2 h intervals, inducing severe and persistent depletions of dopamine as previously described (Jackson-Lewis and Przedborski, 2007). During the experiment, mice were monitored for their physical condition and weight loss. The mortality rate of mice after MPTP injection was 0%–30% in each group and the animals surviving with <20% weight loss were included in the analysis.

$BvPLA_2$ Treatment

One day after the last MPTP injection, MPTP-injected mice were received with either $bvPLA_2$ or phosphate buffered saline (PBS). For administration, $bvPLA_2$ was dissolved in PBS and administered by once daily subcutaneous (s.c.) injections for six consecutive days in the concentration range of 0.01–0.5 mg/kg. Mice treated with commercial standard $bvPLA_2$ (Sigma-Aldrich, St Louis, MO, USA) by s.c. injection at a dose of 0.5 mg/kg for 6 days was used to compare the effect of purified $bvPLA_2$.

Immunohistochemistry

Immunohistochemical analysis was carried out, as previously described with minor modifications (Chung et al., 2015). Briefly, the tissues were incubated with the relevant primary antibody [tyrosine hydroxylase (TH; Mukhopadhyay and Stahl, 1995), Iba1 (1:2,000, Wako Pure Chemic Industries, Osaka, Japan), and ED1 (1:500, Serotec, Oxford, UK)] at 4°C overnight. Then, the tissues were incubated with biotinylated goat anti-secondary antibody (1:200, Vector Laboratories, Burlingame, CA, USA) and horseradish peroxidase (HRP)-conjugated streptavidin-biotin complex (Vectastain Elite ABC kit; Vector Laboratories) and visualized with diaminobenzidine (DAB). The stained cells were analyzed under a bright field microscope (Nikon, Tokyo, Japan).

Unbiased Stereological Estimation

Unbiased stereological estimation of the total number of TH-, ED1-, or H&E-positive cells was made using an optical fractionator as described previously, with minor modifications (West, 1993). In brief, the sections used for counting covered the entire SN from the rostral tip of the SN pars compacta (SNpc) to the caudal end of the SN pars reticulate (SNr). The counting was carried out using the Olympus CAST-Grid system (Olympus, Ballerup, Denmark). The counting frame was placed randomly on the first counting area and moved systematically over all counting areas until the entire delineated area was sampled. The total number of cells was calculated according to the optical fractionator equation (West et al., 1991).

Flow Cytometry

Flow cytometric detection of regulatory T cells was performed using fluorescein isothiocyanate (FITC)-conjugated anti-mouse CD4 (clone GK1.5; eBioscience, San Diego, CA, USA), phycoerythrin (PE)-conjugated anti-mouse CD25 (clone PC61.5; eBioscience, San Diego, CA, USA), and Alexa Fluor 647 anti-mouse Foxp3 (clone MF23; BD Pharmingen^{TM}, San Jose, CA, USA). The single-cell splenocytes were washed with PBS and stained with FITC-conjugated anti-CD4 and PE-labeled anti-CD25 antibodies in staining buffer. The cells were subsequently fixed and stained with Alexa Fluor 647 anti-Foxp3 antibody overnight at 4°C in the dark. After washing, the cells were stored at 4°C in the dark for subsequent detection.

Enzyme-Linked Immunosorbent Assay (ELISA)

To assess $CD4^+$ T helper (Th) cell subsets from splenocytes, we measured cytokine production by enzyme-linked immunosorbent assay (ELISA). First, the splenocytes at a concentration of 1×10^7 cells/ml were prepared from mice. Then, splenic $CD4^+$ T cells were isolated by positive selection using anti-CD4 (L3T4) MicroBeads (Miltenyi Biotec, Bergisch Gladbach, Germany) according to the manufacturer's instructions. The purified splenic $CD4^+$ T cells were stimulated for 12 h with 50 ng/ml of phorbol myristate acetate (Sigma-Aldrich, St Louis, MO, USA) and 1,000 ng/ml of ionomycin (Sigma-Aldrich, St Louis, MO, USA). The supernatants were taken and the levels of IFN-γ, IL-4, and IL-17A were measured from these supernatants by ELISA kits (BD Biosciences, San Jose, CA, USA) according to the supplier's instructions.

Pole Test

The degree of bradykinesia of the mouse was measured by the pole test with a slight modification of a previous protocol (Ogawa et al., 1985). Briefly, a tube of ∼50 cm in length and ∼1 cm in diameter was wrapped in gauze and a wooden pole was attached to the top. The time at which the mice turned completely downward and the total time to climb down the pole were measured with a cut-off limit of 30 s. Each mouse was given five trials, and the average of the best three measurements was used as the result. Trials, where the mouse jumped or slid down the pole, were excluded.

Statistical Analysis

Statistical analysis was performed using GraphPad Prism (v5.0; GraphPad) software. Each data was compared between conditions using unpaired *T*-test or one-way analysis of variance (ANOVA), or Kruskal-Wallis test followed by *post hoc* group comparisons. Data are expressed as the means ± standard error of the mean (SEM); $P < 0.05$ was considered significant.

RESULTS

Standardization of the Manufacturing Process of Bee Venom PLA_2

In the present study, we developed standardized methods for preparing $bvPLA_2$ from active components of European honeybee, *Apis mellifera* (**Figure 1A**). To purify the crude BV, the extract was ultra-filtrated and subsequently concentrated to increase the yield of $bvPLA_2$, as well as to remove undesirable products. Purified standard $bvPLA_2$ were identified and separated using RP-HPLC system with a C18 column (**Figure 1B**). Commercial standard $bvPLA_2$ was also used to identify the separation profiles of purified $bvPLA_2$ and determine the content of purified of $bvPLA_2$. Additionally, the bioactivity

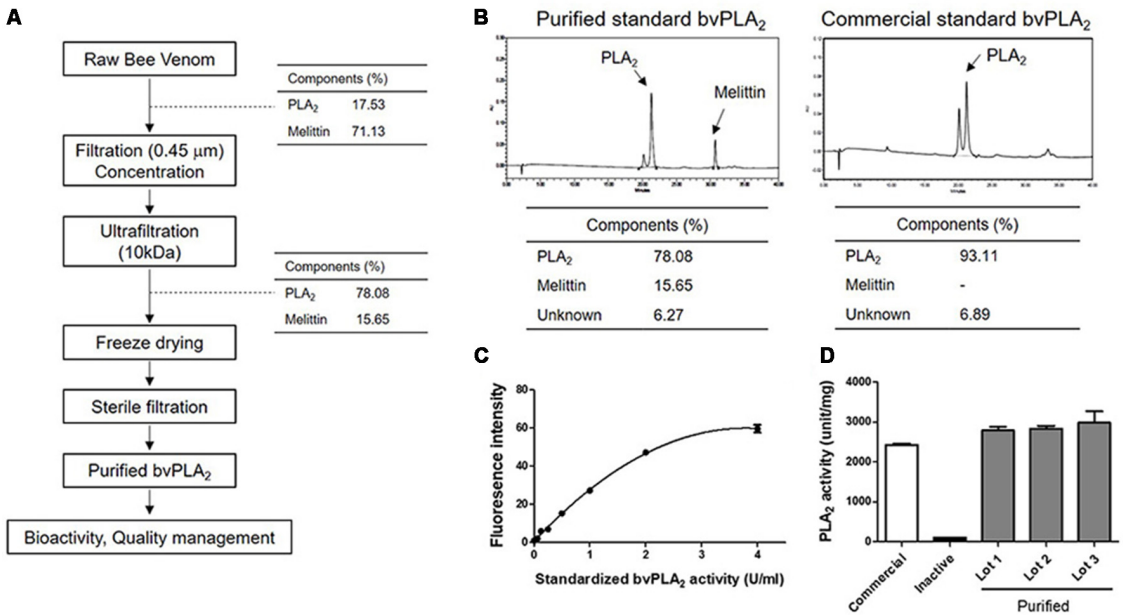

FIGURE 1 | Developing methods for preparing bee venom phospholipase A_2 (bvPLA$_2$) standard reagent from BV. **(A)** Purification and manufacturing process of PLA$_2$ from raw BV at a good manufacturing practice (GMP) facility. **(B)** Identification and determination of the purity of purified and commercial standard bvPLA$_2$. **(C)** Standard curve of purified standard bvPLA$_2$. **(D)** The activity of PLA$_2$ from purified bvPLA$_2$ isolated from BV (Lot 1–3), inactive recombinant mutant bvPLA$_2$ (bvPLA$_2$-H34A), and commercial bvPLA$_2$. Combined results were plotted from at least two independent experiments. The data are expressed as the means ± standard error of the mean (SEM).

test was carried out to test specific PLA$_2$ activity (**Figures 1C,D**). To ensure that purified bvPLA$_2$ was safe, we performed the quality control tests, resulting in that it had an allowable endotoxin level approved by US Food and Drug Administration (FDA; **Table 1**). Therefore, based on these observations, we considered this purified bvPLA$_2$ as properly manufactured and standardized agent.

BvPLA$_2$ Improves Motor Activity in a Dose-Dependent Manner in MPTP-Induced PD Mice

We first examined whether purified standard bvPLA$_2$ protected behavioral deficits in PD mice. As shown in **Figure 2A**, purified bvPLA$_2$ was given to MPTP-treated mice at a dose of 0.01, 0.1, or 0.5 mg/kg for six consecutive days, beginning 1 day after the last MPTP injection. On day 6 after MPTP treatment, MPTP-challenged mice took much longer than the control mice to turn downward (**Figure 2B**) and to descend the pole (**Figure 2C**), indicating basal ganglia-related movement disorders in MPTP-treated mice. Treatment of purified bvPLA$_2$ significantly shortened the time to turn and to down in MPTP-treated mice. However, inactive mutant bvPLA$_2$ (H34A) treatment induced no significant difference compared with

TABLE 1 | Endotoxin analysis of purified standard bee venom phospholipase A_2 (bvPLA$_2$).

Fold-dilution	Spike recovery (%)	CV (%)	Endotoxin value (EU/ml)
10	64	1.82	0.6915
50	98	0.83	0.3776
100	109	<0.01	0.5447
200	123	<0.01	0.6151

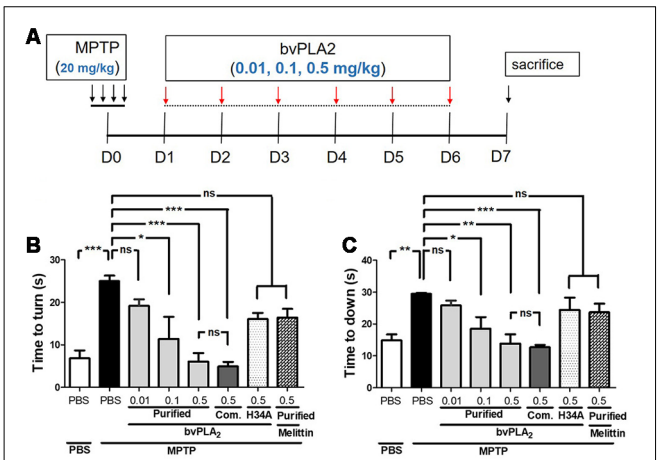

FIGURE 2 | Dose-dependent neuroprotection of purified standard bvPLA$_2$ on motor deficits in MPTP-injected mice. **(A)** Standard bvPLA$_2$ purified from BV (0.01, 0.1, or 0.5 mg/kg), commercial standard bvPLA$_2$ (Com. bvPLA$_2$; 0.5 mg/kg), inactive recombinant mutant bvPLA$_2$ (bvPLA$_2$-H34A; 0.5 mg/kg), or standard melittin purified from BV (0.5 mg/kg) was administered to the mice for 6 days, beginning 1 day after MPTP injection. **(B,C)** The motor ability of mice was evaluated on a pole test on day 6 post-MPTP. Time to orient downward **(B)** and total time to descend **(C)** were measured. The data are expressed as the means ± SEM, n = 5–8 per group; $^{*}p < 0.05$, $^{**}p < 0.01$, $^{***}p < 0.001$, ns, not significant.

MPTP-treated mice. No significant differences were detected between purified standard $bvPLA_2$ group and commercial standard $bvPLA_2$ group treated with the same dose (0.5 mg/kg). As observed, administration of purified standard $bvPLA_2$ improved motor deficits induced by MPTP in a concentration-dependent manner.

$BvPLA_2$ Is a Regulator of Peripheral Regulatory T Cell Differentiation

Growing body of evidence supported the role of regulatory T cells in the disease progression of PD both in human PD patients (Chen et al., 2015) and animal models of PD (Reynolds et al., 2010). Here, we speculated that the action of purified standard $bvPLA_2$ on improving sensorimotor function in PD mice may be related to the induction of Tregs in the periphery.

To address our hypothesis, we first measured the cellular proportions of Tregs in MPTP mice after treatment with different doses of $bvPLA_2$ (**Figure 3**). In fact, no significant difference in $CD4^+CD25^+Foxp3^+$ Treg populations was detected between control and MPTP mice on 7 days after MPTP challenge (**Figure 3B**). Importantly, administration of $bvPLA_2$ at a concentration of 0.1 and 0.5 mg/kg induced an increase in the number of splenic Tregs on MPTP-treated mice, when compared with mice treated with MPTP only. Whereas lower doses of $bvPLA_2$ (0.01 mg/kg) induced no significant differences in the population of Treg cells. Similarly, commercial $bvPLA_2$ (0.5 mg/kg) stimulated Treg induction in the periphery with no significant difference compared with purified standard $bvPLA_2$ (0.5 mg/kg). All these findings support the notion that $bvPLA_2$ induces the expansion of $CD4^+CD25^+Foxp3^+$ Treg in the periphery in PD, which can suppress the inflammatory response.

$BvPLA_2$ Inhibits the Expansion of Th1 and Th17 Effector Cells That Are Associated With PD

Since the balance of $CD4^+$ T cell subsets is highly correlated with disease activity in PD (Chen et al., 2015), we further

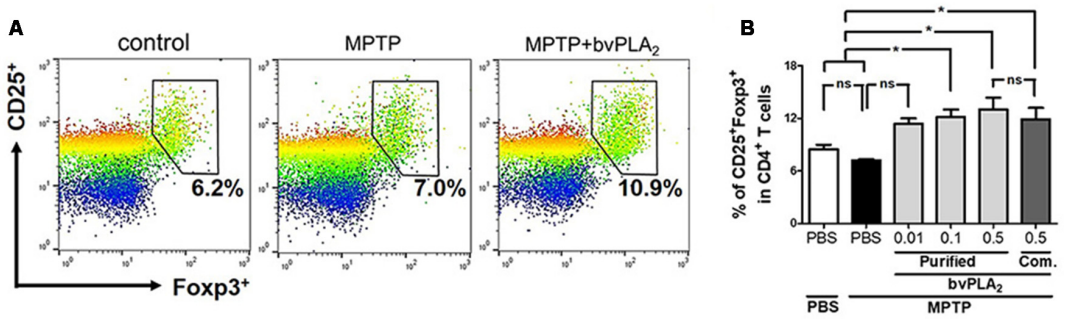

FIGURE 3 | Dose-dependent effect of purified standard $bvPLA_2$ on inducing differentiation of Treg cells in MPTP-treated mice. **(A,B)** On day 7 after MPTP treatment, $CD4^+CD25^+Foxp3^+$ regulatory T cells in splenocytes were analyzed by flow cytometry. The percentage of $CD25^+Foxp3^+$ cells in $CD4^+$ T cells were assessed in MPTP-treated mice with $bvPLA_2$ treatment (purified $bvPLA_2$: 0.01, 0.1, 0.5 mg/kg; commercial (Com.) $bvPLA_2$: 0.5 mg/kg) for consecutive 6 days after 1 day of MPTP challenge. Combined results from two independent experiments with at least three mice per group were plotted. MPTP+$bvPLA_2$ group: standard $bvPLA_2$, purified from crude BV, was injected from Day 1 to Day 6 post-MPTP at a concentration of 0.5 mg/kg. The data are expressed as the means ± SEM; $^*p < 0.05$, $^{**}p < 0.01$, $^{***}p < 0.001$, ns, not significant.

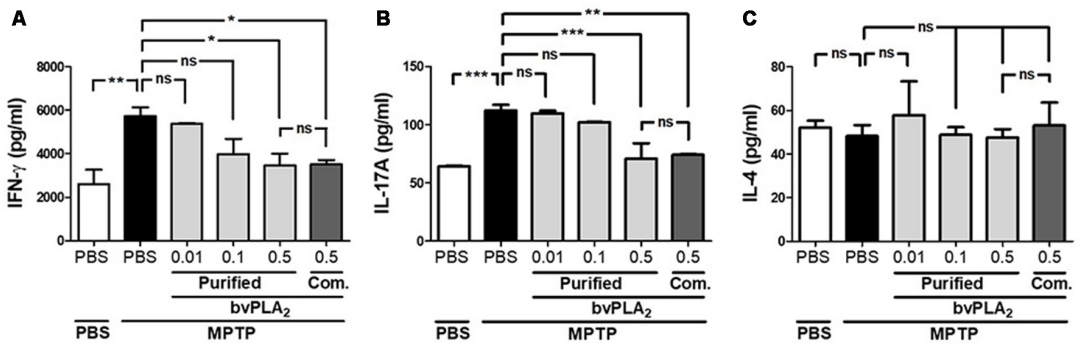

FIGURE 4 | Dose-dependent inhibitory effect of purified standard $bvPLA_2$ on Parkinson's disease (PD)-related Th1 and Th17 polarization. Th1, Th2, and Th17-polarizing conditions were analyzed by enzyme-linked immunosorbent assay (ELISA) of Th1 cytokine (IFN-γ; **A**), Th2 cytokine (IL-4; **C**), and Th17 cytokine (IL-17A; **B**) from the supernatants of splenic $CD4^+$ T cells in MPTP-injected mice treated with purified standard $bvPLA_2$ (0.01, 0.1, or 0.5 mg/kg) or commercial standard $bvPLA_2$ (Com. $bvPLA_2$; 0.5 mg/kg). The data are expressed as the means ± SEM, n = 3–5 per group; $^*p < 0.05$, $^{**}p < 0.01$, $^{***}p < 0.001$, ns, not significant.

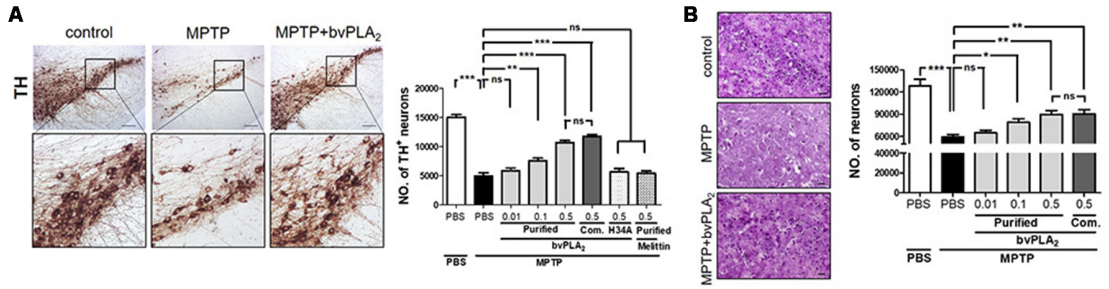

FIGURE 5 | Dose-dependent suppressive effect of purified standard bvPLA$_2$ on neuronal death of MPTP-challenged mice. Immunohistochemical staining for tyrosine hydroxylase (TH; **A**) or H&E **(B)** was carried out on MPTP mice with the treatment of standard bvPLA$_2$ purified from crude BV (0.01, 0.1, or 0.5 mg/kg) or commercial standard bvPLA$_2$ (Com. bvPLA$_2$; 0.5 mg/kg) on day 7 post-MPTP. Representative images of immunohistochemical staining for TH-positive or H&E stained cells in substantia nigra (SN) are shown. The number of stained cells was quantified by using an unbiased stereology. High-magnification images of boxed regions on TH-stained sections are also shown. MPTP+bvPLA$_2$ group: standard bvPLA$_2$, purified from crude BV, was injected from Day 1 to Day 6 post-MPTP at a concentration of 0.5 mg/kg. The data are expressed as the means ± SEM. n = 4–8 per group; $^*p < 0.05$, $^{**}p < 0.01$, $^{***}p < 0.001$, ns, not significant. Scale bar: 100 μm **(A)**; 50 μm **(B)**.

explored whether T helper subset balance was altered in PD. As shown in **Figure 4**, we assessed the differentiation of T helper (Th) cells based on their cytokine signature: IFN-γ-secreting Th1, IL-4-secreting Th2 and IL-17A-producing Th17 cells (Zhu et al., 2010). Obviously, MPTP treatment increased IFN-γ-secreting Th1 cells, but not IL-4-secreting Th2, indicating a shifted Th1/Th2 balance towards Th1 in PD mice (**Figure 4**). Additionally, we asked whether purified standard bvPLA$_2$ could reverse the altered balance of Th subsets in PD mice. Impressively, bvPLA$_2$ treatment significantly reduced the secretion of the two pro-inflammatory cytokines IFN-γ and IL-17A in a dose-dependent fashion (**Figure 4**). Commercial bvPLA$_2$ injection (0.5 mg/kg) also exhibited a similar suppressive effect on Th1- and Th17-polarizing cytokines associated with PD. These results showed that specific CD4$^+$ T subsets, including Th1 and Th17 cells, were markedly differentiated in PD induced by MPTP. Impressively, purified standard bvPLA$_2$ in a dose-dependent manner suppressed MPTP-mediated imbalance of CD4$^+$ T cell subsets.

BvPLA$_2$ Protects Dopaminergic Neurons Against MPTP Neurotoxicity in a Concentration-Dependent Manner

We further evaluated whether purified standard bvPLA$_2$ exhibited a dose-dependent neuroprotection against neuronal degeneration of PD. Expectedly, the immunohistochemistry data revealed apoptotic cell death in H&E stained and loss of dopaminergic neurons in TH stained sections of MPTP-challenged mice (**Figure 5**). In contrast, there was a dramatic neuronal protection in SN of MPTP mice following bvPLA$_2$ treatment in a dose-dependent manner. When administered at a comparative lower dose (0.01 mg/kg), bvPLA$_2$ administration did not significantly rescue MPTP-induced neuronal loss. Similar results were observed in MPTP mice given with commercial bvPLA$_2$ at a dose of 0.5 mg/kg. These data indicate that purified bvPLA$_2$ effectively attenuated the loss of dopaminergic neurons associated with PD in a concentration-dependent way.

BvPLA$_2$ Suppresses Microglial Activation Caused by MPTP in Mice in a Dose-Dependent Manner

Mounting evidence has demonstrated that microglial activation may play a key role in amplifying the neuroinflammatory response, which can exacerbate dopaminergic neuronal death (Kim and Joh, 2006). Hence, we examined the expression levels of microglia markers, such as Iba1 and ED1, to explore whether purified standard bvPLA$_2$ could directly suppress the activation of microglia. As shown in **Figure 6A**, the level of Iba1-positive microglia was markedly increased in the SN of MPTP mice at 7 days after MPTP post-injection, whereas bvPLA$_2$ administration clearly reduced the expression of Iba1 in PD mice a concentration-dependent manner. Similarly, MPTP caused a significant increase in ED1-positive neuronal cells compared with the control group, while administration of purified bvPLA$_2$ markedly reduced the number of ED1$^+$ microglia in the brains of MPTP-challenged mice (**Figures 6B,C**). The effect of commercial standard bvPLA$_2$ (0.5 mg/kg) appeared to be similar to that of 0.5 mg/kg of purified bvPLA$_2$, showing no difference between the two groups. All these findings support the notion that purified bvPLA$_2$ inhibits microglial activation in MPTP-treated mice in a dose-dependent manner.

DISCUSSION

In the present study, we developed an effective method of bvPLA$_2$ purification to create a valid and safe standardized medicine. Using MPTP animal models, we further demonstrated the therapeutic potential of purified standard bvPLA$_2$ against PD. Additionally, we identified the dose-dependent neuroprotective effect of purified standard bvPLA$_2$ on PD mice.

Growing evidence suggests that neuroinflammation is involved in the development and progression of PD (Wang et al., 2015). It is generally suggested that nerve damage in the pathogenesis of PD can be aggravated by the activated microglia producing an excess of pro-inflammatory cytokines.

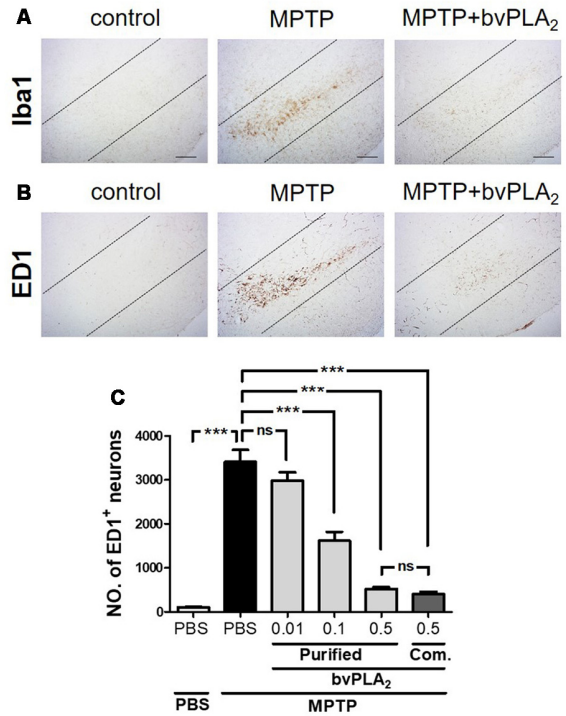

FIGURE 6 | Dose-dependent inhibitory effect of purified standard $bvPLA_2$ on microglial activation in the MPTP mouse model of PD. Immunohistochemical analysis was performed on MPTP-challenged mice treated with standard $bvPLA_2$ purified from crude BV (0.01, 0.1, or 0.5 mg/kg), or commercial standard $bvPLA_2$ (Com. $bvPLA_2$; 0.5 mg/kg) for consecutive 6 days. Representative images of sections containing Iba1- **(A)** or ED1-positive **(B)** neurons are displayed and dotted lines indicate SN pars compacta (SNpc). MPTP+$bvPLA_2$ group: standard $bvPLA_2$, purified from crude BV, was injected from Day 1 to Day 6 post-MPTP at a concentration of 0.5 mg/kg. **(C)** Unbiased stereological estimation for ED1-postive neurons was performed in SN region. The data are expressed as the means ± SEM. n = 3–5 per group; $^{***}p < 0.001$, ns, not significant. Scale bar: 100 μm.

In contrast, some recent studies have proposed that activated microglia, especially M2 microglia, can be beneficial, at least in the early phase of the neurodegeneration process (Hu et al., 2012). Additionally, a growing body of evidence suggests that neuroinflammatory processes can act as a double-edged sword in diverse pathologic conditions linked to neurodegenerative diseases (Wang et al., 2015). Hence, when identifying a novel anti-inflammatory drug for treating neurodegenerative disease, though evaluation to designate a therapeutic window at a minimum effective dose is necessary.

To our knowledge, the present study was the first to present manufacturing process of $bvPLA_2$ from crude BV, as well as to assess its therapeutic efficacy for treatment of PD. We developed effective strategies to isolate and purified $bvPLA_2$ from active components of crude BV at GMP facilities. The separated $bvPLA_2$ displayed bioactivity with showing a specific activity of about 2,000 unit/mg. In order to evaluate translational relevance and therapeutic potential of purified $bvPLA_2$, we examined the therapeutic effect of purified $bvPLA_2$ by injecting three different doses (0.01, 0.1, 0.5 mg/kg) on MPTP-challenged PD mice. Indeed, it is known that high doses of $bvPLA_2$ (2.5 mg/kg) can cause a variety of allergic reactions, while relatively low doses of $bvPLA_2$ (0.25 mg/kg) induce protective effects against inflammatory conditions (Palm et al., 2013). Previously, we also observed that relatively low doses of $bvPLA_2$ (0.2–0.5 mg/kg) could induce anti-inflammatory effects in murine models of atopic dermatitis (Jung et al., 2017) and asthma (Park et al., 2015). Hence, we assumed the biological function of $bvPLA_2$ may differ in a dose-dependent manner, reflecting that at low doses $bvPLA_2$ act more generally to reduce neuroinflammation. Further studies are required to clarify the paradoxical effect and dose-dependent activity of $bvPLA_2$.

In this study, we found a dose-dependent neuroprotective effect of purified standard $bvPLA_2$ containing ∼78% of PLA_2 and ∼15% of melittin. In line with the experiments with purified bvPLA2, we also examined whether melittin caused a neuroprotective effect against PD by isolated from crude BV with high purity (98.5% of melittin). Administration of purified melittin did not induce any neuroprotective effect on PD mice. Additionally, the inactive mutant of $bvPLA_2$ ($bvPLA_2$-H34A) caused an inhibitory effect on the neuronal death and motor deficits in MPTP-challenged mice. Melittin is a major component of BV, comprising around 50% of dry venom. Recently, many studies have reported the therapeutic effects of melittin against cancers, neurodegenerative diseases and chronic inflammatory diseases including rheumatism (Park et al., 2004; Yang et al., 2011; Rady et al., 2017). It has been suggested that the biological activity of $bvPLA_2$ can be enhanced by melittin (Mingarro et al., 1995; Shen et al., 2010). Certainly, more detailed sets of experimental investigations are needed to verify its potential usefulness in the future applications.

The initial study regarding the involvement of inflammation in PD progression over 30 years ago clearly reported activated microglia in the SN of a PD patient (McGeer et al., 1988). Since then accumulated studies support the role of activated microglia and increased inflammatory mediators in the pathology of PD (Collins et al., 2012). In particular, accumulating evidence suggests the important role of adaptive immune system in the development and progression of PD (Ferrari and Tarelli, 2011). Importantly, the cytotoxic $CD4^+$ T cells have been discovered in the SN of PD patients and animal PD models (Brochard et al., 2009; Stone et al., 2009). Indeed, the adaptive immune system would modulate neuroinflammatory response *via* regulation of microglia activation (Tansey and Goldberg, 2010). In this study, we observed the inhibitory effect of $bvPLA_2$ isolated and purified from BV on dopaminergic cell loss of MPTP mice. Impressively, induction of immunosuppressive regulatory T cells was observed in MPTP mice treated with purified standard $bvPLA_2$. These results suggest that $bvPLA_2$ may exert anti-inflammatory action *via* activation of Treg cells, which can suppress the inflammatory process by targeting cytotoxic $CD4^+$ T cells.

In summary, we standardized the purification process to provide standard $bvPLA_2$ from active component of crude BV and observed dose-dependent therapeutic effect of standard $bvPLA_2$ on MPTP-induced PD mice. Based on our results, it appears that $bvPLA_2$ is a potent drug that can promote the survival of dopaminergic neurons, suggesting

a novel therapeutic candidate as an add-on to conventional dopaminergic substitution treatments.

ETHICS STATEMENT

All experiments were performed in accordance with the approved animal protocols and guidelines established by Kyung Hee University.

AUTHOR CONTRIBUTIONS

KK and HB conceived and designed the project. KK, SL, JS, and HJ performed the experiments and analyzed the data. J-TH was in charge of standardization of the manufacturing process of $bvPLA_2$ from crude BV. The manuscript was written by KK and HB.

FUNDING

This work was supported by the Basic Science Research Program through the National Research Foundation (NRF) of South Korea funded by the Ministry of Science, ICT and Future Planning (NRF-2017R1A2B3009574), the Korea Health Technology R&D Project through the Korea Health Industry Development Institute (KHIDI), funded by the Ministry of Health and Welfare, South Korea (HI17C0978).

REFERENCES

Ameratunga, R. V., Hawkins, R., Prestidge, R., and Marbrook, J. (1995). A high efficiency method for purification and assay of bee venom phospholipase A2. *Pathology* 27, 157–160. doi: 10.1080/00313029500169782

Bertram, L., and Tanzi, R. E. (2005). The genetic epidemiology of neurodegenerative disease. *J. Clin. Invest.* 115, 1449–1457. doi: 10.1172/jci24761

Brochard, V., Combadiere, B., Prigent, A., Laouar, Y., Perrin, A., Beray-Berthat, V., et al. (2009). Infiltration of $CD4^+$ lymphocytes into the brain contributes to neurodegeneration in a mouse model of Parkinson disease. *J. Clin. Invest.* 119, 182–192. doi: 10.1172/JCI36470

Chen, Y., Qi, B., Xu, W., Ma, B., Li, L., Chen, Q., et al. (2015). Clinical correlation of peripheral CD4+cell subsets, their imbalance and Parkinson's disease. *Mol. Med. Rep.* 12, 6105–6111. doi: 10.3892/mmr.2015.4136

Chung, E. S., Lee, G., Lee, C., Ye, M., Chung, H. S., Kim, H., et al. (2015). Bee venom phospholipase A2, a novel Foxp3+ regulatory T cell inducer, protects dopaminergic neurons by modulating neuroinflammatory responses in a mouse model of Parkinson's disease. *J. Immunol.* 195, 4853–4860. doi: 10.4049/jimmunol.1500386

Collins, L. M., Toulouse, A., Connor, T. J., and Nolan, Y. M. (2012). Contributions of central and systemic inflammation to the pathophysiology of Parkinson's disease. *Neuropharmacology* 62, 2154–2168. doi: 10.1016/j.neuropharm.2012.01.028

de Lau, L. M., Giesbergen, P. C., de Rijk, M. C., Hofman, A., Koudstaal, P. J., and Breteler, M. M. (2004). Incidence of parkinsonism and Parkinson disease in a general population: the Rotterdam study. *Neurology* 63, 1240–1244. doi: 10.1212/01.wnl.0000140706.52798.be

Ferrari, C. C., and Tarelli, R. (2011). Parkinson's disease and systemic inflammation. *Parkinsons. Dis.* 2011:436813. doi: 10.4061/2011/436813

Habermann, E. (1972). Bee and wasp venoms. *Science* 177, 314–322. doi: 10.1126/science.177.4046.314

Hossen, M. S., Ali, M. Y., Jahurul, M. H. A., Abdel-Daim, M. M., Gan, S. H., and Khalil, M. I. (2017). Beneficial roles of honey polyphenols against some human degenerative diseases: a review. *Pharmacol. Rep.* 69, 1194–1205. doi: 10.1016/j.pharep.2017.07.002

Hossen, M. S., Shapla, U. M., Gan, S. H., and Khalil, M. I. (2016). Impact of bee venom enzymes on diseases and immune responses. *Molecules* 22:E25. doi: 10.3390/molecules22010025

Hu, X., Li, P., Guo, Y., Wang, H., Leak, R. K., Chen, S., et al. (2012). Microglia/macrophage polarization dynamics reveal novel mechanism of injury expansion after focal cerebral ischemia. *Stroke* 43, 3063–3070. doi: 10.1161/strokeaha.112.659656

Jackson-Lewis, V., and Przedborski, S. (2007). Protocol for the MPTP mouse model of Parkinson's disease. *Nat. Protoc.* 2, 141–151. doi: 10.1038/nprot.2006.342

Jeong, J. K., Moon, M. H., Bae, B. C., Lee, Y. J., Seol, J. W., and Park, S. Y. (2011). Bee venom phospholipase A2 prevents prion peptide induced-cell death in neuronal cells. *Int. J. Mol. Med.* 28, 867–873. doi: 10.3892/ijmm.2011.730

Jung, K. H., Baek, H., Kang, M., Kim, N., Lee, S. Y., and Bae, H. (2017). Bee venom phospholipase A2 ameliorates house dust mite extract induced atopic dermatitis like skin lesions in mice. *Toxins* 9:E68. doi: 10.3390/toxins9020068

Kim, Y. S., and Joh, T. H. (2006). Microglia, major player in the brain inflammation: their roles in the pathogenesis of Parkinson's disease. *Exp. Mol. Med.* 38, 333–347. doi: 10.1038/emm.2006.40

Lang, A. E., and Lozano, A. M. (1998). Parkinson's disease. First of two parts. *N. Engl. J. Med.* 339, 1044–1053. doi: 10.1056/NEJM199810083391506

Lee, J. A., Son, M. J., Choi, J., Jun, J. H., Kim, J. I., and Lee, M. S. (2014). Bee venom acupuncture for rheumatoid arthritis: a systematic review of randomised clinical trials. *BMJ Open* 4:e006140. doi: 10.1136/bmjopen-2014-006140

McGeer, P. L., Itagaki, S., Boyes, B. E., and McGeer, E. G. (1988). Reactive microglia are positive for HLA-DR in the substantia nigra of Parkinson's and Alzheimer's disease brains. *Neurology* 38, 1285–1291. doi: 10.1212/wnl.38.8.1285

Mingarro, I., Pérez-Payá, E., Pinilla, C., Appel, J. R., Houghten, R. A., and Blondelle, S. E. (1995). Activation of bee venom phospholipase A2 through a peptide-enzyme complex. *FEBS Lett.* 372, 131–134. doi: 10.1016/0014-5793(95)00964-b

Mukhopadhyay, A., and Stahl, P. (1995). Bee venom phospholipase A2 is recognized by the macrophage mannose receptor. *Arch. Biochem. Biophys.* 324, 78–84. doi: 10.1006/abbi.1995.9926

Ogawa, N., Hirose, Y., Ohara, S., Ono, T., and Watanabe, Y. (1985). A simple quantitative bradykinesia test in MPTP-treated mice. *Res. Commun. Chem. Pathol. Pharmacol.* 50, 435–441.

Palm, N. W., Rosenstein, R. K., Yu, S., Schenten, D. D., Florsheim, E., and Medzhitov, R. (2013). Bee venom phospholipase A2 induces a primary type 2 response that is dependent on the receptor ST2 and confers protective immunity. *Immunity* 39, 976–985. doi: 10.1016/j.immuni.2013.10.006

Park, S., Baek, H., Jung, K. H., Lee, G., Lee, H., Kang, G. H., et al. (2015). Bee venom phospholipase A2 suppresses allergic airway inflammation in an ovalbumin-induced asthma model through the induction of regulatory T cells. *Immun. Inflamm. Dis.* 3, 386–397. doi: 10.1002/iid3.76

Park, H. J., Lee, S. H., Son, D. J., Oh, K. W., Kim, K. H., Song, H. S., et al. (2004). Antiarthritic effect of bee venom: inhibition of inflammation mediator generation by suppression of NF-kappaB through interaction with the p50 subunit. *Arthritis Rheum.* 50, 3504–3515. doi: 10.1002/art.20626

Rady, I., Siddiqui, I. A., Rady, M., and Mukhtar, H. (2017). Melittin, a major peptide component of bee venom and its conjugates in cancer therapy. *Cancer Lett.* 402, 16–31. doi: 10.1016/j.canlet.2017.05.010

Reynolds, A. D., Stone, D. K., Hutter, J. A., Benner, E. J., Mosley, R. L., and Gendelman, H. E. (2010). Regulatory T cells attenuate Th17 cell-mediated nigrostriatal dopaminergic neurodegeneration in a model of Parkinson's disease. *J. Immunol.* 184, 2261–2271. doi: 10.4049/jimmunol.0901852

Sakaguchi, S., Yamaguchi, T., Nomura, T., and Ono, M. (2008). Regulatory T cells and immune tolerance. *Cell* 133, 775–787. doi: 10.1016/j.cell.2008.05.009

Samii, A., Etminan, M., Wiens, M. O., and Jafari, S. (2009). NSAID use and the risk of Parkinson's disease: systematic review and meta-analysis of observational studies. *Drugs Aging* 26, 769–779. doi: 10.2165/11316780-000000000-00000

Shen, L. R., Ding, M. H., Zhang, L. W., Zhang, W. G., Liu, L., and Li, D. (2010). Expression of a bee venom phospholipase A2 from Apis cerana cerana in the baculovirus-insect cell. *J. Zhejiang Univ. Sci. B* 11, 342–349. doi: 10.1631/jzus.b0900254

Stone, D. K., Reynolds, A. D., Mosley, R. L., and Gendelman, H. E. (2009). Innate and adaptive immunity for the pathobiology of Parkinson's disease. *Antioxid. Redox Signal.* 11, 2151–2166. doi: 10.1089/ARS.2009.2460

Tansey, M. G., and Goldberg, M. S. (2010). Neuroinflammation in Parkinson's disease: its role in neuronal death and implications for therapeutic intervention. *Neurobiol. Dis.* 37, 510–518. doi: 10.1016/j.nbd.2009.11.004

Tufekci, K. U., Meuwissen, R., Genc, S., and Genc, K. (2012). Inflammation in Parkinson's disease. *Adv. Protein Chem. Struct. Biol.* 88, 69–132. doi: 10.1016/B978-0-12-398314-5.00004-0

Wang, Q., Liu, Y., and Zhou, J. (2015). Neuroinflammation in Parkinson's disease and its potential as therapeutic target. *Transl. Neurodegener.* 4:19. doi: 10.1186/s40035-015-0042-0

West, M. J. (1993). New stereological methods for counting neurons. *Neurobiol. Aging* 14, 275–285. doi: 10.1016/0197-4580(93)90112-o

West, M. J., Slomianka, L., and Gundersen, H. J. (1991). Unbiased stereological estimation of the total number of neurons in thesubdivisions of the rat hippocampus using the optical fractionator. *Anat. Rec.* 231, 482–497. doi: 10.1002/ar.1092310411

Yang, E. J., Kim, S. H., Yang, S. C., Lee, S. M., and Choi, S. M. (2011). Melittin restores proteasome function in an animal model of ALS. *J. Neuroinflammation* 8:69. doi: 10.1186/1742-2094-8-69

Ye, M., Chung, H. S., Lee, C., Yoon, M. S., Yu, A. R., Kim, J. S., et al. (2016). Neuroprotective effects of bee venom phospholipase A2 in the 3xTg AD mouse model of Alzheimer's disease. *J. Neuroinflammation* 13:10. doi: 10.1186/s12974-016-0476-z

Zhu, J., Yamane, H., and Paul, W. E. (2010). Differentiation of effector CD4 T cell populations*. *Annu. Rev. Immunol.* 28, 445–489. doi: 10.1146/annurev-immunol-030409-101212

Conflict of Interest Statement: J-TH was employed by company Inist ST Co. Ltd.

The remaining authors declare that the research was conducted in the absence of any commercial or financial relationships that could be construed as a potential conflict of interest.

frontiers in Aging Neuroscience

SYSTEMATIC REVIEW
published: 08 May 2019
doi: 10.3389/fnagi.2019.00102

Does Acupuncture Protect Dopamine Neurons in Parkinson's Disease Rodent Model?: A Systematic Review and Meta-Analysis

Jade Heejae Ko[1,2], *Hyangsook Lee*[3,4], *Seung-Nam Kim*[1*] and *Hi-Joon Park*[3,4*]

[1] College of Korean Medicine, Dongguk University, Goyang, South Korea, [2] Graduate School, Dongguk University, Seoul, South Korea, [3] Acupuncture and Meridian Science Research Center, Seoul, South Korea, [4] College of Korean Medicine, Kyung Hee University, Seoul, South Korea

Background: Acupuncture has been reported to have significant effects, not only in alleviating impaired motor function, but also rescuing dopaminergic neuron deficits in rodent models of Parkinson's disease (PD). However, a systemic analysis of these beneficial effects has yet to be performed.

Objective: To evaluate the neuroprotective effect of acupuncture in animal models of PD.

Methods: A literature search of the PubMed, MEDLINE, EMBASE, China National Knowledge Infrastructure, Research Information Service System, and Japan Society of Acupuncture and Moxibustion databases was performed to retrieve studies that investigated the effects of acupuncture on PD. The quality of each included study was evaluated using the 10-item checklist modified from the Collaborative Approach to Meta-Analysis and Review of Animal Data from Experimental Studies. RevMan version 5.3 (Foundation for Statistical Computing, Vienna, Austria) was used for meta-analysis.

Results: The 42 studies included scored between 2 and 7 points, with a mean score of 4.6. Outcome measures included tyrosine hydroxylase (TH) level and dopamine content. Meta-analysis results revealed statistically significant effects of acupuncture for increasing both TH levels (33.97 [95% CI 33.15–34.79]; $p < 0.00001$) and dopamine content (4.23 [95% CI 3.53–4.92]; $p < 0.00001$) compared with that observed in PD control groups. In addition, motor dysfunctions exhibited by model PD animals were also mitigated by acupuncture treatment.

Conclusions: Although there were limitations in the number and quality of the included studies, results of this analysis suggest that acupuncture exerts a protective effect on dopaminergic neurons in rodent models of PD.

Keywords: acupuncture, dopamine neuroprotection, meta analysis, Parkinson's disease, rodent model, systematic review

OPEN ACCESS

Edited by:
Allison B. Reiss,
Winthrop University Hospital,
United States

Reviewed by:
Peggy Bosch,
Radboud University Nijmegen,
Netherlands
Zhe Zhang,
Shandong University of Traditional Chinese Medicine, China

***Correspondence:**
Seung-Nam Kim
snkim@dongguk.edu
Hi-Joon Park
acufind@khu.ac.kr

Received: *28 December 2018*
Accepted: *16 April 2019*
Published: *08 May 2019*

Citation:
Ko JH, Lee H, Kim S-N and Park H-J (2019) Does Acupuncture Protect Dopamine Neurons in Parkinson's Disease Rodent Model?: A Systematic Review and Meta-Analysis. Front. Aging Neurosci. 11:102. doi: 10.3389/fnagi.2019.00102

INTRODUCTION

Parkinson's disease (PD) is a neurodegenerative disorder first described by Dr. James Parkinson in 1817 as a "shaking palsy" (Demaagd and Philip, 2015). PD is characterized by motor symptoms, such as rigidity, resting tremors, and postural instability, and non-motor symptoms including sleep disturbance, hallucinations, and constipation (Demaagd and Philip, 2015). It has been reported that 1–2% of the global population >65 years of age is affected by PD (Alves et al., 2008). In terms of pathology, recent studies have suggested that PD is closely associated with the loss of dopaminergic (DA) neurons in the substantia nigra (SN) pars compacta of the brain caused by familial and/or sporadic factors (Zhou et al., 2008; Surmeier et al., 2010; Blesa et al., 2015). Levodopa has been widely used in recent decades for the management of PD; however, complications following the use of levodopa are considerable.

In East Asian countries, acupuncture has long been used to treat motor dysfunction and brain disorders such as PD (Joh et al., 2010). Moreover, in recent years, it has been shown that acupuncture improves motor function in rodent models of PD via mechanisms including anti-inflammatory and neurotrophic effects (Yu et al., 2010; Rui et al., 2013). Furthermore, the effect of acupuncture on PD has been demonstrated in clinical studies. Improvement in motor function in PD patients who underwent bee venom acupuncture treatment has been reported (Cho et al., 2012), and motor function-associated neural responses with acupuncture have also been shown in PD patients using functional magnetic resonance imaging fMRI (Chae et al., 2009; Yeo et al., 2012). Additionally, a systematic review of clinical studies of acupuncture involving PD patients demonstrated the potential effectiveness of acupuncture (Lam et al., 2008). Accordingly, acupuncture has been suggested as an integrative medicine treatment for PD.

As mentioned earlier, destruction and recovery of DA neurons in the SN, which play critical role in motor functions, is significant in terms of the pathology of PD. Thus, it is important to investigate the extent to which acupuncture treatment affects the recovery of DA neurons. Rodent models have been widely used in PD research because they can provide valuable information in terms of understanding pathogenic processes and developing effective therapies (Duty and Jenner, 2011; Blandini and Armentero, 2012).

Recent rodent-based studies have demonstrated that acupuncture recovered DA neurons in a mouse model of 1-methyl-4-phenyl-1,2,3,6-tetrahydropyridine (MPTP)-induced PD, and in a 6-hydroxydopamine (6-OHDA)-induced PD rat model (Kim et al., 2005; Jeon et al., 2008; Park et al., 2015). In contrast, it was also reported that acupuncture treatment did not demonstrate a neuroprotective effect in an MPTP mouse model (Yang et al., 2017).

Therefore, the present systematic review and meta-analysis aimed to assess the pre-clinical evidence supporting the neuroprotective effects of acupuncture in rodent models of PD.

METHODS

Literature Search

English-language studies that examined the neuroprotective effect of acupuncture in PD rodent models were included in the present study. The PubMed, EMBASE, and MEDLINE, China National Knowledge Infrastructure, Research Information Service System, and Japan Society of Acupuncture and Moxibustion databases were searched from inception until June 2018 using the following search terms: "mouse (mice)" or "rat (rats)," "acupuncture (electroacupuncture)," and "Parkinson's disease."

Inclusion/Exclusion Criteria

Studies were included based on the following criteria: subjects (rodent models of PD); intervention (acupuncture as the main intervention, but limited to manual acupuncture [MA] and electroacupuncture [EA]); and outcomes (tyrosine hydroxylase [TH] and DA neuron level were the main outcomes to evaluate the efficacy of acupuncture). Behavioral test data were the subsequent outcome to evaluate motor functions in PD rodent models. Studies not reporting exact outcome values and full-text articles not published in English were excluded.

Data Extraction

Two authors (Kim and Ko) extracted the data independently. Data extracted from the databases included the following: publication year, name of the first author, and type of rodent PD model; type of acupuncture; results of behavioral tests; and the outcome of treatment in acupuncture-treated groups. Three studies were excluded because exact outcome values were not reported; thus, 42 original research articles were selected for further analysis.

Quality Assessment

The methodological quality of each included study was assessed by two authors (Kim and Ko) using a 10-item checklist modified from the Collaborative Approach to Meta-Analysis and Review of Animal Data from Experimental Studies checklist (Sena et al., 2007): publication in a peer-reviewed journal; statements describing temperature control; random allocation to treatment or control; blinded building of the model; use of aged animal models; blinded assessment of outcome; use of anesthetic without significant intrinsic neuroprotective activity; sample size calculation; compliance with animal welfare regulations; and declarations of any potential conflicts of interest. A sum of the quality scores was recorded for each article, with a possible total score of 10 points.

Statistical Analysis

In each study, densitometry of TH-positive (TH+) staining or stereological cell counting results or dopamine content were considered as continuous data. Because the same comparison was used in the studies (i.e., compared with a control group), the mean differences for effect sizes were estimated based on a fixed-effects model. Publication bias was assessed using a funnel plot. To examine the influence of the type of rodent model

on the outcome measures, specific subgroups were defined: MPTP-induced PD model; 6-OHDA-induced PD model; medial forebrain bundle (MFB)-axotomy-induced PD model; and an alpha-synuclein (α-syn) mutation PD model.

The meta-analysis was performed using RevMan version 5.3 (Foundation for Statistical Computing, Vienna, Austria). The confidence interval was established at 95%, and $p < 0.05$ was considered to be statistically significant. For the assessment of study heterogeneity, the chi-squared distribution and I^2 statistic were used.

RESULTS

Study Inclusion

Among 123 initially identified studies, 78 were excluded because the full-texts were not available in English. Full-text screening was performed for the remaining 45 studies, of which 3 were excluded due to deficiency in exact outcome values. A total of 42 studies were, therefore, included in the present review. A flow diagram of the study selection process is shown in **Figure 1**.

Study Characteristics

Of the 42 studies, 23 used EA and 19 used MA. Of the PD models used in these studies, 21 used an MPTP-induced PD model, 15 used a 6-OHDA-induced PD model; and 5 other studies used an MFB lesion-induced PD model. One study used an A53T α-syn transgenic mouse model.

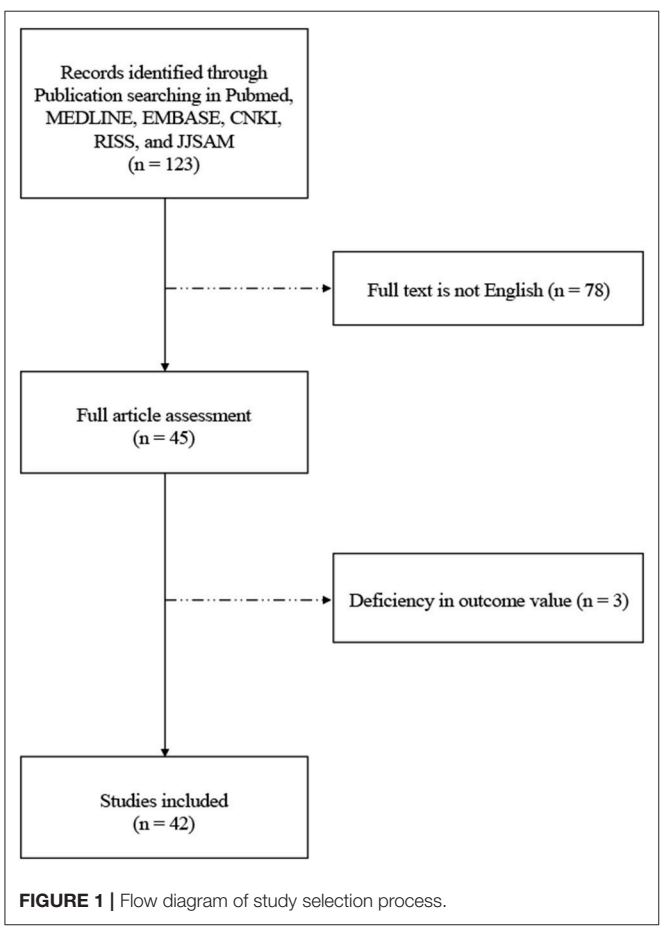

FIGURE 1 | Flow diagram of study selection process.

TABLE 1 | Quality assessment.

References	Q1	Q2	Q3	Q4	Q5	Q6	Q7	Q8	Q9	Q10	Score
Liang et al., 2002	✓		✓				✓				3
Liang et al., 2003	✓		✓				✓		✓		4
Park et al., 2003	✓	✓	✓			✓	✓		✓		6
Kim et al., 2005	✓	✓	✓				✓				4
Kang et al., 2007	✓		✓				✓				3
Jeon et al., 2008	✓		✓				✓		✓	✓	5
Choi et al., 2009	✓		✓				✓				3
Jia et al., 2009	✓		✓			✓	✓				4
Hong et al., 2010	✓	✓	✓						✓		4
Jia et al., 2010	✓		✓						✓		3
Kim et al., 2010	✓		✓						✓		3
Yu et al., 2010	✓	✓	✓			✓	✓		✓		6
Choi et al., 2011a	✓		✓				✓		✓		4
Choi et al., 2011b	✓		✓				✓		✓		4
Kim et al., 2011a	✓		✓			✓			✓	✓	5
Kim et al., 2011b	✓		✓			✓			✓	✓	5
Wang et al., 2011	✓	✓	✓			✓			✓	✓	6
Yeo et al., 2013	✓		✓				✓		✓	✓	5
Huo et al., 2012	✓		✓			✓	✓		✓	✓	6
Sun et al., 2012	✓		✓			✓	✓		✓		5
Rui et al., 2013	✓	✓	✓			✓	✓		✓		6
Wang et al., 2013	✓	✓	✓			✓			✓		5
Yu et al., 2016	✓		✓			✓	✓		✓		5
Kim et al., 2014	✓		✓			✓	✓		✓		5
Deng et al., 2015	✓		✓				✓		✓	✓	5
Lv et al., 2015	✓		✓			✓	✓		✓	✓	6
Park et al., 2015	✓	✓	✓						✓	✓	5
Shen et al., 2015	✓		✓						✓	✓	4
Yeo et al., 2015	✓		✓						✓		3
Jia et al., 2017	✓		✓			✓	✓		✓	✓	6
Sun et al., 2016	✓	✓	✓			✓	✓		✓	✓	7
Tian et al., 2016	✓		✓								2
Yang et al., 2011	✓	✓	✓				✓		✓	✓	6
Yang et al., 2017	✓	✓	✓			✓	✓		✓	✓	6
Park et al., 2017	✓	✓	✓			✓			✓	✓	6
Jeon et al., 2017	✓	✓	✓						✓	✓	5
Lee et al., 2018	✓	✓	✓						✓	✓	5
Lu et al., 2017	✓	✓	✓				✓		✓	✓	6
Li et al., 2017a	✓		✓								2
Li et al., 2017b	✓		✓								2
Lin et al., 2017	✓		✓						✓	✓	4
Wang et al., 2018	✓		✓				✓		✓	✓	5

Q1, publication in a peer-reviewed journal; Q2, statements describing control of temperature; Q3, random allocation to treatment or control; Q4, blinded building of model; Q5, use of aged animal model; Q6, blinded assessment of outcome; Q7, use of anesthetic without significant intrinsic neuroprotective activity; Q8, sample size calculation; Q9, compliance with animal welfare regulations; Q10, declared any potential conflict of interest.

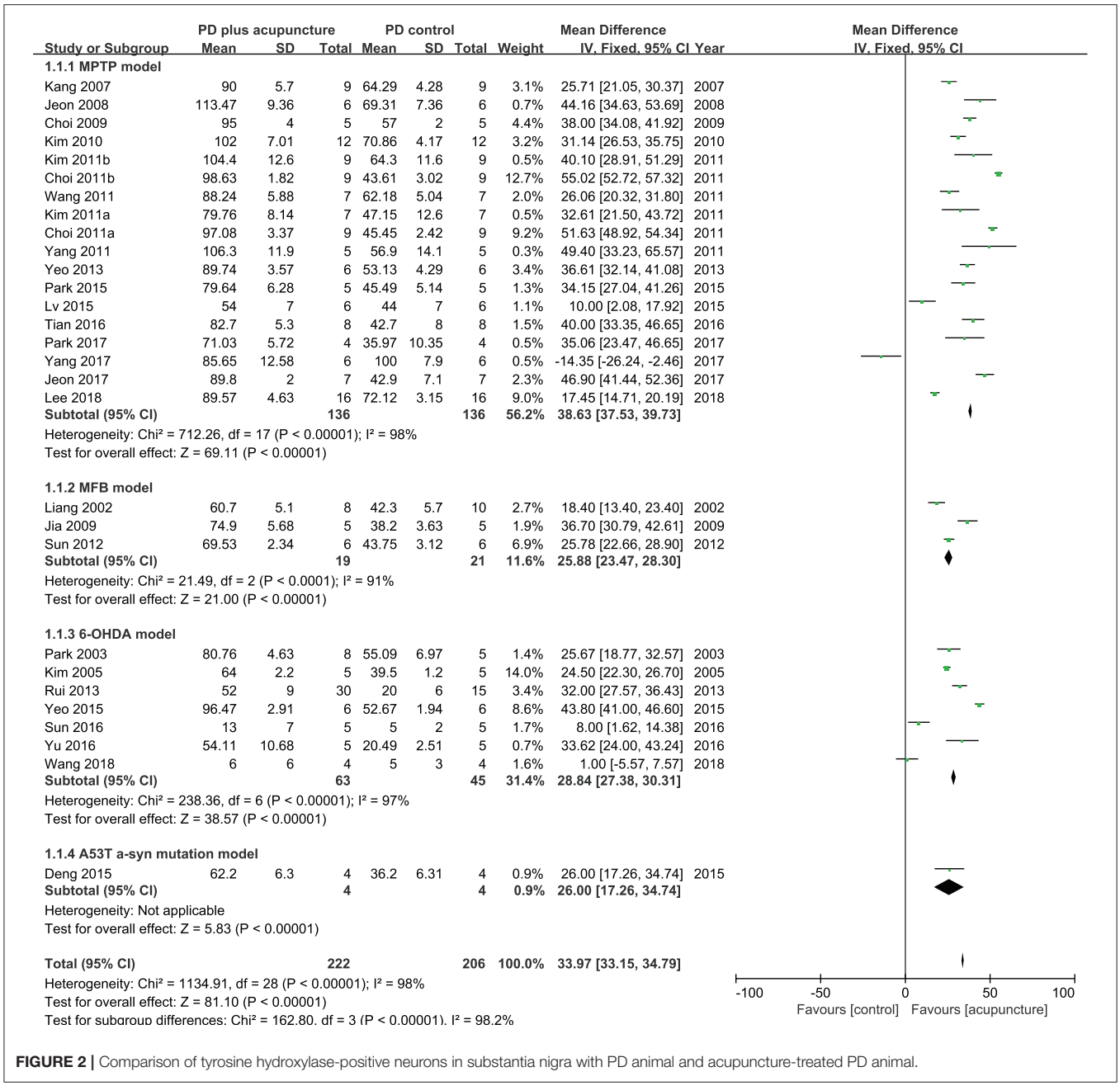

FIGURE 2 | Comparison of tyrosine hydroxylase-positive neurons in substantia nigra with PD animal and acupuncture-treated PD animal.

Quality Assessment

The quality assessment of the included studies is summarized in **Table 1**. The quality score of the included studies ranged from 2 to 7 of a total 10 points. One study scored 7, 11 scored 6, 13 scored 5, 8 scored 4, 6 scored 3, and 3 studies scored 2 points. All the 42 studies were peer-reviewed and included randomly allocated control and acupuncture groups. Fifteen studies included statements describing temperature control, 17 described blinded assessment of outcomes, and 25 reported use of anesthetic without significant intrinsic neuroprotective activity. Thirty-four studies reported compliance with animal welfare regulations and 20 declared potential conflicts of interest. No study conducted blind building of the model or sample size calculation. Finally, no study used aged animals.

Effect of Acupuncture on DA Neuron Protection

TH has a specific role in dopamine synthesis and is abundantly expressed in DA neurons; accordingly, it has been used as a dopamine neuronal marker in PD studies. **Figure 2** shows the meta-analysis of studies with TH+ neurons in the SN of PD model animals. Twenty-nine studies adopted TH+ level as an outcome index. All of the studies reported a positive effect of acupuncture on increasing TH+ levels in the SN of

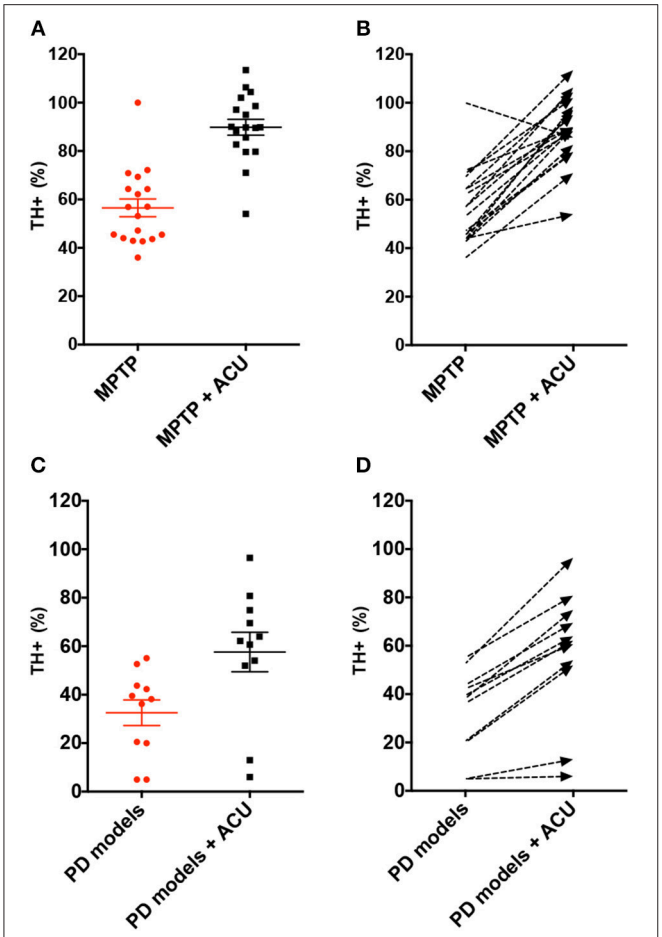

FIGURE 3 | Analysis of difference in TH-positive level between PD rodent and acupuncture treatment group throughout studies. **(A)** Each TH+ level (% control) of MPTP-induced PD (MPTP) group and MPTP plus acupuncture (MPTP + ACU) group. Lines indicates the mean value and error. **(B)** Dashed arrows mean the slope of difference from MPTP to MPTP plus acupuncture group in each study. **(C)** Each TH+ level (% control) of 6-OHDA or MFB-axotomy or a-syn mutation-induced PD (PD models) group and acupuncture-treated PD (PD models + ACU) group. Lines indicates the mean value and error. **(D)** Dashed arrows mean the slope of difference between PD models to PD models plus acupuncture group in each study. Notice the difference of the TH+ level between acupuncture treated group compared to PD rodent model.

acupuncture treated PD models compared with the PD control group except for two studies (Yang et al., 2017; Wang et al., 2018) ($n = 426$; standardized mean difference [SMD] 33.97; 95% CI 33.15–34.79; $p < 0.00001$; heterogeneity $\chi^2 = 162.80$, $I^2 = 98.2\%$, **Figure 2**). Each data point on the plot is shown with group comparisons (**Figure 3**). One study reported decreased TH+ cells in the acupuncture-treated group compared with the MPTP model (**Figures 2**, **3A,B**), and one study demonstrated no difference in TH+ cells between acupuncture and 6-OHDA mouse models (**Figures 2**, **3C,D**). However, TH+ cells were increased after acupuncture in almost all studies, except two that reported no significant difference (**Figures 2**, **3**). Overall, integrated changes of TH+ neurons in PD models demonstrated 35.94% of normal brain and, interestingly, those of acupuncture treated improved these neuronal deficits by 70.43% (**Figure 3**). Additionally, a subgroup analysis of different PD models was performed to examine the effect of acupuncture on TH+ level. The result of the subgroup analysis indicated that acupuncture had a significant effect on MPTP models (SMD 56.2 [95% CI 37.53–39.73]; $p < 0.00001$), MFB models (SMD 25.88 [95% CI 23.47–28.30]; $p < 0.00001$), and 6-OHDA models (SMD 28.84 [95% CI 27.38–30.31]; $p < 0.00001$).

Effect of Acupuncture on Dopamine Content Alteration

DA neuronal deficit leads to decreases in dopamine content in striatal projections. The above analysis indicated that DA neurons in PD model rodents were recovered by acupuncture; thus, it was explored how dopamine content was changed by acupuncture in the studies (**Figure 4**). Twelve studies reported the effect of acupuncture on improving dopamine content in PD models compared with the control PD group. There was no remarkable increase in dopamine content, except in three studies with high increase (Jia et al., 2010; Tian et al., 2016; Yu et al., 2016) ($n = 185$; SMD 4.23 [95% CI 3.53–4.92]; $p < 0.00001$; heterogeneity $\chi^2 = 86.92$, $I^2 = 96.5\%$, **Figure 4**). While three studies reported large increases in the striatal dopamine by acupuncture, overall, studies showed that dopamine content was not significantly altered by acupuncture (**Figures 4**, **5**). In the subgroup analysis of dopamine content, there was a significant effect of acupuncture was observed in MPTP models (SMD 5.83 [95% CI 4.96–6.70]; $p < 0.00001$), MFB models (SMD 16.03 [95% CI 11.24–20.82]; $p < 0.00001$), but no significant difference was found in the 6-OHDA models (SMD 0.18 [95% CI −1.02–1.37]; $p = 0.77$).

Effect of Acupuncture on Motor Function in a PD Model

Table 2 shows how acupuncture affected motor function in PD models by examining the results of behavioral tests. Among the 42 studies, 13 conducted a rotarod test, 3 conducted a pole test, 5 performed the open field test, 11 examined rotational behavior, and the 5 remaining studies performed the Morris Water Maze test, grip strength test, gait analysis, cylinder test, and locomotor test, respectively. For studies that used the rotarod test, it was evident that motor dysfunctions were alleviated in the treatment group compared with the PD rodent model group. For the pole test result, descending time was shortened in the acupuncture-treated group in three studies. In studies that examined rotation behavior between model group and treatment group, acupuncture reduced rotational asymmetry induced by MFB-axotomy or on the side of neurotoxin injection. Based on most studies, it is believed that acupuncture alleviated motor dysfunction in PD rodent models.

DISCUSSION

Summary of Evidence

In this review, we systematically analyzed 42 acupuncture studies that used rodent models of PD to determine whether acupuncture can improve PD symptoms and/or pathology. It is possible to study the progression of PD and therapeutic

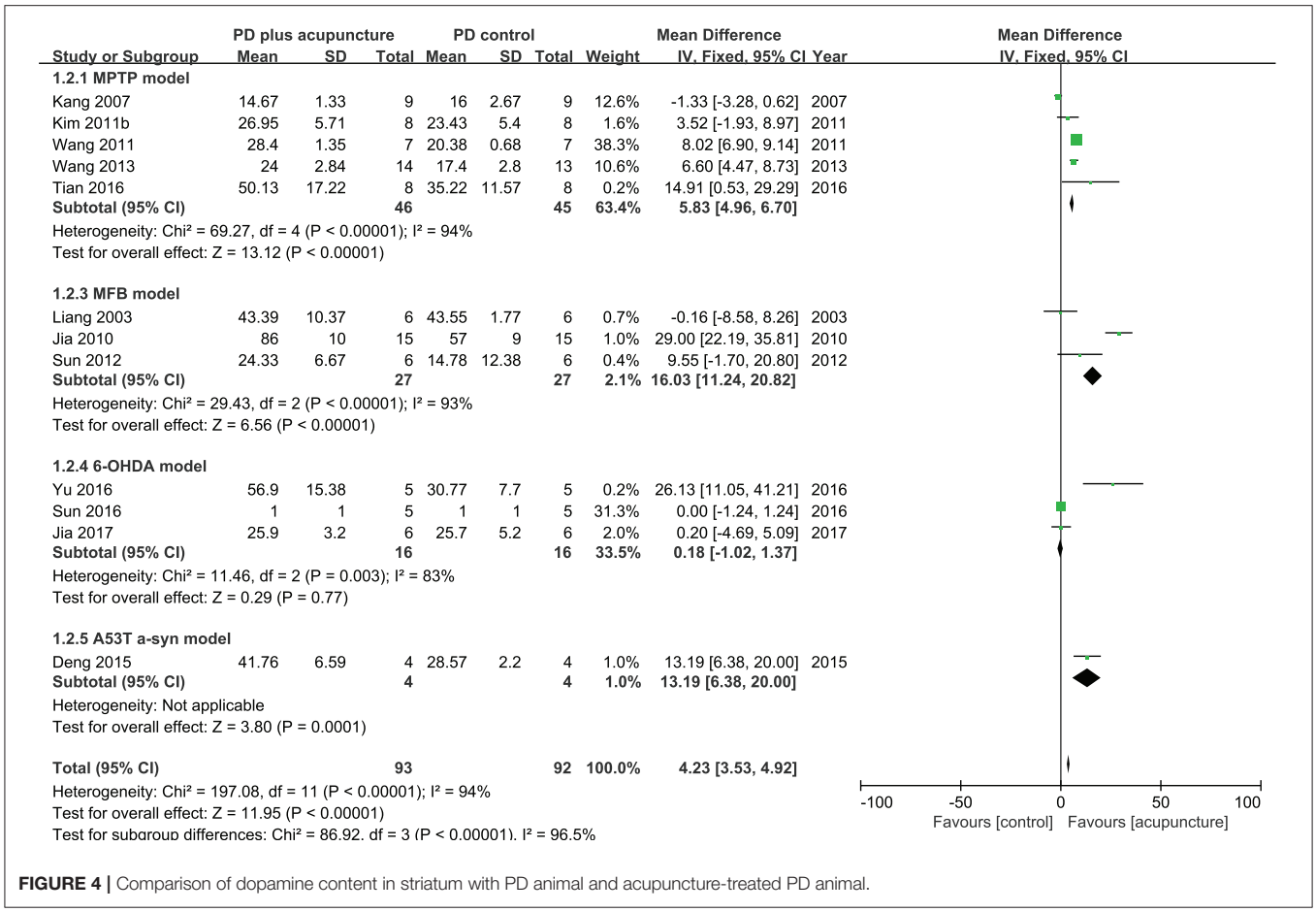

FIGURE 4 | Comparison of dopamine content in striatum with PD animal and acupuncture-treated PD animal.

approaches by using rodent models. However, there is still no experimental rodent model that can perfectly phenocopy the disease (Jagmag et al., 2015). There was a broad range of experimental models used to study PD including MPTP mouse, 6-OHDA-lesioned rat, MFB-axotomy rodent, and an α-syn mutation mouse. In the studies, acupuncture treatment involved MA and EA. Overall, meta-analysis revealed that deficits of both TH+ levels and dopamine content in PD model animals were recovered by acupuncture. Acupuncture treatment in MPTP, MFB, and 6-OHDA models were also found to be effective according to subgroup analyses. Additionally, motor dysfunctions in those PD models were also alleviated by acupuncture.

Possible Mechanism of Neuroprotective Effects

Several mechanisms of acupuncture have been suggested to be involved in recovering DA neuronal deficits. First, the neurotrophic factor-induced cell proliferation pathway was suggested as a potential mechanism to explain the neuroprotective effect of acupuncture. For example, it was found that acupuncture increased brain-derived neurotrophic factor (BDNF) levels, followed by activation of TrkB-related cell proliferation cascade (Liang et al., 2002; Park et al., 2003; Sun et al., 2016). Glial cell-derived neurotrophic factor was also upregulated by acupuncture (Liang et al., 2003), and there was remarkable increase in cyclophilin A levels (Jeon et al., 2008). Additionally, it was found that acupuncture activates hypothalamic melanin-concentrating hormone (MCH), which is involved in neuronal protection by upregulating a downstream pathway related to neuroprotection in the SN of MPTP-induced and A53T α-syn mutant PD mice (Park et al., 2017). Moreover, various researchers have suggested possibilities that acupuncture helps PD patients recover from PD through biological processes such as anti-oxidant (Yu et al., 2010; Wang et al., 2011; Lv et al., 2015; Lee et al., 2018), anti-inflammation (Kang et al., 2007; Jeon et al., 2008; Deng et al., 2015), and regulation of autophagy (Tian et al., 2016). Although all of these processes need to be clinically verified, the scientific evidence revealed strong possibilities of a neuroprotective effect of acupuncture on PD.

Contradictory Results and Plausible Reasons

In contrast, we found that one study reported non-meaningful changes in TH+ levels (Jia et al., 2017) and contradicting results in another study (Yang et al., 2017), which reported that acupuncture is not effective in improving DA neuron protection. In a study by Yang et al., the authors reported that the number

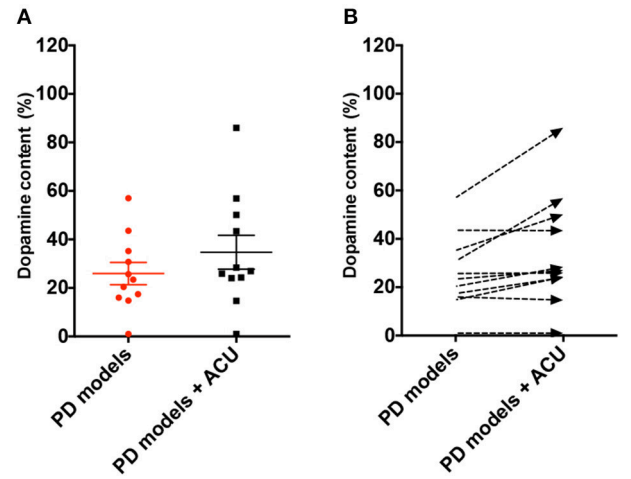

FIGURE 5 | Analysis of difference in dopamine content level between PD rodent and acupuncture treatment group throughout studies. **(A)** Each dopamine content level (% control) of all the PD animal models (PD models) group and acupuncture-treated PD animal models (PD models + ACU) group. Lines indicates the mean value and error. **(B)** Dashed arrows mean the slope of difference from PD models to PD models plus acupuncture group in each study.

of TH+ neurons did not increase as a result of acupuncture treatment compared with PD models. However, this study did not have a normal control group and, as such, it is questionable whether a PD model was successfully established. Although C57/Bl6 mice are the most sensitive to MPTP, there are some cases in which models are not successfully induced (Jackson-Lewis and Przedborski, 2007). This illustrates why thorough controls, such as saline-injected normal mice, are needed for developing reliable rodent models. Therefore, it is doubtful whether their model would be appropriate to examine the effects of acupuncture in PD rodent models. In a study by Jia et al., changes in TH+ neurons were not meaningful but were partially restored. The study used 6-OHDA surgery-induced neuronal depletion model for development of PD. We found that the degree of neuronal deficit by 6-OHDA surgery was worse than neurotoxin injection (28.25 vs. 56.52% normal control TH+ value of 6-OHDA and MPTP, respectively) (**Figure 5**). Such differences among models may also lower the degree of recovery effect of acupuncture (52.33 vs. 89.83% normal control TH+ value of 6-OHDA+ACU and MPTP+ACU, respectively) (**Figure 5**). It also explains why the recent development of PD animal models remains arguable (Duty and Jenner, 2011; Blesa et al., 2012); therefore, it is important to carefully examine studies using various models to induce PD to draw the appropriate conclusions.

Dopamine Content and Possible Mechanisms for Improvements in Motor Function

Studies have shown that dopamine content is recovered, although not as much as neuronal deficits, by acupuncture treatment (**Figures 4**, **5**). These results were unexpected because most studies reported that motor dysfunctions in PD animals were significantly altered after acupuncture (**Table 2**). Studies have reported that partial recovery of DA neurons is not

TABLE 2 | Behavior tests and changes by acupuncture treatment in PD animal studies.

References	Result	Behavior tests
Liang et al., 2002	N/A	
Liang et al., 2003	Improved	Rotational behavior ↓
Park et al., 2003	Improved	Rotational behavior ↓
Kim et al., 2005	Improved	Rotational behavior ↓
Kang et al., 2007	N/A	
Jeon et al., 2008	Improved	Pole test ↓
Choi et al., 2009	N/A	
Jia et al., 2009	Improved	Rotational behavior ↓
Hong et al., 2010	N/A	
Jia et al., 2010	Improved	Rotarod ↑
Kim et al., 2010	N/A	
Yu et al., 2010	Improved	Rotational behavior ↓
Choi et al., 2011a	N/A	
Choi et al., 2011b	N/A	
Kim et al., 2011a	Improved	Rotarod ↑
Kim et al., 2011b	Improved	Rotarod ↑
Wang et al., 2011	N/A	
Yang et al., 2011	Improved	Pole test ↓
Huo et al., 2012	Improved	Rotational behavior ↓
Sun et al., 2012	Improved	Rotarod ↑
Rui et al., 2013	Improved	Rotational behavior ↓
Wang et al., 2013	Improved	Open field ↑
Yeo et al., 2013	N/A	
Kim et al., 2014	N/A	
Deng et al., 2015	Improved	Rotarod ↑ Open field ↑ Grip strength ↑ Gait analysis ↑
Lv et al., 2015	Improved	Open field ↑ (vertical activity)
Park et al., 2015	Improved	Rotarod ↑ Cylinder test ↑
Shen et al., 2015	N/A	
Yeo et al., 2015	N/A	
Jia et al., 2017	Improved	Rotarod ↑
Sun et al., 2016	Improved	Rotarod ↑ Rotational behavior ↓ Open field ↑
Tian et al., 2016	Improved	Rotarod ↑
Yu et al., 2016	Improved	Rotarod ↑ Cylinder test ↑ Locomotion ↑
Yang et al., 2017	N/A	
Park et al., 2017	Improved	Rotarod ↑
Jeon et al., 2017	Improved	Pole test ↓
Lee et al., 2018	Improved	Pole test ↓
Lu et al., 2017	Improved	Morris water maze ↓
Li et al., 2017a	N/A	
Li et al., 2017b	Improved	Rotarod ↑ Open field ↑
Lin et al., 2017	Improved	Rotational behavior ↓ Locomotion ↑
Wang et al., 2018	Improved	Rotarod ↑ Rotational behavior ↓

Improved, motor dysfunction by PD was mitigated by acupuncture; N/A, not applicable; ↑, increase of the value compared to PD model; ↓, decrease of the value compared to PD model.

sufficient to rescue neuronal function completely in terms of dopamine secretion. Instead, studies have suggested that acupuncture treatment has another effect on PD animals, which is improvement of synaptic function in addition to neuronal protection (Jia et al., 2009; Kim et al., 2011b; Yang et al., 2011; Sun et al., 2012; Rui et al., 2013; Yu et al., 2016). Notably, single-photon emission computed tomography imaging has demonstrated that neurotransmission was increased by acupuncture (Yang et al., 2011). Moreover, analysis of synaptic changes showed that dopamine use was enhanced via regulating the D1 dopamine receptor and dopamine transporter (Rui et al., 2013). Additionally, *in vivo* microdialysis results have shown that dopamine availability (Kim et al., 2011b) and other neurotransmitters, such as acetylcholine and glutamate, were mitigated by acupuncture (Sun et al., 2012). Furthermore, postsynaptic cortico-striatal pathway alteration was found after acupuncture (Wang et al., 2018). Based on these results, it is possible to hypothesize that acupuncture can modulate DA synaptic pathways via alteration of neuronal plasticity; however, it rescues less striatal dopamine content itself in PD animal models.

Limitations and Future Direction

There were several limitations in terms of drawing definitive conclusions based on the included studies. First, it is difficult to perform an accurate analysis by including studies using a variety of PD models and acupuncture methods. Nevertheless, it is meaningful that the potential neuroprotective effect of acupuncture treatment was evident in most of the included studies. Second, the number of available studies was not conducive to a thorough systematic review, which reflects the limited research investigating effects of acupuncture. In other words, more studies will enable us to draw more accurate conclusions in the future.

CONCLUSION

Results of the present review and analysis suggest that acupuncture treatment potentially protected DA neurons through various beneficial mechanisms. Nevertheless, resolving the low quality of studies and further research investigating the efficacy of different acupuncture treatment methods in PD rodent models will be needed.

AUTHOR CONTRIBUTIONS

JK analyzed the data. S-NK and H-JP supervised the project. JK, HL, S-NK, and H-JP wrote the paper.

FUNDING

This work was supported by National Research Foundation of Korea funded by the Korea government (MSIT) (NRF-2017R1C1B5018061, NRF-2015M3A9E3052338, and 2017R1A2B4009963) and from the Korea Institute of Oriental Medicine (grant K18182).

REFERENCES

Alves, G., Forsaa, E. B., Pedersen, K. F., Dreetz Gjerstad, M., and Larsen, J. P. (2008). Epidemiology of Parkinson's disease. *J. Neurol.* 255 (Suppl. 5), 18–32. doi: 10.1007/s00415-008-5004-3

Blandini, F., and Armentero, M. T. (2012). Animal models of Parkinson's disease. *FEBS J.* 279, 1156–1166. doi: 10.1111/j.1742-4658.2012.08491.x

Blesa, J., Phani, S., Jackson-Lewis, V., and Przedborski, S. (2012). Classic and new animal models of Parkinson's disease. *J. Biomed. Biotechnol.* 2012:845618. doi: 10.1155/2012/845618

Blesa, J., Trigo-Damas, I., Quiroga-Varela, A., and Jackson-Lewis, V. R. (2015). Oxidative stress and Parkinson's disease. *Front. Neuroanat.* 9:91. doi: 10.3389/fnana.2015.00091

Chae, Y., Lee, H., Kim, H., Kim, C. H., Chang, D. I., Kim, K. M., et al. (2009). Parsing brain activity associated with acupuncture treatment in Parkinson's diseases. *Mov. Disord.* 24, 1794–1802. doi: 10.1002/mds.22673

Cho, S. Y., Shim, S. R., Rhee, H. Y., Park, H. J., Jung, W. S., Moon, S. K., et al. (2012). Effectiveness of acupuncture and bee venom acupuncture in idiopathic Parkinson's disease. *Parkinsonism Relat. Disord.* 18, 948–952. doi: 10.1016/j.parkreldis.2012.04.030

Choi, Y. G., Park, J. H., and Lim, S. (2009). Acupuncture inhibits ferric iron deposition and ferritin-heavy chain reduction in an MPTP-induced parkinsonism model. *Neurosci. Lett.* 450, 92–96. doi: 10.1016/j.neulet.2008.11.049

Choi, Y. G., Yeo, S., Hong, Y. M., Kim, S. H., and Lim, S. (2011a). Changes of gene expression profiles in the cervical spinal cord by acupuncture in an MPTP-intoxicated mouse model: microarray analysis. *Gene* 481, 7–16. doi: 10.1016/j.gene.2011.03.006

Choi, Y. G., Yeo, S., Hong, Y. M., and Lim, S. (2011b). neuroprotective changes of striatal degeneration-related gene expression by acupuncture in an mptp mouse model of parkinsonism: microarray analysis. *Cell. Mol. Neurobiol.* 31, 377–391. doi: 10.1007/s10571-010-9629-2

Demaagd, G., and Philip, A. (2015). Parkinson's disease and its management: part 1: disease entity, risk factors, pathophysiology, clinical presentation, and diagnosis. *P T* 40, 504–532.

Deng, J., Lv, E., Yang, J., Gong, X., Zhang, W., Liang, X., et al. (2015). Electroacupuncture remediates glial dysfunction and ameliorates neurodegeneration in the astrocytic alpha-synuclein mutant mouse model. *J. Neuroinflammation* 12:103. doi: 10.1186/s12974-015-0302-z

Duty, S., and Jenner, P. (2011). Animal models of Parkinson's disease: a source of novel treatments and clues to the cause of the disease. *Br. J. Pharmacol.* 164, 1357–1391. doi: 10.1111/j.1476-5381.2011.01426.x

Hong, M. S., Park, H. K., Yang, J. S., Park, H. J., Kim, S. T., Kim, S. N., et al. (2010). Gene expression profile of acupuncture treatment in 1-methyl-4-phenyl-1,2,3,6-tetrahydropyridine-induced Parkinson's disease model. *Neurol. Res.* 32, 74–78. doi: 10.1179/016164109X12537002794165

Huo, L. R., Liang, X. B., Li, B., Liang, J. T., He, Y., Jia, Y. J., et al. (2012). The cortical and striatal gene expression profile of 100 Hz electroacupuncture treatment in 6-hydroxydopamine-induced Parkinson's disease model. *Evid. Based Complement. Alternat. Med.* 2012:908439. doi: 10.1155/2012/908439

Jackson-Lewis, V., and Przedborski, S. (2007). Protocol for the MPTP mouse model of Parkinson's disease. *Nat. Protoc.* 2, 141–151. doi: 10.1038/nprot.2006.342

Jagmag, S. A., Tripathi, N., Shukla, S. D., Maiti, S., and Khurana, S. (2015). Evaluation of models of Parkinson's disease. *Front. Neurosci.* 9:503. doi: 10.3389/fnins.2015.00503

Jeon, H., Ryu, S., Kim, D., Koo, S., Ha, K. T., and Kim, S. (2017). Acupuncture stimulation at GB34 restores MPTP-induced neurogenesis impairment in the subventricular zone of mice. *Evid. Based Complement. Alternat. Med.* 2017:3971675. doi: 10.1155/2017/3971675

Jeon, S., Kim, Y. J., Kim, S. T., Moon, W., Chae, Y., Kang, M., et al. (2008). Proteomic analysis of the neuroprotective mechanisms of acupuncture

treatment in a Parkinson's disease mouse model. *Proteomics* 8, 4822–4832. doi: 10.1002/pmic.200700955

Jia, J., Li, B., Sun, Z. L., Yu, F., Wang, X., and Wang, X. M. (2010). Electro-acupuncture stimulation acts on the basal ganglia output pathway to ameliorate motor impairment in Parkinsonian model rats. *Behav. Neurosci.* 124, 305–310. doi: 10.1037/a0018931

Jia, J., Sun, Z., Li, B., Pan, Y., Wang, H., Wang, X., et al. (2009). Electro-acupuncture stimulation improves motor disorders in Parkinsonian rats. *Behav. Brain Res.* 205, 214–218. doi: 10.1016/j.bbr.2009.06.024

Jia, Y. J., Deng, J. H., Zhang, W. Z., Sun, Z. L., Yang, J., Yu, Y., et al. (2017). The role of group II metabotropic glutamate receptors in the striatum in electroacupuncture treatment of Parkinsonian rats. *CNS Neurosci. Ther.* 23, 23–32. doi: 10.1111/cns.12587

Joh, T. H., Park, H. J., Kim, S. N., and Lee, H. (2010). Recent development of acupuncture on Parkinson's disease. *Neurol. Res.* 32(Suppl. 1), 5–9. doi: 10.1179/016164109X12537002793643

Kang, J. M., Park, H. J., Choi, Y. G., Choe, I. H., Park, J. H., Kim, Y. S., et al. (2007). Acupuncture inhibits microglial activation and inflammatory events in the MPTP-induced mouse model. *Brain Res.* 1131, 211–219. doi: 10.1016/j.brainres.2006.10.089

Kim, S. N., Doo, A. R., Park, J. Y., Bae, H., Chae, Y., Shim, I., et al. (2011b). Acupuncture enhances the synaptic dopamine availability to improve motor function in a mouse model of Parkinson's disease. *PLoS ONE* 6:e27566. doi: 10.1371/journal.pone.0027566

Kim, S. N., Doo, A. R., Park, J. Y., Choo, H. J., Shim, I., Park, J. J., et al. (2014). Combined treatment with acupuncture reduces effective dose and alleviates adverse effect of L-dopa by normalizing Parkinson's disease-induced neurochemical imbalance. *Brain Res.* 1544, 33–44. doi: 10.1016/j.brainres.2013.11.028

Kim, S. N., Kim, S. T., Doo, A. R., Park, J. Y., Moon, W., Chae, Y., et al. (2011a). Phosphatidylinositol 3-kinase/akt signaling pathway mediates acupuncture-induced dopaminergic neuron protection and motor function improvement in a mouse model of Parkinson's disease. *Int. J. Neurosci.* 121, 562–569. doi: 10.3109/00207454.2011.591515

Kim, S. T., Moon, W., Chae, Y., Kim, Y. J., Lee, H., and Park, H. J. (2010). The effect of electroaucpuncture for 1-methyl-4-phenyl-1,2,3,6-tetrahydropyridine-induced proteomic changes in the mouse striatum. *J. Physiol. Sci.* 60, 27–34. doi: 10.1007/s12576-009-0061-7

Kim, Y. K., Lim, H. H., Song, Y. K., Lee, H. H., Lim, S., Han, S., et al. (2005). Effect of acupuncture on 6-hydroxydopamine-induced nigrostratal dopaminergic neuronal cell death in rats. *Neurosci. Lett.* 384, 133–138. doi: 10.1016/j.neulet.2005.04.068

Lam, Y. C., Kum, W. F., Durairajan, S. S., Lu, J. H., Man, S. C., Xu, M., et al. (2008). Efficacy and safety of acupuncture for idiopathic Parkinson's disease: a systematic review. *J. Altern. Complement. Med.* 14, 663–671. doi: 10.1089/acm.2007.0011

Lee, Y., Choi, G., Jeon, H., Kim, D., Ryu, S., Koo, S., et al. (2018). Acupuncture stimulation at GB34 suppresses 1-methyl-4-phenyl-1,2,3,6-tetrahydropyridine-induced oxidative stress in the striatum of mice. *J. Physiol. Sci.* 68, 455–462. doi: 10.1007/s12576-017-0547-7

Li, M., Li, L., Wang, K., Su, W., and Jia, J. (2017a). The effect of electroacupuncture on proteomic changes in the motor cortex of 6-OHDA Parkinsonian rats. *Brain Res.* 1673, 52–63. doi: 10.1016/j.brainres.2017.07.027

Li, M., Wang, K., Su, W. T., Jia, J., and Wang, X. M. (2017b). Effects of electroacupuncture on metabolic changes in motor cortex and striatum of 6-hydroxydopamine-induced Parkinsonian rats. *Chin. J. Integr. Med.* doi: 10.1007/s11655-017-2975-x. [Epub ahead of print].

Liang, X. B., Liu, X. Y., Li, F. Q., Luo, Y., Lu, J., Zhang, W. M., et al. (2002). Long-term high-frequency electro-acupuncture stimulation prevents neuronal degeneration and up-regulates BDNF mRNA in the substantia nigra and ventral tegmental area following medial forebrain bundle axotomy. *Brain Res. Mol. Brain Res.* 108, 51–59. doi: 10.1016/S0169-328X(02)00513-2

Liang, X. B., Luo, Y., Liu, X. Y., Lu, J., Li, F. Q., Wang, Q., et al. (2003). Electro-acupuncture improves behavior and upregulates GDNF mRNA in MFB transected rats. *Neuroreport* 14, 1177–1181. doi: 10.1097/00001756-200306110-00015

Lin, J. G., Chen, C. J., Yang, H. B., Chen, Y. H., and Hung, S. Y. (2017). electroacupuncture promotes recovery of motor function and reduces dopaminergic neuron degeneration in rodent models of Parkinson's disease. *Int. J. Mol. Sci.* 18:1846. doi: 10.3390/ijms18091846

Lu, K. W., Yang, J., Hsieh, C. L., Hsu, Y. C., and Lin, Y. W. (2017). Electroacupuncture restores spatial learning and downregulates phosphorylated N-methyl-D-aspartate receptors in a mouse model of Parkinson's disease. *Acupunct. Med.* 35, 133–141. doi: 10.1136/acupmed-2015-011041

Lv, E., Deng, J., Yu, Y., Wang, Y., Gong, X., Jia, J., et al. (2015). Nrf2-ARE signals mediated the anti-oxidative action of electroacupuncture in an MPTP mouse model of Parkinson's disease. *Free Radic. Res.* 49, 1296–1307. doi: 10.3109/10715762.2015.1067696

Park, H. J., Lim, S., Joo, W. S., Yin, C. S., Lee, H. S., Lee, H. J., et al. (2003). Acupuncture prevents 6-hydroxydopamine-induced neuronal death in the nigrostriatal dopaminergic system in the rat Parkinson's disease model. *Exp. Neurol.* 180, 93–98. doi: 10.1016/S0014-4886(02)00031-6

Park, J. Y., Choi, H., Baek, S., Jang, J., Lee, A., Jeon, S., et al. (2015). p53 signalling mediates acupuncture-induced neuroprotection in Parkinson's disease. *Biochem. Biophys. Res. Commun.* 460, 772–779. doi: 10.1016/j.bbrc.2015.03.105

Park, J. Y., Kim, S. N., Yoo, J., Jang, J., Lee, A., Oh, J. Y., et al. (2017). Novel neuroprotective effects of melanin-concentrating hormone in Parkinson's disease. *Mol. Neurobiol.* 54, 7706–7721. doi: 10.1007/s12035-016-0258-8

Rui, G., Guangjian, Z., Yong, W., Jie, F., Yanchao, C., Xi, J., et al. (2013). High frequency electro-acupuncture enhances striatum DAT and D1 receptor expression, but decreases D2 receptor level in 6-OHDA lesioned rats. *Behav. Brain Res.* 237, 263–269. doi: 10.1016/j.bbr.2012.09.047

Sena, E., Van Der Worp, H. B., Howells, D., and Macleod, M. (2007). How can we improve the pre-clinical development of drugs for stroke? *Trends Neurosci.* 30, 433–439. doi: 10.1016/j.tins.2007.06.009

Shen, X., Xie, Y. Y., Chen, C., and Wang, X. P. (2015). Effects of electroacupuncture on cognitive function in rats with Parkinson's disease. *Int. J. Physiol. Pathophysiol. Pharmacol.* 7, 145–151.

Sun, M., Wang, K., Yu, Y., Su, W. T., Jiang, X. X., Yang, J., et al. (2016). Electroacupuncture alleviates depressive-like symptoms and modulates BDNF signaling in 6-hydroxydopamine rats. *Evid. Based Complement. Alternat. Med.* 2016:7842362. doi: 10.1155/2016/7842362

Sun, Z., Jia, J., Gong, X., Jia, Y., Deng, J., Wang, X., et al. (2012). Inhibition of glutamate and acetylcholine release in behavioral improvement induced by electroacupuncture in parkinsonian rats. *Neurosci. Lett.* 520, 32–37. doi: 10.1016/j.neulet.2012.05.021

Surmeier, D. J., Guzman, J. N., Sanchez-Padilla, J., and Goldberg, J. A. (2010). What causes the death of dopaminergic neurons in Parkinson's disease? *Prog. Brain Res.* 183, 59–77. doi: 10.1016/S0079-6123(10)83004-3

Tian, T., Sun, Y., Wu, H., Pei, J., Zhang, J., Zhang, Y., et al. (2016). Acupuncture promotes mTOR-independent autophagic clearance of aggregation-prone proteins in mouse brain. *Sci. Rep.* 6:19714. doi: 10.1038/srep19714

Wang, H., Liang, X., Wang, X., Luo, D., Jia, J., and Wang, X. (2013). Electro-acupuncture stimulation improves spontaneous locomotor hyperactivity in MPTP intoxicated mice. *PLoS ONE* 8:e64403. doi: 10.1371/journal.pone.0064403

Wang, H., Pan, Y., Xue, B., Wang, X., Zhao, F., Jia, J., et al. (2011). The antioxidative effect of electro-acupuncture in a mouse model of Parkinson's disease. *PLoS One* 6:e19790. doi: 10.1371/journal.pone.0019790

Wang, Y., Wang, Y., Liu, J., and Wang, X. (2018). Electroacupuncture alleviates motor symptoms and Up-regulates vesicular glutamatergic transporter 1 expression in the subthalamic nucleus in a unilateral 6-hydroxydopamine-lesioned hemi-Parkinsonian rat model. *Neurosci. Bull.* 34, 476–484. doi: 10.1007/s12264-018-0213-y

Yang, H. J., Gao, Y., Yun, J. Y., Kim, Y. E., Ehm, G., Lee, J. Y., et al. (2017). Acupuncture does not protect against 1-methyl-4-phenyl-1,2,3,6-tetrahydropyridine-induced damage of dopaminergic neurons in a preclinical mouse model of Parkinson's disease. *Neuroreport* 28, 50–55. doi: 10.1097/WNR.0000000000000709

Yang, J. L., Chen, J. S., Yang, Y. F., Chen, J. C., Lin, C. H., Chang, R. S., et al. (2011). Neuroprotection effects of retained acupuncture in neurotoxin-induced Parkinson's disease mice. *Brain Behav. Immun.* 25, 1452–1459. doi: 10.1016/j.bbi.2011.05.012

Yeo, S., An, K. S., Hong, Y. M., Choi, Y. G., Rosen, B., Kim, S. H., et al. (2015). Neuroprotective changes in degeneration-related gene expression in the substantia nigra following acupuncture in an MPTP mouse model of Parkinsonism: microarray analysis. *Genet. Mol. Biol.* 38, 115–127. doi: 10.1590/S1415-47573812014013 7

Yeo, S., Choi, Y. G., Hong, Y. M., and Lim, S. (2013). Neuroprotective changes of thalamic degeneration-related gene expression by acupuncture in an MPTP mouse model of Parkinsonism: microarray analysis. *Gene* 515, 329–338. doi: 10.1016/j.gene.2012.12.002

Yeo, S., Lim, S., Choe, I. H., Choi, Y. G., Chung, K. C., Jahng, G. H., et al. (2012). Acupuncture stimulation on GB34 activates neural responses associated with Parkinson's disease. *CNS Neurosci. Ther.* 18, 781–790. doi: 10.1111/j.1755-5949.2012.00363.x

Yu, Y., Wang, K., Deng, J., Sun, M., Jia, J., and Wang, X. (2016). Electroacupuncture produces the sustained motor improvement in 6-hydroxydopamine-lesioned mice. *PLoS ONE* 11:e0149111. doi: 10.1371/journal.pone.0149111

Yu, Y. P., Ju, W. P., Li, Z. G., Wang, D. Z., Wang, Y. C., and Xie, A. M. (2010). Acupuncture inhibits oxidative stress and rotational behavior in 6-hydroxydopamine lesioned rat. *Brain Res.* 1336, 58–65. doi: 10.1016/j.brainres.2010.04.020

Zhou, C., Huang, Y., and Przedborski, S. (2008). Oxidative stress in Parkinson's disease: a mechanism of pathogenic and therapeutic significance. *Ann. N.Y. Acad. Sci.* 1147, 93–104. doi: 10.1196/annals.1427.023

Conflict of Interest Statement: The authors declare that the research was conducted in the absence of any commercial or financial relationships that could be construed as a potential conflict of interest.

frontiers in Neuroscience

ORIGINAL RESEARCH
published: 14 May 2019
doi: 10.3389/fnins.2019.00496

Electro-Acupuncture Ameliorated MPTP-Induced Parkinsonism in Mice via TrkB Neurotrophic Signaling

Yingke Zhao, Dan Luo, Zhipeng Ning, Jianhui Rong and Lixing Lao**

School of Chinese Medicine, Li Ka Shing Faculty of Medicine, The University of Hong Kong, Pok Fu Lam, Hong Kong

Neurotrophins, such as brain-derived neurotrophic factor (BDNF), have shown promise as neuroprotective agents, indicating their potential in therapeutic strategies for neurodegenerative disease. However, the inherent bioactivity and pharmaceutical limitations of BDNF compromise its clinical efficacy. Research has documented the beneficial effects of electroacupuncture (EA) against neurodegeneration, possibly by BDNF-mediated mechanisms. The present study was designed to clarify whether EA can mount a neuroprotective effect in mice lesioned with MPTP (1-methyl-4-phenyl-1,2,3,6-tetrahydropyridine) via stimulation of the BDNF-TrkB signaling pathway. We found that EA not only ameliorated the motor dysfunction but also restored the dopaminergic neuronal function and upregulated BDNF expression in MPTP-lesioned mice. Interestingly, the TrkB inhibitor K252a abolished the neuroprotective effects of EA. Western blot analyses further demonstrated that EA might recover the level of phospho-Akt, phospho-ERK1/2, and BDNF against MPTP neurotoxicity via reversing the imbalance between TrkB FL and TrkB T1. Taken together, the results of the present study show that EA stimulation can ameliorate MPTP-induced parkinsonism in mice. Such a neuroprotective effect may be partially mediated via restoring TrkB neurotrophic signaling.

Keywords: Parkinson's disease, electro-acupuncture, brain-derived neurotrophic factor, TrkB, MPTP

OPEN ACCESS

Edited by:
Hi-Joon Park,
Kyung Hee University, South Korea

Reviewed by:
Federico Herrera,
Instituto de Tecnologia Química e Biológica (ITQB-NOVA), Portugal
Wei Cui,
Ningbo University, China
Yi-Hung Chen,
China Medical University, Taiwan

****Correspondence:***
Jianhui Rong
jrong@hku.hk
Lixing Lao
lxlao1@hku.hk

Specialty section:
This article was submitted to Neurodegeneration, a section of the journal Frontiers in Neuroscience

Received: *19 October 2018*
Accepted: *30 April 2019*
Published: *14 May 2019*

Citation:
Zhao Y, Luo D, Ning Z, Rong J and Lao L (2019) Electro-Acupuncture Ameliorated MPTP-Induced Parkinsonism in Mice via TrkB Neurotrophic Signaling. Front. Neurosci. 13:496. doi: 10.3389/fnins.2019.00496

INTRODUCTION

Parkinson's disease (PD) is characterized by the progressive loss of dopaminergic neurons in the substantia nigra par compacta (SNpc) and by impairments in motor function as well as other autonomic nervous system activities (Dexter and Jenner, 2013; Kalia and Lang, 2016). Although the exact etiology of PD remains elusive, recent studies have revealed that the neuronal functions may be impaired by several risk factors including oxidative stress, neuroinflammation, glutaminergic toxicity, protein misfolding and aggregation, and lack of neurotrophins (Kalia and Lang, 2015). Under oxidative stress, the physiological functions of neurotrophins [e.g., nerve growth factor and brain-derived neurotrophic factor (BDNF)] and the related tyrosine kinase receptors (Trks) are affected, subsequently jeopardizing the survival, differentiation, and patterning of neurons (Yamada et al., 2001; Bruno and Cuello, 2012). Disruption of BDNF biosynthesis failed to support dopaminergic neurons, whereas BDNF polymorphisms are associated with a susceptibility to PD (Hong et al., 2003). Previous studies demonstrated that exogenous BDNF could prevent the neurotoxicity of 1-methyl-4-phenyl-1,2,3,6-tetrahydropyridine (MPTP) and 6-hydroxydopamine

(6-OHDA) in dopaminergic neurons (Frim et al., 1994; Levivier et al., 1995). Interestingly, ectopic overexpression of BDNF ameliorated the motor dysfunction in 6-OHDA-treated animals (Klein et al., 1999). These studies indicate that BDNF is important for preserving the dopaminergic neurons and preventing or retarding neurodegeneration. Moreover, tyrosine kinase receptor type B (TrkB) is well known to mediate the neurotrophic function of BDNF. The TrkB gene encodes different isoforms of the TrkB receptor: full-length (TrkB FL) and splicing truncated isoforms (TrkB T1 or T2) (Otani et al., 2017). Notably, the truncated isoform TrkB T1 is regarded as the dominant negative form and may thereby suppress the neurotrophic activity of BDNF (Gupta et al., 2013). TrkB T1 is upregulated in situations such as stress, hypoxia, excitotoxicity, and neurodegeneration (Ferrer et al., 1999; Vidaurre et al., 2012). Collectively, neuroprotective therapy is needed to recover the balance of TrkB FL and TrkB T1 (Andero et al., 2014).

Acupuncture and electroacupuncture (EA) are well documented for their beneficial effects against various neurological disorders (Ghaffari and Kluger, 2014; Solanki et al., 2016). Accumulating evidence from clinical studies also provides support for the beneficial effect of EA in the management of PD, and clinicians have emphasized its application as a complementary strategy for treating the non-motor symptoms of PD (Jiang et al., 2018). As a non-pharmacological approach, EA has been investigated by several groups for its biological effects against PD (Xiao et al., 2018). EA was found to regulate the levels of various neurotransmitters such as dopamine, glutamate, and acetylcholine (Rui et al., 2013; Li et al., 2017). EA exhibited potent antioxidant properties in PD models, in particular by activating the nuclear factor E2–related factor 2 (Nrf2) signaling pathway (Lv et al., 2015). EA might elicit anti-neuroinflammatory activity through suppressing glial activation (Deng et al., 2015). As for the effects of EA on neurotrophic factors (e.g., BDNF), Liang et al. (2002) observed that EA upregulated the expression of BDNF in 6-OHDA-lesioned rats. Kim et al. (2011) also observed that manual acupuncture intervention could induce the activation of the PI3K/Akt pathway. Interestingly, Lin reported that EA enhanced the activation of BDNF and the phosphorylation of downstream signaling molecules such as Akt and ERK in MPP^+-induced rat models (Lin et al., 2017). These studies suggest the potential of EA in the activation of the BDNF signaling pathway.

In the present study, we propose to further identify the effects of EA on the BDNF-TrkB signaling pathway as a neuroprotective mechanism against MPTP neurotoxicity. We focus on the expression level and the post-translational processing of TrkB within the context of MPTP-induced neurodegeneration.

MATERIALS AND METHODS

Experimental Design

The design of our animal experiments is outlined in **Figure 1A**. To observe the effect of EA on MPTP-triggered parkinsonism symptoms, 30 mice were randomly divided into three groups: vehicle control group, model group (MPTP + sham EA), and EA group (MPTP + EA). Mice in the model and EA groups received MPTP (25 mg/kg/day) via intraperitoneal injection every afternoon for 7 consecutive days, whereas animals in the vehicle control group received the same volume of saline. The EA treatment was carried out every morning, 4 h prior to the MPTP injection, for 7 days, whereas mice from the control group and the model group were subjected to sham EA treatment. The detailed procedures for EA and sham EA are described below. In the next step, to identify the role of the TrkB receptor in the protective effect of EA, we randomly divided the mice in three groups (10 mice/group): model group (MPTP+ sham EA), EA group (MPTP + EA), and K252a group (MPTP + EA + K252a). Prior to EA treatment, mice in the K252a group were pre-treated with K252a (a TrkB inhibitor) via intraperitoneal injection (5 μg/kg/day) 1 h in advance, whereas mice in the other two groups received the equivalent volume of vehicle (saline). Mice from the EA group and the K252a group were treated by EA every morning for 7 days, whereas mice from MPTP group were subjected to sham EA.

Biochemical Reagents

Antibody against tyrosine hydroxylase (TH) was purchased from Merck Millipore (Billerica, MA, United States). Polyclonal rabbit anti-BDNF antibody was purchased from Santa Cruz Biotechnology Inc., (Santa Cruz, CA, United States). Antibodies against TrkB, ERK, phospho-ERK, AKT, phospho-AKT, CREB, phospho-CREB, GAPDH, and Alexa Fluor 594-conjugate anti-rabbit IgG antibody were obtained from Cell Signaling Technology (Boston, MA, United States). Protein assay dye reagent concentrate was purchased from Bio-Rad (Hercules, CA, United States). Enhanced chemiluminescence detection reagents were obtained from GE Healthcare (Uppsala, Sweden). A 3,3-*N*-diaminobenzidine tetrahydrochloride (DAB) substrate kit was purchased from Dako Corporation (Carpintera, CA, United States). Anti-rabbit horseradish peroxidase (HRP)-conjugated IgG secondary antibody and MPTP were purchased from Sigma-Aldrich (St. Louis, MO, United States). Mouse anti-BDNF antibody and proteinase inhibitor K252a were bought from Abcam (Cambridge, United Kingdom). Goat-anti Mouse Alexa-568 was obtained from Invitrogen (Carlsbad, CA, United States).

Animal Husbandry and MPTP-Induced PD Model

Adult C57BL/6N male mice (6–8 weeks, weight 21–25 g) were supplied by the Laboratory Animal Unit, University of Hong Kong. The mice were housed in a 12-h/12-h light/dark cycle under the conditions of constant temperature and humidity. All the experimental procedures were performed according to the regulations of the Hong Kong University Committee on the Use of Live Animals in Teaching and Research (CULATR No. 4196-16). The method of establishing MPTP-induced parkinsonism mice followed our previous work (Zhao et al., 2015). Mice received MPTP (25 mg/kg/day) via intraperitoneal injection every afternoon for 7 consecutive days, whereas animals in the vehicle control group received the same volume of saline. After the last injection of MPTP, mice were kept in isolation for 3 days

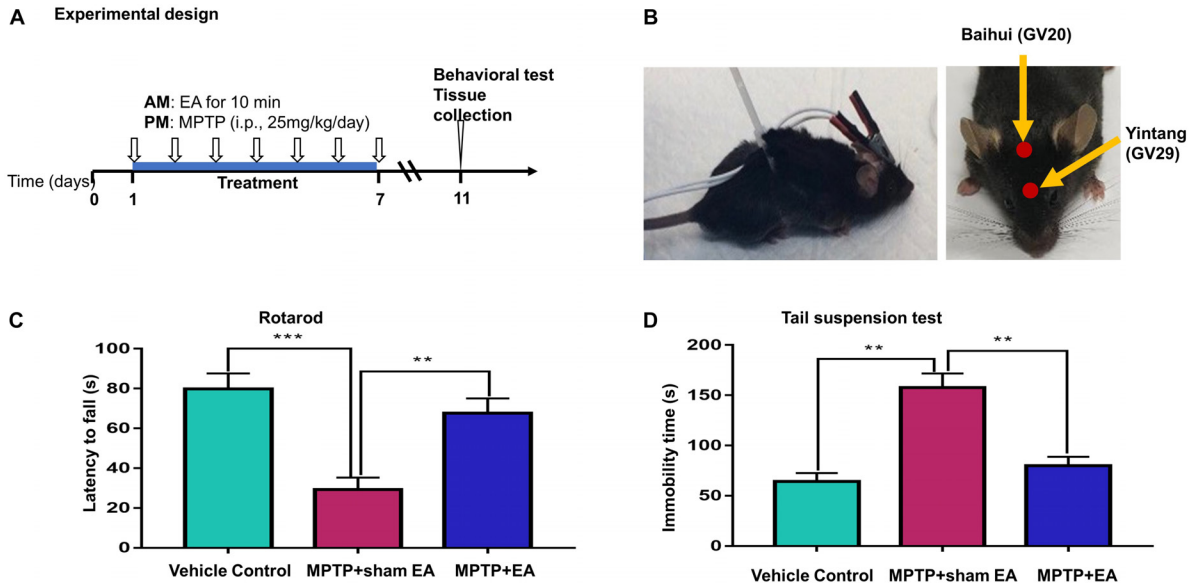

FIGURE 1 | EA ameliorated the deficit of motor functions in MPTP-lesioned mouse model **(A)** Experimental design. Mice were randomly divided into three groups: vehicle control, MPTP+sham EA, MPTP+EA. Mice received MPTP (25 mg/kg/day) for 7 consecutive days. EA treatment was carried out at 4 h before MPTP injection. After one-week treatment, mice were kept for 3 days and assessed by behavioral test and biochemical analysis. **(B)** Diagram for EA stimulation. EA was applied at GV20 and GV29. Needles were inserted into acupoint at 3 mm under the skin. The electrodes were connected to the needles and secured with a plastic wire. EA was carried out for 10 min per session. **(C)** Rotarod test performance to assess the behavior impairments. The on-rotarod time for mice was recorded. **(D)** Tail suspension test. The immobility time for mice was recorded over 6 min. The results were presented as mean ± SEM from 3 independent experiments (n = 10), $^{**}p < 0.01$, $^{***}p < 0.001$.

for potential neurotoxin risk. Finally, mice were moved out, assessed for behavioral performance, and subsequently sacrificed after the 3-day isolation.

EA and Sham EA Procedure

Electroacupuncture treatment was performed at the time point of 4 h prior to daily MPTP injection for 7 consecutive days essentially as previously described (Lao et al., 2004). The acupoints (i.e., GV20, Baihui; GV29, Yintang) were selected in our experiments (shown in **Figure 1B**). The acupoint GV20 is located in the vertex on the midline (5 *cun* posterior to the anterior hairline), whereas the acupoint GV29 is located midway between the medial ends of the eyebrows in humans. The equivalent position in mice was selected to mimic these two acupoints (Yin et al., 2008). Before the experiment, mice had the fur over the acupoints removed and the exposed skin cleaned. During the treatment, disposable intradermal acupunctures (0.22*5 mm, Hwato, China) were inserted into the acupoints to a depth of 3 mm. Electrodes were then connected to the end of each needle; the needles and the electrodes were stabilized by wiring the mouse body. EA stimulation was subsequently performed using an ES-160, six-channel programmable EA stimulator (ITO physiotherapy & rehabilitation Co., Tokyo, Japan), with intensity 1.5 mA, frequency 2 Hz, and pulse width 100 μs for 10 min. During EA stimulation, mice were placed in a plastic chamber without restraint other than a plastic wire around the body to stabilize the electrical wire. Animals from the control and MPTP groups received a sham EA procedure. Briefly, needles were taped onto the surface at the two acupoints, and the electrodes were connected to the ends of the needles, but no electricity stimulation was performed. The same wire stabilization procedure and similar plastic chamber were used during the treatment, to minimize potential confounders.

Behavioral Test

Rotarod Performance Test

Mice were assessed for MPTP-triggered parkinsonism impairments by a rotarod performance test (Harvard apparatus, Holliston, MA, United States). Mice were isolated for 3 days after the last MPTP administration prior to the test. On the day of the behavioral test, mice were first pre-trained on the machine three times for 3 min each. After resting for 2 h, mice were placed on the rotating horizontal rod (constant 15 rpm) for 5 min. The time for each mouse staying on the rod was automatically recorded by the rotarod apparatus. Each mouse was tested for three times, and after each test the mice were put back to their cage for a 30-min intertrial interval.

Tail Suspension Test

The tail suspension test, was conducted 4 h after the rotarod test as previously described (Luo et al., 2018). Briefly, mice were suspended from a bar by adhering a piece of tape to the tail and attaching the other end to the bar. The distance between the mouse's nose and the apparatus was kept to about 20–25 cm. The status of each mouse during a 6-min hanging session was tracked by video; the observers thereafter analyzed the video and recorded the agitation and immobility times of each mouse during the test.

Western Blot Analysis

The expression levels of BDNF, TrkB, and other related proteins were detected by Western blotting as described elsewhere (Zhao et al., 2017). Midbrain tissues were isolated and lysed in RIPA buffer containing a protease inhibitor cocktail. The proteins were recovered by centrifugation at 13,000 rpm for 15 min at 4°C. The protein concentration was determined with protein assay dye reagent. Proteins (20 μg) were resolved on 10% SDS–polyacrylamide gels and transferred onto a PVDF membrane. After 2 h incubation in Tris buffer with 1% Tween-20 and 5% BSA, the membranes were probed with primary antibodies overnight at 4°C, and subsequently detected with goat anti-rabbit IgG-HRP-conjugated secondary antibodies for another 3 h at 4°C. The blots were visualized with ECL under a Bio-Rad GelDoc imaging system (Hercules, CA, United States). The gel images were analyzed by Image Lab^{TM} software 5.1.

Immunohistochemistry

The expression level of TH in the midbrain was detected by immunohistochemical staining as previously described (Zhao et al., 2015). After the behavioral tests, mice were transcardially perfused with saline and 4% paraformaldehyde under anesthetic conditions. The brain tissues were collected and post-fixed in 4% paraformaldehyde overnight at 4°C. The samples were then immersed in 4% paraformaldehyde solution containing 30% sucrose overnight until the tissues sank, for cryoprotection. Tissues were fixed and embedded in Tissue-Tek O.C.T. Compound (Sakura, United States) and stored at −80°C. The cryosections were cut into serial coronal sections with a thickness of 30 μm on a freezing microtome (Model CM-1850, Leica, Germany). After thawing at room temperature for 1 h, the cryostat sections were heated in antigen retrieval citrate buffer for 30 min. After thawing at room temperature for 1 h, the cryostat sections were heated in antigen retrieval citrate buffer for 30 min. The slides were cooled, immersed in 0.3% hydrogen peroxide solution to block endogenous peroxidase, and sequentially blocked with 5% goat serum and 0.5% Triton X-100 in PBS for 30 min at room temperature. The slides were drained on tissue paper, then incubated with anti-TH primary antibody overnight at 4°C. Following several washes, the bound antibodies were detected with HRP-conjugated goat anti-rabbit secondary antibody for 2 h at room temperature. The HRP was then assayed with a DAB substrate kit from Dako (Carpintera, CA, United States). The slices were counterstained with hematoxylin, then observed under an Olympus microscope (Olympus Corp, Tokyo, Japan). The number of TH^+ neurons of each animal was counted within three non-overlapping areas at 10× magnification.

Immunofluorescence Staining

The expression of BDNF in the SNpc was examined by immunofluorescence staining. The cryosections were prepared as described for immunohistochemical analysis. After antigen retrieval, the slides were sequentially immersed in 0.5% Triton X-100 in PBS for 30 min, and then blocked in 5% goat serum for 2 h. The sections were probed with antibody against BDNF overnight at 4°C, washed three times with PBS, and detected with Alexa Fluor 568-conjugated goat anti-mouse IgG secondary antibody. The cell nuclei were stained with 4'-6-diamidino-2-phenylindole for 10 min. Prior to the examination of fluorescence, the slides were mounted with coverslips in mounting medium. The images were then acquired under a Zeiss LSM 780 confocal microscope (Carl-Zeiss, Jena, Germany). The positive cells were enumerated from three different views in each specimen.

Statistical Analysis

Behavioral assessments were represented as means ± SEM, whereas other experiments were expressed in mean ± SD. The difference was analyzed by one-way ANOVA, followed by Dunnett's *post hoc*, using GraphPad Prism software 7.00 (La Jolla, CA, United States). A value of $p < 0.05$ was considered statistically significant.

RESULTS

EA Ameliorated the Deficit of Motor Functions in an MPTP-Lesioned Mouse Model

To assess the effects of EA on the neuronal impairments, mice were treated with MPTP for 7 consecutive days and evaluated by rotarod test and tail suspension test. The time of latency in the rotarod performance test was recorded to indicate motor dysfunction, whereas the immobility time in the tail suspension test was measured for depressive behaviors (Taylor et al., 2010). As shown in **Figures 1C,D**, the rotarod performance test showed that MPTP shortened the time that mice remained on the rotarod (29.3±6.029 s (MPTP + sham EA) vs. 79.8±7.791 s (vehicle control), $n = 10$, $p = 0.0001$). EA treatment effectively prolonged the time on the rotarod for mice compared with the MPTP group (67.7±7.336 s (MPTP + EA) vs. 29.3±6.029 s (MPTP + sham EA), $n = 10$, $p = 0.0014$). The tail suspension test showed that MPTP increased the immobility time of mice compared with vehicle control mice (157.8±13.91 s (MPTP + sham EA) vs. 64.2±8.346 s (vehicle control), $n = 10$, $p = 0.001$). EA treatment successfully reduced the immobility time for MPTP-lesioned mice (79.9±8.877 s (MPTP + EA) vs. 157.8±13.91 s (MPTP + sham EA), $n = 10$, $p = 0.001$). Results from both the rotarod test and tail suspension test showed that the 7-day injection of MPTP triggered a severe motor disability in mice, whereas the EA treatment dramatically ameliorated the impairment observed in both the rotarod performance and tail suspension tests.

EA Reduced the Loss of Dopaminergic Neurons in MPTP-Treated Mice

The key pathological change of PD is dopaminergic neuron loss in the SNpc; therefore, we observed the loss of dopaminergic neurons by detecting the expression of TH. Immunohistochemical analysis and Western blotting

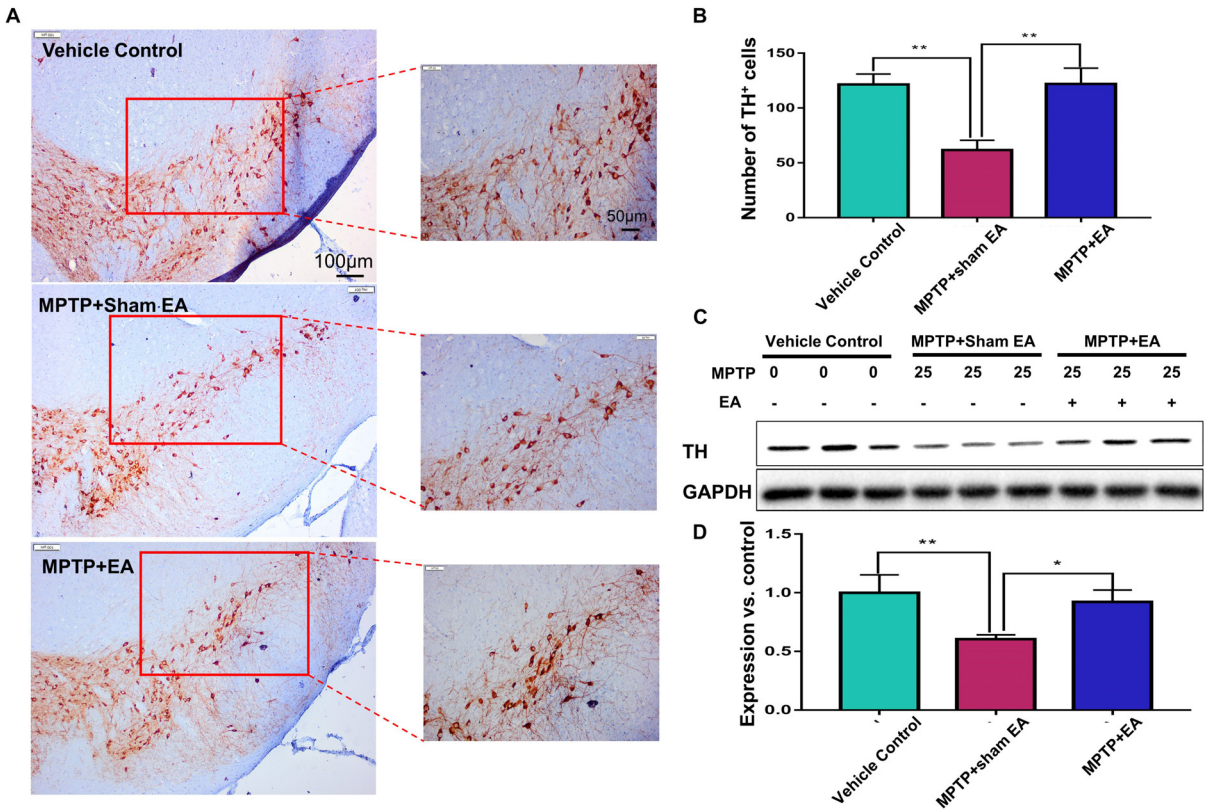

FIGURE 2 | EA reduced the loss of dopaminergic neurons in MPTP-treated mice After behavioral test, midbrain tissues were collected and analyzed by immunohistochemical analysis. The number of TH^+ cells on each slide was counted from three different views at 10× magnification under an Olympus microscope. **(A)** Representative images (with 10× and 20× magnification) were shown. Scale bar represented 100 μm, 50 μm in length, respectively. **(B)** The statistical analysis for the expression of TH^+ cells among each group. The results were presented as mean ± SD ($n = 4$). *$p < 0.05$, **$p < 0.01$. **(C)** TH expression determined by immunoblot. Midbrain tissues were lysed and analyzed by Western blotting with anti-TH and GAPDH (as loading control). Representative blots from three mice of each group were shown. **(D)** Quantification for the immunoblots. The blots were quantified by a densitometric method by ImageLab 5.1 (Bio-Rad). *$p < 0.05$, **$p < 0.01$.

were used in this regard. As shown in **Figures 2A,B**, MPTP downregulated TH expression compared with vehicle controls ($n = 4$, $p = 0.0012$). EA treatment restored the level of TH expression [121.9±14.46 (MPTP + EA) vs. 61.75±8.757 (MPTP + sham EA), $n = 4$, $p = 0.0010$]. Western blot analysis also confirmed that EA effectively restored TH expression in the midbrain compared with MPTP without EA [0.92±0.101 (MPTP + EA) vs. 0.61±0.035 (MPTP + sham EA), $n = 3$, $p = 0.02$] (**Figures 2C,D**). Thus, our results validated that EA treatment not only preserved the expression of TH in the midbrain but also effectively protected the dopaminergic neurons from MPTP neurotoxicity.

EA Preserved the Functions of the BDNF-TrkB Signaling Pathway

To observe the effect of EA on the BDNF-TrkB signaling pathway, we examined the expression levels of BDNF and the activation of its downstream signaling cascades, such as phospho-Akt, Akt, phospho-ERK1/2, ERK1/2, phospho-CREB, and CREB, by Western blotting with specific antibodies. As illustrated in **Figures 3A,C**, MPTP decreased BDNF expression compared with vehicle control [0.56±0.056 (MPTP + sham EA) vs. 1±0.064 (vehicle control), $n = 3$, $p = 0.0069$], whereas EA treatment significantly recovered the level of BDNF expression [0.94±0.19 (MPTP + EA) vs. 0.56±0.056 (MPTP + sham EA), $n = 3$, $p = 0.0136$]. The activation of downstream signaling cascades was also investigated by Western blot analysis (**Figures 3A,B**). After a 7-day administration, MPTP largely inactivated the survival signaling transduction, as indicated by the weaker intensity of the phosphorylated bands in each sample compared with the vehicle control group: phospho-AKT/AKT ($n = 3$, $p = 0.0373$), phospho-ERK/ERK ($n = 3$, $p = 0.0038$), and phospho-CREB/CREB ($n = 3$, $p = 0.0339$). Interestingly, EA stimulation effectively increased the phosphorylation levels of phospho-AKT ($p = 0.0048$), phospho-ERK ($p = 0.0010$), but did not affect phospho-CREB ($p = 0,0695$), compared with that in MPTP-treated animals. BDNF expression in the SN was also verified by immunofluorescence analysis. **Figure 4A** is the representative images of immunofluorescence; as expected, MPTP treatment reduced BDNF-immunoreactive signals in the SNpc [14.8±3.72 (MPTP + sham EA) vs. 37.2±4.02 (vehicle control), $n = 3$, $p = 0.0003$] (**Figure 4B**). Interestingly, EA

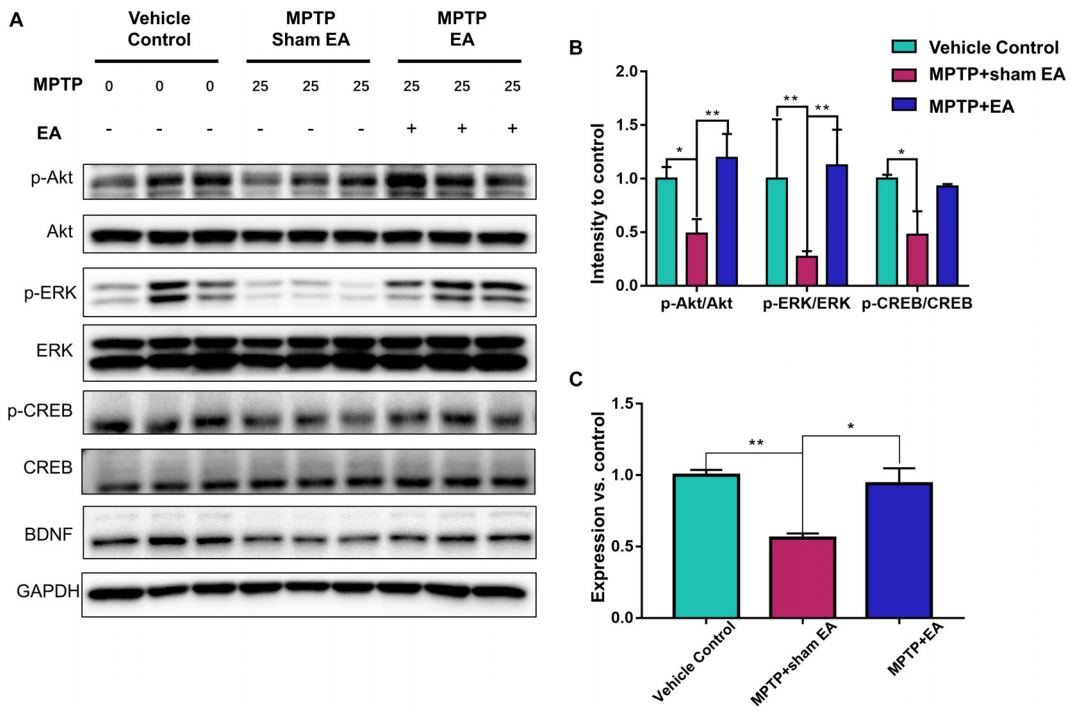

FIGURE 3 | EA preserved the functions of BDNF-TrkB signaling pathway. The midbrain tissues were lysed and analyzed by Western blotting using antibodies against Akt, phospho-Akt, ERK1/2, phospho-ERK1/2, CREB, phospho-CREB, and BDNF, GAPDH serves as loading control. **(A)** Representative blot was presented. **(B)** The quantitative analysis for the phosphorylation of Akt, ERK1/2, and CREB. **(C)** Quantification of the BDNF expression detected by western blot. The signal intensities of protein bands (n = 3) were determined by a densitometric method, and quantitatively analyzed by one-way ANOVA. *$p < 0.05$, **$p < 0.01$.

stimulation elevated the number of $BDNF^{+}$ cells against MPTP-lesioned group [28±2 (MPTP + EA) vs. 14.8±3.72 (MPTP + sham EA), $n = 3$, $p = 0.0053$].

EA Recovered MPTP-Induced Disruption to the Ratio of TrkB FL vs. TrkB T1

To clarify how EA affected TrkB receptors, we next analyzed the levels of two TrkB receptor isoforms by Western blotting. As shown in **Figures 5A,B**, MPTP reduced the level of TrkB FL over the 7-day stimulation compared with vehicle [0.74±0.029 (MPTP + sham EA) vs. 1±0.106 (vehicle control), $n = 4$, $p = 0.0232$]. In contrast, MPTP increased the level of truncated TrkB T1 (**Figure 5A**). Moreover, MPTP eventually disrupted the TrkB FL/TrkB T1 ratio [0.63±0.159 (MPTP + sham EA) vs. 1.02±0.135 (vehicle control), $n = 4$, $p = 0.0176$, **Figure 5C**]. Importantly, EA stimulation upregulated the expression of functional TrkB FL [0.98±0.172 (MPTP + EA) vs. 0.74±0.029 (MPTP + sham EA), $n = 4$, $p = 0.0340$], giving rise to the recovery of the MPTP-disrupted TrkB FL/TrkB T1 ratio [1.09±0.20 (MPTP + EA) vs. 0.63±0.159 (MPTP + sham EA), $n = 4$, $p = 0.0064$].

The Protective Effect of EA Can Be Abrogated With the TrkB Inhibitor K252a

To further confirm the involvement of TrkB in the EA-regulated BDNF elevation, we used the TrkB inhibitor K252a to observe whether it could abrogate the effect of EA. Briefly, 1 h before the EA treatment, the mice in the inhibitor group received an additional injection of K252a (5 μg/kg/day, i.p.). The protective effects of EA (i.e., behavioral change, dopaminergic neuron survival, and BDNF expression) were determined. As shown in **Figure 6A**, K252a abrogated the EA effect, as seen by a reduction in on-rotarod time [37.5±6.718 s (MPTP + EA + K252a) vs. 85.8±8.358 s (MPTP + EA), $p = 0.0007$], resulting in a disruption comparable to that of the MPTP group [37.5±6.718 s (MPTP + EA + K252a) vs. 31±6.206 s (MPTP + sham EA), $p = 0.7474$]. In the tail suspension test, the K252a group prolonged the EA-improved immobility time [146.4±9.976 s (MPTP + EA + K252a) vs. 94.6±13.15 s (MPTP + EA), $p = 0.0451$], showing an immobility time similar to that seen in the MPTP group [146.4±9.976 s (MPTP + EA + K252a) vs. 158.9±13.66 s (MPTP + sham EA), $p = 0.6998$, **Figure 6B**]. The effect of EA on preserving the dopaminergic neurons was also compromised with the K252a injection. The immunohistochemical analysis of TH expression showed a level comparable to MPTP [71.67±2.764 (MPTP + EA + K252a) vs. 112.1±19.7 (MPTP + EA), $p = 0.0046$; 71.67±2.764 (MPTP + EA + K252a) vs. 79.92±13.09 (MPTP + sham EA), $p = 0.6208$, **Figures 7A,B**]; results from the Western blot analysis also showed a trend similar to that obtained with immunohistochemistry [0.9±0.03 (MPTP + EA + K252a) vs. 1.3±0.13 (MPTP + EA), $p = 0.0029$, 0.9±0.03 (MPTP + EA + K252a) vs. 1±0.058 (MPTP + sham EA),

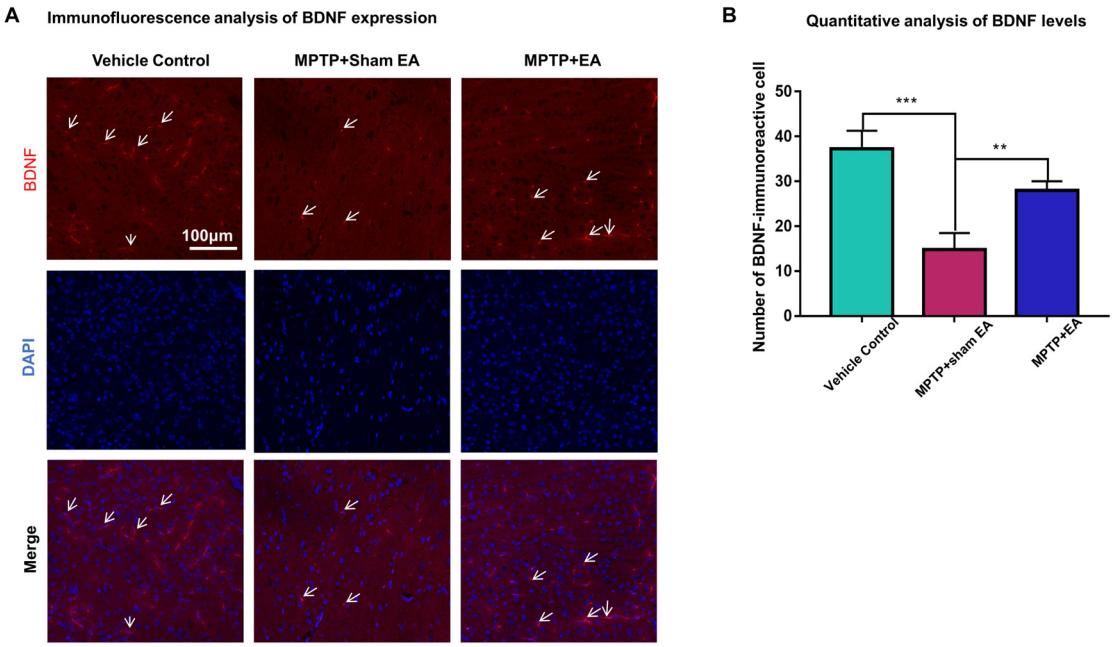

FIGURE 4 | EA reversed the expression of BDNF against MPTP neurotoxicity. Midbrain cryosections were incubated with primary antibody against BDNF and Alexa Fluor 596-conjugated secondary antibody. The cell nuclei were stained with DAPI for 10 min. The SN areas were examined under a Zeiss LSM 780 confocal microscopy. **(A)** Representative images with 20× amplification were shown. Scale bar represents 100 μm in length. **(B)** Quantitative analysis of BDNF expression detected by immunostaining. Numbers of BDNF-immunoreactive cells in the SN region was quantified and expressed in mean ± SD (n = 3). $^{**}p < 0.01$, $^{***}p < 0.001$.

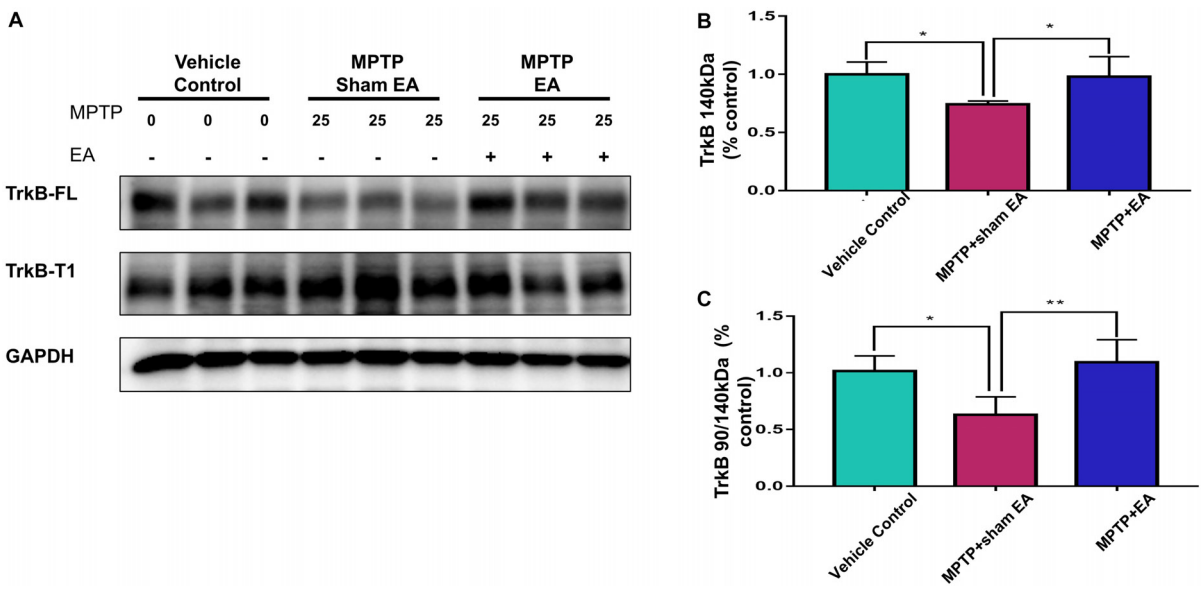

FIGURE 5 | EA recovered MPTP-induced disruption to the ratio of TrkB FL vs. TrkB T1. The mesencephalon proteins were extracted and analyzed by Western blotting for the expression of TrkB FL (140 kDa) and TrkB T1 (90 kDa). GAPDH serves as loading control. **(A)** Representative blots were shown. **(B)** Quantitative analysis for the expression of TrkB FL (140 kDa). **(C)** Ratio of TrkB T1/TrkB FL determined by western blot. The intensity of each band was determined by a densitometric approach. Quantitative analysis (n = 4) were conducted by one-way ANOVA. $^{*}p < 0.05$, $^{**}p < 0.01$.

p = 0.3333, **Figures 7C,D**]. Moreover, the additional utilization of K252a successfully blocked the effect of EA on BDNF expression, as was detected by the Western blot shown in **Figure 8** [0.81±0.076 (MPTP + EA + K252a) vs. 1.9±0.32 (MPTP+ EA), p = 0.0008, 0.81±0.076 (MPTP + EA + K252a) vs. 1±0.049 (MPTP + sham EA), p = 0.4359]. The

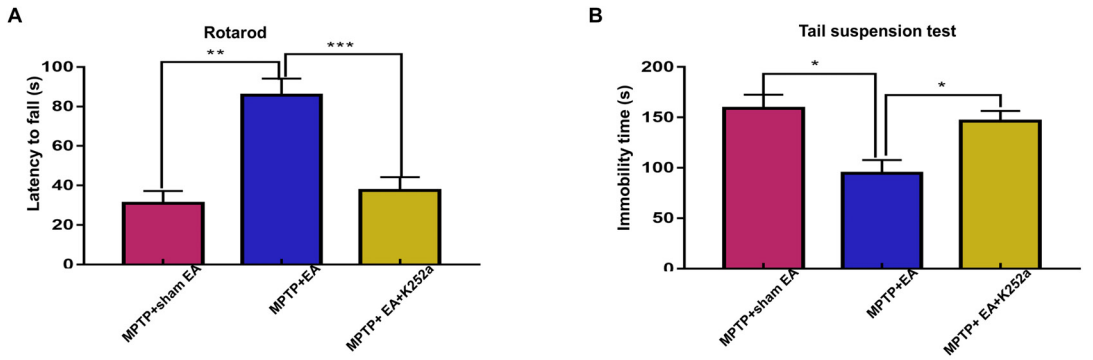

FIGURE 6 | The administration of TrkB inhibitor K252a effectively abolished the effect of EA on MPTP impaired the motor function. 1 h prior to each EA session, K252a (5 μg/kg/day) or vehicle was administered to mice via i.p. injection. **(A)** The effect of K252a on rotarod performance test. The rodding time of each mice were analyzed. **(B)** The behavioral deficits were assessed by tail suspension test. The immobility time of each mice within 6-min were recorded. The results were presented as mean ± SEM from 3 independent experiments (n = 10). *p < 0.05, **p < 0.01, ***p < 0.001.

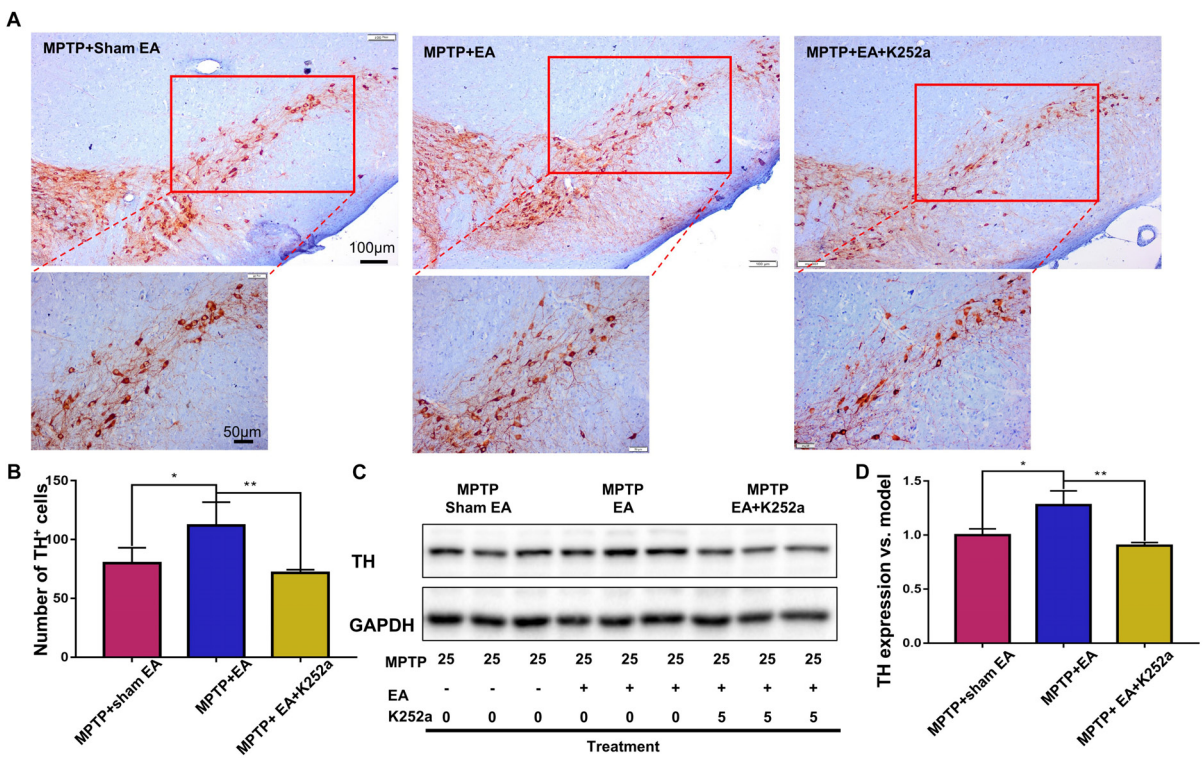

FIGURE 7 | EA preserved dopaminergic neuron survival can be abrogated by K252a. The brain cryosections were sequentially incubated with TH antibody, then visualized by DAB substrate kit. **(A)** The represented photos from each group were shown (with 10× and 20× magnification), scale bar represented 100 μm, 50 μm in length, respectively. **(B)** Statistical analysis for the number of TH^+ cells from each group. The numbers of TH^+ cells of each slide were counted for three non-overlapping areas at 10× magnification via an Olympus microscope. The results were presented as mean ± SD of three independent experiments. **(C)** Midbrain protein were extracted and probed with anti-TH and GAPDH (as loading control) via western blotting technique. The representative blots were shown. **(D)** The quantification for TH expression probed by western blot. The blots were quantified in a densitometric method by ImageLab 5.1 (Bio-Rad). *p < 0.05, **p < 0.01.

activation of the BDNF downstream signaling cascades that was enhanced by EA stimulation was also jeopardized with K252a administration, as shown by a marked decrease in intensity of the phosphorylation of Akt and ERK1/2, but not CREB expression, as compared with the EA-treated group {p-AKT/AKT [p = 0.0204 (MPTP + EA + K252a vs. MPTP+ EA), p = 0.8555 (MPTP + EA + K252a vs. MPTP+ Sham EA)], p-ERK/ERK [p = 0.0001 (MPTP + EA + K252a vs. MPTP+ EA), p = 0.6219 (MPTP + EA + K252a vs. MPTP+ Sham EA)], and p-CREB/CREB [p = 0.4752 (MPTP + EA + K252a vs. MPTP+ EA), p = 0.0732 (MPTP + EA + K252a vs. MPTP+ Sham EA)], **Figures 8A,B**}.

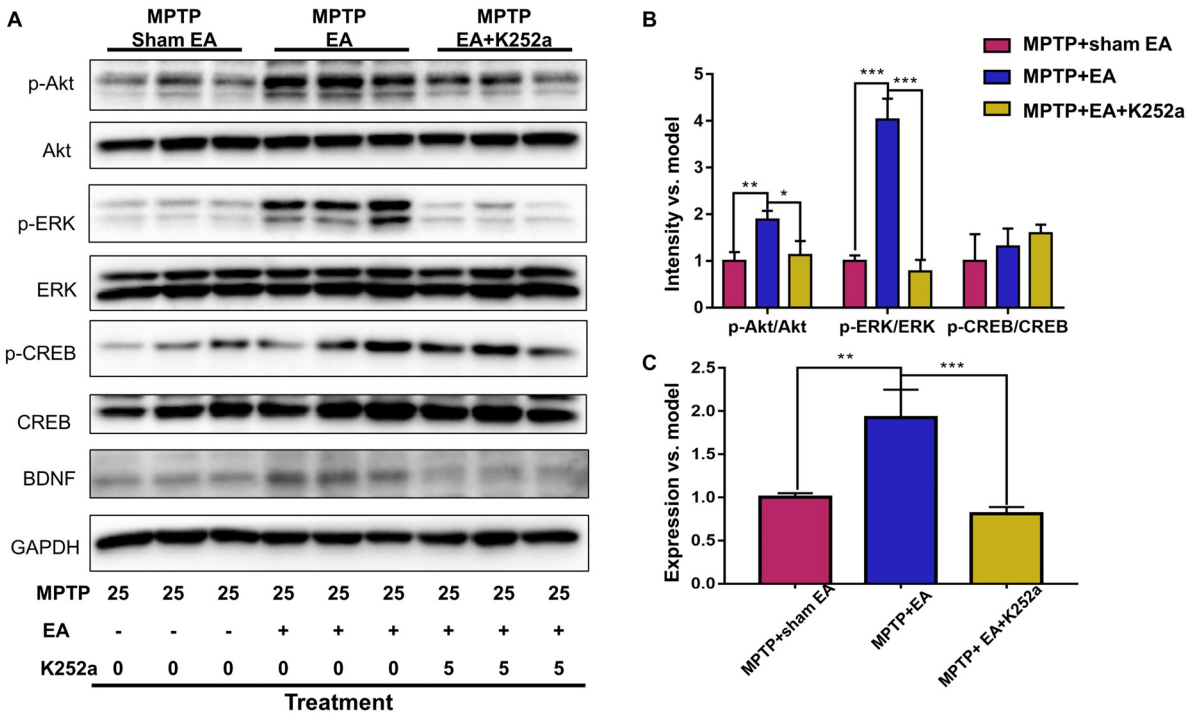

FIGURE 8 | K252a administration can effectively inhibited EA enhanced BDNF signaling pathway transduction. **(A)** The midbrain tissues were lysed and analyzed by Western blotting using antibodies against Akt, phospho-Akt, ERK1/2, phospho-ERK1/2, CREB, phospho-CREB, and BDNF. Representative blot was shown. GAPDH serves as loading control. **(B)** Statistical analysis for the phosphorylation of Akt, ERK1/2, and CREB. **(C)** Quantitative analysis for the expression level of BDNF. The signal intensities of protein bands ($n = 3$) were determined by a densitometric method, and quantitatively analyzed by one-way ANOVA. $^{*}p < 0.05$, $^{**}p < 0.01$, $^{***}p < 0.001$.

DISCUSSION

The disruption of the BDNF-TrkB signaling pathway is implicated in neurodegenerative diseases (Andero et al., 2014). The potential of BDNF-based therapy is hindered by the dose and delivery in translational studies (Nagahara and Tuszynski, 2011). Acupuncture and EA may have potential for treatment to retard or reverse neurodegeneration in PD (Eng et al., 2006; Lei et al., 2016; Kong et al., 2018). Earlier studies suggested a role for BDNF in EA-induced neuroprotection. In the present study, we not only validated the effect of EA on BDNF expression against MPTP neurotoxicity but also determined the effects of EA on the TrkB FL/TrkB T1 ratio and the activation of downstream signals, such as PI3K/Akt and ERK1/2.

Electroacupuncture combines the traditional effects of acupuncture and electrical stimulation for potential neuroprotective properties against parkinsonism symptoms. The earlier study by Liang et al. (2002) reported that EA stimulation on GV20 and GV14 could upregulate the expression of BDNF in 6-OHDA-lesioned rats. Kim et al. (2011) applied manual acupuncture at GB34 to activate the neuroprotective PI3K/Akt pathway. Along the same line of evidence, Lin et al. found that EA stimulation on GB34 and LR3 not only enhanced BDNF expression but also induced the activation of the signaling proteins Akt and ERK in MPP^{+}-induced rat models (Lin et al., 2017). Acupoints such as GB34 (Yang Ling Quan), ST36 (Zu San Li) and GV20 (Bai Hui) are frequently selected to achieve neuroprotective properties. GV20 and GV29 are used as scalp acupuncture for neurological disorders (Lee et al., 2013). More experiments are called for to verify the effectiveness of scalp acupuncture for PD. The present study was designed to observe the therapeutic effect of scalp acupuncture in conscious animals. EA stimulation was performed in mice without restraints. To avoid the disruption of electrical stimulation, we selected two acupoints (GV20 and GV29) on the head.

Brain-derived neurotrophic factor regulates the survival and activity of dopaminergic, motor, and sensory neurons (Hyungju and Mu-Ming, 2012). The reduction of BDNF expression in the striatum and serum was detected in PD patients (Mogi et al., 1999; Scalzo et al., 2010). Nevertheless, the ectopic overexpression of BDNF could protect the neurons against 6-OHDA-induced neurotoxicity in mice (Levivier et al., 1995). Tsukahara et al. also demonstrated the efficacy of BDNF against MPTP-induced damage in non-human primates (Tsukahara et al., 1995). It was previously shown that acupuncture reduced parkinsonism symptoms, rescued dopaminergic neurons, and restored the expression of dopamine transporters against MPTP-induced neurotoxicity (Choi et al., 2011). Moreover, several studies revealed that EA could ameliorate MPTP-induced neurotoxicity by upregulating BDNF, GDNF, and cyclophilin A, thereby ameliorating the pathological changes in PD (Chen et al., 2007; Jeon et al., 2008; Joh et al., 2010). The present study corroborated

that EA could alleviate motor impairments and enhance the survival of dopaminergic neurons against MPTP neurotoxicity. Western blotting and immunofluorescence analysis further verified the effects of EA stimulation on BDNF expression in the SNpc against MPTP-induced disruption. Moreover, apart from the observation of the effect of EA on BDNF expression, we additionally determined the role of the TrkB receptor in EA-regulated neurosurvival.

It is well known that BDNF regulates neuronal survival via interacting with TrkB. However, TrkB exists in two different forms: full-length and truncated. TrkB FL is the high-affinity receptor for BDNF and is widely expressed in different regions in the adult brain, for example, hippocampus, striatum, and cortex (Huang and Reichardt, 2003). Under physiological conditions, BDNF binding induces the dimerization of the functional TrkB FL and elicits tyrosine phosphorylation and related cellular neuroprotective signals. In contrast to TrkB FL, TrkB T1 is a predominantly negative isoform. The upregulation of TrkB T1 often indicates the dysfunction of TrkB FL-mediated signals leading to neurodegeneration (Haapasalo et al., 2002; Danelon et al., 2016). Thus, TrkB T1 was suggested as a potential target for the treatment of neurodegenerative diseases (Ferrer et al., 1999; Vidaurre et al., 2012). A recent study reported that the ratio of TrkB FL vs. TrkB T1 was altered in the SNpc and striatum of patients with PD (Fenner et al., 2014). However, EA stimulation was not examined for its effects on the ratio of TrkB FL vs. TrkB T1 in animal models. In the present study, we examined the levels of two TrkB isoforms following MPTP exposure and EA treatment by Western blotting. The key finding from the present study is that EA stimulation can antagonize the effects of MPTP on the formation of TrkB FL and TrkB T1. The neurotoxin MPTP has been well documented for its effects on mitochondrial function and on the overactivation of calpain (Chera et al., 2002). Calpain activation directly enhanced the expression of TrkB T1 (Danelon et al., 2016). These results eventually revealed the mechanisms by which MPTP increases the level of TrkB T1. Nevertheless, EA stimulation restored the balance between TrkB FL and TrkB T1, probably via preventing the MPTP-induced cleavage of TrkB FL or downregulating the TrkB T1 expression. It is well established that TrkB activation initiates the activation of several signaling pathways involving MAPK, ERK, phospholipase Cγ, and PI3K/Akt (Dolcet et al., 1999). Disruption of the TrkB FL/TrkB T1 ratio often alters the cellular signaling transduction. Our result for the phosphorylation of ERK1/2 and Akt also suggested that EA treatment indeed increased the level of phospho-ERK1/2 and phospho-Akt (shown in **Figures 3A,B**). To further confirm the involvement of the TrkB receptor in EA-induced the neuroprotection, we used the TrkB inhibitor K252a. As expected, K252a completely abrogated the beneficial effect of EA as indicated by behavioral impairments and dopaminergic loss. Moreover, K252a also abolished the effect of EA on the activation of intracellular BDNF/TrkB signal transduction. Together, the current findings suggest that EA-regulated BDNF elevation was accomplished via reversing the imbalance between TrkB FL and TrkB T1.

The present study demonstrated that EA has a protective effect against MPTP-induced neurotoxicity in midbrain dopaminergic neurons and that EA ameliorated the impairments of motor function in a mouse PD model. EA mainly restored the activation of the BDNF-TrkB signaling pathway. Importantly, EA treatment appears to be a promising approach for the management of PD. Considering the general impact of BDNF dysregulation, EA could be a powerful non-pharmacological neuroprotective strategy against PD symptoms. Further work is needed to validate the therapeutic efficacy of EA and elucidate its neuroprotective mechanisms against PD.

ETHICS STATEMENT

All the experimental procedures were performed according to the regulation of the Committee on the Use of Live Animal in Teaching and Research (CULATR No. 4196-16).

AUTHOR CONTRIBUTIONS

YZ, DL, and ZN performed the animal experiments. YZ performed the biological experiments, statistical analysis, and wrote the first draft of the manuscript. LL and JR contributed to the design of the study, coordinated the whole process of the study. All the authors contributed to the manuscript revision and approved the final version.

FUNDING

This work was supported by General Research Fund (GRF) grants (17120915, 17146216, and 17100317) from the Research Grants Council of Hong Kong, National Natural Science Foundation of China (NSFC) grant (21778046), and the Seed Funding (201611159156) for Basic Research Program from University of Hong Kong.

ACKNOWLEDGMENTS

We would like to acknowledge the support of Professor Simon Lee (University of Macau) on the use of rotarod instrument.

REFERENCES

Andero, R., Choi, D. C., and Ressler, K. J. (2014). BDNF-TrkB receptor regulation of distributed adult neural plasticity, memory formation and psychiatric disorders. *Mol. Basis Memory* 122, 169–192. doi: 10.1016/B978-0-12-420170-5.00006-4

Bruno, M. A., and Cuello, A. C. (2012). Cortical peroxynitration of nerve growth factor in aged and cognitively impaired rats. *Neurobiol. Aging* 33, 1927–1937. doi: 10.1016/j.neurobiolaging.2011.09.031

Chen, J., Qi, J.-G., Zhang, W., Zhou, X., Meng, Q.-S., Zhang, W.-M., et al. (2007). Electro-acupuncture induced NGF, BDNF and NT-3 expression in spared L6 dorsal root ganglion in cats subjected to removal of

adjacent ganglia. *Neurosci. Res.* 59, 399–405. doi: 10.1016/j.neures.2007.08.006

Chera, B., Schaecher, K. E., Rocchini, A., Imam, S. Z., Ray, S. K., Ali, S. F., et al. (2002). Calpain upregulation and neuron death in spinal cord of MPTP-induced parkinsonism in mice. *Ann. N. Y. Acad. Sci.* 965, 274–280.

Choi, Y.-G., Yeo, S., Hong, Y.-M., and Lim, S. (2011). Neuroprotective changes of striatal degeneration-related gene expression by acupuncture in an mptp mouse model of Parkinsonism: microarray analysis. *Cell. Mol. Neurobiol.* 31, 377–391. doi: 10.1007/s10571-010-9629-2

Danelon, V., Montroull, L. E., Unsain, N., Barker, P. A., and Masco, D. H. (2016). Calpain-dependent truncated form of TrkB-FL increases in neurodegenerative processes. *Mol. Cell. Neurosci.* 75, 81–92. doi: 10.1016/j.mcn.2016.07.002

Deng, J. H., Lv, E., Yang, J., Gong, X. L., Zhang, W. Z., Liang, X. B., et al. (2015). Electroacupuncture remediates glial dysfunction and ameliorates neurodegeneration in the astrocytic alpha-synuclein mutant mouse model. *J. Neuroinflamm.* 12:103. doi: 10.1186/s12974-015-0302-z

Dexter, D. T., and Jenner, P. (2013). Parkinson disease: from pathology to molecular disease mechanisms. *Free Radic. Biol. Med.* 62, 132–144. doi: 10.1016/j.freeradbiomed.2013.01.018

Dolcet, X., Egea, J., Soler, R. M., Martin-Zanca, D., and Comella, J. X. (1999). Activation of phosphatidylinositol 3-kinase, but not extracellular-regulated kinases, is necessary to mediate brain-derived neurotrophic factor-induced motoneuron survival. *J. Neurochem.* 73, 521–531. doi: 10.1046/j.1471-4159.1999.0730521.x

Eng, M. L., Lyons, K. E., Greene, M. S., and Pahwa, R. (2006). Open-label trial regarding the use of acupuncture and yin tui na in Parkinson's disease outpatients: a pilot study on efficacy, tolerability, and quality of life. *J. Altern. Complement. Med.* 12, 395–399. doi: 10.1089/acm.2006.12.395

Fenner, M. E., Achim, C. L., and Fenner, B. M. (2014). Expression of full-length and truncated trkB in human striatum and substantia nigra neurons: implications for Parkinson's disease. *J. Mol. Histol.* 45, 349–361. doi: 10.1007/s10735-013-9562-z

Ferrer, I., Marin, C., Rey, M. J., Ribalta, T., Goutan, E., Blanco, R., et al. (1999). BDNF and full-length and truncated TrkB expression in Alzheimer disease. Implications in therapeutic strategies. *J. Neuropathol. Exp. Neurol.* 58, 729–739. doi: 10.1097/00005072-199907000-00007

Frim, D. M., Uhler, T. A., Galpern, W. R., Beal, M. F., Breakefield, X. O., and Isacson, O. (1994). Implanted fibroblasts genetically engineered to produce brain-derived neurotrophic factor prevent 1-methyl-4-phenylpyridinium toxicity to dopaminergic neurons in the rat. *Proc. Natl. Acad. Sci. U.S.A.* 91, 5104–5108.

Ghaffari, B., and Kluger, B. (2014). Mechanisms for alternative treatments in parkinson's disease: acupuncture, tai chi, and other treatments. *Current Neurol. Neurosci. Rep.* 14, 1–11. doi: 10.1007/s11910-014-0451-y

Gupta, V. K., You, Y. Y., Gupta, V. B., Klistorner, A., and Graham, S. L. (2013). TrkB receptor signalling: implications in neurodegenerative, psychiatric and proliferative disorders. *Int. J. Mol. Sci.* 14, 10122–10142. doi: 10.3390/ijms140510122

Haapasalo, A., Sipola, L., Larsson, K., Akerman, K. E. O., Stoilov, P., Stamm, S., et al. (2002). Regulation of TRKB surface expression by brain-derived neurotrophic factor and truncated TRIM Isoforms. *J. Biol. Chem.* 277, 43160–43167. doi: 10.1074/jbc.M205202200

Hong, C.-J., Liu, H.-C., Liu, T.-Y., Lin, C.-H., Cheng, C.-Y., and Tsai, S.-J. (2003). Brain-derived neurotrophic factor (BDNF) Val66Met polymorphisms in Parkinson's disease and age of onset. *Neurosci. Lett.* 353, 75–77. doi: 10.1016/j.neulet.2003.09.009

Huang, E. J., and Reichardt, L. F. (2003). Trk receptors: roles in neuronal signal transduction. *Annu. Rev. Biochem.* 72, 609–642. doi: 10.1146/annurev.biochem.72.121801.161629

Hyungju, P., and Mu-Ming, P. (2012). Neurotrophin regulation of neural circuit development and function. *Nat. Rev. Neurosci.* 14, 7–23. doi: 10.1038/nrn3379

Jeon, S., Kim, Y. J., Kim, S. T., Moon, W., Chae, Y., Kang, M., et al. (2008). Proteomic analysis of the neuroprotective mechanisms of acupuncture treatment in a Parkinson's disease mouse model. *Proteomics* 8, 4822–4832. doi: 10.1002/pmic.200700955

Jiang, F., Yang, T., Yin, H., Guo, Y., Namba, H., Sun, Z., et al. (2018). Evidence for the use of acupuncture in treating parkinson's disease: update of information from the past 5 years, a mini review of the literature. *Front. Neurol.* 9:596. doi: 10.3389/fneur.2018.00596

Joh, T. H., Park, H.-J., Kim, S.-N., and Lee, H. (2010). Recent development of acupuncture on Parkinson's disease. *Neurol. Res.* 32, 5–9. doi: 10.1179/016164109X12537002793643

Kalia, L. V., and Lang, A. E. (2015). Parkinson's disease. *Lancet* 386, 896–912. doi: 10.1016/S0140-6736(14)61393-3

Kalia, L. V., and Lang, A. E. (2016). Parkinson disease in 2015: evolving basic, pathological and clinical concepts in PD. *Nat. Rev. Neurol.* 12, 65–66. doi: 10.1038/nrneurol.2015.249

Kim, S.-N., Kim, S.-T., Doo, A.-R., Park, J.-Y., Moon, W., Chae, Y., et al. (2011). Phosphatidylinositol 3-kinase/Akt signaling pathway mediates acupuncture-induced dopaminergic neuron protection and motor function improvement in a mouse model of parkinson's disease. *Int. J. Neurosci.* 121, 562–569. doi: 10.3109/00207454.2011.591515

Klein, R. L., Lewis, M. H., Muzyczka, N., and Meyer, E. M. (1999). Prevention of 6-hydroxydopamine-induced rotational behavior by BDNF somatic gene transfer. *Brain Res.* 847, 314–320. doi: 10.1016/S0006-8993(99)02116-2

Kong, K. H., Ng, H. L., Li, W., Ng, D. W., Tan, S. I., Tay, K. Y., et al. (2018). Acupuncture in the treatment of fatigue in Parkinson's disease: a pilot, randomized, controlled, study. *Brain Behav.* 8:e00897. doi: 10.1002/brb3.897

Lao, L., Zhang, R.-X., Zhang, G., Wang, X., Berman, B. M., and Ren, K. (2004). A parametric study of electroacupuncture on persistent hyperalgesia and Fos protein expression in rats. *Brain Res.* 1020, 18–29. doi: 10.1016/j.brainres.2004.01.092

Lee, H. S., Park, H. L., Lee, S. J., Shin, B. C., Choi, J. Y., and Lee, M. S. (2013). Scalp acupuncture for Parkinson's disease: a systematic review of randomized controlled trials. *Chin. J. Integr. Med.* 19, 297–306. doi: 10.1007/s11655-013-1431-9

Lei, H., Toosizadeh, N., Schwenk, M., Sherman, S., Karp, S., Sternberg, E., et al. (2016). A pilot clinical trial to objectively assess the efficacy of electroacupuncture on gait in patients with parkinson's disease using body worn sensors. *PLoS One* 11:e0155613. doi: 10.1371/journal.pone.0155613

Levivier, M., Przedborski, S., Bencsics, C., and Kang, U. J. (1995). Intrastriatal implantation of fibroblasts genetically engineered to produce brain-derived neurotrophic factor prevents degeneration of dopaminergic neurons in a rat model of Parkinson's disease. *J. Neurol.* 15, 7810–7820.

Li, M., Li, L. J., Wang, K., Su, W. T., Jia, J., and Wang, X. M. (2017). The effect of electroacupuncture on proteomic changes in the motor cortex of 6-OHDA Parkinsonian rats. *Brain Res.* 1673, 52–63. doi: 10.1016/j.brainres.2017.07.027

Liang, X. B., Liu, X. Y., Li, F. Q., Luo, Y., Lu, J., Zhang, W. M., et al. (2002). Long-term high-frequency electro-acupuncture stimulation prevents neuronal degeneration and up-regulates BDNF mRNA in the substantia nigra and ventral tegmental area following medial forebrain bundle axotomy. *Mol. Brain Res.* 108, 51–59. doi: 10.1016/S0169-328x(02)00513-2

Lin, J. G, Chen, C. J., Yang, H. B., Chen, Y. H., and Hung, S. Y. (2017). Electroacupuncture promotes recovery of motor function and reduces dopaminergic neuron degeneration in rodent models of parkinson's disease. *Int. J. Mol. Sci.* 18:E1846. doi: 10.3390/ijms18091846

Luo, D., Zhao, J., Cheng, Y., Lee, S. M., and Rong, J. (2018). N-Propargyl Caffeamide (PACA) ameliorates dopaminergic neuronal loss and motor dysfunctions in MPTP mouse model of parkinson's disease and in MPP(+)-induced neurons via promoting the conversion of proNGF to NGF. *Mol. Neurobiol.* 55, 2258–2267. doi: 10.1007/s12035-017-0486-6

Lv, E., Deng, J., Yu, Y., Wang, Y., Gong, X., Jia, J., et al. (2015). Nrf2-ARE signals mediated the anti-oxidative action of electroacupuncture in an MPTP mouse model of Parkinson's disease. *Free Radic. Res.* 49, 1296–1307. doi: 10.3109/10715762.2015.1067696

Mogi, M., Togari, A., Kondo, T., Mizuno, Y., Komure, O., Kuno, S., et al. (1999). Brain-derived growth factor and nerve growth factor concentrations are decreased in the substantia nigra in Parkinson's disease. *Neurosci. Lett.* 270, 45–48.

Nagahara, A. H., and Tuszynski, M. H. (2011). Potential therapeutic uses of BDNF in neurological and psychiatric disorders. *Nat. Rev. Drug Discov.* 10, 209–219. doi: 10.1038/nrd3366

Otani, K., Okada, M., and Yamawaki, H. (2017). Diverse distribution of tyrosine receptor kinase B isoforms in rat multiple tissues. *J. Vet. Med. Sci.* 79, 1516–1523. doi: 10.1292/jvms.17-0257

Rui, G., Zhang, G. J., Yong, W., Jie, F., Cui, Y. C., Xi, J., et al. (2013). High frequency electro-acupuncture enhances striatum DAT and D1 receptor expression, but decreases D2 receptor level in 6-OHDA lesioned rats. *Behav. Brain Res.* 237, 263–269. doi: 10.1016/j.bbr.2012.09.047

Scalzo, P., Kümmer, A., Bretas, T., Cardoso, F., and Teixeira, A. (2010). Serum levels of brain-derived neurotrophic factor correlate with motor impairment in Parkinson's disease. *J. Neurol.* 257, 540–545. doi: 10.1007/s00415-009-5357-2

Solanki, I., Parihar, P., and Parihar, M. S. (2016). Neurodegenerative diseases: from available treatments to prospective herbal therapy. *Neurochem. Int.* 95, 100–108. doi: 10.1016/j.neuint.2015.11.001

Taylor, T. N., Greene, J. G., and Miller, G. W. (2010). Behavioral phenotyping of mouse models of Parkinson's disease. *Behav. Brain Res.* 211, 1–10. doi: 10.1016/j.bbr.2010.03.004

Tsukahara, T., Takeda, M., Shimohama, S., Ohara, O., and Hashimoto, N. (1995). Effects of brain-derived neurotrophic factor on 1-methyl-4-phenyl-1,2,3,6-tetrahydropyridine-induced parkinsonism in monkeys. *Neurosurgery* 37, 733–739;discussion 739–741.

Vidaurre, O. G., Gascon, S., Deogracias, R., Sobrado, M., Cuadrado, E., Montaner, J., et al. (2012). Imbalance of neurotrophin receptor isoforms TrkB-FL/TrkB-T1 induces neuronal death in excitotoxicity. *Cell Death Dis.* 3:e256. doi: 10.1038/cddis.2011.143

Xiao, L. Y., Wang, X. R., Yang, Y., Yang, J. W., Cao, Y., Ma, S. M., et al. (2018). Applications of acupuncture therapy in modulating plasticity of central nervous system. *Neuromodulation* 21, 762–776. doi: 10.1111/ner.12724

Yamada, M., Tanabe, K., Wada, K., Shimoke, K., Ishikawa, Y., Ikeuchi, T., et al. (2001). Differences in survival-promoting effects and intracellular signaling properties of BDNF and IGF-1 in cultured cerebral cortical neurons. *J. Neurochem.* 78, 940–951. doi: 10.1046/j.1471-4159.2001.00497.x

Yin, C. S., Jeong, H.-S., Park, H.-J., Baik, Y., Yoon, M.-H., Choi, C.-B., et al. (2008). A proposed transpositional acupoint system in a mouse and rat model. *Res. Vet. Sci.* 84, 159–165. doi: 10.1016/j.rvsc.2007.04.004

Zhao, J., Cheng, Y. Y., Fan, W., Yang, C. B., Ye, S. F., Cui, W., et al. (2015). Botanical drug puerarin coordinates with nerve growth factor in the regulation of neuronal survival and neuritogenesis via activating ERK1/2 and PI3K/Akt signaling pathways in the neurite extension process. *CNS Neurosci. Ther.* 21, 61–70. doi: 10.1111/cns.12334

Zhao, J., Luo, D., Liang, Z., Lao, L., and Rong, J. (2017). Plant natural product puerarin ameliorates depressive behaviors and chronic pain in mice with spared nerve injury (SNI). *Mol. Neurobiol.* 54, 2801–2812. doi: 10.1007/s12035-016-9870-x

Conflict of Interest Statement: The authors declare that the research was conducted in the absence of any commercial or financial relationships that could be construed as a potential conflict of interest.

frontiers in Aging Neuroscience

ORIGINAL RESEARCH
published: 28 August 2019
doi: 10.3389/fnagi.2019.00230

Gami–Chunggan Formula Prevents Motor Dysfunction in MPTP/p-Induced and A53T α-Synuclein Overexpressed Parkinson's Disease Mouse Model Though DJ-1 and BDNF Expression

Sora Ahn[1†], Quan Feng Liu[2†], Jae-Hwan Jang[1], Jeonghun Park[1], Ha Jin Jeong[3], Youngman Kim[4], Dong-hee Kim[1], Guwon Jeong[4], Seung Tack Oh[4], Seong-Uk Park[5], Seung-Yeon Cho[5], Hi-Joon Park[1,6] and Songhee Jeon[3]**

[1] Department of Korean Medical Science, Graduate School of Korean Medicine, Kyung Hee University, Seoul, South Korea, [2] Department of Neuropsychiatry, Graduate School of Oriental Medicine, Dongguk University, Gyeongju, South Korea, [3] Department of Biomedical Sciences, Center for Creative Biomedical Scientists, Chonnam National University, Gwangju, South Korea, [4] Research Institute, Dong Kwang Pharmaceutical Co., Ltd., Seoul, South Korea, [5] Stroke and Neurological Disorders Center, Kyung Hee University Hospital at Gangdong, Kyung Hee University, Seoul, South Korea, [6] Studies of Translational Acupuncture Research (STAR), Acupuncture and Meridian Science Research Center (AMSRC), Kyung Hee University, Seoul, South Korea

OPEN ACCESS

Edited by:
Daniel Ortuño-Sahagún, University of Guadalajara, Mexico

Reviewed by:
Hiroyoshi Ariga, Hokkaido University, Japan
Charles K. Meshul, Portland Veterans Affairs Medical Center, United States

***Correspondence:**
Hi-Joon Park
acufind@khu.ac.kr
Songhee Jeon
jsong0304@jnu.ac.kr

[†] These authors have contributed equally to this work

Received: *29 November 2018*
Accepted: *13 August 2019*
Published: *28 August 2019*

Citation:
Ahn S, Liu QF, Jang J-H, Park J, Jeong HJ, Kim Y, Kim D-h, Jeong G, Oh ST, Park S-U, Cho S-Y, Park H-J and Jeon S (2019) Gami–Chunggan Formula Prevents Motor Dysfunction in MPTP/p-Induced and A53T α-Synuclein Overexpressed Parkinson's Disease Mouse Model Though DJ-1 and BDNF Expression. Front. Aging Neurosci. 11:230. doi: 10.3389/fnagi.2019.00230

The Gami–Chunggan formula (GCF) is a modification of the Chunggan (CG) decoction, which has been used to treat movement disorders such as Parkinson's disease (PD) in Traditional East Asian Medicine. To evaluate the neuroprotective effects of GCF in chronic PD animal models, we used either a 5-week treatment of 1-methyl-4-phenyl-1,2,3,6-tetrahydropyridine with probenecid (MPTP/p) or the α-synuclein A53T overexpressed PD mouse model. C57BL/6 mice were treated with MPTP, in combination with probenecid, for 5 weeks. GCF was administered simultaneously with MPTP injection for 38 days. The A53T α-synuclein overexpressed mice were also fed with GCF for 60 days. Using behavioral readouts and western blot analyses, it was observed that GCF prevents motor dysfunction in the MPTP/p-induced and A53T α-synuclein overexpressed mice. Moreover, GCF inhibited the reduction of dopaminergic neurons in the substantia nigra (SN) and fibers in the striatum (ST) against MPTP/p challenge. The expression of DJ-1 was increased but that of α-synuclein was decreased in the SN of PD-like brains by GCF administration. *In vitro* experiments also showed that GCF inhibited 6-OHDA-induced neurotoxicity in SH-SY5Y neuroblastoma cell lines and that it did so to a greater degree than CG. Furthermore, GCF induced BDNF expression through phosphorylation of Akt, ERK, CREB, and AMPK in the SN of PD-like brains. Therefore, use of the herbal medicine GCF offers a potential remedy for neurodegenerative disorders, including Parkinson's disease.

Keywords: Parkinson's disease, traditional medicine, Chunggan extract, chronic disease model, mouse

INTRODUCTION

Parkinson's disease (PD) is a chronic neurodegenerative disorder that is predominantly characterized by three representative motor features: akinesia, stiffness, and tremors (Conley and Kirchner, 1999; Kalia and Lang, 2015). Although the exact pathogenic mechanism of PD remains unknown, one study with PD patients suggested that oxidative stress and inflammatory pathways together induce apoptosis of dopaminergic neurons, eventually leading to manifestation of the disease (Hartmann, 2004). In addition, several genes have been correlated with the development of PD (de Silva et al., 2000). One among them is the presynaptic protein α-synuclein, a fibrillar factor of Lewy bodies that is linked to neuropathological features of PD; several different missense mutations of α-synuclein such as A53T, A30P, and E46K have been linked to early onset PD (Polymeropoulos et al., 1997; Krüger et al., 1998). Overexpression of wild-type or mutant A53T human α-synuclein in mice causes human PD-like symptoms such as neuronal degeneration and movement impairments (van der Putten et al., 2000).

Several toxins or reagents that mimic Parkinsonism both *in vitro* and *in vivo* have been reported in recent times, such as 1-methyl-4-phenyl-1,2,3,6-tetrahydropyridine (MPTP), 6-hydroxydopamine (6-OHDA), and rotenone (Beal, 2001). MPTP specifically targets dopaminergic neurons and causes severe and irreversible PD-like syndrome in non-human primates and humans. These subjects display biochemical and pathological hallmarks of PD (Przedborski et al., 2000) such as the obvious loss of dopaminergic neurons, astrogliosis, and activated microglia in the substantia nigra pars compacta (SNpc) (Beal, 2001). A second reagent, probenecid, can accelerate the mitochondrial toxicity of MPTP by interfering with ATP metabolism (Alvarez-Fischer et al., 2013). In the chronic MPTP/probenecid (MPTP/p) model, approximately 40–45% of dopaminergic neurons in the SNpc are lost within 3 weeks of treatment while 25% are lost in subchronic models without probenecid (Petroske et al., 2001; Meredith et al., 2008). In either case, death of dopaminergic neurons continues for at least 6 months, unlike in the subchronic and acute MPTP models (Petroske et al., 2001; Meredith et al., 2008). 6-OHDA, on the other hand, mimics symptoms of PD by generating free radicals after it is transported by the dopamine transporter, resulting in the cell death of dopaminergic neurons.

Treatment for PD typically comprises L-3,4-dihydroxy-phenylalanine (L-dopa), a dopamine precursor and/or a dopamine agonist. Although this can reduce symptoms of PD, long-term use of the drug reduces its effectiveness and does not in fact stop disease progression (Kostic et al., 1991).

Chunggan (CG) extract has been used for the treatment of motor-related disorders, such as PD, in traditional oriental medicine. It includes six herbs: *Paeonia lactiflora* root, *Angelica gigas* root, *Bupleurum falcatum Linne* root, *Ligusticum chuanxiong* root, *Gardenia jasminoides Ellis* fruit, and *Paeonia suffruticosa Andrews* root bark. We have previously presented evidence for the pharmaceutical effects and mechanism of action of modified CG extract and its combination with L-dopa in the MPTP-induced PD model (Ahn et al., 2017; Chang et al., 2018). Although we already demonstrated the pharmacological properties of CG on acute PD symptoms, we did not examine its effects in a chronic disease model. Therefore, in this study, MPTP/p or α-synuclein A53T overexpression was used to establish a chronic PD mouse model. To improve the treatment efficacy of CG, a modified formula named Gami–Chunggan formula (GCF) was prepared, consisting of CG plus the *Syzygium aromaticum* bud and the *Agastache rugosa O. Kuntze* herb that has strong radical scavenging activities (data not shown). We aim to demonstrate the effect and mechanisms of action of GCF on PD-like phenotypes such as motor symptoms and neuroprotection in the chronic MPTP/p-induced or α-synuclein A53T overexpression induced PD mice models.

MATERIALS AND METHODS

Apparatus, Chemicals, and Reference Compounds

All analytical experiments were conducted with the Shimadzu LC-20AD XR High Performance Liquid Chromatography (HPLC) system and an SPD-M20A Photo Diode Array (PDA) detector (Kyoto, Japan). Acetonitrile and ethanol were obtained from J.T. Baker (PA, United States), and 18.2 MΩ distilled water was purified using Younglin's Aqua Max Ultra 370 (Anyang, South Korea) series. Geniposide, paeoniflorin, tilianin, paeonol, eugenol, saikosaponin A, ligustilide and decursin reference compounds were used for HPLC analysis and all were purchased from ChemFaces (Hubei, China).

Preparation of GCF and CG Extract

All packages of *P. lactiflora* root, *L. chuanxiong* root, *A. gigas* root, *B. falcatum Linne* root, *G. jasminoides Ellis* fruit, *S. aromaticum* bud, *P. suffruticosa Andrews* root bark, and *A. rugosa O. Kuntze* herb were purchased from the Tae-won-dang herb supplier (Daegu, South Korea). The origins of all plant batches were confirmed and deposited at Dongkwang Pharmaceutical Research and Development Center for extraction and HPLC analysis. For extraction of GCF, air-dried *P. lactiflora* root (60 g), *L. chuanxiong* root (40 g), *A. gigas* root (40 g), *B. falcatum Linne* root (32 g), *G. jasminoides Ellis* fruit (16 g), *S. aromaticum* bud (60 g), *P. suffruticosa Andrews* root bark (16 g), and *A. rugosa O. Kuntze* herb (40 g) were uniformly mixed and 30% ethanol (3.24 L) added to make a 30% ethanol mixture (10% w/v). For preparation of CG extract, *S. aromaticum* bud and *A. rugosa O. Kuntze* herb were excluded from GCF. After heating was initialized under reflux and the temperature reached 95 °C, the 30% ethanol mixture was extracted for a further 4 h. The 30% ethanol extract was cooled down for 30 min and filtered with Whatman #2 filter paper. The filtered extract was freeze dried to obtain GCF dried extract powder. The extraction was repeated 10 times.

Preparation of Standards and Samples

For standardization of GCF extract, The Korean Pharmacopoeia and scientific papers were reviewed and its major components

identified (Yun et al., 2008; Tuan et al., 2012; Korean Food and Drug Administration [KFDA], 2015; Baek et al., 2016). One reference compound from each plant component of GCF was selected as a standard; these were geniposide, paeoniflorin, paeonol, eugenol, saikosaponin A, and decursin. For HPLC analysis, each reference compound was dissolved and mixed thoroughly to make stock solution. Individual stock solutions were added in uniform amounts to make working standard mixtures, which were used for the simultaneous separation and determination of compounds. For HPLC analysis, 1 g of freeze-dried GCF extract powder was weighed and added into a 10 mL volumetric flask with HPLC-grade 70% ethanol as solvent. The GCF extract powder was further extracted using an ultra-sonicator for 1 h. After sonication, the extract was filtered and used as GCF extract sample for HPLC analysis.

HPLC Analysis of GCF

All experiments were conducted with the Shimadzu LC-20AD XR HPLC system. GCF extract samples were analyzed under the developed HPLC method and the reference compounds in GCF extract samples were quantified using Shimadzu's Lab Solutions software. Chromatographic separation was accomplished by using a YMC Pack Pro C18 (250 × 4.6 mm, 5 μm) column (YMC Company, Japan) with a flow rate of 1.0 mL/min at 30℃. To optimize detection, the entire UV spectrum of each reference compound was reviewed at different wavelengths. For optimum analysis, we selected 210 nm for saikosaponin A and ligustilide, and 230 nm for geniposide, paeoniflorin, tilianin, paeonol, eugenol and decursin.

MPTP Mouse Model

Male C57BL/6 mice (Central Laboratories Animal Inc., South Korea) with a mean weight of 29.5 g were reared under standard conditions. The experimental processes were approved by the Institutional Animal Treatment Ethical Committee at the Dongguk University Campus (No. 2017-0992) and followed NIH guidelines. Mice were administered with intraperitoneal (i.p.) injections of saline, MPTP (30 mg/kg, dissolved in saline; Sigma-Aldrich, MO, United States), or L-3,4-dihydroxyphenylalanine (L-dopa, Sigma-Aldrich, MO, United States) for 6 days. Mice were allocated to six groups:

(1) Control (saline-injected group, $n = 5$)
(2) MPTP (MPTP + intraorally saline-treated group, $n = 5$)
(3) MPTP + GCF 100 (MPTP + intraorally 100 mg/kg of GCF-treated group, $n = 5$)
(4) MPTP + GCF 200 (MPTP + intraorally 200 mg/kg of GCF-treated group, $n = 5$)
(5) MPTP + GCF 300 (MPTP + intraorally 300 mg/kg of GCF-treated group, $n = 5$)
(6) MPTP + L-dopa (MPTP + intraperitoneally 10 mg/kg of L-dopa-treated group, $n = 5$)

Gami–Chunggan formula or L-dopa treatment was given simultaneously with MPTP injection for 14 days. Behavior tests were done on day 15.

MPTP/p Mouse Model

Protocols for mouse experiments were revised and permitted by the Institutional Animal Care and Use Committee at the Dongguk University Campus (No. 2017-025) and followed NIH guidelines. Mice, excluding the control group, were administered MPTP (25 mg/kg in saline, i.p.) along with probenecid (100 mg/kg in 5% $NaHCO_3$, i.p.) (MPTP/p). These mice were treated with 10 injections of MPTP with probenecid, every 3.5 days for 5 weeks. During the schedule, two of them died after the ninth and tenth injection in the MPTP/p and MPTP/p + GCF (100 mg/kg) groups, respectively. Mice were allocated to five groups:

(1) Control (saline-injected group, $n = 8$)
(2) MPTP/p (MPTP/p + intraorally saline-treated group, $n = 9$)
(3) MPTP/p + GCF 100 (MPTP/p + intraorally 100 mg/kg of GCF -treated group, $n = 9$)
(4) MPTP/p + GCF 200 (MPTP/p + intraorally 200 mg/kg of GCF treated group, $n = 9$)
(5) MPTP/p + GCF 300 (MPTP/p + intraorally 300 mg/kg of GCF-treated group, $n = 9$)

Gami–Chunggan formula was administered intraorally along with MPTP/p injections. Each dose of GCF was dissolved in 0.9% saline and administered once a day for 38 days. The drugs were administered each day at 2:30 p.m.

Transgenic Mice

83Vle mice (Prnp-SNCA*A53T) with a B6C3H background (Jackson Laboratory, Bar Harbor, Maine, United States) were bred at the Dongguk University and animal protocols followed previously described methods (Lee et al., 2017) (No. 2017-0992). A53T hemizygous mice ($n = 22$) at 13–14 months of age were divided into three groups:

(1) Control (intraorally saline-treated group, $n = 7$)
(2) GCF 100 (intraorally 100 mg/kg of GCF -treated group, $n = 7$)
(3) GCF 300 (intraorally 300 mg/kg of GCF-treated group, $n = 8$)

Saline or GCF was orally administered every day for 60 days. Behavior experiments were done on day 60 and the mice were then sacrificed. The feed efficiency ratio (FER) was calculated as total increased weight divived by the total amount of food consumption.

Biochemical Analysis of Blood

For biochemichal blood analysis, total blood was collected with heparin-syringe tubes and centrifuged at 3000 rpm for 15 min at 4°C. Plasma was collected and kept at −70°C. Glucose, total cholesterol, high-density lipoprotein (HDL) cholesterol, GOT (Glutamate Oxaloacetate Transaminase)/GPT (Glutamate Pyruvate Transaminase), and triglyceride (TG) were examined with analysis kits (Asan Pharmaceutical, Seoul, South Korea).

Akinesia

Akinesia was measured as the latency in time taken to move four limbs. The test was administered as previously described (Ahn et al., 2017). The test was repeated four times for each animal.

Catalepsy

Catalepsy was recorded as the time period for which animals retained their front legs, once placed, on a bar suspended above the floor of the test apparatus (Ahn et al., 2017). The time point at which the mice lifted their front paws from the bar marked the end of the time period. This experiment was repeated four times for each animal and mean value was calculated.

Rotarod Test

The rotarod test was used to assess neurological impairment such as motor coordination and balance. The experimental procedure followed was as previously reported (Ahn et al., 2017).

Pole Test

We performed a pole test 60 days after GCF administration, using an instrument 55 cm in height and 1.3 cm in diameter. The mice were held by their tails, with their heads positioned upward near the top of the pole and their forepaw on top of the pole. The time taken by the mouse to fall fully head down (orient down time) and the time taken to reach the bottom (transverse down time) were recorded. Mice were adjusted to the task by performing five trials per day for 3 days before the behavior test.

Brain Immunohistochemistry

Brain tissue preparation and immunohistochemistry methods were performed as per a previous report (Ahn et al., 2017). Briefly, sectioned slices were incubated with rabbit anti-tyrosine hydroxylase (1:1000; Santa-Cruz Biotechnology, TX, United States) overnight at room temperature. They were then stained using ABC methods (Vectastain Elite ABC kit; Vector Laboratories, Inc., CA, United States) and developed with diaminobenzidine (Sigma, MO, United States). The sections were mounted, coverslipped, and imaged using a light microscope (BX51; Olympus Japan Co., Tokyo, Japan).

Western Blot Analysis

The substantia nigra (SN) and striatum (ST) from mice brains were isolated and homogenized with RIPA buffer (Thermo Fisher Scientific, MA, United States). Supernatant from these lysates were mixed with 4X Laemmli's sample buffer and boiled at 99°C for 5 min. The samples were electrophoresed through 10% or 15% Tris-SDS-PAGE and then transferred to an Immobilon-P membrane (Millipore, MA, United States). The blotted membrane was blocked with 5% skim milk in Tris-Buffered Saline containing 0.05% Tween 20 (TBS-T buffer) for 1 h. After washing the membrane with TBS-T, each primary antibody was added and incubated overnight at 4°C. The primary antibodies used were α-synuclein (1:500; Cell Signaling, MA, United States), p-Akt (1:1000; Cell Signaling), Akt (1:1000; Cell Signaling), p-ERK (1:1000; Cell Signaling), ERK (1:1000; Cell Signaling), p-CREB (1:1000; Cell Signaling), CREB (1:1000; Cell Signaling), BDNF (1:500; Santa-Cruz Biotechnology, TX, United States), p-AMPK (1:1000; Cell Signaling), AMPK (1:500; Cell Signaling), DJ-1 (1:1000; Cell Signaling), p-synapsin-1 (1:1000; Cell Signaling), Synapsin-1 (1:1000; Cell Signaling), β-actin (1:4000; Sigma, MO, United States), TNF-α (1:500; Cell Signaling), BCL-2 (1:1000; Cell Signaling) and BAX (1:500; Abcam, Cambridge, MA). The blots were mixed with HRP-conjugated secondary rabbit (Thermo Fisher Scientific, MA, United States) or mouse (Thermo Fisher Scientific) antibodies. Bands were detected using the ChemiDoc XRS + (Bio-Rad, CA, United States) and analyzed using Image Lab software (ver. 2.0.1; Bio-Rad).

Cell Culture

The human neuroblastoma SH-SY5Y cell line was purchased from the American Type Culture Collection (Rockville, MD, United States) and maintained in DMEM containing 10% FBS and 1% antibiotics (Hyclone Laboratories Inc., UT, United States). Serum-deprived cells were treated with GCF for 30 min and then stressed with 200 μM of 6-OHDA (Biosource International, CA, United States) for 24 h. To examine cell viability, 100X of 3-(4,5-dimethylthiazol-2-yl)-2,5-diphenyltetrazolium bromide (MTT) (Sigma) was added to the media and the cells were incubated for 3 h at 37°C in a CO_2 incubator. The media was then removed and remaining dye in the cells solubilized with DMSO. The optical density of each well was calculated using a spectrophotometer (Versamax microplate reader, Molecular Device, CA, United States) at a wavelength of 570 nm.

Statistical Analyses

GraphPad Prism (ver. 5; GraphPad Software, Inc., CA, United States) was used to perform all statistical analyses. One-way ANOVA was used to analyse the data excluding AIMs. Two-way ANOVA was used in AIMs data considering time and group as factors. All data are expressed as means ± SEM. $p < 0.05$ were considered as statistically significant.

RESULTS

Development of the Chemical Profile of GCF and Identification of Major Components

Plants contain hundreds of constituents, some of which are present at very low concentrations. Compositions may vary within different batches of plant material due to factors like freshness, temperature, light, water, time of collection, drying, and storage methods. To minimize this variation, the origins and suppliers of plant materials and the chemical compositions of GCF extract powder were controlled and standardized. One reference compound from each plant source used in GCF was selected for standardization based a thorough literature scan (**Figure 1A**; Yun et al., 2008; Tuan et al., 2012; Korean Food and Drug Administration [KFDA], 2015; Baek et al., 2016). Eight reference compounds were analyzed using the developed HPLC method; all of them were well-resolved and detected in

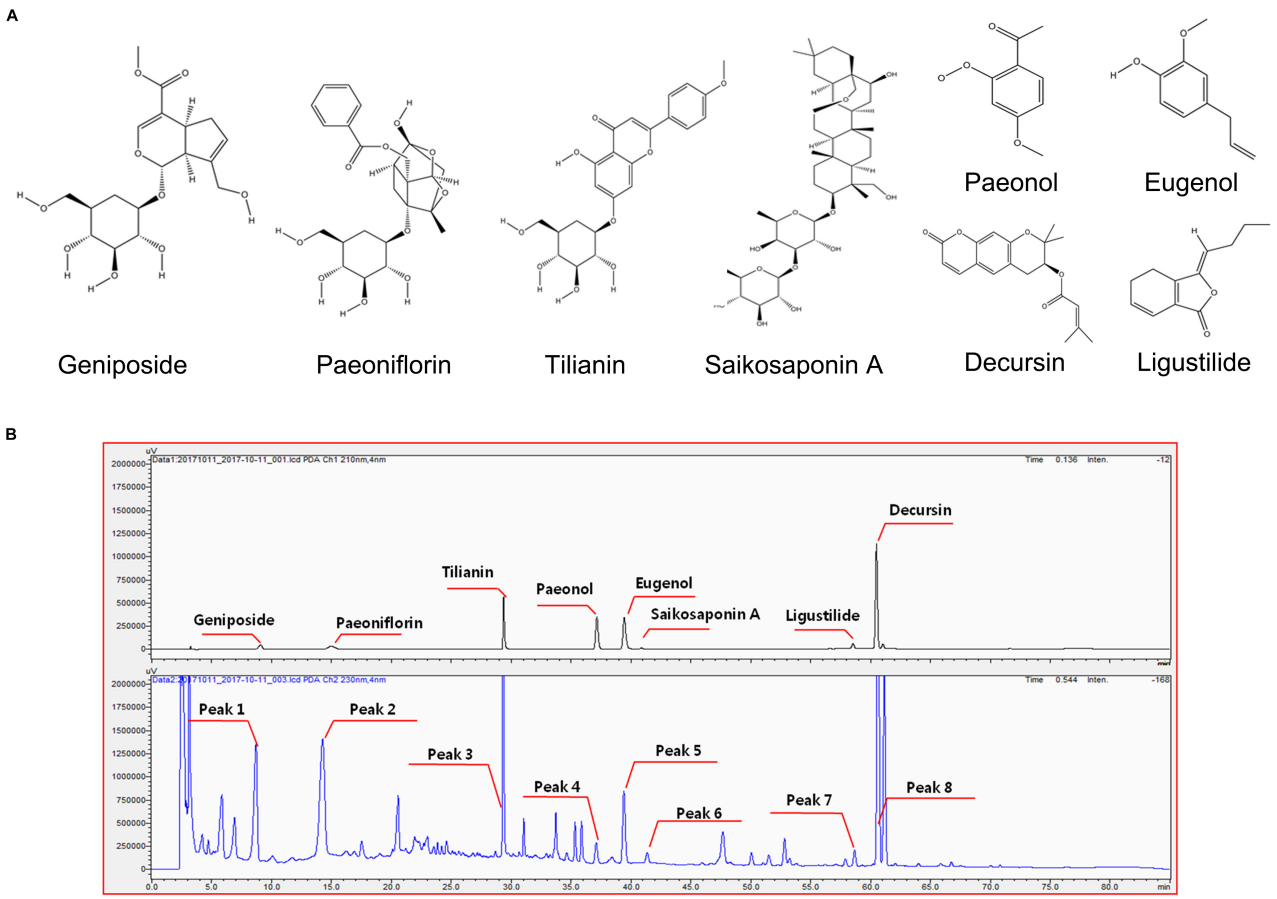

FIGURE 1 | Chemical structure of reference compounds and HPLC chromatograms of GCF samples. **(A)** Chemical structures of the reference compounds were drawn using ChemDraw software. **(B)** Eight reference compounds were selected, and their retention times observed using the Shimadzu PDA system (upper panel). Eight peaks with same retention time were identified from GCF extracts (lower panel).

the chromatograms (**Figure 1B**). The retention times of these compounds were used for identification of those from the GCF extract samples. When the GCF extract samples were analyzed, their chromatograms showed eight peaks matching those of the eight reference compounds (**Figure 1B**). The composition of the eight compounds in GCF extract powder are geniposide (13.97 ± 0.03 mg/g), ligustilide (0.8 ± 0.12 mg/g), tilianin (6.23 ± 0.03 mg/g), eugenol (12.13 ± 0.03 mg/g), saikosaponin A (1.1 ± 0.04 mg/g), paeoniflorin (19.26 ± 0.27 mg/g), paeonol (0.97 ± 0.08 mg/g), and decursin (11.20 ± 0.14 mg/g). No significant differences were found between batches.

GCF Has Neuroprotective Effects on 6-OHDA-Induced Apoptosis in SH-SY5Y Cells

The cytotoxic effect of GCF was tested using the MTT assay (**Figure 2A**) ($F_{(8,22)}$ = 3.15, p < 0.0205). When administered at a concentration of 200 μg/ml, neither CG nor GCF showed any cytotoxicity in SH-SY5Y cells. Treatment with 6-OHDA at a concentration of 200 μM for 24 h reduced cell viability to 76.81 ± 1.53% (n = 3) of the control value (100 ± 2.26%, n = 3) ($F_{(9,25)}$ = 14.82, p < 0.0001) (**Figure 2B**). However, SH-SY5Y cell viability of groups treated with 200 μg/ml CG recovered to 83 ± 2.55% (n = 3) and those of groups treated with 50 μg/ml GCF increased to 95.70 ± 1.98% (n = 3) (**Figure 2B**). These observations indicated that GCF has a stronger protective effect than CG against 6-OHDA toxicity in SH-SY5Y cells. To compare the neuroprotective effects of each component GCF, SH-SY5Y cells were pre-treated with different concentrations of the components or of GCF itself, followed by treatment with vehicle or 200 μM 6-OHDA for 24 h (n = 3). Among the components, tilianin (2.5 μg/ml, 83.00 ± 4.15%), eugenol (10 μg/ml, 86.21 ± 3.99%), saikosaponin A (10 μg/ml, 79.71 ± 4.55%), paeoniflorin (10 μg/ml, 77.92 ± 0.76%), paeonol (10 μg/ml, 78.62 ± 2.97%), and decursin (0.5 μg/ml, 81.52 ± 3.65%) facilitated significant recovery of the 6-OHDA-treated SH-SY5Y cells. ($F_{(28,85)}$ = 7.36, p < 0.0010) (**Figure 2C**).

GCF Inhibits MPTP-Induced Movement Impairments

To verify the protective effect of GCF in a PD animal model, GCF or L-dopa was administered to MPTP-treated mice for

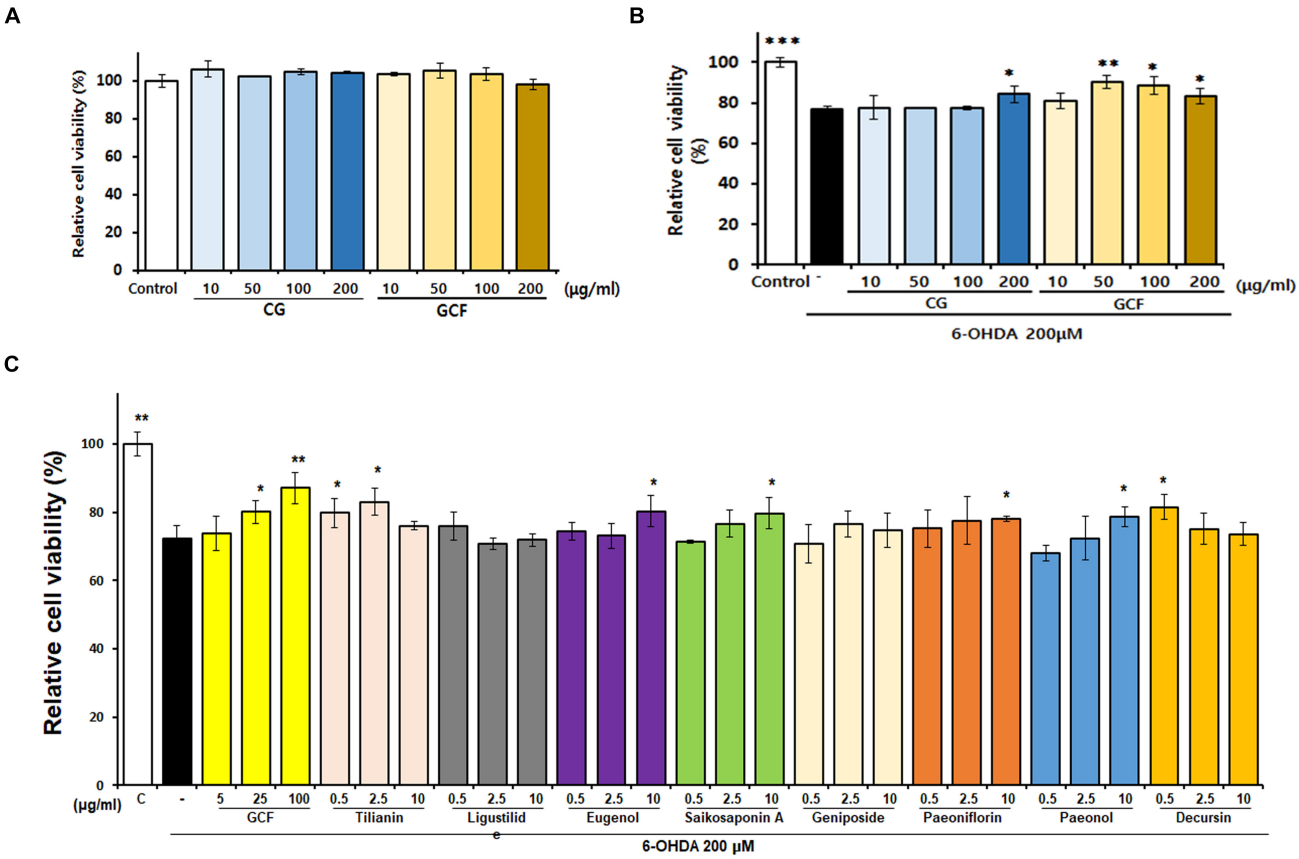

FIGURE 2 | Neuroprotective effects of GCF and its active compounds on SH-SY5Y cells. **(A)** Effect of CG and GCF extracts on viability of SH-SY5Y cells. SH-SY5Y cells were treated with CG and GCF of different concentrations and relative cell viability examined using the MTT assay. **(B)** Neuroprotective effect of CG and GCF extract on 6-OHDA-treated SH-SY5Y cells. **(C)** Neuroprotective effect of GCF on 6-OHDA-treated SH-SY5Y cells. Cell viability was determined using the MTT assay. Data are presented as mean ± SEM (***$p < 0.001$, **$p < 0.01$, *$p < 0.05$ compared with the MPTP group; $n = 3$).

14 days. MPTP induced severe motor impairments in the pole and rotarod tests when compared to the control group. Administration of GCF, however, significantly reduced the orient down time ($F_{(5,35)} = 8.88$, $p < 0.0001$), traverse down time ($F_{(5,34)} = 6.81$, $p < 0.0002$) and increased the time taken to fall from the rod ($F_{(5,35)} = 3.04$, $p < 0.224$). L-dopa-treated mice were used as positive controls and they also recovered movement impairments, but not to the extent of the GCF-treated group (**Figures 3A–C**).

Preventive Effect of GCF on MPTP/p-Induced Movement Impairments and Dopaminergic Neuron Loss

To verify the neuroprotective effects of GCF against motor symptoms, behavioral experiments were conducted on the chronic MPTP/p mouse model. Chronic administration of MPTP/p failed to initiate movement (akinesia, $F_{(4,38)} = 159.30$, $p < 0.0001$) or correct an externally enforced posture (catalepsy, $F_{(4,38)} = 248.00$, $p < 0.0001$) when compared to the control group ($p < 0.0001$ and $p > 0.0001$, respectively). Administration of GCF significantly diminished MPTP/p-induced akinesia and catalepsy (MPTP vs. GCF 100, $p < 0.01$; GCF 200 and 300, $p < 0.001$ each) (**Figures 4A,B**). In the rotarod test ($F_{(4,38)} = 43.60$, $p < 0.0001$), the MPTP/p group dropped from the rod at a significantly higher rate than the control group ($p < 0.001$) (**Figure 4C**), but the GCF-treated group remained on the rod longer than the MPTP/p group (MPTP/p vs. GCF 100, 200, and 300, $p < 0.001$ in all cases), indicating that GCF can reduce MPTP/p-induced hypokinesia.

To examine the effect of GCF on MPTP/p-induced dopaminergic neuronal loss, tyrosin hydroxylase (TH) was stained in the ST and SNpc of mice brains (SN: $F_{(4,15)} = 189.80$, $p < 0.0001$; ST: $F_{(4,15)} = 36.86$, $p < 0.0001$). In the MPTP/p group, the number of TH-positive cells in both the ST and SNpc was decreased and fiber density was lower than that of the control group ($p < 0.001$ and $p < 0.001$, respectively) (**Figures 4D–F**). However, GCF-treated mice (all doses) showed increased numbers of TH-immunopositive cells in the SNpc (MPTP vs. GCF 100, $p < 0.01$; GCF 200 and 300, $p < 0.001$ each) and denser fibers in the ST than those of the MPTP/p group (MPTP/p vs. GCF 100, 200 and 300, each $p < 0.001$) (**Figures 4D–F**). These data are indicative of the protective effect GCF on MPTP/p-induced dopaminergic neuron loss.

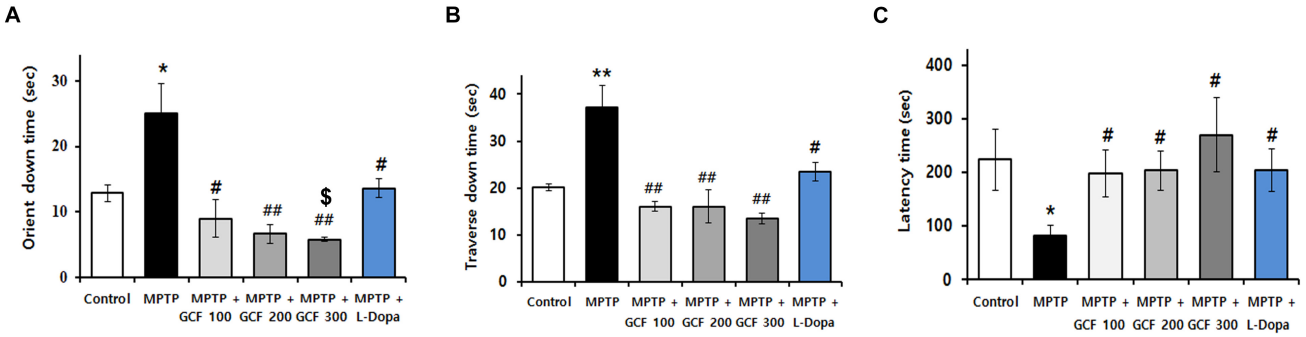

FIGURE 3 | Effects of GCF on MPTP-induced motor behavior dysfunctions and dopamine levels in the ST. Pole test of MPTP-injected PD model **(A)** orient down time and **(B)** transverse down time. **(C)** Latency time in overall rod performance test of MPTP-injected PD model. MPTP: MPTP only; GCF 100: GCF 100 mg/kg; GCF 200: GCF 200 mg/kg; GCF 300: GCF 300 mg/kg. Data are expressed as mean ± SEM ($^{*}p < 0.05$, $^{**}p < 0.01$ compared to control group; $^{\#}p < 0.05$, $^{\#\#}p < 0.01$ compared to MPTP group; $^{\$}p < 0.05$ compared to L-dopa group; $n = 5$).

Suppressive Effect of GCF on the Level of α-Synuclein and TNF-α in the MPTP/p PD Model

The levels of α-synuclein, a Lewy Body marker, were assessed by immunoblotting. Chronic MPTP/p treat m ent significantly enhanced α-synuclein expression in the SN and ST (SN: $F_{(4,15)} = 8666.00$, $p < 0.0001$; ST: $F_{(4,15)} = 3672.00$, $p < 0.0001$) when compared to vehicle treatment ($p < 0.001$, respectively) (**Figures 5A,B**). GCF treatment, on the other hand, significantly and dose-dependently suppressed the MPTP/p-induced α-synuclein expression in both the SN and ST (MPTP/p vs. GCF 100, 200 and 300, $p < 0.001$ in all cases) (**Figures 5A,B**). We also examined the levels of tumor necrosis factor α (TNF-α), a cytokine involved in the inflammatory response and regulation of immune cells, in the SN of chronic MTPT/p mice. The expression level of TNF-α ($F_{(4,15)} = 19.80$, $p < 0.0001$) was significantly increased in the chronic MPTP/p group when compared to the control group ($p < 0.001$). However, treatment with GCF significantly reduced the levels of TNF-α (MPTP vs. GCF 100, $p < 0.01$; GCF 200 and 300, $p < 0.001$ each) (**Figure 5C**).

Changes in Protein Expression Upon GCF Administration in the MPTP/p PD Model

Chronic MPTP/p treatment induced a marked reduction in Akt activation ($F_{(4,15)} = 46.65$, $p < 0.0001$) and extracellular signal-regulated kinase (ERK) activity ($F_{(4,15)} = 48.68$, $p < 0.0001$) in comparison to the control group ($p < 0.001$) (**Figures 6A,B**). Conversely, GCF (200 and 300 mg/kg) significantly blocked the Akt and ERK dephosphorylation seen in the chronic MPTP/p-treated animals ($p < 0.001$ each) (**Figures 6A,B**). In addition, chronic MPTP/p treatment reduced the activation of cAMP response element binding (CREB) ($F_{(4,15)} = 14.93$, $p < 0.0001$) and decreased the expression of brain-derived neuroprotective factor (BDNF) ($F_{(4,15)} = 6.76$, $p < 0.0064$) when compared to controls ($p < 0.001$ each) (**Figures 6C,D**). GCF (200 and 300 mg/kg) also significantly inhibited CREB dephosphorylation and BDNF down-regulation (CREB: $p < 0.001$ each; BDNF: $p < 0.01$ each) (**Figures 6C,D**). Interestingly, the phosphorylation of ERK and expression of BDNF were more dramatic at 200 mg/kg than at 300 mg/kg.

Next, we examined the phosphorylation level of adenosine monophosphate (AMP)-activated protein kinase (AMPK) as a negative regulator of autophagy. Chronic MPTP/p treatment inhibited phosphorylation of AMPK ($F_{(4,15)} = 17.38$, $p < 0.0001$) (**Figure 6E**), but treatment with GCF increased AMPK phosphorylation (**Figure 6E**). Notably, total AMPK levels ($F_{(4,15)} = 19.80$, $p < 0.0001$) were also increased by GCF treatment (MPTP vs. GCF 100, $p < 0.01$; GCF 300, $p < 0.05$) (**Figure 6E**). Furthermore, when DJ-1 expression was investigated, we found that it was significantly reduced in the chronic MPTP/p group ($F_{(4,15)} = 14.67$, $p < 0.0001$) when compared to the control group ($p < 0.001$) or GCF-treated group (200 and 300 mg/kg, $p < 0.001$) (**Figure 6F**). The phosphorylation level of synapsin-1 ($F_{(4,15)} = 7.35$, $p < 0.0017$) was also lower in the chronic MPTP/p group than in the control group ($p < 0.01$), whereas GCF treatment significantly inhibited synapsin-1 dephosphorylation in a dose-dependent manner ($p < 0.01$) (**Figure 6G**).

We then investigated whether the expression of BAX, a critical downstream mediator of apoptosis belonging to the BCL-2 family, was affected by GCF treatment. To check this, we determined the expression levels of the anti-apoptotic protein BCL-2 and apoptotic protein BAX. In the chronic MPTP/p group, the level of BCL-2 ($F_{(4,15)} = 19.80$, $p < 0.0001$) was significantly lower than that of the control group ($p < 0.001$), but GCF treatment inhibited BCL-2 downregulation (MPTP vs. GCF 100, $p < 0.01$; GCF 200, 300, $p < 0.001$) (**Figure 6H**). BAX levels were increased by chronic MPTP/p treatment ($F_{(4,15)} = 19.80$, $p < 0.0001$), but GCF administration blocked this increase (MPTP vs. GCF 100, $p < 0.01$; GCF 200, 300, $p < 0.001$) (**Figure 6H**). When we compared the ratio of BAX to BCL-2 ($F_{(4,15)} = 19.80$, $p < 0.0001$), we found that it was higher in chronic MPTP/p treated mice by 2.5 fold, but reduced in the SN of GCF-treated mice in a dose-dependent manner ($p < 0.001$) (**Figure 6H**).

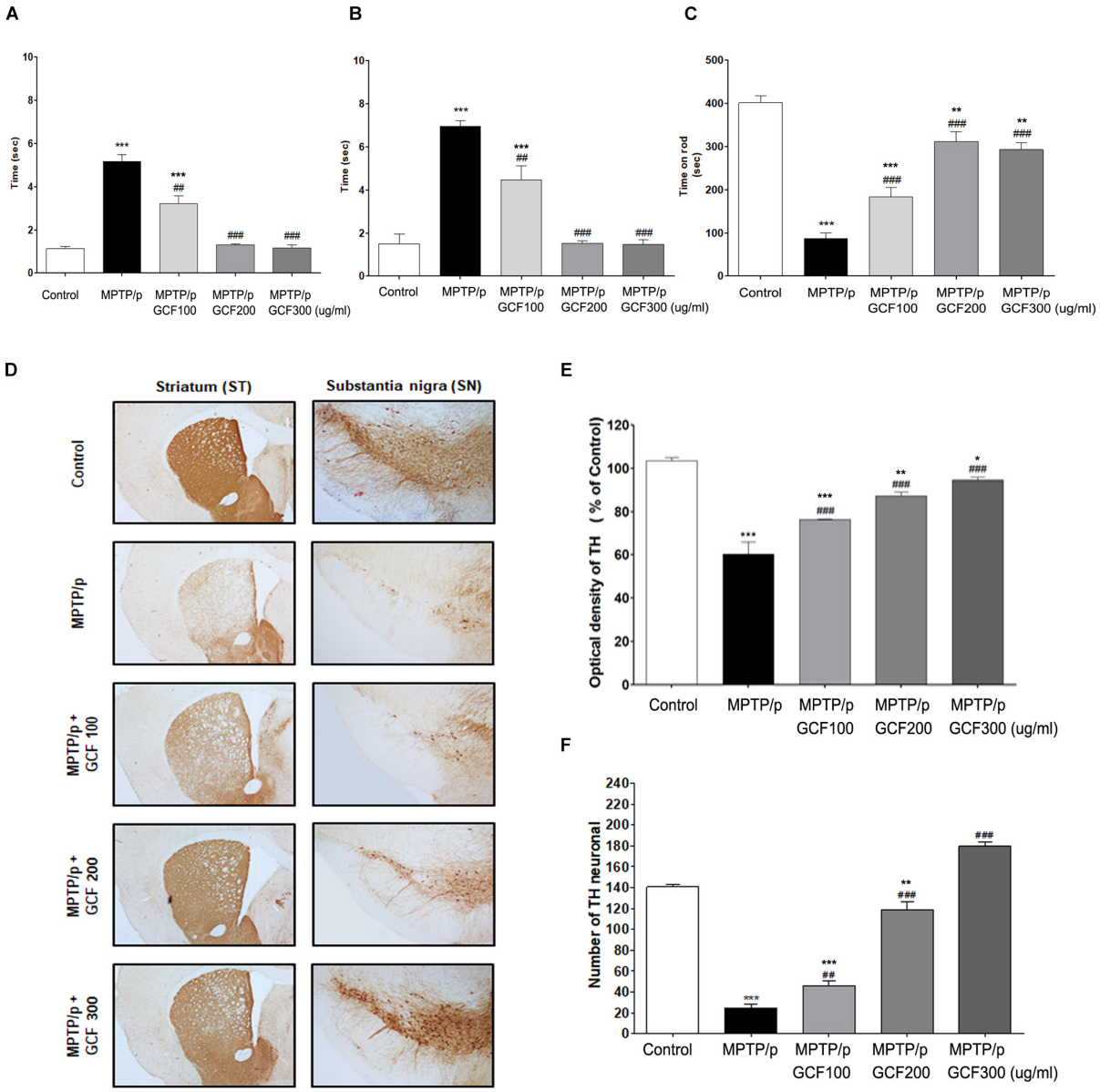

FIGURE 4 | Effects of GCF on MPTP/p-induced motor behavior dysfunctions and other neuroprotective effects. **(A)** Akinesia, **(B)** catalepsy, and **(C)** rotarod test were measured at day 36 post MPTP/p administration in control (n = 8), MPTP/p (n = 9), MPTP/p + GCF 100 (n = 9), MPTP/p + GCF 200 (n = 9), and MPTP/p + GCF 300 (n = 9) mice. **(D)** Brain sections were stained immunohistochemically for TH-positive dopaminergic fibers in the ST and neurons in the SN (scale bar, ST – 200 μm; SN – 100 μm). **(E)** The optical density of TH-positive dopaminergic fibers in the ST is shown in bar graphs. **(F)** Total TH-positive cell numbers in the SN. MPTP/p: MPTP/probenecid; GCF 100: GCF 100 mg/kg; GCF 200: GCF 200 mg/kg; GCF 300: GCF 300 mg/kg. Data are expressed as mean ± SEM (*$p < 0.05$, **$p < 0.01$, ***$p < 0.001$ compared to control group; $^{\#\#}p < 0.01$, $^{\#\#\#}p < 0.001$ compared to MPTP/p group).

Neuroprotective Effect of GCF on A53T α-Synuclein Tg Mice

Recent studies have shown that high blood levels of triglyceride (TG) and LDL-cholesterol have been associated with rapid cognitive decline (Ma et al., 2017). Therefore, we examined the biochemical parameters of plasma obtained from GCF-treated A53T α-synuclein Tg mice. As shown in **Figure 7**, GCF-treated Tg mice showed significantly higher levels of plasma HDL-cholesterol ($F_{(2,13)} = 5.70$, $p < 0.0001$; 100 mg/kg, $p < 0.001$; 300 mg/kg, $p < 0.01$) and significantly lower levels of plasma TG ($F_{(2,13)} = 1.50$, $p < 0.0087$), GOT ($F_{(2,13)} = 12.56$, $p < 0.0009$) and GPT ($F_{(2,13)} = 0.75$, $p < 0.0001$) when compared to control Tg mice ($p < 0.01$). However, the levels of glucose ($F_{(2,13)} = 2.07$, $p < 0.1606$) and total cholesterol ($F_{(2,13)} = 2.52$, $p < 0.1140$) were similar in both groups.

To assess the efficacy of GCF on motor symptoms, we conducted behavior tests on A53T α-synuclein Tg mice. In the pole test, GCF showed a dose-dependent reduction of the

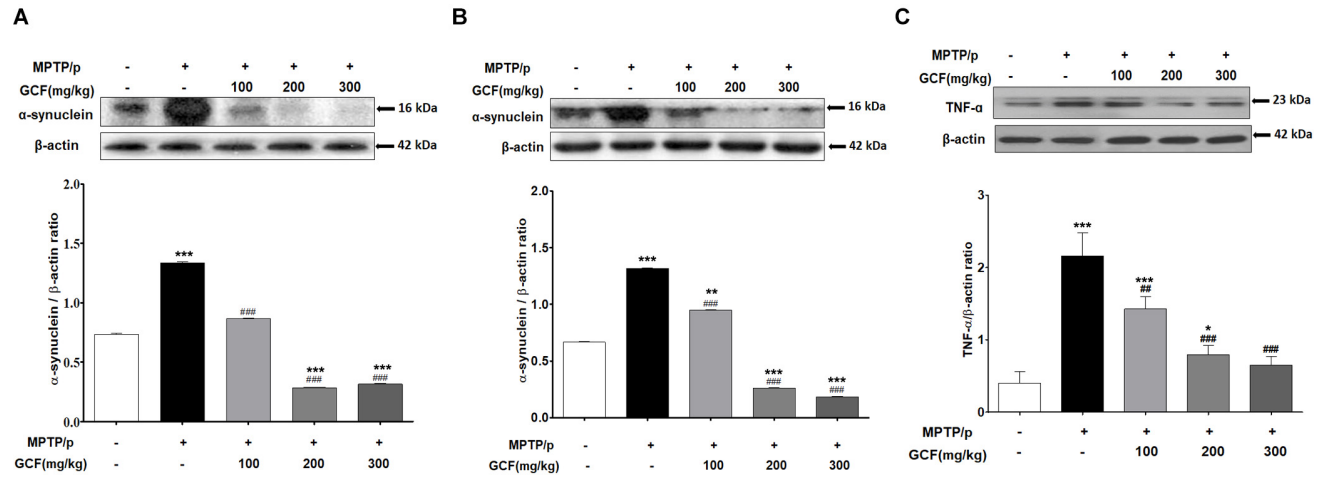

FIGURE 5 | Expression of α-synuclein and TNF-α in MPTP/p-induced mouse brains. Immunoblots assessing the effect of GCF treatment on levels of α-synuclein in **(A)** ST and **(B)** SN and **(C)** the levels of TNF-α in SN of MPTP/p induced mice. Data are expressed as mean ± SEM, (*$p < 0.05$, **$p < 0.01$, ***$p < 0.001$ compared to control group; $^{\#\#}p < 0.01$, $^{\#\#\#}p < 0.001$ compared to MPTP/p group; $n = 4$).

orient down time ($F_{(2,7)} = 3.27$, $p < 0.0857$) and traverse down time ($F_{(2,7)} = 3.00$, $p < 0.1043$) when compared to control Tg mice (each $p < 0.001$) (**Figures 8A,B**). Additionally, in the rotarod test we observed significant improvement of the latency time ($F_{(2,7)} = 4.54$, $p < 0.0431$) in GCF 300 treated mice in comparison to the control mice ($p < 0.01$) (**Figure 8C**).

A53T α-synuclein Tg mice showed no differences in TH expression in the SN as compared to control mice (**Supplementary Figure S1**). This is in agreement with previous reports showing that, in transgenic mice expressing A53T α-synuclein under the tyrosine hydroxylase promoter, the number of nigral neurons and levels of striatal dopamine are unchanged relative to wild-type mice for up to 1 year (Matsuoka et al., 2001). It has also been shown that the total number of SN neurons is not changed between the Tg and wild-type mice (Jia et al., 2018), indicating that dopaminergic cell loss has not yet occurred in the Tg mice. Despite lacking these markers of PD, the A53T mutation was identified in familial cases leading to early onset of parkinsonian symptoms (Athanassiadou et al., 1999), as well as in cases of motor impairment in mice (Uchihara and Giasson, 2016).

Expression of DJ-1 is known to clear the accumulation and toxicity of α-synuclein (Zhou et al., 2011; Zondler et al., 2014). GCF treatment induced DJ-1 ($F_{(2,4)} = 24.69$, $p < 0.0013$; 100 mg/kg, $p < 0.05$; 300 mg/kg, $p < 0.01$) and BDNF ($F_{(2,4)} = 13.53$, $p < 0.0260$; 300 mg/kg, $p < 0.05$) expression in a dose-dependent fashion when compared to control. It also decreased α-synuclein expression ($F_{(2,4)} = 22.04$, $p < 0.0160$; 300 mg/kg, $p < 0.05$) in the SN of A53T α-synuclein Tg mice (**Figure 8D**). Moreover, the GCF 300 group showed significant phosphorylation of Akt ($F_{(2,4)} = 39.24$, $p < 0.0400$), CREB ($F_{(2,4)} = 62.68$, $p < 0.00129$), and ERK ($F_{(2,4)} = 9.81$, $p < 0.0010$) in the SN of A53T α-synuclein Tg mice ($F_{(2,4)} = 13.53$, $p < 0.0260$; 300 mg/kg, $p < 0.05$) (**Figure 8E**). These data suggest that GCF treatment may decrease α-synuclein expression through DJ-1 expression and exercise a neuroprotective effect through BDNF expression.

DISCUSSION

In this study, we demonstrated that administration of GCF significantly improves behavioral impairments in A53T α-synuclein overexpressed mice and blocks the loss of doparminergic neurons in MPTP/p-induced mice, both of which are models of chronic Parkinson's disease. In addition, GCF induces BDNF and DJ-1 expression in the SN and downregulates α-synuclein in PD models.

The CG decoction has been used to improve motor function of PD patients in traditional oriental medicine. GCF is a modification of the CG decoction, consisting of some herbal components in addition to the standard CG mixture. Among the GCF components, paeoniflorin shows the most prominent anti-PD activities (Li et al., 2013). Paeoniflorin comes from the *P. lactiflora* root, which has been used to treat neurodegenerative disorders like PD in traditional medicine clinics. Paeoniflorin has been known to rescue MPP^+ and acidic damage-induced PC12 cell apoptosis through the autophagic pathway (Cao et al., 2010). This treatment also alleviates neurological deficits associated with unilateral striatal 6-OHDA lesion PD models (Liu et al., 2007). It attenuates neuroinflammation and dopaminergic neurodegeneration in PD mouse models by activation of the adenosine A1 receptor (Liu et al., 2006). Geniposide, an active element of *G. jasminoides Ellis*, has tranquilizing effects and is an important herb used in Traditional Chinese Medicine for dementia (Su et al., 2016). It shows neuroprotective effects by suppressing α-synuclein expression (Su et al., 2016), induces growth factors and reduces apoptosis in PD models (Chen et al., 2015). Eugenol, a phenol extracted from cloves, is an antioxidant (Ito et al., 2005), monoamine oxidase (MAO)

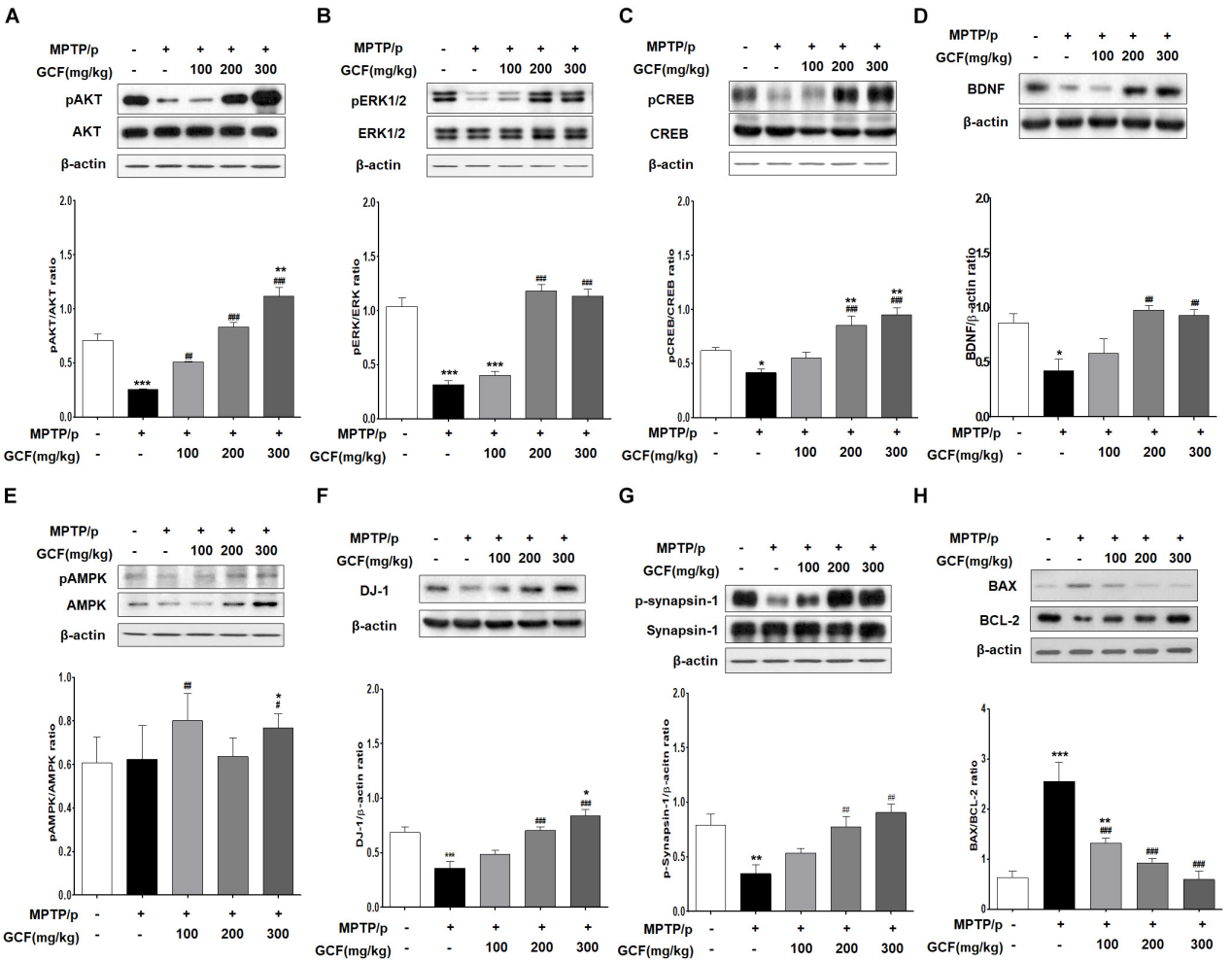

FIGURE 6 | Mechanisms of protective effects of GCF in MPTP/p-induced PD mouse model. Immunoblots of SN extracts probed using the following antibodies: **(A)** pAkt/Akt/β-actin, **(B)** pERK/ERK/β-actin, **(C)** pCREB/CREB/β-actin, **(D)** BDNF/β-actin, **(E)** pAMPK/AMPK/β-actin, **(F)** DJ-1/β-actin, **(G)** pSynapsin-1/Synapsin-1/β-actin, and **(H)** BAX/BCL-2/β-actin. The intensities of protein bands were quantitated by densitometry and the bands indicating phosphorylated protein were normalized against either the total protein or β-actin. Data are expressed as mean ± SEM (*$p < 0.05$, **$p < 0.01$, ***$p < 0.001$ compared to control group; $^{\#\#}p < 0.01$, $^{\#\#\#}p < 0.001$ compared to MPTP/p group; $n = 4$).

inhibitor (Tao et al., 2005), and displays other neuroprotective properties in PD models (Kabuto and Yamanushi, 2011). *A. rugosa*, a medicinal herb of the family *Lamiaceae* native to China, Korea, and Japan, has been used to decrease nausea and vomiting and treat fungal infections. Pharmacological studies have found that *A. rugosa* and one of its components, tilianin, have antiviral (Wang et al., 2009), antimicrobial (Shin, 2004), antioxidant (Guo et al., 2011), cardiovascular (Yuan et al., 2017), anti-inflammatory, anti-diabetic, and anti-hyperlipidemic properties (García-Díaz et al., 2016).

In the present study, we examined six active components (geniposide, paeoniflorin, tilianin, eugenol, saikosaponin A, and decursin) from the GCF mixture using *in vitro* assays, and for the first time demonstrated that tilianin has anti-PD activity in SH-SY5Y neuroblastoma cells. In addition, we showed that GCF has a stronger neuroprotective effect on the neuroblastoma cells than CG or its individual components (**Figure 2C**), suggesting that GCF might be a good formulation to treat PD patients. One possible caveat of this study is that we treated the cells first with GCF and then with 6-OHDA. The antioxidant properties of GCF may have inhibited the oxidation of 6-OHDA, thus weakening its toxicity toward the cells. However, GCF administered at a high concentration of 200 ug/ml did not show cytotoxicity and inhibited the cell death induced by 6-OHDA. This indicated that it most likely did not suppress the oxidation of 6-OHDA, but had a genuine protective effect on the cells.

cAMP response element binding is a transcription factor stimulated by Ser-133 phosphorylation, and it has numerous downstream effecters: protein kinase C (PKC), protein kinase A (PKA), ERK1/2, and several PI3K/Akt/GSK-3β pathways (Adams and Sweatt, 2002; Carlezon et al., 2005). In this study, we found that GCF treatment increased the levels of CREB phosphorylation in the SN of MPTP/p-treated and A53T a-synuclein Tg mice. An upstream activator of CREB, Akt, was

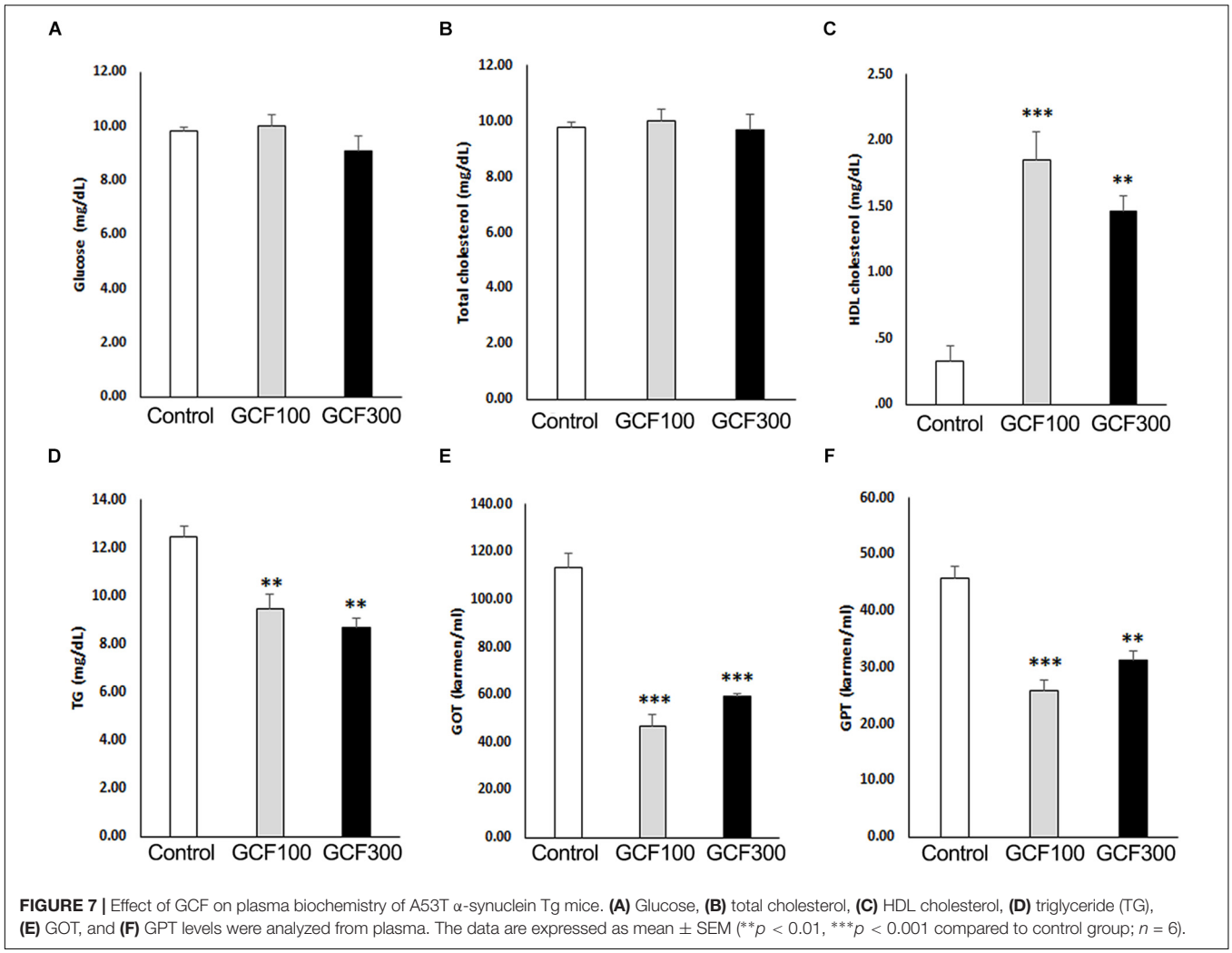

FIGURE 7 | Effect of GCF on plasma biochemistry of A53T α-synuclein Tg mice. **(A)** Glucose, **(B)** total cholesterol, **(C)** HDL cholesterol, **(D)** triglyceride (TG), **(E)** GOT, and **(F)** GPT levels were analyzed from plasma. The data are expressed as mean ± SEM (**$p < 0.01$, ***$p < 0.001$ compared to control group; $n = 6$).

phosphorylated by GCF treatment as well. The observed ERK phosphorylation, however, may be attributed not just to GCF treatment, but to increased proinflammatory cytokine release, which could be neurotoxic in itself (Hua et al., 2002). In addition to these elements, administration of GCF was shown to suppress TNF-α expression (**Figure 5C**). These alterations in protein expression indicate that GCF activates Akt, which in turn enhances CREB activation and exerts neuroprotective effects in the PD model mice.

DJ-1, a sensor of oxidative stress (Canet-Avilés et al., 2004), can decrease the accumulation and toxicity of α-synuclein in PD models (Shendelman et al., 2004; Zhou et al., 2011; Sun et al., 2012; Zondler et al., 2014; Lee et al., 2017). It is also known to activate ERK and Akt pathways to induce cell proliferation and survival (Oh and Mouradian, 2017). In this study, we demonstrated that GCF activates Akt, which might in turn be due to the induction of DJ-1 expression. The final cellular output of these signaling pathways is the reduction of α-synuclein accumulation, relieving the symptoms of PD in animal models.

MPTP-induced oxidative stress induces apoptosis through the activation of BCL-2 family proteins, including anti-apoptotic BCL-2 and pro-apoptotic BAX (Yang et al., 1997; Crompton, 2000). It has been reported that DJ-1 translocates to the mitochondria and binds to BCL-X_L in response to UV-B irradiation, inhibiting both rapid degradation of BCL-X_L and mitochondrial apoptosis (Ren et al., 2011). Specifically, BCL-X_L interacts with BAX to block its oligomerization in the mitochondrial membrane, thereby protecting cells from BAX-induced mitochondrial membrane permeabilization (Yin et al., 1994). In the present study, it was shown that GCF induces DJ-1, which may suppress BCL-2 degradation and BAX expression, resulting in the inhibition of MPTP-induced apoptosis in PD models.

Autophagy is the process of degradation and elimination of aggregated proteins. Inhibition of this process induces neuronal degeneration in the central nervous system (Hara et al., 2006; Komatsu et al., 2006). AMPK activation is linked to the maintenance of autophagy (Mihaylova and Shaw, 2011) and neurogenesis (Dagon et al., 2005). AMPK activity in dopaminergic neurons has also been shown to be necessary for neuroprotection in a mouse model of PD (Bayliss et al., 2016). In addition, neuronal AMPK is part

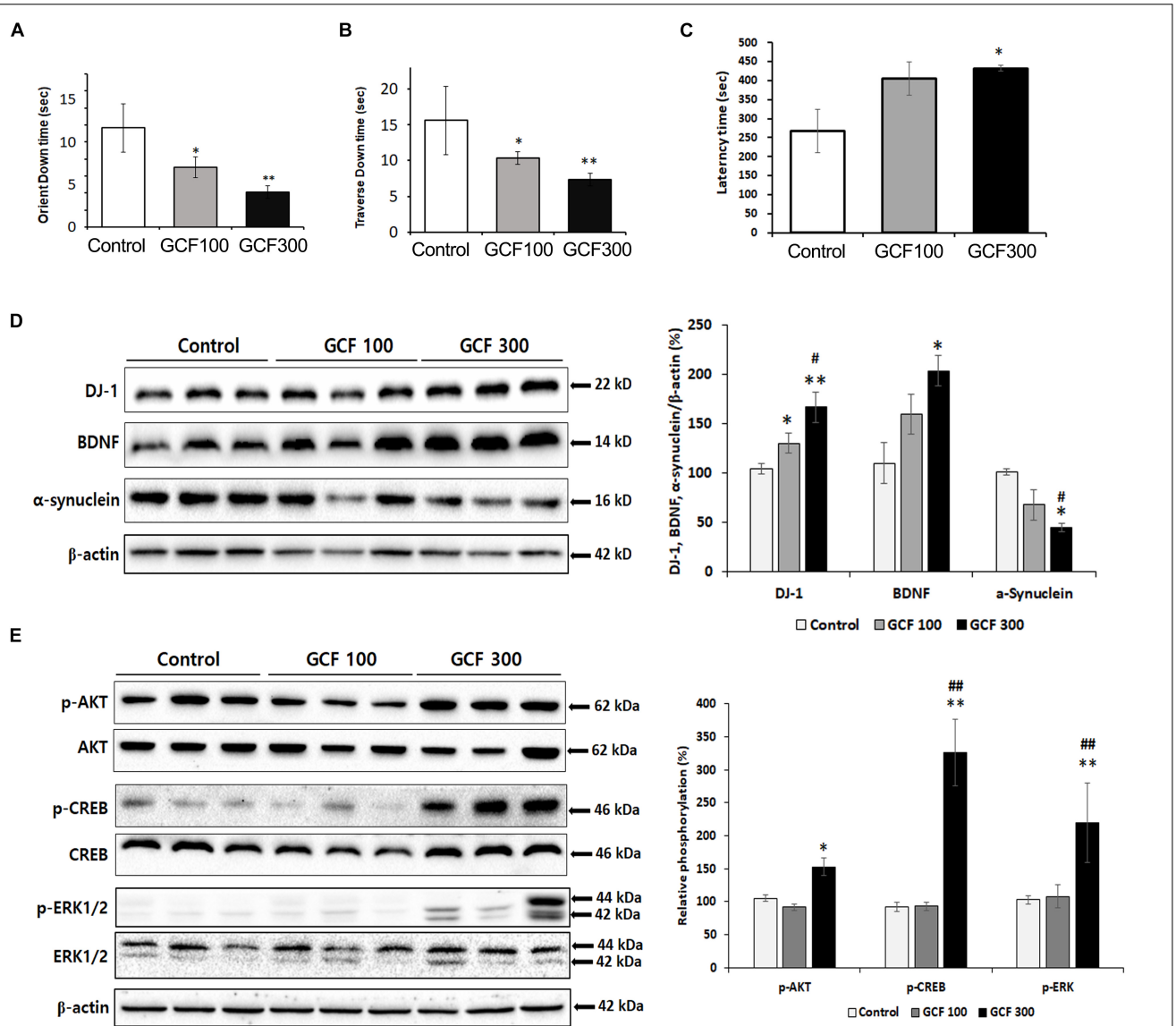

FIGURE 8 | Neuroprotective effect of GCF on A53T α-synuclein Tg mice. **(A)** Orient down time and **(B)** transverse down time of pole test, and **(C)** latency time of overall rotarod performance were measured in each group. The lysates of SN were electrophoresed and immunoblotted with each antibodies against α-synuclein, DJ-1, BDNF, and the phosphorylated forms of Akt, CREB, and ERK. The intensity of each band was normalized to that of β-actin **(D)** or total form and β-actin **(E)** and presented in bar graphs. The data are expressed as mean ± SEM (*$p < 0.05$, **$p < 0.01$ compared to control group; #$p < 0.05$ compared to GCF 100 mg/kg treated group; $n = 7$).

of an important signaling pathway that regulates BDNF, an essential mediator of neurogenesis (Kim and Leem, 2016; Liu et al., 2014). In this context, we demonstrated that treatment with GCF activates AMPK and induces BDNF expression in MPTP/p-induced PD mice models. Thus, this study provides evidence for the neuroprotective effects of GCF through AMPK activation in the SN.

We conducted both *in vitro* and *in vivo* efficacy tests of GCF in SH-SY5Y cells and mouse models. However, we primarily focused on the *in vivo* test to determine the effective doses of GCF in humans. We found that the effective doses in mice were 200 mg/kg and 300 mg/kg and the Human Equivalent Doses (HED) (Reagan-Shaw et al., 2008) were the following: 972.9730 mg/day (200 mg/kg × (3/37) × 60 kg) and 1459.4595 mg/day (300 mg/kg × (3/37) × 60 kg], respectively. In line with this observation, we conducted a 13-week oral toxicity study in Sprague–Dawley (SD) rats to determine the No Observed Adverse Effect Level (NOAEL). Based on this oral toxicity study, the NOAEL was assessed to be 2000 mg/kg/day by the KFDA-certified Good Laboratory Practice (GLP) Contract Research Organization (CRO), ChemOn (Yongin-Si, Gyeonggi, South Korea). The concentrations of GCF that were used in mice are therefore safe for therapeutic usage (data not shown).

Generally, when animals are tested for therapeutic effects of new compounds, the drug is administered simultaneously with disease induction. Therefore in this experiment, medication in the form of GCF was administered at the same time as MPTP, implying that the protective effects of GCF in the MPTP/p study are due to blockage of MPTP metabolism to MPP^+. However, we also examined the neuroprotective effects of GCF after PD induction in the MPTP PD models (data not shown) and in the A53T α-synuclein Tg animal model, and found similar effects to those seen with simultaneous GCF administration. Hence, it can be inferred that GCF is an effective reagent for neuroprotection and regeneration when administered to PD patients.

In this study, we compared the anti-PD effects of GCF with L-dopa in the MPTP PD model (**Figure 3**). Although L-dopa did not recover the loss of dopaminergic cells, it did improve behavioral impairment, which is in concert with previous reports that L-dopa improves abnormal behavior in Parkinson's patients by supplementing deficient dopamine. However, longterm use of L-dopa may induce certain complications such as eventual loss of symptom control, leading to dyskinesia (Hauser, 2009). We found that the effect of GCF was more significant than that of L-dopa in terms of motor control (**Figure 3**), suggesting that GCF may normalize the function of dopaminergic cells in MPTP-treated mice. However, further studies are essential to determine the levels of dopamine and its metabolites in order to fully illustrate the protective effects of GCF.

In summary, the present findings demonstrate the neuroprotective effect of GCF against MPTP- or MPTP/p-induced motor deficits and dopaminergic cell death. In addition, GCF administration diminishes behavioral impairments in α-synuclein A53T overexpressed mice. GCF activates elements of cell survival pathways such as Akt, ERK, and CREB in PD models and induced DJ-1 and BDNF expression. Moreover, GCF decreases α-synuclein expression and pro-apoptotic BAX expression through DJ-1 induction in chronic PD models. Therefore, the use of GCF, a herbal medicine, could be a potential remedy for neurodegenerative disorders such as Parkinson's disease.

ETHICS STATEMENT

The experimental processes were approved from the Institutional Animal Treatment Ethical Committee, Dongguk University Campus (Nos. 2017-0992, 2017-025, and 2017-0992) and followed the NIH guidelines.

AUTHOR CONTRIBUTIONS

All authors were responsible for the study concept and design. SA, J-HJ, and JP carried out the immunoblotting of animal experiments in MPTP/p PD model. QL and HJ carried out the cell study, MPTP PD model, and α-synuclein PD animal experiments. YK, DK, GJ, and SO participated in the extraction of herbal medicine and analytical experiments. S-UP and S-YC organized the oriental medicine prescription. H-JP and SJ conceived the study and wrote the draft manuscript.

FUNDING

This work was supported by a grant of the Korean Health Technology R&D Project, Ministry of Health and Welfare, South Korea (No. HI16C0405) and a grant from the National Research Foundation of Korea funded by the Korean Government (NRF-2017R1A2B4009963).

SUPPLEMENTARY MATERIAL

The Supplementary Material for this article can be found online at: https://www.frontiersin.org/articles/10.3389/fnagi.2019.00230/full#supplementary-material

FIGURE S1 | Tyrosin hydroxylase expression in the SN of WT and A53T α-synuclein Tg mice. **(A)** The lysates of SN were electrophoresed and immunoblotted with TH or β-actin antibody. The intensity of each band was normalized to that of β-actin and presented in bar graphs **(B)**. The data are expressed as mean ± SEM.

REFERENCES

Adams, J. P., and Sweatt, J. D. (2002). Molecular psychology: roles for the ERK MAP kinase cascade in memory. *Annu. Rev. Pharmacol. Toxicol.* 42, 135–163. doi: 10.1146/annurev.pharmtox.42.082701.145401

Ahn, S., Song, T. J., Park, S. U., Jeon, S., Kim, J., Oh, J. Y., et al. (2017). Effects of a combination treatment of KD5040 and (L)-dopa in a mouse model of Parkinson's disease. *BMC. Complement. Altern. Med.* 17:220. doi: 10.1186/s12906-017-1731-2

Alvarez-Fischer, D., Noelker, C., Grünewald, A., Vulinoviæ, F., Guerreiro, S., Fuchs, J., et al. (2013). Probenecid potentiates MPTP/MPP+ toxicity by interference with cellular energy metabolism. *J. Neurochem.* 127, 782–792. doi: 10.1111/jnc.12343

Athanassiadou, A., Voutsinas, G., Psiouri, L., Leroy, E., Polymeropoulos, M. H., Ilias, A., et al. (1999). Genetic analysis of families with Parkinson disease that carry the Ala53Thr mutation in the gene encoding alpha-synuclein. *Am. J. Hum. Genet.* 65, 555–558. doi: 10.1086/302486

Baek, M. E., Seong, G. U., Lee, Y. J., and Won, J. H. (2016). Quantitative analysis for the quality evaluation of active ingredients in cnidium rhizome. *Yakhak Hoeji.* 60, 227–234. doi: 10.17480/psk.2016.60.5.227

Bayliss, J. A., Lemus, M. B., Stark, R., Santos, V. V., Thompson, A., Rees, D. J., et al. (2016). Ghrelin-AMPK signaling mediates the neuroprotective effects of calorie restriction in parkinson's disease. *J. Neurosci.* 36, 3049–3063. doi: 10.1523/JNEUROSCI.4373-15.2016

Beal, M. F. (2001). Experimental models of Parkinson's disease. *Nat. Rev. Neurosci.* 2, 325–334.

Canet-Avilés, R. M., Wilson, M. A., Miller, D. W., Ahmad, R., McLendon, C., Bandyopadhyay, S., et al. (2004). The Parkinson's disease protein DJ-1 is neuroprotective due to cysteine-sulfinic acid-driven mitochondrial localization. *Proc. Natl. Acad. Sci. U.S.A.* 101, 9103–9108. doi: 10.1073/pnas.0402959101

Cao, B. Y., Yang, Y. P., Luo, W. F., Mao, C. J., Han, R., Sun, X., et al. (2010). Paeoniflorin, a potent natural compound, protects PC12 cells from MPP+ and acidic damage via autophagic pathway. *J. Ethnopharmacol.* 131, 122–129. doi: 10.1016/j.jep.2010.06.009

Carlezon, W. A. , Duman, R. S., and Nestler, E. J. (2005). The many faces of CREB. *Trends Neurosci.* 28, 436–445. doi: 10.1016/j.tins.2005.06.005

Chang, Y., Yoo, J., Kim, H., Park, H. J., Jeon, S., and Kim, J. (2018). Salusin-β mediate neuroprotective effects for Parkinson's disease. *Biochem. Biophys. Res. Commun.* 503, 1428–1433. doi: 10.1016/j.bbrc.2018.07.059

Chen, Y., Zhang, Y., Li, L., and Hölscher, C. (2015). Neuroprotective effects of geniposide in the MPTP mouse model of Parkinson's disease. *Eur. J. Pharmacol.* 768, 21–27. doi: 10.1016/j.ejphar.2015.09.029

Conley, S. C., and Kirchner, J. T. (1999).). Parkinson's disease–the shaking palsy. underlying factors, diagnostic considerations, and clinical course. *Postgrad Med.* 106, 39–52. doi: 10.3810/pgm.1999.07.604

Crompton, M. (2000). Bax, Bid and the permeabilization of the mitochondrial outer membrane in apoptosis. *Curr. Opin. Cell Biol.* 12, 414–419. doi: 10.1016/s0955-0674(00)00110-1

Dagon, Y., Avraham, Y., Magen, I., Gertler, A., Ben-Hur, T., and Berry, E. M. (2005). Nutritional status, cognition, and survival: a new role for leptin and AMP kinase. *J. Biol. Chem.* 280, 42142–42148. doi: 10.1074/jbc.m507607200

de Silva, H. R., Khan, N. L., and Wood, N. W. (2000). The genetics of Parkinson's disease. *Curr. Opin. Genet. Dev.* 10, 292–298.

García-Díaz, J. A., Navarrete-Vázquez, G., García-Jiménez, S., Hidalgo-Figueroa, S., Almanza-Pérez, J. C., Alarcón-Aguilar, F. J., et al. (2016). Antidiabetic, antihyperlipidemic and anti-inflammatory effects of tilianin in streptozotocin-nicotinamide diabetic rats. *Biomed. Pharmacother.* 83, 667–675. doi: 10.1016/j.biopha.2016.07.023

Guo, K. J., Xu, S. F., Yin, P., Wang, W., Song, X. Z., Liu, F. H., et al. (2011). Active components of common traditional Chinese medicine decoctions have antioxidant functions. *J. Anim. Sci.* 89, 3107–3115. doi: 10.2527/jas.2010-3831

Hara, T., Nakamura, K., Matsui, M., Yamamoto, A., Nakahara, Y., Suzuki-Migishima, R., et al. (2006). Suppression of basal autophagy in neural cells causes neurodegenerative disease in mice. *Nature* 441, 885–889. doi: 10.1038/nature04724

Hartmann, A. (2004). Postmortem studies in Parkinson's disease. *Dialogues Clin. Neurosci.* 6, 281–293.

Hauser, R. A. (2009). New considerations in the medical management of early Parkinson's disease: impact of recent clinical trials on treatment strategy. *Parkinsonism Relat. Disord.* 15, S17–S21. doi: 10.1016/S1353-8020(09)70772-2

Hua, L. L., Zhao, M. L., Cosenza, M., Kim, M. O., Huang, H., Tanowitz, H. B., et al. (2002). Role of mitogen-activated protein kinases in inducible nitric oxide synthase and TNF alpha expression in human fetal astrocytes. *J. Neuroimmunol.* 126, 180–189. doi: 10.1016/s0165-5728(02)00055-3

Ito, M., Murakami, K., and Yoshino, M. (2005). Antioxidant action of eugenol compounds: role of metal ion in the inhibition of lipid peroxidation. *Food Chem. Toxicol.* 43, 461–466. doi: 10.1016/j.fct.2004.11.019

Jia, F., Song, N., Wang, W., Du, X., Chi, Y., and Jiang, H. (2018). High dietary iron supplement induces the nigrostriatal dopaminergic neurons lesion in transgenic mice expressing mutant A53T human alpha-synuclein. *Front. Aging. Neurosci.* 6:97. doi: 10.3389/fnagi.2018.00097

Kabuto, H., and Yamanushi, T. T. (2011). Effects of zingerone [4-(4-hydroxy-3-methoxyphenyl)-2-butanone] and eugenol [2-methoxy-4-(2-propenyl)phenol] on the pathological progress in the 6-hydroxydopamine-induced Parkinson's disease mouse model. *Neurochem. Res.* 36, 2244–2249. doi: 10.1007/s11064-011-0548-5

Kalia, L. V., and Lang, A. E. (2015). Parkinson's disease. *Lancet* 386, 896–912. doi: 10.1016/S0140-6736(14)61393-3

Kim, D. M., and Leem, Y. H. (2016). Chronic stress-induced memory deficits are reversed by regular exercise via AMPK-mediated BDNF induction. *Neuroscience* 324, 271–285. doi: 10.1016/j.neuroscience.2016.03.019

Komatsu, M., Waguri, S., Chiba, T., Murata, S., Iwata, J., Tanida, I., et al. (2006). Loss of autophagy in the central nervous system causes neurodegeneration in mice. *Nature* 441, 880–884. doi: 10.1038/nature04723

Korean Food and Drug Administration [KFDA], (2015). *The Korean Pharmacopoeia XI*. Seoul: Shinil Books.

Kostic, V., Przedborski, S., Flaster, E., and Sternic, N. (1991). Early development of levodopa-induced dyskinesias and response fluctuations in young-onset Parkinson's disease. *Neurology* 41, 202–205.

Krüger, R., Kuhn, W., Müller, T., Woitalla, D., Graeber, M., Kösel, S., et al. (1998). Ala30Pro mutation in the gene encoding alpha-synuclein in Parkinson's disease. *Nat. Genet.* 18, 106–108.

Lee, S., Oh, S. T., Jeong, H. J., Pak, S. C., Park, H. J., Kim, J., et al. (2017). MPTP-induced vulnerability of dopamine neurons in A53T α-synuclein overexpressed mice with the potential involvement of DJ-1 downregulation. *Korean J. Physiol. Pharmacol.* 21, 625–632. doi: 10.4196/kjpp.2017.21.6.625

Li, X. Z., Zhang, S. N., Liu, S. M., and Lu, F. (2013). Recent advances in herbal medicines treating Parkinson's disease. *Fitoterapia* 84, 273–285. doi: 10.1016/j.fitote.2012.12.009

Liu, D. Z., Zhu, J., Jin, D. Z., Zhang, L. M., Ji, X. Q., Ye, Y., et al. (2007). Behavioral recovery following sub-chronic paeoniflorin administration in the striatal 6-OHDA lesion rodent model of Parkinson's disease. *J. Ethnopharmacol.* 112, 327–332. doi: 10.1016/j.jep.2007.03.022

Liu, H. Q., Zhang, W. Y., Luo, X. T., Ye, Y., and Zhu, X. Z. (2006). Paeoniflorin attenuates euroinflammation and dopaminergic neurodegeneration in the MPTP model of Parkinson's disease by activation of adenosine A1 receptor. *Br. J. Pharmacol.* 148, 314–325. doi: 10.1038/sj.bjp.0706732

Liu, Y., Tang, G., Zhang, Z., Wang, Y., and Yang, G. Y. (2014). Metformin promotes focal angiogenesis and neurogenesis in mice following middle cerebral artery occlusion. *Neurosci. Lett.* 579, 46–51. doi: 10.1016/j.neulet.2014.07.006

Ma, C., Yin, Z., Zhu, P., Luo, J., Shi, X., and Gao, X. (2017). Blood cholesterol in late-life and cognitive decline: a longitudinal study of the Chinese elderly. *Mol. Neurodegener.* 12:24. doi: 10.1186/s13024-017-0167-y

Matsuoka, Y., Vila, M., Lincoln, S., McCormack, A., Picciano, M., LaFrancois, J., et al. (2001). Lack of nigral pathology in transgenic mice expressing human alpha- synuclein driven by the tyrosine hydroxylase promoter. *Neurobiol. Dis.* 8, 535–539. doi: 10.1006/nbdi.2001.0392

Meredith, G. E., Totterdell, S., Potashkin, J. A., and Surmeier, D. J. (2008). Modeling PD pathogenesis in mice: advantages of a chronic MPTP protocol. *Parkinsonism. Relat. Disord.* 2, S112–S115. doi: 10.1016/j.parkreldis.2008.04.012

Mihaylova, M. M., and Shaw, R. J. (2011). The AMPK signalling pathway coordinates cell growth, autophagy and metabolism. *Nat. Cell. Biol.* 13, 1016–1023. doi: 10.1038/ncb2329

Oh, S. E., and Mouradian, M. M. (2017). Regulation of signal transduction by DJ-1. *Adv. Exp. Med. Biol.* 1037, 97–131. doi: 10.1007/978-981-10-6583-5_8

Petroske, E., Meredith, G. E., Callen, S., Totterdell, S., and Lau, Y. S. (2001). Mouse model of Parkinsonism: a comparison between subacute MPTP and chronic MPTP/probenecid treatment. *Neuroscience* 106, 589–601. doi: 10.1016/s0306-4522(01)00295-0

Polymeropoulos, M. H., Lavedan, C., Leroy, E., Ide, S. E., Dehejia, A., Dutra, A., et al. (1997). Mutation in the alpha-synuclein gene identified in families with Parkinson's disease. *Science* 276, 2045–2047. doi: 10.1126/science.276.5321.2045

Przedborski, S., Jackson-Lewis, V., Djaldetti, R., Liberatore, G., Vila, M., Vukosavic, S., et al. (2000). The parkinsonian toxin MPTP: action and mechanism. *Restor. Neurol. Neurosci.* 16, 135–142.

Reagan-Shaw, S., Nihal, M., and Ahmad, N. (2008). Dose translation from animal to human studies revisited. *FASEB J.* 22, 659–661. doi: 10.1096/fj.07-9574lsf

Ren, H., Fu, K., Wang, D., Mu, C., and Wang, G. (2011). Oxidized DJ-1 interacts with the mitochondrial protein BCL-XL. *J. Biol. Chem.* 286, 35308–35317. doi: 10.1074/jbc.M110.207134

Shendelman, S., Jonason, A., Martinat, C., Leete, T., and Abeliovich, A. (2004). DJ-1 is a redox-dependent molecular chaperone that inhibits alpha-synuclein aggregate formation. *PLoS. Biol.* 2:e362. doi: 10.1371/journal.pbio.0020362

Shin, S. (2004). Essential oil compounds from agastache rugosa as antifungal agents against *Trichophyton* species. *Arch. Pharm. Res.* 27, 295–299. doi: 10.1007/bf02980063

Su, C., Yang, X., and Lou, J. (2016). Geniposide reduces α-synuclein by blocking microRNA-21/lysosome-associated membrane protein 2A interaction in Parkinson disease models. *Brain Res.* 1644, 98–106. doi: 10.1016/j.brainres.2016.05.011

Sun, S. Y., An, C. N., and Pu, X. P. (2012). DJ-1 protein protects dopaminergic neurons against 6-OHDA/MG-132-induced neurotoxicity in rats. *Brain Res. Bull.* 88, 609–616. doi: 10.1016/j.brainresbull.2012.05.013

Tao, G., Irie, Y., Li, D. J., and Keung, W. M. (2005). Eugenol and its structural analogs inhibit monoamine oxidase A and exhibit antidepressant-like activity. *Bioorg. Med. Chem.* 13, 4777–4788. doi: 10.1016/j.bmc.2005.04.081

Tuan, P. A., Park, W. T., Xu, H., Park, N. I., and Park, S. U. (2012). Accumulation of tilianin and rosmarinic acid and expression of phenylpropanoid biosynthetic genes in *Agastache rugosa*. *J. Agric. Food Chem.* 60, 5945–5951. doi: 10.1021/jf300833m

Uchihara, T., and Giasson, B. I. (2016). Propagation of alpha-synuclein pathology: hypotheses, discoveries, and yet unresolved questions from experimental and human brain studies. *Acta Neuropathol.* 131, 49–73. doi: 10.1007/s00401-015-1485-1

van der Putten, H., Wiederhold, K. H., Probst, A., Barbieri, S., Mistl, C., Danner, S., et al. (2000). Neuropathology in mice expressing human alpha-synuclein. *J. Neurosci.* 20, 6021–6029.

Wang, K. C., Chang, J. S., Chiang, L. C., and Lin, C. C. (2009). 4-Methoxycinnamaldehyde inhibited human respiratory syncytial virus in a human larynx carcinoma cell line. *Phytomedicine* 16, 882–886. doi: 10.1016/j.phymed.2009.02.016

Yang, J., Liu, X., Bhalla, K., Kim, C. N., Ibrado, A. M., Cai, J., et al. (1997). Prevention of apoptosis by Bcl-2: release of cytochrome c from mitochondria blocked. *Science* 275, 1129–1132. doi: 10.1126/science.275.5303.1129

Yin, X. M., Oltvai, Z. N., and Korsmeyer, S. J. (1994). BH1 and BH2 domains of Bcl-2 are required for inhibition of apoptosis and heterodimerization with Bax. *Nature* 369, 321–323. doi: 10.1038/369321a0

Yuan, Y., Cao, W., Hong, Y., Guo, X., Wang, Y., Wang, Y., et al. (2017). Tilianin pretreatment prevents myocardial ischemia-reperfusion injury via preservation of mitochondrial function in rat heart. *Phytomedicine* 34, 106–114. doi: 10.1016/j.phymed.2017.08.007

Yun, H. J., Yun, S. M., Lee, M. H., and Son, S. W. (2008). Determination of eugenol in Eugenia caryophyllata by high-performance liquid chromatography with photodiode array detection and method validation. *Korean J. Vet. Res.* 48, 9–15.

Zhou, W., Bercury, K., Cummiskey, J., Luong, N., Lebin, J., and Freed, C. R. (2011). Phenylbutyrate up-regulates the DJ-1 protein and protects neurons in cell culture and in animal models of Parkinson disease. *J. Biol. Chem.* 286, 14941–14951. doi: 10.1074/jbc.M110.211029

Zondler, L., Miller-Fleming, L., Repici, M., Gonçalves, S., Tenreiro, S., and Rosado-Ramos, R. (2014). DJ-1 interactions with α-synuclein attenuate aggregation and cellular toxicity in models of Parkinson's disease. *Cell Death Dis.* 5:e1350. doi: 10.1038/cddis.2014.307

Conflict of Interest Statement: The authors declare that the research was conducted in the absence of any commercial or financial relationships that could be construed as a potential conflict of interest.

Advantages of publishing in Frontiers

OPEN ACCESS
Articles are free to read for greatest visibility and readership

FAST PUBLICATION
Around 90 days from submission to decision

HIGH QUALITY PEER-REVIEW
Rigorous, collaborative, and constructive peer-review

TRANSPARENT PEER-REVIEW
Editors and reviewers acknowledged by name on published articles

Frontiers
Avenue du Tribunal-Fédéral 34
1005 Lausanne | Switzerland

Visit us: www.frontiersin.org
Contact us: info@frontiersin.org | +41 21 510 17 00

REPRODUCIBILITY OF RESEARCH
Support open data and methods to enhance research reproducibility

DIGITAL PUBLISHING
Articles designed for optimal readership across devices

FOLLOW US
@frontiersin

IMPACT METRICS
Advanced article metrics track visibility across digital media

EXTENSIVE PROMOTION
Marketing and promotion of impactful research

LOOP RESEARCH NETWORK
Our network increases your article's readership